The genus Ammonia (Foraminifera) in the ecosystems of the Atlantic coasts

Julien Richirt

DOCTORAT SCIENCES BRETAGNE DE LA MER LOIRE ET DU LITTORAL

université angers

THESE DE DOCTORAT DE

L'UNIVERSITE D'ANGERS

ECOLE DOCTORALE N° 598
Sciences de la Mer et du Littoral
Spécialité : Géosciences Marines

Par
Julien RICHIRT

Le genre *Ammonia* (Foraminifères) dans les écosystèmes côtiers de la façade atlantique

Thèse présentée et soutenue à Angers, le 2 Septembre 2020

Unité de recherche : UMR 6112 LPG-BIAF : Bio-Indicateur Actuels et Fossiles, CNRS, Université d'Angers

Rapporteurs avant soutenance :

Ellen THOMAS	Professeure Université de Yale
Gerhard SCHMIEDL	Professeur Université d'Hamburg

Composition du Jury :

Vincent BOUCHET	Maître de conférence Université de Lille
Emmanuelle GESLIN	Professeure Université d'Angers
Nicolaas GLOCK	Docteur GEOMAR
Directeur de thèse : Frans JORISSEN	Professeur Université d'Angers
Co-encadrantes de thèse : Magali SCHWEIZER	Maître de conférence Université d'Angers
Aurélia MOURET	Maître de conférence Université d'Angers

Le genre *Ammonia* (Foraminifères) dans les écosystèmes côtiers de la façade atlantique

REMERCIEMENTS

Je souhaite remercier mon directeur ainsi que mes deux co-encadrantes de thèse. Vous avez su m'indiquer la bonne direction à suivre tout au long de ces quatre années, tout en me laissant l'autonomie dont j'avais besoin. Vous avez été disponibles et à l'écoute. J'imagine qu'il n'est pas facile d'encadrer un étudiant pendant plusieurs années, vous avez pleinement assuré votre mission, j'espère avoir rempli la mienne. J'ai sincèrement aimé travailler avec vous et j'espère avoir l'occasion de continuer à le faire dans le futur.

Mes remerciements vont également à tous mes collègues. Lorsque je suis arrivé, j'étais un peu intimidé, parfois même dérouté. Ici, c'est vivant, on mange tous ensemble, tout le monde se connaît bien, ça blague souvent, ça rigole fort. Parfois le ton monte, mais ça ne dure jamais très longtemps. Cette description ressemble fort à celle d'une famille, et chacun sait que c'est parfois difficile de s'intégrer pour une pièce rapportée. Mais j'ai très rapidement compris que les gens ici étaient chaleureux et bienveillants. Merci à toutes et tous pour votre accueil et cette bonne humeur quotidienne. Je pense qu'il sera difficile de retrouver la même chose autre part. Honnêtement, je me suis senti plutôt bien chez vous.

Je voudrais aussi remercier mes amis. Nous nous suivons depuis de nombreuses années maintenant, j'espère que cela continuera. J'ai la chance d'avoir votre soutien indéfectible. Je vois les deux ou trois du fond qui trouvent ça cucu mais tant pis, vous savez que je vous aime!

Merci à ma famille, qui m'a toujours soutenu dans mes choix. Je suis sûr que sans eux je ne serais pas là où je suis. « Que-ce que tu veux faire plus tard quand tu seras grand ? », c'est toujours plus facile de répondre à cette question lorsque l'on est enfant. On doute plus rarement quand on est jeune. J'avais deux lubies quand j'étais petit, je voulais devenir soit « fabricateur de billes », soit océanographe. Finalement, je ne suis pas tombé si loin, je suis chanceux ! Les dissections de maquereaux chez papy et mamie y sont très certainement pour quelque chose. Merci pour tout.

« *La joie de vivre, la joie de vivre et le jambon, y'a pas trente-six recettes du bonheur!*"

Karadoc, *Kaamelott*, Livre III

CONTENTS

CHAPTER 1

INTRODUCTION

In the last 60 years, the human population has more than doubled, from three billion in 1960 to seven billion in 2012, and is expected to reach 10 billion by 2050. Consequently, anthropogenic pressure is increasing over the planet, with potentially disastrous consequences on all ecosystems (e.g. habitat destructions, eutrophication, loss of biodiversity, species extinctions). Consequently, environmental problems caused by anthropogenic pressure are increasing and start now to occupy a central position in politics. In view of the growing need for conservation and management of terrestrial as well as marine ecosystems, scientists are asked to develop methods to measure environmental quality, and to propose reliable solutions to remediate environmental problems. An essential prerequisite to answer these questions is to understand the functioning of these ecosystems.

Foraminifera are important biotic components in almost all marine settings. Therefore, it is essential to know how they interact with their environment, which ultimately leads to a better understanding of their role in these ecosystems. In line with this topic, the present PhD thesis investigates three phylotypes of the benthic foraminiferal genus *Ammonia*. This genus is a dominant element in coastal areas of mid-latitude, which are strongly menaced by increased anthropogenic impact. Presently, these three phylotypes are very often recognised together as one morphospecies, but they correspond in fact to three well separated pseudocryptic species, with only minor but consistent morphological differences. We will focus on their distinction on the basis of morphological characteristics (Chapter 2), on their distribution around British Isles (Chapter 3), on their temporal response to seasonal anoxic stress (Chapter 4), and on a recent historical record in this area which is strongly impacted by human activities (Chapter 5). Finally, by using a theoretical approach in Chapter 6, we aim to understand the functional morphology of the pore pattern of their tests, which is very different between these three phylotypes.

1. COASTAL AREAS

Coastal areas have always exerted a strong attraction on human populations around the world. The reasons are multiple: richness of natural resources (fish, molluscs, salt, sand, etc.), logistic facilities (navigation, commerce), esthetical considerations, etc. Consequently, a large proportion of human populations worldwide is concentrated in the 100 km bordering the coastline (about one third after Cohen et al., 1997; about one quarter after Small & Nicholls, 2003), and the last two centuries have seen a global inland to coast migration associated with a trend of increasing coastal area urbanisation (Hugo, 2011).

Coastal zones are also among the most productive ecosystems worldwide (Alongi, 1998). Therefore, human societies are highly reliant on these areas (Vitousek et al, 1997, Costanza et al., 1997) and benefit from very important and diverse ecosystemic goods and services (Figure 1, Millenium Ecosystem Assessment, 2005).

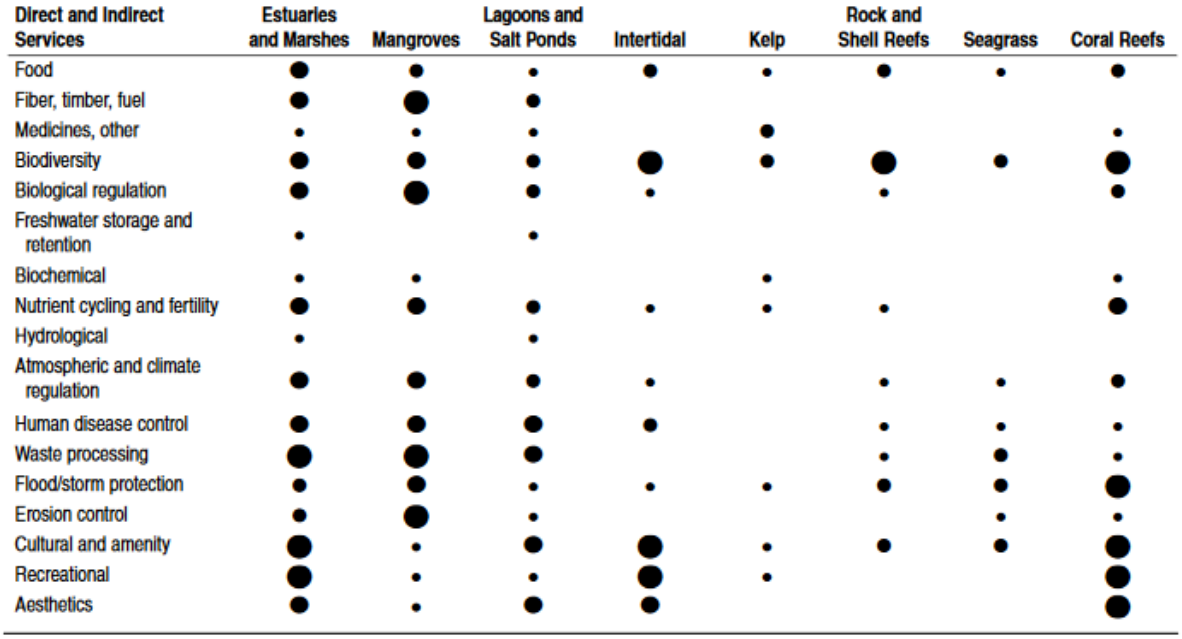

Figure 1. Direct and indirect ecosystem services provided by different types of coastal ecosystems. The size of the black circles represents the relative magnitude of each ecosystem service. The larger the circle the larger the relative magnitude (From Millenium Ecosystem Assessment, 2005).

Coastal areas are very dynamic and complex, with many intertwined processes acting at different spatial and temporal scales (Elliot & Whitfield, 2011), resulting in a relatively high natural variability. At the same time, these environments are affected by important and multiple anthropogenic pressures, which can lead to discrete or diffuse pollutions, originating from one source or originating from widespread anthropogenic activities with no single discrete source, respectively.

As a result, coastal ecosystems often exhibit a combination of high natural variability and important anthropogenic impact. Consequently, it is highly complicated to unravel the ecosystem responses to these interacting factors. Nevertheless, it is now well understood that these ecosystems are particularly fragile and undergo major changes in response to the strong pressures exerted by the mankind (Figure 2; Jackson et al., 2001; Millenium ecosystem assessment, 2005; Harley et al., 2006; Worm et al, 2006; Halpern et al., 2008; IPCC, 2013).

Impact Type	Examples
Physical changes	
Hydrologic changes	Channelization of streams, canals for petroleum production in Mississippi delta,oil exploration, dredging, drainage, harbor dredging, and navigation
Impoundments	
Reclamation	Polders in the Netherlands
Enrichment	
Eutrophication	Algal blooms resulting from agricultural runoff
Organic enrichment	Fish-processing wastes
Thermal additions	Power plants
Toxins	Heavy metals, pesticides, other chemicals such as DDT and PCBs, mercury, exotic organics
Direct changes in species	
Composition	Harvest and overharvest, overfishing
Introduction of exotic species	Striped bass on US west coast, nutria in Louisiana

Figure 2. Classification and examples of human impacts on coastal ecosystems from Day et al. (2012).

As a result, management solutions to maintain the ecosystemic goods and services provided by coastal areas are increasingly urged and formal management strategies emerged in a growing number of countries (Sorensen, 1997; Borja et al., 2008), such as:

- The Clean Water Act/Ocean Act (1972/2000) in the USA.
- The National Water Act (1998) in South Africa.
- The Environment Protection and Biodiversity Conservation Act (1999) in Australia.
- The Water Directive Framework (WFD, 2000) and the Marine Strategy Framework Directive (MSFD, 2008) in Europe.

The WFD as well as the MSFD impose the necessity for a "good" ecological quality status (EQS) of all European water bodies. The EQS is defined by comparing the current state of the ecosystem with a similar ecosystem in pristine state (without any human impact). If the current state deviates too much from the pristine state (i.e. "bad" EQS), management measures must be taken to return to a "good" EQS. This method has the benefit to take into account the natural state of the ecosystems without anthropogenic pressure. However, it has the shortcoming that we need to define a reference state (pristine) for every type of ecosystem. This may be particularly difficult in Europe, where almost all coastal ecosystems are strongly altered by

human activities. An additional complication is that natural ecosystems can be affected by phenomena which are usually considered as bad, such as algal blooms or hypoxia/anoxia (Dolven et al., 2013). Consequently, it is essential to have a better knowledge about the functioning of these coastal ecosystems to provide a good evaluation of the pristine states but also to design efficient management solutions.

Anthropogenic nutrient input is probably one of the major human treats to coastal ecosystems. It results from modern agricultural practices, increased industrial activities, combustion of fossil fuels or direct sewage discharge. All these factors contribute to the increased flow of nitrogen and phosphorus to coastal ecosystems (Diaz et al., 2013).

Increased nutrient supplies generally result in an intensified growth of all auto- and heterotrophic organisms. This increased biological production ultimately leads to enhanced organic matter input ("enrichment") and increased oxygen consumption. This series of events, called eutrophication, is now very strongly amplified by human activities in most places. Eutrophication is a global phenomenon, as shown by the various symptoms observed worldwide, such as harmful algal blooms, loss of habitats and natural resources and oxygen depletion (hypoxia or anoxia), which is probably the most severe problem (Vitousek et al, 1997; Cloern, 2001; Rabalais et al., 2009, 2010; Diaz et al., 2013).

2. HYPOXIA IN COASTAL ECOSYSTEMS

A commonly used definition of hypoxia (also used in this thesis) is a concentration of dissolved oxygen < 2 mg L^{-1}, or 1.4 ml L^{-1}, approx. equivalent to 63 μmol L^{-1} and corresponding to 30% oxygen saturation (sea water at 30°C) (Rabalais et al., 2010), whereas anoxia is defined as an absence of oxygen (i.e. non-detectable). Hypoxia affects numerous environments, including coastal ecosystems, at many different spatial (from < 1 km^2 to > 100 000 km^2) and temporal (from hours to decades) scales. Because human influence is more acute in coastal areas compared to open oceans (where this influence is more diluted), there is more anthropogenic pressure in coastal ecosystems (Figure 3, Rabalais et al. 2010).

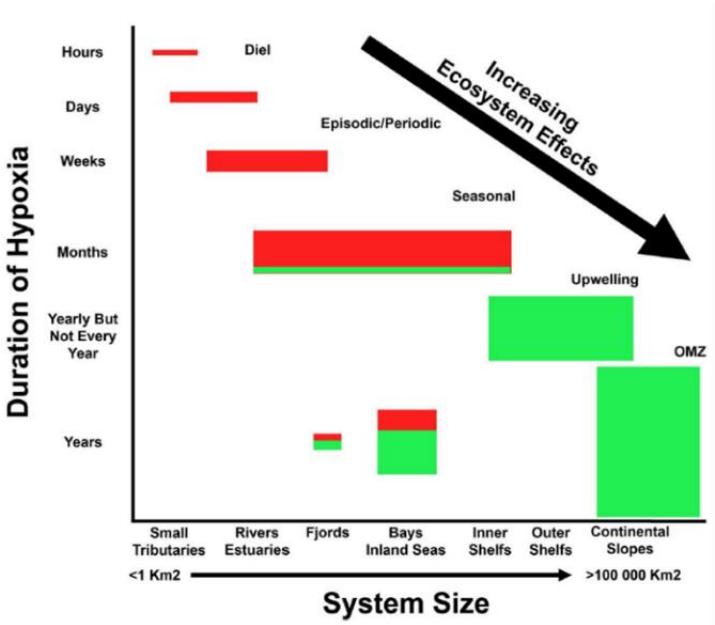

Figure 3. Synthetic scheme of the temporal and spatial variability of hypoxia in different environments. Red and green correspond respectively to human and natural causes (from Rabalais et al. 2010).

Oxygen is fundamental to sustain aerobic life in most modern ecosystems. Its depletion affects the performance and fitness of many organisms and can even be lethal for many of them. As a major threat to ecosystems, hypoxia is responsible for various types of environmental impact (Figure 4, Diaz et al., 2013).

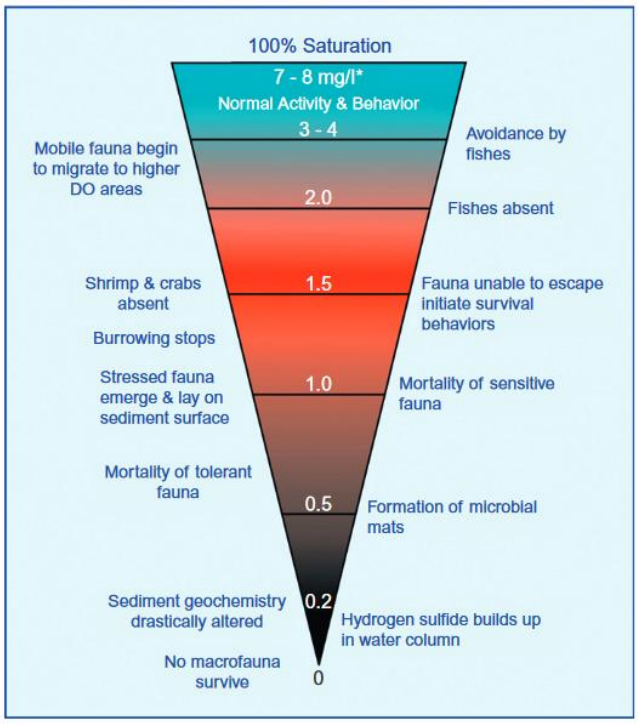

Figure 4. Range of behavioural and environmental impact as dissolved oxygen levels drop from saturation to anoxia (from Diaz et al., 2013).

Oxygen depletion has effects at the individual and population levels, with cascading effects at the community level which can finally lead to an ecosystem collapse (Figure 5, Riedel et al., 2016). Responses of coastal ecosystems to hypoxia concern all compartments of the biocoenosis and ultimately may alter and/or abolish ecosystem functions and services (Riedel et al., 2016).

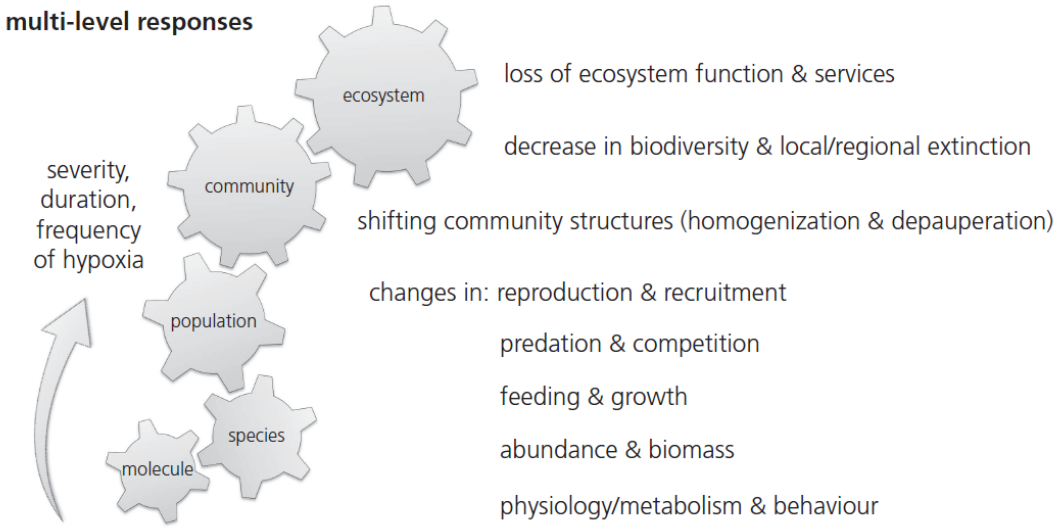

Figure 5. Cascading effects showing the multi-level aspect of the biological responses to oxygen depletion (from Riedel et al., 2016).

Due to increased human activities in coastal zones (e.g. increased nutrient input, building of coastal facilities modifying natural hydrodynamics) coupled with climate change (Rabalais et al., 2009; 2010), hypoxia in coastal waters are increasing in extent, frequency and duration (Figure 6, Schmidko et al., 2017; Diaz & Rosenberg, 2008). Diaz and Rosenberg (1995) already noted that “no other environmental variable of such ecological importance to coastal marine ecosystems as dissolved oxygen has changed so drastically, in such a short period of time”.

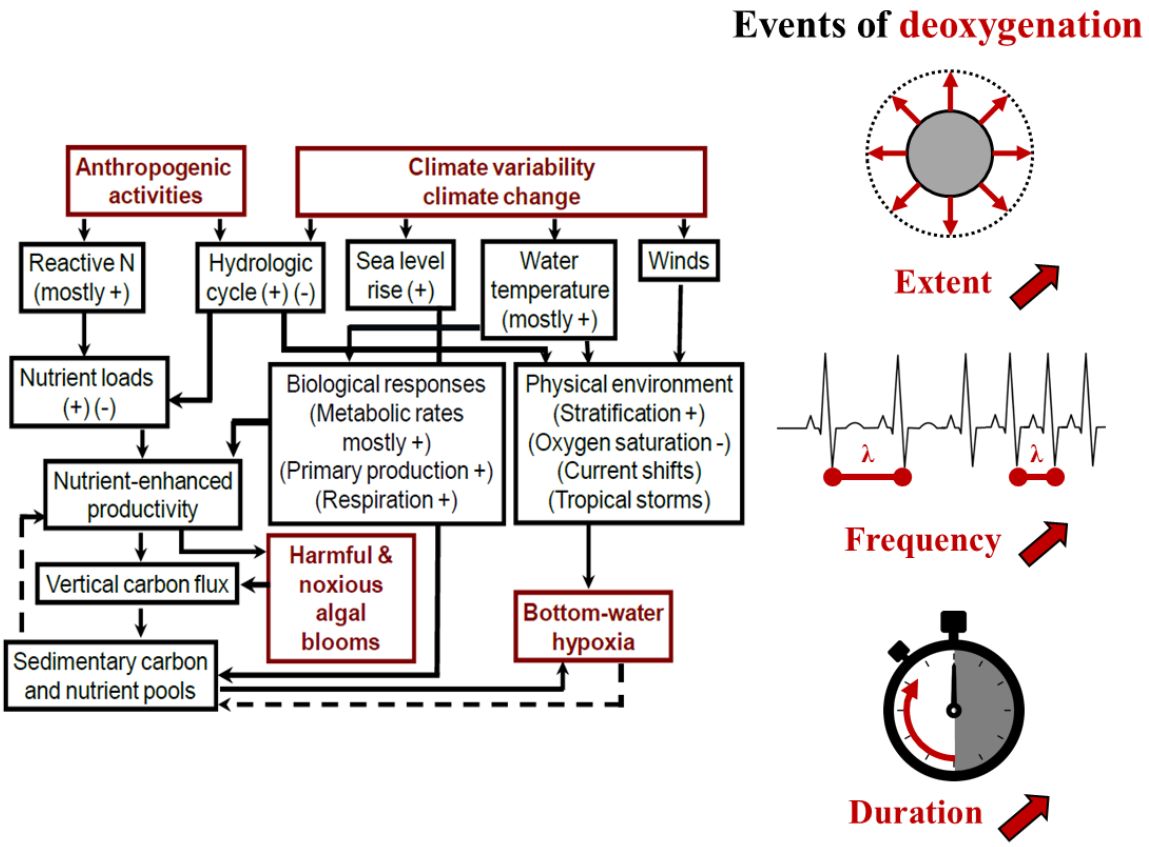

Figure 6. Potential physical and hydrological changes resulting from climate change and their interaction with current and future human activities. The dashed lines represent negative feedback to the system (from Rabalais et al., 2010).

Gilbert et al. (2010) highlighted the fact that the number of hypoxic sites around the world reported in literature increased with the number of papers dealing with coastal hypoxia, which started to appear regularly since the 1970's. Consequently, it is legitimate to ask if the growing number of reports of hypoxic conditions (1) truly reflects a widespread increase of this phenomenon or (2) also reflects a larger community of scientists studying oxygen-depleted environments. Whatsoever, the large amount of studies testifying of coastal hypoxia together constitute a highly convincing body of evidence that hypoxia are strongly related to anthropogenic influence, especially in coastal ecosystems (Rabalais et al, 2010; Diaz et al., 2013; Breitburg et al., 2018). Consequently, there is now a wide consensus in the scientific community that the development and worsening of oxygen depletion in coastal areas is very often a direct consequence of human activities. Hypoxic events are expected to intensify in the future, about ten times faster in coastal areas than in the open ocean (Rabalais et al., 2010; Gilbert et al., 2010).

Other anthropogenic pressures on ecosystems, such as overexploitation of resources, pollutant release, habitat degradation or introduction of invasive species, may exacerbate

ecosystem disruptions due to oxygen depletion (Levin et al., 2009). In fact, increased perturbations from anthropogenic or natural sources may exceed the buffering capacity of ecosystems and lead to abrupt regime shifts. Ultimately, an alteration of ecosystems (sometimes irreversible) results in a degradation in the best case, or in the complete loss of the numerous and vital services they provide in the worst case (Figure 8; Scheffer et al., 2001; Elmqvist et al., 2003, Scheffer et al., 2009).

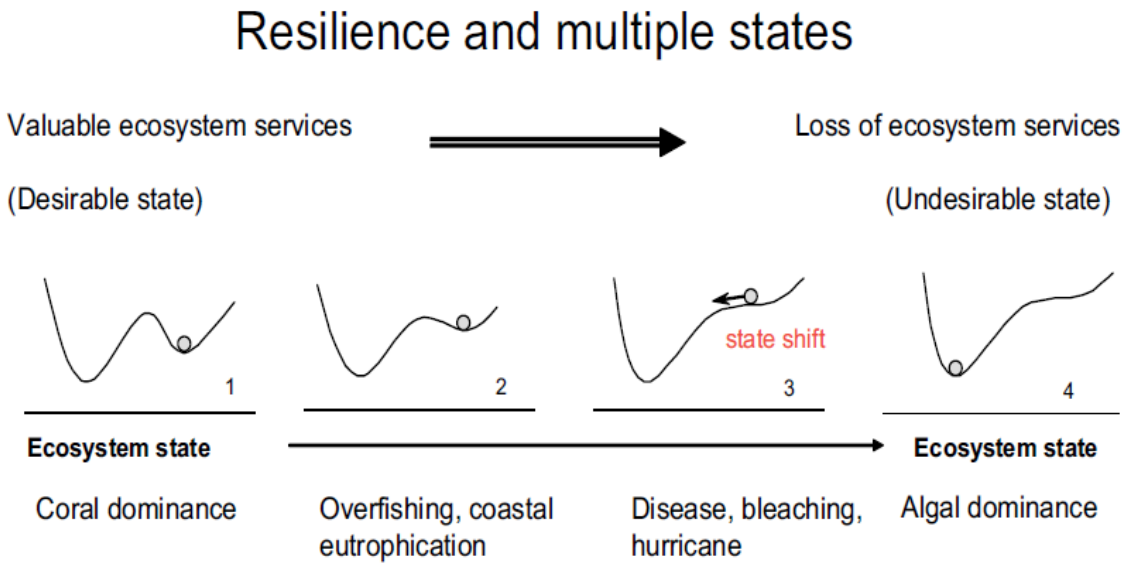

Figure 8. Example of a shift from a desirable to an undesirable state for a coral reef ecosystem, as a consequence of human-induced alteration (from Elmqvist et al., 2003).

In order to adopt correct policies and apply efficient management strategies aiming at conserving the services provided by coastal ecosystems to human societies, it is essential to understand the effects of oxygen depletion on these ecosystems. However, predicting the responses of species, communities or ecosystems to hypoxia in coastal settings clearly requires a good holistic understanding of the ecological context in which these events occur (Levin et al., 2009).

The benthic realm is expected to be the most impacted by oxygen depletion, for two main reasons. First, oxygen depletion essentially occurs in the sediment or in bottom waters, where organic matter is ultimately deposited. Conversely, the upper part of the water column, where most of the organic production takes place, is often saturated in oxygen due to photosynthetic processes and exchanges with the atmosphere. Second, benthic organisms are in general not very motile (or even sessile) and are then condemned to cope with adverse environmental conditions, such as hypoxia.

Diaz and Rosenberg (1995) showed that benthic organisms are indeed very sensitive to oxygen depletion in many different ecosystems. However, meiofauna, especially foraminifera, appears to be less sensitive to oxygen depletion than macrofauna (e.g. Josefson & Widbom, 1988).

3. BENTHIC FORAMINIFERA

One of the first drawings of a foraminifer was probably published by Hooke in 1665 (Figure 9 left, after Cifelli, 1990). While he was looking at sand grains to test several magnification glasses, Hooke found what he described *"to resemble the Shell of a small Water-snail with a flat spiral shell"*. His drawing looks similar to specimens of the genus *Ammonia,* with a spiral shell containing 13 chambers. Later, in a letter dated from June 1700, the Dutch zoologist Antonie van Leeuwenhoek described the content of a shrimp's stomach as "*very little snail-shells, […] no bigger than a coarse sand-grain*" (Figure 9 right, after Dobell, 1932). The presence of clear sutural bridges in these shells makes the resemblance with the genus *Elphidium* striking. These minute organisms were considered as cephalopods (particularly as *Nautilus*) until the early 19th century. In 1825, the French naturalist Alcide d'Orbigny named them Foraminifera, but still classified them within the Cephalopoda (d'Orbigny, 1826). However, in 1834, after his journey to South America, he thought that foraminifera should be removed from cephalopods. Finally, he followed the conclusion of his compatriot, the biologist Félix Dujardin, who showed in 1835 that foraminifera were in fact unicellular organisms (Dujardin, 1835).

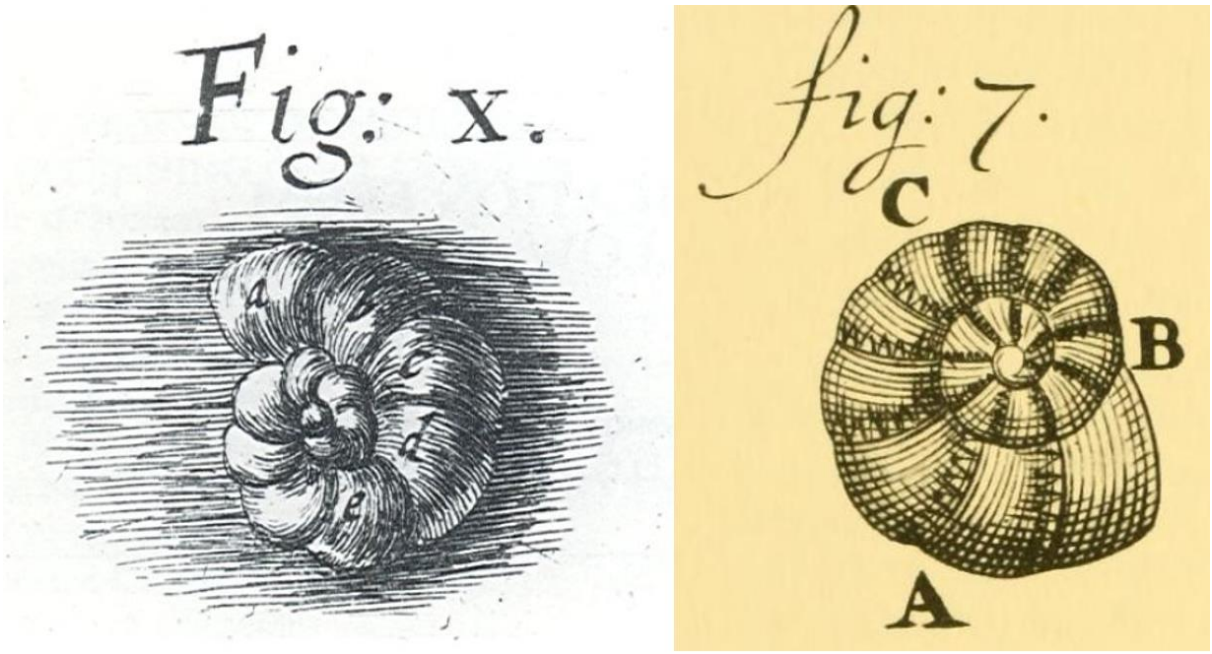

Figure 9. Drawings from Hooke in 1665 on the left (after Cifelli, 1990) and Antonie van Leeuwenhoek in 1700 on the right (after Dobell, 1932).

Marine foraminifera inhabit both the benthic and pelagic realms and are one of the most widespread groups of organisms. Most of them exhibit a shell called a test, and constitute a very diverse group of shelled microorganisms in the modern ocean. Foraminifera have a very rich fossil record, which starts in the Cambrian (Gupta, 2007; Jones, 2013), but their appearance is certainly older as an early radiation of organic shelled (non-fossilised) foraminifera was estimated between 690 and 1150 Ma with a molecular clock calibrated on the fossil record (Pawlowski et al., 2003). Thanks to their wide distribution, high abundances and fast evolution, foraminifera have become a privileged tool in biostratigraphy. They have also been intensively used in paleoceanographic studies and paleoenvironmental reconstructions (e.g. Murray et al., 2006; Milker et al., 2011), while most of our knowledge of the response of past oceans to climate change has been obtained through geochemical measurements of foraminiferal tests (e.g. Thomas & Shackleton; 1996; Zachos et al., 2001; Katz et al., 2010).

Foraminifera show a very high diversity with about 4000 recent living hard shelled species (Murray, 2007). They are among the most tolerant organisms with respect to a wide range of pollutants (Alve, 1995). Recent studies show that they also exhibit a variety of unsuspected adaptations and mechanisms to deal with adverse environmental conditions (e.g. anoxia, euxinia) such as denitrification (Risgaard-Petersen et al., 2006; Piña-Ochoa et al., 2010), dormancy (Ross & Hallock, 2016; LeKieffre, 2017), sequestration of chloroplasts (Lopez 1979; Pillet et al., 2011, Jauffrais et al., 2018a) or symbionts hosting (Bernhard et al., 2010; 2018).

They may represent a significant part of the benthic biomass, particularly in low oxygen ecosystems, and may play a key role in various processes, such as:

- **Carbon cycling,** foraminifera may account for up to 7% of aerobic carbon remineralisation in mudflats (Cesbron et al., 2016) and up to 70% in anaerobic conditions when considering only denitrification (Piña-Ochoa et al., 2010).
- **Nitrate cycling,** foraminifera may account for up to 50% of total benthic denitrification in the Peruvian oxygen minimum zone (Glock et al., 2013), 70% in Chile oxygen minimum zone (Piña-Ochoa et al., 2010) or up to 100% of the total benthic denitrification in the well oxygenated part of the Swedish Gullmar Fjord (Choquel et al., submitted).
- **Carbonate production,** foraminifera may contribute by up to 8% to the total production in reef and shelf areas (Hohenegger, 2006; Langer, 2008).
- **Bioturbation,** the foraminiferal contribution may be comparable to, or exceed, macrofaunal bioturbation (Groß, 2002; Bouchet & Seuront, accepted).

4. THE GENUS *AMMONIA*

Ammonia is probably one of the most widespread genera in coastal areas worldwide, although it does not live in high latitudes. *Ammonia* often dominates benthic foraminiferal communities in temperate to warm European coastal ecosystems, in particular in shallow waters and intertidal mudflats where it proliferates, generally in association with the genera *Haynesina* and *Elphidium* (Murray, 2006). Because of its ubiquitous nature, *Ammonia* is among the most widely studied benthic foraminiferal genera, with various aspects investigated, such as geographic distribution, ecology, behaviour, life cycle, metabolism, morphology or test ultrastructure (Banner &Williams, 1973; Chang & Kaesler, 1974; Schnitker, 1974; Poag, 1978; Walton & Sloan, 1990; Debenay et al., 1998; Stouff et al., 1999a, b; Seuront & Bouchet, 2015; Jauffrais et al., 2016a, b; LeKieffre et al., 2017). Easy to harvest and maintain, the genus is also extensively used in laboratory experiments to investigate biomineralisation (de Nooijer et al., 2009; Nehrke et al., 2013), the response to expected ocean acidification (Charrieau et al., 2018a) or the tolerance to pollutants (Denoyelle et al., 2012; Ciacci et al., 2019; Brouillette Price et al., 2019). Other laboratory experiments have also used *Ammonia* to develop and/or improve palaeoceanographical proxies (Dissard et al., 2010; Barras et al., 2018; Petersen et al., 2018, van Dijk et al., in prep.).

4.1. DISCOVERY

Jacopo Bartolomeo Beccari was the first in 1731 to describe specimens of *Ammonia* from sandy sediment near Bologna in Italy. He ascribed them to "*Cornua Ammonis"* (the Horns of Ammon, Beccari, 1731, p. 66, l. 30–33). The first acurate drawing of *Ammonia* was presented by Plancus in 1739 (Fig. 10), who found many specimens on Rimini beach (Italy) and assigned them to "*Cornu Hammonis"*. In 1758, Linnaeus named them "*Nautilus beccarii*" using his binomial nomenclature. In 1771, the genus "*Ammonia"* was created by Brünnich (1772), who classified it as a cephalopod. In the following two centuries, species that we now include in the genus "*Ammonia*" were assigned to various genera such as "*Rotalia"* (Schultze, 1854; Cushman 1926, 1931; Phleger & Parker 1951), "*Rotalina"* (Williamson, 1858) or "*Streblus"* (Bermúdez 1952; Bradshaw 1957; Hofker 1964). Finally, the name "*Ammonia*" became broadly used worldwide after the publication of Cifelli (1962) in which the author argues that the most ancient available genus name, the one from Brünnich (1772), must be used.

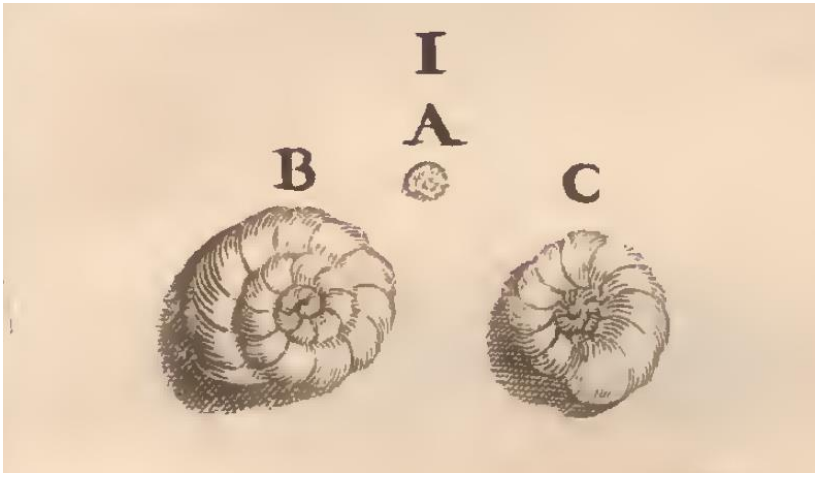

Figure 10. Drawing of *Ammonia* made by Plancus in 1739.

4.2. THE MULTIPLE SPECIES OF *AMMONIA*

The genus *Ammonia* shows a high morphological variability. Coupled with the fact that the genus is ubiquitous worldwide, this led to the description of many species, subspecies, varieties or forms, sometimes based on very subtle morphological differences. As the numerous available descriptions often lack clear illustrations and deposited type material, this have led to an increasing inconsistency in species identification. This inconsistency results from the fact that the classification mainly depends on the judgement of the observer (biased by regional usage) rather than on unambiguously defined criteria (Murray, 2007). In some cases, different names have been proposed in different areas for what is apparently the same morphospecies (making

them junior synonym). It is only by using molecular methods, that one can find out whether these "regional" morphospecies are genetically different (independent phylotypes and therefore different species) or identical (junior synonyms of a morphospecies named before in another area). This tendency to describe morphospecies based on subtle morphological differences has continued (Figure 11), and no less than 63 recent morphospecies of *Ammonia* have been accepted in the WoRMS (World Register of Marine Species) database (Hayward et al., 2020).

4.3. ECOPHENOTYPY

In 1974, Chang & Kaesler suggested that the high morphological variability exhibited by the morphospecies *Ammonia beccarii* was linked to environmental variability, explaining the geographical variation in the morphology of *Ammonia* along the eastern coast of United States. The same year, after undertaking experiments with specimens from the same region, Schnitker (1974) considered that *Ammonia beccarii* was the only "valid" species, and that its great morphological variability was explained by local acclimation. On the basis of his observations, he introduced the concept of ecophenotypy for the genus *Ammonia*, in analogy with Feyling-Hansen (1972), who had used this concept to explain morphological variability in the genus *Elphidium* two years earlier. In the next two decades, this tendency to regroup the previous morphospecies into morphotypes or ecophenotypes with a much larger morphological variability resulted in various new classification schemes, with a reduced number of species, each containing several subspecies, varieties or forms (e.g. Poag, 1978; Wang & Lutze, 1986; Jorissen, 1988; Walton & Sloan, 1990). This led to a major simplification of the nomenclature for *Ammonia*. However, the concept of ecophenotypy in *Ammonia* never became fully consensual in the scientific community (e.g. Haynes, 1992), and researchers continued to assign formal names to the different morphospecies of *Ammonia* based on subtle morphological differences (Figure 11; e.g. Hofker, 1964; Banner & Williams, 1973; Cimerman & Langer, 1991; Colburn & Baskin, 1998). In fact, the disagreement between partisans of these two different concepts of classification for *Ammonia* (and for foraminifera in general) has continued until the beginning of the 21th century.

4.4. MOLECULAR TAXONOMY

Molecular analyses, which have become widely available since the end of the 1980s, are a recent addition to the taxonomical toolbox. Individuals are assigned to phylotypes on the basis of the similarity of their DNA sequences. These phylotypes are mostly considered to be

equivalent to species in traditional taxonomy, but instead of looking at morphological variability, molecular dissimilarity is the conclusive criterion to separate species. The successful development of DNA extraction and PCR amplification for foraminifera started in the mid-1990s. The first sequences of foraminifera were published by Pawlowski et al. (1994) and provided a new (molecular) method, independent of morphological characters, to assign individuals to species for foraminifera.

Pawlowski et al. (1995) were also the first to investigate the nomenclature of the genus *Ammonia* using molecular methods. In the next two decades, the multiplication of molecular studies of *Ammonia* confirmed that most of the different morphological variants previously grouped into ecophenotypes belong to different phylotypes, and should be considered as separate species (e.g. Holzmann et al., 1996; Holzmann, 2000; Holzmann & Pawlowski, 2000; Langer & Leppig, 2000; Hayward et al., 2004; Pawlowski & Holzmann, 2008; Schweizer et al., 2011a, b). However, the number of morphospecies described and accepted in the WoRMS database is still much higher than the number of known *Ammonia* phylotypes (Figure 11), suggesting that this list still contains some junior synonyms and certainly not yet sequenced phylotypes.

As explained before, it is mostly supposed that a phylotype corresponds to a biological species. When different regions of the genome are studied, their evolution rate and evolution history can be different and result in different specimen segregations (e.g. Amato et al., 2007 for diatoms), suggesting that the equivalence of a phylotype with a biological species is maybe not always as straightforward as desired. For the time being, only partial small sub-unit (SSU) and large sub-unit (LSU) of ribosomal DNA sequences were compared for *Ammonia* and the congruence is rather good (e.g. Holzmann, 2000; Schweizer et al., 2011b; Bird et al. 2020).

In summary, molecular identification represents an extremely useful additional tool to identify and classify organisms. It is certainly more objective than traditional, morphology-based taxonomy, which is a major advantage, but still contains an element of subjectivity. The present molecular classification of the highly morphologically variable genus *Ammonia* suggests that the number of species is somewhere between the numerous morphospecies proposed until today and the very few ecophenotypes considered previously (Fig. 11). It is interesting to note that a very similar historical development took place concerning the taxonomy of the genus *Elphidium* (Miller et al., 1982; Pillet et al., 2013; Darling et al., 2016), another main dominant foraminiferal taxon in coastal ecosystems.

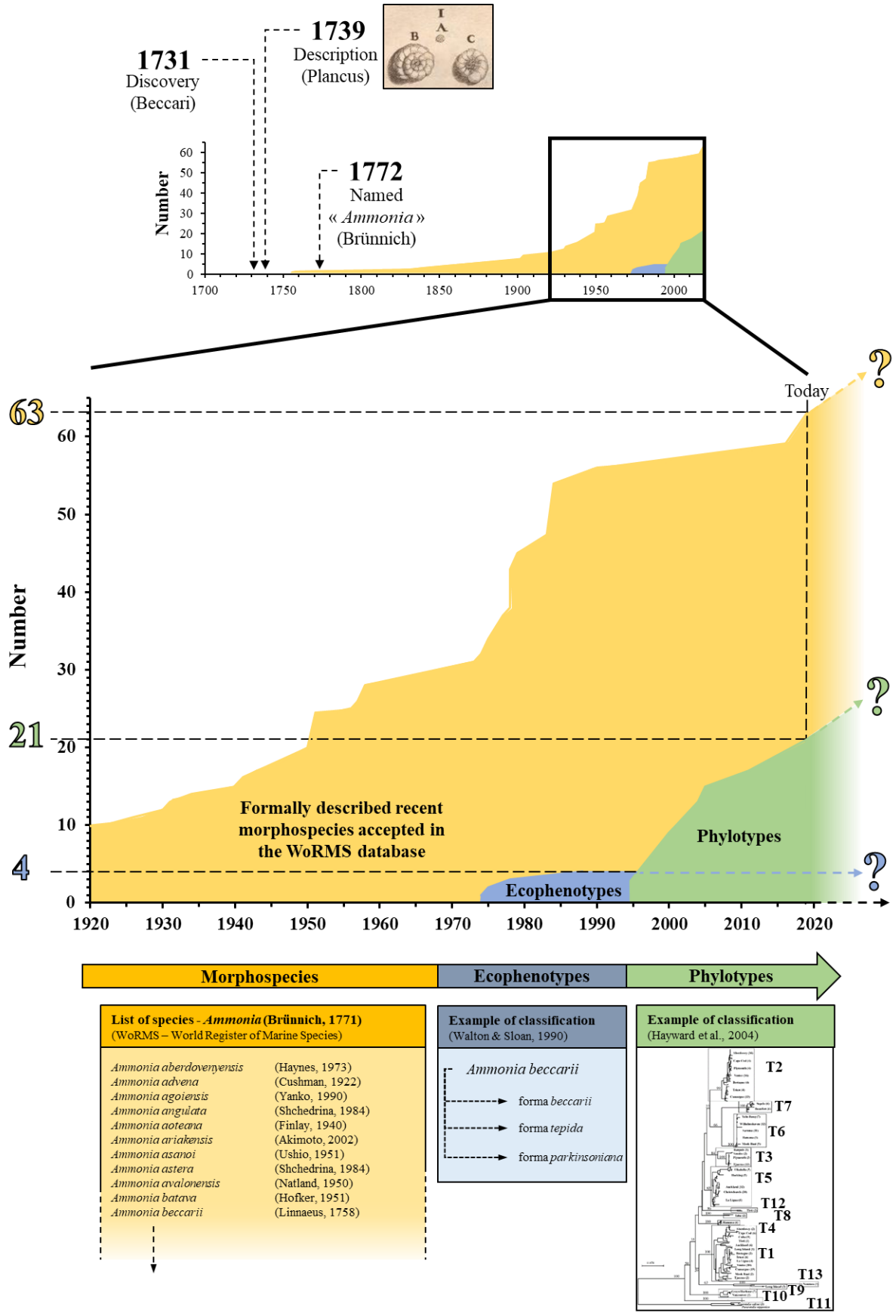

Figure 11. Historical scheme of the discovery and temporal evolution of the number of formally described recent morphospecies (yellow), ecophenotypes (blue) and phylotypes (green) of the genus *Ammonia*. The three curves are not cumulative. Note the non-linearity of the temporal scale. YELLOW: number of recent *Ammonia* species formally described and accepted in WoRMS database,

Hayward et al., 2020). BLUE: number of ecophenotypes described (Chang & Kaesler, 1974; Schnitker, 1974; Seiglie, 1975; Poag, 1978; Vénec-Peyré, 1983; Wand & Lutze, 1986; Jorissen, 1988; Walton & Sloan, 1990). GREEN: number of phylotypes described (Pawlowski, 1995; Holzmann & Pawlowski, 2000; Hayward et al., 2004; Toyofuku et al., 2005; Schweizer et al., 2011a; Hayward et al., 2019; Bird et al., 2020). This scheme is updated until 2019, with 63 formally described species, 4 ecophenotypes and 21 phylotypes.

Since its discovery, the nomenclature of *Ammonia* underwent adaptations and modifications, and has gone through the emergence of different concepts/manners/phases to classify organisms: (1) the first descriptions were made before the binomial nomenclature of Linnaeus, (2) many new formal names were based on subtle morphological differences (morphospecies), (3) the concept of species with a large morphological variability in response to environmental variability (ecophenotypy) and (4) the development of molecular identification (phylotypes). Three centuries after its discovery, the nomenclature of *Ammonia*, which was already considered as "chaotic" by Boltovskoy in 1965 (just as by Haynes in 1992), is still extremely complex.

4.5. DISTRIBUTION OF THE PHYLOTYPES OF *AMMONIA*

Until today, the most extensive study aiming at reconciling molecular (phylotype) and morphological (morphospecies) classifications of *Ammonia* has been published by Hayward et al. (2004). In this study, based on a global inventory, the authors identified 13 molecular types (informally named T1 to T13), which were described morphologically using 37 morphometric parameters. Later, two additional phylotypes were added (T14 and T15), and a subdivision of the phylotype T2 in T2A and T2B was proposed (Schweizer et al., 2011a, b; Bird et al., 2020). Other individuals genetically identified and separated from the previous numbered phylotypes exist such as *A. japonica* and *Ammonia* sp. O (Toyofuku et al., 2005) which branch to the phylotype T8 (Hayward et al. 2019), and *A. corallinarum*, *A. neobeccarii*, and *A. pawlowski* which belong to the T3 clade (Hayward et al., 2019). No numbers have been attributed to these phylotypes, four of which have been assigned to existing species.

Figure 12 shows the worldwide distribution of the 15 phylotypes numbered until now (T1–T15) by Hayward et al. (2004) and Bird et al. (2020). Despite the efforts made by researchers to reconcile traditional morphology-based taxonomy and molecular identification, it is still problematic to attribute an indisputable taxonomic name to each phylotype.

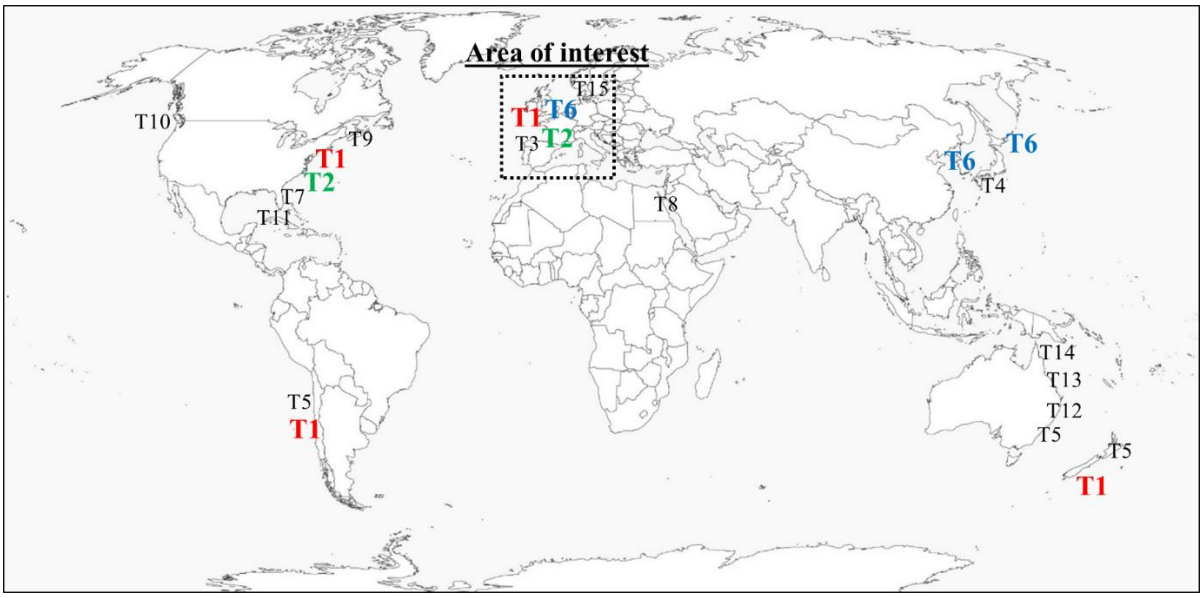

Figure 12. Worldwide distribution of *Ammonia* phylotypes T1 to T15. Phylotypes more specifically investigated in this thesis are indicated: T1 (red), T2 (green) and T6 (blue). Map constructed after Hayward et al., 2004; Pawloski & Holzmann, 2008; Schweizer et al., 2011a; b.

Along the European coasts, two morphologically different groups of *Ammonia* are frequently encountered:

- The *Ammonia beccarii* morphospecies, which contains specimens that are strongly ornamented, and
- The *Ammonia tepida* morphospecies, which contains specimens that are much less ornamented.

These morphospecies are named here after the main two most often used names in the ecophenotypy concept (Poag, 1978; Vénec-Peyré, 1983; Jorissen, 1988; Walton & Sloan, 1990). Each of them contains two to four morphological forms (depending on the authors) with a slightly different morphology, which were considered as species by authors applying a morphospecies concept (e.g. Hofker, 1964; Haynes, 1973; Banner & Williams, 1973). From a molecular perspective, five different phylotypes are encountered in the North East Atlantic: *Ammonia* sp. T1, T2, T3, T6 and T15, if we do not consider sub-types (Figure 12).

Phylotype T1, which has been observed in the north Atlantic (Europe and USA) and south Pacific (New Zealand and Chile), is considered to be cosmopolitan (Holzmann & Pawlowski, 2000). Phylotype T2 has been exclusively encountered along the North Atlantic coasts of Europe and the USA (Hayward et al., 2004). Phylotype T6 shows a disjunct geographical distribution (Hayward et al., 2004; Pawlowski & Holzmann, 2008) with records in Europe (Holzmann & Pawlowski, 2000; Schweizer et al., 2011b) but also around Japan (Toyofuku et al., 2005) and China (Hayward et al., 2004). These three phylotypes present a weak ornamentation (Figure 13) and were traditionally identified as the morphospecies *Ammonia*

tepida. They are morphologically relatively similar, so that a distinction on the basis of morphology alone is difficult. The more ornamented phylotypes T3 and T15 (Figure 13), which were often included in the morphospecies *Ammonia beccarii*, are rather easily distinguishable morphologically from the first three phylotypes and also between them (Hayward et al., 2004; Schweizer et al., 2011a). In short, phylotype T3 shows deeply incised, fissured sutures on the spiral side and a more ornamented umbilical side whereas T15 is characterised by secondary openings at the junction of the radial and spiral sutures on the spiral side (Schweizer et al., 2011a).

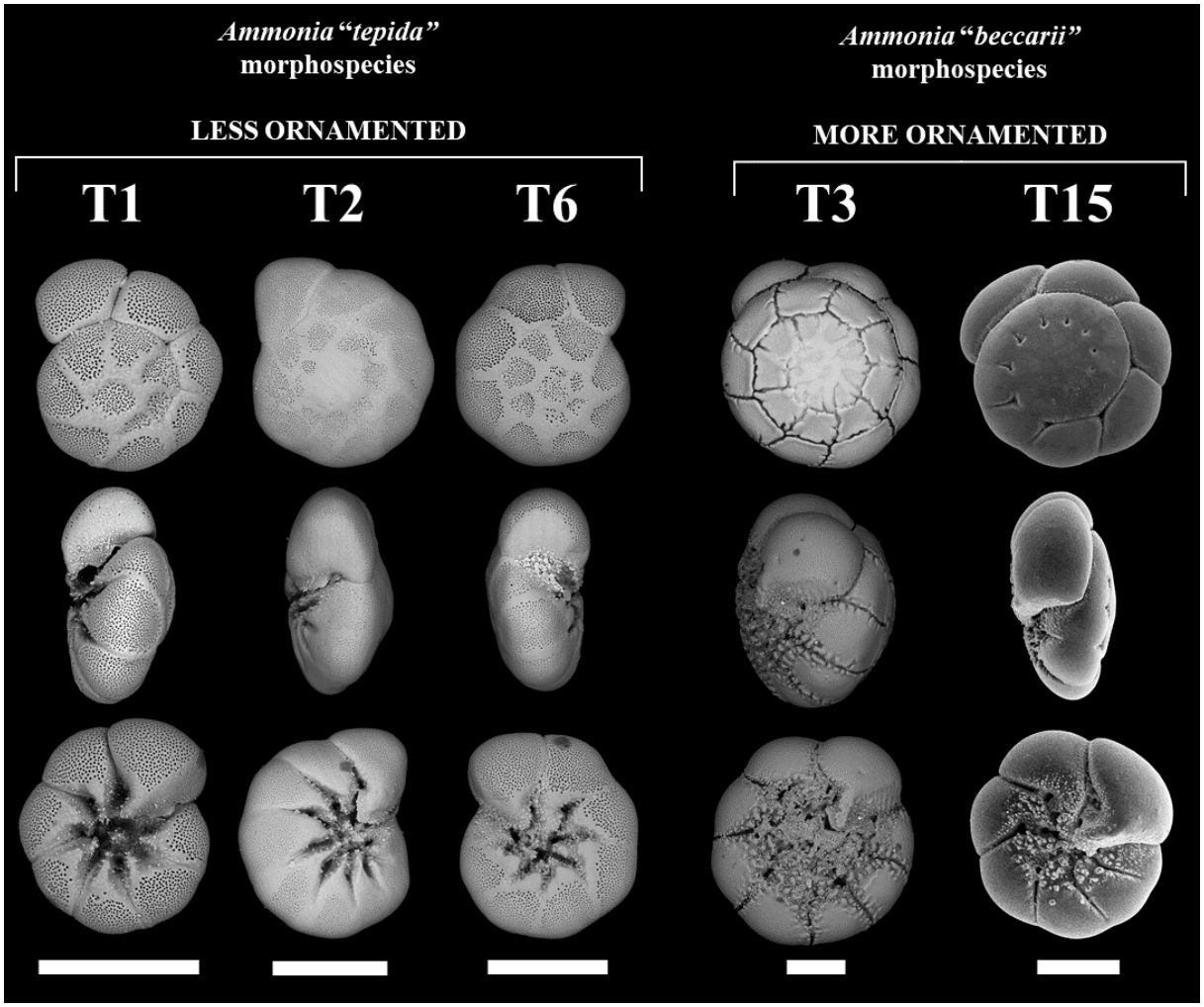

Figure 13. SEM images of the spiral, peripheral and umbilical sides of the less ornamented *Ammonia tepida* morphospecies containing the phylotypes T1, T2 and T6, and the more ornamented *Ammonia beccarii* morphospecies containing T3 and T15 (T15 images from Schweizer et al., 2011a). All scale bars are 200 µm.

Among these five phylotypes, the status of *Ammonia* sp. T6, with its disjunct distribution in Europe and eastern Asia, has been disputed. In fact, *Ammonia* sp. T6 arrived around 2000 in the Kiel fjord (Polovodova et al., 2009; Schweizer et al., 2011b) and was observed in Hanö Bay in 2012 and 2013 (Baltic Sea, Groeneveld et al., 2018 and Charrieau et al., 2018b, respectively), where no *Ammonia* species were present before (Hermelin, 1987;

Murray, 2006). Because of this, and other, as yet unpublished, observations of the recent arrival of this phylotype in other areas (e.g. Loire estuary), in Europe it is often considered as an allochthonous, exotic species originating from eastern Asia. It appears that phylotype T6 progressively replaces the other two phylotypes (T1 and T2) along the European coasts. If true, this could have major consequences for the functioning of the concerned ecosystems.

5. CONTEXT OF THE PHD THESIS AND PREVIOUS FINDINGS

In the general context of the increasing need to better understand European coastal ecosystems, the INSU-CNRS EC2CO-LEFE project "AMTEP" started in 2015 for two years. This project aimed to better understand the role of the morphospecies *Ammonia tepida*, which encompasses the phylotypes T1, T2 and T6 in the mid-latitude Eastern Atlantic. The research presented in this PhD thesis started as an integral part of this project.

For the purpose of the AMTEP project, several European sites were sampled in the North Sea (the Netherlands), the English Channel (France), the Atlantic (Ireland, France and Spain) and the Mediterranean Sea (France and Italy). In addition, samples from Japan, USA (Connecticut), Madagascar and Israel were examined. More than 1000 individuals were extracted for molecular analyses, from which about 500 specimens were successfully amplified, sequenced and assigned to a phylotype. These new molecular data show the existence of sites where only one of the three phylotype is present, as well as sites with all possible combinations of the three phylotypes. A comparison of the phylotype distribution with the available environmental data (e.g. temperature, salinity, oxygen penetration depth in the sediment) did not yet allow to fully understand the spatial distribution of the three phylotypes.

For all sequenced specimens, SEM (Scanning Electron Microscope) images were acquired prior to DNA extraction in order to investigate the morphological variability, and if possible, to identify the morphological variations (and eventual overlaps) of the three phylotypes. In order to measure pore patterns (earlier, Holzmann & Pawlowski, 1997 and Hayward et al., 2004, suggested that pore size was a discriminating feature), a standardised method was developed by Petersen et al. in 2016. This method allowed the production of a large dataset for samples from Lake Grevelingen (the Netherlands), which showed a clear relationship between pore density and pore size. Moreover, the preliminary record of a long core sampled at the same site showed that during the last 50 years, specimens with small pores have been replaced by specimens with bigger pores (Figure 14).

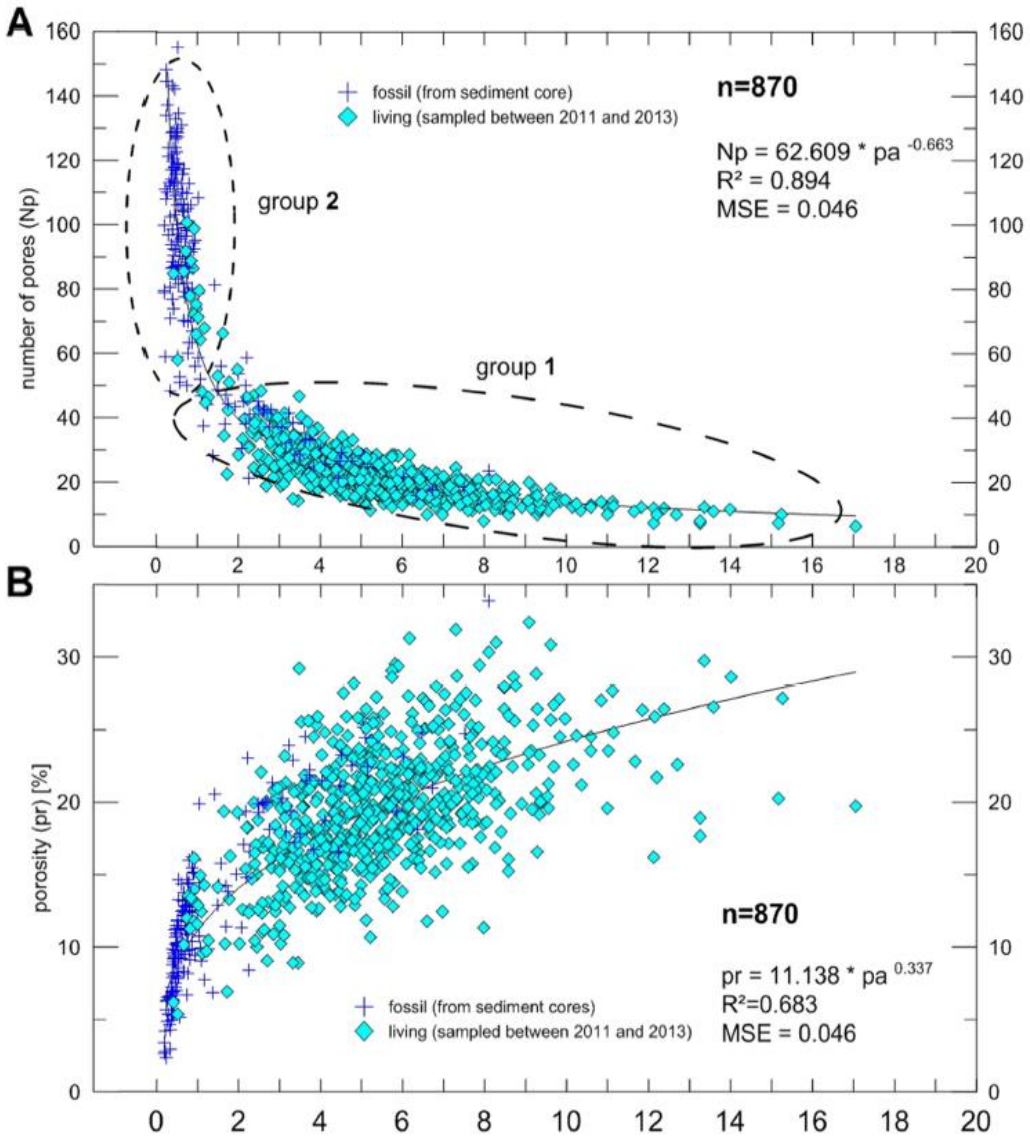

Figure 14. The relationship between pore area and number of pores and porosity (%) from Petersen et al. (2016). Dead *Ammonia* specimens from Lake Grevelingen are represented by crosses and tend to have many small pores and low porosity, whereas recent specimens, represented by diamonds, have fewer larger pores and higher porosity.

6. OBJECTIVES OF THE PHD THESIS

The research undertaken during this PhD thesis is the next logical step of the studies described in the previous paragraph. At the beginning of the PhD, in September 2016, five main research objectives were defined, each of them being the subject of the five subsequent chapters of this PhD thesis.

6.1. RECONCILING TRADITIONAL TAXONOMY AND MOLECULAR IDENTIFICATION

As previously explained, *Ammonia* is one of the earliest described foraminiferal genera, and is often dominant in coastal ecosystems in Europe. Although regularly used in a broad range of fundamental and applied research, its taxonomy is still unclear. **Chapter 2** aims to disentangle the taxonomical uncertainties concerning the *Ammonia "tepida*" morphospecies in the North-East Atlantic. Previous visual inspections of tests from phylotypes T1, T2 and T6 suggested that there were some minor morphological differences, especially concerning pore size (Holzmann & Pawlowski, 1997; Hayward et al., 2004). If true, the three phylotypes would correspond to three pseudocryptic species (that have been morphologically recognized as such only after other methods have unveiled their existence, molecular identification in our case, Luttikhuizen & Dekker, 2010). If we could assign the various specimens reliably and systematically to their phylotype on the basis of morphological criteria alone, it would become possible to avoid the time-consuming and expensive molecular identifications. This would then give the possibility to rapidly generate large and precise datasets about these three phylotypes for (1) recent living or dead material (for studies on ecology or biodiversity) and (2) sub-recent and fossil material (essential for determining pristine conditions or historical evolution of coastal areas). In order to achieve this, we measured 61 morphometric parameters on SEM images of the spiral, peripheral and umbilical sides of the tests, plus a 1000 times magnification of the pore pattern (following Petersen et al., 2016) of 96 specimens of *Ammonia* from 22 different locations along the French and Dutch coasts. The previously imaged specimens have been assigned to phylotypes T1, T2 and T6 by molecular methods. Next, we used a multivariate approach to determine the most adequate morphometric features allowing us to discriminate the three phylotypes. We finally compared the results of this morphometric method with the molecular data, in order to have a quantitative assessment of the reliability of the morphometric method.

6.2. APPLICATION OF THE MORPHOMETRIC DETERMINATION TO MATERIAL COLLECTED AROUND THE BRITISH ISLES - BIOGEOGRAPHY

Recently, Saad & Wade (2016) investigated the distribution of phylotypes T1, T2 and T6 in coastal and transitional environments around Great Britain on the basis of molecular assignation. Because they used a non-destructive method of DNA extraction, the tests (shells) of most of the individuals used in their study were still available, and were very generously put

at our disposal by the authors. This provided us with the unique chance to follow simultaneously two research paths in **Chapter 3**. First, it allowed us to test the consistency of the morphometric discrimination method developed in Chapter 2. Next, the individuals studied by Saad & Wade (2016) were added to the dataset of the AMTEP project along the Dutch and French Atlantic coasts, and to the recently published database of Bird et al. (2020), to constitute a much larger data set. This composite dataset has a wider spatial coverage, and allowed us to investigate the biogeography of the three phylotypes around the British Isles and in the English Channel.

6.3. RESPONSE OF FORAMINIFERAL COMMUNITIES TO EUXINIA IN LAKE GREVELINGEN

Environmental conditions at the local and regional scales must constitute a pre-requisite for the settlement of the three different phylotypes, and their ecological requirements should play a fundamental role in their distribution. However, the environmental parameters controlling their distribution pattern are not well known yet. In order to contribute to this topic, we investigated the response of the foraminiferal community to seasonal anoxia with co-occurring sulphides at two sites in the Den Osse Basin, Lake Grevelingen (**Chapter 4)**. The study area, which is a former branch of the Maas-Rhine-Scheldt estuary where *Ammonia* sp. T6 is one of the dominant species, was sampled bimonthly in 2012. We examined the foraminiferal response to euxinic conditions in late summer/early autumn at two contrasted stations, to investigate how the different durations and intensities of adverse conditions would affect the foraminiferal communities. We also compared the tolerance of *Ammonia* sp. T6 with that of other dominant taxa, which mainly belong to the genus *Elphidium*. This study aimed to obtain some indications about the reasons behind the apparently highly successful recent expansion of *Ammonia* sp. T6 along the east Atlantic coasts.

6.4. HISTORICAL EVOLUTION OF THE FORAMINIFERAL COMMUNITY IN LAKE GREVELINGEN

Until 1965, Lake Grevelingen was an active part of the Maas-Rhine-Scheldt estuary. Due to the construction of two dams in 1965 (landward) and 1971 (seaward), it became the largest salt-water lake in Europe. In order to study the impact of these anthropogenic modifications and as a basis for management decisions, Lake Grevelingen has been intensively monitored since its closure in 1971. In the deepest part of the Den Osse Basin, at one of the same sites where the foraminiferal community has been studied (Chapter 4), a sediment core covering the

last 50 years was sampled. A preliminary study of this core suggested that in this period, Ammonia specimens with smaller pores had been replaced by individuals with larger pores (Petersen et al., 2016). In **Chapter 5**, we present a more detailed analysis of the foraminiferal succession in this core, focussing on the overall species composition, and determining the three *Ammonia* phylotypes, using the method developed in Chapter 2. We interpreted the main foraminiferal community changes observed in this high resolution historical record (40 samples covering ~ 50 years) by comparing them with the main human-induced modifications of the lake, such as the successive closure and re-openings of the landward and/or seaward sluices. We also focused on the putatively exotic and invasive *Ammonia* sp. T6 to investigate its arrival date and dispersal in the eastern Atlantic with this very detailed record.

6.5. POROSITY MODEL – WHAT IS DRIVING POROSITY IN *AMMONIA*?

Through the research presented in this PhD thesis, it became evident that the pore patterns are an essential trait to discriminate phylotypes of the *Ammonia "tepida"* morphospecies. Phylotypes T1, T2 and T6 show a very large variability in pore density and pore surface, and it turned out that the pore pattern is the primary character to distinguish these three phylotypes. The different spatial distributions of these three phylotypes, at various scales of the ecosystems, suggest that they adapt to different environmental conditions, because of different ecological requirements. Since the pore pattern appeared to be an important distinctive character between these three phylotypes, the functional morphology of the pore patterns should be linked to their ecological requirements, possibly to their tolerance to low oxygen conditions. Although the functions of pores in foraminifera are not very well known yet, there is a certain consensus that a higher porosity should lead to a larger exchange surface with the surrounding media, and hence, to more intensive gas exchanges. Until now, no capacity to shift to alternative types of metabolism has been shown for *Ammonia*, so that it very likely is a strictly aerobic genus. For an aerobic species, oxygen uptake should be particularly important. It is therefore likely that the observed differences in pore patterns between the three phylotypes T1, T2 and T6 reflect different adaptations to oxygen levels, with phylotype exhibiting higher porosity being possibly more resistant to low oxygen than species with lower porosity. This is corroborated by our observations of the historical record for the last ~ 50 years presented in Chapter 5. However, it is evident that there must be a higher limit for porosity values, because the test must maintain a certain mechanical integrity. In **Chapter 6**, we investigate this topic by using a physical scaling law model to explore how gas exchanges (metabolic needs) and mechanical constraints

(shell robustness) interact to control foraminiferal pore patterns. The comparison of the predictions derived from our mathematical model with a large empirical dataset of pore patterns measured on many specimens from various sampling sites will inform us to what extent the physical laws used in our model reflect what is found in nature.

REFERENCES

Alongi, D.M. (Daniel M.), 1998. Coastal ecosystem processes. Boca Raton : CRC Press, 458 p.

Alve, E., 1995. Benthic foraminiferal responses to estuarine pollution; a review. Journal of Foraminiferal Research 25, 190–203. https://doi.org/10.2113/gsjfr.25.3.190

Amato, A., Kooistra, W.H.C.F., Levialdi Ghiron, J.H., Mann, D.G., Pröschold, T., Montresor, M., 2007. Reproductive Isolation among Sympatric Cryptic Species in Marine Diatoms. Protist 158, 193–207. https://doi.org/10.1016/j.protis.2006.10.001

Banner, F.T., Williams, E., 1973. Test structure, organic skeleton and extrathalamous cytoplasm of Ammonia Bruennich. Journal of Foraminiferal Research 3, 49–69. https://doi.org/10.2113/gsjfr.3.2.49

Barras, C., Mouret, A., Nardelli, M.P., Metzger, E., Petersen, J., La, C., Filipsson, H.L., Jorissen, F., 2018. Experimental calibration of manganese incorporation in foraminiferal calcite. Geochimica et Cosmochimica Acta 237, 49–64. https://doi.org/10.1016/j.gca.2018.06.009

Beccari, J.B., 1731. De bononiensi arena quadam, De Bononiensis Scientiarum et Artium Instituto atque Academia Commentarii. Bononiae, 647 p.

Bermúdez, P.J., 1952. Estudio sistematico de los foraminiferos rotaliformes. Ed. Sucre, 230 p.

Bernhard, J.M., Goldstein, S.T., Bowser, S.S., 2010. An ectobiont-bearing foraminiferan, Bolivina pacifica, that inhabits microxic pore waters: cell-biological and paleoceanographic insights. Environ. Microbiol. 12, 2107–2119. https://doi.org/10.1111/j.1462-2920.2009.02073.x

Bernhard, J.M., Tsuchiya, M., Nomaki, H., 2018. Ultrastructural observations on prokaryotic associates of benthic foraminifera: Food, mutualistic symbionts, or parasites? Marine Micropaleontology, Benthic Foraminiferal Ultrastructure Studies 138, 33–45. https://doi.org/10.1016/j.marmicro.2017.09.001

Bird, C., Schweizer, M., Roberts, A., Austin, W.E.N., Knudsen, K.L., Evans, K.M., Filipsson, H.L., Sayer, M.D.J., Geslin, E., Darling, K.F., 2020. The genetic diversity, morphology, biogeography, and taxonomic designations of Ammonia (Foraminifera) in the Northeast Atlantic. Marine Micropaleontology 155, 101726. https://doi.org/10.1016/j.marmicro.2019.02.001

Boltovskoy, E., 1965. Twilight of Foraminiferology. Journal of Paleontology 39, 383–390.

Borja, A., Bricker, S.B., Dauer, D.M., Demetriades, N.T., Ferreira, J.G., Forbes, A.T., Hutchings, P., Jia, X., Kenchington, R., Marques, J.C., Zhu, C., 2008. Overview of integrative tools and methods in assessing ecological integrity in estuarine and coastal systems worldwide. Marine Pollution Bulletin 56, 1519–1537. https://doi.org/10.1016/j.marpolbul.2008.07.005

Bouchet V.M.P., Seuront, L., 2020. Strenght may lie in numbers: intertidal foraminifera non-negligible contribution to surface sediment reworking. Accepted in Open Journal of Marine Science.

Bradshaw, J.S., 1957. Laboratory Studies on the Rate of Growth of the Foraminifer, "Streblus beccarii (Linné) var. tepida (Cushman)." Journal of Paleontology 31, 1138–1147.

Breitburg, D., Levin, L.A., Oschlies, A., Grégoire, M., Chavez, F.P., Conley, D.J., Garçon, V., Gilbert, D., Gutiérrez, D., Isensee, K., Jacinto, G.S., Limburg, K.E., Montes, I., Naqvi, S.W.A., Pitcher, G.C., Rabalais, N.N., Roman, M.R., Rose, K.A., Seibel, B.A., Telszewski, M., Yasuhara, M., Zhang, J., 2018. Declining oxygen in the global ocean and coastal waters. Science 359. https://doi.org/10.1126/science.aam7240

Brouillette Price, E., Kabengi, N., Goldstein, S.T., 2019. Effects of heavy-metal contaminants (Cd, Pb, Zn) on benthic foraminiferal assemblages grown from propagules, Sapelo Island, Georgia (USA). Marine Micropaleontology 147, 1–11. https://doi.org/10.1016/j.marmicro.2019.01.004

Brünnich, M.T. (Morten T., Stejneger, L., 1772. M. Th. Brünnichii Zoologiae fundamenta praelectionibus academicis accommodata = Grunde i dyrelaeren. Hafniae ; et Lipsiae : Apud Frider. Christ. Pelt, 254 p.

Cesbron, F., Geslin, E., Jorissen, F.J., Delgard, M.L., Charrieau, L., Deflandre, B., Jézéquel, D., Anschutz, P., Metzger, E., 2016. Vertical distribution and respiration rates of benthic foraminifera: Contribution to aerobic remineralization in intertidal mudflats covered by *Zostera noltei* meadows. Estuarine, Coastal and Shelf Science, Special Issue: Functioning and dysfunctioning of Marine and Brackish Ecosystems 179, 23–38. https://doi.org/10.1016/j.ecss.2015.12.005

Chang, Y.M., Kaesler, R.L., 1974. Morphological variation of the foraminifer Ammonia beccarii (Linné) from the Atlantic coast of the United States.

Charrieau, L.M., Filipsson, H.L., Nagai, Y., Kawada, S., Ljung, K., Kritzberg, E., Toyofuku, T., 2018a. Decalcification and survival of benthic foraminifera under the combined impacts of varying pH and salinity. Marine Environmental Research 138, 36–45. https://doi.org/10.1016/j.marenvres.2018.03.015

Charrieau, L.M., Filipsson, H.L., Ljung, K., Chierici, M., Knudsen, K.L., Kritzberg, E., 2018b. The effects of multiple stressors on the distribution of coastal benthic foraminifera: A case study from the Skagerrak-Baltic Sea region. Marine Micropaleontology 139, 42–56. https://doi.org/10.1016/j.marmicro.2017.11.004

Ciacci, C., Grimmelpont, M.V., Corsi, I., Bergami, E., Curzi, D., Burini, D., Bouchet, V.M.P., Ambrogini, P., Gobbi, P., Ujiié, Y., Ishitani, Y., Coccioni, R., Bernhard, J.M., Frontalini, F., 2019. Nanoparticle-Biological Interactions in a Marine Benthic Foraminifer. Scientific Reports 9, 1–10. https://doi.org/10.1038/s41598-019-56037-2

Cifelli, R., 1990. A History of the classification of Foraminifera, (1826-1933). PART I. Cushman Foundation for Foraminiferal Research 27, 119 p.

Cifelli, R., 1962. The morphology and structure of *Ammonia beccarii* (Linné). Contributions from the Cushman foundation for foraminiferal research XIII, 119–126.

Cimerman, F., Langer, M., 1991. Mediterranean Foraminifera. Academia Scientiarum et Artium Slovenica, Ljubljana 30, 210 p.

Cloern, J.E., 2001. Our evolving conceptual model of the coastal eutrophication problem. Marine Ecology Progress Series 210, 223–253. https://doi.org/10.3354/meps210223

Cohen, J.E., Small, C., Mellinger, A., Gallup, J., Sachs, J., 1997. Estimates of Coastal Populations. Science 278, 1209–1213. https://doi.org/10.1126/science.278.5341.1209c

Colburn, D.F., Baskin, J.A., 1998. Morphological Study of *Ammonia Parkinsoniana* from Laguna Madre and Baffin Bay. Gulf coast association of geological societies transactions, 48, 11–19.

Costanza, R., d'Arge, R., Groot, R. de, Farber, S., Grasso, M., Hannon, B., Limburg, K., Naeem, S., O'Neill, R.V., Paruelo, J., Raskin, R.G., Sutton, P., Belt, M. van den, 1997. The value of the world's ecosystem services and natural capital. Nature 387, 253–260. https://doi.org/10.1038/387253a0

Cushman, J.A., 1926. Recent Foraminifera from Porto Rico. Carnegie Institution of Washington 344, 73–84.

Darling, K.F., Schweizer, M., Knudsen, K.L., Evans, K.M., Bird, C., Roberts, A., Filipsson, H.L., Kim, J.-H., Gudmundsson, G., Wade, C.M., Sayer, M.D.J., Austin, W.E.N., 2016. The genetic diversity, phylogeography and morphology of Elphidiidae (Foraminifera) in the Northeast Atlantic. Marine Micropaleontology 129, 1–23. https://doi.org/10.1016/j.marmicro.2016.09.001

Day, J.W., Yáñez-Arancibia, A., Kemp, W.M., 2012. Human Impact and Management of Coastal and Estuarine Ecosystems, in: Estuarine Ecology. John Wiley & Sons, Ltd, pp. 483–495. https://doi.org/10.1002/9781118412787.ch19

de Nooijer, L.J., Langer, G., Nehrke, G., Bijma, J., 2009. Physiological controls on seawater uptake and calcification in the benthic foraminifer *Ammonia tepida*. Biogeosciences 6, 2669–2675. https://doi.org/10.5194/bg-6-2669-2009

Debenay, J.-P., Bénéteau, E., Zhang, J., Stouff, V., Geslin, E., Redois, F., Fernandez-Gonzalez, M., 1998. *Ammonia beccarii* and *Ammonia tepida* (Foraminifera): morphofunctional arguments for their distinction. Marine Micropaleontology 34, 235–244. https://doi.org/10.1016/S0377-8398(98)00010-3

Denoyelle, M., Geslin, E., Jorissen, F.J., Cazes, L., Galgani, F., 2012. Innovative use of foraminifera in ecotoxicology: A marine chronic bioassay for testing potential toxicity of drilling muds. Ecological Indicators, Marine Benthic Indicators 12, 17–25. https://doi.org/10.1016/j.ecolind.2011.05.011

Diaz, R.J., Eriksson-Hägg, H., Rosenberg, R., 2013. Hypoxya, in: Managing Ocean Environments in a Changing Climate: Sustainability and Economic Perspectives. Elsevier, Burlington, MA, pp. 67–96.

Diaz, R.J., Rosenberg, R., 2008. Spreading Dead Zones and Consequences for Marine Ecosystems. Science 321, 926–929. https://doi.org/10.1126/science.1156401

Diaz, R.J., Rosenberg, R., 1995. Marine benthic hypoxia: a review of its ecological effects and the behavioural responses of benthic macrofauna. Oceanographic Literature Review 12, 245–303.

Dissard, D., Nehrke, G., Reichart, G.J., Bijma, J., 2010. Impact of seawater pCO2 on calcification and Mg/Ca and Sr/Ca ratios in benthic foraminifera calcite: results from culturing experiments with *Ammonia tepida*. Biogeosciences 7, 81–93. https://doi.org/10.5194/bg-7-81-2010

Dobell, C., 1932. Antony van Leeuwenhoek and his "Little animals"; being some account of the father of protozoology and bacteriology and his multifarious discoveries in these disciplines; New York, Harcourt, Brace and company, 436 p.

Dolven, J.K., Alve, E., Rygg, B., Magnusson, J., 2013. Defining past ecological status and in situ reference conditions using benthic foraminifera: A case study from the Oslofjord, Norway. Ecological Indicators 29, 219–233. https://doi.org/10.1016/j.ecolind.2012.12.031

D'Orbigny, A.D., 1826. Tableau méthodique de la classe des Céphalopodes, in Annales des sciences naturelles : comprenant La physiologie animale et végétale, l'anatomie comparée des deux règnes, la zoologie, la botanique, la minéralogie et la géologie. Crochard, Paris, 468 p.

Dujardin, F., 1835. Annales des sciences naturelles. Crochard, Paris, 312–314.

Elliott, M., Whitfield, A.K., 2011. Challenging paradigms in estuarine ecology and management. Estuarine, Coastal and Shelf Science 94, 306–314. https://doi.org/10.1016/j.ecss.2011.06.016

Elmqvist, T., Folke, C., Nyström, M., Peterson, G., Bengtsson, J., Walker, B., Norberg, J., 2003. Response diversity, ecosystem change, and resilience. Frontiers in Ecology and the Environment 1, 488–494. https://doi.org/10.1890/1540-9295(2003)001[0488:RDECAR]2.0.CO;2

Feyling-Hanssen, R.W., 1972. The Foraminifer *Elphidium excavatum* (Terquem) and Its Variant Forms. Micropaleontology 18, 337–354. https://doi.org/10.2307/1485012

Gilbert, D., Rabalais, N.N., Diaz, R.J., Zhang, J., 2010. Evidence for greater oxygen decline rates in the coastal ocean than in the open ocean. Biogeosciences 2283–2296.

Glock, N., Schönfeld, J., Eisenhauer, A., Hensen, C., Mallon, J., Sommer, S., 2013. The role of benthic foraminifera in the benthic nitrogen cycle of the Peruvian oxygen minimum zone. Biogeosciences 10, 4767–4783. https://doi.org/10.5194/bg-10-4767-2013

Groeneveld, J., Filipsson, H.L., Austin, W.E.N., Darling, K., McCarthy, D., Krupinski, N.B.Q., Bird, C., Schweizer, M., 2018. Assessing proxy signatures of temperature, salinity, and hypoxia in the Baltic Sea through foraminifera-based geochemistry and faunal assemblages. Journal of Micropalaeontology 37, 403–429.

Groß, O., 2002. Sediment interactions of Foraminifera: implications for food degradation and bioturbation processes. Journal of Foraminiferal Research 32, 414–424. https://doi.org/10.2113/0320414

Gupta, B.K.S., 2007. Modern Foraminifera. Springer Science & Business Media, 371 p.

Halpern, B.S., Walbridge, S., Selkoe, K.A., Kappel, C.V., Micheli, F., D'Agrosa, C., Bruno, J.F., Casey, K.S., Ebert, C., Fox, H.E., Fujita, R., Heinemann, D., Lenihan, H.S., Madin, E.M.P., Perry, M.T., Selig, E.R., Spalding, M., Steneck, R., Watson, R., 2008. A Global Map of Human Impact on Marine Ecosystems. Science 319, 948–952. https://doi.org/10.1126/science.1149345

Harley, C.D.G., Hughes, A.R., Hultgren, K.M., Miner, B.G., Sorte, C.J.B., Thornber, C.S., Rodriguez, L.F., Tomanek, L., Williams, S.L., 2006. The impacts of climate change in coastal marine systems. Ecology Letters 9, 228–241. https://doi.org/10.1111/j.1461-0248.2005.00871.x

Haynes, J.R., 1992. Supposed pronounced ecophenotypy in foraminifera. Journal of Micropalaeontology 11, 59–63. https://doi.org/10.1144/jm.11.1.59

Haynes, J.R., 1973. Cardigan Bay Recent Foraminifera: Cruise of the R.V."Antur", 1962-64. Natural History Museum Publications.

Hayward, B.W., Holzmann, M., Grenfell, H.R., Pawlowski, J., Triggs, C.M., 2004. Morphological distinction of molecular types in *Ammonia* – towards a taxonomic revision of the world's most commonly misidentified foraminifera. Marine Micropaleontology 50, 237–271. https://doi.org/10.1016/S0377-8398(03)00074-4

Hayward, B.W., Holzmann, M., Tsuchiya, M., 2019. Combined Molecular and Morphological Taxonomy of the *Beccarii*/T3 Group of the Foraminiferal Genus *Ammonia*. Journal of Foraminiferal Research 49, 367–389. https://doi.org/10.2113/gsjfr.49.4.367

Hayward, B.W., Le Coze, F., Vachard, D., Gross, O., 2020. World Foraminifera Database. *Ammonia* Brünnich, 1771. Accessed through: World Register of Marine Species at: http://www.marinespecies.org/aphia.php?p=taxdetails&id=112078 on 2020-04-06.

Hermelin, J.O.R., 1987. Distribution of Holocene benthic foraminifera in the Baltic Sea. Journal of Foraminiferal Research 17, 62–73. https://doi.org/10.2113/gsjfr.17.1.62

Hofker, J., 1964. Foraminifera from the tidal zone in the Netherlands Antilles and other West Indian Islands. Studies on the Fauna of Curaçao and other Caribbean Islands 21, 1–119.

Hohenegger, J., 2006. The importance of symbiont-bearing benthic foraminifera for West Pacific carbonate beach environments. Marine Micropaleontology, Foraminifera and Environmental Micropaleontology 61, 4–39. https://doi.org/10.1016/j.marmicro.2006.05.007

Holzmann, M., 2000. Species Concept in Foraminifera: *Ammonia* as a Case Study. Micropaleontology 46, 21–37.

Holzmann, M., Pawlowski, J., 2000. Taxonomic relationships in the genus *Ammonia* (Foraminifera) based on ribosomal DNA sequences. Journal of Micropalaeontology 19, 85–95. https://doi.org/10.1144/jm.19.1.85

Holzmann, M., Pawlowski, J., 1997. Molecular, morphological and ecological evidence for species recognition in *Ammonia* (Foraminifera). Journal of Foraminiferal Research 27, 311–318. https://doi.org/10.2113/gsjfr.27.4.311

Holzmann, M., Piller, W., Pawlowski, J., 1996. Sequence variations in the large-subunit ribosomal RNA gene of *Ammonia* (foraminifera, protozoa) and their evolutionary implications. Journal of Molecular Evolution 43, 145–151. https://doi.org/10.1007/BF02337359

Hugo, G., 2011. Future demographic change and its interactions with migration and climate change. Global Environmental Change, Migration and Global Environmental Change – Review of Drivers of Migration 21, S21–S33. https://doi.org/10.1016/j.gloenvcha.2011.09.008

Jackson, J.B.C., Kirby, M.X., Berger, W.H., Bjorndal, K.A., Botsford, L.W., Bourque, B.J., Bradbury, R.H., Cooke, R., Erlandson, J., Estes, J.A., Hughes, T.P., Kidwell, S., Lange, C.B., Lenihan, H.S., Pandolfi, J.M., Peterson, C.H., Steneck, R.S., Tegner, M.J., Warner, R.R., 2001. Historical Overfishing and the Recent Collapse of Coastal Ecosystems. Science 293, 629–637. https://doi.org/10.1126/science.1059199

Jauffrais, T., Jesus, B., Metzger, E., Mouget, J.-L., Jorissen, F., Geslin, E., 2016a. Effect of light on photosynthetic efficiency of sequestered chloroplasts in intertidal benthic foraminifera (*Haynesina germanica* and *Ammonia tepida*). Biogeosciences 13, 2715–2726. https://doi.org/10.5194/bg-13-2715-2016

Jauffrais, T., Jesus, B., Geslin, E., Briand, F., Jézéquel, V.M., 2016b. Locomotion speed of the benthic foraminifer *Ammonia tepida* exposed to different nitrogen and carbon sources. Journal of Sea Research, Recent and past sedimentary, biogeochemical and benthic ecosystem evolution of the Loire Estuary (Western France) 118, 52–58. https://doi.org/10.1016/j.seares.2016.07.001

Jauffrais, T., LeKieffre, C., Koho, K.A., Tsuchiya, M., Schweizer, M., Bernhard, J.M., Meibom, A., Geslin, E., 2018. Ultrastructure and distribution of kleptoplasts in benthic foraminifera from shallow-water (photic) habitats. Marine Micropaleontology, Benthic Foraminiferal Ultrastructure Studies 138, 46–62. https://doi.org/10.1016/j.marmicro.2017.10.003

Jones, R.W., 2013. Foraminifera and their Applications. Cambridge University Press, 391 p.

Jorissen, F.J., 1988. Benthic foraminifera from the Adriatic Sea: principles of phenotypic variation. State University of Utrecht, 176 p.

Josefson, A.B., Widbom, B., 1988. Differential response of benthic macrofauna and meiofauna to hypoxia in the Gullmar Fjord basin. Marine Biology 100, 31–40. https://doi.org/10.1007/BF00392952

Katz, M.E., Cramer, B.S., Franzese, A., Hönisch, B., Miller, K.G., Rosenthal, Y., Wright, J.D., 2010. Traditional and emerging geochemical proxies in foraminifera. Journal of Foraminiferal Research 40, 165–192. https://doi.org/10.2113/gsjfr.40.2.165

Langer, M., Leppig, U., 2000. Molecular phylogenetic status of *Ammonia catesbyana* (D'Orbigny, 1839), an intertidal foraminifer from the North Sea. Neues Jahrbuch fur Geologie und Palaontologie Monatshefte 9, 545–556.

Langer, M.R., 2008. Assessing the Contribution of Foraminiferan Protists to Global Ocean Carbonate Production1. Journal of Eukaryotic Microbiology 55, 163–169. https://doi.org/10.1111/j.1550-7408.2008.00321.x

LeKieffre, C., Spangenberg, J., Mabilleau, G., Escrig, S., Meibom, A., Geslin, E., 2017. Surviving anoxia in marine sediments: The metabolic response of ubiquitous benthic foraminifera (*Ammonia tepida*). PLoS ONE 12, e0177604. https://doi.org/10.1371/journal.pone.0177604

Levin, L.A., Ekau, W., Gooday, A.J., Jorissen, F., Middelburg, J.J., Naqvi, S.W.A., Neira, C., Rabalais, N.N., Zhang, J., 2009. Effects of natural and human-induced hypoxia on coastal benthos. Biogeosciences 6, 2063–2098. https://doi.org/10.5194/bg-6-2063-2009

Linné, C. von, 1758. Systema Naturae. 824 p.

Lopez, E., 1979. Algal chloroplasts in the protoplasm of three species of benthic foraminifera: taxonomic affinity, viability and persistence. Marine Biology 53, 201–211. https://doi.org/10.1007/BF00952427

Luttikhuizen, P.C., Dekker, R., 2010. Pseudo-cryptic species *Arenicola defodiens* and *Arenicola marina* (Polychaeta: *Arenicolidae*) in Wadden Sea, North Sea and Skagerrak: Morphological and molecular variation. Journal of Sea Research 63, 17–23. https://doi.org/10.1016/j.seares.2009.09.001

Milker, Y., Schmiedl, G., Betzler, C., 2011. Paleobathymetric history of the Western Mediterranean Sea shelf during the latest glacial period and the Holocene: Quantitative reconstructions based on foraminiferal transfer functions. Palaeogeography, Palaeoclimatology, Palaeoecology 307, 324–338. https://doi.org/10.1016/j.palaeo.2011.05.031

Millennium Ecosystem Assessment (Program), 2005. Chapter 19: Coastal Systems, in Ecosystems and Human Well Being: Current State & Trends, Washington DC: Island Press, 513–549

Miller, A.A.L., Scott, D.B., Medioli, F.S., 1982. *Elphidium excavatum* (Terquem); ecophenotypic versus subspecific variation. Journal of Foraminiferal Research 12, 116–144. https://doi.org/10.2113/gsjfr.12.2.116

Murray, J.W., 2007. Biodiversity of living benthic foraminifera: How many species are there? Marine Micropaleontology 64, 163–176. https://doi.org/10.1016/j.marmicro.2007.04.002

Murray, J.W., 2006. Ecology and Applications of Benthic Foraminifera. Cambridge University Press, 426 p.

Nehrke, G., Keul, N., Langer, G., de Nooijer, L.J., Bijma, J., Meibom, A., 2013. A new model for biomineralization and trace-element signatures of Foraminifera tests. Biogeosciences 10, 6759–6767. https://doi.org/10.5194/bg-10-6759-2013

Pawlowski, J., Bolivar, I., Fahrni, J., Zaninetti, L., 1994. Taxonomic Identification of Foraminifera Using Ribosomal DNA Sequences. Micropaleontology 40, 373–377. https://doi.org/10.2307/1485942

Pawlowski, J., Bolivar, I., Farhni, J., Zaninetti, L., 1995. DNA analysis of "*Ammonia beccarii*" morphotypes: one or more species? Marine Micropaleontology 26, 171–178. https://doi.org/10.1016/0377-8398(95)00022-4

Pawlowski, J., Holzmann, M., 2008. Diversity and geographic distribution of benthic foraminifera: a molecular perspective. Biodiversity and Conservation 17, 317–328. https://doi.org/10.1007/s10531-007-9253-8

Pawlowski, J., Holzmann, M., Berney, C., Fahrni, J., Gooday, A.J., Cedhagen, T., Habura, A., Bowser, S.S., 2003. The evolution of early Foraminifera. PNAS 100, 11494–11498. https://doi.org/10.1073/pnas.2035132100

Petersen, J., Barras, C., Bézos, A., La, C., de Nooijer, L.J., Meysman, F.J.R., Mouret, A., Slomp, C.P., Jorissen, F.J., 2018. Mn/Ca intra- and inter-test variability in the benthic foraminifer *Ammonia tepida*. Biogeosciences 15, 331–348. https://doi.org/10.5194/bg-15-331-2018

Petersen, J., Riedel, B., Barras, C., Pays, O., Guihéneuf, A., Mabilleau, G., Schweizer, M., Meysman, F.J.R., Jorissen, F.J., 2016. Improved methodology for measuring pore patterns in the benthic foraminiferal genus *Ammonia*. Marine Micropaleontology 128, 1–13. https://doi.org/10.1016/j.marmicro.2016.08.001

Phleger, F.B., Parker, F.L., 1951. Ecology of Foraminifera, north-west Gulf of Mexico. Part II. Foraminifera species. New York, Geological Society of America.

Pillet, L., de Vargas, C., Pawlowski, J., 2011. Molecular Identification of Sequestered Diatom Chloroplasts and Kleptoplastidy in Foraminifera. Protist 162, 394–404. https://doi.org/10.1016/j.protis.2010.10.001

Pillet, L., Voltski, I., Korsun, S., Pawlowski, J., 2013. Molecular phylogeny of Elphidiidae (foraminifera). Marine Micropaleontology 103, 1–14. https://doi.org/10.1016/j.marmicro.2013.07.001

Piña-Ochoa, E., Høgslund, S., Geslin, E., Cedhagen, T., Revsbech, N.P., Nielsen, L.P., Schweizer, M., Jorissen, F., Rysgaard, S., Risgaard-Petersen, N., 2010. Widespread occurrence of nitrate storage and denitrification among Foraminifera and Gromiida. PNAS 107, 1148–1153. https://doi.org/10.1073/pnas.0908440107

Plancus, 1739. De conchis minvs notis liber : cvi accessit specimen aestvs reciproci maris svperi ad littvs portvmqve Arimini. Venetiis : typis Joannis Baptistae Pasqvali.

Poag, C.W., 1978. Paired Foraminiferal Ecophenotypes in Gulf Coast Estuaries: Ecological and Paleoecological Implications 28, 395–421.

Polovodova, I., Nikulina, A., Schönfeld, J., Dullo, W.-C., 2009. Recent benthic foraminifera in the Flensburg Fjord (Western Baltic Sea). Journal of Micropalaeontology 28, 131–142. https://doi.org/10.1144/jm.28.2.131

Rabalais, N.N., Díaz, R.J., Levin, L.A., Turner, R.E., Gilbert, D., Zhang, J., 2010. Dynamics and distribution of natural and human-caused hypoxia. Biogeosciences 7, 585–619. https://doi.org/10.5194/bg-7-585-2010

Rabalais, N.N., Turner, R.E., Díaz, R.J., Justić, D., 2009. Global change and eutrophication of coastal waters. International Council for the Exploration of the Sea Journal of Marine Science 66, 1528–1537. https://doi.org/10.1093/icesjms/fsp047

Riedel, B., Diaz, R., Rosenberg, R., Stachowitsch, M., 2016. The ecological consequences of marine hypoxia: from behavioural to ecosystem responses, in Stressors in the marine environment: physiological responses and ecological implication. Martin Solan, Nia M. Whiteley, Oxford University Press. ed, pp. 175–194.

Risgaard-Petersen, N., Langezaal, A.M., Ingvardsen, S., Schmid, M.C., Jetten, M.S.M., Camp, H.J.M.O. den, Derksen, J.W.M., Piña-Ochoa, E., Eriksson, S.P., Nielsen, L.P., Revsbech, N.P., Cedhagen, T., Zwaan, G.J. van der, 2006. Evidence for complete denitrification in a benthic foraminifer. Nature 443, 93–96. https://doi.org/10.1038/nature05070

Ross, B.J., Hallock, P., 2016. Dormancy in the Foraminifera: A Review. Journal of Foraminiferal Research 46, 358–368. https://doi.org/10.2113/gsjfr.46.4.358

Saad, S.A., Wade, C.M., 2016. Biogeographic distribution and habitat association of *Ammonia* genetic variants around the coastline of Great Britain. Marine Micropaleontology 124, 54–62. https://doi.org/10.1016/j.marmicro.2016.01.004

Scheffer, M., Bascompte, J., Brock, W.A., Brovkin, V., Carpenter, S.R., Dakos, V., Held, H., Nes, E.H. van, Rietkerk, M., Sugihara, G., 2009. Early-warning signals for critical transitions. Nature 461, 53–59. https://doi.org/10.1038/nature08227

Scheffer, M., Carpenter, S., Foley, J.A., Folke, C., Walker, B., 2001. Catastrophic shifts in ecosystems. Nature 413, 591–596. https://doi.org/10.1038/35098000

Schmidtko, S., Stramma, L., Visbeck, M., 2017. Decline in global oceanic oxygen content during the past five decades. Nature 542, 335–339. https://doi.org/10.1038/nature21399

Schnitker, D., 1974. Ecotypic variation in *Ammonia beccarii* (Linne). Journal of Foraminiferal Research 4, 217–223. https://doi.org/10.2113/gsjfr.4.4.217

Schultze, M.J.S., 1854. Uber den Organismus der Polythalamien (Foraminiferen) nebst Bemerkungen über die Rhizopoden im Allgemeinen.

Schweizer, M., Jorissen, F., Geslin, E., 2011a. Contributions of molecular phylogenetics to foraminiferal taxonomy: General overview and example of *Pseudoeponides falsobeccarii* Rouvillois, 1974. Comptes Rendus Palevol 10, 95–105. https://doi.org/10.1016/j.crpv.2011.01.003

Schweizer, M., Polovodova, I., Nikulina, A., Schönfeld, J., 2011b. Molecular identification of *Ammonia* and *Elphidium* species (Foraminifera, Rotaliida) from the Kiel Fjord (SW Baltic Sea) with rDNA sequences. Helgoland Marine Research 65, 1–10. https://doi.org/10.1007/s10152-010-0194-3

Seiglie, G.A., 1975. Foraminifers of Guayanilla Bay and their use as environmental indicators. Revista Espanola de Micropaleontologia 7, 453–487.

Seuront, L., Bouchet, V.M.P., 2015. The devil lies in details: new insights into the behavioural ecology of intertidal Foraminifera. Journal of Foraminiferal Research 45, 390–401. https://doi.org/10.2113/gsjfr.45.4.390

Small, C., Nicholls, R.J., 2003. A Global Analysis of Human Settlement in Coastal Zones. Journal of Coastal Research 19, 584–599.

Sorensen, J., 1997. National and international efforts at integrated coastal management: Definitions, achievements, and lessons. Coastal Management 25, 3–41. https://doi.org/10.1080/08920759709362308

Stouff, V., Geslin, E., Debenay, J.-P., Lesourd, M., 1999a. Origin of Morphological Abnormalities in Ammonia (foraminifera): Studies in Laboratory and Natural Environments. Journal of Foraminiferal Research 29, 152–170. https://doi.org/10.2113/gsjfr.29.2.152

Stouff, V., Lesourd, M., Debenay, J.-P., 1999b. Laboratory Observations on Asexual Reproduction (schizogony) and Ontogeny of Ammonia Tepida with Comments on the Life Cycle. Journal of Foraminiferal Research 29, 75–84. https://doi.org/10.2113/gsjfr.29.1.75

Thomas, E., Shackleton, N.J., 1996. The Paleocene-Eocene benthic foraminiferal extinction and stable isotope anomalies. Geological Society, London, Special Publications 101, 401–441. https://doi.org/10.1144/GSL.SP.1996.101.01.20

Toyofuku et al, 2005. Phylogenetic relationships among genus *Ammonia* (Foraminifera) based on ribosomal DNA sequences which are distributed in the vicinity of the Japanese Islands.

Vénec-Peyré, M.-T., 1983. Étude de la croissance et de la variabilité chez un foraminifère benthique littoral *Ammonia beccarii* (Linné), en Méditerranée occidentale /. Éditions du Centre national de la recherche scientifique, Paris, 31 p.

Vitousek, P.M., Mooney, H.A., Lubchenco, J., Melillo, J.M., 1997. Human Domination of Earth's Ecosystems. Science 277, 494–499. https://doi.org/10.1126/science.277.5325.494

Walton, W.R., Sloan, B.J., 1990. The genus *Ammonia* Brünnich, 1772; its geographic distribution and morphologic variability. Journal of Foraminiferal Research 20, 128–156. https://doi.org/10.2113/gsjfr.20.2.128

Wang, P., Lutze, G.F., 1986. Inflated later chambers; ontogenetic changes of some Recent hyaline benthic foraminifera. Journal of Foraminiferal Research 16, 48–62. https://doi.org/10.2113/gsjfr.16.1.48

Williamson, W.C., 1858. On the recent Foraminifera of Great Britain. London, Printed for the Ray society.

Worm, B., Barbier, E.B., Beaumont, N., Duffy, J.E., Folke, C., Halpern, B.S., Jackson, J.B.C., Lotze, H.K., Micheli, F., Palumbi, S.R., Sala, E., Selkoe, K.A., Stachowicz, J.J., Watson, R., 2006. Impacts of Biodiversity Loss on Ocean Ecosystem Services. Science 314, 787–790. https://doi.org/10.1126/science.1132294

Zachos, J., Pagani, M., Sloan, L., Thomas, E., Billups, K., 2001. Trends, Rhythms, and Aberrations in Global Climate 65 Ma to Present. Science 292, 686–693. https://doi.org/10.1126/science.105941

CHAPTER 2

MORPHOLOGICAL DISTINCTION OF THREE *AMMONIA* PHYLOTYPES OCCURRING ALONG THE EUROPEAN COASTS

JULIEN RICHIRT[1,*], MAGALI SCHWEIZER[1], VINCENT M. P. BOUCHET[2], AURELIA MOURET[1], SOPHIE QUINCHARD[1] AND FRANS J. JORISSEN[1]

[1] UMR 6112 LPG-BIAF Recent and Fossil Bio-Indicators, Angers University, 2 Boulevard Lavoisier, F-49045 Angers, France
[2] Univ. Lille, CNRS, Univ. Littoral Côte d'Opale, UMR 8187, LOG, Laboratoire d'Océanologie et de Géosciences, F 62930, Wimereux, France

*Correspondence author: richirt.julien@gmail.com

Published in Journal of Foraminiferal Research, v. 49, no. 1, p. 76–93, January 2019

Received 16 April 2018
Accepted 9 July 2018

ABSTRACT

The high morphological variability observed in the genus *Ammonia*, together with its global distribution, led to the description of a plethora of species, subspecies and varieties. Until today, many researchers have used a limited number of (morpho-)species, and have considered the numerous varieties as ecophenotypes. Recently, molecular studies have shown that these putative ecophenotypes are in reality well separated genetically, and should rather be considered as separate species. This study aims to investigate the morphological characteristics of three phylotypes (T1, T2 and T6) belonging to the genus *Ammonia*, encountered along the European coasts. For this purpose, *Ammonia* specimens were sampled at 22 different locations between 2014 and 2016, and were imaged using an environmental SEM (Scanning Electron Microscope). For 96 specimens, images of the spiral, umbilical and peripheral sides were obtained and pore features were investigated using 1000x magnified images of the penultimate chamber on the spiral side. Sixty-one morphometric parameters were measured for each individual. In order to assign each specimen to a phylotype, molecular analyses have been performed using a SSU (Small Sub-Unit) rDNA fragment. A multivariate approach (Factorial Analysis of Mixed Data, FAMD), allowing the joint analysis of quantitative and qualitative measurements, was performed to determine the most reliable morphometric parameters to discriminate the three phylotypes. Our results show that the use of only two morphological characteristics is sufficient to differentiate the three pseudocryptic species: the raised or flush character of the sutures on the central part of the spiral side and the mean pore diameter. These two criteria, which can be observed with a standard stereomicroscope, provide an efficient method to discriminate T1, T2 and T6 with at least 90% accuracy. We consider that there is still insufficient information to reliably assign previously defined formal scientific names to the three phylotypes, and therefore we recommend to continue using the phylotype designations T1, T2 and T6. Our results make it possible to study the distribution of these three pseudocryptic species (T1, T2 and T6) on the basis of stereomicroscope examination alone. This opens the possibility to discriminate these species also in dead/fossil assemblages. Among other things, this will allow verification in sediment cores the putative recent introduction in European coastal areas of T6, which is often considered as an exotic species, originating from East Asia.

1. INTRODUCTION

Ammonia Brünnich 1772 is an extant foraminiferal genus that appeared during the Early Miocene (Loeblich & Tappan, 1987) and inhabits shallow and intertidal coastal areas, including estuaries (e.g., Cifelli, 1962; Walton & Sloan, 1990). Known for well over two centuries (e.g., Plancus, 1739; Linné, 1758), this genus exhibits a worldwide distribution and occurs with high abundances in shallow marine and estuarine ecosystems of temperate to tropical regions, but is absent at high latitudes (Sen Gupta, 2007; Murray, 2014). *Ammonia* is one of the most widely studied benthic foraminiferal genera. Studies on this genus concern many different aspects, such as geographic distribution, ecology, behavior, life cycle, metabolism, morphology, or test ultrastructure (Banner &Williams, 1973; Chang & Kaesler, 1974; Schnitker, 1974; Poag, 1978; Walton & Sloan, 1990; Debenay et al., 1998; Stouff et al., 1999a, b; Seuront & Bouchet, 2015;

Jauffrais et al., 2016; LeKieffre et al., 2017). Since *Ammonia* is relatively easy to obtain and maintain in laboratory conditions, the genus is also extensively used for laboratory experiments aiming to better understand foraminiferal biomineralization (e.g., de Nooijer et al., 2009; Nehrke et al., 2013) and to improve palaeoceanographical proxies based on the chemical composition of foraminiferal test carbonate (e.g., Dissard et al., 2010; Barras et al., 2018; Petersen et al., 2018).

The high morphological variability observed in *Ammonia* led to the description of numerous species, subspecies, and varieties, many of which suffer from an inadequate illustration and/or a lack of type material. Many of the proposed taxa have mainly been used in specific regions and are the result of a tendency for "splitting" (i.e., describing species based on rather small morphological differences) in the first half of the 20th century. Presently, no less than 60 recent species of Ammonia have been accepted in the World Register of Marine Species (WoRMS) database (Hayward et al., 2018). Since species descriptions often show overlaps, many species names are only used regionally, and no real consensus exists concerning the morphological criteria to distinguish the different Ammonia species. For these reasons, the taxonomy of the genus Ammonia is still confusing and has been described as "nomenclatural chaos" by Boltovskoy (1965) and Haynes (1992).

In 1974, two studies suggested that the high morphological variability exhibited by *Ammonia* was probably linked to environmental variability of their ecological niches (Chang & Kaesler, 1974; Schnitker, 1974). Following this idea, numerous species previously described were subsequently considered ecophenotypes and assigned to a limited number of species (Schnitker, 1974). This approach substantially simplified the taxonomy of the genus. *Ammonia beccarii* Linné, 1758 (historically the first species described in the genus *Ammonia*) was often considered a "super-species" with an important morphological plasticity. In the two following decades, this "lumping" vision resulted in several classification schemes (e.g., Poag, 1978; Wang & Lutze, 1986; Jorissen, 1988; Walton & Sloan, 1990). However, the more traditional "splitters" continued to assign formal names to the different morphotypes (e.g., Hofker, 1964; Banner & Williams, 1973; Cimerman & Langer, 1991; Loeblich & Tappan, 1994; Colburn & Baskin, 1998). The opposition between "lumpers" and "splitters" has continued since then (Pawlowski & Holzmann, 2008).

Some studies have investigated the morphological variability of *Ammonia* using a morphometric approach (Cifelli 1962; Chang & Kaesler, 1974; Vénec-Peyré, 1983; Wang & Lutze, 1986). Although Haynes (1992) already questioned the existence of ecophenotypy in *Ammonia* on the basis of theoretical considerations, the confirmation that many of the

morphotypes should indeed be considered as separate species came with molecular studies initiated by Pawlowski et al. (1995) and continued since then (e.g., Holzmann et al., 1996; Holzmann, 2000; Holzmann & Pawlowski, 2000; Langer & Leppig, 2000; Schweizer et al., 2011a,b). Subsequently, it appeared that studies combining morphometric approaches and molecular biology were needed to define distinctive morphological features for all phylotypes (Holzmann, 2000).

Today, 20 years after the first molecular studies of *Ammonia*, the classification of this genus is still partly inaccurate, despite the efforts made by researchers to reconcile traditional morphology-based taxonomy (i.e., morphometric approach) and molecular biology (i.e., molecular phylogenetic approach; Holzmann & Pawlowski, 1997; Holzmann et al., 1998).Hayward et al. (2004) published one of the most extensive combined (morphologic/molecular phylogenetic) studies of this genus using 37 parameters to morphologically distinguish the 13 molecular groups resulting from a global inventory available at that time. However, many phylotypes were morphologically close and remained difficult to distinguish on the basis of morphology.

In the present study, we investigated three *Ammonia* phylotypes encountered abundantly along European coasts. While phylotype T1 is considered to be cosmopolitan (Holzmann & Pawlowski, 2000), T2 has been exclusively encountered along the North Atlantic coasts of Europe and the USA (Hayward et al., 2004); phylotype T6 shows a disjunct geographical distribution (Hayward et al., 2004; Pawlowski & Holzmann, 2008) with records in the North Sea (Holzmann & Pawlowski, 2000; Schweizer et al., 2011b) and also around Japan (Toyofuku et al., 2005) and China (Hayward et al., 2004). At the 22 investigated sites, we also sporadically encountered phylotype T3 and *Ammonia falsobeccarii* (Rouvillois, 1974), which are easily distinguishable morphologically from the other three (Hayward et al., 2004; Schweizer et al., 2011a) and are therefore not further studied here. In short, T3 shows deeply incised, fissured sutures on the spiral side and a more ornamented umbilical side whereas *A. falsobeccarii* is characterized by secondary openings at the junction of the radial and spiral sutures on the spiral side (Schweizer et al., 2011a). Phylotypes T1, T2, and T6 are morphologically very similar, and until now, their discrimination on the basis of morphological criteria without molecular analysis has been very difficult, if not impossible.

The objective of this study was to identify simple morphological criteria that would allow for the discrimination of these three phylotypes. To achieve this aim, we adopted an approach combining high-resolution morphological measurements performed on SEM (Scanning Electron Microscope) images and molecular biology (to identify the various phylotypes).

We think that the ability to distinguish these three phylotypes of *Ammonia* on the basis of morphological criteria alone constitutes a major advancement for the study of coastal environments in which these species occur in high densities. First of all, the proposed morphological method eludes molecular analysis, which may be expensive and time-consuming. More importantly, once the ecological characteristics of the three phylotypes are better known, their morphological discrimination (1) may increase the taxonomic resolution in routine studies on the quality of recent coastal environments, leading to more precise measurements of diversity and biotic indices; (2) will improve experimental studies by considering one phylotype at a time, instead of having a mix of cryptic species; and (3) will increase the resolution of biostratigraphical and/or palaeoecological studies of ancient coastal environments for which only fossil material is available and molecular analyses are difficult or impossible. Finally, we hope that this study will help lessen the "taxonomical chaos" in the genus *Ammonia*.

2. MATERIALS AND METHODS

2.1. BIOLOGICAL MATERIAL

Specimens of *Ammonia* that were morphologically similar to T1, T2, and T6 were collected at 22 different locations between 2014 and 2016. All sites are intertidal mudflats, which were sampled at low tide (mainly on the French Atlantic coast; Fig. 1, Table 1). Sediment samples were obtained by spooning off the surface layer (1 cm at most). Samples were sieved at 100 µm and *Ammonia* specimens were picked and cleaned with a brush under a stereomicroscope and transferred in a Petri dish. Live specimens were distinguished from dead ones by their pseudopodial activity. After introducing them on a thin layer of fine sediment (<38 µm) in the Petri dish, if locomotion (i.e., pseudopodial network or movement) was discerned after 1 hour, individuals were considered alive. Living individuals were cleaned, dried, and stored on micropalaeontological slides.

2.2. SEM IMAGES ACQUISITION AND MORPHOLOGICAL MEASUREMENTS

The dried *Ammonia* specimens were imaged using an environmental SEM (Scanning ElectronMicroscope, Zeiss EVO LS10) prior to DNA extraction and test destruction. For each individual, four images were taken: a 1000x magnification of the penultimate chamber of the

spiral side, to observe and measure porosity features (Fig. 2a), and full specimens in spiral, umbilical, and peripheral views (Fig. 2b–d).

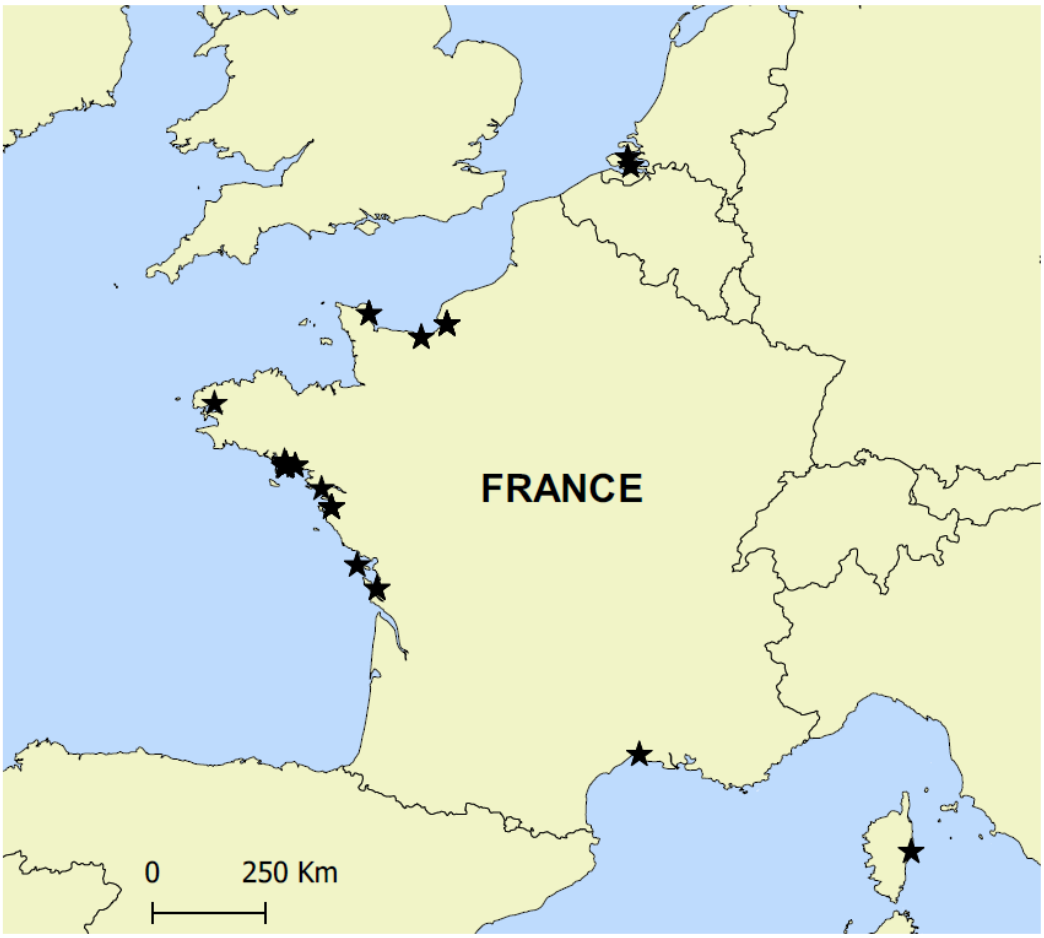

Figure 1. Sampling sites (black stars) in Europe.

To investigate the morphological variability of the specimens, 61 morphological parameters (Fig. 3, Appendix-Table 1) were measured on the SEM images using ImageJ software (Schneider et al., 2012). The parameters measured on the 1000x image of the penultimate chamber concerned the pore features and were obtained following the semi-automated method described in detail by Petersen et al. (2016). Some parameters have been used in previous morphometric studies [e.g., maximum diameter, thickness, diameter of the proloculus, number of chambers (Cifelli, 1962); lobateness index (Chang & Kaesler, 1974) or umbilical ornamentation (Vénec-Peyré, 1983)] whereas others are specific to this study (e.g., the relative length of the last chamber compared to the test diameter in the umbilical view).

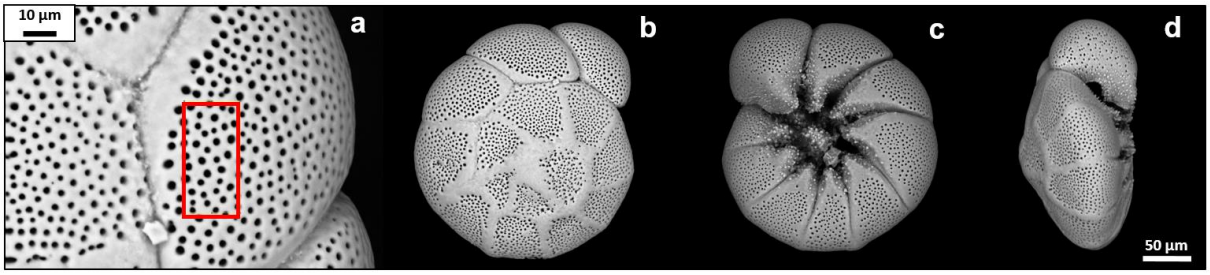

Figure 2. SEM images of (a) a 1000x magnification of the penultimate chamber on the spiral siden (b) spiral, (c) umbilical and (d) peripheral views of an *Ammonia* specimen (Au502 from Auray River – Gulf of Morbihan). The red rectangle (a) represents the area considered for the porosity measurements.

2.3. PHYLOTYPE ASSIGNATION

The DNA extraction was performed by crushing each specimen individually in a microtube filled with DOC buffer and warmed at 60°C for one hour (Pawlowski, 2000). The amplification of a fragment of approximatively 500 bp (base pairs) at the 3' end of the SSU (Small Sub-Unit) rDNA was achieved in two steps with a nested PCR (Polymerase Chain Reaction, Appendix-Fig. 1).

The first step consisted of the amplification of a fragment of 1000 bp using the primers s14F3 and J2 (Pawlowski, 2000; Darling et al., 2016). The PCR setup was 1 min at 95°C followed by 40 cycles of 30 sec at 94°C, 30 sec at 50°C, and 1 min 30 sec at 72°C with a terminal cycle of 3 min at 72°C. The second step of the nested PCR was performed using the primers s14F1 and N6 (Pawlowski, 2000; White et al., 1990). The PCR conditions were 1 min at 95°C followed by 25 cycles of 30 sec at 94°C, 30 sec at 50°C, and 1 min at 72°C with a terminal cycle of 5 min at 72°C.

Positive amplifications obtained with the nested PCR were then sequenced either with the Sanger (directly, without cloning) or the High Throughput Sequencing (HTS) methods (Appendix-Table 2). For the Sanger method, samples were sent to GATC Biotech in Cologne for sequencing (deposited in the GenBank database, accession numbers MH200642–MH200706; Appendix-Table 2). Samples sequenced through HTS with a MiSeq (Illumina) at the Molecular Systematics & Environmental Genomics Laboratory (University of Geneva) will be published elsewhere (Apothéloz-Perret-Gentil et al., unpublished data).

Sequences were obtained for 96 specimens and were automatically aligned with a set of sequences published in GenBank using the ClustalO algorithm (Sievers et al., 2011) using Seaview software version 4 (Gouy et al., 2010). To assign a phylotype to each specimen sequenced in this study, the sequences were aligned and compared with GenBank sequences

previously identified as phylotypes T1, T2, and T6 (Langer & Leppig, 2000; Ertan et al., 2004; Schweizer et al., 2011b; Pawlowski & Holzmann, unpublished data).

Table 1. Name, location, coordinates (from North to South) and number of individuals for each sampling site used in this study.

Location	Station	Latitude	Longitude	Number of individuals
North Sea, Netherlands	Zandkreek	51°33′12.24″N	3°52′25.34″E	2
North Sea, Netherlands	Biezelingse Ham	51°26′53.40″N	3°55′49.79″E	3
English Channel, France	Saint Vaast	49°34′38.60″N	1°16′38.80″W	4
English Channel, France	Estuaire de la Seine	49°26′31.30″N	0°16′25.20″E	13
English Channel, France	Ouistreham	49°16′16.40″N	0°14′12.20″W	3
East Atlantic, France	Rade de Brest	48°24′13.10″N	4°21′16.00″W	1
East Atlantic, France	Rivière du Bono	47°38′4.71″N	2°57′36.27″W	1
East Atlantic, France	Pointe de Toulvern	47°35′39.95″N	2°55′35.80″W	3
East Atlantic, France	Kerouarc'h 2	47°34′60.00″N	2°57′17.20″W	5
East Atlantic, France	Locmariaquer 1	47°34′12.12″N	2°56′32.40″W	15
East Atlantic, France	Locmariaquer 2	47°34′11.58″N	2°56′26.58″W	11
East Atlantic, France	Locmariaquer 3	47°34′11.29″N	2°56′21.38″W	7
East Atlantic, France	Ile Bailleron est	47°34′38.07″N	2°44′45.25″W	4
East Atlantic, France	Saint Pierre Lopérec	47°33′44.77″N	2°58′23.02″W	1
East Atlantic, France	Saint Nazaire	47°15′56.75″N	2°13′20.79″W	1
East Atlantic, France	Baie de Bourgneuf	47°0′56.38″N	2°1′31.00″W	8
East Atlantic, France	Ile de Ré	46°13′23.13″N	01°30′46.27″W	2
East Atlantic, France	Baie de l'Aiguillon	45°53′60.00″N	1°7′0.00″W	4
Mediterranean, France	Camargue	43°33′9.306″N	4°6′15.112″E	2
Mediterranean, France	Corsica DIA5	42°8′7.44″N	09°31′59.04″E	2
West Pacific, Japan	Yokohama, Tokyo Bay	35°19′21″N	139°38′6″E	3
Madagascar	Zoostera meadow	23°21′33.74″S	43°39′29.859″E	1

2.4. STATISTICAL TREATMENT / ANALYSIS

2.4.1. Data Pre-Treatment

To investigate morphological variability and to determine the morphological features allowing discrimination among the phylotypes, we first deleted all variables involved in the calculation of ratios from the initial morphological data matrix, including both the primary measurements and their ratios that would introduce redundant information (e.g., 8 and 9 were deleted because they were used to calculate 17, see Fig. 3 and Appendix-Tables 1, 3).

Although all four views were available for all 96 *Ammonia* individuals used in this study, in a few cases some individual data were missing, for instance due to inaccurate test orientation or adherence of dirt particles, which made certain measurements difficult or even impossible to perform. To deal with missing data, the mean of the molecular group was assigned to such specimens in case of quantitative variables and the mode of the molecular group in case of qualitative variables (following Legendre & Legendre, 2012).

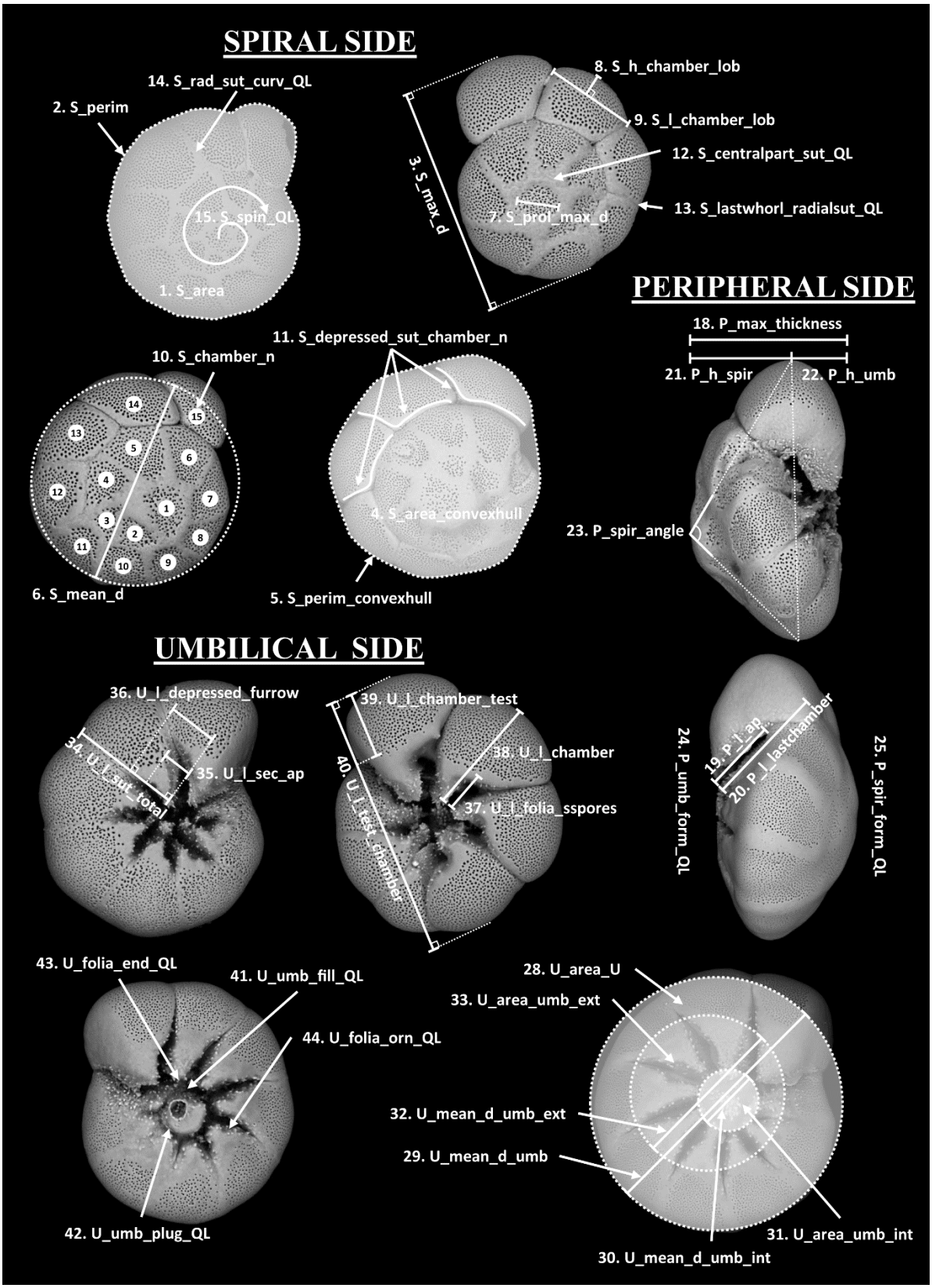

Figure 3. Morphological parameters measured on the spiral (S), umbilical (U), and peripheral (P) faces. For a more detailed description of the measured variables, see also Appendix-Table 1.

To account for the ontogenic stage of the specimens (size parameters are generally dependent on ontogenic stage; e.g., Stouff et al., 1999a; Hottinger, 2000), all variables that were significantly correlated with the total number of chambers (Pearson correlations with Bonferroni correction applied on p-value, Appendix-Table 4) were divided by "10. S_chamber_n". All quantitative variables were then standardized (i.e., subtracting the mean and dividing by the standard deviation) to give the same weight to all variables in the further analyses.

To investigate relationships between the variables and to eliminate redundant information (Joliffe, 1972), Pearson correlations were performed for each pair of quantitative variables and homogeneity Chi² tests were used for qualitative variables. To assess the significance of the relationship between variables, we applied a Bonferroni correction for multiple comparisons. For each pair of quantitative variables showing an absolute Pearson coefficient of correlation > 0.7 (threshold subjectively chosen following Chang & Kaesler, 1974) and each pair of qualitative variables that were significantly linked (p-value < 0.05), we eliminated one of the two variables. The main criterion used to choose the retained variable was the ease of observation under a stereomicroscope (Appendix-Tables 5, 6). Following the data pretreatment procedure, a total of 20 variables were retained for further analysis.

2.4.2. Multivariate Analysis

To determine the most discriminant variables for the three considered phylotypes, we applied a Factorial Analysis of Mixed Data (FAMD; Pagès, 2004) using the FactoMineR package (Husson et al., 2008) implemented in R software (R Core Team, 2018) on the morphological parameters matrix. The selection of the variables was based on the respective contribution of the variables issued from the FAMD. To account for the variability explained by each variable, we determined the "total weighted contribution" to the first two dimensions, the "total weighted contribution" being defined as the sum of the product of the variable contribution to a dimension and the percentage of the total variability explained by this dimension.

First step: selection of the most contributing variables. The first step of our procedure consisted in the selection of the variables that showed the highest sum of weighted contributions (for dimensions 1–2) and together represented at least 50% of the cumulative sum of the total weighted contributions.

Second step: removal of the least contributing variables. During the second step of the procedure, we performed another FAMD on the restrained set of variables (i.e., those selected by the previous step) and eliminated the one that had the weakest weighted contribution to dimensions 1 and 2 together. This step was repeated until a minimum number of variables was obtained with which the three phylotypes could be discriminated reliably.

To assess the ability of the different sets of variables to discriminate the three phylotypes, we applied Hierarchical Clustering on Principal Components (HCPC; Husson et al., 2010) on the components from FAMD (all components of the analysis were included in this procedure). We continued the variable selection procedure until the number of variables to be considered was the lowest possible, and the error rate on the HCPC analysis did not substantially increase.

3. RESULTS

3.1. PHYLOTYPE ASSIGNATION

Of the 96 specimens studied, 34 were assigned to T1, 30 to T2, and 32 to T6. Six sequences belonging to phylotype T2 were of relatively poor quality (i.e., Co006, Au491, Au467, Ma030, ZK020, and ZK023), but their identification through alignment with known sequences was still highly reliable. All the sequences assigned to T1 and T6 were of good quality.

Among the 34 T1 specimens, 31 were sequenced with the Sanger method and three were sequenced using HTS. Among T2, 22 specimens were sequenced using Sanger and 8 using HTS. For T6, 22 sequences were determined using Sanger and 10 using HTS.

3.2. MORPHOLOGICAL STUDY

In the first stage of selecting the most important variables, the three phylotypes separated on the first two dimensions of the FAMD analysis, which explained 24% of the total variability (Fig. 4). Six variables, which together represented 54% of the total weighted contributions of the variables on dimensions 1–2, were then retained for further analyses (Fig. 3, Table 2): 11 (11%), 50 (10%), 42 (9%), 12 (9%), 23 (8%) and 61 (7%).

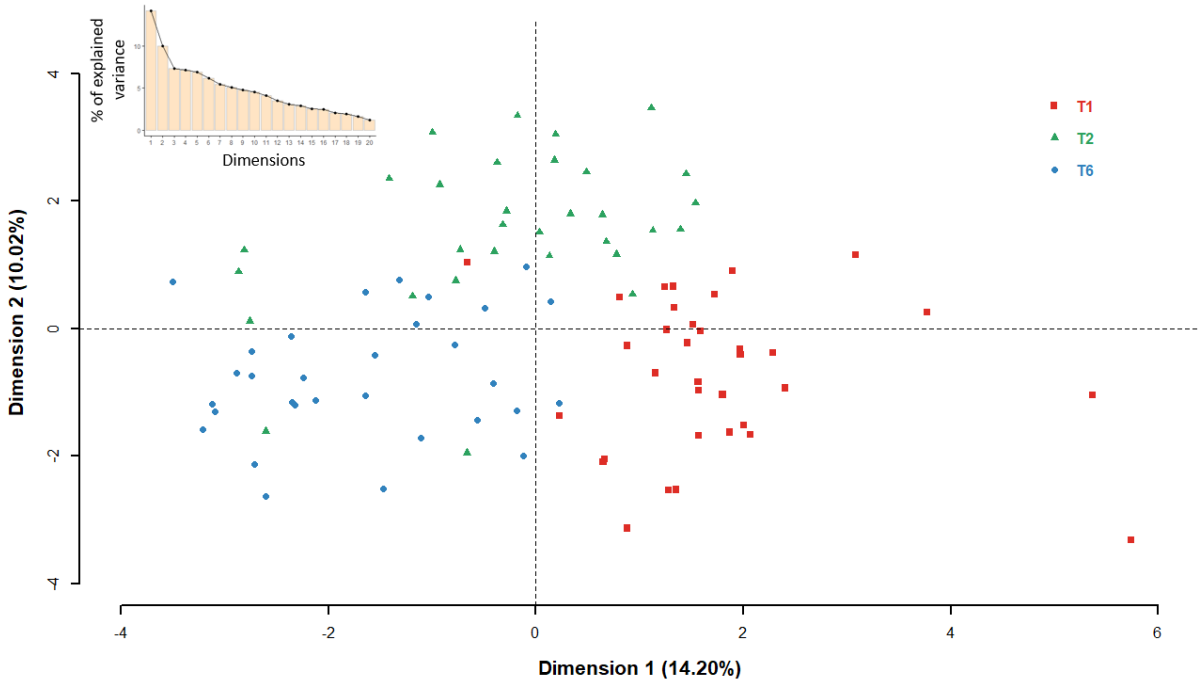

Figure 4. Scatter plot of the first two dimensions issued from the FAMD analysis (20 variables). Each specimen and its associated phylotype are represented: T1 (red squares), T2 (green triangles), and T6 (blue dots).

Table 2. Contributions as determined by the FAMD (first stage selection procedure). Variables in bold represent at least 50% of the total weighted contribution on dimensions 1–2 and are retained for further analyses. Variables are defined in Appendix-Table 1.

		Contributions		Weighted contributions				
	Variables	Dim1	Dim2	Dim1	Dim2	sum(Dim1+Dim2)	Cumulative sum(Dim1+Dim2)	Cumulative % sum(Dim1+Dim2)
FAMD STAGE 1	**S_depressed_sut_chamber_n**	**16.13**	**3.12**	**229.08**	**31.28**	**260.36**	**260.36**	**10.75**
	U_ind_l_depressed_furrow	**14.67**	**2.44**	**208.38**	**24.53**	**232.92**	**493.29**	**20.36**
	U_umb_plug_QL	**10.22**	**7.82**	**145.17**	**78.37**	**223.54**	**716.83**	**29.59**
	S_centralpart_sut_QL	**12.46**	**4.36**	**177.05**	**43.72**	**220.77**	**937.61**	**38.71**
	P_spir_angle	**11.32**	**3.07**	**160.85**	**30.82**	**191.68**	**1129.3**	**46.62**
	pores_d	**2.06**	**14.85**	**29.36**	**148.86**	**178.22**	**1307.52**	**53.98**
	U_ind_l_chamber_test	2.16	14.15	30.67	141.88	172.55	1480.07	61.1
	U_ind_l_flat_suture	9.67	2.95	137.44	29.6	167.05	1647.13	68
	U_ind_d_umb_ext	0	14.11	0.06	141.43	141.49	1788.62	73.84
	U_ind_l_folia_sspores	0.36	12.22	5.13	122.44	127.57	1916.2	79.11
	S_rad_sut_curv_QL	5.38	0.03	76.5	0.34	76.85	1993.06	82.28
	U_ind_d_umb_int	4.42	1.11	62.86	11.21	74.07	2067.13	85.34
	S_ind_prol	3.06	2.7	43.55	27.15	70.7	2137.84	88.26
	P_umb_form_QL	0.64	5.75	9.15	57.7	66.85	2204.7	91.02
	U_folia_orn_QL	0.08	5.49	1.21	55.04	56.26	2260.96	93.35
	S_chamber_n	3.41	0.2	48.44	2.02	50.46	2311.43	95.43
	U_ind_l_sec_ap	2.77	0.07	39.43	0.79	40.23	2351.66	97.09
	P_Indice_aperture	0.73	2.38	10.38	23.9	34.28	2385.95	98.51
	U_folia_end_QL	0.26	1.6	3.7	16.12	19.82	2405.78	99.33
	S_mean_d	0.1	1.46	1.5	14.7	16.21	2421.99	100

Table 3 presents the results of the four successive steps of the second stage, which identified the least contributing variables. The variables that were sequentially removed (i.e., during each step the one with the weakest weighted contribution to dimensions 1 and 2) were 50, 11, 42, and 23, respectively. The phylotypes remained well separated on the plot of the first two dimensions after each step.

The error rate of the classification resulting from HCPC analysis (Table 3) decreased (from 17% to 6%) when five instead of six variables were included in the FAMD, indicating that the

removed parameter (i.e., 50) was responsible for high background noise. When one more parameter was removed (11), the error rate remained very low, although a slight increase was observed (from 6% to 8%, Table 3), probably indicative of a slight loss of information. Finally, when only two parameters were considered, no further increase of the error rate was observed (error rate 8%, Table 3). The two last retained variables were the average pore diameter (61) and the character of the sutures in the central part of the spiral side (12), which is a discrete variable representing raised or flush sutures (Appendix-Fig. 2).

Table 3. Contributions of the retained morphological parameters during the second stage procedure and assignation error for the HCPC performed on the components issued from FAMD. Variables in bold represent the set of variables retained between step n and n+1. Variables in italics are the variables removed between step n and n+1. Variables are defined in Appendix Table 1.

		Contribution		Weighted contribution			
	Variables	Dim1	Dim2	Dim1	Dim2	sum(Dim1+Dim2)	HCPC assignation error number (rate)
	pores_d	**3.58**	**60.39**	**147.41**	**1212.6**	**1360.01**	**16 errors (16.7%)**
FAMD	**S_centralpart_sut_QL**	**21.79**	**11.61**	**896.28**	**233.07**	**1129.36**	
STAGE 2	**U_umb_plug_QL**	**17.61**	**16.83**	**724.3**	**337.85**	**1062.15**	
STEP 1	**S_depressed_sut_chamber_n**	**19.98**	**9.2**	**821.77**	**184.66**	**1006.43**	
	P_spir_angle	**22.06**	**1.37**	**907.58**	**27.51**	**935.09**	
	U_ind_l_depressed_furrow	*14.99*	*0.61*	*616.65*	*12.31*	*628.97*	
	pores_d	**3.53**	**61.75**	**156.2**	**1483.81**	**1640.01**	**6 errors (6.3%)**
FAMD	**S_centralpart_sut_QL**	**26.58**	**9.9**	**1175.51**	**237.85**	**1413.35**	
STAGE 2	**U_umb_plug_QL**	**20.32**	**18.89**	**898.51**	**454.02**	**1352.53**	
STEP 2	**P_spir_angle**	**27.93**	**0.68**	**1234.9**	**16.34**	**1251.24**	
	S_depressed_sut_chamber_n	*21.64*	*8.78*	*956.89*	*210.99*	*1167.88*	
	pores_d	**8.95**	**60.63**	**422.33**	**1702.98**	**2125.31**	**8 errors (8.3%)**
FAMD	**S_centralpart_sut_QL**	**27.36**	**23.45**	**1291.02**	**658.81**	**1949.83**	
STAGE 2	**P_spir_angle**	**32.88**	**6.69**	**1551.44**	**187.81**	**1739.24**	
STEP 3	*U_umb_plug_QL*	*30.8*	*9.23*	*1453.21*	*259.4*	*1712.61*	
FAMD	**pores_d**	**1.85**	**93.3**	**93.88**	**3164.76**	**3258.64**	**8 errors (8.3%)**
STAGE 2	**S_centralpart_sut_QL**	**47.5**	**6.35**	**2405.82**	**215.34**	**2621.17**	
STEP 4	*P_spir_angle*	*50.65*	*0.35*	*2565.3*	*11.9*	*2577.19*	

The results indicated a gradient in the average pore diameter: T2 presented relatively small pores (1.06 ± 0.33 µm), which contrasted with the much larger pores in T6 (2.69 ± 0.44 µm), while T1 had pores of intermediate size (1.96 ± 0.34 µm).While there was some overlap in pore size between T1 and T6, T2 was well separated from the two other groups (Table 4). The raised character of the sutures on the spiral side allowed us to discriminate between T1 (raised sutures) and both T2 and T6 (flush sutures).

Table 4. Number of specimens showing raised or flush sutures on the central part of the spiral side and mean ± sd pore diameter values (µm) for the three phylotypes. NA = the number of individuals for which the data were missing.

Phylotype	Sutures	Pores mean diameter (µm)
T1 (n = 34)	raised (28) - flush (5) - NA (1)	1.96 ± 0.34 (NA = 1)
T2 (n = 30)	flush (29) - raised (1)	1.06 ± 0.33 (NA = 1)
T6 (n = 32)	flush (32)	2.69 ± 0.44

The dendrogram issued from the HCPC shows that for each of the three phylotypes, the majority of the individuals cluster together (Fig. 5). Only 8 of the 96 individuals (8%, Table 3)

were not morphologically assigned to the phylotype determined by the molecular approach (i.e., Au453, RB007, Au411, Au407, ZK023, Au485, ZK020, andMa142; see Fig. 5).

3.3. PORE DIAMETER THRESHOLD DETERMINATION

To determine the morphometric threshold between T2 ("small pores"), T1 ("intermediate pores"), and T6 ("large pores"), we constructed a Receiver Operating Characteristic (ROC) curve. This empirical procedure consists of plotting a graph that illustrates the diagnostic ability of a binary classification system (i.e., small vs. intermediate/large pores, Appendix-Fig. 3, left panel) as a function of the value of the discrimination threshold (i.e., mean pore diameter). The ROC curve is created after a contingency table computation by plotting, for various pore diameter threshold values, the sensitivity [equation (1): proportion of true positives, i.e., individuals genetically defined as T2 with small pores] versus the specificity [equation (2): proportion of true negatives, i.e., individuals genetically defined as T1 or T6 with larger pores]. The threshold value yielding the highest accuracy [equation (3): percentage of correctly classified specimens] is considered the most accurate. The same procedure was performed to determine a threshold value to distinguish between large (T6) and intermediate/small pores (T1 and T2, Appendix-Fig. 3, right panel).

$$Sensitivity = \frac{TP}{TP + FN} \quad (1)$$

TP: True Positive
FN: False Negative

$$Specificity = \frac{TN}{TN + FP} \quad (2)$$

TN: True Negative
FP: False Positive

$$Accuracy = \frac{TP + TN}{N + P} \quad (3)$$

N: Negative
P: Positive

Results show that the optimal threshold (i.e., best accuracy) to distinguish between small (T2) and intermediate/ large pores (T1 and T6) is situated between 1.32 and 1.51 µm (Fig. 6, Appendix-Table 7). We propose using a threshold of 1.4 µm, corresponding to an accuracy of 0.97 (sensitivity = 0.93; specificity = 0.98).

The highest accuracy to distinguish between T6 (large pores) and T1 and T2 (intermediate and small pores) was found for pore diameters between 2.33 and 2.42 µm (Fig. 6, Appendix-Table 7). We propose to use a threshold value of 2.4 µm, corresponding to an accuracy of 0.91 (sensitivity = 0.88; specificity = 0.89).

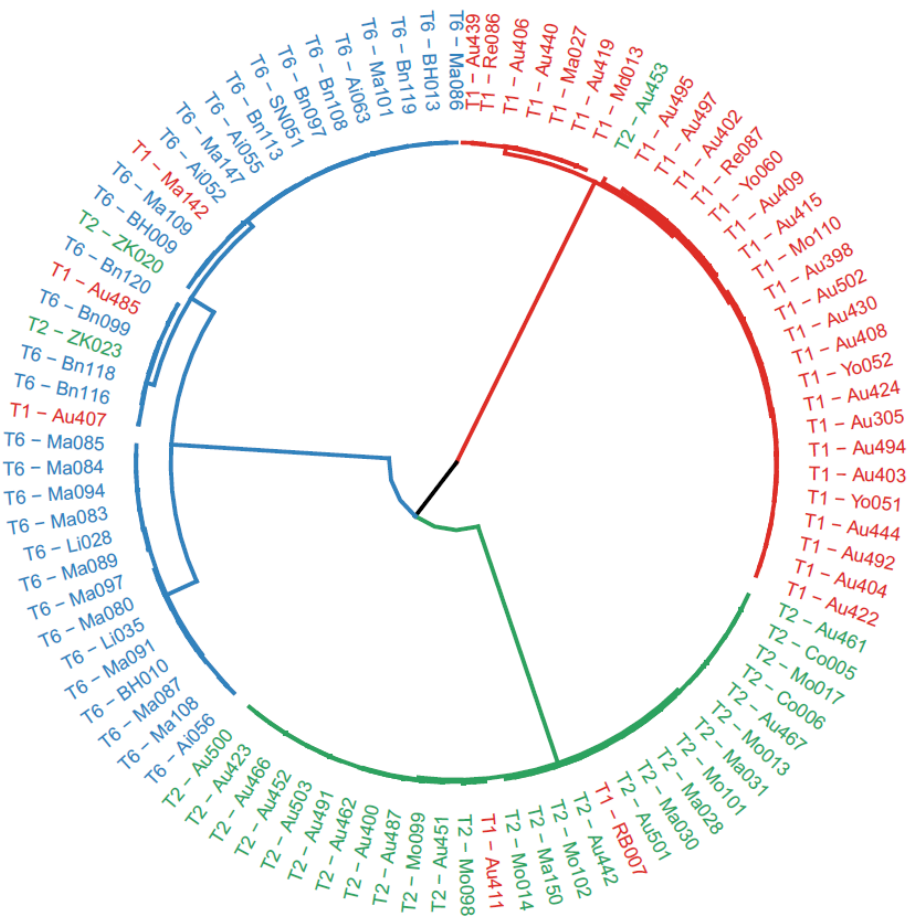

Figure 5. Circular dendrogram issued from the HCPC (morphometric analysis) compared to molecular attributions (red = T1; green = T2; blue = T6).

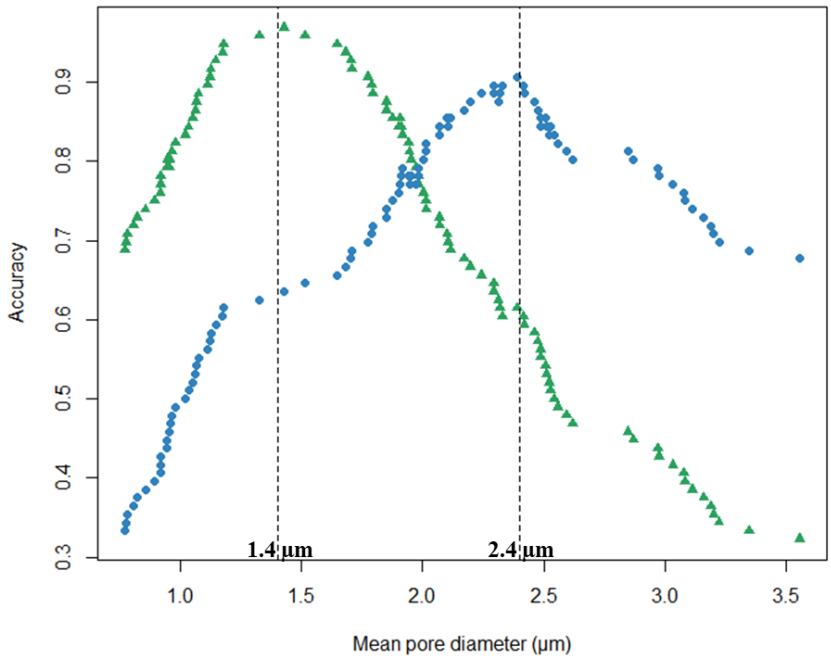

Figure 6. Graph representing the accuracy of the assignation in function of various pore diameter thresholds. Accuracy is calculated as (TP + TN)/(P + N). Green triangles = T2 or small pores vs. others and blue dots = T6 or large pores vs. others. Vertical dotted lines represent the proposed thresholds showing the highest accuracy to discriminate between T2 or small pores vs. others (1.4 µm) and T6 or large pores vs. others (2.4 µm).

4. DISCUSSION

4.1. MORPHOMETRIC DISCRIMINATION OF PHYLOTYPES T1, T2 AND T6

Phylotypes T1, T2, and T6 can be distinguished morphologically by considering only two features: the average diameter of the pores (i.e., of the penultimate chamber) and the raised or flush character of the sutures in the central part of the test on the spiral side (Figs. 7, 8). The T1 phylotype shows pores of intermediate size (1.96 ± 0.34 μm) and raised sutures. The T2 phylotype shows smaller pores (1.06 ± 0.33 μm) and flush sutures. The T6 phylotype exhibits larger pores (2.69 ± 0.44 μm) associated with flush sutures. These two morphometric parameters are already visible under a stereomicroscope at 40x magnification: (1) small pores are usually not discernible while individuals with intermediate/large pores clearly show a porous wall, and (2) the raised character of the sutures is apparent when observed with oblique light. Figure 7 presents SEM images of the three views (i.e., spiral, peripheral, and umbilical) plus a magnification of the porous region of the penultimate chamber on the spiral side, for typical individuals of each phylotype.

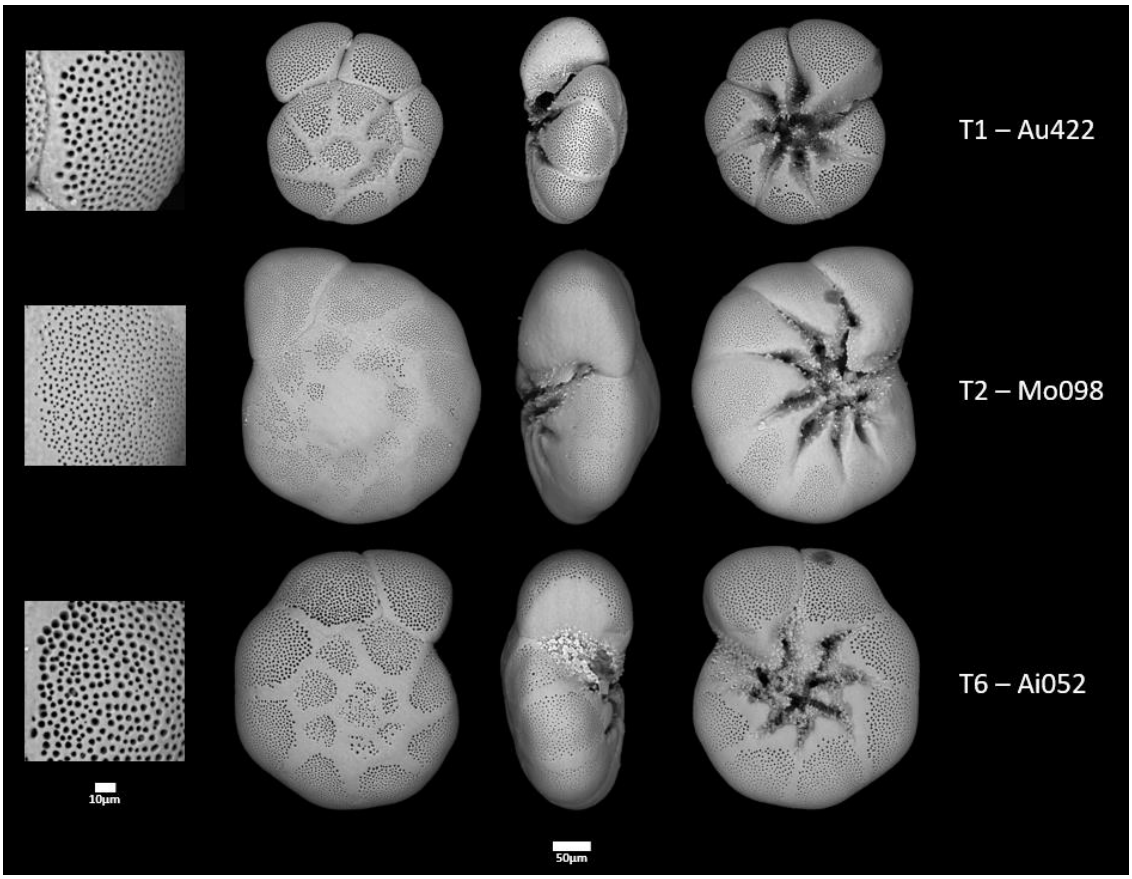

Figure 7. Views (penultimate chamber magnification, spiral, peripheral, and umbilical) of representative specimens for T1, T2, and T6 phylotypes. Note the raised sutures on the central part of the spiral side for T1 (flush on T6 and T2) and the small size of the pores for T2 (intermediate for T1 and large for T6).

One of the first studies presenting quantitative measurements of *Ammonia*, using a statistical approach to assess morphological variability, was conducted by Chang & Kaesler (1974). This study focused on the link between morphological variability and biogeographical distribution along the eastern coast of United States. The authors considered that all specimens belonged to a single species (i.e., *Ammonia beccarii*, Linneaus, 1758). Conversely, in the same area, Schnitker (1974) recognized three morphologically different "species" [*Ammonia beccarii*, *Ammonia tepida* (Cushman, 1926), and *Ammonia parkinsoniana* (d'Orbigny, 1839)]. A number of studies investigating morphological variability of *Ammonia* in other areas reached similar conclusions (i.e., ecophenotypy), including Vénec-Peyré (1983), Wang & Lutze (1986), and Jorissen (1988). Later, Hayward et al. (2004) identified various phylotypes along the North Atlantic coast of America (i.e., from north to south, T2 from Cape Cod; T1 and T9 from Long Island, NY; T7 from North Carolina and Georgia), showing that the large morphological variation, which Chang & Kaesler (1974) attributed to ecophenotypy, was in fact the result of the existence of different species inhabiting different ecological niches. In view of the presently available genetic and morphological evidence (e.g., Hayward et al., 2004), most of the ecophenotypes of earlier studies represent different species.

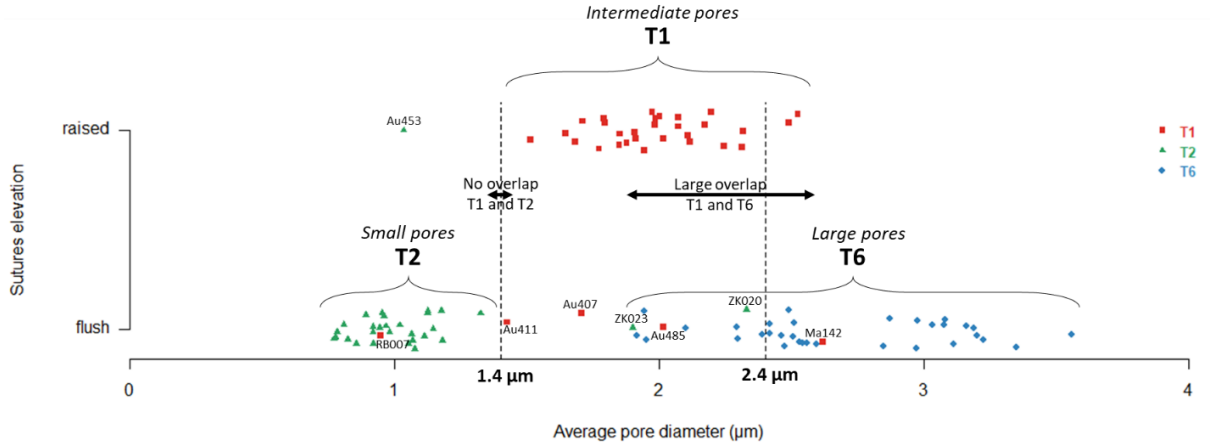

Figure 8. Suture elevation (flush or raised) and average pore diameter (in µm) for the three phylotypes (red squares: T1; green triangles: T2; and blue points: T6). For specimens with a putatively wrong assignment (see discussion in the text), the individual IDs are indicated. Average pore diameter thresholds are indicated by the vertical dotted lines.

The first study that investigated *Ammonia* with a mixed morphological (based on SEM images) and molecular approach was carried out by Holzmann & Pawlowski (1997). *Ammonia* sp. 1 was characterized by "distinct spiral sutures" and "large pores" (1.468 µm diameter on average), while *Ammonia* sp. 2 was characterized by "less distinct sutures" and "fine pores" [0.778 µm diameter on average; see plate 1 in Holzmann & Pawlowski (1997) and plate 1 in Holzmann & Pawlowski (2000)]. According to the present informal molecular phylogenetic

classification, these taxa correspond to T1 and T2, respectively (Holzmann & Pawlowski, 2000).

Hayward et al. (2004) provided a much more exhaustive study of *Ammonia*. Among many other characteristics, the authors also assessed the elevation of the sutures on the spiral side ("spicac = development of raised thickened calcite over central spiral area"). For this character, they noted a difference between T1 ("weak-medium") and T2 and T6 ("none-very weak"). However, this study included other molecular types (i.e., phylotypes) for which this character was much more pronounced, such as types B or T5A [see plate IV in Hayward et al. (2004)]. The consequence of the much larger overall variability in this character very likely explains why T1 could not be easily distinguished from T2 and T6 in their multivariate analysis. Differences in pore diameter were also highlighted in their study (variable "mnpore"): the mean diameter for T2 ranged from 0.7–1.0 μm and for T1 and T6 from 1.3–2.2 μm and 1.4–2.0 μm, respectively. These earlier measurements are very similar to ours, except that T6 shows much larger pores in our study. The difference could result from different protocols used to measure the pore diameter [e.g., only 10 pores measured per individual by Hayward et al. (2004) versus 20–80 in our study] or from the smaller number of measured individuals (8 T1, 6 T2, and 6 T6 individuals versus 33 T1, 29 T2 and 32 T6 in our study).

Toyofuku et al. (2005) investigated the genus *Ammonia* along the Japanese coast. Their SEM images suggest that T6 (*A. beccarii* forma 1) has flush sutures on the dorsal side (plates 1, 2) and relatively large pores (plate 2), while T1 (*Ammonia* sp. S) shows raised sutures on the spiral side (plate 1).

In summary, the two morphological criteria retained by our analysis allowed us to efficiently distinguish between T1, T2, and T6 (>90% correct assignations), and our results appear to be consistent with previous studies that were based on less detailed analyses of fewer specimens.

4.2. MISMATCH BETWEEN MORPHOMETRIC AND MOLECULAR ASSIGNATIONS

Previous phylogenetic analyses of the genus *Ammonia* (Holzmann & Pawlowski, 2000; Pawlowski & Holzmann, 2002, 2008; Hayward et al., 2004; Schweizer et al., 2011a,b; Saad &Wade, 2016) showed a clear separation between phylotypes T1, T2, and T6, even when using different genes of the rDNA array [i.e., Large and Small Sub-Units, Holzmann & Pawlowski (2000)]. At present, 14 phylotypes of *Ammonia* have been identified worldwide (Hayward et al., 2004; Schweizer et al., 2011a). In these molecular studies, T1, T2, and T6 were well

separated genetically, but it was difficult to discriminate them morphologically with morphometric analyses (Hayward et al., 2004).

As indicated before, eight of our 96 investigated individuals were incorrectly assigned to a phylotype on the basis of the two retained morphological characters (Fig. 8, Appendix-Figs. 4–6: individuals Au453, RB007, Au411, Au407, ZK023, Au485, ZK020, and Ma142). These inconsistent classifications fall into two groups: 1) individuals where the wrong classification seems to be the result of an erroneous molecular assignation, and 2) individuals for which the wrong classification seems to result from a wrong interpretation of the SEM images.

For three of our specimens (i.e., RB007, ZK020, and ZK023), the discrepancy between genetic and morphologic assignment appears to be due to an error during molecular analyses. In all three cases, the specimens exhibited morphological characteristics highly typical for one of the three phylotypes and completely outside of the range of morphological variability observed for the (other) phylotype to which they were assigned on the basis of molecular analyses (Fig. 8). This was the case for individual RB007, phylotyped as T1, but which shows flush sutures and especially, a pore diameter much smaller than all other T1 specimens. Similarly, specimens ZK020 and ZK023, phylotyped as T2, had pore diameters almost twice as large as the range observed for all other T2 specimens.

Erroneous phylotype assignments may arise in several ways. A first possibility concerns sites where several phylotypes co-occur. Here, erroneous assignments may result from the presence of exogenous biological material on the surface or within the tests (environmental contamination), such as prey particles (if feeding on another phylotype) or very small specimens (propagules or juveniles) of another phylotype (Hemleben et al., 1989). This could concern the three specimens mentioned above. At the Rade de Brest (RB007), T1 and T2 co-occur whereas at Zandkreek (ZK020 and ZK023), T2 and T6 are found together. Another possibility is laboratory contamination occurring during molecular manipulations, especially during the amplification and re-amplification phases. The simultaneous analysis of multiple specimens and the very high quantity of rDNA amplified might result in cross-contamination, even if we used a partitioned bench for the PCR set-up and post-PCR analyses (Weiner et al., 2016). If there is indeed an erroneous phylotype determination for these three specimens, the rate of successful phylotype assignation based on morphological criteria would rise to almost 95%.

Potentially wrong interpretations of the SEM images in the other five cases (i.e., Au411, Au407, Au485, Ma142, and Au453) were related to the suture elevation criterion (Fig. 8). In four T1 specimens, the raised character of the dorsal sutures was poorly developed and not recognized as such. Based upon the average pore diameter, these specimens were

morphologically determined as T2 (Au411) or T6 (Au407, Au485, and Ma142; Fig. 8). The inverse situation (i.e., of raised sutures in phylotype T2), which should have flush sutures, concerns a single specimen (Au453; Fig. 8).

When analyzing these five specimens retrospectively, it appears that the wrong assignments can be explained in several ways. First, the morphology of all three phylotypes is still variable, and extreme individuals may deviate from the general morphological characteristics used to define the phylotypes. This appears to be the case for individuals Au411 and Au485, in which the raised character of the sutures is not visible, and specimen Au453, which appears to have raised sutures; this is normally not the case in T2 (Fig. 8). Next, some of the wrong assignments seem to be due to partial dissolution of the test, which may have suppressed the raised character of the sutures (Au411; Fig. 8) and may also have increased the pore diameter (Ma142; Fig. 8). This dissolution may come from the acidification of the pore waters due to anaerobic organic matter remineralization, as is often observed in mudflat environments (Cesbron et al., 2016). Finally, more careful inspection (when the phylogenetic assignment is known) suggests that in a single case, sutures may have been considered wrongly as flush (Au407).

Of course, for some specimens, a combination of these factors can result in a wrong assignment. An important question is how to minimize erroneous assignments based upon morphological criteria. As we showed, most erroneous assignments were based on a wrong interpretation of the character of the sutures in the central part of the dorsal side. In this context, a well oriented image of the peripheral view is very helpful. Next, for doubtful specimens, the average pore diameter should be a decisive argument. Specimens with a pore diameter <1.4 μm should always be assigned to T2, even when the sutures are apparently raised. Similarly, specimens with a pore diameter between 1.4 and 1.9 μm (never observed for T6), should be assigned to T1, even if the sutures are apparently flush. Next, in case of doubt, it may be very useful to look at an additional criterion: the presence or absence of incised sutures on the dorsal side for the last two to five chambers. This is a recurrent characteristic of T1 whereas in T6, only the last one or two chambers sometimes show this (Fig. 7). The application of these criteria would have led unambiguously to the correct assignation of specimens Au453, Au411, and Au407 whereas the consideration of strong dissolution in specimenMa142 (which apparently had increased pore diameter), in combination with the strongly depressed sutures in the last five chambers, should have allowed us to assign this specimen correctly as well.

To summarize, on the basis of the character of the dorsal sutures and the average pore diameter, the majority of specimens (>90%) were correctly assigned. Wrong assignments can be further reduced if the observed ranges of pore diameter for each phylotype is taken into

account and if a supplementary character, the incised dorsal sutures for the last two to five chambers (in T1), is considered. As more specimens are analyzed, the variability of pore diameter for each phylotype can be better defined.

4.3. COMBINED MORPHOLOGICAL/MOLECULAR STUDIES – CRYPTIC AND PSEUDOCRYPTIC SPECIES

Studies combining morphometric measurements and phylogenetic data diminish taxonomic uncertainty. Taxonomic issues concern not only *Ammonia*, but other foraminiferal genera as well. The genus *Elphidium*, for which 17 different phylotypes have been described and morphologically investigated (Pillet et al., 2013; Darling et al., 2016), is another good example. In this genus, pseudocryptic (i.e., differentiation based on subtle, unseen, or previously overlooked morphological differences) as well as cryptic (i.e., inability to discriminate two species morphologically) morphological variability was observed, concerning several phylotypes (Darling et al., 2016). Roberts et al. (2016) determined the key diagnostic features for a single phylotype, S1 (the morphospecies *Elphidium williamsoni* Haynes, 1973), by a combined molecular/morphometric approach and highlighted the importance of such integrated studies to unravel the taxonomic complexity of benthic foraminifera. Similar approaches combining morphological and molecular methods have been adopted for the genera *Bulimina* (Tsuchiya et al., 2008), *Cibicides/Cibicidoides* (Schweizer et al., 2009, 2011c, 2012), and *Uvigerina* (Schweizer et al., 2005).

Planktonic foraminiferal genera are also affected by taxonomic issues, with the number of phylotypes recognized in individual morphospecies varying from one to seven (Darling & Wade, 2008). For example, a phylogenetic/morphological study of the *Globorotalia truncatulinoides* (d'Orbigny, 1839) species complex, for which the morphological variability was previously ascribed to ecophenotypy, showed the presence of four genetically distinct species with different morphological features and ecological preferences (de Vargas et al., 2001). Similarly, three pseudocryptic species were recognized in *Orbulina universa* d'Orbigny, 1839, with porosity differences and distinct geographic distributions (de Vargas et al., 1999; Morard et al., 2009). These authors suggested that species with an apparently "simple" morphology might hide a large genetic complexity, which would affect species diversity. For *Globigerinoides ruber* (d'Orbigny, 1839), traditionally seen as a single species with phenotypic plasticity attributed to habitat parameters (i.e., ecophenotypy), several authors (e.g., Darling et al., 1997; Aurahs et al., 2011) showed that the two chromotypes (pink and white) should be considered as separate species on the basis of phylogenetic analyses.

Traditionally, the high morphologic variability displayed by the genus *Ammonia* has led to major difficulties in species identification and induced numerous discussions about its taxonomy (e.g., Schnitker, 1974; Poag, 1978;Wang & Lutze, 1986; Haynes, 1992). Recent studies using the molecular approach have shown a high amount of cryptic and/or pseudocryptic diversity in this genus (Pawlowski et al., 1995; Holzmann et al., 1996; Langer & Leppig, 2000; Hayward et al., 2004). Our study has highlighted the fact that three *Ammonia* phylotypes (i.e., T1, T2, and T6) routinely encountered on the European coasts, which were never separated in studies based on morphological criteria until now, can in fact be distinguished rather confidently through a morphometric analysis. Our results confirm that T1, T2, and T6 are pseudocryptic, that is, they can be discriminated morphologically when using the appropriate criteria, rather than being truly cryptic species that cannot be distinguished morphologically.

4.4. FORMAL LINNEAN NOMENCLATURE

Concerning the genus *Ammonia*, most original species descriptions only include quantitative information for a limited number of parameters, such as test diameter, the number of chambers, the number of whorls, and the proloculus diameter (Table 5). All these parameters show large variability within each phylotype, and in our case, their values overlap between T1, T2, and T6. In spite of the difficulty to link detailed quantitative information concerning the phylotypes with much less detailed morphological formal species descriptions, previous studies have proposed formal names for the various phylotypes (Holzmann et al., 1998; Holzmann & Pawlowski, 2000; Hayward et al., 2004).

Among the five phylotypes encountered along the European coasts (*A. falsobeccarii*, T1, T2, T3, and T6), T3 can easily be distinguished by its deeply incised sutures and heavy ornamentation on the dorsal side, and *A. falsobeccarii* by its secondary openings on the dorsal side. The remaining pseudocryptic phylotypes (T1, T2, T6), which form the subject of our study, have traditionally been considered superspecies, which we will refer to as "*Ammonia tepida* group" in the following discussion.

To investigate the possibility to use formal names for the three pseudocryptic phylotypes studied here, we compared their morphology with the diagnosis of the formally described morphospecies that have been used for the representatives of the "*A. tepida* group". We retained the following species: *Ammonia catesbyana* (d'Orbigny, 1839), *Ammonia parkinsoniana* (d'Orbigny, 1839), *Ammonia veneta* (Schultze, 1854), *Ammonia tepida* (Cushman, 1926), *Ammonia flevensis* (Hofker, 1930), *Ammonia sobrina* (Shupack, 1934), *Ammonia aomoriensis*

(Asano, 1951), *Ammonia limnetes* (Todd & Bronnimann, 1957), *Ammonia compacta* (Hofker, 1964), and *Ammonia aberdoveyensis* (Haynes, 1973). These morphospecies were originally described in the Caribbean and along European and Japanese coasts, where T1, T2, and T6 occur (Hayward et al., 2004). In Table 5, we present an overview of the main morphological characteristics of the original descriptions, and in some cases of later uses (if these differ from the original description), of these morphospecies as well as of our phylotypes.

Unfortunately, the two distinctive characters of our three phylotypes, the pore size and the raised or flush character of the sutures on the dorsal side, are almost never mentioned in the original species descriptions. Consequently, our phylotypes cannot be assigned to formal species on the basis of these characters, and other more commonly described but less distinctive characters must be used. Furthermore, for many morphospecies, there are large discrepancies between the original description and the species concept that has later been generally accepted. This is clearly the case for the oldest species of this group, *A. catesbyana* (originally described with a large number of chambers in the last whorl) and *A. parkinsoniana* (originally described as having a highly lobulate test). Ideally, species assignments must be strictly based on the characters of the holotype and original description, and not on subsequent, altered species concepts that have come into use later.

Ammonia catesbyana is the oldest species described potentially belonging to the "*A. tepida* group." In 1839, d'Orbigny described this species from the Caribbean, where both T1 and T11 have been observed. This morphospecies stands out by the absence of an umbilical plug and the large number of chambers in the final whorl (10 chambers in the type figure). This is different from T1 and T11 (6–7 chambers for both phylotypes in Hayward et al., 2004; and 7.85 ± 0.68 for T1 in this study). Additionally, we found small umbilical plugs in T1 for 23 of the 34 individuals studied here. It appears therefore that the name *A. catesbyana* is not suitable for the phylotypes T1 and T11 found in the Caribbean. The use of this name in theWadden Sea for specimens with a lobulated periphery (Langer et al., 1989; Langer & Leppig, 2000), later attributed to T6 (Schweizer et al., 2011a), seems even less appropriate.

Ammonia parkinsoniana, also described by d'Orbigny in 1839, is a morphospecies with a prominent umbilical boss. In fact, small plugs are common in T1 and T2, but rare in T6 (Appendix-Table 8). A major problem is that *A. parkinsoniana* has been originally described as having a lobulate test (see d'Orbigny, 1839, plate IV, figs. 25–27) whereas Schnitker (1974) and many subsequent authors have used it for morphotypes with a rounded test. Although *A. parkinsoniana* was described in his monograph on foraminifera from Cuba, d'Orbigny doubted of the origin of the single described specimen and noticed that this morphospecies inhabits the

European Atlantic coasts. In spite of the doubt concerning the origin of the specimen figured by d'Orbigny, it appears that *A. parkinsoniana* could be a suitable name for T1, which is the only phylotype described from Europe as well as from the Caribbean. Unfortunately, following the publication of Schnitker (1974) and supported by the description of a neotype belonging to the d'Orbigny collection from Cuba by Le Calvez in 1977, the name *A. parkinsoniana* has been mainly used for forms with a rounded periphery. The use of this name for T1, which often shows a lobulate periphery, would therefore mean a radical break with the morphological criteria established for this taxon. *Ammonia compacta*, described by Hofker (1964) from the Caribbean, is another potential candidate for T1, when considering the description and the figures (especially fig. 242 a–c, which show a strong similarity with our specimens). However, it seems highly improbable that thismorphospecies, which is very common along the Atlantic European and Caribbean coasts, was not described earlier than 1964.

Ammonia veneta, from the Adriatic Sea, was described with a strongly lobulate outline, a lunate chamber form and arcuate sutures on the spiral side. This does not fit with T1 and T2, which have both been encountered in the Adriatic Sea. Additionally, its size is smaller (160 µm test diameter for adult individuals) than the range measured for T1 and T2 (220–400 µm and 290–510 µm in Hayward et al., 2004; and 265 ± 39 µm and 272 ± 54 µm in our study, for T1 and T2, respectively). Finally, the figures and description of Schultze (1854) cast some doubt on whether *A. veneta* really belongs to the genus *Ammonia* or is rather a *Rosalina*. For all these reasons, and in spite of the fact that *A. veneta* is without doubt the oldest name available for representatives of the "*A. tepida* group" in Europe, the use of this name is problematic.

The T6 phylotype is characterized by the almost systematic absence of an umbilical plug and by large adult specimens with many chambers (16.5 ± 2.9). Pawlowski & Holzmann (2008) and Schweizer et al. (2011b) suggested that this species originates from East Asia and was introduced recently in the Eastern Atlantic. However, there is currently no convincing proof for this. Although *A. aomoriensis* has a (rather incomplete) description which could fit T6, the type specimens of this morphospecies have a Pliocene age (Asano, 1951), which is out of reach for molecular studies. Therefore, the name *A. aomoriensis* is, in our opinion, not suitable for recent T6. The description of the morphospecies *A. aberdoveyensis* from Cardigan Bay by Haynes (1973) shows a striking similarity with the quantitative morphological data we obtained for phylotype T6. However, Hayward et al. (2004) sequenced topotypes from Aberdovey (Wales, UK) and determined them as T2. In view of this discrepancy, it seems problematic to use *A. aberdoveyensis*, either for T2 or for T6. Concerning the very widely-used morphotype *A. tepida* described by Cushman (1926), the re-description of a lectotype from the Cushman Collection

by Hayward et al. (2003) did not fit morphologically with any of the three phylotypes T1, T2, and T6. In fact, the latter study suggested that *A. tepida* is restricted to tropical, equatorial-shallow water environments, while T1, T2, and T6 prefer more temperate waters encountered along the European coastline, for example (Hayward et al., 2004; Schweizer et al., 2011b; Saad & Wade, 2016).

To summarize, in our opinion, it is too early to definitively attribute species names to these three phylotypes and consequently, we recommend the continued use of the informal phylotype designations T1, T2, and T6. More exhaustive molecular studies have to be performed in the type areas of the most logical candidates, such as topotype sequencing, and the question of whether T6 is an exotic species has yet to be settled.

Table 5. Morphological information concerning formal species, identified by their Linnean names, potentially belonging to the "*A. tepida* group," and morphometric characters of phylotypes T1, T2, and T6 from Hayward et al. (2004) and this study.

FORMAL SPECIES NAMES													
Actual formal name	Date	Original description	Sensu	Area	Possible phylotype (type area)	Diameter (µm)	Number of chambers in last whorl (dorsal side)	Total number of chambers	Outline	Umbilical plug	Form of chambers	Convexity of the test	Remarks
A. catesbyana	1839	d'Orbigny		Caribbean	T1, T11	333 µm	10	29	rounded	no	rectangular	moderate	
A. catesbyana			Hofker, 1964	Caribbean	T1, T11	max 700 µm	6.5–9	17–21	(slightly) lobulate	no	rectangular	moderate	
A. catesbyana			Langer et al., 1989	Wadden Sea	sequenced as T6	?	8.5	18	lobulate	no	rectangular	moderate	
A. parkinsoniana	1839	d'Orbigny		Caribbean	T1, T11	333 µm	9	19	very lobulate	prominent	lunate	very compressed	
A. parkinsoniana			Phleger & Parker, 1951	Gulf of Mexico	T1, T11	?	9	27	slightly lobulate	yes	rectangular	?	Authors doubt of their determination. they refer to Kornfeld (1931) their specimen does not correspond to the original description
A. parkinsoniana			Schnitker, 1974	US Atlantic	T1, T2, T7, T9	?	?	?	rounded	yes	rectangular	?	
A. parkinsoniana			Le Calvez, 1977	Cuba	T1, T11	500 µm	9	?	rounded	very prominent	rectangular	slightly convex dorsally	Neotype description
A. veneta	1854	Schultze		Adriatic	T1, T2	160 µm	6–7(–8)	12–13	strongly lobulate	no	lunate	very compressed	Resembles *Rosalina*?
A. veneta			Boltovskoy, 1980	SW Atlantic	?	100–230 µm	7–8	?	rounded somewhat lobate	?		somewhat convex dorsally	Sutures limbate, arcuate and depressed on spiral side. Finely and densely perforate. Pores in clusters of 3-5. There are but a few specimens of this species and no sections were made to determine if it is truly an *Ammonia*.

Table 5. Continued

FORMAL SPECIES NAMES

Actual formal name	Date	Original description	Sensu	Area	Possible phylotype (type area)	Diameter (µm)	Number of chambers in last whorl (dorsal side)	Total number of chambers	Outline	Umbilical plug	Form of chambers	Convexity of the test	Remarks
A. tepida	1926	Cushman		Caribbean	T1, T11	≤350 µm	6–7	?	rounded (to lobulate)	no	?	?	
A. tepida			Parker et al., 1953	Gulf of Mexico	T1, T11	?	6	15–16	slightly lobulate	no	elongated rectangular	?	
A. tepida			Bradshaw, 1957	Gulf of Mexico	T1, T11	?	6.5	19	strongly lobulate	no	elongated rectangular	planoconvex	
A. tepida			Hayward et al., 2003	Puerto Rico	T1, T11	almost 300 µm	6.5	17?	lobulate	no	square to rectangular	slightly convex dorsally	Lectotype description
A. flevensis	1930	Hofker		Wadden Sea	T1, T6	250–300 µm	(5–)7.5–8	13–17	slightly to very lobulate	no	square	slightly convex dorsally	Original description very incomplete. Refers to description in Hofker, 1922.
A. sobrina	1934	Shupack		US Atlantic	T1, T2, T7, T9	300–650 µm	9	18	rounded	large plug	square	biconvex	
A. paucilocalata	1951	Phleger & Parker		Gulf of Mexico	T1, T11	<290 µm	5.5	18	slightly lobulate	no	rectangular	?	
A. aomoriensis	1951	Asano		Japan, Pliocene	T1, T4, T6	≤500 µm	7	14?	slightly lobulate	no	elongated rectangular	slightly convex dorsally	
A. limnetes	1957	Todd & Bronnimann		Caribbean	T1, T11	320–420 µm	7	21?	rounded	no	square	compressed	
A. limnetes			Haynes, 1973	Great Britain, brackish water	T1, T2, T6	320 µm	5.5–6.5	14–17	slightly lobulate	no	rectangular	very compressed	
A. compacta	1964	Hofker		Caribbean	T1, T11	≤550 µm	7–8.5	14–22	rounded	no	rectangular	dorsally convex	

Table 5. Continued

FORMAL SPECIES NAMES												
Actual formal name	Date	Original description	Sensu	Area	Possible phylotype (type area)	Diameter (µm)	Number of chambers in last whorl (dorsal side)	Total number of chambers	Outline	Umbilical plug	Form of chambers	Convexity of the test	Remarks
A. aberdoveyensis	1973	Haynes		Great Britain, brackish water	T1, T2, T6	400 µm	8–9	23–29	rounded (to slightly lobulate)	no	square to elongated rectangular	biconvex	"Differs from *A. batava* by its convex dorsal side". "Differs from *A. tepida* by the larger number of chambers visible on the ventral side (8–9 instead of 6–7)."

HAYWARD et al., 2004									
Phylotype	Figured / sequenced specimen	General distribution	Diameter (µm)	Number of chambers in last whorl on dorsal side	Total number of chambers	Outline	Umbilical plug	Form of chambers	Convexity of the test	Remarks
T1	Cuba	Cosmopolitan	220-400 µm	6–7		lobulate	no	elongated rectangular	compressed	
T2	Adriatic Sea	Western Atlantic, Eastern Atlantic, Mediterranean	290-510 µm	7–8		very lobulate	no	lunate	compressed	
T6	China	Eastern Atlantic, Japan	310-430 µm	6–7		lobulate	no	elongated rectangular	compressed	

THIS STUDY								
Phylotype	Figured / sequenced specimen	Diameter (µm)	Number of chambers in last whorl on dorsal side	Total number of chambers	Outline	Umbilical plug	Form of chambers	Convexity of the test	Remarks
T1	Japan, Madagascar, Mediterranean, Eastern Atlantic	265 ± 39 µm 208–391 µm	7.85 ± 0.68 7–9	13.79 ± 2.66 8–21	very lobulate to rounded	yes (23) no (10) NA (1)	square to rarely elongated rectangular	dorsally highly convex (16) or convex (10)	
T2	Mediterranean, Eastern Atlantic	272 ± 54 µm 182–397 µm	7.83 ± 0.84 6–9	14.97 ± 2.37 11–21	very lobulate to rounded	yes (17) no (9) NA (4)	square	dorsally convex (11) or compressed (10)	
T6	Eastern Atlantic	362 ± 68 µm 270–565 µm	7.59 ± 0.73 6–9	16.53 ± 2.91 11–23	very lobulate to rounded	yes (2) no (30)	Square rectangular	compressed (17) dorsally convex (11) to highly convex (4)	

5. CONCLUSION

In this study, we investigated the morphological characteristics of phylotypes T1, T2, and T6, belonging to the genus *Ammonia*. A combined molecular/morphometric approach is necessary to distinguish pseudocryptic species of the genus *Ammonia* as well as for the other genera of foraminifera with a large genetic and morphological variability. Concerning *Ammonia*, this combined approach allowed us to identify two morphological parameters to discriminate phylotypes T1, T2, and T6 with a high degree of accuracy: the raised or flush character of the sutures on the spiral side and the mean pore diameter.

We also investigated the possibility to assign formal scientific names to T1, T2, and T6. Unfortunately, the traditional morphological characters described in the original species diagnoses are highly variable and discrepancies exist between first descriptions and the morphospecies concepts used subsequently. Due to the lack of detailed morphological descriptions of the formally described species, we refrain from attributing formal scientific names to the three investigated phylotypes. More combined molecular/morphometric studies are needed in the type areas where the morphospecies have been described. Awaiting such supplementary information, we recommend using the phylotype designations T1, T2, and T6.

The possibility to recognize T1, T2, and T6 on the basis of morphological criteria alone, not only increases the precision in studies of biodiversity and species ecology, but also offers the possibility to study the distribution of these phylotypes in dead and fossil assemblages. Among other things, this should allow us to definitely establish whether phylotype T6 originated from eastern Asia and was introduced recently in the eastern Atlantic.

ACKNOWLEDGMENTS

This study comprised part of the research project AMTEP, financed by the CNRS-INSU program EC2CO. We are grateful to Romain Mallet and the team of the SCIAM imaging facility at the University of Angers. We gratefully acknowledge the help of many colleagues who provided samples: Christine Barras, Eric Bénéteau, Thibaut Bernard, Jean-Pierre Bouchet, Pascal Bouchet, Julie Garnier, Emmanuelle Geslin, Hélène Howa, Dylan Hurblain, Thierry Jauffrais, Liesbeth Jorissen, Charlotte LeKieffre, Edouard Metzger, Maria Pia Nardelli, Briz Parent, Jan Pawlowski, Aubin Thibault de Chanvalon, and Takashi Toyofuku. We also thank Bruce Hayward and an anonymous reviewer for their very valuable comments and suggestions to improve our manuscript.

REFERENCES

Asano, K., 1951, Illustrated catalogue of Japanese Tertiary smaller foraminifera, *in* Stach, L. W. (ed), Part 14: Rotaliidae: Hosokawa Printing, Tokyo, p. 1–21.

Aurahs, R., Treis, Y., Darling, K., and Kucera, M., 2011, A revised taxonomic and phylogenetic concept for the planktonic foraminifer species *Globigerinoides ruber* based on molecular and morphometric evidence: Marine Micropaleontology, v. 79, p. 1–14.

Banner, F. T., and Williams, E., 1973, Test structure, organic skeleton and extrathalamous cytoplasm of *Ammonia* Brünnich: Journal of Foraminiferal Research, v. 3, p. 49–69.

Barras, C., Mouret, A., Nardelli, M. P., Metzger, E., Petersen, J., La, C., Filipsson, H., L., Jorissen, F., 2018, Experimental calibration of manganese incorporation in foraminiferal calcite: Geochimica et Cosmochimica Acta, v. 237, p. 49–64.

Boltovskoy, E., 1965, Twilight of foraminiferology: Journal of Paleontology, v. 39, p. 383–390.

Cesbron, F., Geslin, E., Jorissen, F. J., Delgard, M. L., Charrieau, L., Deflandre, B., Jézéquel, D., Anschutz, P., and Metzger, E., 2016, Vertical distribution and respiration rates of benthic foraminifera: Contribution to aerobic remineralization in intertidal mudflats covered by *Zostera noltei* meadows: Estuarine, Coastal and Shelf Science, v. 179, p. 23–38.

Chang, Y. M., and Kaesler, R. L., 1974, Morphological variation of the foraminifer *Ammonia beccarii* (Linné) from the Atlantic coast of the United States: The University of Kansas Paleontolongical Contributions, pap. 69, p. 1–23.

Cifelli, R., 1962, The morphology and structure of *Ammonia beccarii* (Linné): Contributions from the Cushman Foundation for Foraminiferal Research, v. 13, p. 119–126.

Cimerman, F., and Langer, M., 1991, Mediterranean foraminifera: Academia Scientiarum et Artium Slovenica, Ljubljana, 210 p.

Colburn, D. F., and Baskin, J. A., 1998, Morphological study of *Ammonia parkinsoniana* from Laguna Madre and Baffin Bay, Texas: Gulf coast Association of Geological Societies Transactions, v. 48, p. 11–19.

Cushman, J. A., 1926, Recent foraminifera from Porto Rico: Publications of the Carnegie Institution of Washington, v. 342, p. 73–84.

Darling, K. F., Schweizer, M., Knudsen, K. L., Evans, K. M., Bird, C., Roberts, A., Filipsson, H. L., Kim, J. -H., Gudmundsson, G., Wade, C. M., Sayer, M. D. J., and Austin, W. E. N., 2016, The genetic diversity, phylogeography and morphology of *Elphidiidae* (foraminifera) in the Northeast Atlantic: Marine Micropaleontology, v. 129, p. 1–23.

Darling, K. F., and Wade, C. M., 2008, The genetic diversity of planktic foraminifera and the global distribution of ribosomal RNA genotypes: Marine Micropaleontology, v. 67, p. 216–238.

Darling, K. F., Wade, C. M., Kroon, D., and Brown, A. J. L., 1997, Planktic foraminiferal molecular evolution and their polyphyletic origins from benthic taxa: Marine Micropaleontology, v. 30, p. 251–266.

Debenay, J. -P., Bénéteau, E., Zhang, J., Stouff, V., Geslin, E., Redois, F., and Fernandez-Gonzalez, M., 1998, *Ammonia beccarii* and *Ammonia tepida* (foraminifera): morphofunctional arguments for their distinction: Marine Micropaleontology, v. 34, p. 235–244.

de Nooijer, L. J., Langer, G., Nehrke, G., and Bijma, J., 2009, Physiological controls on seawater uptake and calcification in the benthic foraminifer *Ammonia tepida*: Biogeosciences, v. 6, p. 2669–2675.

de Vargas, C., Norris, R., Zaninetti, L., Gibb, S. W., and Pawlowski, J., 1999, Molecular evidence of cryptic speciation in planktonic foraminifers and their relation to oceanic provinces: PNAS, v. 96, p. 2864–2868.

de Vargas, C., Renaud, S., Hilbrecht, H., and Pawlowski, J., 2001, Pleistocene adaptive radiation in *Globorotalia truncatulinoides*: genetic, morphologic, and environmental evidence: Paleobiology, v. 27, p. 104–125.

Dissard, D., Nehrke, G., Reichart, G. J., and Bijma, J., 2010, Impact of seawater pCO2 on calcification and Mg/Ca and Sr/Ca ratios in benthic foraminifera calcite: results from culturing experiments with *Ammonia tepida*: Biogeosciences, v. 7, p. 81–93.

d'Orbigny, A. D., 1839, Foraminifères, *in* Sagra, R. D. L., Histoire physique, politique et naturelle de l'ile de Cuba, Bertrand, A. (ed), Paris, 224 p.

Ertan, K. T., Hemleben, V., and Hemleben, C., 2004, Molecular evolution of some selected benthic foraminifera as inferred from sequences of the small subunit ribosomal DNA: Marine Micropaleontology, v. 53, p. 367–388.

Gouy, M., Guindon, S., and Gascuel, O., 2010, SeaView version 4: a multiplatform graphical user interface for sequence alignment and phylogenetic tree building: Molecular Biology and Evolution, v. 27, p. 221–224.

Haynes, J. R., 1973, Cardigan Bay recent foraminifera: cruise of the R.V. Antur, 1962–64: Natural History Museum Publications, London, 246 p.

Haynes, J. R., 1992, Supposed pronounced ecophenotypy in foraminifera: Journal of Micropalaeontology, v. 11, p. 59–63.

Hayward, B. W., Buzas, M. A., Buzas-Stephens, P., and Holzmann, M., 2003, The lost type of *Rotalia beccarii* var. *tepida* Cushman 1926: Journal of Foraminiferal Research, v. 33, p. 352–354.

Hayward, B. W., Holzmann, M., Grenfell, H. R., Pawlowski, J., and Triggs, C. M., 2004, Morphological distinction of molecular types in *Ammonia* – towards a taxonomic revision of the world's most commonly misidentified foraminifera: Marine Micropaleontology, v. 50, p. 237–271.

Hayward, B. W., Le Coze, F., and Gross, O., 2018, World foraminifera database, *Ammonia* Brünnich, 1772, accessed through: World Register of Marine Species at: http://www.marinespecies.org/aphia.php?p=taxdetails&id=112078 on 2018-02-24.

Hemleben, C., Spindler, M., and Anderson, O. R., 1989, Modern planktonic foraminifera: Springer Science & Business Media, New York, 363 p.

Hofker, J., 1930, Der Generationswechsel von *Rotalia beccarii* var. flevensis, nov. var: Z. Zellforsch, v. 10, p. 756–768.

Hofker, J., 1964, Foraminifera from the tidal zone in the Netherlands Antilles and other West Indian Islands: Studies on the Fauna of Curaçao and other Caribbean Islands, v. 21, p. 1–119.

Holzmann, M., 2000, Species concept in foraminifera: *Ammonia* as a case study: Micropaleontology, v. 46, p. 21–37.

Holzmann, M., and Pawlowski, J., 2000, Taxonomic relationships in the genus *Ammonia* (foraminifera) based on ribosomal DNA sequences: Journal of Micropalaeontology, v. 19, p. 85–95.

Holzmann, M., and Pawlowski, J., 1997, Molecular, morphological and ecological evidence for species recognition in *Ammonia* (foraminifera): Journal of Foraminiferal Research, v. 27, p. 311–318.

Holzmann, M., Piller, W., and Pawlowski, J., 1996, Sequence variations in the large-subunit ribosomal RNA gene of *Ammonia* (foraminifera, protozoa) and their evolutionary implications: Journal of Molecular Evolution, v. 43, p. 145–151.

Holzmann, M., Piller, W. E., Zaninetti, L., Fenner, R., Martini, R., Serandrei-Barbero, R., and Pawlowski, J., 1998, Molecular versus morphologic variability in *Ammonia* spp. (foraminifera, protozoa) from the Lagoon of Venice, Italy: Revue de Micropaléontologie, v. 41, p. 59–69.

Hottinger, L. C., 2000, Functional morphology of benthic foraminiferal shells, envelopes of cells beyond measure: Micropaleontology, v. 46, p. 57–86.

Husson, F., Josse, J., and Le, S., 2008, FactoMineR: an R package for multivariate analysis: Journal of Statistical Software, v. 25, p. 1–18.

Husson, F., Josse, J., and Pages, J., 2010, Principal component methods—hierarchical clustering—partitional clustering: why would we need to choose for visualizing data? Applied Mathematics Department, Technical Report, Agrocampus.

Jauffrais, T., Jesus, B., Metzger, E., Mouget, J. -L., Jorissen, F., and Geslin, E., 2016, Effect of light on photosynthetic efficiency of sequestered chloroplasts in intertidal benthic foraminifera (*Haynesina germanica* and *Ammonia tepida*): Biogeosciences v. 13, p. 2715–2726.

Jolliffe, I. T., 1972, Discarding variables in a principal component analysis. I: artificial data: Journal of the Royal Statistical Society, Series C (Applied Statistics), v. 21, p. 160–173.

Jorissen, F. J., 1988, Benthic foraminifera from the Adriatic Sea: principles of phenotypic variation: Utrecht Micropaleontological Bulletins, Utrecht, v. 37, 176 p.

Langer, M., Hottinger, L. and Huber, B.,1989, Functional morphology in low-diverse benthic foraminiferal assemblages from tidal-flats of the North Sea: Senckenbergiana Maritima, v. 20, p. 81–99.

Langer, M., and Leppig, U., 2000, Molecular phylogenetic status of *Ammonia catesbyana* (d'Orbigny, 1839), an intertidal foraminifer from the North Sea: Neues Jahrbuch fur Geologie und Palaontologie Monatshefte, v. 9, p. 545–556.

Le Calvez, Y., 1977, Foraminifères de l'Île de Cuba: Cahier de Micropaléontologie, v. 2, p. 92–94.

LeKieffre, C., Spangenberg, J., Mabilleau, G., Escrig, S., Meibom, A., and Geslin, E., 2017, Surviving anoxia in marine sediments: the metabolic response of ubiquitous benthic foraminifera (*Ammonia tepida*): Plos One, v. 12, no. 5, p. e0177604.

Legendre, P., and Legendre, L. F. J., 2012, Numerical Ecology: Elsevier, 1007 p.

Linné, C. von, 1758, Systema naturæ per regna tria naturæ, secundum classes, ordines, genera, species, cum characteribus, differentiis, synonymis, locis, *in* Systema naturæ editio decima reformata, Tomus I, Holmiæ, 824 p.

Loeblich, A. R. Jr., and Tappan, H., 1994, Foraminifera of the Sahul Shelf and Timor Sea: Cushman Foundation for Foraminiferal Research, Special Publication, v. 31, p. 1–661.

Loeblich, A. R. Jr., and Tappan, H., 1987, Foraminiferal genera and their classification: Springer US, 970 p.

Morard, R., Quillévéré, F., Escarguel, G., Ujiie, Y., de Garidel-Thoron, T., Norris, R. D., and de Vargas, C., 2009, Morphological recognition of cryptic species in the planktonic foraminifer *Orbulina universa*: Marine Micropaleontology, v. 71, p. 148–165.

Murray, J. W., 2014, Ecology and palaeoecology of benthic foraminifera: Routledge, 408 p.

Nehrke, G., Keul, N., Langer, G., de Nooijer, L. J., Bijma, J., and Meibom, A., 2013, A new model for biomineralization and trace-element signatures of foraminifera tests: Biogeosciences, v. 10, p. 6759–6767.

Pagès, J., 2004, Analyse factorielle de données mixtes : Revue de statistique appliquée, v. 52, p. 93–111.

Pawlowski, J., 2000, Introduction to the molecular systematics of foraminifera: Micropaleontology, v. 46, p. 1–12.

Pawlowski, J., Bolivar, I., Farhni, J., and Zaninetti, L., 1995, DNA analysis of "*Ammonia beccarii*" morphotypes: one or more species? Marine Micropaleontology, v. 26, p. 171–178.

Pawlowski, J., and Holzmann, M., 2008, Diversity and geographic distribution of benthic foraminifera: a molecular perspective: Biodiversity and Conservation, v. 17, p. 317–328.

Pawlowski, J., and Holzmann, M., 2002, Molecular phylogeny of foraminifera a review: European Journal of Protistology, v. 38, p. 1–10.

Petersen, J., Riedel, B., Barras, C., Pays, O., Guihéneuf, A., Mabilleau, G., Schweizer, M., Meysman, F. J. R., and Jorissen, F. J., 2016, Improved methodology for measuring pore patterns in the benthic foraminiferal genus *Ammonia*: Marine Micropaleontology, v. 128, p. 1–13.

Petersen, J., Barras, C., Bézos, A., La, C., de Nooijer, L. J., Meysman, F. J. R., Mouret, A., Slomp, C. P., and Jorissen, F. J., 2018, Mn/Ca intra- and inter-test variability in the benthic foraminifer *Ammonia tepida*: Biogeosciences, v. 15, p. 331–348.

Pillet, L., Voltski, I., Korsun, S., and Pawlowski, J., 2013, Molecular phylogeny of *Elphidiidae* (foraminifera): Marine Micropaleontology, v. 103, p. 1–14.

Plancus, J., 1739, Jani Planci Ariminensis de conchis minus notis liber: Cui assessit specimen aestus reciproci maris superi ad littus portumque Arimini: Venice, Italy.

Poag, C. W., 1978, Paired foraminiferal ecophenotypes in gulf coast estuaries: ecological and paleoecological implications: Gulf Coast Association of Geological Societies, v. 28, p. 395–421.

R Core Team, 2018, R: A language and environment for statistical computing: R Foundation for Statistical Computing, Vienna, Austria, https://www.R-project.org/.

Roberts, A., Austin, W., Evans, K., Bird, C., Schweizer, M., and Darling, K., 2016, A new integrated approach to taxonomy: the fusion of molecular and morphological systematics with type material in benthic foraminifera: Plos One, v. 11, no. 7, p. e0158754.

Saad, S. A., and Wade, C.M., 2016, Biogeographic distribution and habitat association of *Ammonia* genetic variants around the coastline of Great Britain: Marine Micropaleontology, v. 124, p. 54–62.

Schneider, C. A., Rasband, W. S., and Eliceiri, K. W., 2012, NIH Image to ImageJ: 25 years of image analysis: Nature Methods, v. 9, p. 671–675.

Schnitker, D., 1974. Ecotypic variation in *Ammonia beccarii* (Linne): Journal of Foraminiferal Research, v. 4, p. 217–223.

Schultze, M. J. S., 1854, Uber den organismus der polythalamien (foraminiferen) nebst Bemerkungen über die Rhizopoden im Allgemeinen: Leipzig.

Schweizer, M., Pawlowski, J., Duijnstee, I. A. P., Kouwenhoven, T. J., and van der Zwaan, G. J., 2005, Molecular phylogeny of the foraminiferal genus *Uvigerina* based on ribosomal DNA sequences: Marine Micropaleontology, v. 57, p. 51–67.

Schweizer, M., Pawlowski, J., Kouwenhoven, T., van der Zwaan, B., 2009, Molecular phylogeny of common *Cibicidids* and related *Rotaliida* (foraminifera) based on small subunit rDNA sequences: Journal of Foraminiferal Research, v. 39, p. 300–315.

Schweizer, M., Jorissen, F., and Geslin, E., 2011a, Contributions of molecular phylogenetics to foraminiferal taxonomy: general overview and example of *Pseudoeponides falsobeccarii* Rouvillois, 1974: Comptes Rendus Palevol, v. 10, p. 95–105.

Schweizer, M., Polovodova, I., Nikulina, A., and Schönfeld, J., 2011b. Molecular identification of *Ammonia* and *Elphidium* species (foraminifera, *Rotaliida*) from the Kiel Fjord (SW Baltic Sea) with rDNA sequences: Helgoland Marine Research, v. 65, p. 1–10.

Schweizer, M., Fontaine, D., and Pawlowski, J., 2011c, Phylogenetic position of two Patagonian *Cibicididae* (*Rotaliida*, foraminifera): *Cibicidoides dispars* (d'Orbigny, 1839) and *Cibicidoides variabilis* (d'Orbigny, 1826): Revue de Micropaléontologie, v. 54, p. 175–182.

Schweizer, M., Bowser, S. S., Korsun, S., and Pawlowski, J., 2012, Emendation of *Cibicides Antarcticus* (Saidova, 1975) based on molecular, morphological, and ecological data: Journal of Foraminiferal Research, v. 42, p. 340–344.

Sen Gupta, B. K., 2007, Modern foraminifera: Kluwer Academic Publisher, Dordrecht, 371 p.

Seuront, L., and Bouchet, V. M. P., 2015, The devil lies in details: new insights into the behavioural ecology of intertidal foraminifera, Journal of Foraminiferal Research v. 45, p. 390–401.

Shupack, B., 1934, Some foraminifera from western Long Island and New York harbor: American Museum Novitates, Foraminifera from New York Harbor, no. 737.

Sievers, F., Wilm, A., Dineen, D., Gibson, T. J., Karplus, K., Li, W., Lopez, R., McWilliam, H., Remmert, M., Söding, J., Thompson, J. D., and Higgins, D. G., 2011, Fast, scalable generation of high-quality protein multiple sequence alignments using Clustal Omega: Molecular Systems Biology, v. 7, p. 539.

Stouff, V., Lesourd, M., and Debenay, J. -P., 1999a, Laboratory observations on asexual reproduction (schizogony) and ontogeny of *Ammonia tepida* with comments on the life cycle: Journal of Foraminiferal Research, v. 29, p. 75–84.

Stouff, V., Geslin, E., Debenay, J. -P., and Lesourd, M., 1999b, Origin of morphological abnormalities in *Ammonia* (foraminifera): studies in laboratory and natural environments: Journal of Foraminiferal Research, v. 29, p. 152–170.

Todd, R., and Bronnimann, P., 1957, Recent foraminifera and Thecamoebina from the Eastern Gulf of Paria: Cushman Foundation for Foraminiferal Research, Special publication, Ithaca, N. Y.

Toyofuku, M., S., Kitazato, H., and Tsuchiya, M., 2005. Phylogenetic relationships among genus *Ammonia* (foraminifera) based on ribosomal DNA sequences which are distributed in the vicinity of the Japanese Islands: Frontier Research on Earth Evolution, v. 2, p. 1–9.

Tsuchiya, M., Tazume, M., and Kitazato, H., 2008, Molecular characterization of the non-costate morphotypes of *buliminid* foraminifers based on internal transcribed region of ribosomal DNA (ITS rDNA) sequence data: Marine Micropaleontology, v. 69, p. 212–224.

Vénec-Peyré, M. -T., 1983, Étude de la croissance et de la variabilité chez un foraminifère benthique littoral *Ammonia beccarii* (Linné), en Méditerranée occidentale: Cahiers de Micropaléontologie, v. 2, p. 5–32.

Walton, W. R., and Sloan, B. J., 1990, The genus *Ammonia* Brünnich, 1772; its geographic distribution and morphologic variability: Journal of Foraminiferal Research, v. 20, p. 128–156.

Wang, P., and Lutze, G. F., 1986, Inflated later chambers; ontogenetic changes of some recent hyaline benthic foraminifera: Journal of Foraminiferal Research, v. 16, p. 48–62.

Weiner, A. K. M., Morard, R., Weinkauf, M. F. G., Darling, K. F., André, A., Quillévéré, F., Ujiie, Y., Douady, C. J., de Vargas, C., and Kucera, M., 2016, Methodology for single-cell genetic analysis of planktonic foraminifera for studies of protist diversity and evolution: Frontiers in Marine Science, v. 3, p. 255.

White, T. J., Bruns, T. D., Lee, S. B., and Taylor, J. W., 1990, Amplification and direct sequencing of fungal ribosomal RNA genes for phylogenetics. PCR protocols: a guide to methods and applications, Academic Press, New York, v. 18, p. 315–322.

APPENDIX

The appendix, consisting of eight supplementary data tables and six figures, can be found on the Cushman Foundation website in the JFR Article Data Repository (https://cushmanfoundation.allenpress.com/ JournalofForaminiferal Research/DataRepository) as item number JFR_DR_2019005.

Appendix-Table 1. List of the morphological parameters measured or calculated for each *Ammonia* specimen. Face S: spiral; P: peripheral; U: umbilical.

N	FACE	VARIABLE	DESCRIPTION	CALCULATION
1	S	area	Total area of the spiral side of the test	
2	S	perim	Perimeter of the spiral side of the test	
3	S	max_d	Maximum diameter of the spiral side of the test	
4	S	area_convexhull	Area of the test fitted convex hull	
5	S	perim_convexhull	Perimeter of the test fitted convex hull	
6	S	mean_d	Mean diameter of the test. Diameter of the test fitted circle	
7	S	prol_max_d	Maximum diameter of the proloculus	
8	S	h_chamber_lob	Height of the lobulate part of the n-1 chamber.	
9	S	l_chamber_lob	Length between the radial sutures on peripheral part of the n-1 chamber	
10	S	chamber_n	Number of chambers of the test	
11	S	depressed_sut_chamber_n	Number of chambers where spiral sutures are depressed in the last whorl	
12	S	centralpart_sut_QL	Qualitative. Relief of the sutures in central part of the test. flush/raised	
13	S	lastwhorl_radialsut_QL	Qualitative. Relief of the radial sutures in the last whorl of the test. Depressed/flush/raised	
14	S	rad_sut_curv_QL	Qualitative. Curvature of the suture between n-1 and n-2 chamber. None/weak/medium/strong	
15	S	spin_QL	Qualitative. Direction of the test spin. Senestre(s)/dextral(d)	
16	S	ind_prol	Proloculus maximum diameter relative to test maximum diameter	$\frac{prol\_\max\_d}{\max\_d}$
17	S	ind_lob	Indicates the lobateness of the n-1 chamber. The higher the value, the higher the lobateness	$\frac{h\_chamber\_lob}{l\_chamber\_lob}$
18	P	max_thickness	Maximum thickness of the test	
19	P	l_ap	Length of the principal aperture	
20	P	l_lastchamber	Length between the aperture start on the umbilical side and the length of the last chamber (parallel to aperture)	
21	P	h_spir	Height of the spiral part of the test. Measured from apertural orientation	
22	P	h_umb	Height of the umbilical part of the test. Measured from apertural orientation	
23	P	spir_angle	Angle of the spiral side	
24	P	umb_form_QL	Qualitative. Umbilical part of the test concavity of convexity. Concave/flat/convex	
25	P	spir_form_QL	Qualitative. Spiral part of the test concavity of convexity. Concave/flat/convex/high convex	
26	P	Indice_aperture	Length of the aperture relative to the last chamber length	$\frac{l\_ap}{l\_lastchamber}$
27	P	Indice_spiral_haut	Length of the spiral part relative to the umbilical part of the test	$\frac{h\_spir}{h\_umb}$
28	U	area_U	Total area of the umbilical side of the test	
29	U	mean_d_umb	Mean diameter of the umbilical side of the test. Diameter of the test fitted circle	
30	U	mean_d_umb_int	Mean diameter of the intern umbilical part (ends of folia to ends of folia)	
31	U	area_umb_int	Area of the intern umbilical part (ends of folia to ends of folia)	
32	U	mean_d_umb_ext	Mean diameter of the extern umbilical part (ends of depressed radial sutures to ends of depressed radial sutures)	
33	U	area_umb_ext	Area of the extern umbilical part (ends of depressed radial sutures to ends of depressed radial sutures)	
34	U	l_sut_total	Length of the radial suture between the n-1 and n-2 chamber (measured between the end of n-1 chamber's folia end and the end of radial suture between n-1 and n-2 chamber at the periphery)	
35	U	l_sec_ap	Length of the secondary aperture between n-1 and n-2 chamber (start at the n-1 chamber's folia end)	
36	U	l_depressed_furrow	Length of the depressed furrow part between end of n-1 and n-2 (start at the n-1 chamber's folia end)	

37	U	l_folia_sspores	Length of the n-1 chamber's folia without pores (start at the n-1 chamber's folia end)	
38	U	l_chamber	Length of the n-1 chamber (between the n-1 chamber's folia end and the maximum height of the chamber)	
39	U	l_chamber_test	Length of the last chamber relative to the length of the test	
40	U	l_test_chamber	Length of test relative to the length last chamber	
41	U	umb_fill_QL	Qualitative. Filling of the umbilicus. Umbilical part is full (umbilical aperture non visible, umbilicus full) or empty (umbilical aperture visible, umbilicus empty). Umbilical plug(s) excluded. Empty/medium/full	
42	U	umb_plug_QL	Qualitative. Presence of umbilical plug(s). Yes/no	
43	U	folia_end_QL	Qualitative. Form of the ends of the folia. Blunt/medium/sharp	
44	U	folia_orn_QL	Qualitative. Refer to the ornamentation on folia and folia furrows. Weak/medium/strong	
45	U	ind_d_umb_int	Mean diameter of the intern umbilical part (ends of depressed radial sutures to ends of depressed radial sutures) relative to the mean diameter of the umbilical side	$\frac{mean\_d\_umb\_int}{mean\_d\_umb}$
46	U	ind_d_umb_ext	Mean diameter of the extern umbilical part (ends of depressed radial sutures to ends of depressed radial sutures) relative to the mean diameter of the umbilical side	$\frac{mean\_d\_umb\_ext}{mean\_d\_umb}$
47	U	ind_area_umb_int	Area of the intern umbilical part (ends of folia to ends of folia) relative to the total area of the umbilical side	$\frac{area\_umb\_int}{area\ U}$
48	U	ind_area_umb_ext	Area of the extern umbilical part (ends of folia to ends of folia) relative to the total area of the umbilical side	$\frac{area\_umb\_ext}{area\ U}$
49	U	ind_l_sec_ap	Relative length of the secondary aperture to total suture length (chamber n-1)	$\frac{l\_\mathrm{sec}\_ap}{l\ sut\ total}$
50	U	ind_l_depressed_furrow	Relative length of the depressed furrow (exclude secondary aperture) to total suture length (chamber n-1)	$\frac{l\_depressed\_furrow - l\_\mathrm{sec}\_ap}{l\_sut\_total}$
51	U	ind_l_flat_suture	Relative length of flushing part of the suture (exclude secondary aperture and depressed furrow) to total suture length (chamber n-1)	$\frac{l\_sut\_total - l\_\mathrm{depressed}\_furrow}{l\_sut\_total}$
52	U	ind_l_folia_sspores	Relative length of the folia part without pores to chamber length	$\frac{l\_folia\_sspores}{l\ chamber}$
53	U	ind_l_chamber_test	Relative length of the last chamber to the test diameter	$\frac{l\_chamber\_test}{l\ test\ chamber}$
54	pores	count	Number of pores	
55	pores	total_area	Total area of pores	
56	pores	average_size	Average size of pores (i.e., mean area of pores)	
57	pores	area_percent	Area covered by pores (percent). Equivalent to porosity.	
58	pores	perimeter	Mean perimeter of pores	
59	pores	count_reworked	Number of pores corrected	$count - exc\_small - (\frac{partiel}{2} + double + triple * 2)$
60	pores	mean_area_reworked	Mean area of pores corrected	$\frac{count\_reworked}{total\ area}$
61	pores	d	Mean diameter of the pores	$\sqrt{(\frac{mean\_area\_reworked}{\pi})} * 2$

Appendix-Table 2. Sampling stations, phylotype assignation and sequencing method (HTS = High Throughput Sequencing) for each specimen, identified by their ID. Published sequences are specified by their accession number (deposited in the GenBank data base).

Specimen ID	Station	Phylotype assignation	Sequencing method	Accession number
Mo110	Rivière du Bono	T1	HTS	-
Re086	Ile de Ré	T1	Sanger	MH200642
Re087	Ile de Ré	T1	Sanger	MH200643
Au430	Kerouarc'h 2	T1	Sanger	MH200644
Au439	Kerouarc'h 2	T1	Sanger	MH200645
Au440	Kerouarc'h 2	T1	Sanger	MH200646
Au444	Kerouarc'h 2	T1	Sanger	MH200647
Au404	Locmariaquer 1	T1	Sanger	MH200648
Au409	Locmariaquer 1	T1	Sanger	MH200649
Au415	Locmariaquer 1	T1	Sanger	MH200650
Au422	Locmariaquer 1	T1	Sanger	MH200651
Au424	Locmariaquer 1	T1	Sanger	MH200652
Au398	Locmariaquer 1	T1	Sanger	MH200653
Au402	Locmariaquer 1	T1	Sanger	MH200654
Au403	Locmariaquer 1	T1	Sanger	MH200655
Au406	Locmariaquer 1	T1	Sanger	MH200656
Au407	Locmariaquer 1	T1	Sanger	MH200657
Au408	Locmariaquer 1	T1	Sanger	MH200658
Au411	Locmariaquer 1	T1	Sanger	MH200659
Au419	Locmariaquer 1	T1	Sanger	MH200660
Au485	Locmariaquer 2	T1	Sanger	MH200661
Au492	Locmariaquer 2	T1	Sanger	MH200662
Au494	Locmariaquer 2	T1	Sanger	MH200663
Au495	Locmariaquer 2	T1	Sanger	MH200664
Au497	Locmariaquer 2	T1	Sanger	MH200665
Au502	Locmariaquer 2	T1	Sanger	MH200666
Md013	Zoostera meadow	T1	Sanger	MH200667
Ma142	Ouistreham	T1	Sanger	MH200668
RB007	Rade de Brest	T1	HTS	-
Au305	Saint Pierre Lopérec	T1	Sanger	MH200669
Ma027	Saint Vaast	T1	HTS	-
Yo060	Yokohama, Tokyo Bay	T1	Sanger	MH200670
Yo051	Yokohama, Tokyo Bay	T1	Sanger	MH200671
Yo052	Yokohama, Tokyo Bay	T1	Sanger	MH200672
Mo098	Ile Bailleron est	T2	HTS	-
Mo102	Ile Bailleron est	T2	HTS	-
Mo099	Ile Bailleron est	T2	HTS	-
Mo101	Ile Bailleron est	T2	HTS	-
Co005	Corsica DIA5	T2	Sanger	MH200673
Co006	Corsica DIA5	T2	Sanger	-
Au442	Kerouarc'h 2	T2	Sanger	MH200674
Au400	Locmariaquer 1	T2	Sanger	MH200675

Au423	Locmariaquer 1	T2	Sanger	-
Au491	Locmariaquer 2	T2	Sanger	-
Au500	Locmariaquer 2	T2	Sanger	-
Au503	Locmariaquer 2	T2	Sanger	-
Au487	Locmariaquer 2	T2	Sanger	MH200676
Au501	Locmariaquer 2	T2	Sanger	MH200677
Au451	Locmariaquer 3	T2	Sanger	-
Au453	Locmariaquer 3	T2	Sanger	MH200678
Au462	Locmariaquer 3	T2	Sanger	MH200679
Au452	Locmariaquer 3	T2	Sanger	MH200680
Au461	Locmariaquer 3	T2	Sanger	MH200681
Au466	Locmariaquer 3	T2	Sanger	MH200682
Au467	Locmariaquer 3	T2	Sanger	-
Ma150	Ouistreham	T2	Sanger	MH200683
Ma028	Saint Vaast	T2	HTS	-
Ma031	Saint Vaast	T2	Sanger	MH200684
Ma030	Saint Vaast	T2	Sanger	-
Mo013	Pointe de Toulvern	T2	HTS	-
Mo017	Pointe de Toulvern	T2	HTS	-
Mo014	Pointe de Toulvern	T2	HTS	-
ZK020	Zandkreek	T2	Sanger	-
ZK023	Zandkreek	T2	Sanger	-
Ai052	Baie de l'Aiguillon	T6	Sanger	MH200685
Ai055	Baie de l'Aiguillon	T6	Sanger	MH200686
Ai056	Baie de l'Aiguillon	T6	Sanger	MH200687
Ai063	Baie de l'Aiguillon	T6	Sanger	MH200688
BH009	Biezelingse Ham	T6	HTS	-
BH010	Biezelingse Ham	T6	Sanger	MH200689
BH013	Biezelingse Ham	T6	Sanger	MH200690
Bn097	Baie de Bourgneuf	T6	Sanger	MH200691
Bn099	Baie de Bourgneuf	T6	Sanger	MH200692
Bn108	Baie de Bourgneuf	T6	Sanger	MH200693
Bn113	Baie de Bourgneuf	T6	Sanger	MH200694
Bn116	Baie de Bourgneuf	T6	Sanger	MH200695
Bn118	Baie de Bourgneuf	T6	Sanger	MH200696
Bn119	Baie de Bourgneuf	T6	Sanger	MH200697
Bn120	Baie de Bourgneuf	T6	Sanger	MH200698
Li028	Camargue	T6	Sanger	MH200699
Li035	Camargue	T6	Sanger	MH200700
Ma080	Estuaire de la Seine	T6	Sanger	MH200701
Ma083	Estuaire de la Seine	T6	Sanger	MH200702
Ma084	Estuaire de la Seine	T6	HTS	-
Ma085	Estuaire de la Seine	T6	HTS	-
Ma086	Estuaire de la Seine	T6	HTS	-
Ma087	Estuaire de la Seine	T6	HTS	-
Ma089	Estuaire de la Seine	T6	HTS	-

Ma091	Estuaire de la Seine	T6	HTS	-
Ma094	Estuaire de la Seine	T6	HTS	-
Ma097	Estuaire de la Seine	T6	HTS	-
Ma101	Estuaire de la Seine	T6	Sanger	MH200703
Ma108	Estuaire de la Seine	T6	Sanger	MH200704
Ma109	Estuaire de la Seine	T6	Sanger	MH200705
Ma147	Ouistreham	T6	HTS	-
SN051	Saint Nazaire	T6	Sanger	MH200706

Appendix-Table 3. List of the 23 variables that were not included in statistical analyses because they were involved in the calculation of ratios.

Variable deleted	Reason	Variable deleted	Reason
S_prol_max_d	Used in a ratio	U_area_umb_ext	Used in a ratio
S_h_chamber_lob	Used in a ratio	U_l_sut_total	Used in a ratio
S_l_chamber_lob	Used in a ratio	U_l_sec_ap	Used in a ratio
P_l_ap	Used in a ratio	U_l_depressed_furrow	Used in a ratio
P_l_lastchamber	Used in a ratio	U_l_folia_sspores	Used in a ratio
P_h_spir	Used in a ratio	U_l_chamber	Used in a ratio
P_h_umb	Used in a ratio	U_l_chamber_test	Used in a ratio
U_area_U	Used in a ratio	U_l_test_chamber	Used in a ratio
U_mean_d_umb	Used in a ratio	pores_count	Used in a ratio
U_mean_d_umb_int	Used in a ratio	pores_total_area	Used in a ratio
U_area_umb_int	Used in a ratio	pores_average_size	equivalent to pores_mean_area_reworked
U_mean_d_umb_ext	Used in a ratio		

Appendix-Table 4. List of variables that were significantly correlated (Pearson) with the number of chambers.

Number of chambers	Variables divided by S_chamber_n	Coefficient of correlation (Pearson)	p-value (Bonferroni correction)
S_chamber_n	P_max_thickness	0.66	0.00
	U_area_U	0.49	0.00
	U_max_d_umb	0.44	0.00
	S_area	0.72	0.00
	S_area_convexhull	0.72	0.00
	S_max_d	0.71	0.00
	S_mean_d	0.73	0.00
	S_perim	0.68	0.00
	S_perim_convexhull	0.73	0.00

Appendix-Table 5. List of quantitative variables that were correlated (Pearson) and the deleted vs. retained variables.

Retained variable	Deleted variable	Coefficient of correlation (Pearson)	p-value (Bonferroni correction)
S_mean_d	P_max_thickness	0.85	0.00
	S_ind_lob	0.78	0.00
	S_area	0.81	0.00
	S_area_convexhull	0.81	0.00
	S_max_d	0.99	0.00
	S_perim	0.97	0.00
	S_perim_convexhull	1.00	0.00
P_spir_angle	P_Indice_spiral_haut	–0.84	0.00
U_ind_d_umb_ext	U_ind_area_umb_ext	0.97	0.00
U_ind_d_umb_int	U_ind_area_umb_int	0.99	0.00
pores_d	pores_area_percent	0.85	0.00
	pores_count_reworked	–0.92	0.00
	pores_mean_area_reworked	0.98	0.00
	pores_perimeter	0.99	0.00

Appendix-Table 6. List of qualitative variables that were significantly linked (homogeneity Chi² test) and the deleted vs. retained variables.

Retained variable	Deleted variable	Statistical test (Chi^2)	p-value (Bonferroni correction)
S_centralpart_sut_QL	S_lastwhorl_radialsut_QL	34.89	0.00
	P_spir_form_QL	19.33	0.00
S_rad_sut_curv_QL	S_lastwhorl_radialsut_QL	31.30	0.00
U_folia_orn_QL	S_spin_QL	13.99	0.04
U_umb_plug_QL	U_umb_fill_QL	16.43	0.01

Appendix-Table 7. Accuracy calculated for various pore diameter thresholds (all available values). In bold the highest accuracy to discriminate between small pores T2 vs. others (1.43 µm) and large pores T6 vs. others (about 2.39 µm).

Pore diameter (µm)	Accuracy (T2 vs. others)	Accuracy (T6 vs. others)	Pore diameter (µm)	Accuracy (T2 vs. others)	Accuracy (T6 vs. others)	Pore diameter (µm)	Accuracy (T2 vs. others)	Accuracy (T6 vs. others)
Inf	0.31	0.67	2.29	0.64	0.89	1.51	0.96	0.65
3.56	0.32	0.68	2.29	0.65	0.9	**1.43**	**0.97**	0.64
3.35	0.33	0.69	2.24	0.66	0.89	1.32	0.96	0.63
3.22	0.34	0.7	2.2	0.67	0.88	1.18	0.95	0.61
3.2	0.35	0.71	2.17	0.68	0.86	1.18	0.94	0.6
3.19	0.36	0.72	2.12	0.69	0.85	1.15	0.93	0.59
3.16	0.38	0.73	2.11	0.7	0.84	1.13	0.92	0.58
3.11	0.39	0.74	2.1	0.71	0.85	1.12	0.91	0.57
3.08	0.4	0.75	2.07	0.72	0.84	1.11	0.9	0.56
3.08	0.41	0.76	2.07	0.73	0.83	1.07	0.89	0.55
3.03	0.42	0.77	2.02	0.74	0.82	1.07	0.88	0.54
2.98	0.43	0.78	2.01	0.75	0.81	1.06	0.86	0.53
2.97	0.44	0.79	2	0.76	0.8	1.05	0.85	0.52
2.87	0.45	0.8	1.99	0.77	0.79	1.03	0.84	0.51
2.85	0.46	0.81	1.98	0.78	0.78	1.02	0.83	0.5
2.62	0.47	0.8	1.97	0.79	0.77	0.98	0.82	0.49
2.59	0.48	0.81	1.95	0.8	0.78	0.97	0.81	0.48
2.56	0.49	0.82	1.94	0.81	0.77	0.96	0.8	0.47
2.54	0.5	0.83	1.94	0.82	0.78	0.95	0.79	0.46
2.53	0.51	0.84	1.92	0.83	0.79	0.95	0.8	0.45
2.52	0.52	0.83	1.91	0.84	0.78	0.94	0.79	0.44
2.51	0.53	0.84	1.91	0.85	0.77	0.92	0.78	0.43
2.51	0.54	0.85	1.9	0.84	0.76	0.92	0.77	0.42
2.49	0.55	0.84	1.88	0.85	0.75	0.92	0.76	0.41
2.49	0.56	0.85	1.85	0.86	0.74	0.89	0.75	0.4
2.47	0.57	0.86	1.85	0.88	0.73	0.86	0.74	0.39
2.46	0.58	0.88	1.79	0.89	0.72	0.82	0.73	0.38
2.42	0.59	0.89	1.79	0.9	0.71	0.81	0.72	0.36
2.42	0.6	0.9	1.77	0.91	0.7	0.78	0.71	0.35
2.39	0.61	**0.91**	1.71	0.92	0.69	0.78	0.7	0.34
2.33	0.6	0.9	1.7	0.93	0.68	0.77	0.69	0.33
2.32	0.61	0.89	1.68	0.94	0.67			
2.31	0.63	0.88	1.65	0.95	0.66			

Appendix-Table 8. Morphometric measurements for the 61 variables for the three phylotypes. Quantitative variables: mean ± sd (length/area measurements are in µm/µm²); and qualitative variables: level (occurrence).

N	Variable	T1 (n=34)	T2 (n=30)	T6 (n=32)
1	S_area	55321.8 ± 16793.16	58854.96 ± 21117.17	103852.88 ± 39503.9
2	S_perim	974.52 ± 129.16	992.62 ± 189.94	1310.58 ± 255.3
3	S_max_d	287.53 ± 41.52	299.26 ± 57.26	397.32 ± 72.95
4	S_area_convexhull	56538.37 ± 17096.53	60431.5 ± 21962.56	106429.02 ± 40431.53
5	S_perim_convexhull	847.22 ± 123.51	871.35 ± 171.37	1127.39 ± 284.83
6	S_mean_d	265.69 ± 39.06	272.29 ± 53.9	361.9 ± 68.3
7	S_prol_max_d	57.61 ± 14.34	44.45 ± 11.78	44.95 ± 13.09
8	S_h_chamber_lob	22.63 ± 6.32	21.28 ± 11.69	29 ± 8.5
9	S_l_chamber_lob	107.95 ± 16.47	108.72 ± 26.62	144.56 ± 24.75
10	S_chamber_n	13.79 ± 2.66	14.97 ± 2.37	16.53 ± 2.91
11	S_depressed_sut_chamber_n	2.47 ± 1.29	1 ± 0.83	0.91 ± 0.69
12	S_centralpart_sut_QL	raised (28) - flush (5)	flush (29) - raised (1)	flush (32)
13	S_lastwhorl_radialsut_QL	flush (17) - raised (13) - depressed (3)	flush (30)	flush (32)
14	S_rad_sut_curv_QL	weak (17) - none (15) - medium (2)	none (15) - weak (13) - medium (2)	none (22) - weak (10)
15	S_spin_QL	d (18) - s(15)	s (18) - d (12)	d (21) - s (11)
16	S_ind_prol	0.08 ± 0.02	0.07 ± 0.03	0.07 ± 0.02
17	S_ind_lob	8.01 ± 1.4	7.3 ± 1.64	8.9 ± 1.63
18	P_max_thickness	158 ± 32.15	152.53 ± 33.12	202.71 ± 42.83
19	P_l_ap	44.77 ± 17.41	51.62 ± 17.13	67.27 ± 13.92
20	P_l_lastchamber	82.15 ± 18.21	86.23 ± 25.88	118.04 ± 23.61
21	P_h_spir	87.6 ± 23.01	77.35 ± 21.18	96.72 ± 30.96
22	P_h_umb	70.4 ± 13.92	75.18 ± 17.01	105.99 ± 16.08
23	P_spir_angle	117.15 ± 7.23	125.35 ± 7.64	129.58 ± 7.14
24	P_umb_form_QL	flat (18) - concave (7) - convex (2)	flat (17) - convex (3) - concave (1)	flat (29) - concave (3)
25	P_spir_form_QL	convex (16) - highconvex (10) - flat (1)	convex (11) - flat (10) - highconvex (1)	flat (17) - convex (11) - highconvex (4)
26	P_Indice_aperture	0.54 ± 0.13	0.6 ± 0.09	0.57 ± 0.05
27	P_Indice_spiral_haut	0.55 ± 0.06	0.5 ± 0.07	0.47 ± 0.06
28	U_area_U	53365.45 ± 18565.86	59358.73 ± 20275.59	105272.85 ± 40358.83
29	U_mean_d_umb	260.46 ± 38.57	270.99 ± 50.11	360.7 ± 68.49
30	U_mean_d_umb_int	69.58 ± 13.76	67.03 ± 13.85	88.56 ± 23.74
31	U_area_umb_int	3898.42 ± 1615.69	3629.22 ± 1503.04	6479.78 ± 3564.69
32	U_mean_d_umb_ext	122.66 ± 28.48	136.87 ± 24.94	164.66 ± 36.7
33	U_area_umb_ext	12111.15 ± 5941.67	15092.43 ± 5190.46	22114.84 ± 9794.99
34	U_l_sut_total	104.11 ± 22.44	108.7 ± 24.11	152.61 ± 33.56
35	U_l_sec_ap	38.39 ± 19.98	42.08 ± 24.05	58.58 ± 26.73
36	U_l_depressed_furrow	87.09 ± 20.61	85.79 ± 27.61	101.93 ± 37.11
37	U_l_folia_sspores	41.62 ± 11.52	51.17 ± 15.81	56.7 ± 18.8
38	U_l_chamber	109.56 ± 23.42	110.64 ± 27.2	161.52 ± 38.66
39	U_l_chamber_test	76.01 ± 21.18	95.1 ± 18.12	117.76 ± 26.05
40	U_l_test_chamber	280.99 ± 42.3	292 ± 55.39	392.59 ± 71.51
41	U_umb_fill_QL	medium (14) - full (11) - empty (8)	medium (14) - full (7) - empty (6)	medium (19) - empty (11) - full (1)

42	**U_umb_plug_QL**	yes (23) - no (10)	yes (17) - no (9)	no (30) - yes (2)
43	**U_folia_end_QL**	sharp (14) - medium (13) - blunt (7)	medium (13) - sharp (11) - blunt (4)	blunt (11) - sharp (11) - medium (10)
44	**U_folia_orn_QL**	medium (15) - weak (11) - strong (8)	medium (11) - strong (11) - weak (5)	strong (11) - medium (11) - weak (10)
45	**U_ind_d_umb_int**	0.27 ± 0.04	0.25 ± 0.04	0.25 ± 0.05
46	**U_ind_d_umb_ext**	0.47 ± 0.07	0.51 ± 0.05	0.46 ± 0.04
47	**U_ind_area_umb_int**	0.1 ± 0.14	0.07 ± 0.02	0.06 ± 0.02
48	**U_ind_area_umb_ext**	0.3 ± 0.51	0.26 ± 0.05	0.27 ± 0.37
49	**U_ind_l_sec_ap**	0.37 ± 0.18	0.39 ± 0.22	0.38 ± 0.16
50	**U_ind_l_depressed_furrow**	0.48 ± 0.19	0.39 ± 0.25	0.29 ± 0.25
51	**U_ind_l_flat_suture**	0.15 ± 0.17	0.21 ± 0.18	0.33 ± 0.2
52	**U_ind_l_folia_sspores**	0.38 ± 0.09	0.47 ± 0.1	0.35 ± 0.09
53	**U_ind_l_chamber_test**	0.27 ± 0.06	0.33 ± 0.04	0.3 ± 0.05
54	**pores_count**	44.61 ± 9.7	87.76 ± 18.82	28.25 ± 7.7
55	**pores_total_area**	113.31 ± 23.22	68.42 ± 21.34	126.1 ± 21.64
56	**pores_average_size**	2.69 ± 0.89	0.88 ± 0.65	4.76 ± 1.38
57	**pores_area_percent**	20.17 ± 4.13	12.18 ± 3.8	22.45 ± 3.85
58	**pores_perimeter**	6.08 ± 1.11	3.27 ± 0.99	7.9 ± 1.25
59	**pores_count_reworked**	38.94 ± 9.2	81.31 ± 18.32	23.44 ± 6.87
60	**pores_mean_area_reworked**	3.09 ± 1	0.97 ± 0.77	5.82 ± 1.85
61	**pores_d**	1.96 ± 0.34	1.06 ± 0.33	2.69 ± 0.44

Appendix-Figure 1. Locations of the primers used to amplify the SSU rDNA fragment of interest.

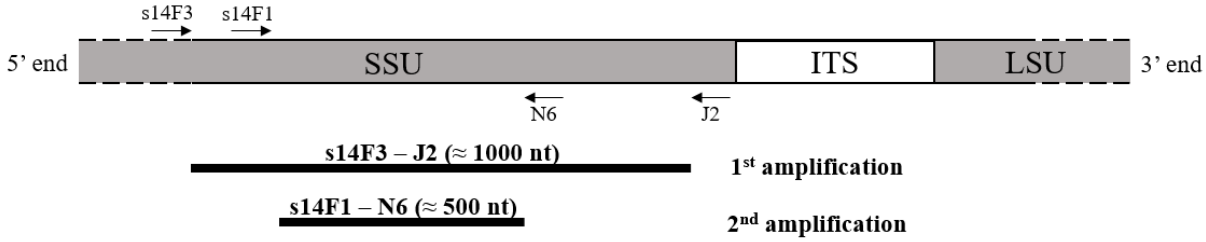

Appendix-Figure 2. Scatter plot of the first two dimensions issued from the FAMD analysis for the last two variables (mean pore diameter and the raised of flush character of the sutures in the central part of the spiral side). All specimens and their associated phylotypes are represented: T1 (red squares), T2 (green triangles) and T6 (blue dots). Variables are represented by the black arrows according to the FAMD output.

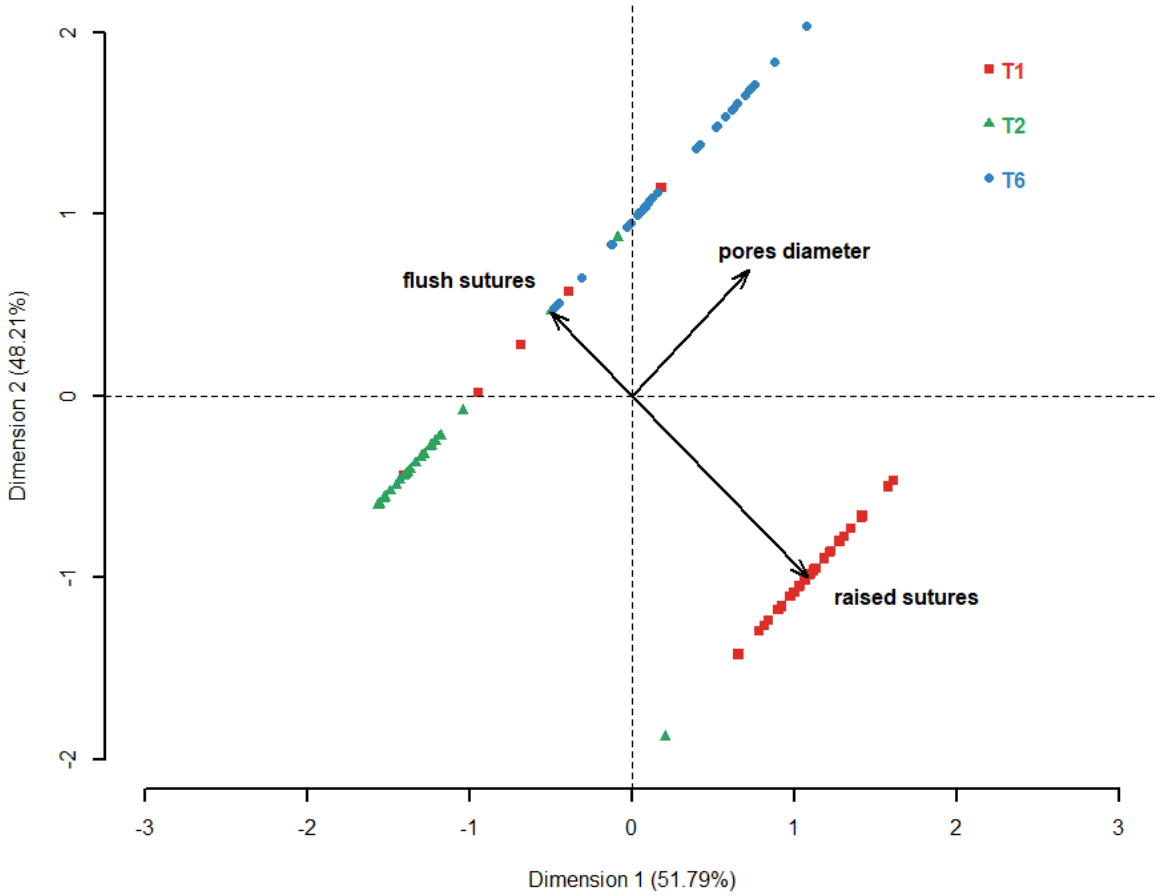

Appendix-Figure 3. ROC curves issued from the calculation of the sensibility and specificity for various pore diameters. The point located on the upper left corner of the ROC space represents the value of pore diameter for which the sensibility and specificity are maximal. Left panel (T2 vs. others) and right panel (T6 vs. others).

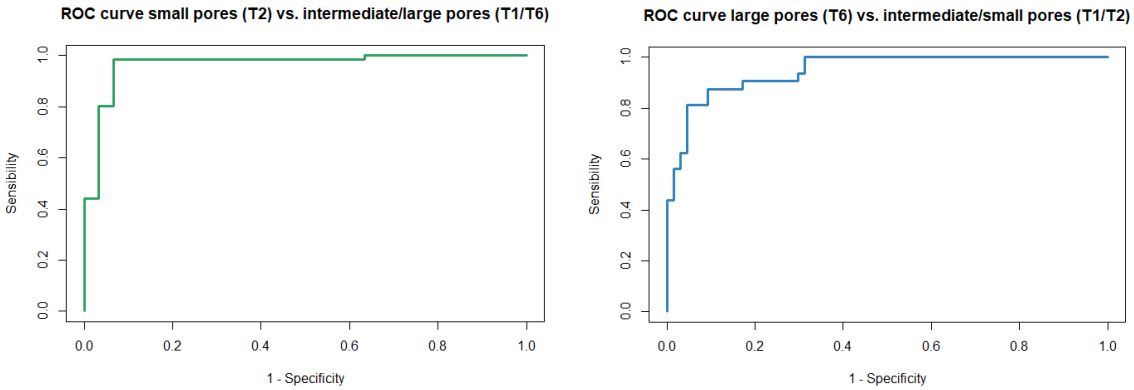

Appendix-Figure 4. SEM images of the 34 specimens phylotyped T1 used in this study.

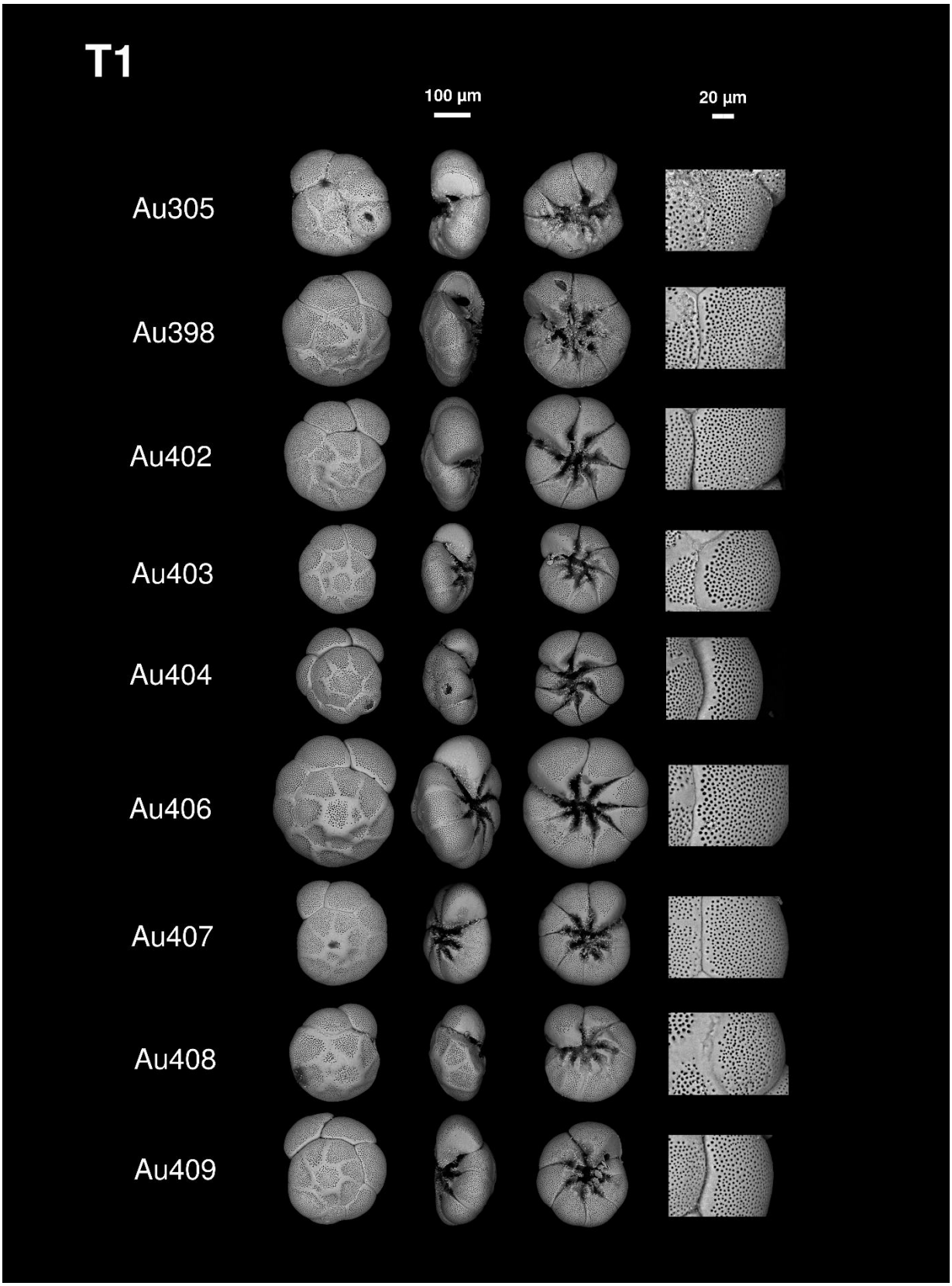

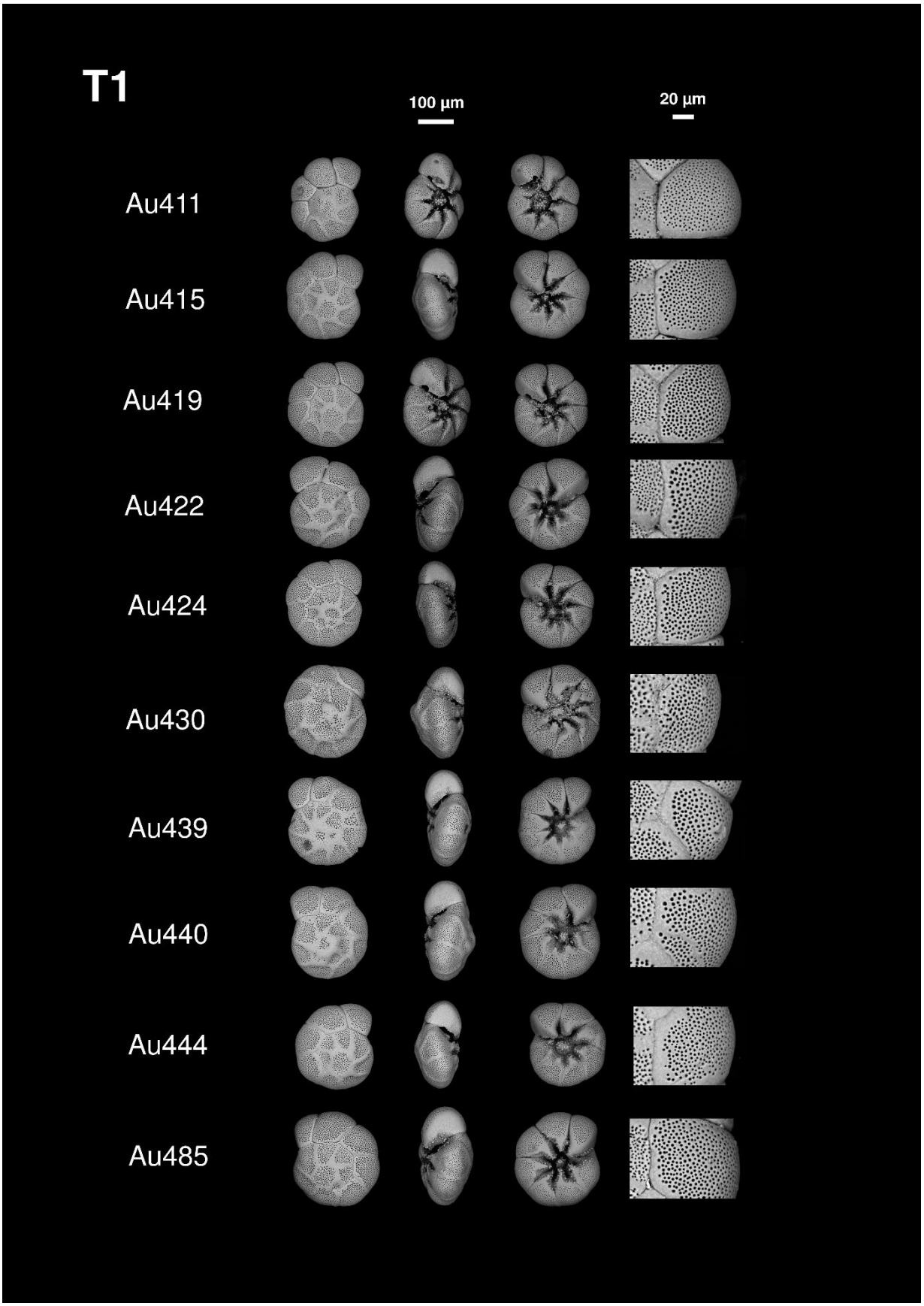
T1
100 µm
20 µm
Au411
Au415
Au419
Au422
Au424
Au430
Au439
Au440
Au444
Au485

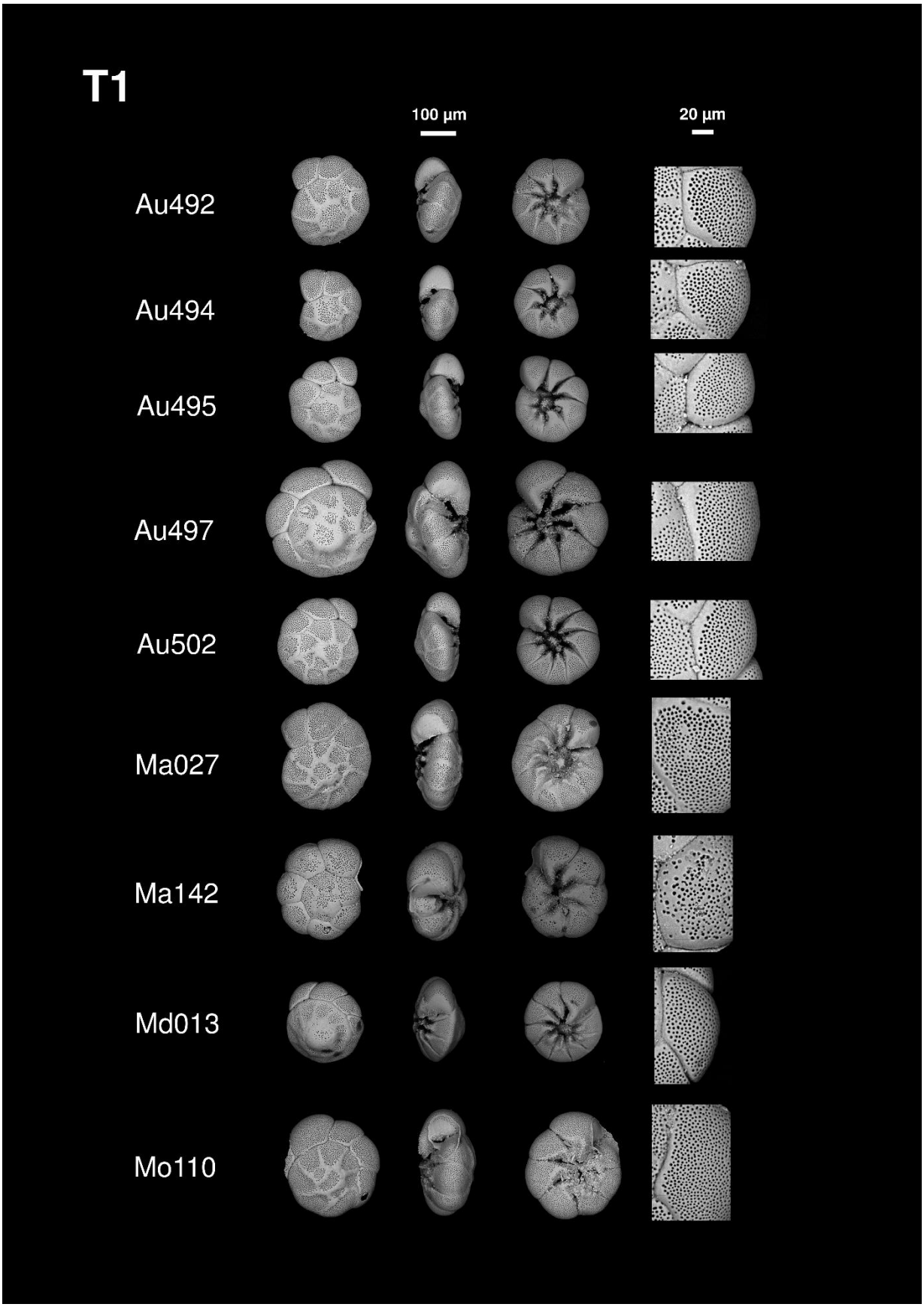
T1
100 µm
20 µm
Au492
Au494
Au495
Au497
Au502
Ma027
Ma142
Md013
Mo110

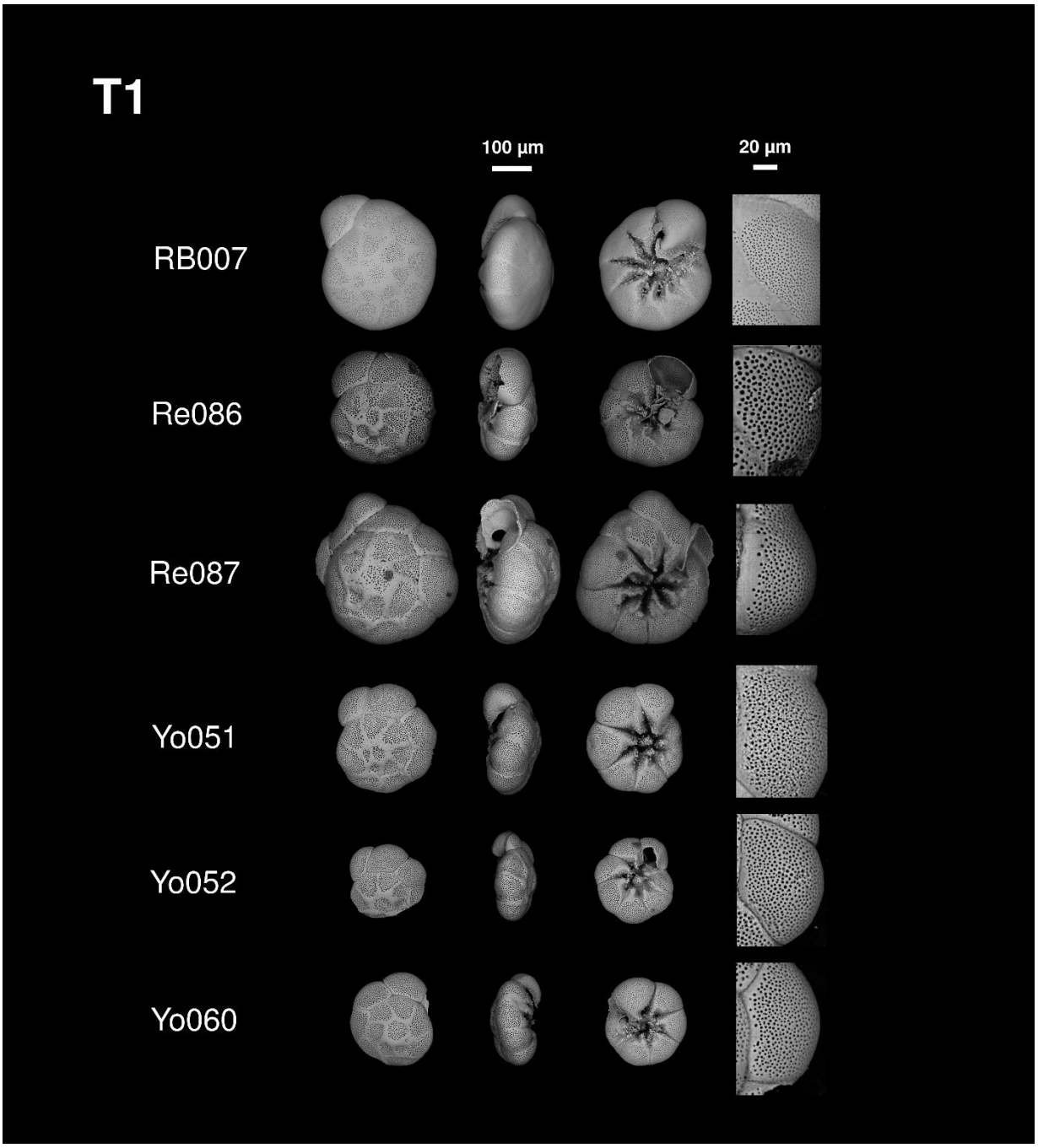
T1
100 µm
20 µm
RB007
Re086
Re087
Yo051
Yo052
Yo060

Appendix-Figure 5. SEM images of the 30 specimens phylotyped T2 used in this study.

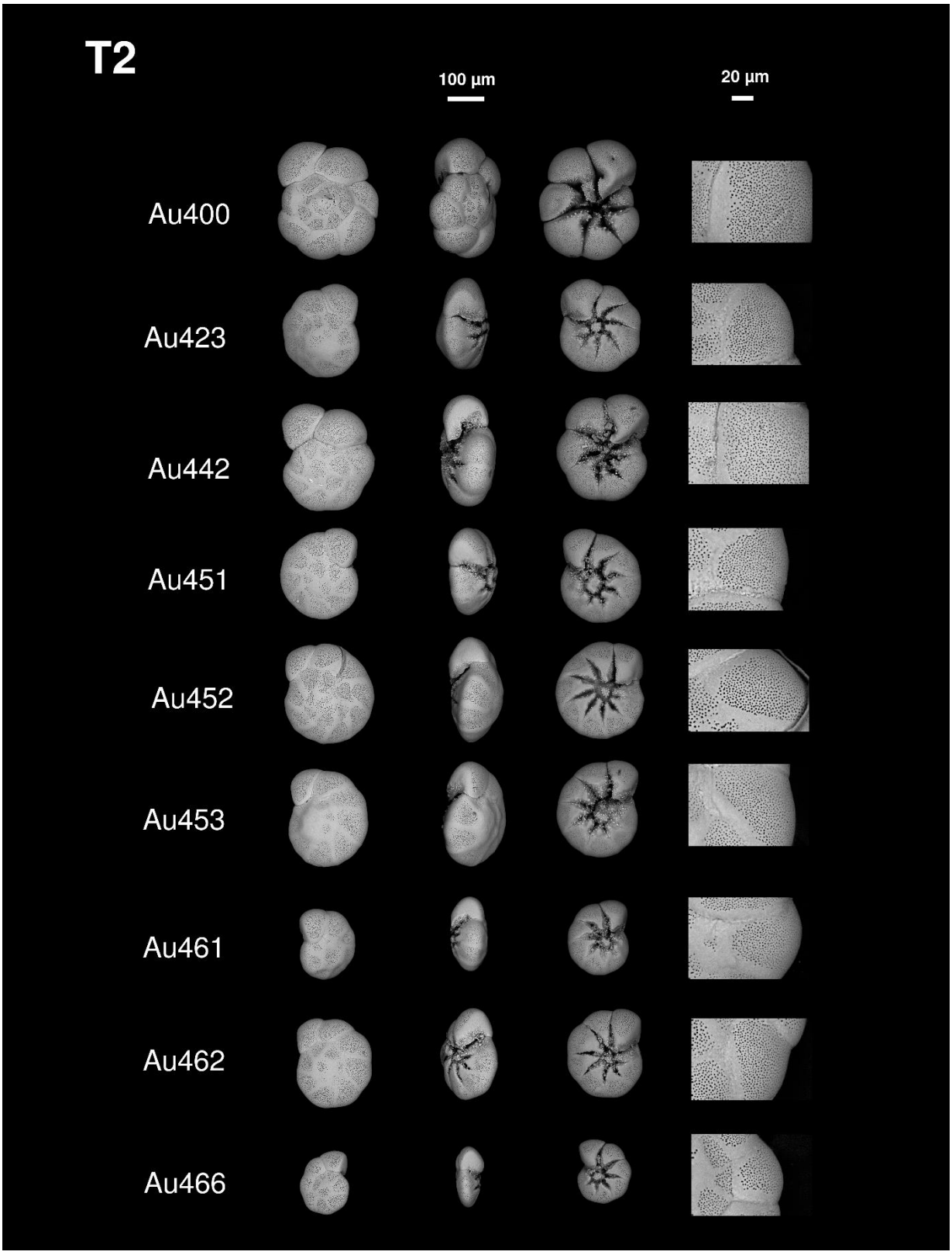

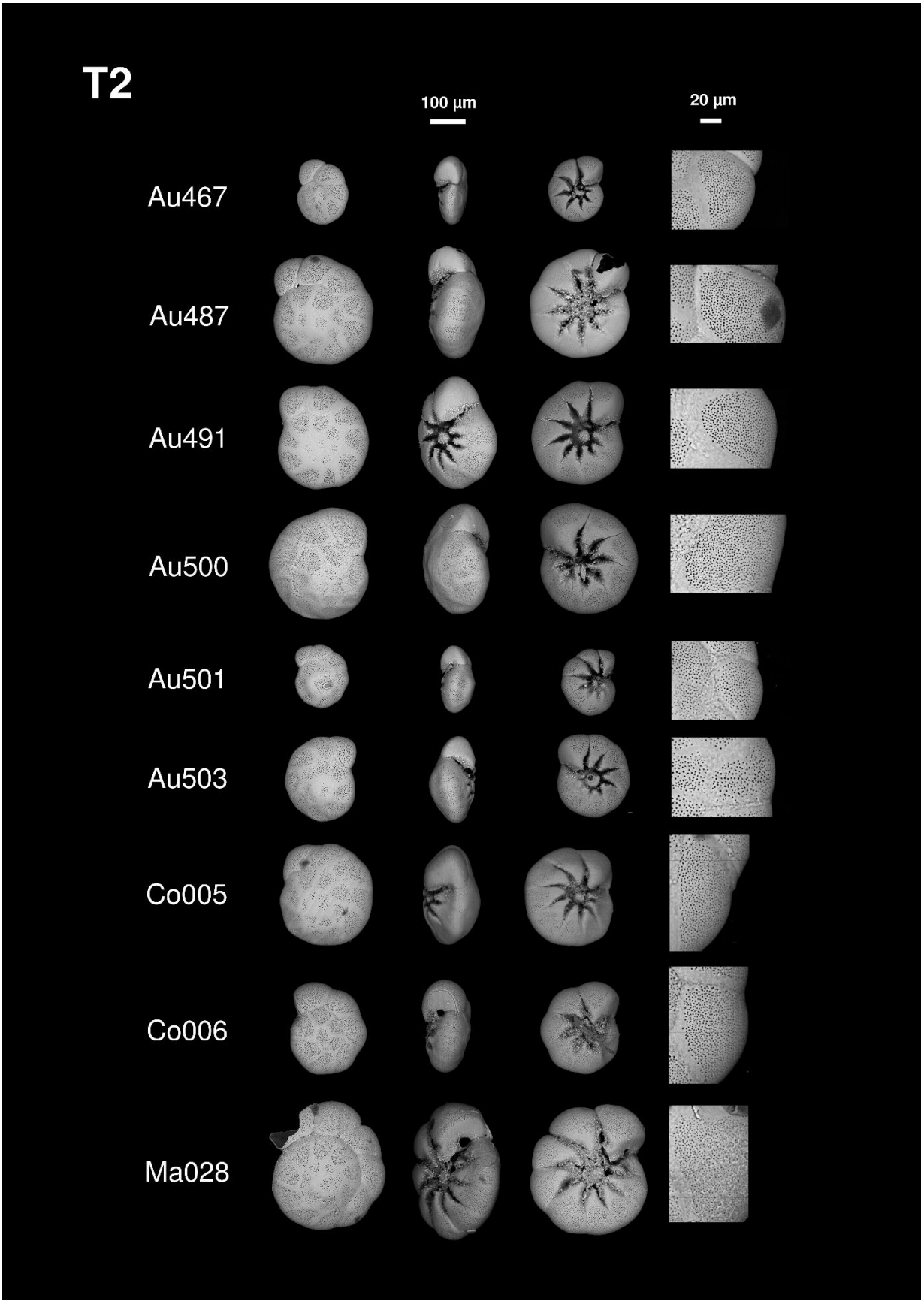
T2
100 µm
20 µm
Au467
Au487
Au491
Au500
Au501
Au503
Co005
Co006
Ma028

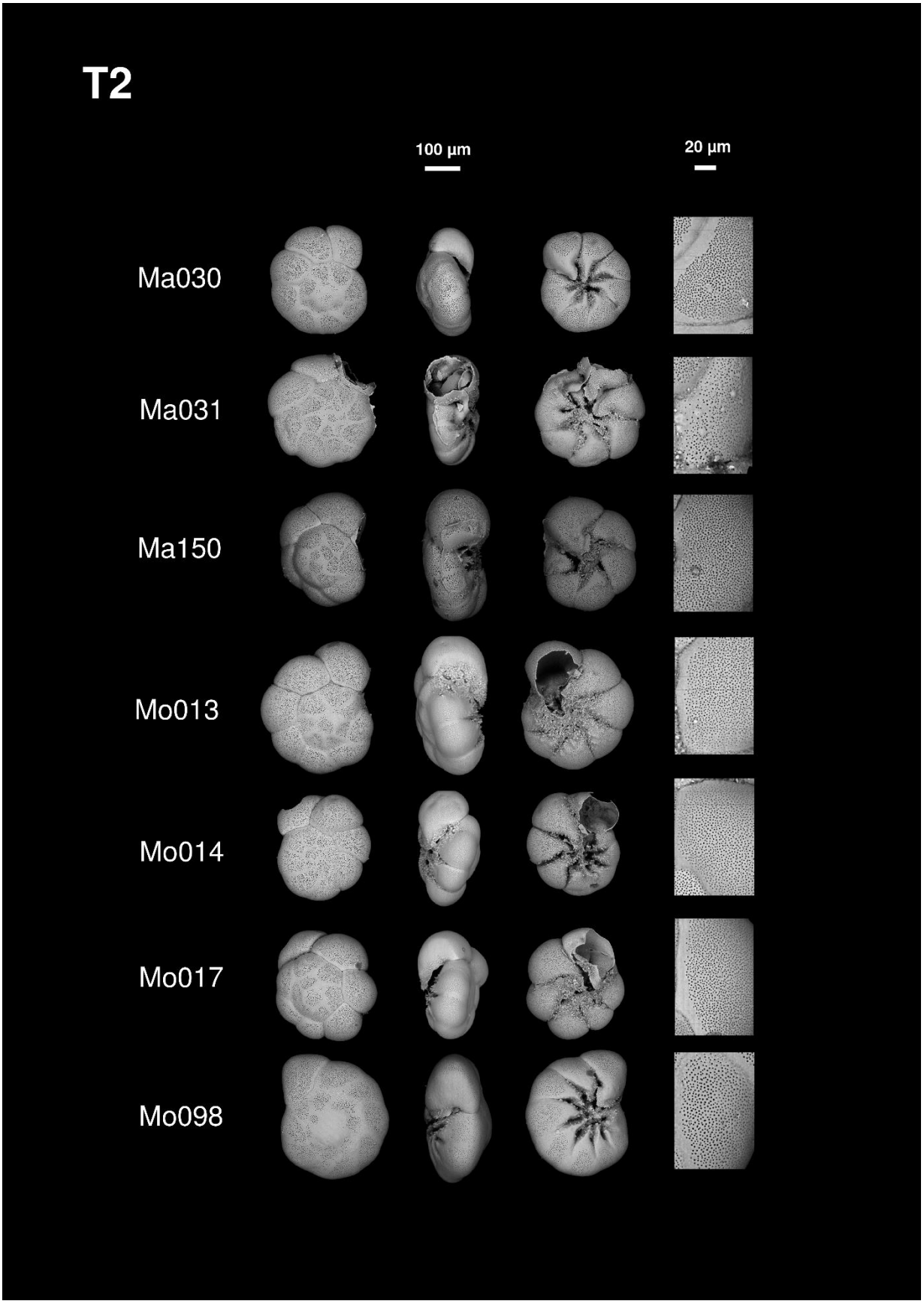
T2
100 µm
20 µm
Ma030
Ma031
Ma150
Mo013
Mo014
Mo017
Mo098

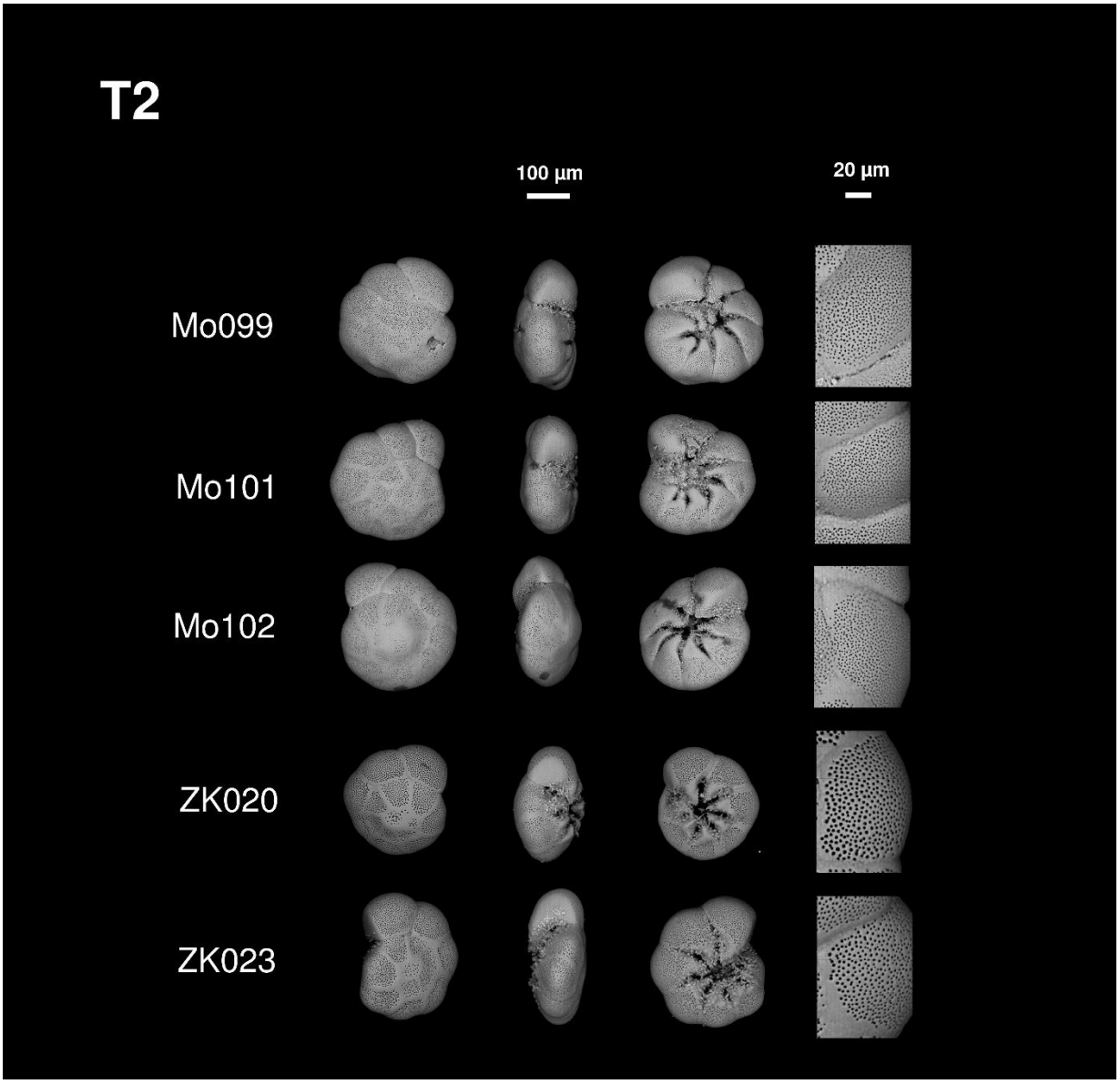
T2
100 µm
20 µm
Mo099
Mo101
Mo102
ZK020
ZK023

Appendix-Figure 6. SEM images of the 32 specimens phylotyped T6 used in this study.

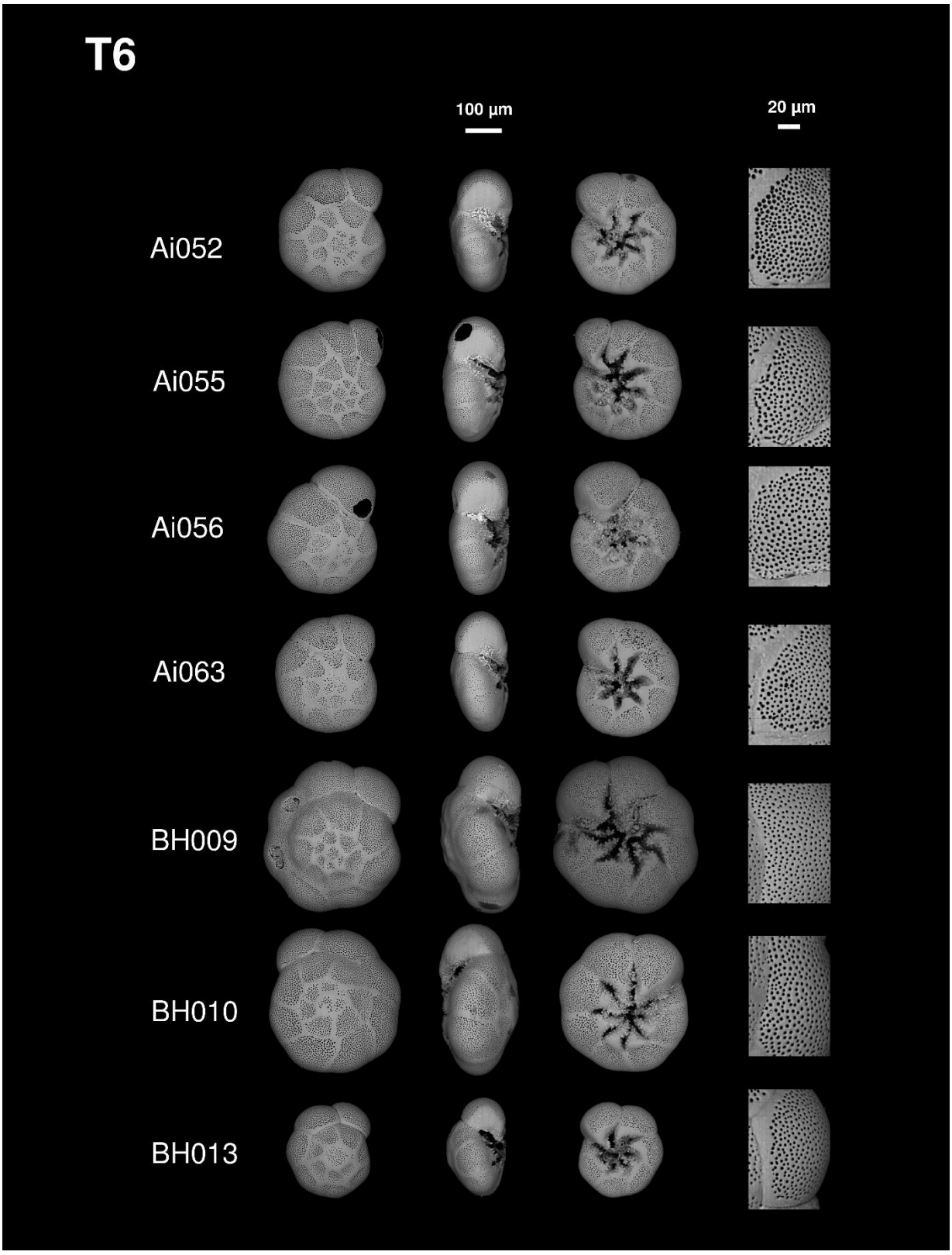

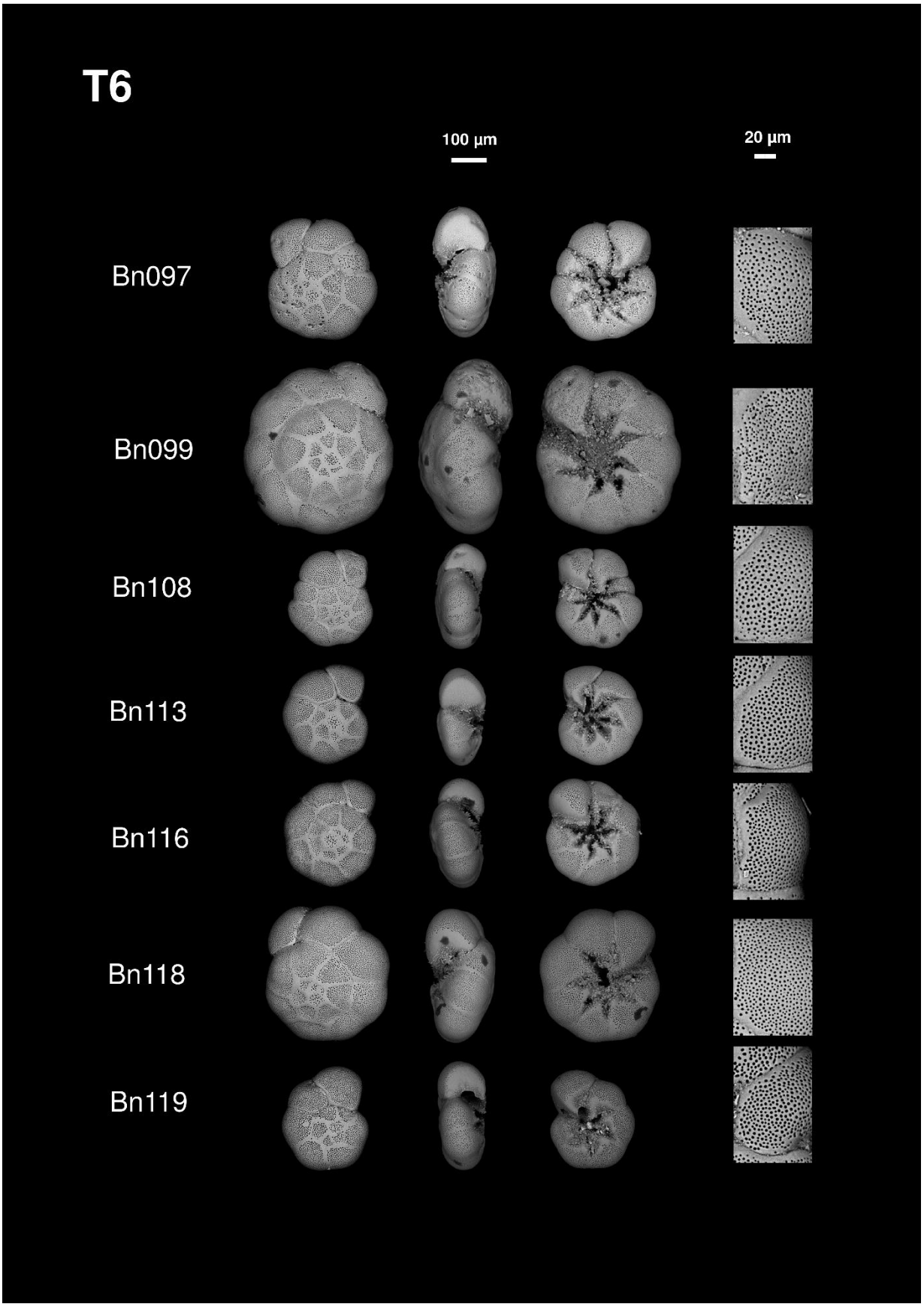
T6
100 µm
20 µm
Bn097
Bn099
Bn108
Bn113
Bn116
Bn118
Bn119

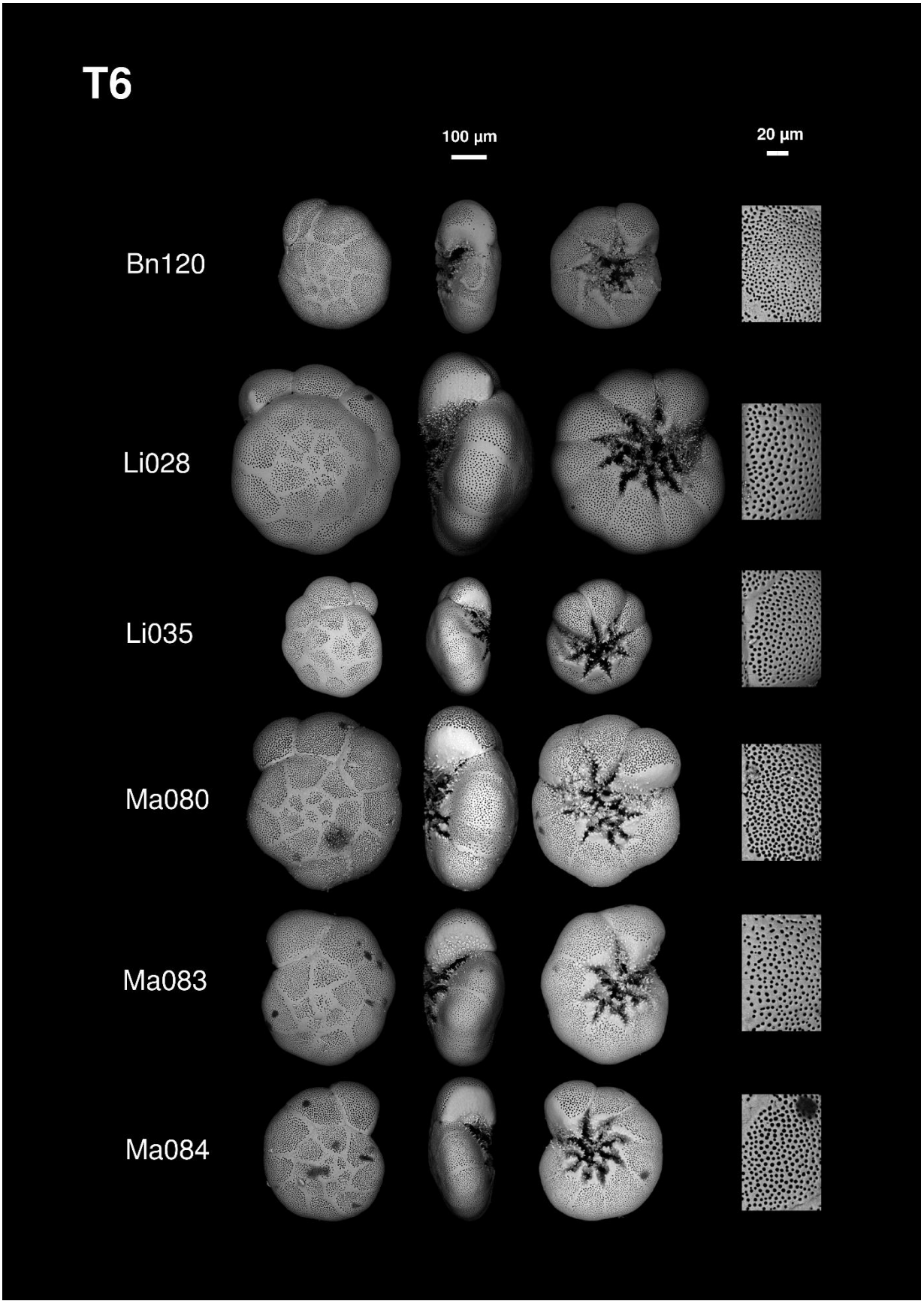
T6
100 µm
20 µm
Bn120
Li028
Li035
Ma080
Ma083
Ma084

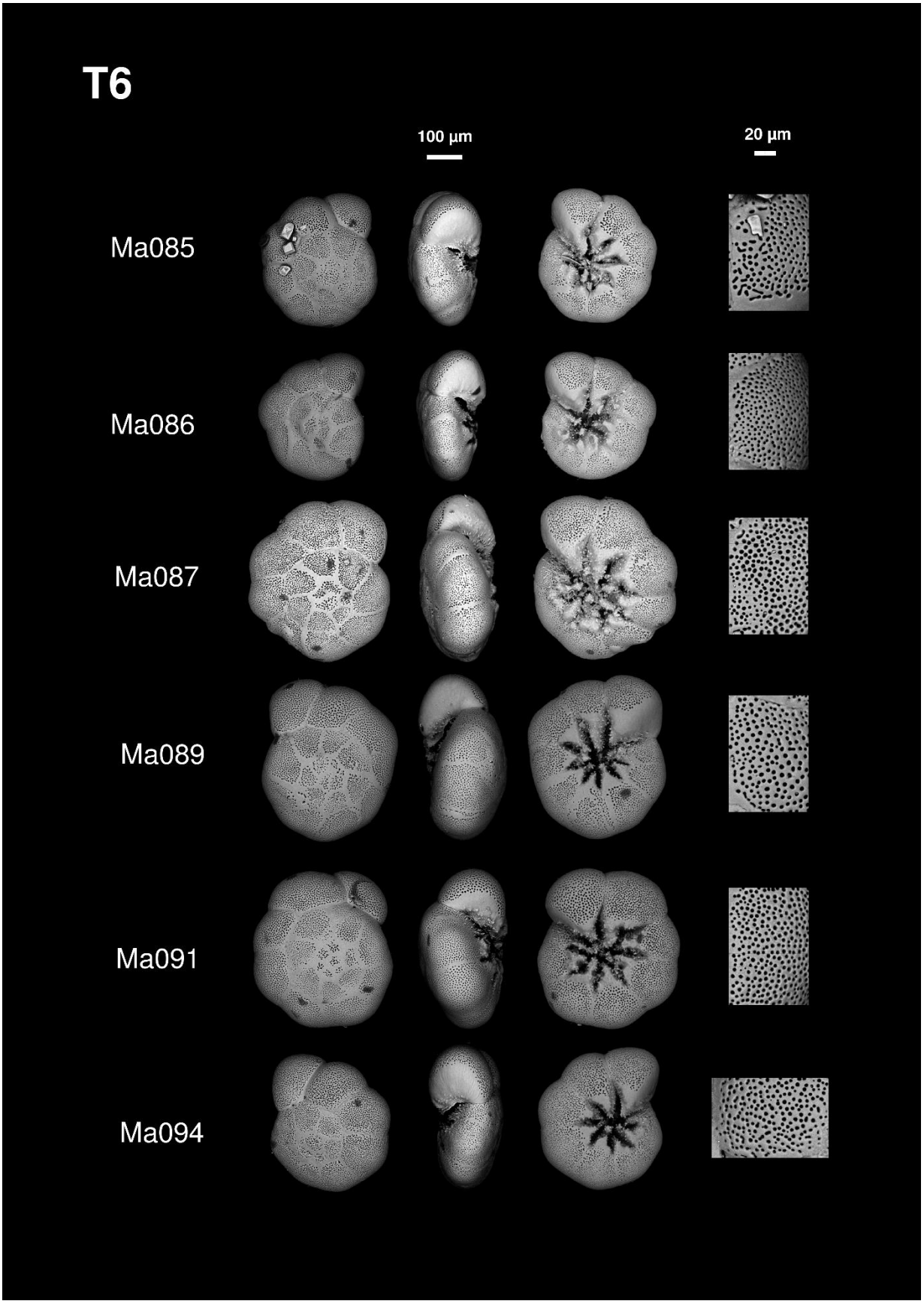
T6
100 µm
20 µm
Ma085
Ma086
Ma087
Ma089
Ma091
Ma094

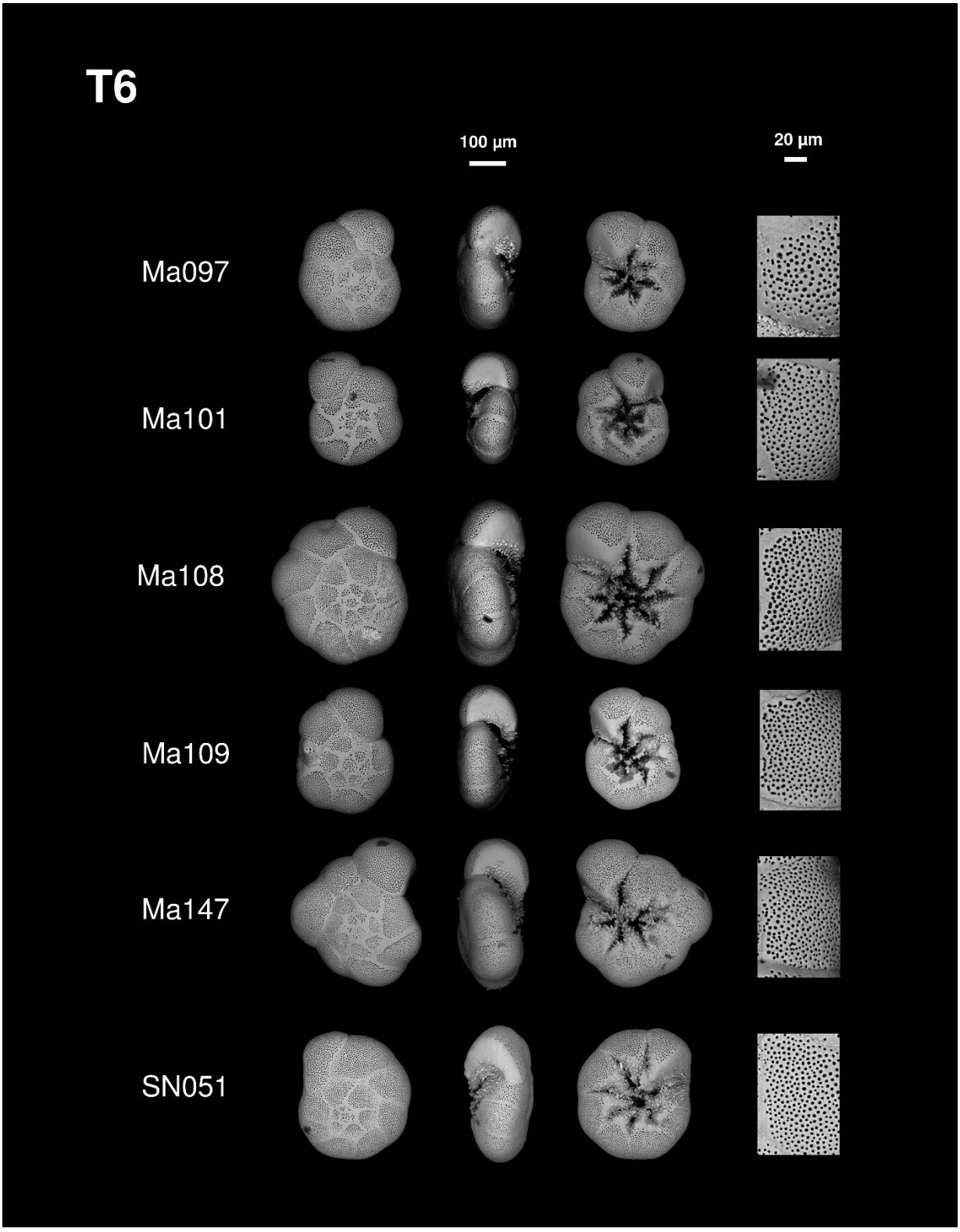
T6
100 µm
20 µm
Ma097
Ma101
Ma108
Ma109
Ma147
SN051

CHAPTER 3

BIOGEOGRAPHIC DISTRIBUTION OF THREE PHYLOTYPES (T1, T2 AND T6) OF *AMMONIA* (FORAMINIFERA, RHIZARIA) AROUND GREAT BRITAIN: NEW INSIGHTS USING A COMBINATION OF MOLECULAR AND MORPHOLOGICAL RECOGNITION

JULIEN RICHIRT[1], MAGALI SCHWEIZER[1], AURELIA MOURET[1], SOPHIE QUINCHARD[1], SALHA A. SAAD[2], VINCENT BOUCHET[3], CHRISTOPHER M. WADE[2] AND FRANS J. JORISSEN[1]

[1]UMR 6112 LPG-BIAF Recent and Fossil Bio-Indicators, University of Angers, University of Nantes, 2 Boulevard Lavoisier, F-49045 Angers, France
[2]School of Life Sciences, University of Nottingham, University Park, Nottingham NG7 2RD, UK
[3]UMR 8187, LOG, Laboratoire d'Océanologie et de Géosciences, University of Lille, CNRS, University of Littoral Côte d'Opale, F 62930 Wimereux, France

*Corresponding author: richirt.julien@gmail.com

ABSTRACT

***Ammonia* is one of the most widespread foraminiferal genera worldwide. Three phylotypes (*Ammonia* sp. T1, T2 and T6), commonly encountered in the Northeast Atlantic, are usually associated with the morphospecies *Ammonia "tepida"*. The biogeographic distribution of these three types was recently investigated in coastal environments around Great Britain based on genetic assignations. A new method was recently developed to recognize these three phylotypes based on morphological criteria (i.e., pore size and suture elevation on spiral side), avoiding the previously necessary molecular analyses to identify them. The results presented here allow us to validate the consistency of the morphometric determination method but also to define more precisely the pore size variability of each of the three phylotypes, which is a main criterion for their recognition. Moreover, these results, combined with earlier molecular and morphological data, enable us to refine the biogeographic distribution previously established by genetic analyses alone. The biogeographical distribution pattern presented here supports the putatively invasive character of *Ammonia* sp. T6, by suggesting that this phylotype is currently spreading out over large areas, and is supplanting autochthonous phylotypes (T1 and T2) at the outskirt of its present distributional areas along the coastlines of the British Isles and Northern France. In fact, only the south coast of England, Ireland and the northwest coast of France have not been colonised by *Ammonia* sp. T6 yet. Our results also suggest that within the areas colonised by phylotype T6, T2 may find refuges in the inner parts of estuaries. We further suggest that the absence of *Ammonia* sp. T6 in the western part of the English Channel may be explained by the general surface current circulation pattern, which impedes further expansion. The high reliability of the determination method of phylotypes T1, T2 and T6 based on morphology also allows us to quickly generate large data sets in sub-recent/fossil material. This new method will make it possible to gain understanding about the ecological differences between the three phylotypes and about the historical changes in their distribution patterns (for example due to changing anthropogenic factors). Finally, it will allow us to confirm or invalidate the putative invasive character of phylotype T6.**

1. INTRODUCTION

Discovered in the 18th century, foraminifera are unicellular eukaryotes with a very rich fossil record (Gupta, 2007; Jones, 2013) and consequently, they have been widely used for biostratigraphy and palaeoreconstructions. For example, the biogeochemistry of their shells is largely used in palaeoceanographic studies to evaluate conditions of the past oceans related to climate change (see Katz et al., 2010, for an overview). The fact that foraminifera represent a very valuable tool in palaeoecological reconstructions and more recently also in bio-monitoring of recent ecosystems has led to a strongly increasing interest in their ecology during the second half of the 20th century.

Among Foraminifera, *Ammonia* is one of the most widespread genera, and is present from temperate to tropical regions in shallow marine as well as estuarine ecosystems. In view of its apparently large tolerance to different types of environmental stress (*e.g.*, Bradshaw, 1957;

Alve, 1995; Bouchet, 2007; Geslin et al., 2014), this genus is an important tool for paleoecological reconstructions and bio-monitoring of coastal ecosystems. However, *Ammonia* suffers from taxonomical uncertainties, since traditional taxonomy (based on morphological criteria, *i.e.*, morphospecies) and molecular identification (based on DNA sequences, *i.e.*, phylotype) often give contradictory evidence and are sometimes difficult to reconcile (*e.g.*, Holzmann & Pawlowski, 1997; Hayward et al., 2004; Bird et al., 2020). A part of the problem is the fact that much of the type material is lost and first descriptions are often too imprecise for many morphospecies to allow comparison with present detailed morphometric measurements, such as with pore size data (Hayward et al., 2004; Petersen et al., 2016; Richirt et al., 2019a). In addition, some of the commonly used morphospecies, such as *Ammonia tepida* or *Ammonia beccarii*, are a mixture of different phylotypes, which are now considered as separated species (Pawlowski et al., 1995; Holzmann et al., 1996; Holzmann, 2000; Langer & Leppig, 2000; Hayward et al. 2004; Schweizer et al., 2011a, b).

In the Northeast Atlantic, five *Ammonia* phylotypes are frequently encountered and have been named T1, T2, T3, T6 and T15 (Hayward et al., 2004; Bird et al., 2020). Phylotypes T3 and T15 are easily distinguishable from the other three (T1, T2 and T6; Hayward et al., 2004; Schweizer et al, 2011a; Bird et al., 2020) and are usually associated with the more ornamented *Ammonia "beccarii"* morphospecies complex. Phylotypes T1, T2 and T6 are more difficult to discriminate because they are morphologically very close; they are commonly associated with the less ornamented *Ammonia "tepida"* morphospecies complex.

Here we will consider only phylotypes T1, T2 and T6, which are very common in the intertidal areas of Northeast Atlantic. Until recently, their morphological discrimination was difficult, and knowledge of their distribution in this area, which required molecular identification, was restricted to a limited number of specimens and sites (*e.g.*, Holzmann & Pawlowski, 2000; Hayward et al., 2004; Pawlowski & Holzmann, 2008; Schweizer et al. 2011b; Saad & Wade, 2016; Bird et al., 2020). Recently, Richirt et al. (2019a) described a new method to distinguish T1, T2 and T6 on the basis of morphological criteria. Consequently, as molecular analysis is no longer needed, it is now possible to quickly determine morphologically large numbers of specimens.

The biogeography of phylotypes T1, T2 and T6 in the Northeast Atlantic area was earlier investigated on the basis of molecular data by Schweizer et al (2011b), Saad & Wade (2016) and Bird et al. (2020), respectively in the Wadden and Baltic Seas and along the coastline of the British Isles. However, no clear pattern emerged from these studies, with all three phylotypes inhabiting contrasting coastal ecosystems such as shallow marine, intertidal and

subtidal, estuarine and saltmarsh environments as well as harbours (Schweizer et al., 2011b; Saad & Wade, 2016; Bird et al., 2020). Consequently, the factors controlling their distribution are still not fully understood.

This study proposes to apply the morphometric criteria proposed by Richirt et al. (2019) to discriminate T1, T2 and T6 on the specimens that were described and identified molecularly by Saad & Wade (2016). Our first aim is to verify the reliability of the morphometric discrimination method developed in Richirt et al. (2019a) by comparing it with molecular identification, on an independent dataset, which was not used to develop the morphometric method. In case of discrepancies between the results of the different assignment methods (molecular *versus* morphometric), the possible reasons for these inconsistencies will be investigated. Our second aim is to use this new morphometric dataset to better constrain the variability of the average pore size for each of the three phylotypes, as described by Richirt et al. (2019a), which is one of the two essential parameters used to discriminate them. The final aim of this study is to re-analyse the biogeographic distribution pattern of the three phylotypes around the British Isles. In order to do this, we expanded the data set as much as possible, by including: (1) the morphometric determinations of the 137 specimens earlier identified by genetic analyses and coming from 17 on the 19 sites in Saad & Wade (2016), (2) the genetic data published by Saad and Wade (2016) from the two remaining sites for which morphometric identification was not possible (South Queensferry and Brancaster Staithe - low marsh sites), and (3) the molecular data for 116 supplementary specimens, sampled at eight additional sites in the English Channel, Netherlands and in Northern France. This final merged dataset includes 27 sampling sites from Great Britain, Ireland, the Netherlands and Northern France. Lastly, we compare the distribution pattern we obtained with the one from Bird et al. (2020) who investigated the biogeographic distribution of *Ammonia* phylotypes in many other sites along Northeast Atlantic margins.

2. MATERIALS AND METHODS

In this study, several data sets will be used, some of them already published, others new. In the next paragraphs, we will briefly present each of them.

2.1. Molecular and morphometric investigation of the specimens studied by Saad & Wade (2016)

2.1.1. Sampling and DNA sequencing

The specimens investigated morphometrically here have been earlier studied by Saad & Wade (2016) using molecular methods; in their article, they present a detailed description of the sampling procedure (including the general environmental characteristics of the sampling sites) and the analytical protocol used for molecular identification. Thanks to their non-destructive DNA extraction procedure, the tests of almost all specimens were preserved, and could be used for morphometric analyses. Except for two sites of the original publication (South Queensferry and Brancaster Staithe - low marsh) for which the specimens were no longer available, only some scarce individuals were broken or lost. In all, 137 of the 162 specimens, which were originally sequenced, could be investigated morphometrically (Table 1; Supplementary Table 1).

Table 1. Site, sites ID, geographic coordinates and number of individuals which were identified genetically (from Saad & Wade, 2016) and morphometrically (this study).

Site	Site ID	Latitude	Longitude	N individuals genotyped (Saad & Wade, 2016)	N individual morphologically investigated (this study)
Bangor	Ban	53°14'2.41"N	4°7'4.26"W	5	4
Barmouth	Bar	52°43'17.26"N	4°2'27.43"W	10	10
Barrow-in-Furness	BIF	54°5'24.16"N	3°14'29.61"W	9	9
Barton-upon-Humber	Hull	53°41'50.86"N	0°26'40.08"W	9	9
Brancaster Staithe (high marsh)	4A	52°58'11.78"N	0°40'05.05"E	8	7
Brancaster Staithe (low marsh)	1A	52°58'6.76"N	0°40'5.08"E	10	0
Braunton	Brs	51°5'55.09"N	4°9'52.15"W	10	10
Burnham-Overy-Staithe	2A	52°57'55.74"N	0°44'48.51"E	10	10
Galmpton	Bix	50°23'31.53"N	3°34'31.15"W	8	4
Hambleton	Ham	53°52'40.15"N	2°57'52.46"W	2	2
Lymington	LM	50°45'16.36"N	1°31'39.34"W	10	10
Pembroke Dock	Pem	51°41'59.66"N	4°55'14.72"W	9	9
Pen Clawdd	Lan	51°38'36.28"N	4°6'20.18"W	10	10
Queenborough	Que	51°25'1.47"N	0°44'21.15"E	9	11
Severn Beach	SB	51°33'17.99"N	2°40'11.37"W	8	6
Shoreham-by-Sea	Sho	50°49'49.04"N	0°16'30.79"W	10	10
South Queensferry	Quf	55°59'34.28"N	3°24'38.18"W	6	0
St Osyth	IPS	51°47'54.83"N	1°3'50.32"E	9	9
Thornham	5A	52°57'59.35"N	0°34'20.09"E	10	7
			TOTAL	162	137

In addition, 16 specimens were newly collected at Thornham in September 2018 for comparison with earlier molecular identifications from Saad & Wade (2016). They were put in a Guanidine buffer and extracted individually for DNA, following the protocol of guanidine extraction with shell destruction (protocol 2 in Pawlowski, 2000). The eight samples positively amplified were then sent to GATC Biotech in Cologne for Sanger sequencing.

2.1.2. SEM imaging and morphometric measures

For all available 137 individuals, we acquired Scanning Electron Microscopy (SEM) overview images of the spiral side as well as detailed images of the penultimate chamber (at 1000x magnification). These images were used to document the suture elevation in the central part of the test and the pore size, respectively (Supplementary Plate1). Pore size measurements were performed following the method of Petersen et al. (2016). These two criteria allow discriminating phylotypes T1, T2 and T6 with a success rate of > 92 % (Richirt et al. 2019a). In practice, the morphological criteria were hierarchised according to the following flow chart (Figure 1):

(1) If the average pore diameter is < 1.4 µm, the specimen is a T2. If the average pore diameter is > 1.4 µm, go to (2),

(2) If the sutures in the central part of the spiral side are raised (elevated), the specimen is a T1; if the sutures are flush, the specimen is a T6. If this character is not visible (damaged specimen) or ambiguous, go to (3),

(3) If the average pore diameter is > 2.4 µm, the specimen is a T6. If the average pore diameter is comprised between 1.4 µm and 2.4 µm, go to (4),

(4) If the number of chamber(s) with incised sutures in the last whorl on the spiral side is > 2, the specimen is a T1. If it is ≤ 2, it is not possible to assign the specimen unambiguously to a phylotype.

When the use of the main criteria (1) and (2) is not sufficient (for example when the test is too damaged), additional criteria (3) and (4) are applied. In some very rare cases in which this checklist does not yield a conclusive response, phylotype assignation is impossible. In this study, 135 specimens were determined using the main criteria (1) and (2), one specimen using the additional criterion (3) (*i.e.*, 5A-15) and phylotype assignation was only impossible for a

single specimen (*i.e.*, Pem-140). The morphological identifications obtained were then compared with the molecular identifications made for the same specimens by Saad & Wade (2016).

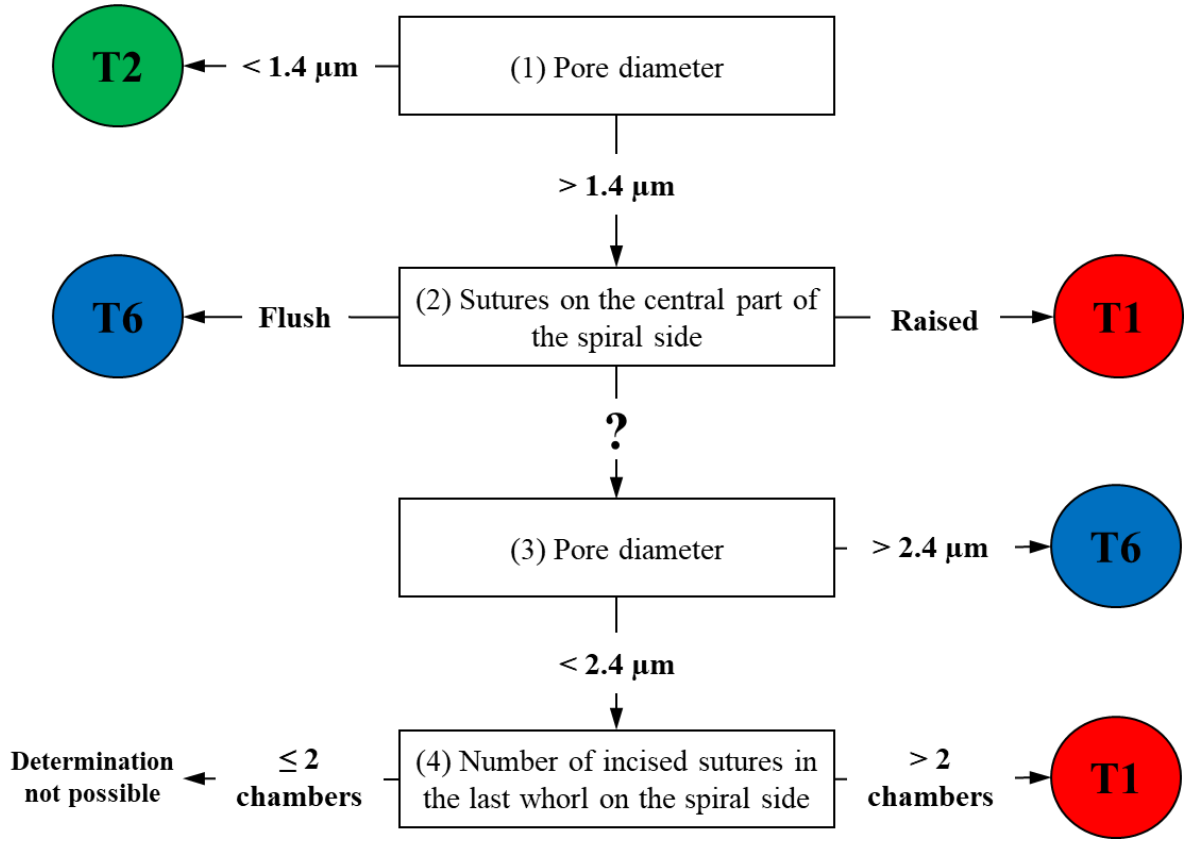

Figure 1. Dichotomous procedure to discriminate T1, T2 and T6.

The eight new specimens re-sampled at Thornham in September 2018, which were successfully amplified and molecularly assigned to a phylotype, were not investigated morphologically, because no SEM images were available.

2.2. THE AMTEP PROJECT DATASET

In order to extend our dataset, we included 116 individuals which were sampled and sequenced from five sites along the French north coast (*i.e.*, Authie, Seine estuary, St. Vaast, Ouistreham and Rade de Brest) and three from the Netherlands (Biezelingse Ham, Grevelingen and Veerse Meer; Table 2 and Supplementary Table 2). These specimens were collected in the context of the CNRS EC2CO-LEFE project AMTEP. All specimens were individually extracted, amplified and sequenced as in Richirt et al. (2019a). The sequences were aligned and compared with a set of sequences previously identified as phylotypes T1, T2 and T6 published on GenBank.

Table 2. Location, geographic coordinates and number of individuals genetically investigated at the sites of the AMTEP project.

Localisation	Latitude	Longitude	N individuals genotyped
Authie	50°22'23.80"N	1°35'44.00"E	4
Biezelingse Ham	51°26'53.40"N	3°55'49.79"E	51
Grevelingen	51°44'50.04"N	3°53'24.06"E	7
Ouistreham	49°16'16.40"N	0°14'12.20"W	7
Rade de Brest	48°24'13.10"N	4°21'16.00"W	2
Seine estuary	49°26'31.30"N	0°16'25.20"E	32
St. Vaast	49°34'38.60"N	1°16'38.80"W	4
Veerse Meer	51°33'12.24"N	3°52'25.34"E	9
		Total	116

3. DATASET OF BIRD ET AL. (2020)

In order to see how the distribution patterns we obtain fit with the larger scale picture based on molecular identification, we included data from 16 sites studied by Bird et al. (2020). These authors investigated the distribution of phylotypes T1, T2A, T2B, T3S, T3V (two sub-phylotypes belonging to T3) and T15. Because the morphometric method does not allow us to discriminate between T2A and T2B sub-phylotypes yet, we merged them for further interpretation, in order to obtain results comparable with our data. Finally, we did not consider T3S, T3V and T15 in this study. The data for the remaining phylotypes are reproduced in Table 3.

Table 3. Location, geographic coordinates and number of individuals genetically identified as T1, T2A, T2B and T6 for the 16 sites of Bird et al., 2020.

Site	latitude	longitude	T1	T2A	T2B	T6	Total
Cromarty (CR)	57°40'45.59"N	04°02'28.12"W	0	1	0	0	1
Loch Sunart (SU)	56°39'56.80"N	05°52'02.10"W	1	0	0	0	1
Dunstaffnage (DF)	56°27'06.1"N	05°27'27.9"W	1	0	0	0	1
Torry Bay (TB)	56°03'28.3"N	03°35'02.5"W	0	0	0	8	8
Cramond (Cd)	55°58'54.2"N	03°17'56.5"W	0	0	0	52	52
Loch na Cille (LK)	55°57'36.00"N	05°41'24.00"W	0	13	0	0	13
Whiterock (WR)	54°29'05.42"N	05°39'12.58"W	0	18	0	0	18
Den Oever (F)	52°56'24.8"N	05°01'30.6"E	0	0	0	1	1
Norfolk (NF)	52°49'02.41"N	00°21'46.16"E	0	1	0	30	31
Laugharne Castle (LC)	51°46'12.00"N	04°27'00.00"W	0	0	0	2	2
Grevelingen (Gv)	51°44'50.04"N	03°53'24.06"E	0	0	0	2	2
Cork (CK)	51°38'29.40"N	08°45'44.50"W	2	0	28	0	30
Cardiff (CF)	51°29'25.40"N	03°07'19.50"W	0	0	0	20	20
Dartmouth (DM) - Upper shore	50°21'04.84"N	03°34'11.33"W	0	6	0	0	6
Dartmouth (DM) - Mid shore	50°21'04.84"N	03°34'11.33"W	2	12	0	0	14
Dartmouth (DM) - Lower shore	50°21'04.84"N	03°34'11.33"W	2	49	0	0	51
		Total	8	100	28	115	251

4. RESULTS

4.1. MORPHOMETRIC IDENTIFICATION OF THE SPECIMENS STUDIED BY SAAD & WADE (2016)

From the 137 specimens published by Saad &Wade (2016), which could be analysed molecularly as well as morphologically, the first two morphological criteria (pore diameter and the suture elevation on the spiral side) were sufficient to reliably assign 135 individuals to a phylotype. Criterion (3) of the procedure described in Figure 1 was only used for one individual (5A-15), because the central part of the spiral side was damaged. Finally, a last specimen could not be assigned on the basis of morphological criteria (Pem-140), because the test was too heavily damaged. Among the 136 specimens identified morphologically, T6 was the dominant phylotype with 94 individuals (69%), followed by T2 with 28 individuals (21%), whereas T1 was least represented with 14 individuals (10%).

The correspondence between the genetic identifications of Saad & Wade (2016) and the morphological discriminations performed here is shown in Figure 2. Of the 136 specimens, 117 were assigned identically (86%) by the molecular and morphological methods, whereas 19 (14%) were assigned differently by both methods. Fourteen of these 19 specimens came from two sites only, Thornham (5A) and Shoreham-by-Sea (Sho).

At Thornham, the seven specimens analysed morphologically (5A-15, 5A-34, 5A-37, 5A-38, 5A-39, 5A-40 and 5A-62) were all determined as T6. However, six were identified genetically as T2 and a single one as T6 (5A-15, Figure 2).

At Shoreham-by-Sea, 10 specimens were genetically assigned to T6, but only two specimens (Sho-3 and Sho-8) were identified as such morphologically. Of the remaining eight specimens, seven were determined morphologically as T2 (Sho-2, Sho-4, Sho-6, Sho-10, Sho-11, Sho-12 and Sho-13), whereas a single specimen (Sho-7) was determined as T1 (Figure 2).

The other five discrepancies concern isolated specimens from different sites: 4A-7 (Brancaster high-marsh), Bix-202 (Galmpton), IPS-4 (St Osyth), Bar-236 (Barmouth) and Lan-25 (Pen Clawdd). In all these five cases, the isolated specimen was genetically identified differently from all other specimens of the considered site, whereas it was morphologically identified as the same phylotype as all other specimens of the considered site.

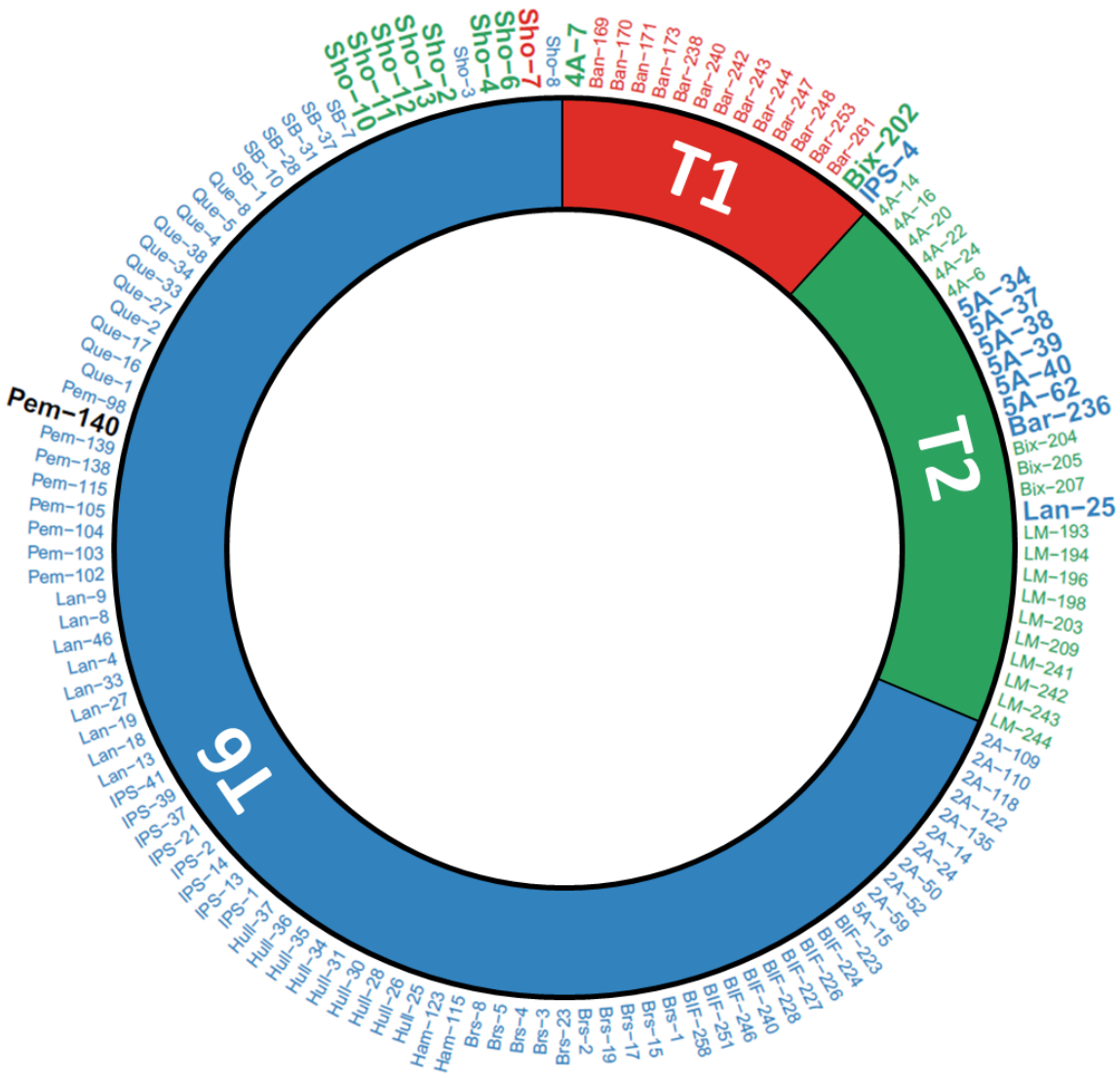

Figure 2. Circular diagram comparing molecular identification (internal part of the diagram, from Saad & Wade, 2016) with morphological determination (external part of the diagram) for the 137 individuals investigated in this study (ordered by molecular identification and their ID's). Red: T1, green: T2, blue: T6. Not determined morphologically: black. Specimens for which molecular and morphological assignations mismatch or for which morphological determination was not possible are indicated in bold with a greater font size.

Figure 3 shows the position and IDs of the mismatching individuals on the graph representing suture elevation and average pore diameter. All data concerning average pore diameter, determination of the sutures character (flush/raised) as well as SEM images of the spiral side and of the penultimate chamber at 1000x magnification for the 137 specimens investigated in this study are available in the supplementary Table 1 and Plate 1.

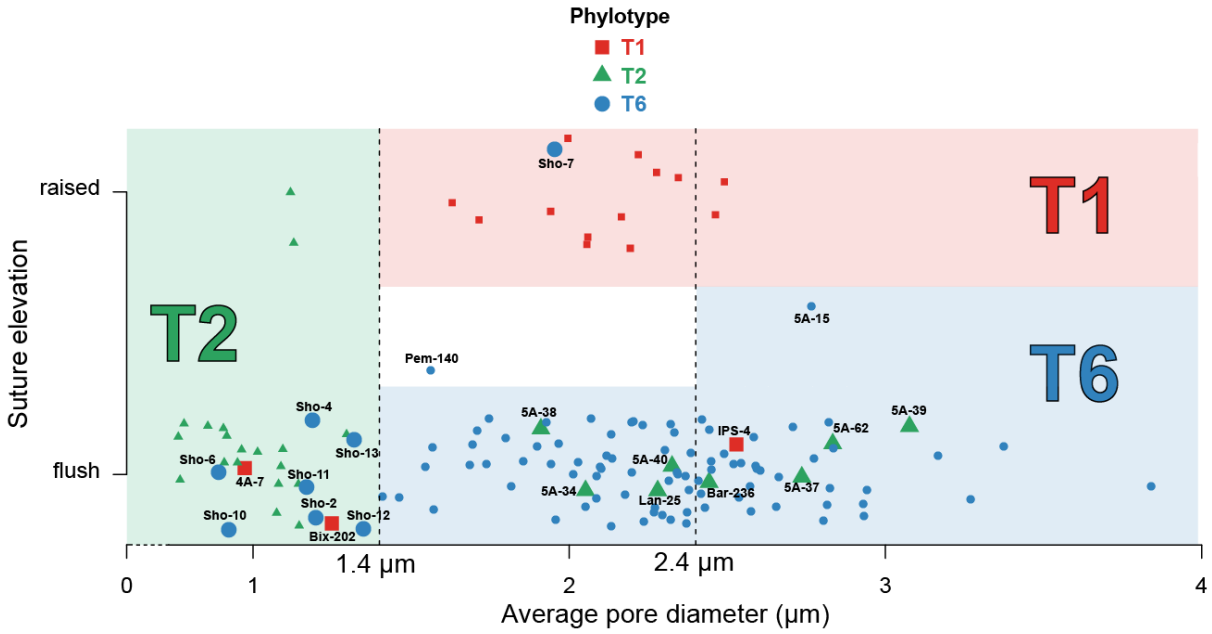

Figure 3. Average pore diameter (µm) and suture elevation (flush/raised) for the 137 individuals investigated morphologically. Individuals genotyped as T1 (red squares), T2 (green triangles) and T6 (blue circles) are represented in the graph which separates the three phylotypes on the basis of their average pore diameter and suture elevation following Richirt et al., 2019a (red area for T1, green area for T2 and blue area for T6). Individuals for which genetic and morphological identification are mismatching are represented with bigger marks and associated with their ID's (see supplementary material). Pem-140 was too damaged to be morphologically determined (white area). 5A-15 is the only specimen for which we used criterion (3) of the dichotomous procedure indicated in Figure 1. The (random) vertical dispersion was artificially added in order to better visualize all specimens separately. Vertical dotted lines represent the thresholds to discriminate between the phylotypes as determined by Richirt et al., 2019a.

4.2. THE AMTEP PROJECT DATASET

Of the 116 individuals sampled in eight sites from the AMTEP project (Table 4), 26 were part of the 96 specimens used by Richirt et al. (2019a) to develop and test the morphometric assignment method, and sequences of 10 individuals have already been published in GenBank (Supplementary Table 2). Seven more individuals, from Lake Grevelingen, presented by Richirt et al. (2020) have also been deposited in the GenBank database (accession numbers MN190684–MN190690). The sequences of other specimens have not been published previously and will be published elsewhere.

Among the 26 individuals published by Richirt et al. (2019a), 23 were classified similarly by molecular and morphometric methods. The authors argued that three individuals had been incorrectly classified by molecular analysis. For these three specimens, we will further use the morphological identification. Although the sub-phylotypes T2A and T2B were distinguished (Table 4, Supplementary Table 2), they have been merged here, because it is impossible yet to discriminate them morphologically (cryptic species). Phylotype T6 is the only phylotype

occurring at Authie (4 ind.), Biezelingse Ham (51 ind.), Grevelingen (7 ind.) and in the Seine estuary (32 ind.). Phylotype T2 is the only phylotype found at the Rade de Brest (2 ind.). Two sites yielded two phylotypes: at St. Vaast, a single T1 and three T2, and at the Veerse Meer five T2 and four T6 were found. Ouistreham is the only site were the three phylotypes were found together (five T6 *versus* a single T1 and T2).

Table 4. Location, geographic coordinates and number of individuals genetically identified as T1, T2A, T2B and T6 at the sites of the AMTEP project and from Thornham.

Localisation	Latitude	Longitude	T1	T2a	T2b	T6	Total
Authie	50°22'23.80"N	1°35'44.00"E	0	0	0	4	4
Biezelingse Ham	51°26'53.40"N	3°55'49.79"E	0	0	0	51	51
Grevelingen	51°44'50.04"N	3°53'24.06"E	0	0	0	7	7
Ouistreham	49°16'16.40"N	0°14'12.20"W	1	0	1	5	7
Rade de Brest	48°24'13.10"N	4°21'16.00"W	0	2	0	0	2
Seine estuary	49°26'31.30"N	0°16'25.20"E	0	0	0	32	32
St. Vaast	49°34'38.60"N	1°16'38.80"W	1	3	0	0	4
Veerse Meer	51°33'12.24"N	3°52'25.34"E	0	5	0	4	9
		Total	2	10	1	103	116

5. DISCUSSION

5.1. RELIABILITY OF THE MORPHOMETRIC ASSIGNMENT METHOD

Of the 136 individuals of Saad & Wade (2016) identified morphologically, molecular and morphometric analyses yielded the same result for 86 % of the individuals.

The differences between both methods concern 19 specimens (14 %). Although these specimens come from seven different locations, the main discrepancies between both methods mainly concern two sites, Shoreham by Sea and Thornham, which account together for 14 of the 19 registered discrepancies.

The five diverging identifications concerning isolated individuals (i.e., 4A-7, Bix-202, IPS-4, Bar-236 and Lan-25) show a similar pattern. In all five cases, the disagreement concerns a single individual, genetically assigned to a different phylotype compared to a homogeneous group of specimens belonging to a single other phylotype. These five specimens are indicated with their ID number in Figure 3 and discussed separately hereafter:

(1) Specimen 4A-7. Brancaster Staithe high marsh – genotyped as T1 – morphologically assigned to T2. This individual has a mean pore diameter of 0.97 µm, far lower than the observed range of T1 (1.51–2.62 µm in Richirt et al., 2019a) and flush sutures. This

strongly suggests that this specimen is a T2, like all other specimens from this locality, for which genetic and morphometric identification are in agreement.

(2) Specimen Bix-202. Galmpton – genotyped as T1 – morphologically assigned to T2. This individual has a mean pore diameter of 1.25 µm, within the range of T2 (i.e., lower than 1.4 µm) and flush sutures, so that it is unlikely to be a T1. All other specimens investigated from this location are genotyped and morphologically assigned to T2.

(3) Specimen IPS-4. St. Osyth – genotyped as T1 – morphologically assigned to T6. This individual has an average pore diameter of 2.53 µm (> 2.4 µm) and clearly flush sutures, which are defining morphological traits of T6. The eight other individuals from this site were also morphologically assigned to T6, in agreement with molecular identification.

(4) Specimen Lan-25. Pen Clawdd – genotyped as T2 – morphologically assigned to T6. The mean pore diameter of Lan-25 (2.28 µm), is far too high for a T2 (< 1.4 µm), and additionally, the sutures in the central part of the spiral side are clearly flush, strongly suggesting that this is a T6. At this location, the other nine specimens were all identified as T6 by molecular and morphometric methods. It is interesting to note that among all the specimens investigated by Saad & Wade (2016) for which the sequences were deposited on GenBank (accession numbers KT153369 to KT153528), this individual (accession number KT153419) is the only one attributed to phylotype T2B by Bird et al. (2020). Otherwise, in the studied area, phylotype T2B has only been observed in Cork (south coast of Ireland, Bird et al., 2020).

(5) Specimen Bar-236. Barmouth – genotyped as T2 – morphologically assigned to T6. Bar-236 both has a mean pore diameter of 2.44 µm, far higher than the T2 range (< 1.4 µm), and clearly flush sutures, strongly suggesting that it is a T6 rather than a T2. Unlike the previously discussed individuals, this specimen is the only one morphologically assigned to T6 in a group of nine specimens which are all identified as T1 by molecular and morphometric methods.

Erroneous morphological assignments exist, especially in the case of damaged specimens, explaining why the rate of corresponding identification between molecular and morphological is not 100% (Richirt et al., 2019a). However, incorrect identification may also happen with molecular determination. Here, different causes are possible, such as 1) environmental contamination, which is impossible to control (presence of exogenous material on/in the shell,

e.g., propagules from another phylotype, maybe remains of preys if feeding on another phylotype (Hemleben et al., 1989) or 2) laboratory cross-contamination, that cannot be totally eliminated, even in case of very careful laboratory practice (Weiner et al., 2016).

For the five specimens discussed above, morphological observations (often based on more than one characteristic) and distributional evidence strongly suggests that in these cases the morphological determinations are correct:

(1) for four of the specimens (4A-7, Bix-202, Lan-25 and Bar-236), the pore diameter was completely out of the observed range of the phylotype as determined by Richirt et al. (2019a). In three of the specimens (4A-7, Bix-202 and IPS-4), suture elevation yielded an additional argument in favour of the morphological identification.

(2) In the first four specimens (4A-7, Bix-202, IPS-4, Lan-25), unlike the molecular determination, the morphological determination was the same as the molecular and morphometric determination of all other specimens of the assemblage, which were according to our observations morphologically always very similar as the individual in dissent.

At Shoreham-by-Sea, the ten individuals were all genetically assigned to T6 (Saad & Wade, 2016). When using the morphometric method, one specimen was assigned to T1 (Sho-7), seven to T2 (Sho-2, Sho-4, Sho-6 and Sho10-13), and two to T6 (Sho-3 and Sho-8). Among these individuals, Sho-8 was identified as T6 because of its average pore diameter of 1.41 µm, which is very close to the empirical threshold of 1.40 µm (Richirt et al., 2019a). However, it looks very much like a T2. Firstly, the average pore diameter is closer to T2 (< 1.40 µm) than to T6 (1.51–2.62 µm) according to Richirt et al. (2019a). Secondly, the chambers of this specimen are not inflated and very lunate (Supplementary Plate 1), which is a common feature in T2, but rarely encountered in T6, which generally shows more inflated and rectangular chambers. If this specimen is not a T6 but a T2 with slightly larger pores than the upper limit of 1.40 µm defined earlier, this would mean that the range of pore diameters exhibited by T2 has been slightly under-estimated by Richirt et al. (2019a). Conversely, it appears that individual Sho-3, with an average pore diameter of 1.57 µm, and inflated later chambers, is a real T6.

At Thornham, the seven specimens investigated here were all genetically assigned to T2 (Saad & Wade, 2016), except for 5A-15 which was genetically assigned to T6. Conversely, all specimens were assigned to T6 using the morphometric method; their average pore diameter

(1.91 to 3.08 µm) was largely above the empirical upper threshold of T2 of 1.4 µm, as determined by Richirt et al. (2019a).

While genetic misidentification may occur for single specimens, the systematic discrepancy observed in Shoreham-by-Sea and Thornham sites, which concerns nearly all specimens, suggests a different explanation. When using morphological criteria, seven of the specimens of Shoreham-by-Sea (eight if we include Sho-8 which has a pore diameter of 1.41 µm) were unambiguously attributed to T2, on the basis of their average pore diameter (< 1.40 µm), whereas they were genotyped as T6. Inversely, six of the seven specimens of Thornham were unambiguously attributed morphologically to T6 (average pore diameter > 1.4 µm and clearly flush sutures), whereas they were all genotyped as T2.

As shown in Richirt et al. (2019a), the mean pore diameter is a very efficient criterion to discriminate between T2 and T1/T6 with a very high accuracy (97 %), sensitivity (93 %) and specificity (98 %). All specimens (except Sho-8) are far away from the threshold value of 1.40 µm, so that it seems highly improbable that the morphological determination is incorrect. The fact that the molecular determinations give exactly the opposite results (T6 instead of T2 at one site, T2 instead of T6 at the other site) made us wonder whether the samples of these two sites could not have been inverted for molecular analyses. This would explain the observed discrepancies and restore the high consistency between genetic and morphological assignation methods.

In order to unravel this question, we sequenced eight new individuals from Thornham in September 2018. The sequences for these eight specimens are deposited in GenBank under accession numbers MN165720 to MN165727. All eight individuals were molecularly identified as T6 after comparison with earlier published T6 sequences and were also identified as T6 morphologically under a stereomicroscope using criteria described in Richirt et al. (2019a). These new sequences strongly suggest that T6 is the only phylotype present at this location (as suggested by morphological identification), and corroborates our hypothesis that molecular samples of Thornham and Shoreham-by-Sea have been inverted.

If we do not consider the Shoreham-by-Sea (10 individuals) and Thornham (7 individuals) sites, the comparison of the morphometric identification and the genetic assignment for the 119 remaining individuals indicates that only five individuals were misidentified (i.e., 4A-7, Bix-202, IPS-4, Bar-236 and Lan-25). This would increase the rate of identical phylotype assignation for the genetic and morphological methods to about 96 %, in accordance with the success rate of Richirt et al. (2019a).

The range of measured average pore diameter for the 28 individuals of T2 was very close to that given by Richirt et al., 2019a (0.76–1.41 µm for this study compared to 0.77–1.32 µm). However, a single specimen (Sho-8, with an average pore diameter of 1.41 µm) surpassed the empirical threshold of 1.40 µm defined by Richirt et al. (2019a) and used to discriminate T2 and T1/T6. This suggests that the threshold value for average pore diameter should be slightly increased, up to 1.45 µm, to include the whole variability observed until now. For the 14 specimens of T1, the range of average pore diameter was very close to the range observed by Richirt et al., 2019a: 1.63–2.49 µm in this study compared to 1.51–2.62 µm. Finally, for T6, the range of observed mean pore diameters (1.46 to 3.84 µm) includes some slightly higher values than the range described by Richirt et al. (2019a; 1.92–3.55 µm). This confirms that more morphometric studies are necessary to have a better knowledge of pore size variability between different populations across geographical ranges.

5.2. GEOGRAPHICAL DISTRIBUTION OF T1, T2 AND T6 AROUND THE BRITISH ISLES

In this section we will present an update of the distributional data for the three investigated phylotypes. We will base our inventory both on genetic and morphometric determinations, but will favour morphological determinations in case of discrepancy (*i.e.*, as discussed for the Saad & Wade dataset in the previous section, and for some individuals used in Richirt et al., 2019a, see Material and Methods section for details).

Figure 4 presents a composite map of the three datasets aggregating (1) the 136 specimens of Saad & Wade (2016), which were determined here by morphological criteria, (2) the 116 individuals investigated in the context of the AMTEP project and (3) the 251 individuals investigated by Bird et al. (2020). Together, the three datasets represent 503 individuals of 38 different sites (the three sites from Dartmouth in Bird et al., in press are considered as a single location, and the Grevelingen site is present in both AMTEP and Bird et al., 2020 datasets). These 503 individuals account for 312 specimens belonging to phylotype T6, 167 to phylotype T2 (with T2A and T2B merged) and 24 to phylotype T1.

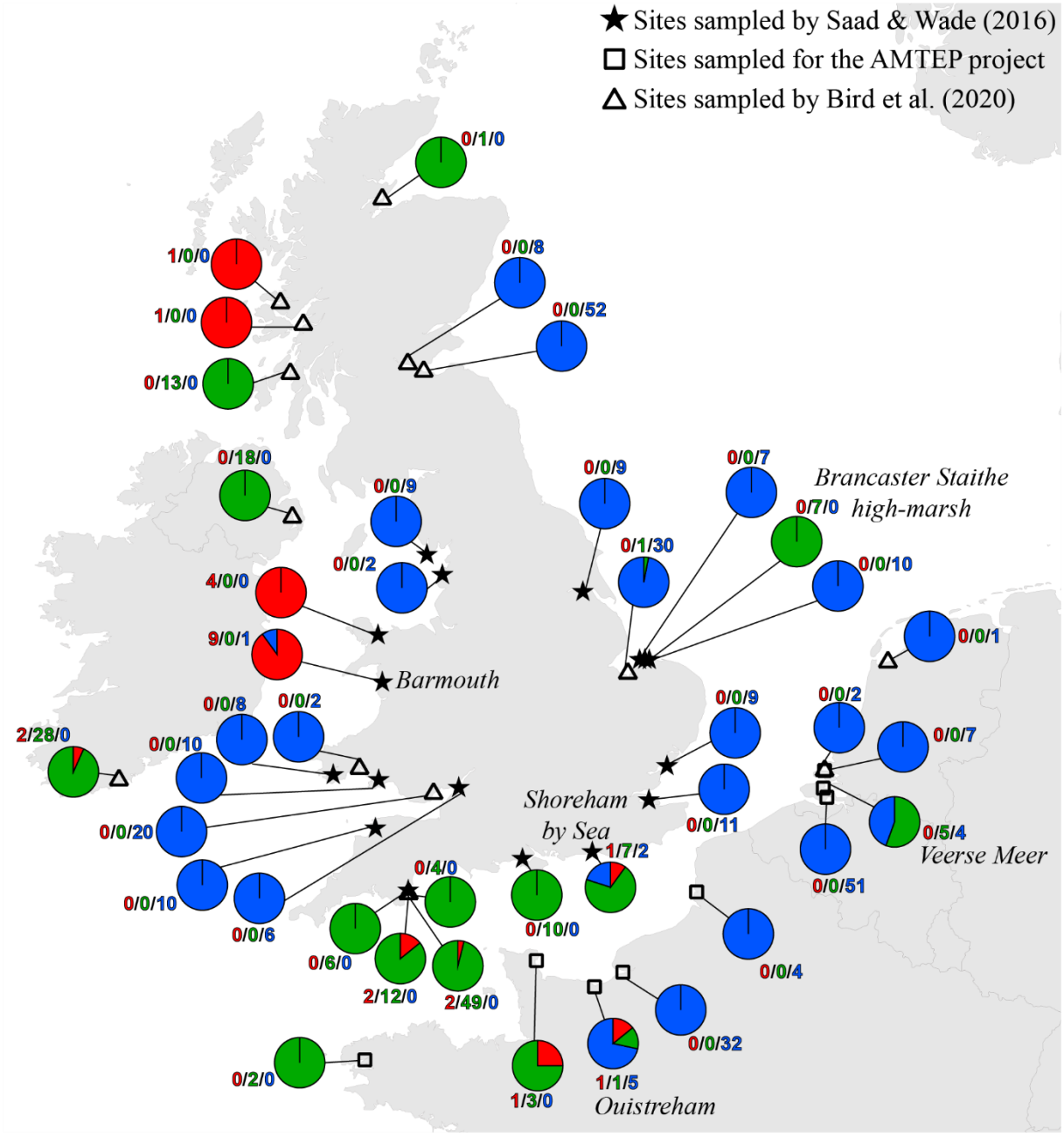

Figure 4. Distribution map showing the number of individuals for the three phylotypes (T1/T2/T6), combining the data from this study (stars, morphological identification of the available individuals from Saad & Wade, 2016), from the AMTEP project (squares, based on genetic identification and morphology for specimens used in Richirt et al., 2019a) and from Bird et al., in press (triangles, based on genetic identification). The peculiar sites discussed in the text later - i.e., Barmouth, Ouistreham, Shoreham-by-Sea, Brancaster Staithe high-marsh and Veerse Meer are indicated in italic.

Figure 4 presents a highly consistent biogeographical pattern, which was not fully recognised by earlier authors (Saad & Wade, 2016; Bird et al., 2020). Phylotype T6 is strongly dominant on the eastern coast of England, as well as in the Bay of Liverpool and Bristol Channel. Phylotype T2 is dominant on the English Channel coast (both on the south coast of England and on the northwest coast of France). It is also dominant at two sites in Ireland and one site in west Scotland, whereas a single individual was genotyped at a site in north Scotland.

Furthermore, T2 is also dominant at two isolated sites, where it is surrounded by T6 populations, one on the Norfolk coast (*i.e.*, Brancaster Staithe high-marsh) and one in the Netherlands (*i.e.*, Veerse Meer, inner part of the Eastern Scheldt estuary). Finally, phylotype T1 is dominant at two sites in Wales (*i.e.*, Barmouth and Bangor), whereas two single individuals were found at two sites in Scotland. The two sites in Wales are bordered by T6 populations both in the north and south (Bay of Liverpool and Bristol Channel, respectively).

It is interesting to note that the co-occurrence of different phylotypes at the same site is rare; only nine of the 40 sites show a co-occurrence of at least two phylotypes. In all cases, one of the phylotypes is strongly dominant. The single exception is the Veerse Meer site in the Netherlands, where T2 and T6 are found in similar proportions (5 and 4 individuals, respectively). Since the three phylotypes are now considered as separated species (Pawlowski et al, 1995; Holzmann et al., 1996; Holzmann, 2000; Holzmann & Pawlowski, 2000; Langer & Leppig, 2000; Schweizer et al., 2011a, b), it may be expected that their ecological niches are slightly different. This suggests that at each individual site, one of the three phylotypes should be favoured by the environmental conditions, explaining its strong dominance.

However, if entire estuaries are considered, the co-occurrence of several phylotypes (at different locations within the estuary) appears to be common, such as observed at the Brancaster Staithe high and low-marsh sites, dominated by T2 and T6, respectively (Saad & Wade, 2016). Other examples are the Vie estuary and the Auray river (Gulf of Morbihan) both on the French Atlantic coast, where both phylotypes T1 and T2 are found, but in different proportions, depending on the exact location in the estuary (Fouet et al., Schweizer et al., work in progress).

At a global scale, phylotype T1 is considered cosmopolitan, whereas T2 seems to be restricted to the north Atlantic (Holzmann & Pawlowski, 2000; Hayward et al., 2004). Concerning T6, because of its disjoint global distribution (*i.e.*, Asia and Europe), it has been suggested that it has its origins in Asia and may be allochthonous in Europe. In fact, T6 arrived around 2000 in the Kiel fjord (Polovodova et al., 2009; Schweizer et al., 2011b) and in Hanö Bay in Baltic Sea (Bird et al., 2020), where no *Ammonia* species were present before (Hermelin, 1987; Murray, 2006). It may have been introduced by an anthropogenic vector such as ship ballast water (Pawlowski & Holzmann, 2008), as already hypothesized for *Haynesina germanica* (Calvo-Marcilese & Langer, 2010) or together with imported Japanese oysters (after mass mortality of local oysters in Europe in the 1960s, Wolff & Reise, 2002).

If phylotype T6 is indeed invasive, it may be expected that it has spread out progressively and has replaced autochthonous phylotypes T1 and/or T2 at most sites where it is found now. The fact that “only” 55 % of the sampled sites are dominated by T6 could mean that the

autochthonous phylotypes T1 and T2 are better adapted to the environmental conditions at some of the remaining sites. For example, the two sites with T2 populations surrounded by T6 dominated faunas in Brancaster Staithe high-marsh and in the Veerse Meer are positioned at higher elevation, and in the inner part of the estuary, respectively. This could suggest that a weaker marine influence is unfavourable for T6.

Alternatively, the observed pattern could also suggest that the replacement of the autochthonous phylotypes by T6 is not yet finished, and that T6 may further extend its distributional area in the near future. This hypothesis is corroborated by the localisation of the sites where T6 is co-occuring with T1 and/or T2. These sites are (1) Shoreham-by-Sea, where two T6 specimens were found in a community dominated by T2, (2) Barmouth, where one T6 was found in an assemblage composed only of T1, and (3) Ouistreham, where five T6 are found with one T1 and one T2 (Figure 4). Although the low numbers of observed specimens make it impossible to make firm conclusions, it is remarkable that these three sites are all bordered on one side by sites exclusively inhabited by T6 (eastward for Shoreham-by-Sea and Ouistreham, and southward for Barmouth, Figure 4). If we assume that phylotype T6 is indeed invasive, and progressively takes over the niches of the autochthonous phylotypes, these localities could represent its "front of progression".

5.3. PUTATIVE HYDRODYNAMIC CONTROL ON THE GEOGRAPHICAL DISTRIBUTION OF *AMMONIA* PHYLOTYPES

Because of their small size and inability for active displacement over large distances, foraminifera migration will probably mainly depend on propagule dispersal by mesoscale spatial hydrodynamic features (*e.g.*, tidal residual currents, wind-driven currents, gyres; Ellien et al., 2000). These features have earlier been identified as decisive for the transport of microorganisms over long distances (Salomon & Breton, 1993; Bailly du Bois & Dumas, 2005). In the case of benthic foraminifera, reports of their presence in sediment traps (Brunner & Biscaye, 1997; 2003; Kuhnt et al., 2013) and planktonic eDNA samples (Morard et al., 2019) suggest that transport in the water column may be rather common. The fact that foraminiferal propagules may be dormant for several years (Alve & Goldstein, 2010) further increases their dispersal potential. In view of this, it appears that the direction and intensity of bottom as well as water column currents could be determinant for the transport of foraminiferal propagules away from their source populations.

The English Channel is famous for its strong tidal currents, including currents with a periodicity of the order of one week to one year (*i.e.*, residual tidal currents, Salomon & Breton,

1993). Although the main water mass circulation through the Channel is NE-ward, from the open Atlantic Ocean to the North Sea, numerous secondary gyres generated by tidal currents are present, especially around the Cotentin Peninsula along the French coast, limiting exchanges between the eastern and the western part of the peninsula (Salomon & Breton, 1991, 1993; Cugier & Le Hir, 2002). Previously, the English Channel has been divided into two basins by Dauvin (2012), the Western and the Eastern Basin, with a boundary at the Cotentin Peninsula (Figure 5). This subdivision was based on differences in general oceanographic characteristics, biological components and human activity. In fact, many studies on the hydrodynamics and larval dispersal in the English Channel have shown that there is a major biogeographic boundary which strongly limits larvae transport between the areas to the east and west of the Cotentin Peninsula (*e.g.*, Ellien et al., 2000; Lefebvre et al., 2003; Dupont et al., 2003; 2007). Additionally, transport between French and English coasts seems strongly limited in the western part of the English Channel, but was shown to occur in the eastern part (Barnay et al., 2003, Lefebvre et al., 2003).

If we hypothesize that *Ammonia* sp. T6 is an invasive phylotype which is still expanding, the major biogeographical boundary in the English Channel, which appears to be related to the overall current pattern, could explain why T6 has not yet colonised the south England Coast and the French western part of the English Channel. The remaining sites dominated by T2 in the Irish Sea could be the consequence of similar biogeographic barriers (See Supplementary Figure 1). Evidently, as it is not yet proved that T6 is indeed an invasive exotic phylotype, this hypothesis is still speculative.

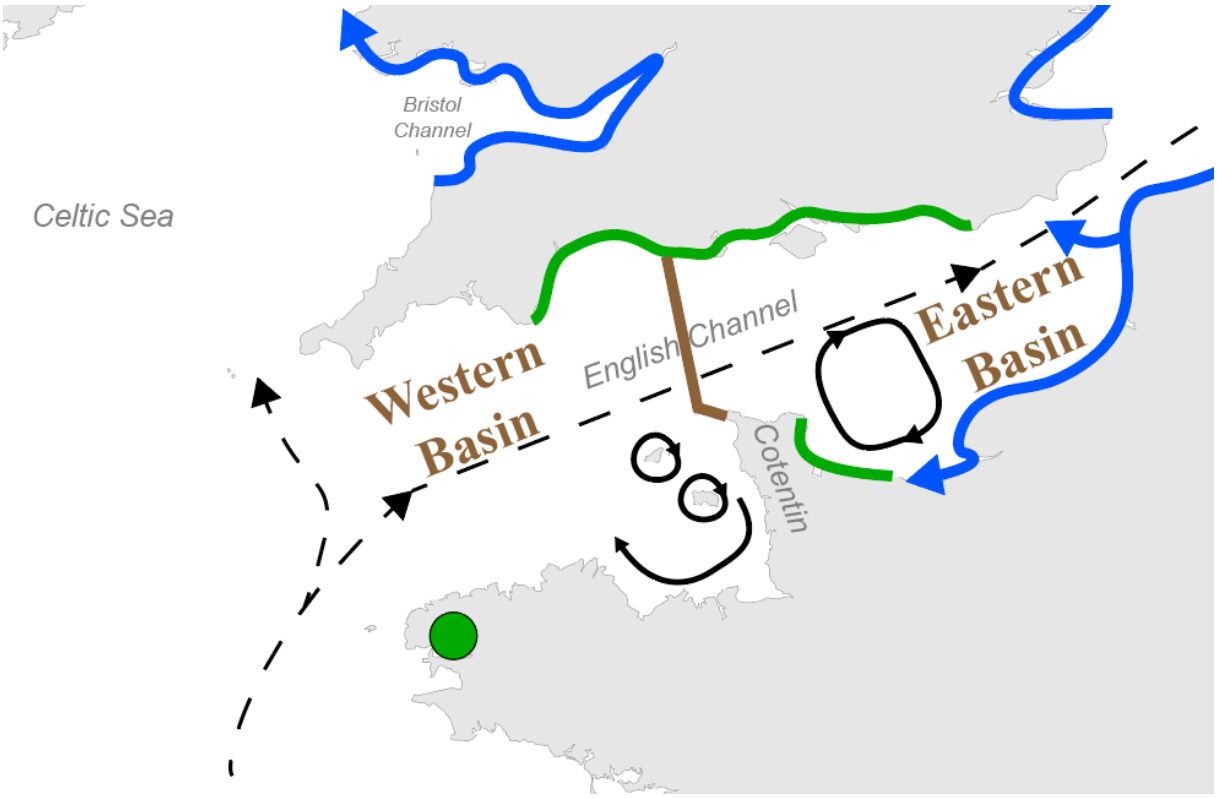

Figure 5. Map displaying the general circulation of water masses in the English Channel. Black dashed arrows represent the residual currents and black plain arrows represent the main gyres in the Channel (Salomon & Breton, 1993; Dupont et al., 2007). The separation between the Western and Eastern Basins of the English Channel is represented by the red line (from Dauvin, 2012). The putative distributional area of phylotypes T2 and T6 are represented by green and blue lines, respectively. Blue arrows indicate the hypothesised direction of progression of the phylotype T6.

5.4. LIMITATIONS OF THE PRESENT STUDY

5.4.1. Geographical sampling coverage.

Although the 503 individuals sampled at 38 different sites give a good general overview of the geographical distribution of T1, T2 and T6, it is evident that the sampling coverage is far too limited to allow a detailed analysis of the geographical distribution and ecological preferences of each of the three phylotypes. In fact, the present data set suffers from two main limitations, which are largely due to the fact that molecular identification is a rather expensive and time-consuming method:

(1) there is usually only one sample per estuary, whereas the scarce available data show that in many estuaries, two or even three phylotypes are present, which occupy different parts of the estuary.

(2) in most cases, only a few individuals were sampled at each site (rarely more than 10 individuals), which is insufficient to draw firm conclusions about the eventual co-occurrence of two or even three phylotypes at a single sampling site.

Fortunately, now that it has been shown that the three phylotypes can be distinguished by morphometric analysis with a high degree of reliability (about 95 %, Richirt et al., 2019a; results of this study), it has become possible to rapidly generate large amounts of data. The combination with eDNA surveys of the same areas (work in progress, Schweizer et al. in prep.) could also speed up the sampling coverage. Consequently, the biogeographical patterns presented here will certainly be refined (and where necessary, corrected) in the next few years.

5.4.2. Temporal scale

The absolute and relative densities of the three phylotypes may show a large seasonal and inter-annual variability, as has been shown by most of the temporal studies of estuarine foraminiferal faunas (*e.g.*, Lutze, 1968; Wefer, 1976; Murray, 1983; Cearreta, 1988; Murray, 1992; Gustafsson & Nordberg, 1999; Murray & Alve, 2000; Korsun & Hald, 2000; Morvan et al., 2006; Horton & Murray, 2007; Papaspyrou et al., 2013; Saad & Wade, 2017; Richirt et al., 2019b, Choquel et al., in prep.). Although different species appear to show different reproduction and growth periods, this has not yet been demonstrated for the *Ammonia* phylotypes. It is evident that temporal studies at a seasonal scale are needed to investigate this aspect. The presence of such putative seasonal or inter-annual differences between phylotypes will also inform us about their ecological preferences.

5.4.3. Ecological niches

The environmental conditions at local and regional scales favouring the three phylotypes will constitute a pre-requisite for their settlement. However, at this very moment, no clear correlation between the distribution pattern (both at a regional scale and within single estuaries) of the three phylotypes and associated environmental conditions has emerged (Saad & Wade, 2016; Bird et al., 2020; present study). This highlights the fact that the controlling parameters of the distribution patterns of the different phylotype are not well known yet and need to be studied in more detail.

6. CONCLUSION

The results of this study support the reliability of the morphometric method to distinguish phylotypes T1, T2 and T6 of the genus *Ammonia*. If we do not consider two sites for which genetic assignation is questionable (Thornham and Shoreham by Sea), the correspondence between morphometric and molecular identification is ~ 95 %. This study represents the first large scale application of the morpholometric determination method to discriminate the *Ammonia* phylotypes T1, T2 and T6. The combined morphological-molecular dataset presented here unveils the presence of a clear and coherent distribution pattern around the British Isles coasts, which was not fully recognised by previous molecular studies. The overall distribution pattern suggests that the supposedly invasive phylotype T6 progressively extends its distributional area and replaces the autochthonous T1 and T2 phylotypes. However, in the area where T6 is strongly dominant, phylotype T2 seems to subsist in refuges, positioned in higher and more inward parts of estuaries. The large-scale general distribution pattern suggests that the spreading of T6 in the English Channel may be slowed down or hampered by the presence of a major biogeographical boundary, related to the dominant current patterns. Finally, the confirmation of the strong reliability of the morphometric determination method should allow us to work confidently on foraminiferal material, avoiding systematic molecular identification of specimens, which is both expensive and time-consuming. This will allow us to rapidly generate large data sets, and thereby gain insight in the ecological differences between the three phylotypes. The morphometric analysis of sub-recent/fossil material, for which molecular study is still very difficult, if not impossible, will allow us to study historical changes in distribution patterns (for instance due to changing anthropogenic pressure) and to verify the putative invasive character of phylotype T6.

ACKNOWLEDGEMENTS

This study has partly been financed by the CNRS/INSU program EC2CO-LEFE. We are grateful to Romain Mallet and the team of the SCIAM imaging facility at the University of Angers for the SEM images. We gratefully acknowledge the help of many colleagues who provided samples.

REFERENCES

Alve, E., 1995. Benthic foraminiferal responses to estuarine pollution; a review. Journal of Foraminiferal Research 25, 190–203. https://doi.org/10.2113/gsjfr.25.3.190

Alve, E., Goldstein, S.T., 2010. Dispersal, survival and delayed growth of benthic foraminiferal propagules. Journal of Sea Research 63, 36–51. https://doi.org/10.1016/j.seares.2009.09.003

Bailly Du Bois, P., Dumas, F., Bailly Du Bois, P., Dumas, F., 2005. TRANSMER, hydrodynamic model for medium- and long-term simulation of radionuclides transfers in the English Channel and southern North Sea. Radioprotection 40. https://doi.org/10.1051/radiopro:2005s1-084

Barnay, A., Ellien, C., Gentil, F., Thiébaut, E., 2003. A model study on variations in larval supply: are populations of the polychaete Owenia fusiformis in the English Channel open or closed? Helgoland Marine Research 56, 229. https://doi.org/10.1007/s10152-002-0122-2

Bird, C., Schweizer, M., Roberts, A., Austin, W.E.N., Knudsen, K.L., Evans, K.M., Filipsson, H.L., Sayer, M.D.J., Geslin, E., Darling, K.F., 2020. The genetic diversity, morphology, biogeography, and taxonomic designations of Ammonia (Foraminifera) in the Northeast Atlantic. Marine Micropaleontology 155, 101726. https://doi.org/10.1016/j.marmicro.2019.02.001

Bouchet, V.M.P., Debenay, J.-P., Sauriau, P.-G., Radford-Knoery, J., Soletchnik, P., 2007. Effects of short-term environmental disturbances on living benthic foraminifera during the Pacific oyster summer mortality in the Marennes-Oléron Bay (France). Marine Environmental Research 64, 358–383. https://doi.org/10.1016/j.marenvres.2007.02.007

Bradshaw, J.S., 1957. Laboratory Studies on the Rate of Growth of the Foraminifer, "Streblus beccarii (Linné) var. tepida (Cushman)." Journal of Paleontology 31, 1138–1147.

Brunner, C.A., Biscaye, P.E., 2003. Production and resuspension of planktonic foraminifers at the shelf break of the Southern Middle Atlantic Bight. Deep Sea Research Part I: Oceanographic Research Papers 50, 247–268. https://doi.org/10.1016/S0967-0637(02)00165-6

Brunner, C.A., Biscaye, P.E., 1997. Storm-driven transport of foraminifers from the shelf to the upper slope, southern Middle Atlantic Bight. Continental Shelf Research 17, 491–508. https://doi.org/10.1016/S0278-4343(96)00043-X

Calvo-Marcilese, L., Langer, M.R., 2010. Breaching biogeographic barriers: the invasion of Haynesina germanica (Foraminifera, Protista) in the Bahía Blanca estuary, Argentina. Biol Invasions 12, 3299–3306. https://doi.org/10.1007/s10530-010-9723-x

Cearreta, A., 1988. Population dynamics of benthic foraminifera in the Santoña estuary, Spain. Revue de Paléobiologie 2, 721–724.

Cugier, P., Le Hir, P., 2002. Development of a 3D Hydrodynamic Model for Coastal Ecosystem Modelling. Application to the Plume of the Seine River (France). Estuarine, Coastal and Shelf Science 55, 673–695. https://doi.org/10.1006/ecss.2001.0875

Dauvin, J.-C., 2012. Are the eastern and western basins of the English Channel two separate ecosystems? Marine Pollution Bulletin 64, 463–471. https://doi.org/10.1016/j.marpolbul.2011.12.010

Dupont, L., Ellien, C., Viard, F., 2007. Limits to gene flow in the slipper limpet Crepidula fornicata as revealed by microsatellite data and a larval dispersal model. Marine Ecology Progress Series 349, 125–138. https://doi.org/10.3354/meps07098

Dupont, L., Jollivet, D., Viard, F., 2003. High genetic diversity and ephemeral drift effects in a successful introduced mollusc (Crepidula fornicata: Gastropoda). Marine Ecology Progress Series 253, 183–195. https://doi.org/10.3354/meps253183

Ellien, C., Thiebaut, É., Barnay, A.-S., Dauvin, J.-C., Gentil, F., Salomon, J.-C., 2000. The influence of variability in larval dispersal on the dynamics of a marine metapopulation in the eastern Channel. Oceanologica Acta 23, 423–442. https://doi.org/10.1016/S0399-1784(00)00136-5

Geslin, E., Barras, C., Langlet, D., Nardelli, M.P., Kim, J.-H., Bonnin, J., Metzger, E., Jorissen, F.J., 2014. Survival, Reproduction and Calcification of Three Benthic Foraminiferal Species in Response to Experimentally Induced Hypoxia, in: Kitazato, H., M. Bernhard, J. (Eds.), Approaches to Study Living Foraminifera: Collection, Maintenance and Experimentation, Environmental Science and Engineering. Springer Japan, Tokyo, pp. 163–193. https://doi.org/10.1007/978-4-431-54388-6_10

Gupta, B.K.S., 2007. Modern Foraminifera. Springer Science & Business Media.371 p.

Gustafsson, M., Nordberg, K., 1999. Benthic foraminifera and their response to hydrography, periodic hypoxic conditions and primary production in the Koljö fjord on the Swedish west coast. Journal of Sea Research 41, 163–178. https://doi.org/10.1016/S1385-1101(99)00002-7

Hayward, B.W., Holzmann, M., Grenfell, H.R., Pawlowski, J., Triggs, C.M., 2004. Morphological distinction of molecular types in Ammonia – towards a taxonomic revision of the world's most

commonly misidentified foraminifera. Marine Micropaleontology 50, 237–271. https://doi.org/10.1016/S0377-8398(03)00074-4
Hemleben, C., Spindler, M., Anderson, O.R., 1989. Modern Planktonic Foraminifera. Springer-Verlag.363 p.
Hermelin, J.O.R., 1987. Distribution of Holocene benthic foraminifera in the Baltic Sea. Journal of Foraminiferal Research 17, 62–73. https://doi.org/10.2113/gsjfr.17.1.62
Holzmann, M., 2000. Species Concept in Foraminifera: Ammonia as a Case Study. Micropaleontology 46, 21–37.
Holzmann, M., Pawlowski, J., 2000. Taxonomic relationships in the genus Ammonia (Foraminifera) based on ribosomal DNA sequences. Journal of Micropalaeontology 19, 85–95. https://doi.org/10.1144/jm.19.1.85
Holzmann, M., Pawlowski, J., 1997. Molecular, morphological and ecological evidence for species recognition in Ammonia (Foraminifera). Journal of Foraminiferal Research 27, 311–318. https://doi.org/10.2113/gsjfr.27.4.311
Holzmann, M., Piller, W., Pawlowski, J., 1996. Sequence variations in the large-subunit ribosomal RNA gene of ammonia (foraminifera, protozoa) and their evolutionary implications. J Mol Evol 43, 145–151. https://doi.org/10.1007/BF02337359
Horton, B.P., Murray, J.W., 2007. The roles of elevation and salinity as primary controls on living foraminiferal distributions: Cowpen Marsh, Tees Estuary, UK. Marine Micropaleontology 63, 169–186. https://doi.org/10.1016/j.marmicro.2006.11.006
Jones, R.W., 2013. Foraminifera and their Applications. Cambridge University Press.391 p.
Katz, M.E., Cramer, B.S., Franzese, A., Hönisch, B., Miller, K.G., Rosenthal, Y., Wright, J.D., 2010. Traditional and emerging geochemical proxies in foraminifera. Journal of Foraminiferal Research 40, 165–192. https://doi.org/10.2113/gsjfr.40.2.165
Korsun, S., Hald, M., 2000. Seasonal dynamics of benthic foraminifera in a glacially fed fjord of Svalbard, European arctic. Journal of Foraminiferal Research 30, 251–271. https://doi.org/10.2113/0300251
Kuhnt, T., Howa, H., Schmidt, S., Marié, L., Schiebel, R., 2013. Flux dynamics of planktic foraminiferal tests in the south-eastern Bay of Biscay (northeast Atlantic margin). Journal of Marine Systems, XII International Symposium on Oceanography of the Bay of Biscay 109–110, S169–S181. https://doi.org/10.1016/j.jmarsys.2011.11.026
Langer, M., Leppig, U., 2000. Molecular phylogenetic status of Ammonia catesbyana (D'Orbigny, 1839), an intertidal foraminifer from the North Sea. Neues Jahrbuch fur Geologie und Palaontologie Monatshefte 9, 545–556.
Lefebvre, A., Ellien, C., Davoult, D., Thiébaut, E., Salomon, J.C., 2003. Pelagic dispersal of the brittle-star Ophiothrix fragilis larvae in a megatidal area (English Channel, France) examined using an advection/diffusion model. Estuarine, Coastal and Shelf Science 57, 421–433. https://doi.org/10.1016/S0272-7714(02)00371-2
Lutze, G.F., 1968. Jahresgang der Foraminiferen-Fauna in der Bottsand-Lagune (westliche Ostsee). Meyniana 18, 13–20. https://doi.org/10.2312/meyniana.1968.18.13
Morard, R., Vollmar, N.M., Greco, M., Kucera, M., 2019. Unassigned diversity of planktonic foraminifera from environmental sequencing revealed as known but neglected species. Plos One 14, e0213936. https://doi.org/10.1371/journal.pone.0213936
Morvan, J., Debenay, J.-P., Jorissen, F., Redois, F., Bénéteau, E., Delplancke, M., Amato, A.-S., 2006. Patchiness and life cycle of intertidal foraminifera: Implication for environmental and paleoenvironmental interpretation. Marine Micropaleontology, Foraminifera and Environmental Micropaleontology 61, 131–154. https://doi.org/10.1016/j.marmicro.2006.05.009
Murray, J.W., 2006. Ecology and Applications of Benthic Foraminifera. Cambridge University Press. 426 p.
Murray, J.W., 1992. Distribution and population dynamics of benthic foraminifera from the southern North Sea. Journal of Foraminiferal Research 22, 114–128. https://doi.org/10.2113/gsjfr.22.2.114
Murray, J.W., 1983. Population dynamics of benthic foraminifera; results from the Exe Estuary, England. Journal of Foraminiferal Research 13, 1–12. https://doi.org/10.2113/gsjfr.13.1.1
Murray, J.W., Alve, E., 2000. Major aspects of foraminiferal variability (standing crop and biomass) on a monthly scale in an intertidal zone. Journal of Foraminiferal Research 30, 177–191. https://doi.org/10.2113/0300177
Papaspyrou, S., Diz, P., García-Robledo, E., Corzo, A., Jimenez-Arias, J.-L., 2013. Benthic foraminiferal community changes and their relationship to environmental dynamics in intertidal muddy sediments (Bay of Cádiz, SW Spain). Marine Ecology Progress Series 490, 121–135. https://doi.org/10.3354/meps10447

Pawlowski, J., 2000. Introduction to the Molecular Systematics of Foraminifera. Micropaleontology 46, 1–12.

Pawlowski, J., Bolivar, I., Farhni, J., Zaninetti, L., 1995. DNA analysis of "Ammonia beccarii" morphotypes: one or more species? Marine Micropaleontology 26, 171–178. https://doi.org/10.1016/0377-8398(95)00022-4

Pawlowski, J., Holzmann, M., 2008. Diversity and geographic distribution of benthic foraminifera: a molecular perspective. Biodiversity and Conservation 17, 317–328. https://doi.org/10.1007/s10531-007-9253-8

Petersen, J., Riedel, B., Barras, C., Pays, O., Guihéneuf, A., Mabilleau, G., Schweizer, M., Meysman, F.J.R., Jorissen, F.J., 2016. Improved methodology for measuring pore patterns in the benthic foraminiferal genus Ammonia. Marine Micropaleontology 128, 1–13. https://doi.org/10.1016/j.marmicro.2016.08.001

Polovodova, I., Nikulina, A., Schönfeld, J., Dullo, W.-C., 2009. Recent benthic foraminifera in the Flensburg Fjord (Western Baltic Sea). Journal of Micropalaeontology 28, 131–142. https://doi.org/10.1144/jm.28.2.131

Richirt, J., Schweizer, M., Bouchet, V.M.P., Mouret, A., Quinchard, S., Jorissen, F.J., 2019. Morphological distinction of three Ammonia phylotypes occurring along European coasts. Journal of Foraminiferal Research 49, 77–94.

Saad, S.A., Wade, C.M., 2017. Seasonal and spatial variations of saltmarsh benthic foraminiferal communities from North Norfolk, England. Microbial Ecology 73, 539–555. https://doi.org/10.1007/s00248-016-0895-5

Saad, S.A., Wade, C.M., 2016. Biogeographic distribution and habitat association of Ammonia genetic variants around the coastline of Great Britain. Marine Micropaleontology 124, 54–62. https://doi.org/10.1016/j.marmicro.2016.01.004

Salomon, J.-C., Breton, M., 1993. An atlas of long-term currents in the channel. Oceanologica Acta 16, 439–448.

Schweizer, M., Jorissen, F., Geslin, E., 2011a. Contributions of molecular phylogenetics to foraminiferal taxonomy: General overview and example of Pseudoeponides falsobeccarii Rouvillois, 1974. Comptes Rendus Palevol 10, 95–105. https://doi.org/10.1016/j.crpv.2011.01.003

Schweizer, M., Polovodova, I., Nikulina, A., Schönfeld, J., 2011b. Molecular identification of Ammonia and Elphidium species (Foraminifera, Rotaliida) from the Kiel Fjord (SW Baltic Sea) with rDNA sequences. Helgoland Marine Research 65, 1–10. https://doi.org/10.1007/s10152-010-0194-3

Wefer, G., 1976. Umwelt, Produktion und Sedimentation benthischer Foraminiferen in der westlichen Ostsee. PhD dissertation, Christian-Albrechts-University in Kiel.

Weiner, A.K.M., Morard, R., Weinkauf, M.F.G., Darling, K.F., André, A., Quillévéré, F., Ujiie, Y., Douady, C.J., de Vargas, C., Kucera, M., 2016. Methodology for single-cell genetic analysis of planktonic foraminifera for studies of protist diversity and evolution. Frontiers in Marine Science 3:255. https://doi.org/10.3389/fmars.2016.00255

Wolff, W.J., Reise, K., 2002. Oyster imports as a vector for the introduction of alien species into Northern and Western European coastal waters, in: Leppäkoski, E., Gollasch, S., Olenin, S. (Eds.), Invasive Aquatic Species of Europe. Distribution, Impacts and Management. Springer Netherlands, Dordrecht, pp. 193–205. https://doi.org/10.1007/978-94-015-9956-6_21

SUPPLEMENTARY INFORMATION

Supplementary Table 1. Site, ID, genetic identification, average pore diameter, sutures and morphological identification of all the individuals from Saad & Wade (2016) investigated in this study.

Site	ID_ind	Genetic identification (from Saad & Wade, 2016)	Average pore diameter (µm)	Sutures (raised/flush)	Morphological identification
Bangor	Ban-167	T1	ND	ND	ABSENT
Bangor	Ban-169	T1	2.35	raised	T1
Bangor	Ban-170	T1	1.71	raised	T1
Bangor	Ban-171	T1	2.28	raised	T1
Bangor	Ban-173	T1	2.46	raised	T1
Barmouth	Bar-236	T2	2.44	flush	T6
Barmouth	Bar-238	T1	2.06	raised	T1
Barmouth	Bar-240	T1	1.63	raised	T1
Barmouth	Bar-242	T1	1.94	raised	T1
Barmouth	Bar-243	T1	2.19	raised	T1
Barmouth	Bar-244	T1	2.06	raised	T1
Barmouth	Bar-247	T1	2.16	raised	T1
Barmouth	Bar-248	T1	2.22	raised	T1
Barmouth	Bar-253	T1	2.00	raised	T1
Barmouth	Bar-261	T1	2.49	raised	T1
Barrow-in-Furness	BIF-223	T6	2.34	flush	T6
Barrow-in-Furness	BIF-224	T6	2.60	flush	T6
Barrow-in-Furness	BIF-226	T6	2.13	flush	T6
Barrow-in-Furness	BIF-227	T6	3.37	flush	T6
Barrow-in-Furness	BIF-228	T6	2.37	flush	T6
Barrow-in-Furness	BIF-240	T6	2.05	flush	T6
Barrow-in-Furness	BIF-246	T6	2.13	flush	T6

Barrow-in-Furness	BIF-251	T6	2.20	flush	T6
Barrow-in-Furness	BIF-258	T6	2.01	flush	T6
Barton-Upon-Humber	Hull-25	T6	2.37	flush	T6
Barton-Upon-Humber	Hull-26	T6	1.57	flush	T6
Barton-Upon-Humber	Hull-28	T6	2.38	flush	T6
Barton-Upon-Humber	Hull-30	T6	2.33	flush	T6
Barton-Upon-Humber	Hull-31	T6	2.10	flush	T6
Barton-Upon-Humber	Hull-34	T6	1.69	flush	T6
Barton-Upon-Humber	Hull-35	T6	1.85	flush	T6
Barton-Upon-Humber	Hull-36	T6	2.59	flush	T6
Barton-Upon-Humber	Hull-37	T6	1.55	flush	T6
Brancaster (high marsh)	4A-14	T2	0.91	flush	T2
Brancaster (high marsh)	4A-16	T2	0.86	flush	T2
Brancaster (high marsh)	4A-20	T2	0.78	flush	T2
Brancaster (high marsh)	4A-21	T2	ND	ND	ABSENT
Brancaster (high marsh)	4A-22	T2	0.77	flush	T2
Brancaster (high marsh)	4A-24	T2	0.76	flush	T2
Brancaster (high marsh)	4A-6	T2	0.92	flush	T2
Brancaster (high marsh)	4A-7	T1	0.97	flush	T2
Brancaster (low marsh)	1A-53	T6	ND	ND	ABSENT
Brancaster (low marsh)	1A-56	T6	ND	ND	ABSENT
Brancaster (low marsh)	1A-57	T6	ND	ND	ABSENT
Brancaster (low marsh)	1A-59	T6	ND	ND	ABSENT
Brancaster (low marsh)	1A-63	T6	ND	ND	ABSENT
Brancaster (low marsh)	1A-64	T6	ND	ND	ABSENT
Brancaster (low marsh)	1A-69	T6	ND	ND	ABSENT + NO IMAGE in original pub
Brancaster (low marsh)	1A-70	T6	ND	ND	ABSENT
Brancaster (low marsh)	1A-71	T6	ND	ND	ABSENT
Brancaster (low marsh)	1A-72	T6	ND	ND	ABSENT
Braunton	Brs-1	T6	1.97	flush	T6

Braunton	Brs-15	T6	2.59	flush	T6
Braunton	Brs-17	T6	2.45	flush	T6
Braunton	Brs-19	T6	3.27	flush	T6
Braunton	Brs-2	T6	2.20	flush	T6
Braunton	Brs-23	T6	2.32	flush	T6
Braunton	Brs-3	T6	1.46	flush	T6
Braunton	Brs-4	T6	2.27	flush	T6
Braunton	Brs-5	T6	2.32	flush	T6
Braunton	Brs-8	T6	3.84	flush	T6
Burnham-Overy-Staithe	2A-109	T6	2.23	flush	T6
Burnham-Overy-Staithe	2A-110	T6	1.93	flush	T6
Burnham-Overy-Staithe	2A-118	T6	2.42	flush	T6
Burnham-Overy-Staithe	2A-122	T6	2.82	flush	T6
Burnham-Overy-Staithe	2A-135	T6	2.10	flush	T6
Burnham-Overy-Staithe	2A-14	T6	2.03	flush	T6
Burnham-Overy-Staithe	2A-24	T6	2.65	flush	T6
Burnham-Overy-Staithe	2A-50	T6	2.27	flush	T6
Burnham-Overy-Staithe	2A-52	T6	2.45	flush	T6
Burnham-Overy-Staithe	2A-59	T6	2.80	flush	T6
Galmpton	Bix-202	T1	1.25	flush	T2
Galmpton	Bix-204	T2	1.13	raised	T2
Galmpton	Bix-205	T2	0.96	flush	T2
Galmpton	Bix-207	T2	1.12	raised	T2
Galmpton	Bix-221	T2	ND	ND	ABSENT
Galmpton	Bix-223	T1	ND	ND	ABSENT
Galmpton	Bix-225	T2	ND	ND	ABSENT
Galmpton	Bix-227	T2	ND	ND	ABSENT
Hambleton	Ham-115	T6	2.82	flush	T6
Hambleton	Ham-123	T6	1.94	flush	T6
Lymington	LM-193	T2	1.09	flush	T2

Lymington	LM-194	T2	1.08	flush	T2
Lymington	LM-196	T2	1.07	flush	T2
Lymington	LM-198	T2	0.95	flush	T2
Lymington	LM-203	T2	1.30	flush	T2
Lymington	LM-209	T2	1.14	flush	T2
Lymington	LM-241	T2	0.91	flush	T2
Lymington	LM-242	T2	1.09	flush	T2
Lymington	LM-243	T2	1.15	flush	T2
Lymington	LM-244	T2	1.01	flush	T2
Pembrock dock	Pem-102	T6	2.32	flush	T6
Pembrock dock	Pem-103	T6	2.93	flush	T6
Pembrock dock	Pem-104	T6	2.82	flush	T6
Pembrock dock	Pem-105	T6	2.24	flush	T6
Pembrock dock	Pem-115	T6	2.49	flush	T6
Pembrock dock	Pem-138	T6	2.57	flush	T6
Pembrock dock	Pem-139	T6	3.17	flush	T6
Pembrock dock	Pem-140	T6	1.56	NA	ND
Pembrock dock	Pem-98	T6	2.44	flush	T6
Pen clawdd	Lan-13	T6	2.09	flush	T6
Pen clawdd	Lan-18	T6	2.14	flush	T6
Pen clawdd	Lan-19	T6	1.75	flush	T6
Pen clawdd	Lan-25	T2	2.28	flush	T6
Pen clawdd	Lan-27	T6	2.41	flush	T6
Pen clawdd	Lan-33	T6	1.70	flush	T6
Pen clawdd	Lan-4	T6	2.12	flush	T6
Pen clawdd	Lan-46	T6	2.71	flush	T6
Pen clawdd	Lan-8	T6	2.37	flush	T6
Pen clawdd	Lan-9	T6	2.66	flush	T6
Queenborough	Que-1	T6	2.83	flush	T6
Queenborough	Que-16	T6	2.77	flush	T6

Queenborough	Que-17	T6	1.71	flush	T6
Queenborough	Que-2	T6	2.57	flush	T6
Queenborough	Que-27	T6	1.96	flush	T6
Queenborough	Que-33	T6	2.20	flush	T6
Queenborough	Que-34	T6	2.30	flush	T6
Queenborough	Que-38	T6	2.38	flush	T6
Queenborough	Que-4	T6	2.58	flush	T6
Queenborough	Que-5	T6	2.43	flush	T6
Queenborough	Que-8	T6	2.93	flush	T6
Severn_Beach	SB-1	T6	2.09	flush	T6
Severn_Beach	SB-10	T6	2.30	flush	T6
Severn_Beach	SB-28	T6	1.74	flush	T6
Severn_Beach	SB-31	T6	1.82	flush	T6
Severn_Beach	SB-37	T6	2.94	flush	T6
Severn_Beach	SB-7	T6	2.07	flush	T6
Severn_Beach	SB-51	T6	ND	ND	ABSENT
Severn_Beach	SB-53	T6	ND	ND	ABSENT
Shoreham-by-Sea	Sho-10	T6	0.92	flush	T2
Shoreham-by-Sea	Sho-11	T6	1.17	flush	T2
Shoreham-by-Sea	Sho-12	T6	1.35	flush	T2
Shoreham-by-Sea	Sho-13	T6	1.32	flush	T2
Shoreham-by-Sea	Sho-2	T6	1.20	flush	T2
Shoreham-by-Sea	Sho-3	T6	1.57	flush	T6
Shoreham-by-Sea	Sho-4	T6	1.19	flush	T2
Shoreham-by-Sea	Sho-6	T6	0.89	flush	T2
Shoreham-by-Sea	Sho-7	T6	1.95	raised	T1
Shoreham-by-Sea	Sho-8	T6	1.41	flush	T6
South Queensferry	Quf-5	T6	ND	ND	ABSENT + NO IMAGE in original pub
South Queensferry	Quf-8	T6	ND	ND	ABSENT + NO IMAGE in original pub
South Queensferry	Quf-16	T6	ND	ND	ABSENT + NO IMAGE in original pub

South Queensferry	Quf-24	T6	ND	ND	ABSENT + NO IMAGE in original pub
South Queensferry	Quf-34	T6	ND	ND	ABSENT + NO IMAGE in original pub
South Queensferry	Quf-37	T6	ND	ND	ABSENT + NO IMAGE in original pub
St Osyth	IPS-1	T6	2.18	flush	T6
St Osyth	IPS-13	T6	2.54	flush	T6
St Osyth	IPS-14	T6	1.90	flush	T6
St Osyth	IPS-2	T6	1.80	flush	T6
St Osyth	IPS-21	T6	2.54	flush	T6
St Osyth	IPS-37	T6	2.42	flush	T6
St Osyth	IPS-39	T6	2.34	flush	T6
St Osyth	IPS-4	T1	2.53	flush	T6
St Osyth	IPS-41	T6	2.52	flush	T6
Thornham	5A-15	T6	2.77	ND	ND
Thornham	5A-32	T6	ND	ND	ABSENT
Thornham	5A-35	T2	ND	ND	ABSENT + NO IMAGE in original pub
Thornham	5A-34	T2	2.05	flush	T6
Thornham	5A-37	T2	2.74	flush	T6
Thornham	5A-38	T2	1.91	flush	T6
Thornham	5A-39	T2	3.08	flush	T6
Thornham	5A-40	T2	2.33	flush	T6
Thornham	5A-62	T2	2.83	flush	T6
Thornham	5A-63	T2	ND	ND	ABSENT

Supplementary Table 2. Site, coordinates, specimen ID, accession number, list of individuals used in Richirt et al., 2019, genetic and morphological identification of the individuals issed from the AMTEP project.

Location	Latitude	Longitude	Specimen ID	Accession number (GenBank)	Used in Richirt et al., 2019a	Used in Richirt et al., 2019b	Phylotype	Morphologic identification
St Vaast	49°34'38.60"N	1°16'38.80"W	Ma027		X		T1	T1
St Vaast	49°34'38.60"N	1°16'38.80"W	Ma028		X		T2A	T2
St Vaast	49°34'38.60"N	1°16'38.80"W	Ma030		X		T2A	T2
St Vaast	49°34'38.60"N	1°16'38.80"W	Ma031	MH200684	X		T2A	T2
Seine estuary	49°26'31.30"N	0°16'25.20"E	Ma080	MH200701	X		T6	T6
Seine estuary	49°26'31.30"N	0°16'25.20"E	Ma081				T6	
Seine estuary	49°26'31.30"N	0°16'25.20"E	Ma082				T6	
Seine estuary	49°26'31.30"N	0°16'25.20"E	Ma083	MH200702	X		T6	T6
Seine estuary	49°26'31.30"N	0°16'25.20"E	Ma084		X		T6	T6
Seine estuary	49°26'31.30"N	0°16'25.20"E	Ma085		X		T6	T6
Seine estuary	49°26'31.30"N	0°16'25.20"E	Ma086		X		T6	T6
Seine estuary	49°26'31.30"N	0°16'25.20"E	Ma087		X		T6	T6
Seine estuary	49°26'31.30"N	0°16'25.20"E	Ma088				T6	
Seine estuary	49°26'31.30"N	0°16'25.20"E	Ma089		X		T6	T6
Seine estuary	49°26'31.30"N	0°16'25.20"E	Ma090				T6	
Seine estuary	49°26'31.30"N	0°16'25.20"E	Ma091		X		T6	T6
Seine estuary	49°26'31.30"N	0°16'25.20"E	Ma093				T6	
Seine estuary	49°26'31.30"N	0°16'25.20"E	Ma094		X		T6	T6
Seine estuary	49°26'31.30"N	0°16'25.20"E	Ma095				T6	
Seine estuary	49°26'31.30"N	0°16'25.20"E	Ma096				T6	
Seine estuary	49°26'31.30"N	0°16'25.20"E	Ma097		X		T6	T6
Seine estuary	49°26'31.30"N	0°16'25.20"E	Ma098				T6	
Seine estuary	49°26'31.30"N	0°16'25.20"E	Ma099				T6	
Seine estuary	49°26'31.30"N	0°16'25.20"E	Ma100				T6	

Seine estuary	49°26'31.30"N	0°16'25.20"E	Ma101	MH200703	X		T6	T6
Seine estuary	49°26'31.30"N	0°16'25.20"E	Ma102				T6	
Seine estuary	49°26'31.30"N	0°16'25.20"E	Ma103				T6	
Seine estuary	49°26'31.30"N	0°16'25.20"E	Ma104				T6	
Seine estuary	49°26'31.30"N	0°16'25.20"E	Ma105				T6	
Seine estuary	49°26'31.30"N	0°16'25.20"E	Ma106				T6	
Seine estuary	49°26'31.30"N	0°16'25.20"E	Ma107				T6	
Seine estuary	49°26'31.30"N	0°16'25.20"E	Ma108	MH200704	X		T6	T6
Seine estuary	49°26'31.30"N	0°16'25.20"E	Ma109	MH200705	X		T6	T6
Ouistreham	49°16'16.40"N	0°14'12.20"W	Ma142	MH200668	X		T1	T1
Ouistreham	49°16'16.40"N	0°14'12.20"W	Ma144				T6	
Ouistreham	49°16'16.40"N	0°14'12.20"W	Ma145				T6	
Ouistreham	49°16'16.40"N	0°14'12.20"W	Ma146				T6	
Ouistreham	49°16'16.40"N	0°14'12.20"W	Ma147		X		T6	T6
Ouistreham	49°16'16.40"N	0°14'12.20"W	Ma148				T6	
Ouistreham	49°16'16.40"N	0°14'12.20"W	Ma150	MH200683	X		T2B	T2
Authie	50°22'23.80"N	1°35'44.00"E	Ma173				T6	
Authie	50°22'23.80"N	1°35'44.00"E	Ma174				T6	
Authie	50°22'23.80"N	1°35'44.00"E	Ma175				T6	
Seine estuary	49°26'31.30"N	0°16'25.20"E	Ma176				T6	
Seine estuary	49°26'31.30"N	0°16'25.20"E	Ma181				T6	
Seine estuary	49°26'31.30"N	0°16'25.20"E	Ma182				T6	
Authie	50°22'23.80"N	1°35'44.00"E	Ma189				T6	
Rade de Brest	48°24'13.10"N	4°21'16.00"W	RB006				T2A	
Rade de Brest	48°24'13.10"N	4°21'16.00"W	RB007		X		T1	T2
Biezelingse Ham	51°26'53.40"N	3°55'49.79"E	BH006				T6	
Biezelingse Ham	51°26'53.40"N	3°55'49.79"E	BH007				T6	
Biezelingse Ham	51°26'53.40"N	3°55'49.79"E	BH008				T6	

Biezelingse Ham	51°26'53.40"N	3°55'49.79"E	BH009		X	T6	T6
Biezelingse Ham	51°26'53.40"N	3°55'49.79"E	BH010	MH200689	X	T6	T6
Biezelingse Ham	51°26'53.40"N	3°55'49.79"E	BH013	MH200690	X	T6	T6
Biezelingse Ham	51°26'53.40"N	3°55'49.79"E	BH014			T6	
Biezelingse Ham	51°26'53.40"N	3°55'49.79"E	BH017			T6	
Biezelingse Ham	51°26'53.40"N	3°55'49.79"E	BH018			T6	
Biezelingse Ham	51°26'53.40"N	3°55'49.79"E	BH024			T6	
Biezelingse Ham	51°26'53.40"N	3°55'49.79"E	BH025			T6	
Biezelingse Ham	51°26'53.40"N	3°55'49.79"E	BH026			T6	
Biezelingse Ham	51°26'53.40"N	3°55'49.79"E	BH027			T6	
Biezelingse Ham	51°26'53.40"N	3°55'49.79"E	BH028			T6	
Biezelingse Ham	51°26'53.40"N	3°55'49.79"E	BH029			T6	
Biezelingse Ham	51°26'53.40"N	3°55'49.79"E	BH030			T6	
Biezelingse Ham	51°26'53.40"N	3°55'49.79"E	BH031			T6	
Biezelingse Ham	51°26'53.40"N	3°55'49.79"E	BH032			T6	
Biezelingse Ham	51°26'53.40"N	3°55'49.79"E	BH034			T6	
Biezelingse Ham	51°26'53.40"N	3°55'49.79"E	BH035			T6	
Biezelingse Ham	51°26'53.40"N	3°55'49.79"E	BH040			T6	
Biezelingse Ham	51°26'53.40"N	3°55'49.79"E	BH041			T6	
Biezelingse Ham	51°26'53.40"N	3°55'49.79"E	BH042			T6	
Biezelingse Ham	51°26'53.40"N	3°55'49.79"E	BH043			T6	
Biezelingse Ham	51°26'53.40"N	3°55'49.79"E	BH044			T6	
Biezelingse Ham	51°26'53.40"N	3°55'49.79"E	BH045			T6	
Biezelingse Ham	51°26'53.40"N	3°55'49.79"E	BH046			T6	
Biezelingse Ham	51°26'53.40"N	3°55'49.79"E	BH047			T6	
Biezelingse Ham	51°26'53.40"N	3°55'49.79"E	BH069			T6	
Biezelingse Ham	51°26'53.40"N	3°55'49.79"E	BH071			T6	
Biezelingse Ham	51°26'53.40"N	3°55'49.79"E	BH074			T6	

Biezelingse Ham	51°26'53.40"N	3°55'49.79"E	BH075				T6	
Biezelingse Ham	51°26'53.40"N	3°55'49.79"E	BH077				T6	
Biezelingse Ham	51°26'53.40"N	3°55'49.79"E	BH078				T6	
Biezelingse Ham	51°26'53.40"N	3°55'49.79"E	BH079				T6	
Biezelingse Ham	51°26'53.40"N	3°55'49.79"E	BH080				T6	
Biezelingse Ham	51°26'53.40"N	3°55'49.79"E	BH081				T6	
Biezelingse Ham	51°26'53.40"N	3°55'49.79"E	BH082				T6	
Biezelingse Ham	51°26'53.40"N	3°55'49.79"E	BH083				T6	
Biezelingse Ham	51°26'53.40"N	3°55'49.79"E	BH084				T6	
Biezelingse Ham	51°26'53.40"N	3°55'49.79"E	BH085				T6	
Biezelingse Ham	51°26'53.40"N	3°55'49.79"E	BH086				T6	
Biezelingse Ham	51°26'53.40"N	3°55'49.79"E	BH087				T6	
Biezelingse Ham	51°26'53.40"N	3°55'49.79"E	BH088				T6	
Biezelingse Ham	51°26'53.40"N	3°55'49.79"E	BH095				T6	
Biezelingse Ham	51°26'53.40"N	3°55'49.79"E	BH096				T6	
Biezelingse Ham	51°26'53.40"N	3°55'49.79"E	BH097				T6	
Biezelingse Ham	51°26'53.40"N	3°55'49.79"E	BH098				T6	
Biezelingse Ham	51°26'53.40"N	3°55'49.79"E	BH103				T6	
Biezelingse Ham	51°26'53.40"N	3°55'49.79"E	BH106				T6	
Biezelingse Ham	51°26'53.40"N	3°55'49.79"E	BH108				T6	
Grevelingen	51°44'50.04"N	03°53'24.06"E	Gv145	MN190684		X	T6	
Grevelingen	51°44'50.04"N	03°53'24.06"E	Gv147	MN190685		X	T6	
Grevelingen	51°44'50.04"N	03°53'24.06"E	Gv152	MN190686		X	T6	
Grevelingen	51°44'50.04"N	03°53'24.06"E	Gv155	MN190687		X	T6	
Grevelingen	51°44'50.04"N	03°53'24.06"E	Gv160	MN190688		X	T6	
Grevelingen	51°44'50.04"N	03°53'24.06"E	Gv162	MN190689		X	T6	
Grevelingen	51°44'50.04"N	03°53'24.06"E	Gv164	MN190690		X	T6	
Veerse Meer	51°33'12.24"N	3°52'25.34"E	ZK020		X		T2A	T6

Veerse Meer	51°33'12.24"N	3°52'25.34"E	ZK023	X	T2A	T6
Veerse Meer	51°33'12.24"N	3°52'25.34"E	ZK034		T2A	
Veerse Meer	51°33'12.24"N	3°52'25.34"E	ZK039		T2A	
Veerse Meer	51°33'12.24"N	3°52'25.34"E	ZK042		T2A	
Veerse Meer	51°33'12.24"N	3°52'25.34"E	ZK043		T6	
Veerse Meer	51°33'12.24"N	3°52'25.34"E	ZK044		T2A	
Veerse Meer	51°33'12.24"N	3°52'25.34"E	ZK047		T6	
Veerse Meer	51°33'12.24"N	3°52'25.34"E	ZK049		T2A	

Plates 1. ID of each individual and the associated SEM images of the spiral side (all scale bars 50 µm) and a magnification (1000x) of the penultimate chamber used for pore measurements. Individuals are ordered by location.

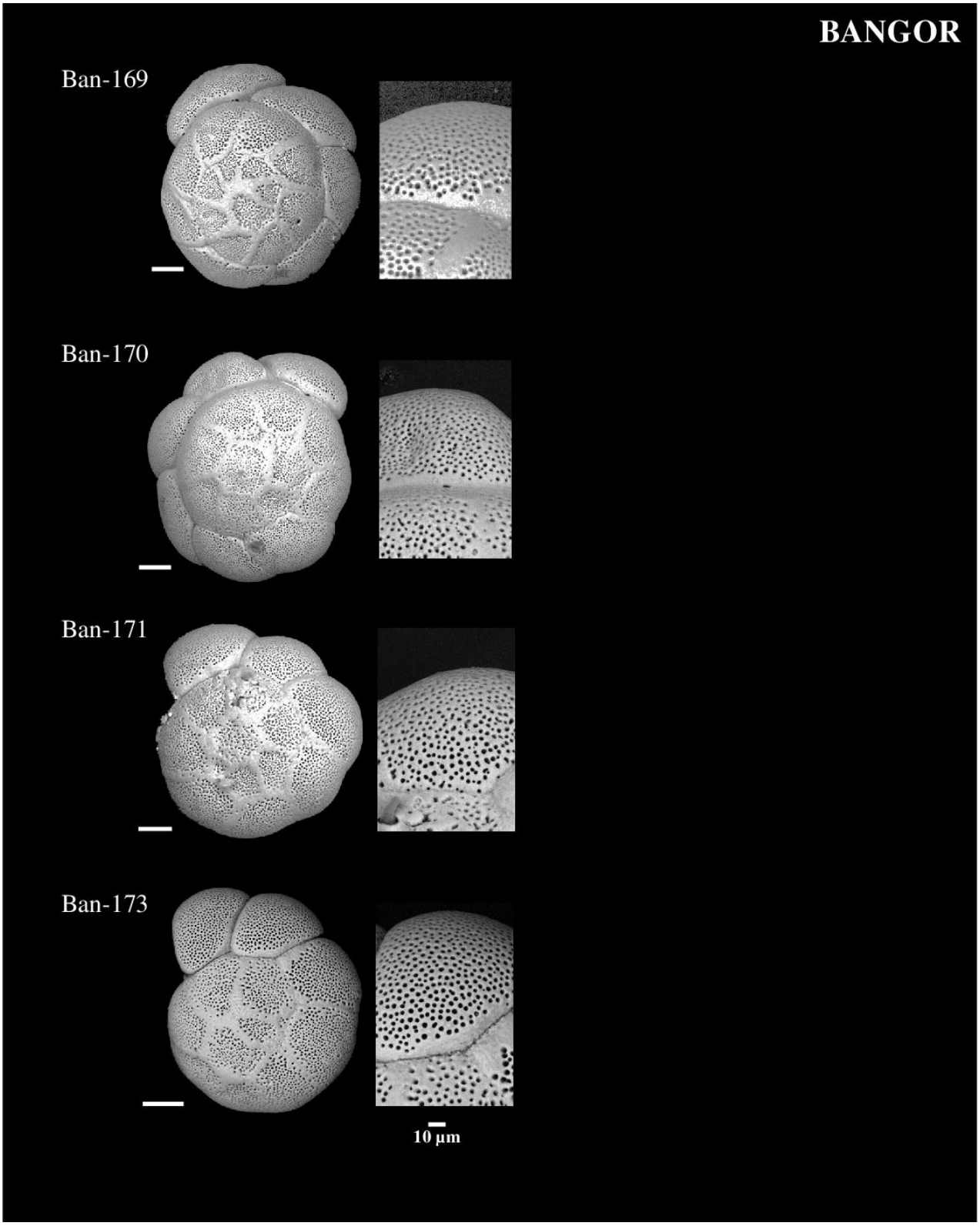

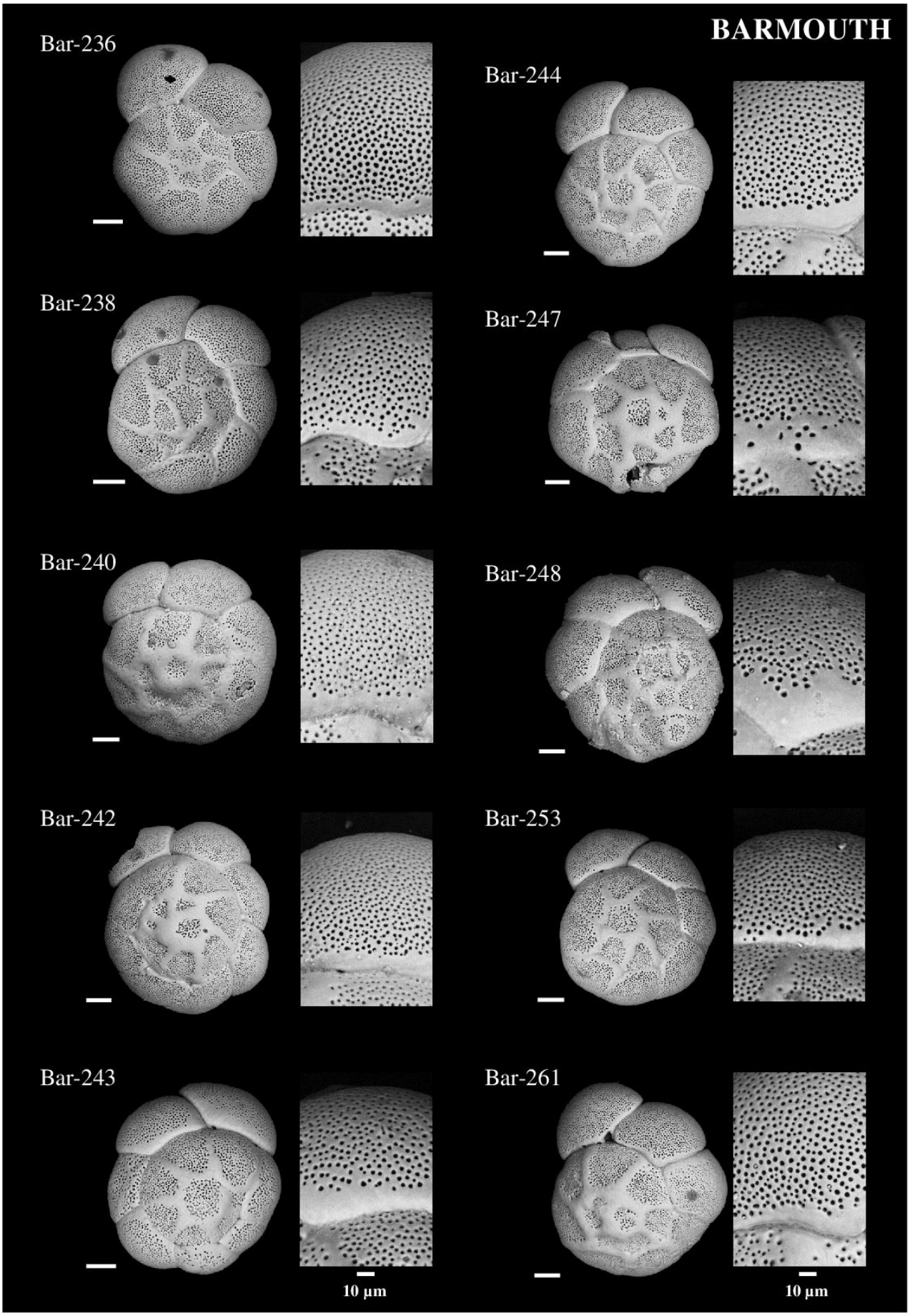
BARMOUTH
Bar-236
Bar-244
Bar-238
Bar-247
Bar-240
Bar-248
Bar-242
Bar-253
Bar-243
Bar-261
10 µm
10 µm

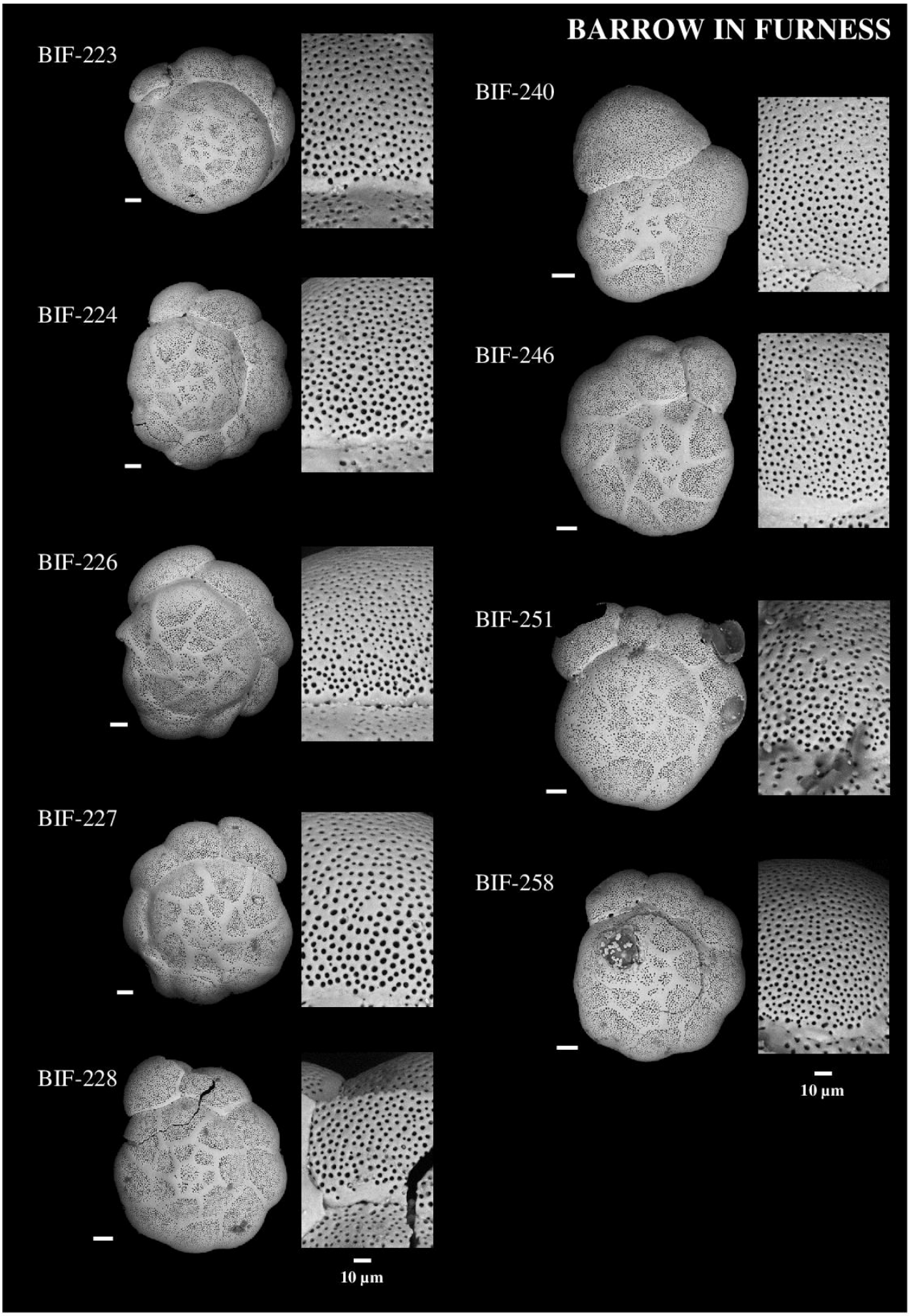
BARROW IN FURNESS
BIF-223
BIF-224
BIF-226
BIF-227
BIF-228
BIF-240
BIF-246
BIF-251
BIF-258
10 µm
10 µm

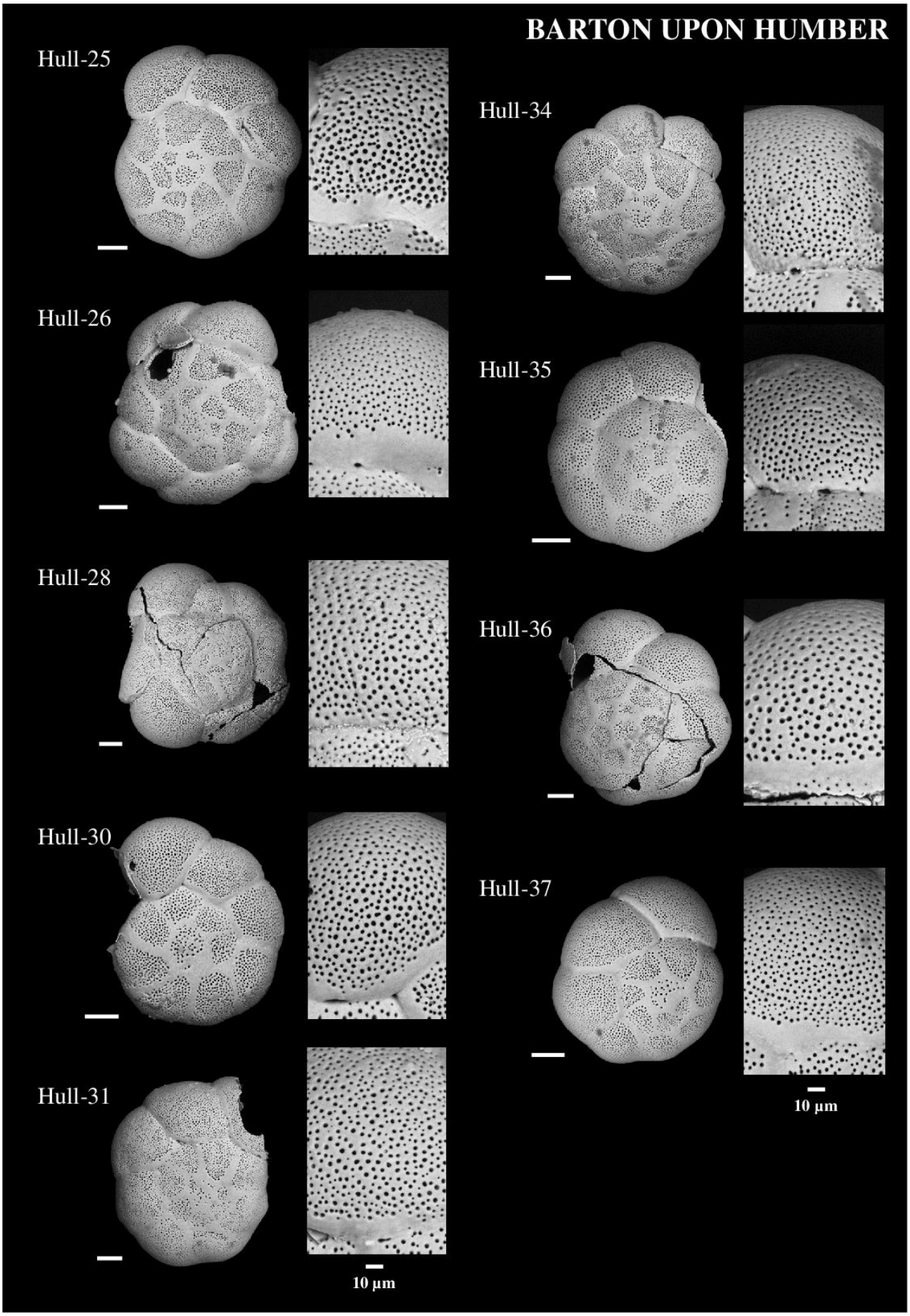
BARTON UPON HUMBER
Hull-25
Hull-26
Hull-28
Hull-30
Hull-31
Hull-34
Hull-35
Hull-36
Hull-37
10 µm
10 µm

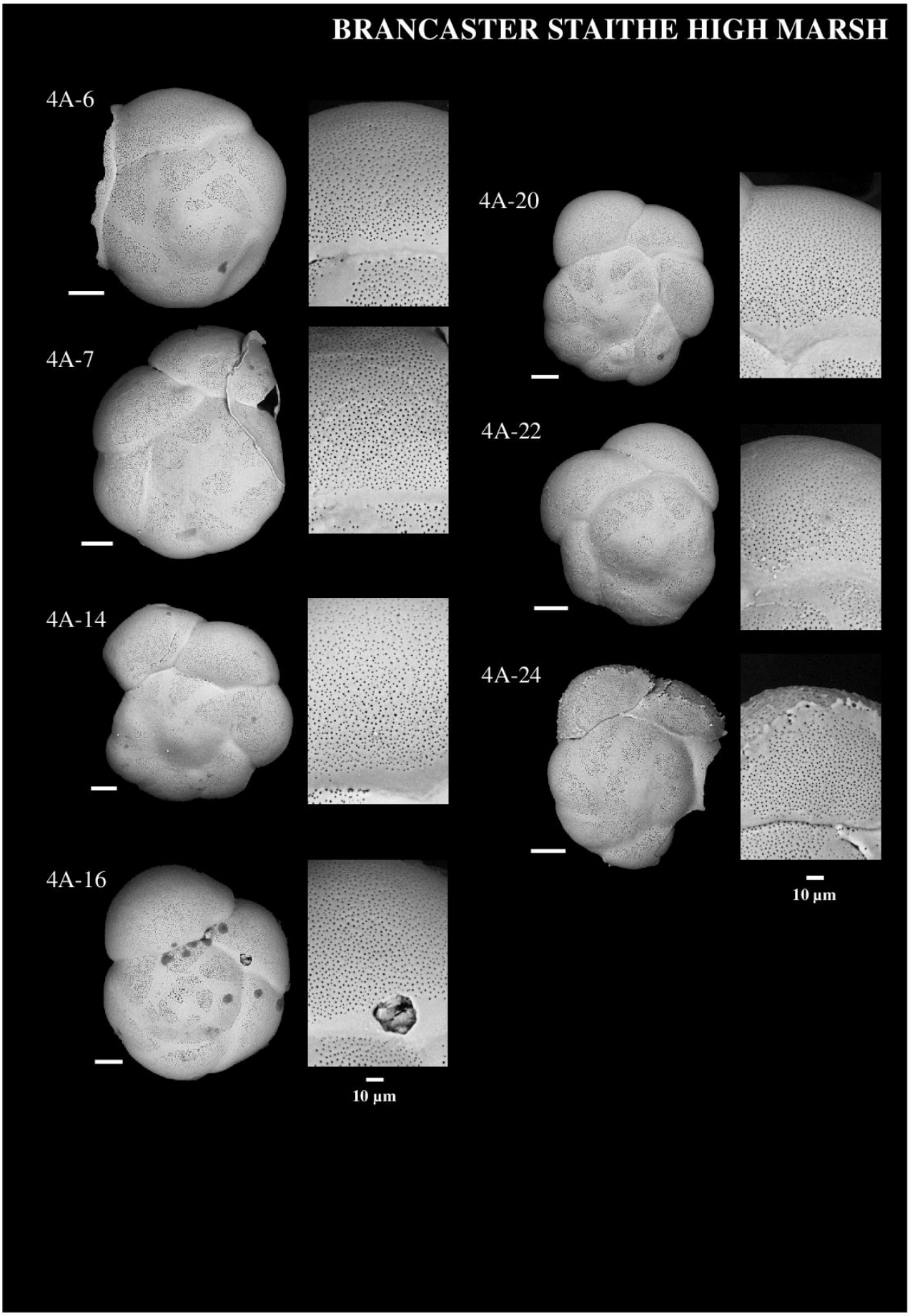
BRANCASTER STAITHE HIGH MARSH
4A-6
4A-7
4A-14
4A-16
4A-20
4A-22
4A-24
10 µm
10 µm

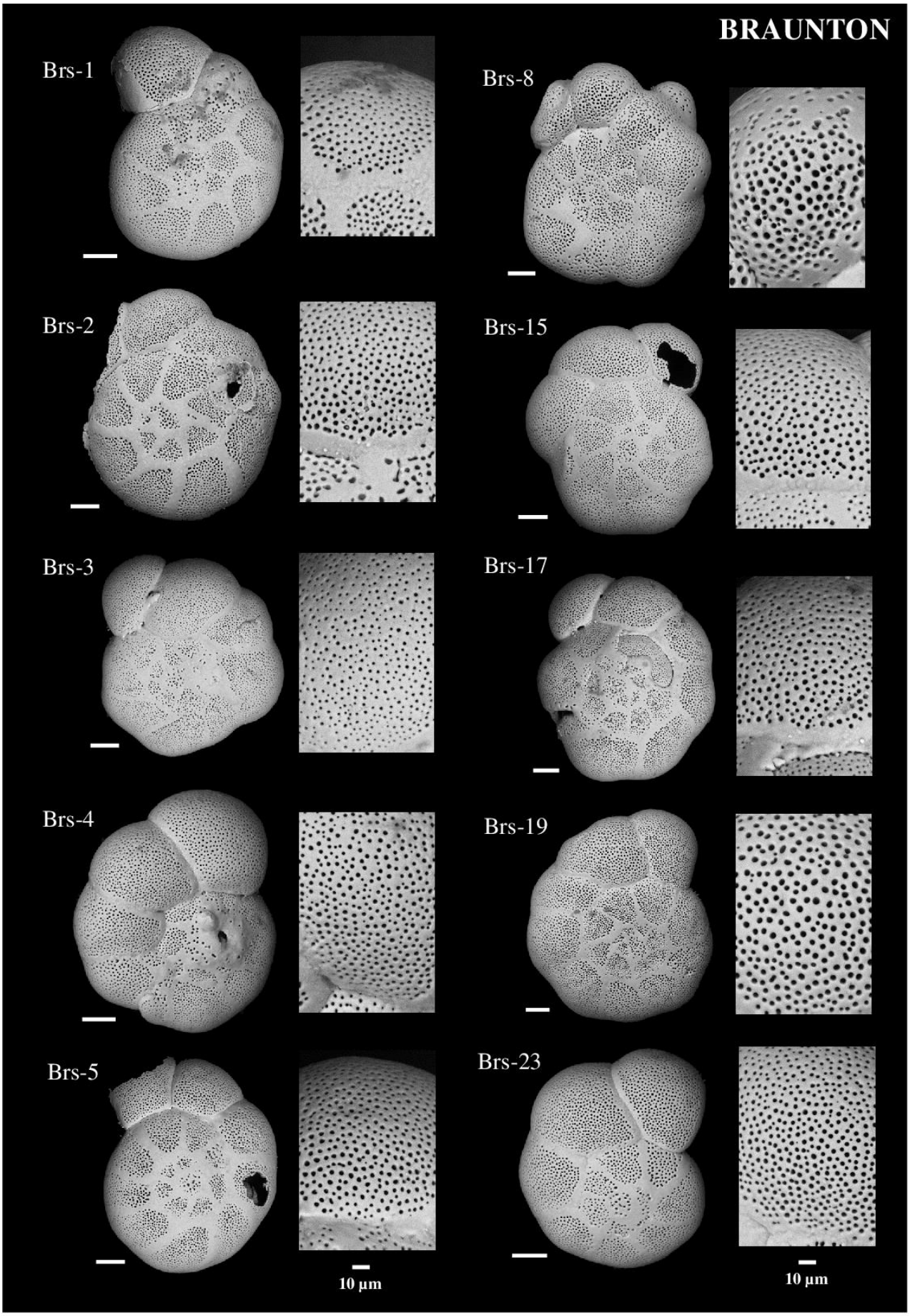
BRAUNTON
Brs-1
Brs-8
Brs-2
Brs-15
Brs-3
Brs-17
Brs-4
Brs-19
Brs-5
Brs-23
10 µm
10 µm

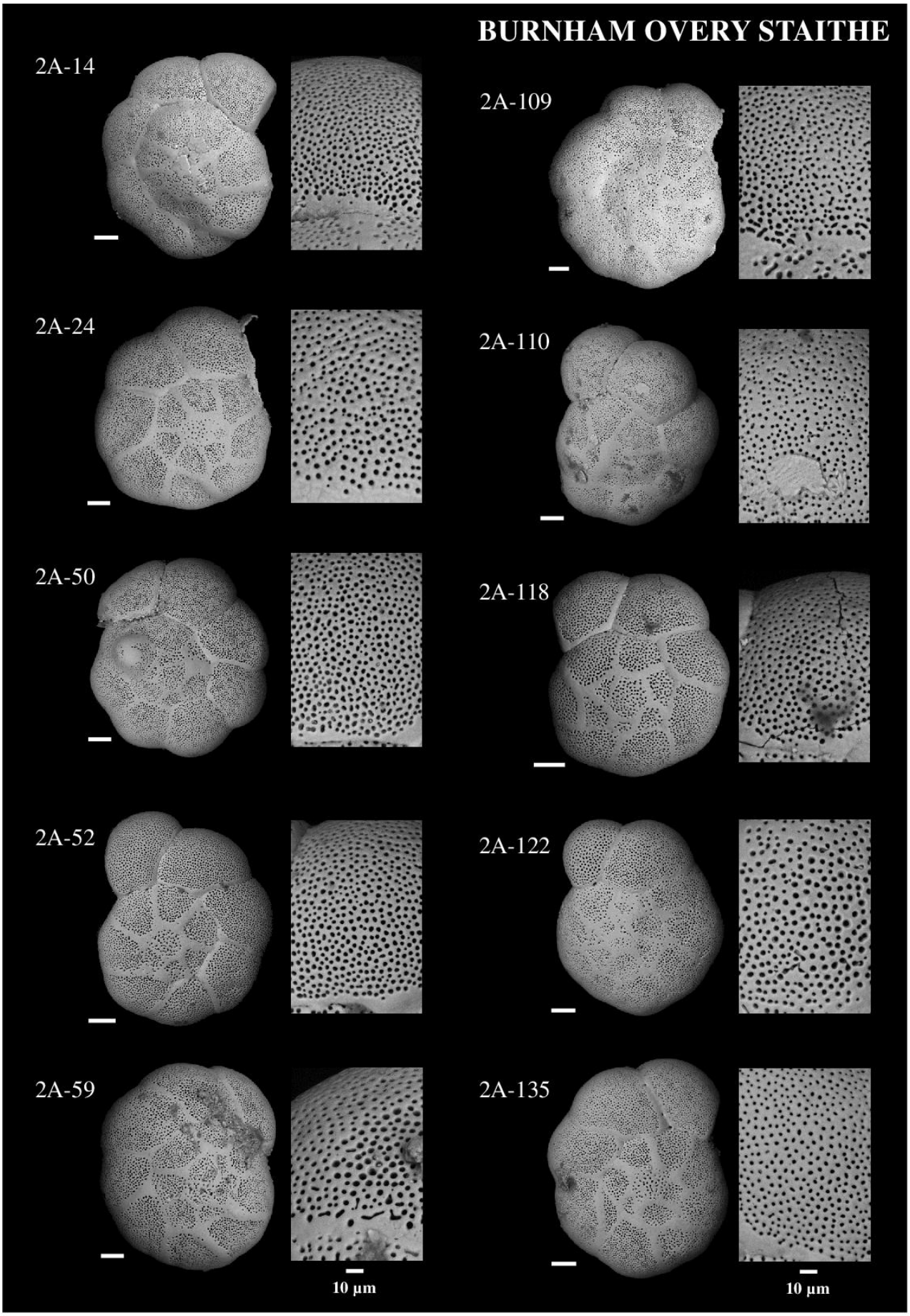
BURNHAM OVERY STAITHE
2A-14
2A-109
2A-24
2A-110
2A-50
2A-118
2A-52
2A-122
2A-59
2A-135
10 µm
10 µm

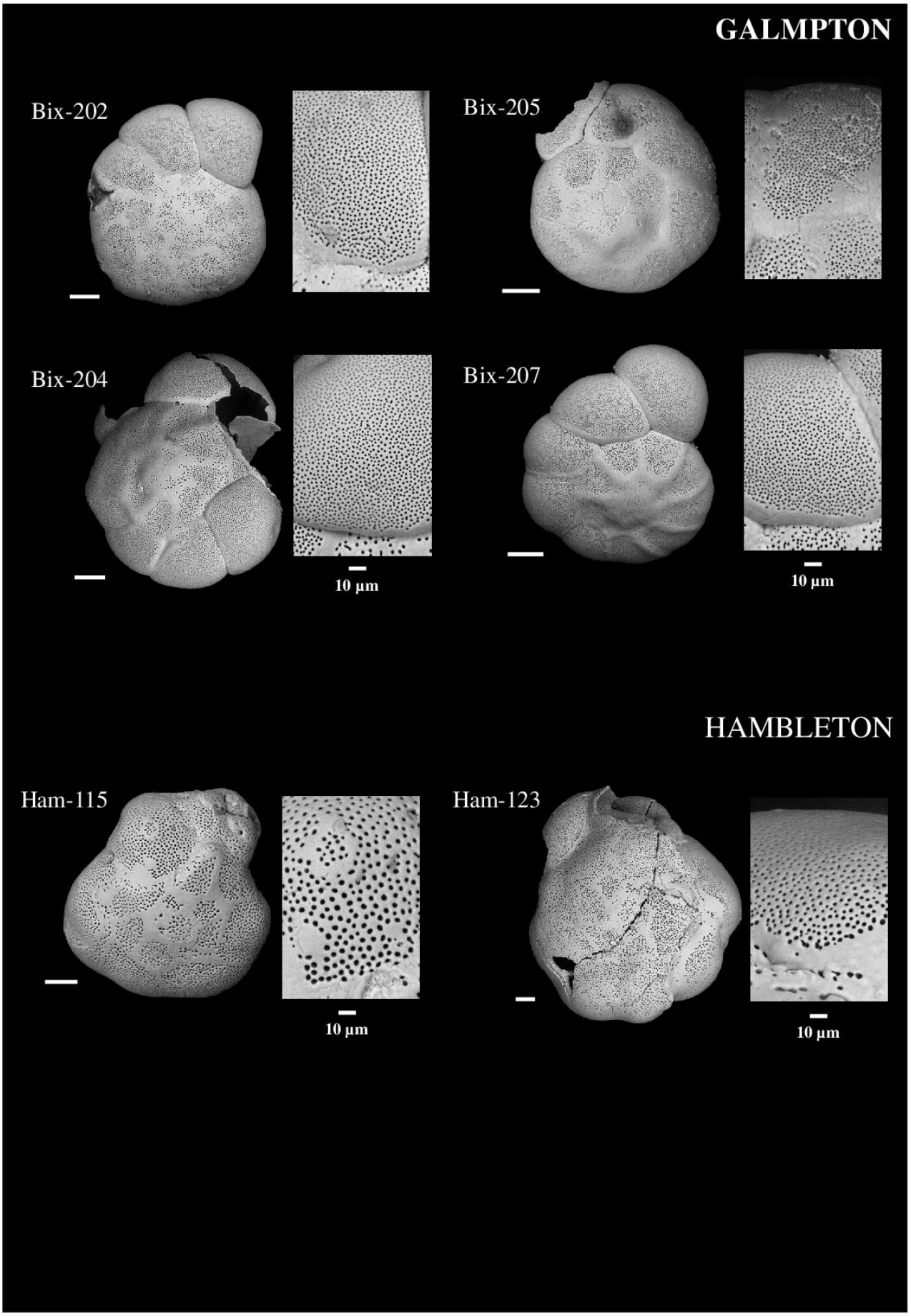
GALMPTON
Bix-202
Bix-205
Bix-204
Bix-207
10 µm
10 µm
HAMBLETON
Ham-115
Ham-123
10 µm
10 µm

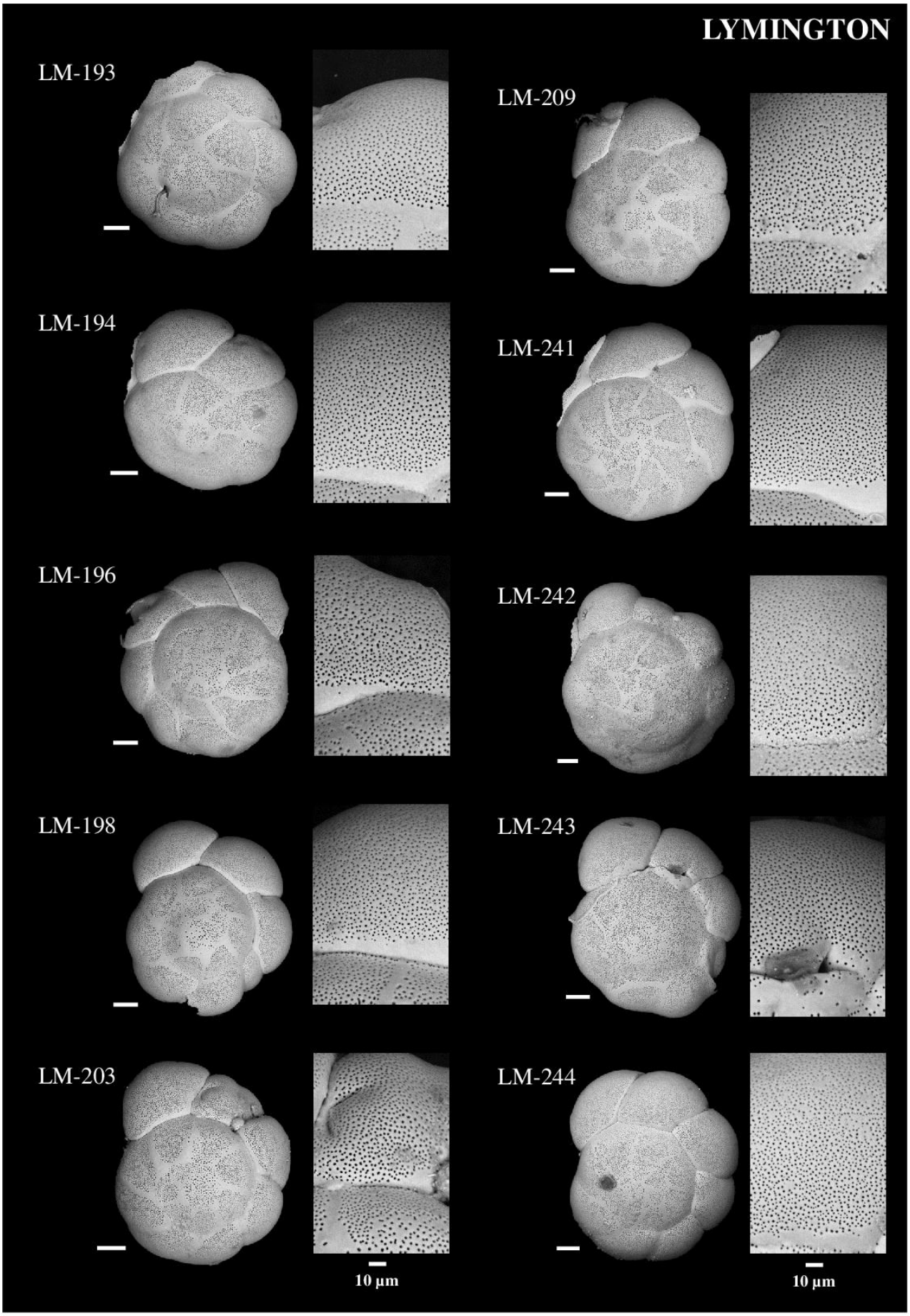
LYMINGTON
LM-193
LM-209
LM-194
LM-241
LM-196
LM-242
LM-198
LM-243
LM-203
LM-244
10 µm
10 µm

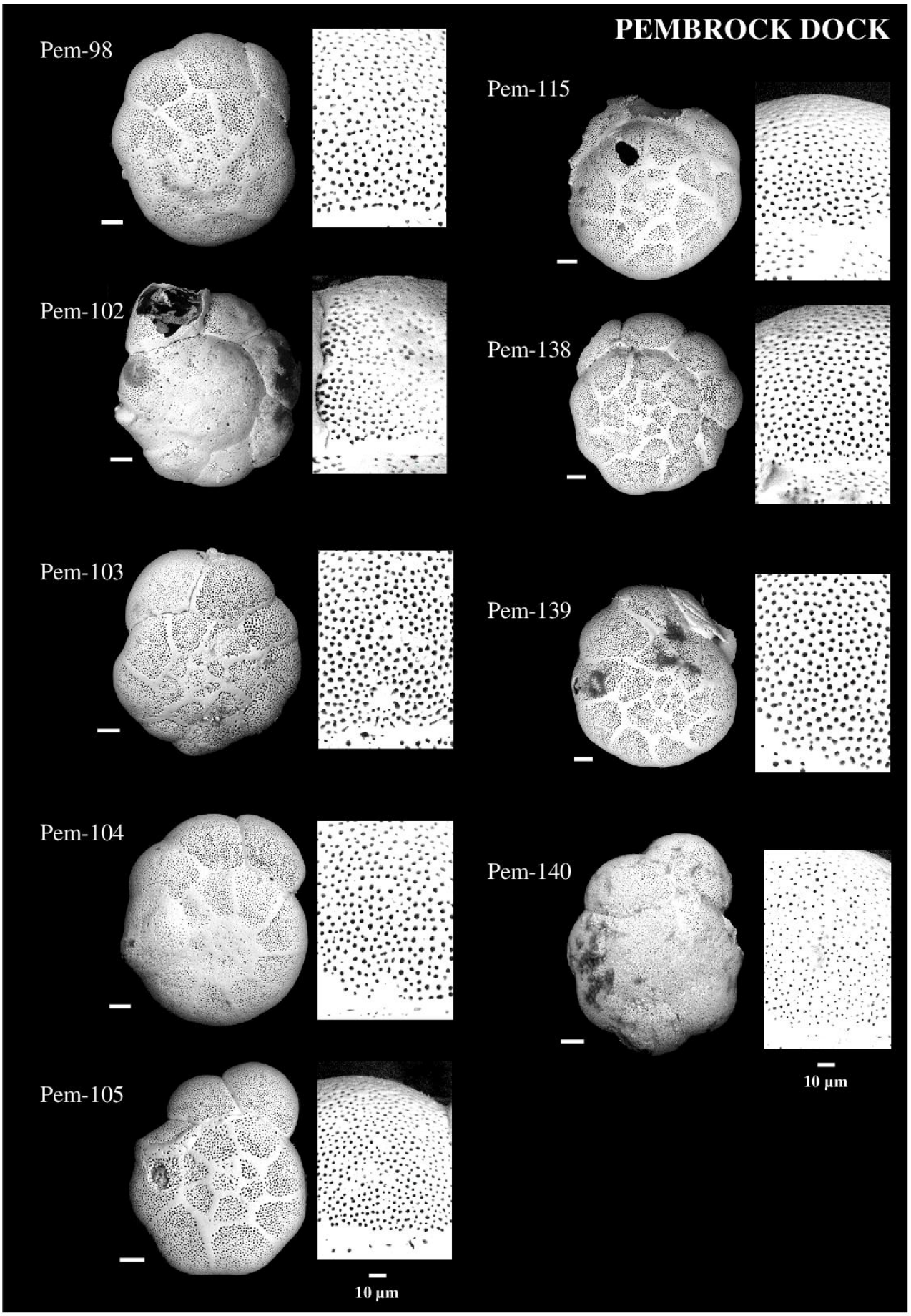
PEMBROCK DOCK
Pem-98
Pem-102
Pem-103
Pem-104
Pem-105
Pem-115
Pem-138
Pem-139
Pem-140
10 µm
10 µm

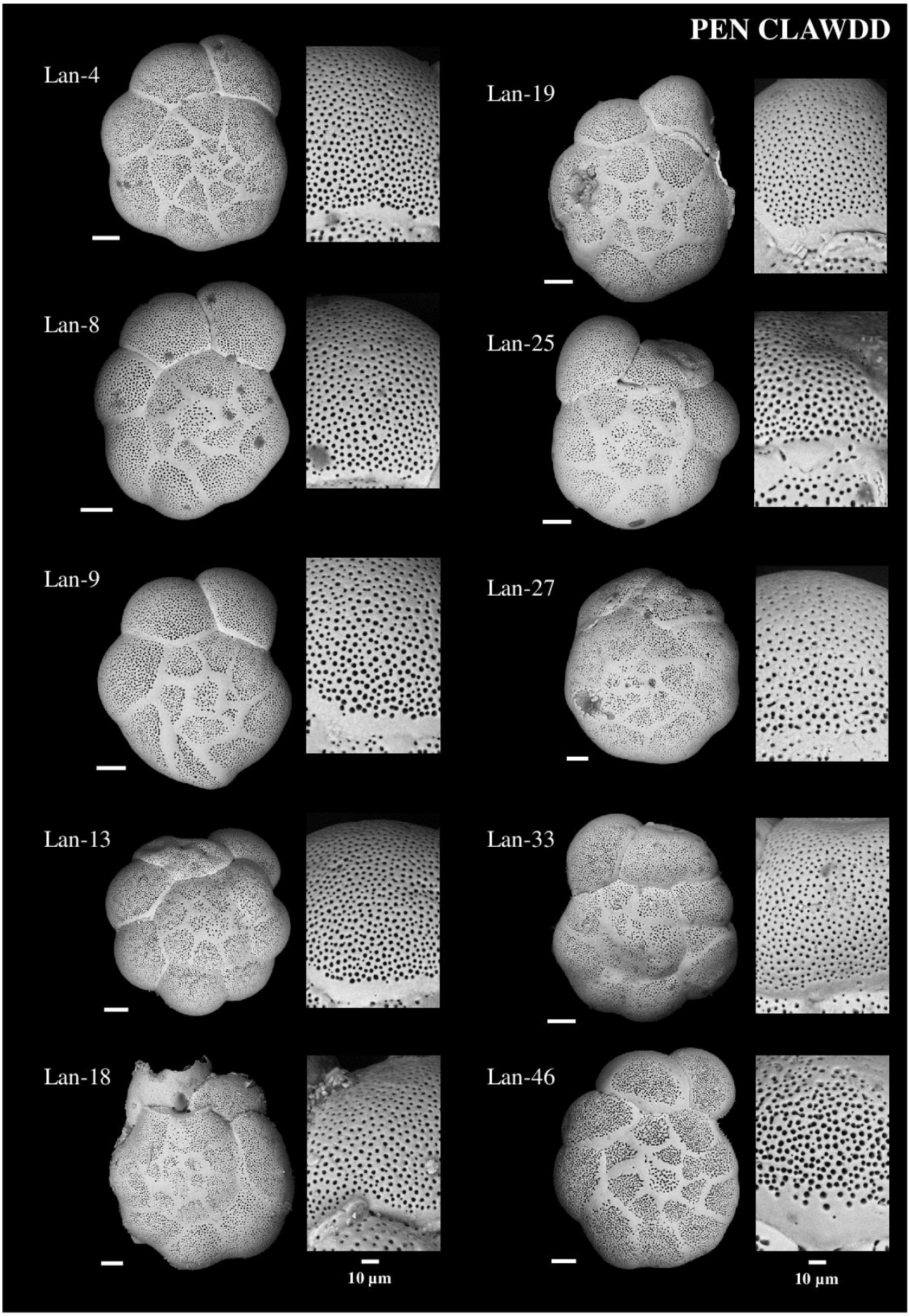
PEN CLAWDD
Lan-4
Lan-19
Lan-8
Lan-25
Lan-9
Lan-27
Lan-13
Lan-33
Lan-18
Lan-46
10 µm
10 µm

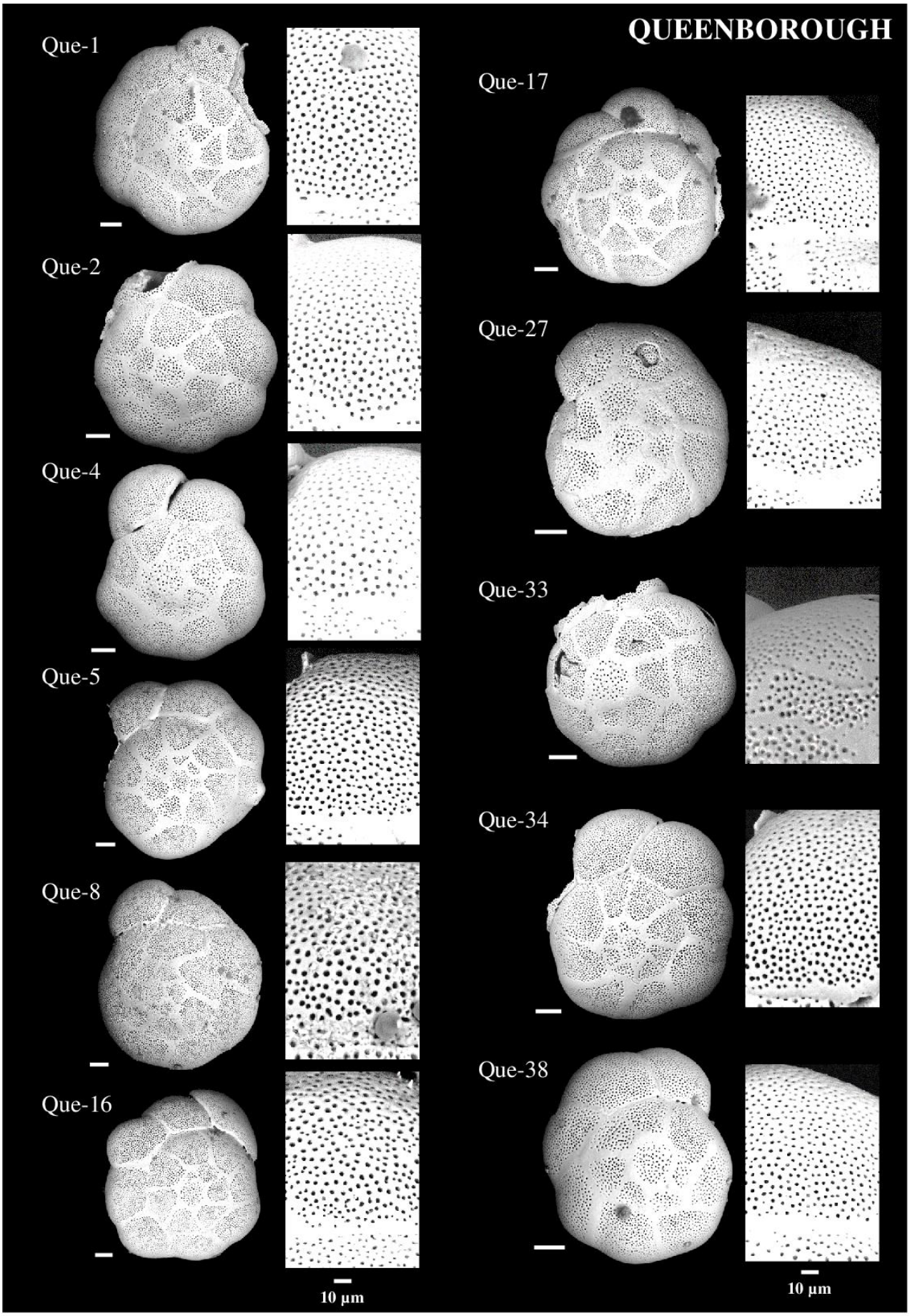
QUEENBOROUGH
Que-1
Que-2
Que-4
Que-5
Que-8
Que-16
Que-17
Que-27
Que-33
Que-34
Que-38
10 µm
10 µm

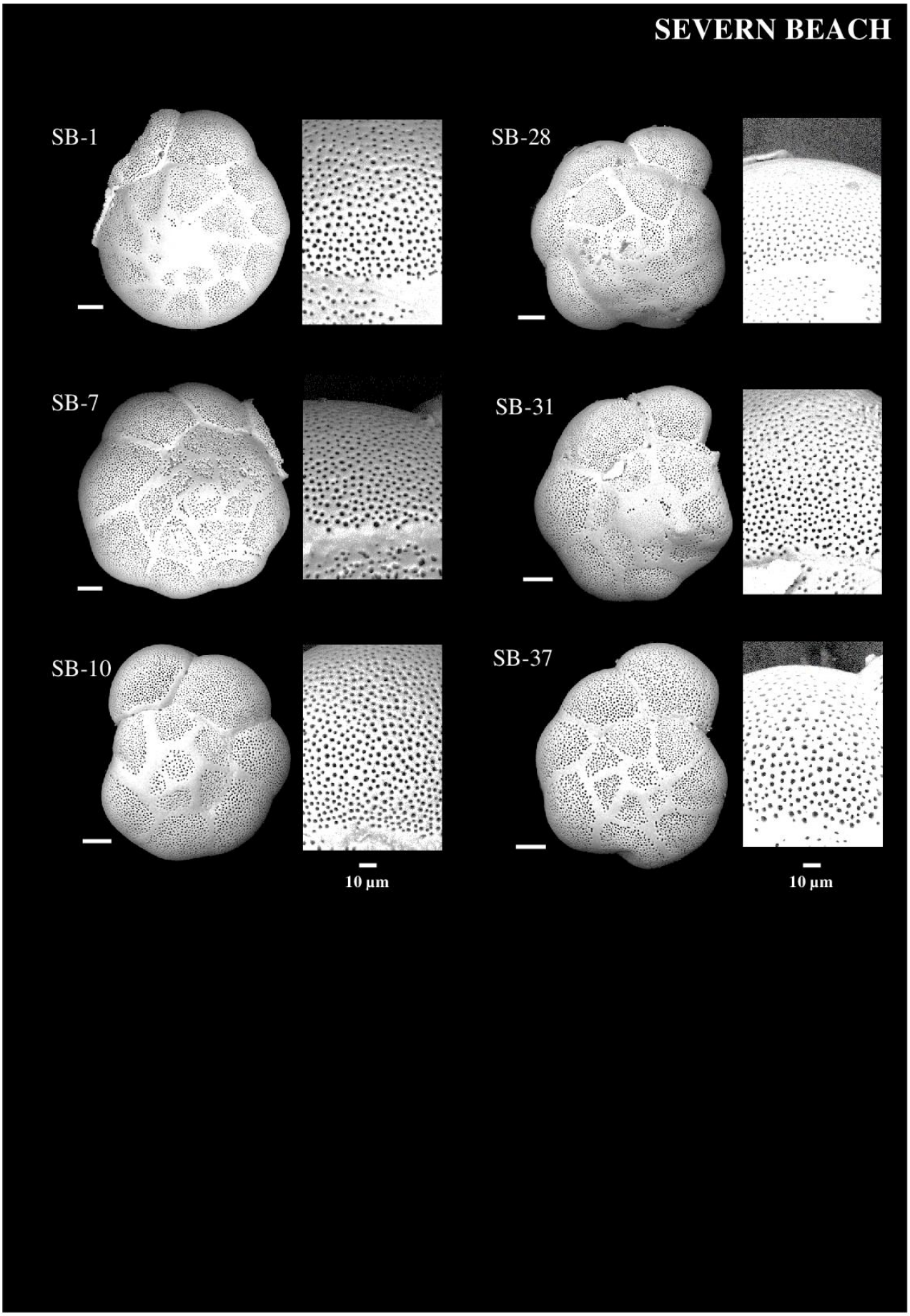
SEVERN BEACH
SB-1
SB-28
SB-7
SB-31
SB-10
SB-37
10 µm
10 µm

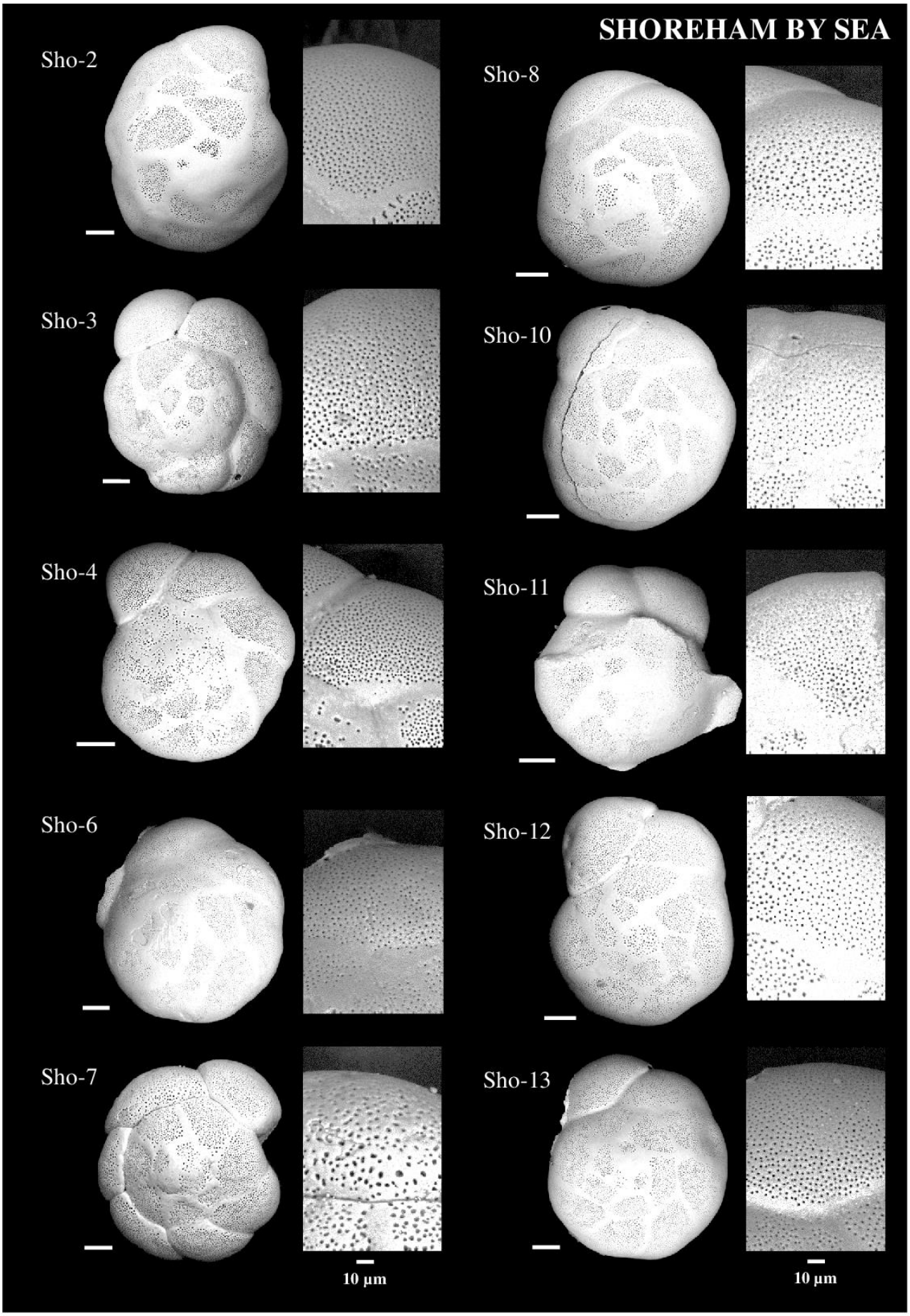
SHOREHAM BY SEA
Sho-2
Sho-3
Sho-4
Sho-6
Sho-7
Sho-8
Sho-10
Sho-11
Sho-12
Sho-13
10 µm
10 µm

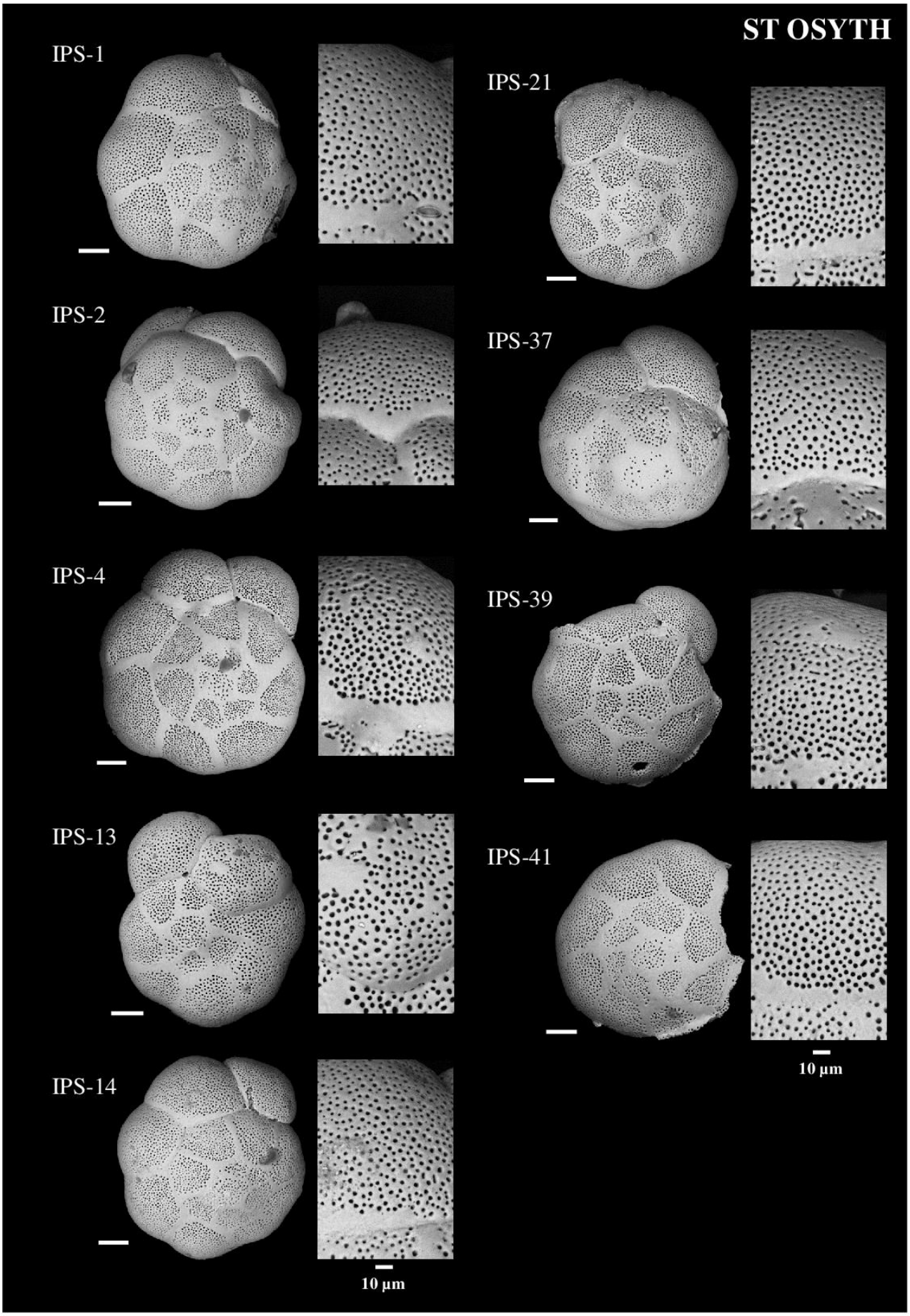
ST OSYTH
IPS-1
IPS-21
IPS-2
IPS-37
IPS-4
IPS-39
IPS-13
IPS-41
IPS-14
10 µm
10 µm

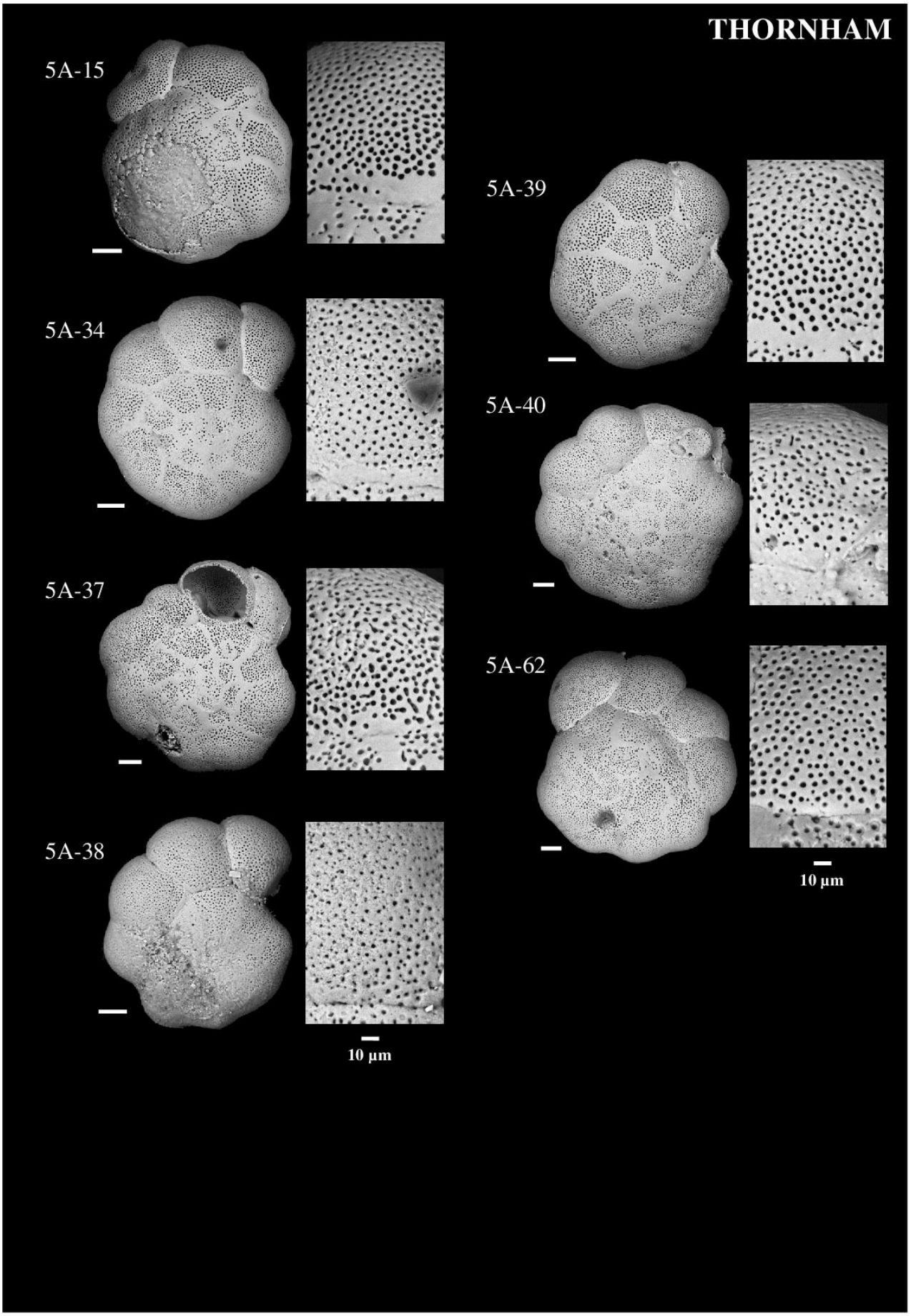
THORNHAM
5A-15
5A-34
5A-37
5A-38
5A-39
5A-40
5A-62
10 µm
10 µm

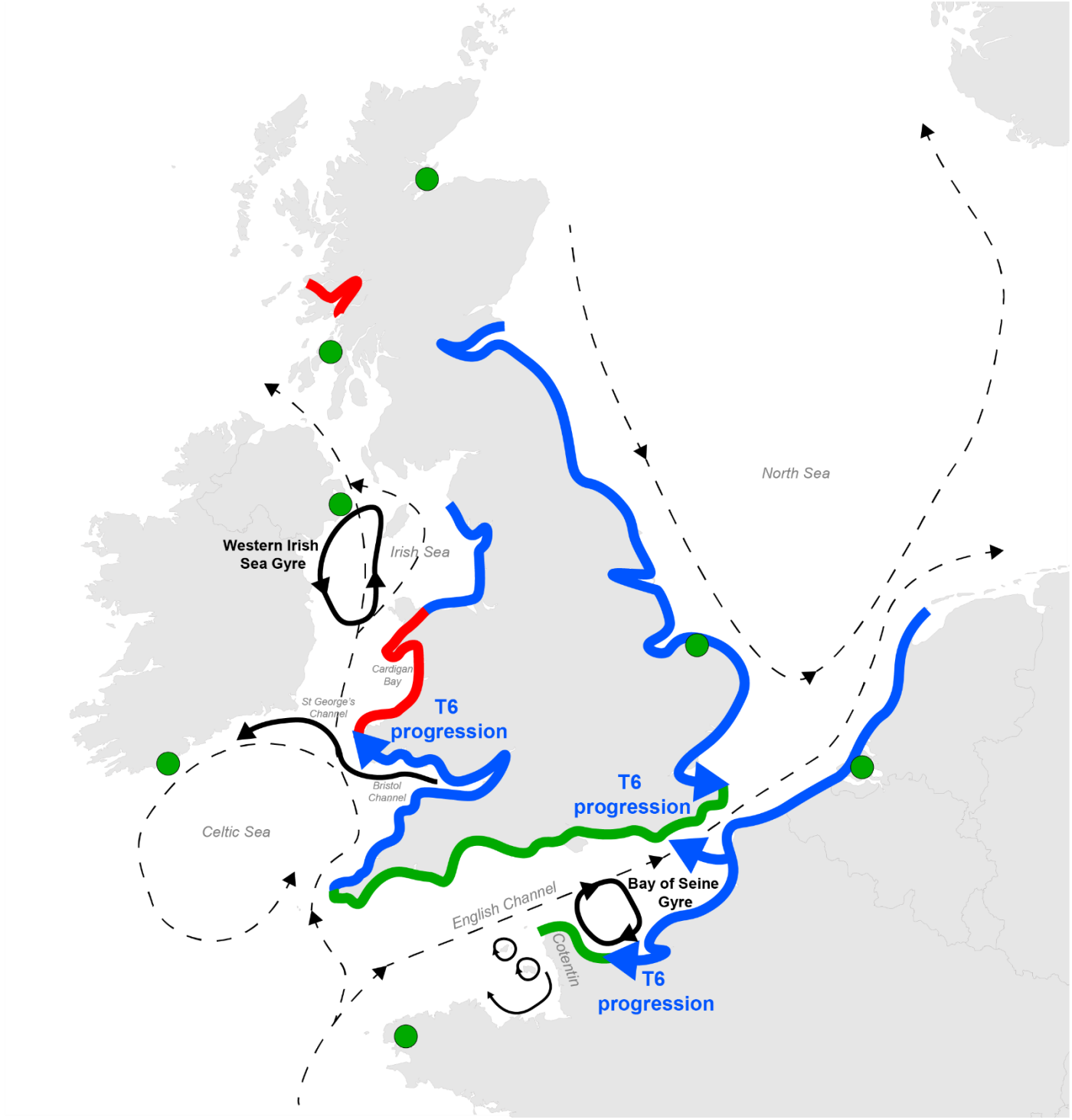

Supplementary Figure 1. Map showing the interpolated distribution of T1 (red), T2 (green) and T6 (blue) based on dominant phylotypes at each site. Blue arrows show the possible colonisation pathway of T6. Black doted arrows represent the general circulation of water masses in the seas of North-western Europe (from Salomon & Breton, 1993 and Bailly du Bois & Dumas, 2005). Black arrows represent the different gyres and strong residual currents. Residual currents and gyres were compiled from Brown et al., 2003, Coscia et al., 2013 and Robins et al., 2013 for the current from Bristom Channel to south Ireland and for the Western Irish Sea Gyre; Salomon & Breton, 1991, 1993 and Dupont et al. 2007 for the Bay of Seine Gyre and gyres on the west side of the Cotentin peninsula.

Bailly Du Bois, P., Dumas, F., Bailly Du Bois, P., Dumas, F., 2005. TRANSMER, hydrodynamic model for medium- and long-term simulation of radionuclides transfers in the English Channel and southern North Sea. Radioprotection 40. https://doi.org/10.1051/radiopro:2005s1-084

Brown, J., Carrillo, L., Fernand, L., Horsburgh, K.J., Hill, A.E., Young, E.F., Medler, K.J., 2003. Observations of the physical structure and seasonal jet-like circulation of the Celtic Sea and St. George's Channel of the Irish Sea. Continental Shelf Research 23, 533–561. https://doi.org/10.1016/S0278-4343(03)00008-6

Coscia, I., Robins, P.E., Porter, J.S., Malham, S.K., Ironside, J.E., 2013. Modelled larval dispersal and measured gene flow: seascape genetics of the common cockle Cerastoderma edule in the southern Irish Sea. Conserv Genet 14, 451–466. https://doi.org/10.1007/s10592-012-0404-4

Dupont, L., Ellien, C., Viard, F., 2007. Limits to gene flow in the slipper limpet Crepidula fornicata as revealed by microsatellite data and a larval dispersal model. Marine Ecology Progress Series 349, 125–138. https://doi.org/10.3354/meps07098

Robins, P.E., Neill, S.P., Giménez, L., Jenkins, S.R., Malham, S.K., 2013. Physical and biological controls on larval dispersal and connectivity in a highly energetic shelf sea. Limnology and Oceanography 58, 505–524. https://doi.org/10.4319/lo.2013.58.2.0505

Salomon, J.-C., Breton, M., 1993. An atlas of long-term currents in the channel. Oceanologica Acta 16, 439–448.

Salomon, J.-C., Breton, M., 1991. Courants résiduels de marée dans la Manche. Oceanologica Acta 11, 47–53.

CHAPTER 4

FORAMINIFERAL COMMUNITY RESPONSE TO SEASONAL ANOXIA IN LAKE GREVELINGEN (THE NETHERLANDS)

JULIEN RICHIRT[1,*], BETTINA RIEDEL[1,2], AURÉLIA MOURET[1], MAGALI SCHWEIZER[1], DEWI LANGLET[1,3], DORINA SEITAJ[4], FILIP J. R. MEYSMAN[5,6], CAROLINE P. SLOMP[7] AND FRANS J. JORISSEN[1]

[1]UMR 6112 LPG-BIAF Recent and Fossil Bio-Indicators, University of Angers, 2 Boulevard Lavoisier, 49045 Angers, France
[2]First Zoological Department, Vienna Museum of Natural History, Burgring 7, 1010 Vienna, Austria
[3]Univ. Lille, CNRS, Univ. Littoral Côte d'Opale, UMR8187, LOG, Laboratoire d'Océanologie et de Géosciences, 62930 Wimereux, France
[4]Department of Ecosystem Studies, Royal Netherlands Institute for Sea Research (NIOZ), Yerseke, the Netherlands
[5]Department of Biology, University of Antwerp, Universiteitsplein 1, 2610 Wilrijk, Belgium
[6]Department of Biotechnology, Delft University of Technology, 2629 HZ Delft, the Netherlands
[7]Department of Earth Sciences (Geochemistry), Faculty of Geosciences, Utrecht University, Princetonlaan 8a, 3584 CB Utrecht, the Netherlands

*Correspondence author: richirt.julien@gmail.com

Published in Biogeosciences, 17, 1415–1435, 2020

Received 23 September 2019
Accepted 10 February 2020

ABSTRACT

Over the last decades, hypoxia in marine coastal environments has become more and more widespread, prolonged and intense. Hypoxic events have large consequences for the functioning of benthic ecosystems. In severe cases, they may lead to complete anoxia and the presence of toxic sulfides in the sediment and bottom-water, thereby strongly affecting biological compartments of benthic marine ecosystems. Within these ecosystems, benthic foraminifera show a high diversity of ecological responses, with a wide range of adaptive life strategies. Some species are particularly resistant to hypoxia–anoxia, and consequently it is interesting to study the whole foraminiferal community as well as species specific responses to such events. Here we investigated the temporal dynamics of living benthic foraminiferal communities (recognised by CellTracker™ Green) at two sites in the saltwater Lake Grevelingen in the Netherlands. These sites are subject to seasonal anoxia with different durations and are characterised by the presence of free sulfide (H_2S) in the uppermost part of the sediment. Our results indicate that foraminiferal communities are impacted by the presence of H_2S in their habitat, with a stronger response in the case of longer exposure times. At the deepest site (34 m), in summer 2012, 1 to 2 months of anoxia and free H_2S in the surface sediment resulted in an almost complete disappearance of the foraminiferal community. Conversely, at the shallower site (23 m), where the duration of anoxia and free H_2S was shorter (1 month or less), a dense foraminiferal community was found throughout the year except for a short period after the stressful event. Interestingly, at both sites, the foraminiferal community showed a delayed response to the onset of anoxia and free H_2S, suggesting that the combination of anoxia and free H_2S does not lead to increased mortality, but rather to strongly decreased reproduction rates. At the deepest site, where highly stressful conditions prevailed for 1 to 2 months, the recovery time of the community takes about half a year. In Lake Grevelingen, *Elphidium selseyense* and *Elphidium magellanicum* are much less affected by anoxia and free H_2S than *Ammonia* sp. T6. We hypothesise that this is not due to a higher tolerance for H_2S, but rather related to the seasonal availability of food sources, which could have been less suitable for *Ammonia* sp. T6 than for the elphidiids.

1. INTRODUCTION

Hypoxia affects numerous marine environments, from the open ocean to coastal areas. Over the last decades, a general decline in oxygen concentration was observed in marine waters (Stramma et al., 2012), with an extent varying between the concerned regions. In coastal areas, oxygen concentrations have been estimated to decrease 10 times faster than in the open ocean, with indications of a recent acceleration, expressed by increasing frequency, intensity, extent and duration of hypoxic events (Diaz and Rosenberg, 2008; Gilbert et al., 2010). This is due to the combination of (1) global warming, which is strengthening seasonal stratification of the water column and decreasing oxygen solubility, and (2) eutrophication resulting from increased anthropogenic nutrient and/or organic matter input, which is enhancing benthic oxygen consumption in response to increased primary production (Diaz and Rosenberg, 2008). Bottom-

water hypoxia has serious consequences for the functioning of all benthic ecosystem compartments (see Riedel et al., 2016, for a review). Benthic faunas are strongly impacted by these events (Diaz and Rosenberg, 1995), even though the meiofauna, especially foraminifera, appears to be less sensitive to low dissolved oxygen (DO) concentrations than the macrofauna (e.g. Josefson and Widbom, 1988). Many foraminiferal taxa are able to withstand seasonal hypoxia–anoxia (see Koho et al., 2012, for a review), and consequently they can play a major role in carbon cycling in ecosystems affected by seasonal low-oxygen concentrations (Woulds et al., 2007). Anoxia is often accompanied by free sulfide (H_2S) in pore and/or bottom waters (e.g. Jørgensen, 1982; Seitaj et al., 2015), which is considered very harmful for the benthic macrofauna (Wang and Chapman, 1999). Neutral molecular H_2S can diffuse through cellular membranes and inhibits the functioning of cytochrome *c* oxidase (a mitochondrial enzyme involved in ATP production), finally inhibiting aerobic respiration (Nicholls and Kim, 1982; Khan et al., 1990; Dorman et al., 2002).

Lake Grevelingen (southwestern Netherlands) is a former branch of the Rhine–Meuse–Scheldt estuary, which was closed in its eastern part (riverside) by the Grevelingen Dam in 1964 and in its western part (seaside) by the Brouwers Dam in 1971. The resulting saltwater lake, with a surface of 115 km^2, is one of the largest saline lakes in western Europe. Lake Grevelingen is characterised by a strongly reduced circulation (even after the construction of a small sluice in 1978) with a strong thermal stratification occurring in the main channels in summer, leading to seasonal bottom-water hypoxia–anoxia in late summer and early autumn (Bannink et al., 1984). This situation results in a rise of the H_2S front in the uppermost part of the sediment, sometimes up to the sediment–water interface.

These observations especially concern the Den Osse Basin (i.e. one of the deeper basins, maximum depth 34 m; Hagens et al., 2015), which has been intensively monitored over the last decades, so that a large amount of environmental data are available (e.g. Wetsteijn, 2011; Donders et al., 2012). The annual net primary production in the Den Osse Basin (i.e. 225 gC m^{-2} yr^{-1}; Hagens et al., 2015) is comparable to other estuarine systems in Europe (Cloern et al., 2014). However, there is almost no nutrient input from external sources; thus primary production is largely based on autochthonous recycling (> 90 %; Hagens et al., 2015), both in the water column and in the sediment, with a very strong pelagic–benthic coupling (de Vries and Hopstaken, 1984). The benthic environment is characterised by the presence of two antagonistic groups of bacteria, with contrasting seasonal population dynamics (i.e. cable bacteria in winter–spring and *Beggiatoaceae* in autumn–winter), which have a profound impact on all biogeochemical cycles in the sediment column (Seitaj et al., 2015; Sulu-Gambari et al.,

2016a, b). The combination of hypoxia–anoxia with sulfidic conditions, which is rather unusual in coastal systems without external nutrient input, and the activity of antagonistic bacterial communities makes Lake Grevelingen a very peculiar environment. In the Den Osse Basin, seasonal anoxia coupled with the presence of H_2S at or very close to the sediment–water interface occurs in summer (i.e. between July–September). However, euxinia (i.e. diffusion of free H_2S in the water column) does not occur, because of cable bacterial activity (Seitaj et al., 2015).

Although the tolerance of foraminifera towards low DO contents and long-term anoxia (from weeks to 10 months) has been well documented for many species from different types of environments in laboratory culture (e.g. Moodley and Hess, 1992; Alve and Bernhard, 1995; Bernhard and Alve, 1996; Moodley et al., 1997; Duijnstee et al., 2003, 2005; Geslin et al., 2004, 2014; Ernst et al., 2005; Pucci et al., 2009; Koho et al., 2011) as well as in field studies (e.g. Piña-Ochoa et al., 2010b; Langlet et al., 2013, 2014), their tolerance of free H2S is still debated. In the vast majority of previous studies, no decrease in the total abundances of living foraminifera (i.e. strongly increased mortality) was observed during anoxic events. Unfortunately, studies on foraminiferal response in systems affected by seasonal hypoxia–anoxia with sulfidic conditions are still very sparse. The few available observations are not conclusive, but they suggest that H_2S could be toxic for foraminifera even on fairly short timescales (Bernhard, 1993; Moodley et al., 1998b; Panieri and Sen Gupta, 2008; Langlet et al., 2014).

To our knowledge, all earlier studies show that the foraminiferal response to hypoxia–anoxia is species-specific (e.g. Bernhard and Alve, 1996; Ernst et al., 2005; Bouchet et al., 2007; Geslin et al., 2014; Langlet et al., 2014). However, this species-specific response generally follows the same scheme (usually decrease in density, reduction of growth and/or reproduction), with different response intensities. Duijnstee et al. (2005) suggested that oxic stress leads to an increased mortality and inhibited growth and reproduction. The suggestion of inhibited growth is supported by LeKieffre et al. (2017), who observed that the morphospecies *Ammonia tepida* (probably *Ammonia* sp. T6) showed minimal or no growth under anoxia. Conversely, Geslin et al. (2014) and Nardelli et al. (2014) suggested that, in the same morphospecies, reproduction was strongly reduced, but growth would not be affected by hypoxic and/or short anoxic events. Additionally, under low-oxygen conditions, some species are able to shift to anaerobic metabolism (i.e. denitrification; Risgaard-Petersen et al., 2006; Piña-Ochoa et al., 2010a), to sequester chloroplast (i.e. kleptoplastidy; Jauffrais et al., 2018), to

associate with bacterial symbionts (Bernhard et al., 2010) or to enter into a state of dormancy (Ross and Hallock, 2016; LeKieffre et al., 2017).

The highly peculiar environmental context of Lake Grevelingen offers an excellent opportunity to study this still poorly known aspect of foraminiferal ecology.

The conventional method to discriminate between live and dead foraminifera uses Rose Bengal, a compound which stains proteins (i.e. organic matter). This method was proposed for foraminifera by Walton (1952) and is based on the assumption that "the presence of protoplasm is positive indication of a living or very recently dead organism". The author already noted that this assumption implied that the rate of degradation of organic material should be relatively high. Previous studies of living benthic foraminifera in environments subjected to hypoxia–anoxia were almost all based on Rose Bengal-stained samples (e.g. Gustafsson and Nordberg, 1999, 2000; Duijnstee et al., 2004; Panieri, 2006; Schönfeld and Numberger, 2007; Polovodova et al., 2009; Papaspyrou et al., 2013). However, foraminiferal protoplasm may remain stainable from several weeks to months after their death (Corliss and Emerson, 1990), especially under low dissolved oxygen concentrations where organic matter degradation may be very slow (Bernhard, 1988; Hannah and Rogerson, 1997; Bernhard et al., 2006). The Rose Bengal staining method is therefore not suitable for studies in environments affected by hypoxia–anoxia. Consequently, the results of foraminiferal studies in low-oxygen environments based on this method have to be considered with reserve. In order to avoid this problem, we used CellTracker™ Green (CTG) to recognise living foraminifera. CTG is a fluorescent probe which marks only living individuals with cytoplasmic (i.e. enzymatic) metabolic activity (Bernhard et al., 2006). Since metabolic activity stops after the death of the organism, CTG should give a much more accurate assessment of the living assemblages at the various sampling times and thereby avoid overestimation of the live foraminiferal abundances.

In this study, samples were collected in August and November 2011 and then every month through the year 2012, at two different stations in the Den Osse Basin, with two replicates dedicated to foraminifera. The two stations were chosen in contrasted environments regarding water depth (34 and 23 m, respectively) and duration of seasonal hypoxia–anoxia and sulfidic conditions. Living foraminiferal assemblages were studied in the uppermost sediment and size distributions were determined in order to get insight into the possible moment(s) of reproduction or accelerated growth in test size. The seasonal variability study of the foraminiferal community allows us (1) to better understand the foraminiferal tolerance of seasonal hypoxia–anoxia with the presence of free H_2S in their microhabitat and (2) to obtain information about the responses of the various species to adverse conditions. This knowledge

will be useful for the development of indices assessing environmental quality (i.e. biomonitoring) and may also improve palaeoecological interpretations of coastal records (e.g. Murray, 1967; Gustafsson and Nordberg, 1999).

2. MATERIALS AND METHODS

2.1. STUDIED AREA – ENVIRONMENTAL SETTINGS IN THE DEN OSSE BASIN

Lake Grevelingen is a part of the former Rhine–Meuse–Scheldt estuary, in the southwestern Netherlands. This former estuarine branch was turned into an artificial saltwater lake during the Delta Works project. In Lake Grevelingen, the water circulation is strongly limited by the construction of dams (in the early 1970s) and only a small sluice allows water exchanges with open seawater (i.e. very weak hydrodynamics). In the lake, development of bottom-water hypoxia–anoxia occurs in the deepest part of the basin in summer (i.e. July–September) to early autumn (i.e. October–December; Bannink et al., 1984; Hagens et al., 2015). In the literature, the terminology and threshold values used to describe oxygen depletion are highly variable (e.g. oxic, dysoxic, hypoxic, suboxic, microxic, postoxic; see Jorissen et al., 2007; Altenbach et al., 2012). In this study we defined hypoxia as a concentration of oxygen < 63 μmol L^{-1} (1.4 mL L^{-1} or 2 mg L^{-1}) whereas anoxia is defined as no detectable oxygen (following Rabalais et al., 2010).

In Den Osse Basin, the nutrient input from external sources is very low and pelagic–benthic coupling is essential, as already noted by de Vries and Hopstaken (1984). In 2012, phytoplankton blooms occurred in April–May and July (Hagens et al., 2015) in response to the increasing solar radiation and nutrient availability in the water column following organic matter recycling in winter. This led to an increased food availability in the benthic compartment in the same periods. In general, Chl *a* concentrations in Den Osse Basin are below 10 μg L^{-1}, excluding very short peaks during blooms in April–May and July which did not exceed 30 μg L^{-1} in 2012 (Hagens et al., 2015). Thermal stratification of the water column and increased oxygen consumption due to organic matter input (i.e. from phytoplankton blooms) are both responsible for the development of seasonal bottom-water hypoxia–anoxia in summer (i.e. July–September). Although euxinia (i.e. the presence of free H_2S in the water column) does not occur in the Den Osse Basin due to cable bacterial activity in winter, free H_2S is present in the uppermost layer of the sediment in summer (Seitaj et al., 2015). Summarising, in the benthic ecosystem, increased food availability in summer is counterbalanced by strongly decreasing

oxygen contents, sometimes accompanied by the presence of free sulfides in the topmost sediment.

2.2. FIELD SAMPLING

The two studied sites are located along a depth gradient in the Den Osse Basin of Lake Grevelingen. Both station 1 (51°44.8340' N, 3°53.4010' E) and station 2 (51°44.9560' N, 3°53.8260' E) are located in the main channel, at 34 and 23 m depth, respectively (Fig. 1).

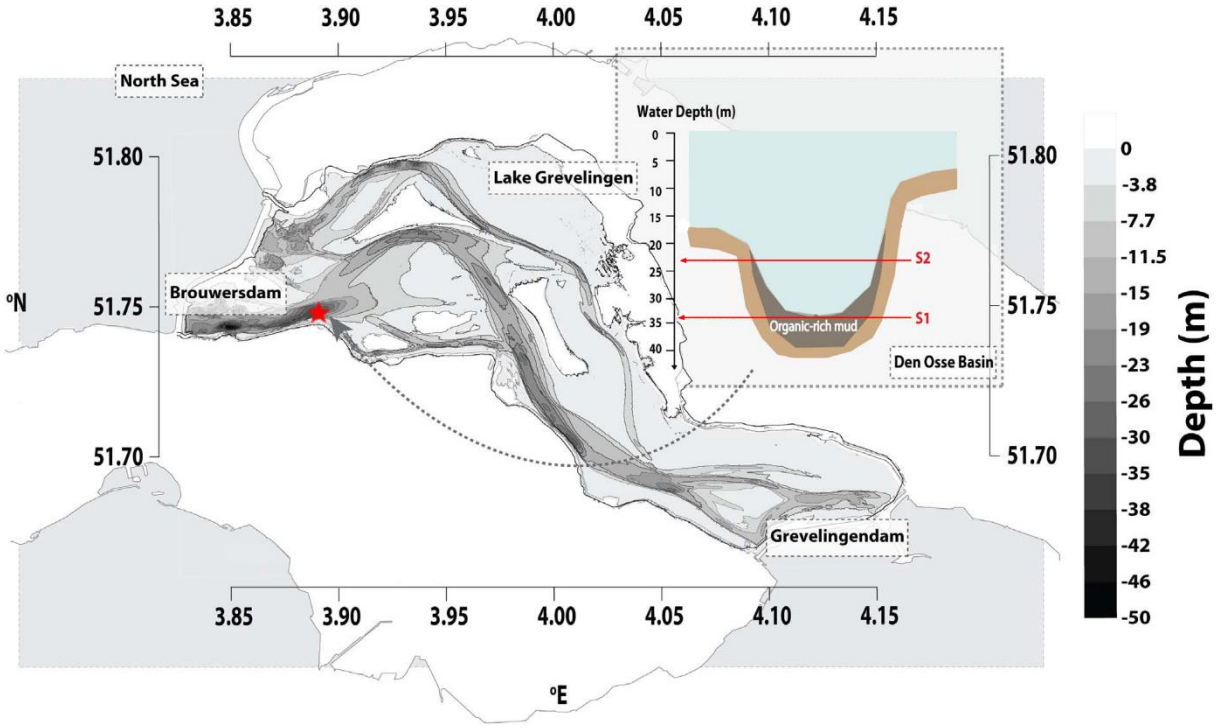

Figure 1. Map of Lake Grevelingen showing the location of the two sampled stations in the Den Osse Basin (red star). The transversal section of the Den Osse Basin (top right) shows the depth at which station 1 (S1) and station 2 (S2) were sampled (34 and 23 m depth, respectively). This figure was modified from Sulu-Gambari et al. (2016b).

Measurements of bottom-water oxygen (BWO) concentrations were performed at 2m above the sediment–water interface and are from Donders et al. (2012), whereas the data for 2012 were published in Hagens et al. (2015). Sediment cores were collected monthly in 2012 using a single core gravity corer (UWITEC, Austria) using PVC core liners (6 cm inner diameter, 60 cm length). All cores were inspected upon retrieval and only visually undisturbed sediment cores were used for further analysis (Seitaj et al., 2017). Oxygen penetration depth (OPD) and depth of free H_2S detection were determined by Seitaj et al. (2015) using profiling microsensors for station 1. The data for station 2 (Supplement Table S1) were acquired similarly and during

the same cruises but never published; for further details about the sampling method, see Seitaj et al. (2015).

Two replicate sediment cores dedicated to the foraminiferal study were sampled in August and November 2011 using the same gravity corer (UWITEC, Austria) and then monthly throughout the year 2012 at the same sampling time as for BWO concentration and OPD and H_2S measurements in the sediment (see Seitaj et al., 2015). Consequently, for 2012 at stations 1 and 2, OPD and H_2S were measured in the sediment column at the same time as foraminifera were sampled (Seitaj et al., 2015). For each replicate, the uppermost centimetre (0–1 cm) of the core was then transferred on board in a vial of 250 mL, and 30 mL of seawater (at the same temperature as in situ) was added to the vial. Then we labelled the samples with CellTracker™ Green CMFDA (CTG, 5-chloromethylfluorescein diacetate, final concentration of 1 μmol L^{-1} following Bernhard et al., 2006) and slowly agitated manually to allow the CTG diffusion in the whole sample. Samples were then fixed in 5 % sodium-borate-buffered formalin after 24 h of incubation in the dark.

2.3. SAMPLE TREATMENT

All samples were sieved over 315, 150 and 125 μm meshes, and foraminiferal assemblages were studied in all three size fractions. Individuals were picked wet under an epifluorescence stereomicroscope (Olympus SZX12, light fluorescent source Olympus URFL-T, excitation/emission wavelengths: 492 nm/517 nm) and placed on micropalaeontological slides. Only specimens that fluoresced brightly green were considered living and were identified to the (morpho)species level when possible. Since picking foraminifera under an epifluorescence stereomicroscope is particularly time-consuming, we decided to study samples only every 2 months for the year 2012. At a later stage, in view of the large differences in foraminiferal abundances between the samples of September and November 2012 at station 2, we decided to study the October and December 2012 samples as well for this station. The sampling dates investigated in this study are listed in Table 1.

Table 1. Sampling dates of the samples which were investigated for living foraminifera for stations 1 and 2. X: one core investigated; O: no core investigated.

Year	Month	Day	Station 1	Station 2
2011	August	22	X X	X X
2011	November	15	X X	X X
2012	January	23	X X	X X
2012	March	12	X X	X X
2012	May	30	X X	X X
2012	July	24	X X	X X
2012	September	20	X X	X X
2012	October	18	O	X X
2012	November	2	X X	X X
2012	December	3	O	X X

Abundances were then standardised to a volume of 10 cm^3. The abundances of living foraminifera for each sampling time and replicate are listed in Tables S2 and S3. The mean abundance and standard deviation ($\bar{x} \pm$ SD) for the two replicates for each sampling date were calculated for both the total living assemblage and the individual species, as an indication of spatial patchiness.

2.4. TAXONOMY OF DOMINANT SPECIES

Four dominant species (> 1 % of the total assemblage) were present in our material: *Ammonia* sp. T6, *Elphidium magellanicum* (Heron-Allen and Earland, 1932), *Elphidium selseyense* (Heron-Allen and Earland, 1911) and *Trochammina inflata* (Montagu, 1808). As we identified these species on the basis of morphological criteria, we will use them as "morphospecies".

Concerning the genus *Ammonia*, two living specimens collected at Grevelingen station 1 were molecularly identified (by DNA barcoding) as phylotype T6 by Bird et al. (2019). At the same site, we genotyped seven other living *Ammonia* specimens, which were all T6. Their sequences were deposited in GenBank (accession numbers MN190684 to MN190690), and Supplement Fig. S1 shows scanning electron microscope (SEM) images of the spiral side and of the penultimate chamber at 1000x magnification for four individuals. A morphological screening based on the criteria proposed by Richirt et al. (2019) confirmed that T6 accounts for the vast majority (> 98 %) of *Ammonia* individuals, whereas phylotypes T1, T2, T3 and T15 are only present in very small amounts (Table S3).

The specimens of *Elphidium magellanicum* were identified exclusively on the basis of morphological criteria, as there are no molecular data available yet. This morphospecies,

although rare, is regularly recognised in Boreal and Lusitanian provinces of Europe (e.g. Gustafsson and Nordberg, 1999; Darling et al., 2016; Alve et al., 2016). However, as the type species was described from the Strait of Magellan (Southern Chile), the European specimens may represent a different species and further studies involving DNA sequencing of both populations are needed to confirm or disprove this taxonomic attribution (see Roberts et al., 2016).

Elphidium selseyense has often been considered an ecophenotype of *Elphidium excavatum* (Terquem, 1875) and has been identified as *E. excavatum* forma *selseyensis* (e.g. Feyling-Hanssen, 1972; Miller et al., 1982). Four living specimens were already sampled for DNA analysis at station 1 and were all identified as the species *E. selseyense* (phylotype S5, Darling et al., 2016). We only observed minor morphological variations in our material, especially concerning the number of small bosses in the umbilical region, which we considered to be intraspecific variability. Consequently, we identified all our specimens as *E. selseyense*. The specimens attributed to *Trochammina inflata* were also identified exclusively on the basis of morphological criteria, as no molecular data are available yet.

2.5. SIZE DISTRIBUTION MEASUREMENT

In order to detect periods of increased growth and/or reproduction, size measurements were performed on all samples of 2012. The measurements were made for all species (4176 individuals for station 1 and 19624 individuals for station 2), and trochospiral species were all orientated spiral side up prior to measurements. High-resolution images (3648 pixels x 2736 pixels) of all micropalaeontological slides were taken with a stereomicroscope (Leica S9i, 10x magnification) and individual measurements were processed using ImageJ software (Schneider et al., 2012, Fig. S2).

Each individual was isolated (Fig. S2) and its maximum diameter was measured (i.e. Feret's diameter). We represented all size distributions using histograms with 20 μm classes (the best compromise between the total number of individuals and the size range (Fig. S3). As we only examined the size fractions > 125 μm, our analysis mainly concerns adult specimens and does not include juveniles. This limitation should be kept in mind when interpreting the results.

Assuming that the size distribution was a sum of Gaussian curves, each of them representing a cohort, we tried to identify the approximate mode for the Gaussian curves (i.e. cohorts) using the changes in slope (i.e. inflexion points) of the second-order derivative of the

total size distribution (Gammon et al., 2017). Unfortunately, this tentative attempt to distinguish cohorts by using a deconvolution method was not conclusive. The main problem was the lack of information concerning individuals smaller than 125 μm, so that our size distributions were systematically skewed toward small individuals. Because the identification of individual cohorts was not successful, a study of population dynamics was not possible. For this reason, the data are only shown in Figs. S2 and S3. Nevertheless, the size distribution data give some clues concerning the possible moment(s) of reproduction or intensified test growth for the different species.

2.6. ENCRUSTED FORMS OF *E. MAGELLANICUM*

In our samples, we found abundant encrusted forms of *E. magellanicum* at station 1 (May 2012) and station 2 (May, July, September and December 2012, Fig. 2). Most individuals were totally encrusted (Fig. 2a), others only partly (Fig. 2b). These crusts were hard, firmly stuck to the shell (difficult to remove with a brush), thin (Fig. 2c–e) and rather coarse. In order to determine if the crust matrix is constituted of carbonate, we placed some specimens in microtubes and exposed them to 0.1 M of EDTA (ethylenediaminetetraacetic acid) diluted in 0.1 M cacodylate buffer (acting as a carbonate chelator). After an exposition of 24 h, we checked under a stereomicroscope if the crust was still cohesive (no carbonate in the crust) or was disaggregated (crust contains carbonate).

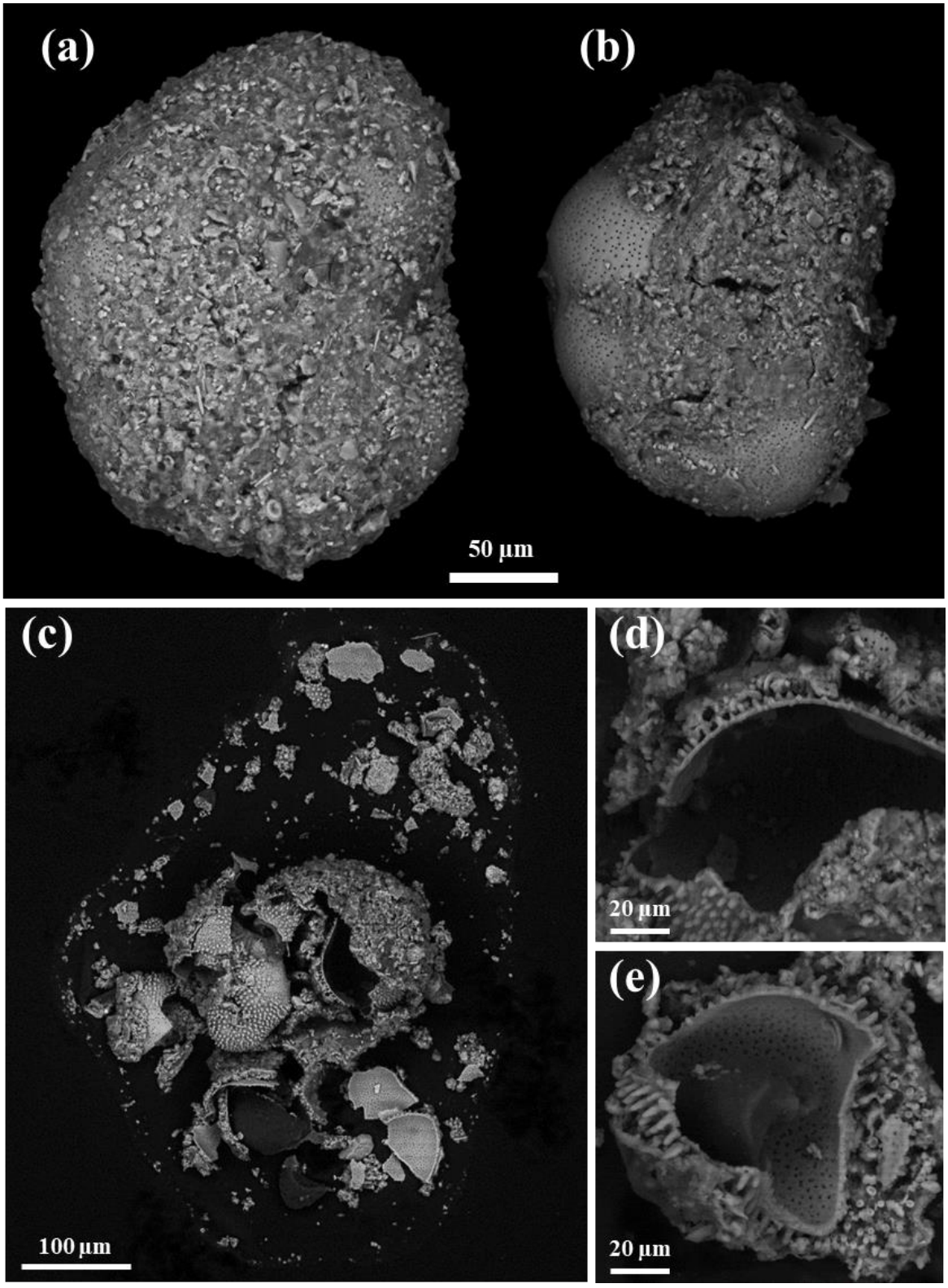

Figure 2. SEM images of fully encrusted specimen (a), partially encrusted specimen (b) and crushed encrusted specimen of *Elphidium magellanicum* (c). Note the thinness of the crust and the spinose structures in (d) and (e).

3. RESULTS

3.1. TOTAL ABUNDANCES OF FORAMINIFERAL ASSEMBLAGES

Averaged total abundances varied between 1.1 ± 1.5 and 449.9 ± 322.1 ind. 10 cm^{-3} for station 1 and between 91.1 ± 25.0 and 604.8 ± 3.5 ind. 10 cm^{-3} for station 2 (Fig. 3 and Table 2). For every studied month, the total density was higher at station 2 than at station 1. The seasonal succession is very different between the two sites (Fig. 3). Station 1 shows very low total foraminiferal abundances for most months, contrasting with much higher densities in May and July. Conversely, station 2 shows high total foraminiferal abundances throughout the year, with somewhat lower values in November 2011 and October and November 2012 (Fig. 3).

Table 2. Mean living foraminiferal absolute (ind. 10 cm^{-3}) and relative abundances (percentage of the total fauna, in parentheses) of the dominant species. Last column: absolute abundance of the total fauna.

Year	Month	*Elphidium selseyense*	*Ammonia* sp. T6	*Elphidium magellanicum*	*Trochammina inflata*	Others	Total
Station 1							
2011	Aug	1.2 (36.8)	1.2 (36.8)	0.0 (0.0)	0.0 (0.0)	0.9 (26.3)	3.4
2011	Nov	0.5 (50.0)	0.4 (33.3)	0.0 (0.0)	0.0 (0.0)	0.2 (16.7)	1.1
2012	Jan	5.1 (44.6)	3.2 (27.7)	0.2 (1.5)	1.2 (10.8)	1.8 (15.4)	11.5
2012	Mar	23.9 (38.5)	12.9 (20.8)	21.6 (34.8)	1.4 (2.3)	2.3 (3.7)	62.1
2012	May	336.5 (74.8)	9.2 (2.0)	96.4 (21.4)	1.8 (0.4)	6.0 (1.3)	449.9
2012	Jul	162.0 (90.2)	10.3 (5.7)	3.7 (2.1)	0.0 (0.0)	3.5 (2.0)	179.5
2012	Sep	29.7 (87.5)	2.3 (6.8)	0.0 (0.0)	0.4 (1.0)	1.6 (4.7)	34.0
2012	Nov	1.1 (66.7)	0.4 (22.2)	0.0 (0.0)	0.0 (0.0)	0.2 (11.1)	1.6
Sum		560.0 (75.4)	39.8 (5.4)	121.8 (16.4)	4.8 (0.6)	16.4 (2.2)	742.9
Station 2							
2011	Aug	74.8 (43.0)	82.1 (47.2)	0.0 (0.0)	14.7 (8.4)	2.5 (1.4)	174.0
2011	Nov	52.3 (40.7)	60.8 (47.3)	0.0 (0.0)	11.8 (9.2)	3.7 (2.9)	128.7
2012	Jan	161.8 (30.9)	226.2 (43.2)	0.9 (0.2)	121.5 (23.2)	13.3 (2.5)	523.6
2012	Mar	214.7 (38.2)	214.0 (38.1)	48.8 (8.7)	75.0 (13.3)	9.9 (1.8)	562.3
2012	May	288.2 (47.7)	147.1 (24.3)	116.0 (19.2)	36.1 (6.0)	17.3 (2.9)	604.8
2012	Jul	282.6 (53.2)	158.4 (29.8)	37.8 (7.1)	31.5 (5.9)	21.2 (4.0)	531.6
2012	Sep	365.5 (64.4)	102.4 (18.0)	72.0 (12.7)	16.1 (2.8)	11.5 (2.0)	567.5
2012	Oct	98.7 (46.7)	99.0 (46.8)	1.8 (0.8)	7.4 (3.5)	4.6 (2.2)	211.5
2012	Nov	30.9 (34.0)	48.1 (52.8)	4.1 (4.5)	3.7 (4.1)	4.2 (4.7)	91.1
2012	Dec	252.2 (66.7)	78.0 (20.6)	25.5 (6.7)	12.7 (3.4)	9.5 (2.5)	377.9
Sum		1821.8 (48.3)	1216.1 (32.2)	306.8 (8.1)	330.5 (8.8)	97.7 (2.6)	3773.0

At station 1, almost no individuals were present in August ($\overline{x} = 3.4 \pm 1.3$) and November 2011 ($\overline{x} = 1.1 \pm 1.5$). In 2012, total abundances were very low in January ($\overline{x} = 11.5 \pm 9.3$), showed a slight increase in March ($\overline{x} = 62.1 \pm 19.3$) and reached a maximal abundance in May ($\overline{x} = 449.9 \pm 322.1$). Total abundances then progressively decreased from May to September ($\overline{x} = 34.0 \pm 17.0$) and almost no foraminifera were present in November ($\overline{x} = 1.6 \pm 0.3$).

At station 2, total abundances were comparatively low in August and November 2011 ($\overline{x} = 174.0 \pm 48.0$ and $\overline{x} = 128.7 \pm 25.0$ ind. 10 cm^{-3}, respectively). In 2012, total abundances

were relatively high and stable from January to September (between $\overline{x} = 523.6 \pm 30.7$ and $\overline{x} = 604.8 \pm 3.5$), then decreased in October ($\overline{x} = 211.5 \pm 8.0$) and November ($\overline{x} = 91.1 \pm 25.3$) and finally increased again in December ($\overline{x} = 377.9 \pm 38.8$).

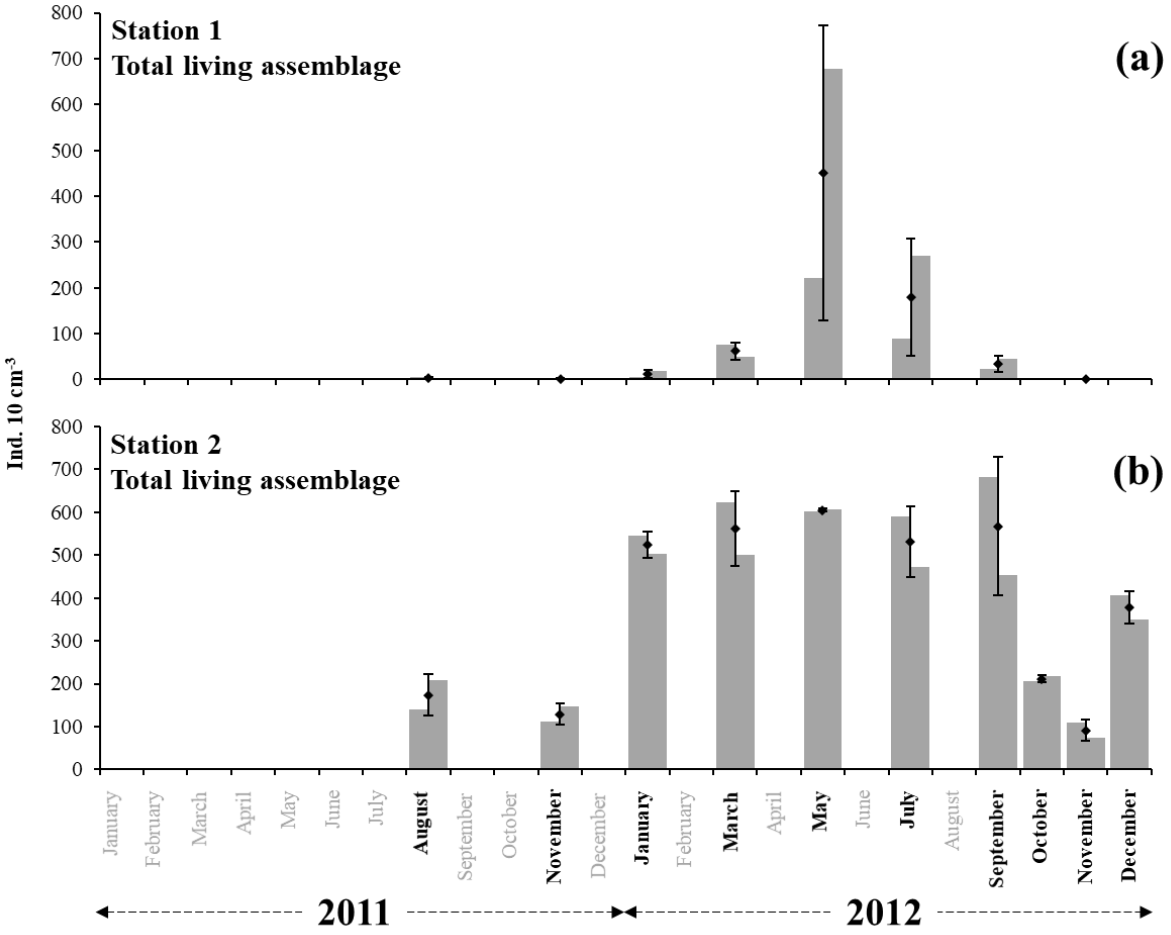

Figure 3. The grey bars represent the living foraminiferal abundances for the two replicates. The mean abundances (diamonds) and standard deviations (black error bars) were calculated for the two replicates for stations 1 (34 m depth, a) and 2 (23 m depth, b). All abundance values are for the 0–1 cm layer and were standardised to 10 cm^3. Months where foraminiferal communities were investigated are indicated in bold (excluding October and December at station 1).

3.2. DOMINANT SPECIES

At station 1, the major species were, in order of decreasing abundances, *Elphidium selseyense* (Fig. 4a–b), *Elphidium magellanicum* (Fig. 4c–d) and *Ammonia* sp. T6 (Fig. 4e–g). In Figure 4, we added *Trochammina inflata* (Fig. 4h–j) to facilitate comparison with station 2, where this species is among the dominant ones. The "other species" account only for 2.2 % of the total assemblage at station 1. The fact that they are well represented in some months (e.g. 26.3 % of the assemblage in August 2011) is due to the extremely low number of individuals (see Fig. 3 and Table 2). At station 2, the dominant species, in order of decreasing abundances,

were *E. selseyense*, *Ammonia* sp. T6, *E. magellanicum* and *T. inflata* (Table 2). Here, "other species" account only for 2.6 % of the total assemblage. Whereas *E. selseyense* and *E. magellanicum* were dominant species at both stations, both *Ammonia* sp. T6 and *T. inflata* were present in much higher abundances at station 2 compared to station 1, where the latter species was almost absent (Figs. 5–6).

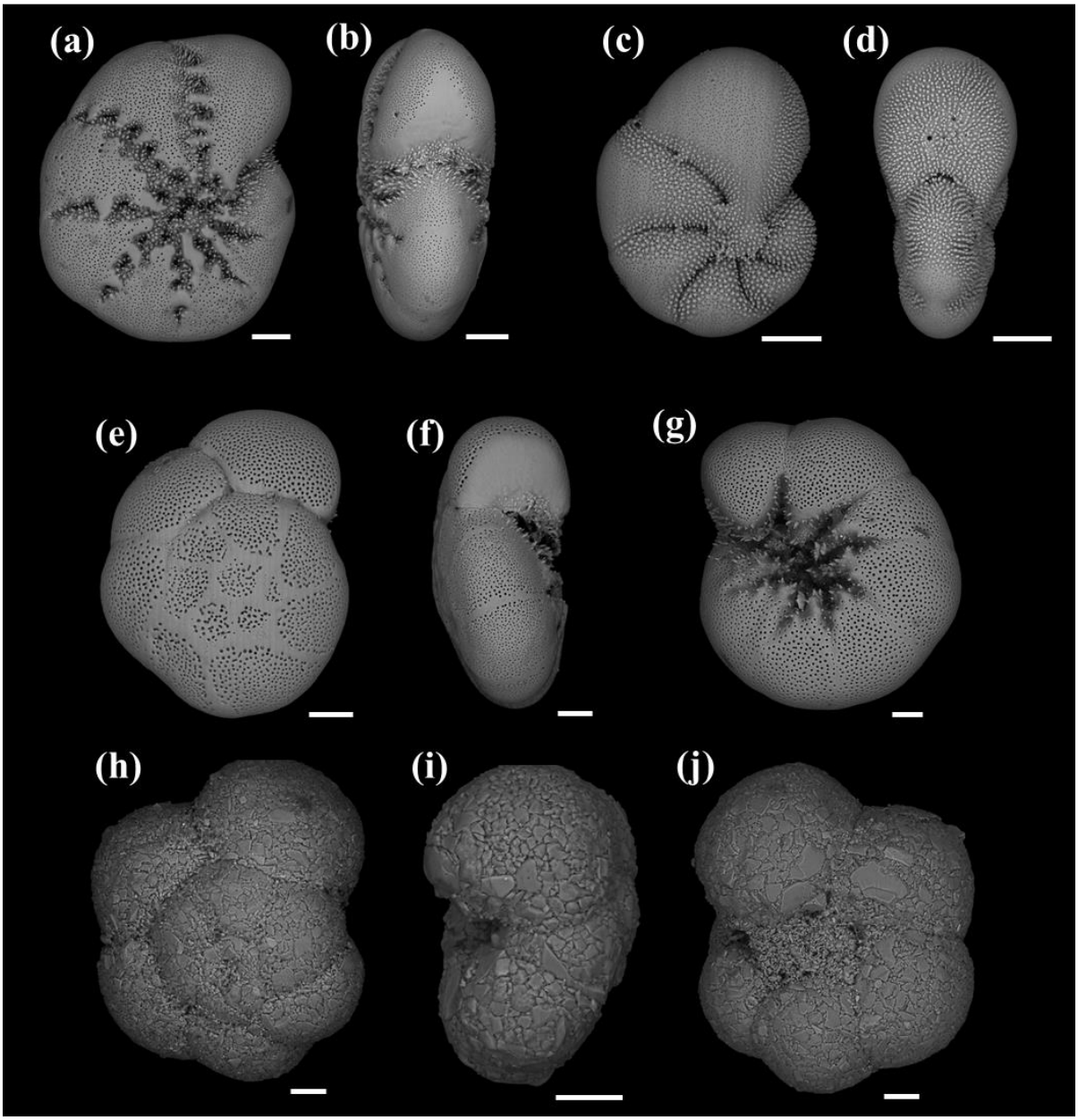

Figure 4. SEM images of *Elphidium selseyense* in lateral (a) and peripheral (b) views; *Elphidium magellanicum* in lateral (c) and peripheral (d) views; *Ammonia* sp. T6 in spiral (e), peripheral (f) and umbilical (g) views; and *Trochammina inflata* in spiral (h), peripheral (i) and umbilical (j) views. All scale bars are 50 μm.

At station 1, only some very scarce individuals of *E. selseyense* were observed in August and November 2011 (Fig. 5 and Table 2). In 2012, *E. selseyense* abundances were very low in

January and started to increase in March ($\overline{x} = 23.9 \pm 6.8$), reaching maximal values in May ($\overline{x} = 336.5 \pm 275.8$). In July, values for *E. selseyense* were still high ($\overline{x} = 162.0 \pm 121.5$) and further decreased until an almost total absence in November 2012. No specimen of *E. magellanicum* was observed in 2011 (Fig. 5 and Table 2). The abundance of *E. magellanicum* was very low in January 2012, started to increase in March ($\overline{x} = 21.6 \pm 11.0$), reaching maximal values in May ($\overline{x} = 96.4 \pm 47.3$) and then strongly decreased in July ($\overline{x} = 3.7 \pm 0.3$). The species was absent from samples in September and November 2012. *Ammonia* sp. T6 was almost absent in August and November 2011 and present with very few specimens in January 2012 ($\overline{x} = 3.2 \pm 3.5$). Maximum abundances were reached between March and July 2012 (ranging between $\overline{x} = 9.2 \pm 6.5$ and $\overline{x} = 12.9 \pm 1.3$). Then abundances rapidly decreased until the species was almost absent in November. *Trochammina inflata* was absent in 2011 and was only present in very low abundances from January to May and in September 2012.

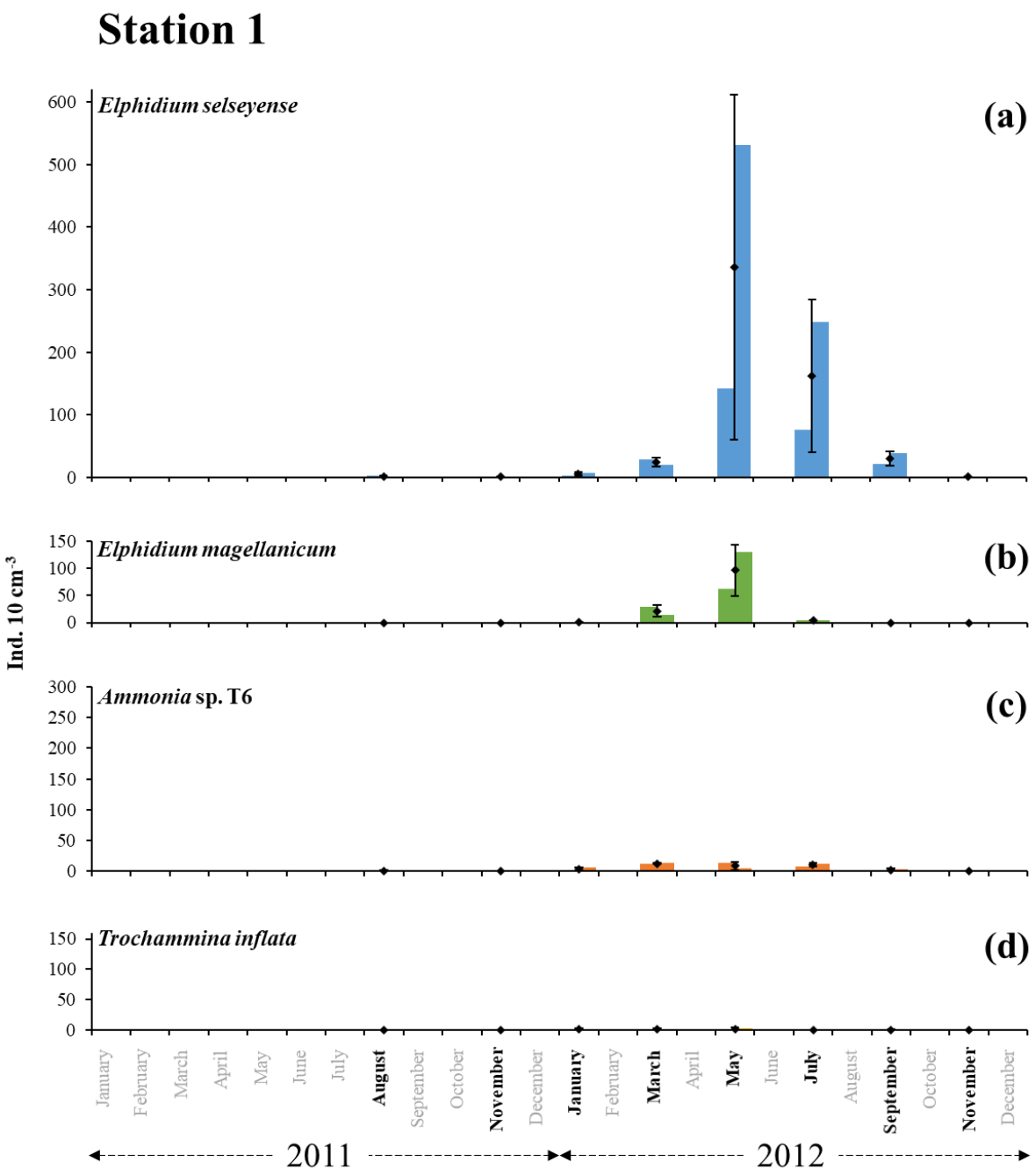

Figure 5. The bars represent the living foraminiferal abundances for the two replicates for *Elphidium selseyense* (a), *Elphidium magellanicum* (b), *Ammonia* sp. T6 (c) and *Trochammina inflata* (d) at station 1 in 2011 and 2012. The mean abundances (diamonds) and standard deviations (black error bars) were calculated for the two replicates. All abundance values are for the 0–1 cm layer and were standardised to 10 cm^3. Months when foraminiferal communities were investigated are indicated in bold. Scales were chosen in order to facilitate comparison with station 2.

At station 2, the two dominant species were *E. selseyense* and *Ammonia* sp. T6, which together always represented at least 70 % of the total assemblage (Fig. 6 and Table 2). These two species showed a different seasonal pattern over the considered period. Abundances of *E. selseyense* were comparable in August ($\overline{x} = 74.8 \pm 29.8$) and November 2011 ($\overline{x} = 52.3 \pm 27.0$) and then showed a progressive increase until a maximum in September 2012 ($\overline{x} =$

365.5 ± 70.3 . Abundances then showed a sharp decrease in October and November (respectively $\overline{x} = 98.7 \pm 8.5$ and $\overline{x} = 30.9 \pm 2.3$) to increase again in December ($\overline{x} = 252.2 \pm 41.0$). For *Ammonia* sp. T6, abundances strongly increased between November 2011 ($\overline{x} = 60.8 \pm 1.5$) and January 2012 ($\overline{x} = 226.2 \pm 52.3$) and then progressively decreased until the end of 2012 ($\overline{x} = 48.1 \pm 26.0$ in November 2012). *Trochammina inflata* showed an analogous pattern to *Ammonia* sp. T6. Abundances strongly increased between November 2011 ($\overline{x} = 11.8 \pm 1.8$) and January 2012 ($\overline{x} = 121.5 \pm 29.8$) and then progressively decreased until very low abundances in November ($\overline{x} = 3.7 \pm 3.0$). *E. magellanicum* was completely absent in August and November 2011, almost absent in January 2012 ($\overline{x} = 0.9 \pm 0.3$) and then suddenly increased until a maximum of $\overline{x} = 116.0 \pm 6.5$ in May. Abundances stayed relatively high in July ($\overline{x} = 37.8 \pm 2.5$) and September ($\overline{x} = 72.0 \pm 35.8$) and then drastically decreased until minimum numbers in October and November. Finally, like all other species, *E. magellanicum* abundances increased again in December ($\overline{x} = 25.5 \pm 13.0$).

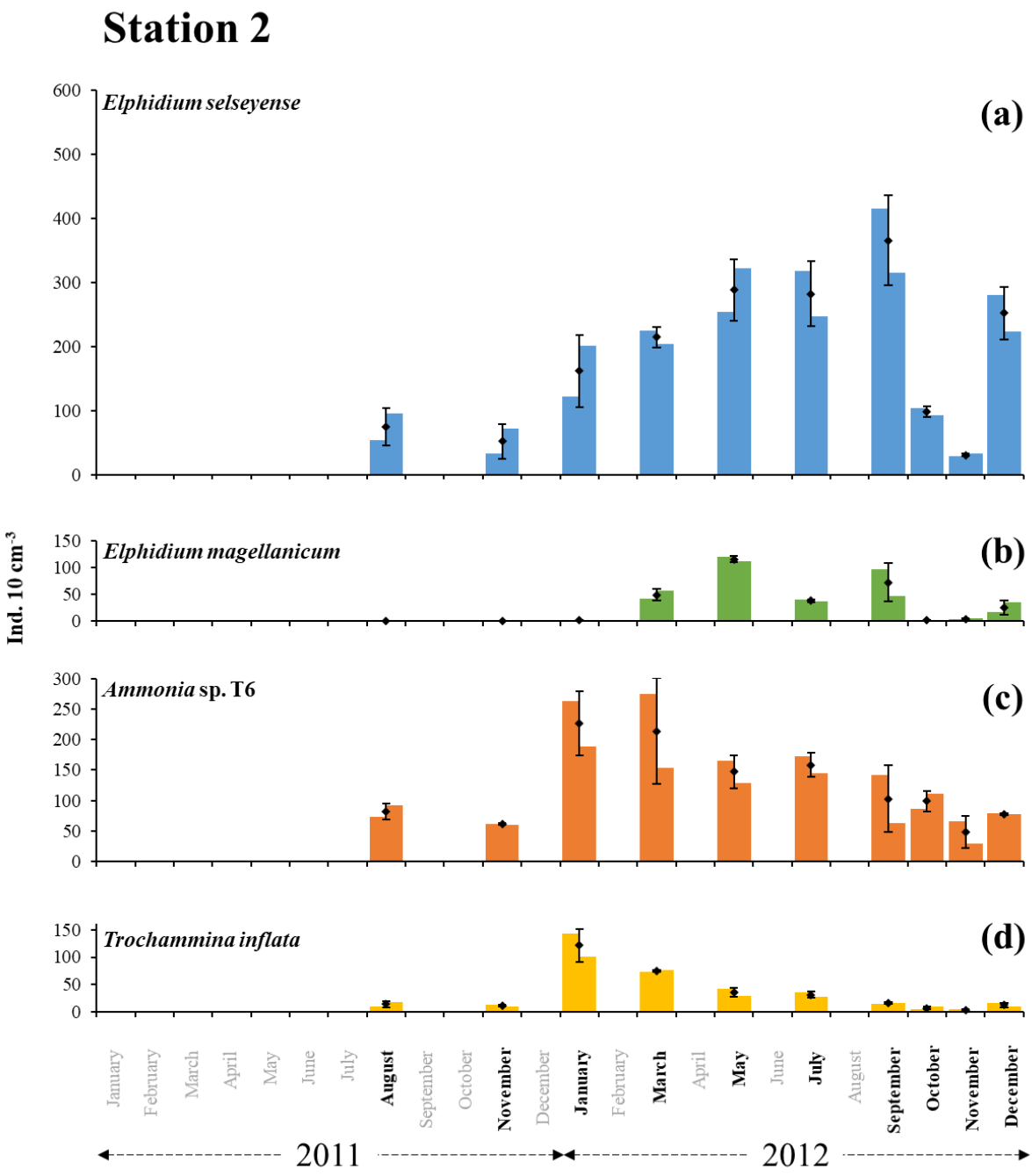

Figure 6. The bars represent the living foraminiferal abundances for the two replicates for *Elphidium selseyense* (a), *Elphidium magellanicum* (b), *Ammonia* sp. T6 (c) and *Trochammina inflata* (d) at station 2 in 2011 and 2012. The mean abundances (diamonds) and standard deviations (black error bars) were calculated for the two replicates. All abundances values are for the 0–1 cm layer and were standardised to 10 cm^3. Months when foraminiferal communities were investigated are indicated in bold. Scales were chosen in order to facilitate comparison with station 1.

3.3. ENCRUSTED FORMS OF *E. MAGELLANICUM*

After exposition to 0.1 M of EDTA diluted in 0.1 M cacodylate buffer, the crusts remained cohesive, indicating that they do not consist of carbonate and suggesting that they are composed

of sediment particles cemented by an organic matrix.

At station 1, encrusted forms of *E. magellanicum* were present in moderate proportions in May (26.8 % of the total *E. magellanicum* population, Fig. 7) and July (47.6 %); the species disappeared thereafter. At station 2, encrusted forms strongly dominated the *E. magellanicum* population from May (72.3 %) to December (88.0 %, Fig. 7).

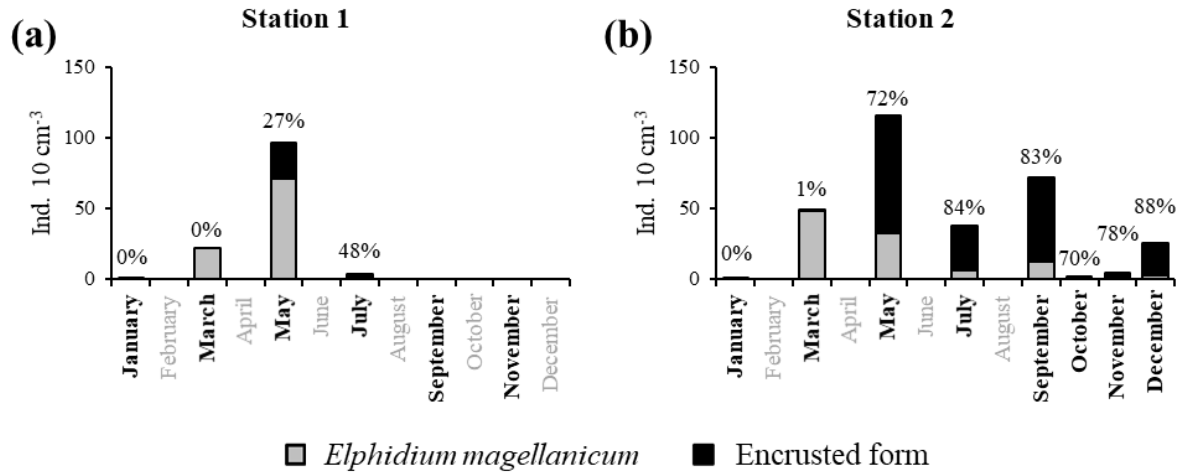

Figure 7. Mean abundances (ind. 10 cm^{-3}) of non-encrusted (grey) and encrusted forms (black) of *Elphidium magellanicum* in 2012, at stations 1 (a) and 2 (b), with proportion of encrusted forms above each bar (%). Investigated months are indicated in bold.

4. DISCUSSION

4.1. TOLERANCE OF FORAMINIFERAL COMMUNITIES TOWARDS ANOXIA AND FREE SULFIDE

At station 1, bottom waters were hypoxic in July 2012 and became anoxic in August (Fig. 8). Both in July and in August, oxygen penetration into the sediment was null, whereas it was 0.7 ± 0.1 mm depth in September. In all 3 months (July to September 2012), sulfidic conditions were observed very close to the sediment–water interface (1 mm or less, Fig. 8 and Table S1). In view of these results, the duration of anoxic and sulfidic conditions in the uppermost sediment layer can be estimated as 1 to 2 months (in July and August, Fig. 8).

After the strong increase in foraminiferal densities in May 2012, there was a decrease starting in July, leading to a near absence of foraminifera at station 1 in November (Fig. 8). The most probable cause of the strong decline of the foraminiferal community appears to be a prolonged presence of sulfides in the foraminiferal microhabitat. However, the fact that foraminiferal abundances reached almost zero only in September (about 2 months after the first occurrence of anoxic and sulfidic conditions in the upper sediment, in July) suggests that the

presence of H_2S did not cause instantaneous mortality, but that the disappearance of the foraminiferal community was a delayed response, probably caused by inhibited reproduction and, eventually, increased mortality. Inhibited reproduction has previously been suggested as a response to hypoxic–short anoxic (Geslin et al., 2014) and sulfidic conditions (Moodley et al., 1998b).

Such a time lag between a change in foraminiferal abundances and changes in environmental parameters affecting reproduction and/or growth of foraminifera has been suggested previously by Duijnstee et al. (2004). These authors highlighted that the density patterns of some foraminiferal species showed a higher correlation with measured environmental parameters (e.g. oxygenation or temperature) when a time lag of about 3 months was applied.

For 2011, at station 1, no pore-water O_2 and H_2S measurements are available. However, severe hypoxia was observed in the bottom waters from May to August, with anoxia in June 2011 (Fig. 8). We therefore assume that, like in 2012, anoxic and probably co-occurring sulfidic conditions were responsible for the very low standing stocks in August and November 2011 and January 2012.

Our observations confirm the suggestion in previous studies that the foraminiferal community is severely affected by a long-term presence of H_2S in its habitat but does not show instant mortality. In fact, after a 66 d incubation in euxinic conditions (a maximum of 11.9 ± 0.4 μmol L^{-1} of H_2S in the overlying water) of foraminiferal assemblages collected at a 19 m deep site in the Adriatic Sea, Moodley et al. (1998a) found a strong decrease in the total density of Rose Bengal stained foraminifera. After 21 d, living specimens were still observed, whereas after 42 and 66 d, the live checks (based on protoplasm movement) gave only negative results. Langlet et al. (2013, 2014) performed an in situ experiment with closed benthic chambers at a 24 m deep site in the Gulf of Trieste, in the Adriatic Sea. They observed a decrease in living foraminiferal density (labelled with CTG), but they also found that almost all species survived after 10 months of anoxia and periodically co-occurring H_2S in the sediment and overlying water. However, the duration of sulfidic conditions, which was estimated to be several weeks, could not be assessed precisely (Metzger et al., 2014). The suggestion that short exposure to euxinic conditions is not directly lethal for foraminifera is confirmed by the experimental results of Bernhard (1993), who found that foraminiferal activity (as determined by ATP content) was not significantly affected after 30 d exposure to euxinia (32.6 ± 8.6 % of active individuals, n = 174 in control conditions versus 29.5 ± 6.2 %, n = 173 in sulfidic conditions).

After the 2011 hypoxia–anoxia, standing stocks at station 1 only started to increase in March 2012, indicating a very long recovery time (about 6 months) of the foraminiferal faunas after a temporary near-extinction due to anoxic and sulfidic conditions. This confirms observations of relatively long recovery times in the literature (e.g. Alve, 1995, 1999; Gustafsson and Nordberg, 2000; Hess et al., 2005). For instance, Gustafsson and Nordberg (1999) showed that in the Koljö Fjord, at comparable water depths, foraminiferal populations responded with increased densities only 3 months after a renewal of sea-floor oxygenation following hypoxic conditions in the bottom waters. However, in that case, the disappearance of the foraminiferal population was only partial and not nearly as complete as in our study.

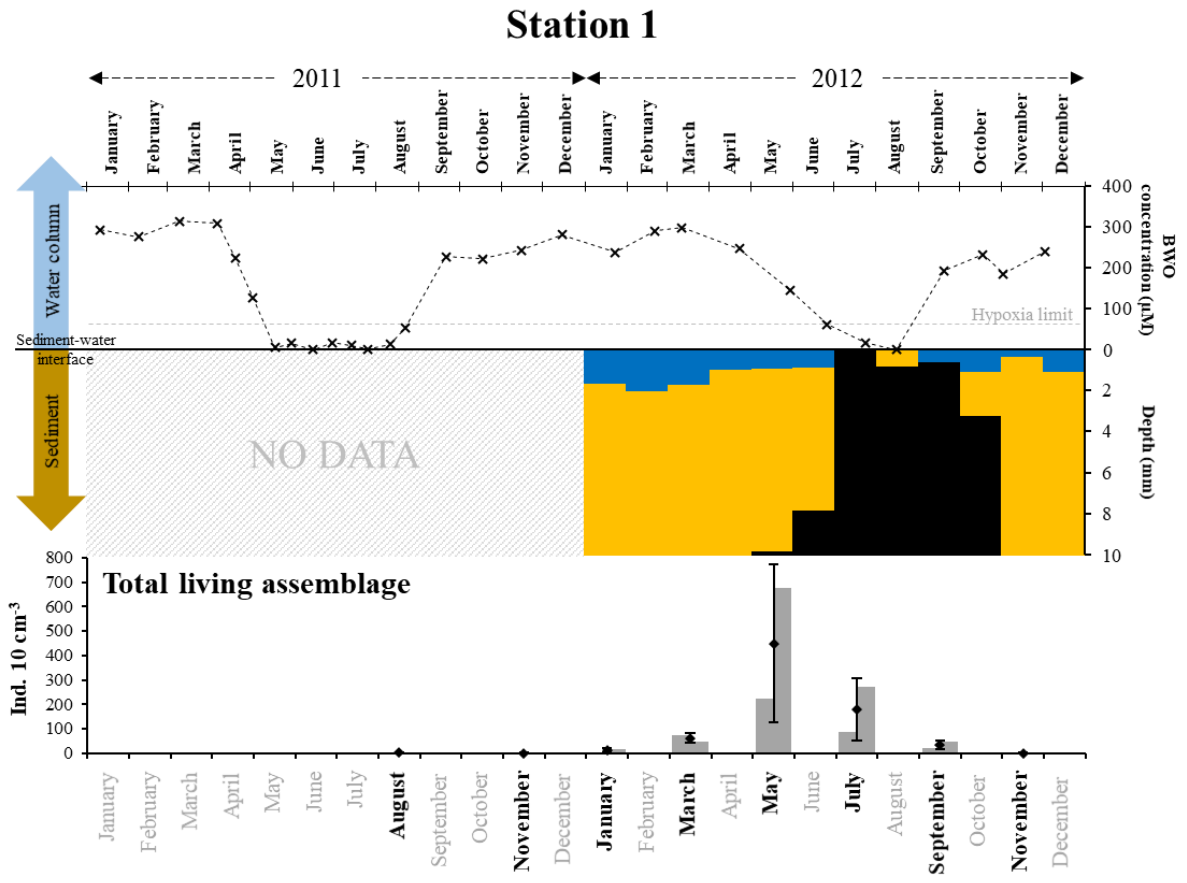

Figure 8. The top panel represents bottom-water oxygen concentrations (µmol L^{-1}) in 2011 and 2012 at station 1, from Donders et al. (2012) and Seitaj et al. (2017). The grey horizontal dotted line indicates the hypoxia limit (63 µmol L^{-1}). The middle panel represents the depth (mm) distribution of the oxic zone (blue), absence of oxygen and sulfides (orange), and sulfidic zone (black) within the sediment in 2012, from Seitaj et al. (2015). The bottom panel shows the total living foraminiferal abundances for both replicates (grey bars), mean abundances (diamonds) and standard deviations (black error bars) calculated for the two replicates, for all investigated months (in bold) in 2011 and 2012.

At station 2, in 2012, hypoxia was only observed in August, when the OPD was zero, and sulfidic conditions were observed in the superficial sediment (i.e. from 0.4 ± 0.2 mm downwards, Fig. 9, Table S1). Both in July and in September, oxygen penetrated more than 1

mm into the sediment (1.3 ± 0.4 and 1.2 ± 0.2 mm, respectively). However, free H_2S was still detected at about 1 mm depth in the sediment (1.1 ± 0.8 mm in July and 0.8 ± 0.2 mm in September). Although the sampling plan does not allow us to be very precise about the duration of anoxic and sulfidic conditions, we can estimate their duration to be 1 month or less (Fig. 9).

Foraminiferal abundances showed a strong decrease in October and November 2012, about 2 months after the presence of anoxic and sulfidic conditions in the topmost part of the sediment (Fig. 9). Like at station 1, this temporal offset between the presence of anoxia–sulfidic conditions at station 2 (in August) and the strong decrease in faunal densities may be explained as a delayed response, mainly due to inhibited reproduction during the anoxic–sulfidic event. If true, the mortality of adults did not strongly increase in the months following the H_2S production in the uppermost sediment. Nevertheless, there was no replacement in the > 125 μm fraction by growing juveniles, probably because reproduction was interrupted when H_2S was present in the foraminiferal microhabitat. A renewed recruitment after the last stage of sulfidic conditions somewhere in September would then explain why the faunal density in the > 125 μm fraction increased again in December 2012 (Fig. S3).

In 2011, at station 2, bottom waters oscillated between hypoxic and oxic conditions between May and August (Fig. 9). Although we have no measurements of H_2S in the pore waters for this year, it seems probable that bottom-water hypoxia was accompanied by the presence of free H_2S very close to the sediment surface, strongly affecting the foraminiferal communities. If we assume that, like in 2012, rich foraminiferal fauna was present in May–July 2011 at both stations, the low faunal densities observed in August and November 2011 could suggest that foraminifera may have also shown a delayed response to sulfidic conditions in 2011.

It is interesting to note that the foraminiferal densities observed at station 2 were lower in August 2011 than in July or September 2012. This may be a consequence of the repetition of short hypoxic events in the bottom water between May and August 2011 (probably associated with anoxia and maybe H_2S in the uppermost part of the sediment), which possibly affected the foraminiferal community more substantially in 2011 than in 2012, when a hypoxic event was recorded in August only.

The important decrease in total standing stocks at station 2 in October and November 2012 (Fig. 9) suggests that, in spite of the shorter duration of anoxia and sulfide conditions (compared to station 1; 1 month or less compared to 1 to 2 months), the foraminiferal faunas were still strongly affected. However, at station 2, foraminiferal abundances increased again in December 2012, suggesting a recovery time of about 2 months, which is likely much shorter than at station

1, where standing stocks in the > 125 µm fraction only increased 6 months after the presence of anoxia and free sulfides.

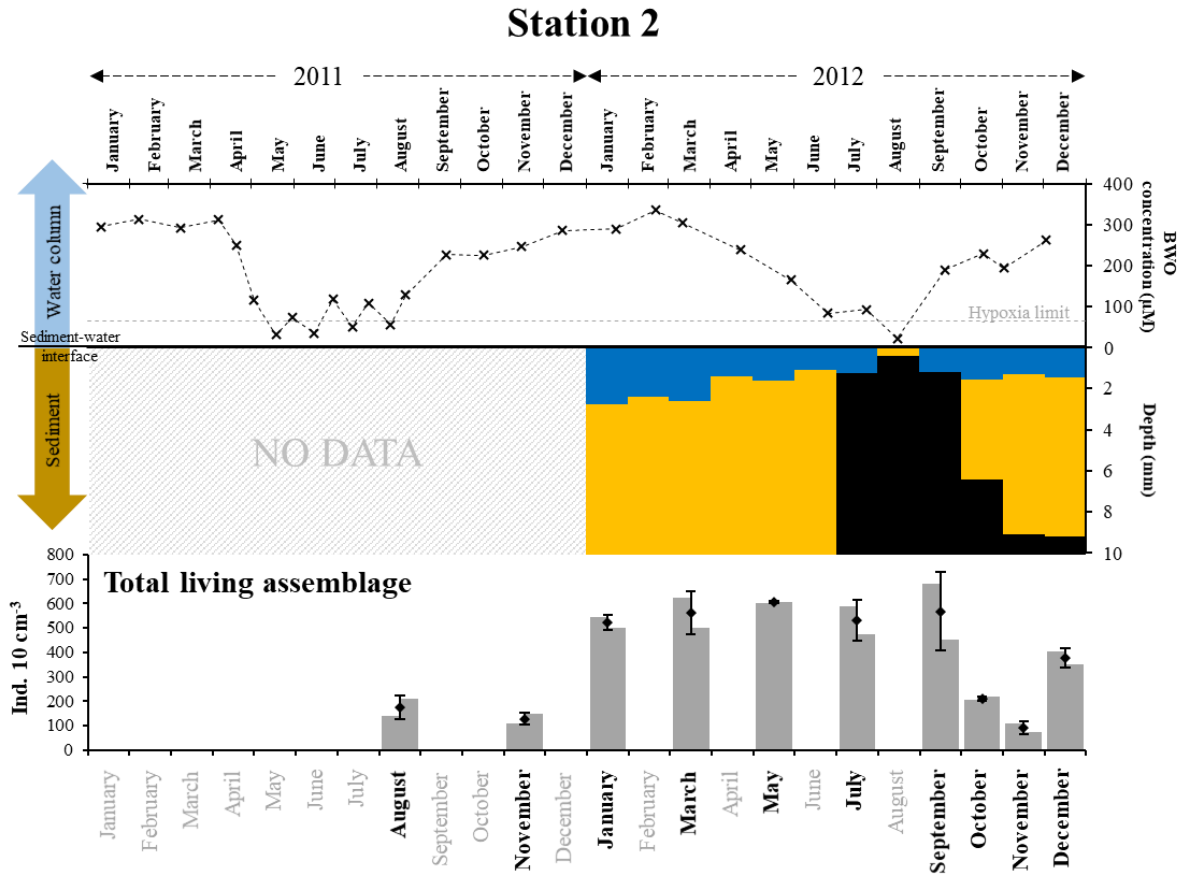

Figure 9. The top panel represents bottom-water oxygen concentrations (µmol L^{-1}) in 2011 and 2012 at station 2, from Donders et al. (2012) and Seitaj et al. (2017). The grey horizontal dotted line indicates the hypoxia limit (63 µmol L^{-1}). The middle panel represents the depth (mm) distribution of the oxic (blue), suboxic (orange, absence of oxygen and sulfides) and sulfidic (black) zones within the sediment in 2012. The bottom panel shows the total living foraminiferal abundances for both replicates (grey bars), mean abundances (diamonds) and standard deviations (black error bars) calculated for the two replicates, for all investigated months (in bold) in 2011 and 2012.

Summarising, the foraminiferal communities of both stations 1 and 2 seem strongly impacted by the anoxic and sulfidic conditions developing in the uppermost part of the sediment in summer (i.e. July–September). However, at station 1, where anoxic and sulfidic conditions lasted for 1 to 2 months, the response is much stronger, leading ultimately (in November) to almost complete disappearance of the foraminiferal fauna. The delayed response at both stations shows that instantaneous mortality was limited and suggests that the decreasing standing stocks might rather be the result of inhibited reproduction and, eventually, increased mortality. Recovery is much faster at station 2 (about 2 months) than at station 1 (about 6 months), probably because at station 1 (in contrast to station 2) the foraminiferal extinction was nearly complete, and the site had to be recolonised (e.g. possibly by nearby sites or by the remaining

few individuals) after reoxygenation of the sediment. At station 2, a reduced but significant foraminiferal community remained present, explaining the faster recovery.

4.2. SPECIES-SPECIFIC RESPONSE TO ANOXIA, SULFIDE AND FOOD AVAILABILITY IN LAKE GREVELINGEN

The comparison of the different seasonal patterns of the major species at the two investigated stations allows us to draw some conclusions about interspecific differences in the response to seasonal anoxic and sulfidic conditions.

First, there is a clear faunal difference between the two stations. Station 1 is dominated by *E. selseyense* and *E. magellanicum* while at station 2 these two taxa are accompanied by *Ammonia* sp. T6 and *T. inflata*. The latter species is almost absent at station 1, where *Ammonia* sp. T6 is present with low densities. At first glance, the dominance of the two *Elphidium* species at station 1 would suggest that they have a greater tolerance of the seasonal anoxic and sulfidic conditions, which lasted much longer there. It is interesting to note that the temporal evolution of standing stocks at station 1 is different for the two *Elphidium* species. *Elphidium magellanicum* shows a strong drop in absolute density in July 2012, at the onset of H_2S presence in the uppermost part of the sediment, whereas the diminution of *E. selseyense* is more progressive and the species disappears almost completely only in November (Fig. 5). This strongly suggests that *E. magellanicum* is more affected by increased mortality than *E. selseyense* in response to the combined effects of anoxic and sulfidic conditions. This hypothesis is confirmed by the patterns observed at station 2, where the drop in standing stocks in October–November is also more drastic in *E. magellanicum* than in *E. selseyense* (Fig. 6).

As mentioned earlier, certain species of foraminifera can use an anaerobic metabolism (i.e. denitrification; Risgaard-Petersen et al., 2006; Piña-Ochoa et al., 2010a), sequester chloroplasts (i.e. kleptoplastidy; Jauffrais et al., 2018), host bacterial symbionts (Bernhard et al., 2010) or enter dormancy (Ross and Hallock, 2016; LeKieffre et al., 2017) to deal with low-oxygen conditions. Concerning the species found in this study, although the presence of intracellular nitrate was shown for *Ammonia*, denitrification tests yielded negative results (Piña-Ochoa et al., 2010a; Nomaki et al., 2014). Similarly, the presence of active symbionts was previously suggested for *Ammonia* but never confirmed (Nomaki et al., 2016; Bernhard et al., 2018). To our knowledge, denitrification or the presence of bacterial symbionts was never shown for *Elphidium* either. In conclusion, a shift to an alternative anaerobic metabolism or an association with bacterial symbionts has never been shown conclusively for the dominant foraminiferal species found in Lake Grevelingen.

The greater tolerance of *E. selseyense* towards low-oxygen conditions could be explained by the fact that it is able to sequester chloroplasts from ingested diatoms and keep them active for several days to weeks, in contrast to *Ammonia* sp. T6 (Jauffrais et al., 2018). These active chloroplasts could serve as an alternative source of oxygen and/or food through photosynthesis (Bernhard and Alve, 1996) or another metabolic pathway (Jauffrais et al., 2019) and thereby increase the capability of this species to survive anoxic events. Although sequestration of chloroplasts was never investigated for *E. magellanicum*, its abundant spinose ornamentation in the umbilical region and in the vicinity of the aperture (Fig. 4c–d) suggests that this species is capable of crushing diatom frustules like some kleptoplastic species (Bernhard and Bowser, 1999; Austin et al., 2005). Hagens et al. (2015) observed that the light penetration depth in the Den Osse Basin never exceeded 15 m in 2012, and therefore photosynthesis by kleptoplasts (Bernhard and Alve, 1996) appears unlikely for both our aphotic stations (34 and 23 m depth). However, other foraminifera from aphotic and anoxic environments such as deep fjords are kleptoplastic and use these kleptoplasts for a yet unknown purpose (Jauffrais et al., 2019).

Rather surprisingly, the drop in foraminiferal densities at station 2 in October–November, which we interpreted as a delayed response to sulfidic conditions, is less strong for *Ammonia* sp. T6 than for the two *Elphidium* species, suggesting that this species is less affected. However, this does not agree with our previous suggestion that the two *Elphidium* species would be more tolerant to anoxic and sulfidic conditions. As already proposed by LeKieffre et al. (2017), *Ammonia* seems to be able to deal with anoxia (up to 28 d, but with no sulfide) by reducing its metabolic activity, but this ability was never shown for *Elphidium* species. If *E. selseyense* and *E. magellanicum* are indeed unable to resist anoxia by reducing their metabolism or by entering a dormancy state, this could explain their stronger decrease in density at station 2 compared to *Ammonia* sp. T6. Nevertheless, further studies about the ability and mechanisms of the two *Elphidium* species to resist anoxic–sulfidic conditions are necessary.

Another remarkable observation is that *Ammonia* sp. T6 (and T. inflata) shows maximum densities in January–March, contrasting with the two *Elphidium* species, which have their density maxima later in the year (May–September). This temporal offset could possibly be explained by a difference in preferential food source, with food particles available in winter (January–March) being more suitable for *Ammonia* sp. T6 (and *T. inflata*) and food particles available later in the year, resulting from phytoplankton blooms, being more favourable for *E. selseyense* and *E. magellanicum*.

In our study, for *E. selseyense* (and *E. magellanicum*), the continuous presence of a high proportion of small-sized specimens and progressively increasing densities between January

and September 2012 strongly suggest ongoing and continuous reproduction (Fig. S3a). Continuous reproduction during the year has been described earlier for different foraminiferal genera, such as *Elphidium*, *Ammonia*, *Haynesina*, *Nonion* and *Trochammina* (e.g. Jones and Ross, 1979; Murray, 1983, 1992; Cearreta, 1988; Basson and Murray, 1995; Gustafsson and Nordberg, 1999; Murray and Alve, 2000). Conversely, for *Ammonia* sp. T6, a decrease in densities coupled with a rapid increase in overall test size between March and May 2012 (small sized specimens remain present but in smaller proportions) could be indicative of a period of reduced recruitment (Fig. S3b).

In fact, foraminifera exhibit a large range of feeding strategies, with several species showing selective feeding with specific food particles (Muller, 1975; Suhr et al., 2003; Chronopoulou et al., 2019). Hagens et al. (2015) reported that in Lake Grevelingen the phytoplankton composition was different between April–May and July 2012. In April–May, the phytoplankton bloom was mainly composed of the haptophyte *Phaeocystis globosa* (Scherffel, 1899), whereas it was dominated by the dinoflagellate *Prorocentrum micans* (Ehrenberg, 1834) in July. *Elphidium* was reported to be able to feed on various food sources (e.g. diatoms, dinoflagellates, green algae; Correia and Lee, 2002; Pillet et al., 2011). However, diatoms are a major food source for kleptoplastic species (Bernhard and Bowser, 1999), such as *E. selseyense* (Jauffrais et al., 2018; Chronopoulou et al., 2019). *Ammonia* spp. seem able to feed on very diverse food sources including microalgae, diatoms, bacteria or even metazoans (Lee et al., 1969; Moodley et al., 2000; Dupuy et al., 2010; Jauffrais et al., 2016; Chronopoulou et al., 2019). Recently, Chronopoulou et al. (2019) showed different feeding preferences for *Ammonia* sp. T6 and *E. selseyense* in intertidal environments in the Dutch Wadden Sea. Although diatoms are ingested by both species (but much more by *E. selseyense*), dinoflagellates were consumed by *E. selseyense* but not by *Ammonia* sp. T6. The latter species is also capable of feeding on metazoans by active predation (Dupuy et al., 2010).

These observations suggest that at station 2 the different seasonal density patterns of *Ammonia* sp. T6 and the two *Elphidium* species are not the consequence of a large difference in tolerance of anoxia–sulfides, but rather a different adjustment to the seasonal cycle of food availability. At station 1, the very low densities of *Ammonia* sp. T6 could possibly be explained by a recolonisation starting in January, when food conditions were favourable for this taxon (as testified by the strong density increase in January 2012 at station 2). However, once a more abundant pioneer population had developed (in March–May), food conditions may have been no longer favourable for *Ammonia* sp. T6, explaining why its density did not show a further increase. Conversely, the food conditions may have become optimal for the two *Elphidium*

species, explaining their strong density increase between March and May 2012. If true, this would mean that the lower densities of *Ammonia* sp. T6 would not be due to a lower resistance to anoxia and free sulfides, but rather due to an unfavourable seasonal succession of food availability. Previous studies already suggested that hypoxic–anoxic conditions coupled with increased food input from autumnal phytoplankton blooms (composed of diatoms and dinoflagellates) would favour the development of *E. magellanicum* (Gustafsson and Nordberg, 1999). The fact that also at station 2 this species was mainly observed between March and September 2012 corroborates our conclusion of its dependence on a specific food regime.

Finally, encrusted forms of *E. magellanicum* were observed at both stations from May until the end of the year but were absent in the samples of March 2012. In view of the fact that the crusts consist mainly of organic matter, the encrusted individuals appear to be specimens with preserved feeding cysts. The precise functions of cysts observed around foraminifera are not clear and include feeding, reproduction, chamber formation, protection or resting (Cedhagen, 1996; Heinz et al., 2005). Concerning the cysts of *E. magellanicum* described here, very similar observations have been made for *Elphidium incertum* at different locations (Norwegian Greenland Sea and Baltic Sea in Linke and Lutze, 1993; Koljö Fjord in Gustafsson and Nordberg, 1999; Kiel Bight in Polovodova et al., 2009). If we assume that encrusted specimens indeed present the remains of feeding cysts, the observation of abundant encrusted specimens corroborates our conclusion that the surface water phytoplankton bloom in May 2012 (i.e. probably mainly *Phaeocystis globosa*) provided a food source particularly well suited to the nutritional preferences of this species.

5. CONCLUSION

In this study we examined the foraminiferal community response to different durations of seasonal anoxia coupled with the presence of sulfide in the uppermost layer of sediment at two stations in Lake Grevelingen. In both stations investigated, foraminiferal communities are highly impacted by the combination of anoxia and H_2S in their habitat. The foraminiferal response varied depending on the duration of adverse conditions and led to a near extinction at station 1, where anoxic and sulfidic conditions were present for 1 to 2 months, compared to a drop in standing stocks at station 2, where these conditions lasted for 1 month or less. At both sites, foraminiferal communities showed a 2-month delay in the response to anoxic and sulfidic conditions, suggesting that the presence of H_2S inhibited reproduction, whereas mortality was not necessarily increased. The duration of the subsequent recovery depended on whether the

foraminiferal community was almost extinct (station 1) or remained present with reduced numbers (station 2). In the former case, 6 months were needed for faunal recovery, whereas in the latter case, it took only 2 months. We hypothesise that the dominance of *E. selseyense* and *E. magellanicum* at station 1 is not due to a lower tolerance of *Ammonia* sp. T6 towards anoxic and sulfidic conditions, but is rather the consequence of a different adjustment between the two *Elphidium* species and *Ammonia* sp. T6 with respect to the seasonal cycle of food availability.

ACKNOWLEDGMENTS

We are very grateful to Sandra Langezaal for inviting us to study the fascinating environments of the Grevelingenmeer. We acknowledge the support of Pieter van Rijswijk, Mathilde Hagens, Anton Tramper and the crew of the R/V Luctor (Peter Coomans and Marcel Kristalijn) during the sampling campaigns. We are grateful to Romain Mallet and the team of the SCIAM imaging facility at the University of Angers. We acknowledge Jassin Petersen for his help with recovering some of the environmental data and Thierry Jauffrais and Charlotte LeKieffre for discussion about alternative metabolisms. This paper benefited from the comments and suggestions of Laurie M. Charrieau and the two anonymous reviewers.

REFERENCES

Altenbach, A. V., Bernhard, J. M. and Seckbach, J., Eds.: Anoxia: evidence for eukaryote survival and paleontological strategies, Springer, Dordrecht, 648 pp., 2012.

Alve, E.: Benthic foraminiferal distribution and recolonization of formerly anoxic environments in Drammensfjord, southern Norway, Mar. Micropaleontol., 25, 169–186, doi:10.1016/0377-8398(95)00007-N, 1995.

Alve, E.: Colonization of new habitats by benthic foraminifera: a review, Earth-Sci. Rev., 46, 167–185, doi:10.1016/S0012-8252(99)00016-1, 1999.

Alve, E. and Bernhard, J. M.: Vertical migratory response of benthic foraminifera to controlled oxygen concentrations in an experimental mesocosm, Mar. Ecol. Prog. Ser., 116, 137–151, ISSN:0171-8630, 1995.

Alve, E., Korsun, S., Schönfeld, J., Dijkstra, N., Golikova, E., Hess, S., Husum, K. and Panieri, G.: Foram-AMBI: A sensitivity index based on benthic foraminiferal faunas from North-East Atlantic and Arctic fjords, continental shelves and slopes, Mar. Micropaleontol., 122, 1–12, doi:10.1016/j.marmicro.2015.11.001, 2016.

Austin, H. A., Austin, W. E. N. and Paterson, D. M.: Extracellular cracking and content removal of the benthic diatom Pleurosigma angulatum (Quekett) by the benthic foraminifera Haynesina germanica (Ehrenberg), Mar. Micropaleontol., 57, 68–73, doi:10.1016/j.marmicro.2005.07.002, 2005.

Bannink, B. A., Van der Meulen, J. H. M. and Nienhuis, P. H.: Lake grevelingen: From an estuary to a saline lake. An introduction, Neth. J. Sea Res., 18, 179–190, doi:10.1016/0077-7579(84)90001-2, 1984.

Basson, P. W. and Murray, J. W.: Temporal Variations in Four Species of Intertidal Foraminifera, Bahrain, Arabian Gulf, Micropaleontology, 41, 69–76, doi:10.2307/1485882, 1995.

Bernhard, J. M.: Postmortem vital staining in benthic foraminifera; duration and importance in population and distributional studies, J. Foraminifer. Res., 18, 143–146, doi:10.2113/gsjfr.18.2.143, 1988.

Bernhard, J. M.: Experimental and field evidence of Antarctic foraminiferal tolerance to anoxia and hydrogen sulfide, Mar. Micropaleontol., 20, 203–213, doi:10.1016/0377-8398(93)90033-T, 1993.

Bernhard, J. M. and Alve, E.: Survival, ATP pool, and ultrastructural characterization of benthic foraminifera from Drammensfjord (Norway): response to anoxia, Mar. Micropaleontol., 28, 5–17, doi:10.1016/0377-8398(95)00036-4, 1996.

Bernhard, J. M. and Bowser, S. S.: Benthic foraminifera of dysoxic sediments: chloroplast sequestration and functional morphology, Earth-Sci. Rev., 46, 149–165, doi:10.1016/S0012-8252(99)00017-3, 1999.

Bernhard, J. M., Ostermann, D. R., Williams, D. S. and Blanks, J. K.: Comparison of two methods to identify live benthic foraminifera: A test between Rose Bengal and CellTracker Green with implications for stable isotope paleoreconstructions, Paleoceanography, 21, PA4210, doi:10.1029/2006PA001290, 2006.

Bernhard, J. M., Goldstein, S. T. and Bowser, S. S.: An ectobiont-bearing foraminiferan, Bolivina pacifica, that inhabits microxic pore waters: cell-biological and paleoceanographic insights, Environ. Microbiol., 12, 2107–2119, doi:10.1111/j.1462-2920.2009.02073.x, 2010.

Bernhard, J. M., Tsuchiya, M. and Nomaki, H.: Ultrastructural observations on prokaryotic associates of benthic foraminifera: Food, mutualistic symbionts, or parasites?, Marine Micropaleontology, 138, 33–45, doi:10.1016/j.marmicro.2017.09.001, 2018.

Bird, C., Schweizer, M., Roberts, A., Austin, W. E. N., Knudsen, K. L., Evans, K. M., Filipsson, H. L., Sayer, M. D. J., Geslin, E. and Darling, K. F.: The genetic diversity, morphology, biogeography, and taxonomic designations of Ammonia (Foraminifera) in the Northeast Atlantic, Mar. Micropaleontol., 155, 101726, doi:10.1016/j.marmicro.2019.02.001, 2019.

Bouchet, V. M. P., Debenay, J.-P., Sauriau, P.-G., Radford-Knoery, J. and Soletchnik, P.: Effects of short-term environmental disturbances on living benthic foraminifera during the Pacific oyster summer mortality in the Marennes-Oléron Bay (France), Mar. Environ. Res., 64, 358–383, doi:10.1016/j.marenvres.2007.02.007, 2007.

Cearreta, A.: Population dynamics of benthic foraminifera in the Santoña estuary, Spain, Revue de Paleobiologie, 2, 721–724, ISSN:0253-6730, 1988.

Cedhagen, T.: Foraminiferans as food for cephalaspideans (Gastropoda: Opisthobranchia), with notes on secondary tests around calcareous foraminiferans. Phuket Marine Biological Center Special Publication, 16, 279–290, 1996.

Chronopoulou, P.-M., Salonen, I., Bird, C., Reichart, G.-J. and Koho, K. A.: Metabarcoding Insights Into the Trophic Behavior and Identity of Intertidal Benthic Foraminifera, Front. Microbiol., 10, 1169, doi:10.3389/fmicb.2019.01169, 2019.

Cloern, J. E., Foster, S. Q. and Kleckner, A. E.: Phytoplankton primary production in the world's estuarine-coastal ecosystems, Biogeosciences, 11, 25, doi:10.5194/bg-11-2477-2014, 2014.

Corliss, B. H. and Emerson, S.: Distribution of rose bengal stained deep-sea benthic foraminifera from the Nova Scotian continental margin and Gulf of Maine, Deep Sea Res. Part Oceanogr. Res. Pt. A, 37, 381–400, doi:10.1016/0198-0149(90)90015-N, 1990.

Correia, M. and Lee, J. J.: Fine structure of the plastids retained by the foraminifer Elphidium excavatum (Terquem), Symbiosis, 32, 15–26, ISSN:03345114, 2002.

Darling, K. F., Schweizer, M., Knudsen, K. L., Evans, K. M., Bird, C., Roberts, A., Filipsson, H. L., Kim, J.-H., Gudmundsson, G., Wade, C. M., Sayer, M. D. J. and Austin, W. E. N.: The genetic diversity, phylogeography and morphology of Elphidiidae (Foraminifera) in the Northeast Atlantic, Mar. Micropaleontol., 129, 1–23, doi:10.1016/j.marmicro.2016.09.001, 2016.

Diaz, R. J. and Rosenberg, R.: Marine benthic hypoxia: a review of its ecological effects and the behavioural responses of benthic macrofauna, Oceanogr. Mar. Biol., 33, 245–303, 1995.

Diaz, R. J. and Rosenberg, R.: Spreading Dead Zones and Consequences for Marine Ecosystems, Science, 321, 926–929, doi:10.1126/science.1156401, 2008.

Donders, T. H., Guasti, E., Bunnik, F. P. M. and van Aken, H.: Impact van de Brouwersdam op zuurstofcondities in de Grevelingen; reconstructies uit natuurlijke sediment archieven, TNO-report TNO-060-UT-2011-02116, Utrecht, the Netherlands, 2012.

Dorman, D. C., Moulin, F. J.-M., McManus, B. E., Mahle, K. C., James, R. A. and Struve, M. F.: Cytochrome Oxidase Inhibition Induced by Acute Hydrogen Sulfide Inhalation: Correlation with Tissue Sulfide Concentrations in the Rat Brain, Liver, Lung, and Nasal Epithelium, Toxicol. Sci., 65, 18–25, doi:10.1093/toxsci/65.1.18, 2002.

Duijnstee, I., de Lugt, I., Vonk Noordegraaf, H. and van der Zwaan, B.: Temporal variability of foraminiferal densities in the northern Adriatic Sea, Mar. Micropaleontol., 50, 125–148, doi:10.1016/S0377-8398(03)00069-0, 2004.

Duijnstee, I. a. P., Ernst, S. R. and Zwaan, G. J. van der: Effect of anoxia on the vertical migration of benthic foraminifera, Mar. Ecol. Prog. Ser., 246, 85–94, doi:10.3354/meps246085, 2003.

Duijnstee, I. a. P., Nooijer, L. J. de, Ernst, S. R. and Zwaan, G. J. van der: Population dynamics of benthic shallow-water foraminifera: effects of a simulated marine snow event, Mar. Ecol. Prog. Ser., 285, 29–42, doi:10.3354/meps285029, 2005.

Dupuy, C., Rossignol, L., Geslin, E. and Pascal, P.-Y.: Predation of mudflat meio-macrofaunal metazoans by a calcareous foraminifer, Ammonia tepida (cushman, 1926), J. Foraminifer. Res., 40, 305–312, doi:10.2113/gsjfr.40.4.305, 2010.

Ernst, S., Bours, R., Duijnstee, I. and Zwaan, B. van der: Experimental effects of an organic matter pulse and oxygen depletion on a benthic foraminiferal shelf community, J. Foraminifer. Res., 35, 177–197, doi:10.2113/35.3.177, 2005.

Feyling-Hanssen, R. W.: The Foraminifer Elphidium excavatum (Terquem) and Its Variant Forms, Micropaleontology, 18, 337–354, doi:10.2307/1485012, 1972.

Gammon, P. R., Neville, L. A., Patterson, R. T., Savard, M. M. and Swindles, G. T.: A log-normal spectral analysis of inorganic grain-size distributions from a Canadian boreal lake core: Towards refining depositional process proxy data from high latitude lakes, Sedimentology, 64, 609–630, doi:10.1111/sed.12281, 2017.

Geslin, E., Heinz, P., Jorissen, F. and Hemleben, Ch.: Migratory responses of deep-sea benthic foraminifera to variable oxygen conditions: laboratory investigations, Mar. Micropaleontol., 53, 227–243, doi:10.1016/j.marmicro.2004.05.010, 2004.

Geslin, E., Barras, C., Langlet, D., Nardelli, M. P., Kim, J.-H., Bonnin, J., Metzger, E. and Jorissen, F. J.: Survival, Reproduction and Calcification of Three Benthic Foraminiferal Species in Response to Experimentally Induced Hypoxia, in Approaches to Study Living Foraminifera: Collection, Maintenance and Experimentation, edited by H. Kitazato and J. M. Bernhard, pp. 163–193, Springer Japan, Tokyo., 2014.

Gilbert, D., Rabalais, N. N., Diaz, R. J. and Zhang, J.: Evidence for greater oxygen decline rates in the coastal ocean than in the open ocean, Biogeosciences, 2283–2296, doi:10.5194/bg-7-2283-2010, 2010.

Gustafsson, M. and Nordberg, K.: Benthic foraminifera and their response to hydrography, periodic hypoxic conditions and primary production in the Koljö fjord on the Swedish west coast, J. Sea Res., 41, 163–178, doi:10.1016/S1385-1101(99)00002-7, 1999.

Gustafsson, M. and Nordberg, K.: Living (Stained) Benthic Foraminifera and their Response to the Seasonal Hydrographic Cycle, Periodic Hypoxia and to Primary Production in Havstens Fjord on the Swedish West Coast, Estuar. Coast. Shelf Sci., 51, 743–761, doi:10.1006/ecss.2000.0695, 2000.

Hagens, M., Slomp, C. P., Meysman, F. J. R., Seitaj, D., Harlay, J., Borges, A. V. and Middelburg, J. J.: Biogeochemical processes and buffering capacity concurrently affect acidification in a seasonally hypoxic coastal marine basin, Biogeosciences, 12, 1561–1583, doi:10.5194/bg-12-1561-2015, 2015.

Hannah, F. and Rogerson, A.: The Temporal and Spatial Distribution of Foraminiferans in Marine Benthic Sediments of the Clyde Sea Area, Scotland, Estuar. Coast. Shelf Sci., 44, 377–383, doi:10.1006/ecss.1996.0136, 1997.

Heinz, P., Geslin, E. and Hemleben, C.: Laboratory observations of benthic foraminiferal cysts, Marine Biology Research, 1(2), 149–159, doi:10.1080/17451000510019114, 2005.

Hess, S., Jorissen, F. J., Venet, V. and Abu-Zied, R.: Benthic foraminiferal recovery after recent turbidite deposition in Cap Breton canyon, Bay of Biscay, J. Foraminifer. Res., 35, 114–129, doi:10.2113/35.2.114, 2005.

Jauffrais, T., Jesus, B., Geslin, E., Briand, F. and Jézéquel, V. M.: Locomotion speed of the benthic foraminifer Ammonia tepida exposed to different nitrogen and carbon sources, J. Sea Res., 118, 52–58, doi:10.1016/j.seares.2016.07.001, 2016.

Jauffrais, T., LeKieffre, C., Koho, K. A., Tsuchiya, M., Schweizer, M., Bernhard, J. M., Meibom, A. and Geslin, E.: Ultrastructure and distribution of kleptoplasts in benthic foraminifera from shallow-water (photic) habitats, Mar. Micropaleontol., 138, 46–62, doi:10.1016/j.marmicro.2017.10.003, 2018.

Jauffrais, T., LeKieffre, C., Schweizer, M., Geslin, E., Metzger, E., Bernhard, J. M., Jesus, B., Filipsson, H. L., Maire, O. and Meibom, A.: Kleptoplastidic benthic foraminifera from aphotic habitats: insights into assimilation of inorganic C, N and S studied with sub-cellular resolution, Environ. Microbiol., 21, 125–141, doi:10.1111/1462-2920.14433, 2019.

Jones, G. D. and Ross, C. A.: Seasonal Distribution of Foraminifera in Samish Bay, Washington, J. Paleontol., 53, 245–257, ISSN:0022-3360, 1979.

Jørgensen, B. B., Postgate, J. R., Postgate, J. R. and Kelly, D. P.: Ecology of the bacteria of the sulphur cycle with special reference to anoxic—oxic interface environments, Philosophical Transactions of the Royal Society of London. B, Biological Sciences, 298, 543–561, doi:10.1098/rstb.1982.0096, 1982.

Jorissen, F. J., Fontanier, C. and Thomas, E.: Chapter Seven Paleoceanographical Proxies Based on Deep-Sea Benthic Foraminiferal Assemblage Characteristics, in Developments in Marine Geology, vol. 1, edited by C. Hillaire–Marcel and A. De Vernal, pp. 263–325, Elsevier, 2007.

Josefson, A. B. and Widbom, B.: Differential response of benthic macrofauna and meiofauna to hypoxia in the Gullmar Fjord basin, Mar. Biol., 100, 31–40, doi:10.1007/BF00392952, 1988.

Khan, A. A., Schuler, M. M., Prior, M. G., Yong, S., Coppock, R. W., Florence, L. Z. and Lillie, L. E.: Effects of hydrogen sulfide exposure on lung mitochondrial respiratory chain enzymes in rats, Toxicol. Appl. Pharmacol., 103, 482–490, doi:10.1016/0041-008X(90)90321-K, 1990.

Koho, K. A. and Piña-Ochoa, E.: Benthic Foraminifera: Inhabitants of Low-Oxygen Environments, in Anoxia: Evidence for Eukaryote Survival and Paleontological Strategies,

edited by A. V. Altenbach, J. M. Bernhard, and J. Seckbach, pp. 249–285, Springer Netherlands, Dordrecht., 2012.
Koho, K. A., Piña-Ochoa, E., Geslin, E. and Risgaard-Petersen, N.: Vertical migration, nitrate uptake and denitrification: survival mechanisms of foraminifers (Globobulimina turgida) under low oxygen conditions, FEMS Microbiol. Ecol., 75, 273–283, doi:10.1111/j.1574-6941.2010.01010.x, 2011.
Langlet, D., Geslin, E., Baal, C., Metzger, E., Lejzerowicz, F., Riedel, B., Zuschin, M., Pawlowski, J., Stachowitsch, M. and Jorissen, F. J.: Foraminiferal survival after long-term in situ experimentally induced anoxia, Biogeosciences, 10, 7463–7480, doi:10.5194/bg-10-7463-2013, 2013.
Langlet, D., Baal, C., Geslin, E., Metzger, E., Zuschin, M., Riedel, B., Risgaard-Petersen, N., Stachowitsch, M. and Jorissen, F. J.: Foraminiferal species responses to in situ, experimentally induced anoxia in the Adriatic Sea, Biogeosciences, 11, 1775–1797, doi:10.5194/bg-11-1775-2014, 2014.
Lee, J. J., Muller, W. A., Stone, R. J., McEnery, M. E. and Zucker, W.: Standing crop of foraminifera in sublittoral epiphytic communities of a Long Island salt marsh, Mar. Biol., 4, 44–61, doi:10.1007/BF00372165, 1969.
LeKieffre, C., Spangenberg, J., Mabilleau, G., Escrig, S., Meibom, A. and Geslin, E.: Surviving anoxia in marine sediments: The metabolic response of ubiquitous benthic foraminifera (Ammonia tepida), PLoS ONE, 12, e0177604., doi:10.1371/journal.pone.0177604, 2017.
Linke, P. and Lutze, G. F.: Microhabitat preferences of benthic foraminifera—a static concept or a dynamic adaptation to optimize food acquisition?, Mar. Micropaleontol., 20, 215–234, doi:10.1016/0377-8398(93)90034-U, 1993.
Metzger, E., Langlet, D., Viollier, E., Koron, N., Riedel, B., Stachowitsch, M., Faganeli, J., Tharaud, M., Geslin, E. and Jorissen, F.: Artificially induced migration of redox layers in a coastal sediment from the Northern Adriatic, Biogeosciences, 11, 2211–2224, doi:10.5194/bg-11-2211-2014, 2014.
Miller, A. A. L., Scott, D. B. and Medioli, F. S.: Elphidium excavatum (Terquem); ecophenotypic versus subspecific variation, J. Foraminifer. Res., 12, 116–144, doi:10.2113/gsjfr.12.2.116, 1982.
Moodley, L. and Hess, C.: Tolerance of Infaunal Benthic Foraminifera for Low and High Oxygen Concentrations, Biol. Bull., 183, 94–98, doi:10.2307/1542410, 1992.
Moodley, L., Zwaan, G. J. van der, Herman, P. M. J., Kempers, L. and Breugel, P. van: Differential response of benthic meiofauna to anoxia with special reference to Foraminifera (Protista: Sarcodina), Mar. Ecol. Prog. Ser., 158, 151–163, doi:10.3354/meps158151, 1997.
Moodley, L., van der Zwaan, G. J., Rutten, G. M. W., Boom, R. C. E. and Kempers, A. J.: Subsurface activity of benthic foraminifera in relation to porewater oxygen content: laboratory experiments, Mar. Micropaleontol., 34, 91–106, doi:10.1016/S0377-8398(97)00044-3, 1998a.
Moodley, L., Schaub, B. E. M., Zwaan, G. J. van der and Herman, P. M. J.: Tolerance of benthic foraminifera (Protista: Sarcodina) to hydrogen sulphide, Mar. Ecol. Prog. Ser., 169, 77–86, doi:10.3354/meps169077, 1998b.
Moodley, L., Boschker, H. T. S., Middelburg, J. J., Pel, R., Herman, P. M. J., Deckere, E. de and Heip, C. H. R.: Ecological significance of benthic foraminifera: 13C labelling experiments, Mar. Ecol. Prog. Ser., 202, 289–295, doi:10.3354/meps202289, 2000.
Muller, W. A.: Competition for food and other niche-related studies of three species of salt-marsh foraminifera, Mar. Biol., 31, 339–351, doi:10.1007/BF00392091, 1975.
Murray, J. W.: Production in benthic foraminiferids, J. Nat. Hist., 1, 61–68, doi:10.1080/00222936700770631, 1967.

Murray, J. W.: Population dynamics of benthic foraminifera; results from the Exe Estuary, England, J. Foraminifer. Res., 13, 1–12, doi:10.2113/gsjfr.13.1.1, 1983.

Murray, J. W.: Distribution and population dynamics of benthic foraminifera from the southern North Sea, J. Foraminifer. Res., 22, 114–128, doi:10.2113/gsjfr.22.2.114, 1992.

Murray, J. W. and Alve, E.: Major aspects of foraminiferal variability (standing crop and biomass) on a monthly scale in an intertidal zone, J. Foraminifer. Res., 30, 177–191, doi:10.2113/0300177, 2000.

Nardelli, M. P., Barras, C., Metzger, E., Mouret, A., Filipsson, H. L., Jorissen, F. and Geslin, E.: Experimental evidence for foraminiferal calcification under anoxia, Biogeosciences, 11(, 4029–4038, doi:10.5194/bg-11-4029-2014, 2014.

Nicholls, P. and Kim, J. K.: Sulphide as an inhibitor and electron donor for the cytochrome c oxidase system, Can. J. Biochem., 60, 613–623, doi:10.1139/o82-076, 1982.

Nomaki, H., Chikaraishi, Y., Tsuchiya, M., Toyofuku, T., Ohkouchi, N., Uematsu, K., Tame, A. and Kitazato, H.: Nitrate uptake by foraminifera and use in conjunction with endobionts under anoxic conditions, Limnology and Oceanography, 59, 1879–1888, doi:10.4319/lo.2014.59.6.1879, 2014.

Nomaki, H., Bernhard, J. M., Ishida, A., Tsuchiya, M., Uematsu, K., Tame, A., Kitahashi, T., Takahata, N., Sano, Y. and Toyofuku, T.: Intracellular Isotope Localization in Ammonia sp. (Foraminifera) of Oxygen-Depleted Environments: Results of Nitrate and Sulfate Labeling Experiments, Front. Microbiol., 7, 163, doi:10.3389/fmicb.2016.00163, 2016.

Panieri, G.: Foraminiferal response to an active methane seep environment: A case study from the Adriatic Sea, Mar. Micropaleontol., 61, 116–130, doi:10.1016/j.marmicro.2006.05.008, 2006.

Panieri, G. and Sen Gupta, B. K.: Benthic Foraminifera of the Blake Ridge hydrate mound, Western North Atlantic Ocean, Mar. Micropaleontol., 66, 91–102, doi:10.1016/j.marmicro.2007.08.002, 2008.

Papaspyrou, S., Diz, P., García-Robledo, E., Corzo, A. and Jimenez-Arias, J.-L.: Benthic foraminiferal community changes and their relationship to environmental dynamics in intertidal muddy sediments (Bay of Cádiz, SW Spain), Mar. Ecol. Prog. Ser., 490, 121–135, doi:10.3354/meps10447, 2013.

Pillet, L., de Vargas, C. and Pawlowski, J.: Molecular Identification of Sequestered Diatom Chloroplasts and Kleptoplastidy in Foraminifera, Protist, 162, 394–404, doi:10.1016/j.protis.2010.10.001, 2011.

Piña-Ochoa, E., Koho, K. A., Geslin, E. and Risgaard-Petersen, N.: Survival and life strategy of the foraminiferan Globobulimina turgida through nitrate storage and denitrification, Mar. Ecol. Prog. Ser., 417, 39–49, doi:10.3354/meps08805, 2010a.

Piña-Ochoa, E., Høgslund, S., Geslin, E., Cedhagen, T., Revsbech, N. P., Nielsen, L. P., Schweizer, M., Jorissen, F., Rysgaard, S. and Risgaard-Petersen, N.: Widespread occurrence of nitrate storage and denitrification among Foraminifera and Gromiida, Proc. Natl. Acad. Sci., 107, 1148–1153, doi:10.1073/pnas.0908440107, 2010b.

Polovodova, I., Nikulina, A., Schönfeld, J. and Dullo, W.-C.: Recent benthic foraminifera in the Flensburg Fjord (Western Baltic Sea), J. Micropalaeontology, 28, 131–142, doi:10.1144/jm.28.2.131, 2009.

Pucci, F., Geslin, E., Barras, C., Morigi, C., Sabbatini, A., Negri, A. and Jorissen, F. J.: Survival of benthic foraminifera under hypoxic conditions: Results of an experimental study using the CellTracker Green method, Mar. Pollut. Bull., 59, 336–351, doi:10.1016/j.marpolbul.2009.08.015, 2009.

Rabalais, N. N., Díaz, R. J., Levin, L. A., Turner, R. E., Gilbert, D. and Zhang, J.: Dynamics and distribution of natural and human-caused hypoxia, Biogeosciences, 7, 585–619, doi:10.5194/bg-7-585-2010, 2010.

Richirt, J., Schweizer, M., Bouchet, V. M. P., Mouret, A., Quinchard, S. and Jorissen, F. J.: Morphological distinction of three Ammonia phylotypes occurring along european coasts, J. Foraminifer. Res., 49, 77–94, 2019.

Riedel, B., Diaz, R., Rosenberg, R. and Stachowitsch, M.: The ecological consequences of marine hypoxia: from behavioural to ecosystem responses, in: Stressors in the marine environment: physiological responses and ecological implication, edited by Martin Solan and Nia M. Whiteley., Oxford University Press., 175–194, 2016.

Risgaard-Petersen, N., Langezaal, A. M., Ingvardsen, S., Schmid, M. C., Jetten, M. S. M., Camp, H. J. M. O. den, Derksen, J. W. M., Piña-Ochoa, E., Eriksson, S. P., Nielsen, L. P., Revsbech, N. P., Cedhagen, T. and Zwaan, G. J. van der: Evidence for complete denitrification in a benthic foraminifer, Nature, 443, 93–96, doi:10.1038/nature05070, 2006.

Roberts, A., Austin, W., Evans, K., Bird, C., Schweizer, M. and Darling, K.: A New Integrated Approach to Taxonomy: The Fusion of Molecular and Morphological Systematics with Type Material in Benthic Foraminifera, PLOS ONE, 11, e0158754, doi:10.1371/journal.pone.0158754, 2016.

Ross, B. J. and Hallock, P.: Dormancy in the Foraminifera: A Review, J. Foraminifer. Res., 46, 358–368, doi:10.2113/gsjfr.46.4.358, 2016.

Schneider, C. A., Rasband, W. S. and Eliceiri, K. W.: NIH Image to ImageJ: 25 years of image analysis, Nat. Methods, 9, 671–675, doi:10.1038/nmeth.2089, 2012.

Schönfeld, J. and Numberger, L.: Seasonal dynamics and decadal changes of benthic foraminiferal assemblages in the western Baltic Sea (NW Europe), J. Micropalaeontology, 26, 47–60, doi:10.1144/jm.26.1.47, 2007.

Seitaj, D., Schauer, R., Sulu-Gambari, F., Hidalgo-Martinez, S., Malkin, S. Y., Burdorf, L. D. W., Slomp, C. P. and Meysman, F. J. R.: Cable bacteria generate a firewall against euxinia in seasonally hypoxic basins, Proc. Natl. Acad. Sci., 112, 13278–13283, doi:10.1073/pnas.1510152112, 2015.

Seitaj, D., Sulu-Gambari, F., Burdorf, L. D. W., Romero-Ramirez, A., Maire, O., Malkin, S. Y., Slomp, C. P. and Meysman, F. J. R.: Sedimentary oxygen dynamics in a seasonally hypoxic basin, Limnol. Oceanogr., 62, 452–473, doi:10.1002/lno.10434, 2017.

Stramma, L., Oschlies, A. and Schmidtko, S.: Mismatch between observed and modeled trends in dissolved upper-ocean oxygen over the last 50 yr, Biogeosciences, 9, 4045–4057, doi:10.5194/bg-9-4045-2012, 2012.

Suhr, S. B., Pond, D. W., Gooday, A. J. and Smith, C. R.: Selective feeding by benthic foraminifera on phytodetritus on the western Antarctic Peninsula shelf: evidence from fatty acid biomarker analysis, Mar. Ecol. Prog. Ser., 262, 153–162, doi:10.3354/meps262153, 2003.

Sulu-Gambari, F., Seitaj, D., Meysman, F. J. R., Schauer, R., Polerecky, L. and Slomp, C. P.: Cable Bacteria Control Iron–Phosphorus Dynamics in Sediments of a Coastal Hypoxic Basin, Environ. Sci. Technol., 50, 1227–1233, doi:10.1021/acs.est.5b04369, 2016a.

Sulu-Gambari, F., Seitaj, D., Behrends, T., Banerjee, D., Meysman, F. J. R. and Slomp, C. P.: Impact of cable bacteria on sedimentary iron and manganese dynamics in a seasonally-hypoxic marine basin, Geochim. Cosmochim. Acta, 192, 49–69, doi:10.1016/j.gca.2016.07.028, 2016b.

de Vries, I. and Hopstaken, C. F.: Nutrient cycling and ecosystem behaviour in a salt-water lake, Neth. J. Sea Res., 18(3), 221–245, doi:10.1016/0077-7579(84)90003-6, 1984.

Walton, W. R.: Techniques for recognition of living foraminifera, Contrib. Cushman Found. Foraminifer. Res., 3, 56–60, 1952.

Wang, F. and Chapman, P. M.: Biological implications of sulfide in sediment—a review focusing on sediment toxicity, Environ. Toxicol. Chem., 18, 2526–2532, doi:10.1002/etc.5620181120, 1999.

Wetsteijn, L. P. M. J.: Grevelingenmeer: meer kwetsbaar? Een beschrijving van de ecologische ontwikkelingen voor de periode 1999 t/m 2008-2010 in vergelijking met de periode 1990 t/m 1998., RWS Waterdienst., Lelystad 2011, 2011.

Woulds, C., Cowie, G. L., Levin, L. A., Andersson, J. H., Middelburg, J. J., Vandewiele, S., Lamont, P. A., Larkin, K. E., Gooday, A. J., Schumacher, S., Whitcraft, C., Jeffreys, R. M. and Schwartz, M.: Oxygen as a control on sea floor biological communities and their roles in sedimentary carbon cycling, Limnol. Oceanogr., 52, 1698–1709, doi:10.4319/lo.2007.52.4.1698, 2007.

AUTHOR CONTRIBUTIONS

BR, DL and JR produced the foraminiferal data. DS, AM and CPS provided and interpreted geochemical data. MS provided, verified and integrated all available genetic information concerning the foraminiferal taxa of Lake Grevelingen. FJRM and CPS coordinated a much larger research project concerning Lake Grevelingen, of which this foraminiferal study is a part. They were also responsible for the foraminiferal sampling and provided environmental data. FJJ designed the foraminiferal study and directed the postdoctoral research of BR and, together with AM and MS, the PhD thesis of JR. All authors contributed actively to the several successive versions of the manuscript.

SUPPLEMENTARY INFORMATION

Table S1. Oxygen Penetration Depth ± sd and free H2S detection depth ± sd for each month in 2012 for both stations 1 and 2 (in mm).

Station	Month	OPD (mm)	H_2S depth (mm)
Station 1	January	1.7 ± 0.3	16.5 ± 3.2
	February	2 ± 0.4	17.1 ± 2.8
	March	1.7 ± 0.3	17.5 ± 0.7
	April	1 ± 0.2	18.6 ± 4.8
	May	1 ± 0.1	9.9 ± 2.2
	June	0.9 ± 0.1	7.9 ± 5.3
	July	0 ± 0	0.1 ± 0.1
	August	0 ± 0	0.9 ± 1.1
	September	0.7 ± 0.1	0.3 ± 0.2
	October	1.1 ± 0.1	3.3 ± 1.1
	November	0.4 ± 0	10.3 ± 1.9
	December	1.1 ± 0.2	13.4 ± 1.8
Station 2	January	2.8 ± 0	19.6 ± 2
	February	2.4 ± 0.2	15.8 ± 1.2
	March	2.6 ± 0.6	20.3 ± 3.3
	April	1.4 ± 0.2	23.3 ± 0.3
	May	1.6 ± 0	26.4 ± 1
	June	1.1 ± 0.4	17.1 ± 0.4
	July	1.3 ± 0.4	1.1 ± 0.8
	August	0 ± 0	0.4 ± 0.2
	September	1.2 ± 0.2	0.8 ± 0.2
	October	1.6 ± 0.3	6.4 ± 2.9
	November	1.3 ± 0.2	9.1 ± 3.3
	December	1.5 ± 0.2	9.2 ± 0.7

Table S2. Living foraminiferal abundances for each replicate for the dominant species and total assemblage (ind. $10cm^{-3}$).

STATION 1

Species		*Elphidium selseyense*		*Ammonia* sp. T6		*Elphidium magellanicum*		*Trochammina inflata*		Total assemblage	
Year	**Month**	**A**	**B**	**A**	**B**	**A**	**B**	**A**	**B**	**A**	**B**
2011	August	2.1	0.4	1.4	1.1	0.0	0.0	0.0	0.0	4.2	2.5
2011	November	0.0	1.1	0.0	0.7	0.0	0.0	0.0	0.0	0.0	2.1
2012	January	2.8	7.4	0.7	5.7	0.0	0.4	0.4	2.1	5.0	18.0
2012	March	28.6	19.1	12.0	13.8	29.4	13.8	2.1	0.7	75.7	48.5
2012	May	141.5	531.6	13.8	4.6	63.0	129.8	0.4	3.2	222.1	677.6
2012	July	76.0	247.9	8.1	12.4	3.9	3.5	0.0	0.0	88.4	270.6
2012	September	21.2	38.2	0.7	3.9	0.0	0.0	0.0	0.7	21.9	46.0
2012	November	0.7	1.4	0.4	0.4	0.0	0.0	0.0	0.0	1.4	1.8

STATION 2

Species		*Elphidium selseyense*		*Ammonia* sp. T6		*Elphidium magellanicum*		*Trochammina inflata*		Total assemblage	
Year	**Month**	**A**	**B**	**A**	**B**	**A**	**B**	**A**	**B**	**A**	**B**
2011	August	53.8	95.8	72.5	91.6	0.0	0.0	10.6	18.7	140.1	208.0
2011	November	33.2	71.4	61.9	59.8	0.0	0.0	13.1	10.6	111.1	146.4
2012	January	122.0	201.6	263.1	189.2	1.1	0.7	142.5	100.4	545.4	501.9
2012	March	225.6	203.7	275.2	152.8	41.0	56.6	73.9	76.0	624.2	500.5
2012	May	254.6	321.8	165.9	128.4	120.6	111.4	42.1	30.1	602.3	607.3
2012	July	318.3	246.9	172.2	144.7	39.6	36.1	35.4	27.6	589.9	473.2
2012	September	415.2	315.8	141.1	63.7	97.3	46.7	14.9	17.3	681.2	453.8
2012	October	104.7	92.7	87.0	111.1	2.1	1.4	5.3	9.5	205.8	217.2
2012	November	29.4	32.5	66.5	29.7	3.9	4.2	5.0	2.5	108.9	73.2
2012	December	281.2	223.2	78.9	77.1	16.3	34.7	15.9	9.5	405.3	350.5

Table S3. Living foraminiferal abundances for each replicate, year and month for all the species of the assemblage (ind. $10cm^{-3}$). Empty cases represent the absence in the sample. Last column: absolute abundance of the total fauna.

Year	Station	Replicate	Month	*Ammonia falsobeccarii*	*Ammonia* sp. T1	*Ammonia* sp. T2	*Ammonia* sp. T3	*Ammonia* sp. T6	*Bulimina denudata*	*Bulimina elongata*	*Bulimina marginata*	*Bulimina* sp.	*Cassidulina* sp.	*Elphidium selseyense*	*Elphidium magellanicum*	*Elphidium magellanicum* (encrusted)	*Elphidium margaritaceum*	*Elphidium* sp.	*Epistominella* sp.	*Haynesina depressula*	*Haynesina germanica*	*Hopkinsina* sp.	*Leptohalysis* sp.	Non determined	*Nonion* sp.	*Nonionella* sp.	*Quinqueloculina leavigata*	*Quinqueloculina* sp.	*Stainforthia* sp.	*Textularia* sp.	*Trochammina inflata*	Total
2011	1	A	August					1.4						2.1										0.4				0.4				4.2
2011	1	A	November																													
2012	1	A	January					0.7						2.8						1.1											0.4	5.0
2012	1	A	March	0.4		1.1		12.0	0.4					28.6	29.4			0.4		0.4								0.7		0.4	2.1	75.7
2012	1	A	May					13.8	1.1		0.4			141.5	47.7	15.2								0.4		0.4	1.1		0.4		0.4	222.1
2012	1	A	July					8.1						76.0	1.8	2.1													0.4			88.4
2012	1	A	September					0.7						21.2																		21.9
2012	1	A	November			0.4		0.4						0.7																		1.4
2011	1	B	August					1.1						0.4			1.1															2.5
2011	1	B	November					0.7						1.1														0.4				2.1
2012	1	B	January			0.7		5.7						7.4	0.4		0.4										1.1	0.4			2.1	18.0
2012	1	B	March					13.8						19.1	13.8					0.4				0.4			0.4				0.7	48.5
2012	1	B	May					4.6	0.4					531.6	93.4	36.4	0.4		0.7	0.4				2.1		0.4	0.4	1.1	2.5	0.4	3.2	677.6
2012	1	B	July			0.4		12.4	0.4		0.7			247.9	2.1	1.4	1.4	0.4						0.7			0.7	0.4	1.8			270.6
2012	1	B	September					3.9						38.2			0.4												2.5	0.4	0.7	46.0
2012	1	B	November					0.4						1.4																		1.8
2011	2	A	August					72.5						53.8			0.7				0.4		1.1			0.4		0.4		0.4	10.6	140.1
2011	2	A	November					61.9						33.2			0.7							1.1				1.1			13.1	111.1
2012	2	A	January	0.7		2.5	8.8	263.1		1.1				122.0	1.1		0.7	0.4	1.1						0.7	0.4				0.4	142.5	545.4
2012	2	A	March			1.4		275.2				1.8		225.6	40.0	1.1	0.4		0.4						0.7	0.7		1.4		1.8	73.9	624.2

2012	2	A	May			1.1		165.9			0.4	3.9		254.6	38.6	82.1	0.4		1.4							3.2	0.4	2.1	1.4	5.0	42.1	602.3
2012	2	A	July			1.8		172.2	6.0	2.1	0.4	0.4		318.3	3.9	35.7	1.4		0.4	0.7						0.4		7.1	1.8	2.1	35.4	589.9
2012	2	A	September		0.7			141.1		1.4	0.4			415.2	16.3	81.0	0.4	0.4	3.2			1.4						0.4	1.4	3.2	14.9	681.2
2012	2	A	October		0.4	0.7		87.0	1.1	2.5	0.4			104.7		2.1							0.4							1.4	5.3	205.8
2012	2	A	November					66.5	0.7		0.4			29.4		3.9	0.4					2.1							0.7		5.0	108.9
2012	2	A	December	0.7		1.8		78.9	1.1	0.7	1.4			281.2	0.4	15.9			0.7	0.4		1.8		0.4		0.4		0.4	0.4	3.2	15.9	405.3
2011	2	B	August					91.6				0.4		95.8						0.7	0.4			0.4							18.7	208.0
2011	2	B	November					59.8				0.4		71.4			1.1			1.1				1.1				1.1			10.6	146.4
2012	2	B	January		0.4	2.1		189.2		0.4				201.6	0.7			1.1										5.7		0.4	100.4	501.9
2012	2	B	March			1.1		152.8	0.4			2.1		203.7	56.2	0.4	1.1	0.7	1.4						1.1	0.4		1.8	0.7	0.7	76.0	500.5
2012	2	B	May			1.4		128.4	2.1		0.7		0.4	321.8	25.8	85.6			0.4	0.4				1.8		2.8	1.1	0.7	1.1	2.8	30.1	607.3
2012	2	B	July		1.1	1.4		144.7	0.4	1.8	1.8	2.1		246.9	8.1	27.9	0.7		1.1	1.1						0.4	2.1	1.1	0.7	2.5	27.6	473.2
2012	2	B	September			0.4		63.7	1.8	0.7				315.8	8.1	38.6	1.4	0.4	2.1		0.4							0.4	1.4	1.4	17.3	453.8
2012	2	B	October		0.7	1.1		111.1	0.4					92.7	1.1	0.4			0.4												9.5	217.2
2012	2	B	November			0.4		29.7	1.1		0.4			32.5	1.8	2.5	0.4		0.7									0.4	0.4	0.7	2.5	73.2
2012	2	B	December					77.1	1.4	0.7				223.2	5.7	29.0	1.1		1.4			0.4					0.4	0.4		0.4	9.5	350.5

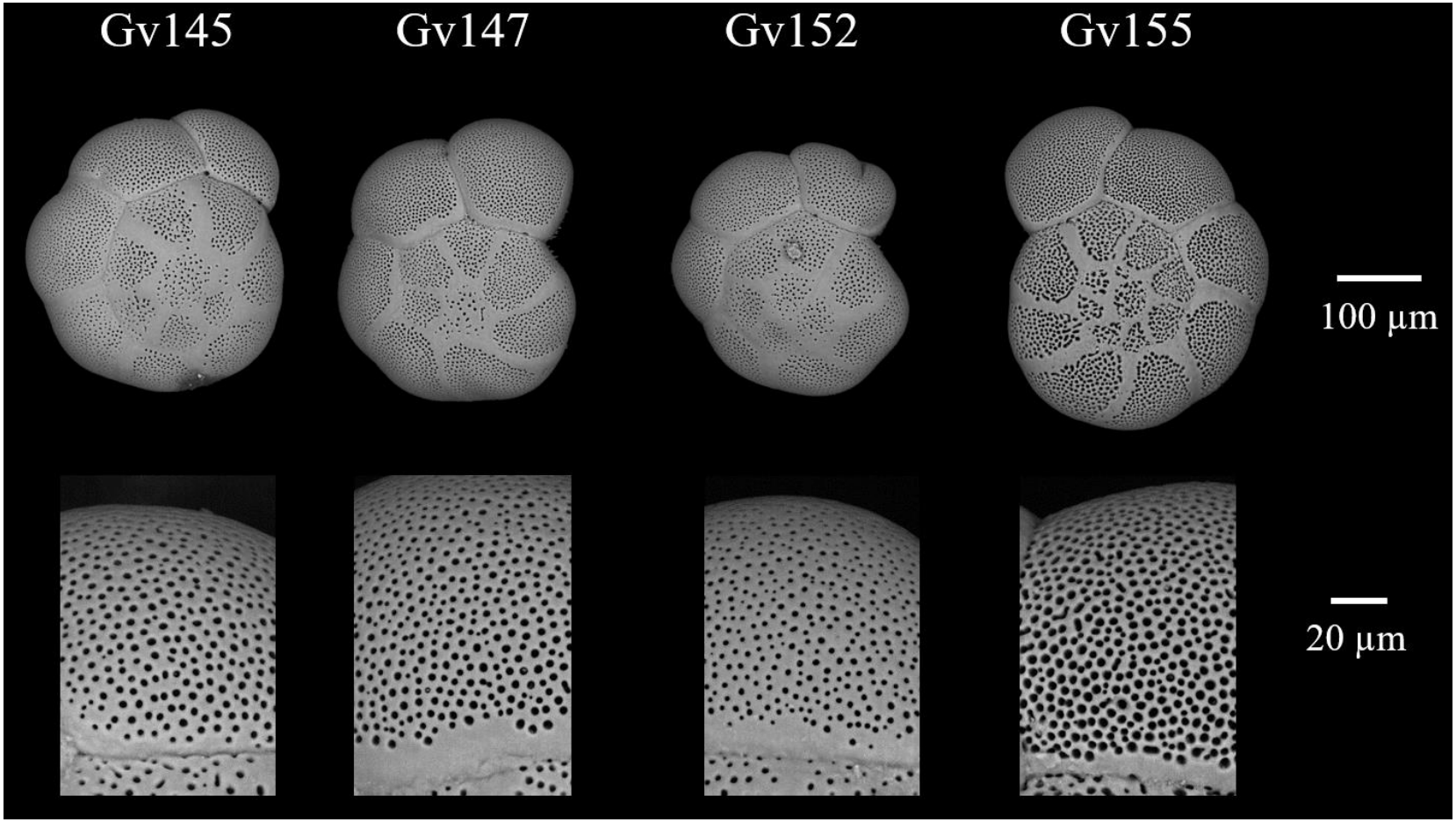

Figure S1. SEM images of spiral side and a 1000x magnification of the penultimate chamber for four individuals from Grevelingen station 1 identified T6 by molecular identification.

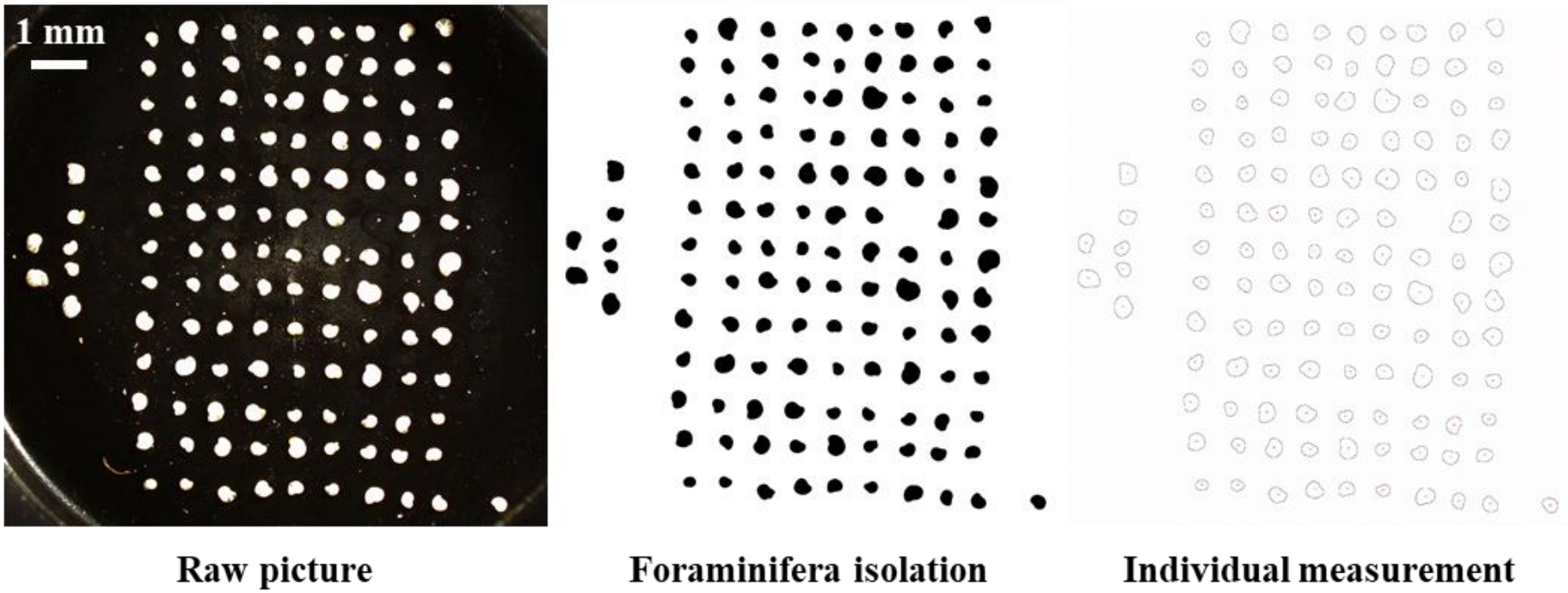

Figure S2. Numerical treatment used for the size measurement for each image performed with ImageJ software. The three size fractions (125–150, 150–315, >315 µm) were analysed together for the size distribution analyses. The left figure shows the untreated image, the middle figure presents the next step, when all individual foraminifera are depicted. Finally, the figure on the right shows the individual foraminiferal outlines which were measured.

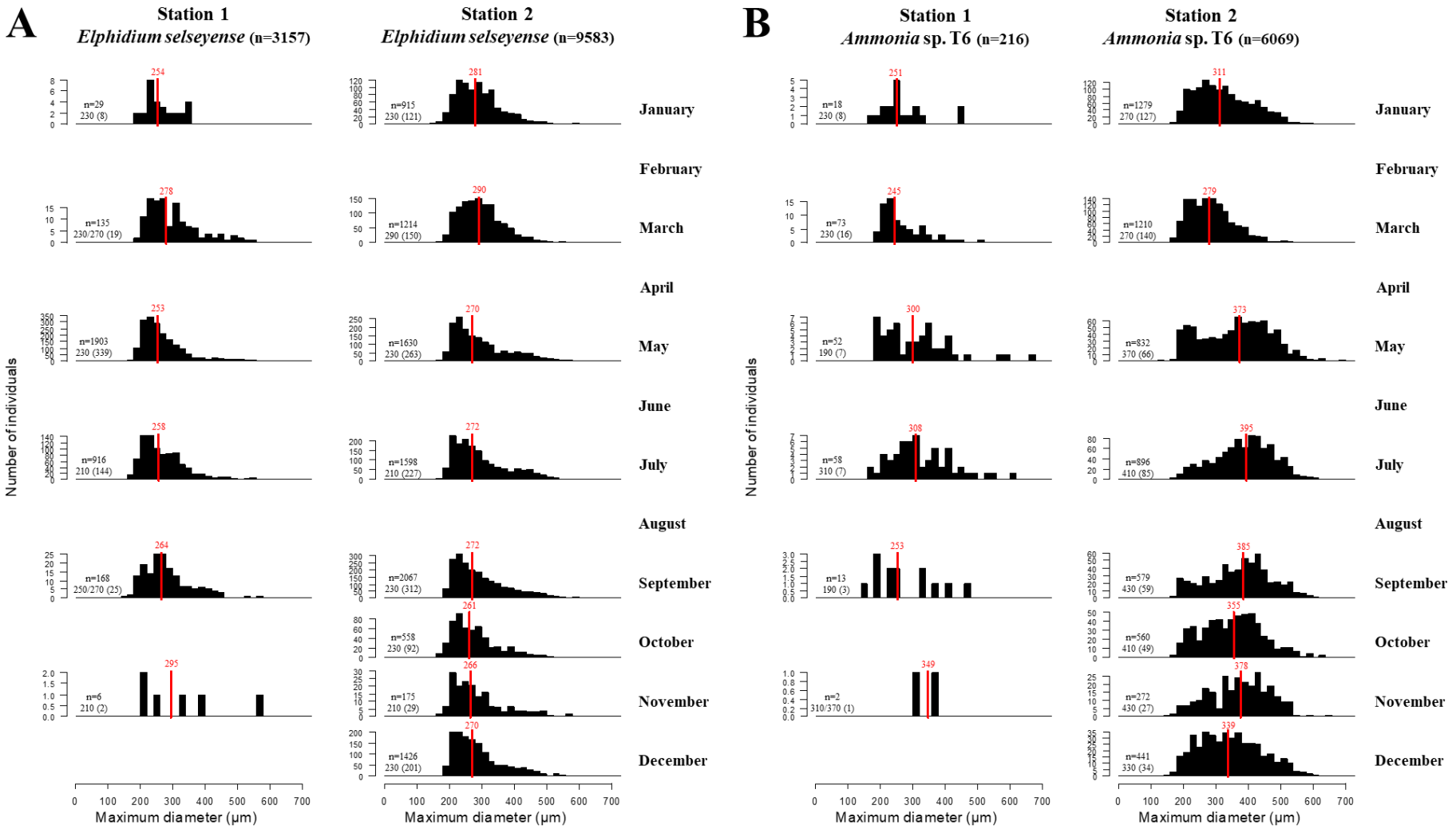

Figure S3. A: size distribution (maximum diameter for each individual in µm) of *Elphidium selseyense* for stations 1 (left) and 2 (right) in 2012. B: size distribution (maximum diameter for each individual in µm) of *Ammonia* sp. T6 for stations 1 (left) and 2 (right) in 2012. For each month, the number of individuals (n), the mode and the number of individuals associated to the mode (between brackets) are indicated in black. The medians are indicated by the red bars in each panel. In order to base our analysis on a sufficiently high number of specimens, we focused on *E. selseyense* and *Ammonia* sp. T6. As explained

before, we only considered specimens retained on a 125 µm mesh meaning that juvenile specimens are not represented. Only the samples taken in 2012 were considered. The size distribution of *E. selseyense* was relatively similar between the two stations regarding the median, ranging from 253 µm (in May) to 295 µm (in November) at station 1 and from 261 µm (in October) to 290 µm (in March) at station 2. At both stations, we observed the presence of an abundant group of smaller specimens, with a mode that never exceeded 250 µm, except in March at station 2, when it is difficult to separate this subpopulation from the larger specimens. The main difference between the two stations was the higher proportion of larger individuals (>400 µm) at station 2, which was visible through the better-developed tails at the right side of the distribution graphs. The low number of *Ammonia* sp. T6 individuals at station 1 did not allow us to draw any firm conclusion concerning the size distribution at this station (Supplementary Figure 3). At station 2, a group of individuals with smaller diameters (< 300 µm) was always present. The overall size distribution showed a clear shift to higher diameters between March (median = 279 µm) and May (median = 373 µm, Fig. 7), which is also evidenced by the much higher proportion of larger individuals. Specimens larger than 400 µm were abundantly found until November (median = 378 µm), but started to diminish in December, as is also shown by the decrease of the median to 339 µm. Our tentative to distinguish cohorts by using a deconvolution method to separate the total size distributions into a sum of Gaussian curves was not conclusive. The main problem was the fact that we did not have any information concerning individuals smaller than 125 µm, so that our size distributions were systematically skewed on the left side (i.e. toward small individuals). An additional problem was the large number of smaller specimens which were always present. Because the identification of individual cohorts was not successful, parameters like reproduction rate, growth rate or lifespan were not assessable. Nevertheless, the size distribution data give some clues concerning the population dynamics of the two dominant species.

CHAPTER 5

BENTHIC FORAMINIFERAL HISTORICAL RECORD IN THE SEASONALLY ANOXIC LAKE GREVELINGEN, THE NETHERLANDS

JULIEN RICHIRT[1], ANAÏS GUIHENEUF[1], AURELIA MOURET[1], MAGALI SCHWEIZER[1], CAROLINE P. SLOMP[2] AND FRANS J. JORISSEN[1]

[1]UMR 6112 LPG-BIAF Recent and Fossil Bio-Indicators, University of Angers, 2 Boulevard Lavoisier, 49045 Angers, France
[2]Department of Earth Sciences (Geochemistry), Faculty of Geosciences, Utrecht University, Princetonlaan 8a, 3584 CB Utrecht, the Netherlands

*Correspondence author: richirt.julien@gmail.com

ABSTRACT

Lake Grevelingen is a former branch of the Rhine-Meuse-Scheldt estuary artificially transformed into a salt-water lake by a dam, in order to avoid flooding events. This transformation induced profound changes in the biocoenoses of the basin which have been described as an ecodisaster, with hypoxic/anoxic events occurring seasonally in the deepest parts of the lake. Here, we investigate a sediment record sampled in 2012 in the Den Osse Basin (34 m depth), spanning the last ~ 50 years, including the transition from estuary to salt-water lake. The record of molybdenum (Mo) concentrations in the sediment core was used to refine an existing age model based on ^{210}Pb, and gave us an estimated precision of ± 3 years. The benthic foraminiferal succession reflects the anthropogenic modifications made in Lake Grevelingen, and allowed us to recognise four successive stages: 1) before the seaward closure in 1971, when the system was estuarine; 2) 1971 to 1978, when the system rapidly changed into an enclosed brackish water lake; 3) 1978 (construction of a seaward sluice opened in winter) to 1999 and 4) the period from 1999 (year-round opening of the sluice, doubling of water exchanges) to today. The foraminiferal record also highlights the appearance of the putatively exotic *Ammonia* phylotype T6 in the mid 1980s, which thereafter progressively replaced the congeneric autochthonous phylotype T2. Finally, we hypothesise that the activity of cable bacteria, S-oxidising prokaryotes which today develop in the first half of the year in the Den Osse Basin, causes dissolution of foraminiferal tests by decreasing the pore water carbonate saturation state in the anoxic upper part of the sediment. This explains the contrast between the dense living faunas and the very low numbers of foraminiferal shells in the top ~ 15 cm of the sediment core.

1. INTRODUCTION

Lake Grevelingen is a former estuary of the Scheldt-Meuse-Rhine delta, in the Netherlands. After a devastating storm in 1953, which caused large scale flooding and more than 1800 casualties, it was decided to construct dams landward (1965) and seaward (1971), in order to avoid such disasters in future. The transformation of the Grevelingen from an estuary to a salt-water lake induced profound changes of its biocoenoses. These modifications took place at ecosystem (e.g. habitat losses, trophic relationships), community (e.g. decrease of biodiversity, replacement of marine by estuarine species) as well as species level (e.g. change of life cycles, densities) (Nienhuis, 1978; Nienhuis & Veld, 1984). More specifically, the suppression of tidal currents and decrease of salinity just after its full closure strongly affected marine benthic animals (e.g. sponges, sea anemones, tunicates). Mass mortality of these animals contributed to increased food availability, insufficient removal of decomposition products and finally oxygen depletion. This "ecodisaster" induced a large simplification of the ecosystem in both structure and functioning (Nienhuis & Veld, 1984; Bannink et al., 1984). Within a few years after closure of the estuary, seasonal bottom water hypoxia/anoxia started to occur, followed by mass

mortality of the remaining marine benthic populations (e.g. molluscs, worms), especially in the deeper parts of the basin (Nienhuis & Veld, 1984).

In 1978, a sluice was opened seaward (Brouwersdam) in winter, to limit water column stratification. Consequently, several species, common at the time of the Grevelingen estuary, which had disappeared when the estuary was closed, were observed again (e.g. some species of jellyfish and crab; Nienhuis and Veld, 1984). In 1999, it was decided to open the sluice all year round (except during a few weeks of rough weather in autumn). Despite these managements, seasonal bottom water oxygen depletion continued to occur every year, as is still the case today, especially in the deepest parts of Lake Grevelingen, such as in the Den Osse Basin, the subject of this study (Wetsteyn, 2011; Sulu-Gambari et al. 2017). Lake Grevelingen has been monitored since the late 1950s, thus a large amount of environmental information is available (Wetsteijn, 2011).

Foraminifera are among the most widespread groups of marine unicellular eukaryotes and constitute one of the most diverse group of shelled organisms. For this reason, they have a very rich fossil record and are widely used for paleoenvironmental reconstructions and paleoecological interpretations (Murray, 2006; Katz et al., 2010). Thanks to the preservation of foraminiferal faunas in the sediment record, Lake Grevelingen provides a unique opportunity to study the benthic foraminiferal response to the progressive transformation of the ecosystem from an estuary to a salt water lake. Recently, a study investigated the temporal response of living foraminiferal communities to recent seasonal anoxia in the Den Osse Basin (Richirt et al. 2020). The authors highlighted the fact that the deepest part of the Den Osse Basin shows a severe decline in foraminiferal faunas in the months following late summer–early autumn anoxia. They explained this by the presence of sulphides in the foraminiferal habitat, which would inhibit foraminiferal reproduction and growth. In the shallower parts of the Den Osse Basin, where the duration of anoxia is shorter, there was not such a major faunal decline.

The living community of the Den Osse Basin is largely dominated by *Elphidium selseyense*, *Elphidium magellanicum* and *Ammonia* sp. T6. The latter species, *Ammonia* sp. T6, is often considered as an exotic and/or invasive species, originating from East Asia (e.g. Pawlowski & Holzmann, 2008; Schweizer et al, 2011; Bird et al., 2020). *Ammonia* sp. T6, which is almost the only representative of the genus *Ammonia* in the recent faunas (Richirt et al., 2020), is characterised by very large pores (Richirt et al., 2019a). Interestingly, a preliminary study of a long core sampled in the Den Osse Basin showed a clear shift from specimens with small pores to specimens with bigger pores in recent times (Petersen et al., 2016), suggesting that in a recent past, *Ammonia* sp. T6 has progressively replaced *Ammonia* sp. T2 (and/or T1) in Lake

Grevelingen. Richirt et al. (2019b) suggested that an increase in overall porosity could be an adaptation to low oxygen concentrations. The putative replacement of *Ammonia* sp. T2 (and/or T1) by *Ammonia* sp. T6 could therefore be due to the larger tolerance of the latter species to hypoxia. The study of the sedimentary foraminiferal record should enable us to shed more light on this important faunal take-over.

In this study, we investigate foraminiferal assemblages of a 90 cm long sediment core sampled in the deepest part of the Den Osse Basin, representing the last ~ 50 years. We will especially address the following questions:

1) How did the foraminiferal community change in response to the closure of Lake Grevelingen in the 1970s and the subsequent management changes of the basin?

2) Has there been a substitution of the supposed autochthonous *Ammonia* phylotypes (T1 and T2) by the putative allochthonous phylotype T6, and, if so, is it the result of an overall spreading of phylotype *Ammonia* sp. T6 across Europe, or rather of a better adaptation of this phylotype to seasonal hypoxia/anoxia?

2. STUDY AREA

Lake Grevelingen is a former estuary in the Scheldt-Meuse-Rhine delta area. After an extreme stormflood event which hit the southern North Sea in February 1953, it was decided to close the main estuaries by dams in order to avoid repetition of flooding events (i.e. Delta Plan, Bannink et al., 1984).

In 1965, the former Grevelingen estuary was closed landward (Grevelingendam) and became a semi-enclosed embayment without river input. A second dam was constructed seaward in 1971 (Brouwersdam), closing the former Grevelingen estuary completely. This stopped the inflow of salt waters from the North Sea and increased the water residence time in the Grevelingen Lake up to three to six years (instead of a few days when the system was estuarine, Nienhuis, 1978; Bannink et al., 1984).

In 1978, in order to remedy eutrophication phenomena and seasonal hypoxia, the connection with the North Sea has been partly reopened by the construction of an underwater sluice in the Brouwersdam (capacity of about 100–140 $m^3 s^{-1}$, initially only opened in winter, Bannink et al. 1984; Muelen et al., 1984). This partial reopening improved bottom water oxygenation in the Den Osse Basin and decreased water residence times to about half a year. A second, landward sluice (siphon) was opened in 1983 (at the Grevelingendam) to ensure a weak (compared to the

natural situation without a dam) fresh water inflow (about 100 m^3 s^{-1}, Bannink et al., 1984; Muelen et al., 1984).

In 1999, the water exchanges between the Lake and the North Sea were doubled (from 1245–1255.10^6 m^3 to 2688–2864.10^6 m^3 per year, Wetsteijn, 2011) by opening the Brouwersdam sluice the whole year, except for a few weeks in autumn and during storm events. This allowed a further decrease of the average water residence time in the Lake from 164 to 72 days and limited water stratification due to high temperatures in summer (Wetsteijn, 2011). However, this situation is still very different compared to the estuarine situation before 1965, when the water residence time was estimated a few days (Nienhuis, 1978; Bannink et al., 1984) and average flood and ebb discharges at the location of the present Brouwersdam were about 126.10^9 and 135.10^9 m^3 per year (in 1959, Louters et al., 1998), respectively, about 50 times higher than the current water exchanges.

To summarize, Lake Grevelingen, a former estuarine system, was completely closed in 1971 (Figure 1). The ensuing strong increase of water residence time, bottom water stagnation and lower salinity caused a major biotope shift in Lake Grevelingen, and led to strong modifications at species and community levels (Nienhuis, 1978).

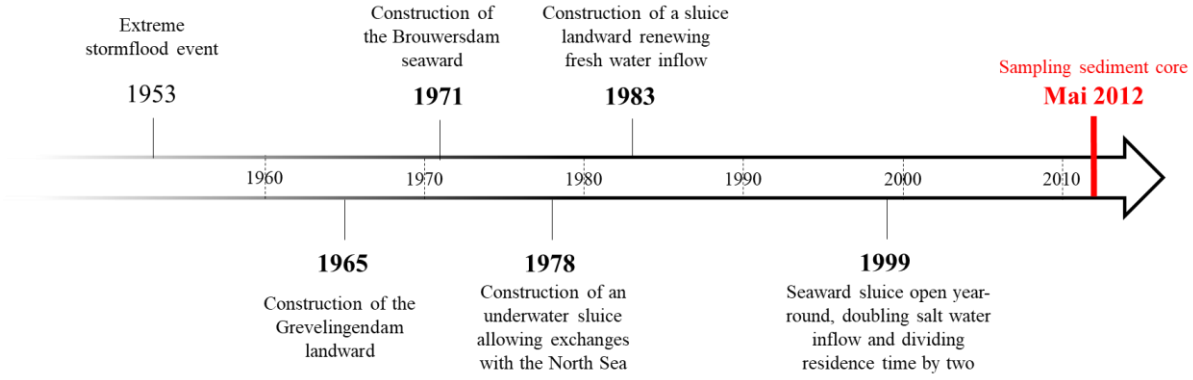

Figure 1. Timeline of the human-induced modifications following the Delta Plan at Lake Grevelingen. The sediment core used to investigate dead foraminiferal assemblages was sampled in Mai 2012 (red line).

3. MATERIALS AND METHODS

3.1. SAMPLING AND LABORATORY TREATMENT

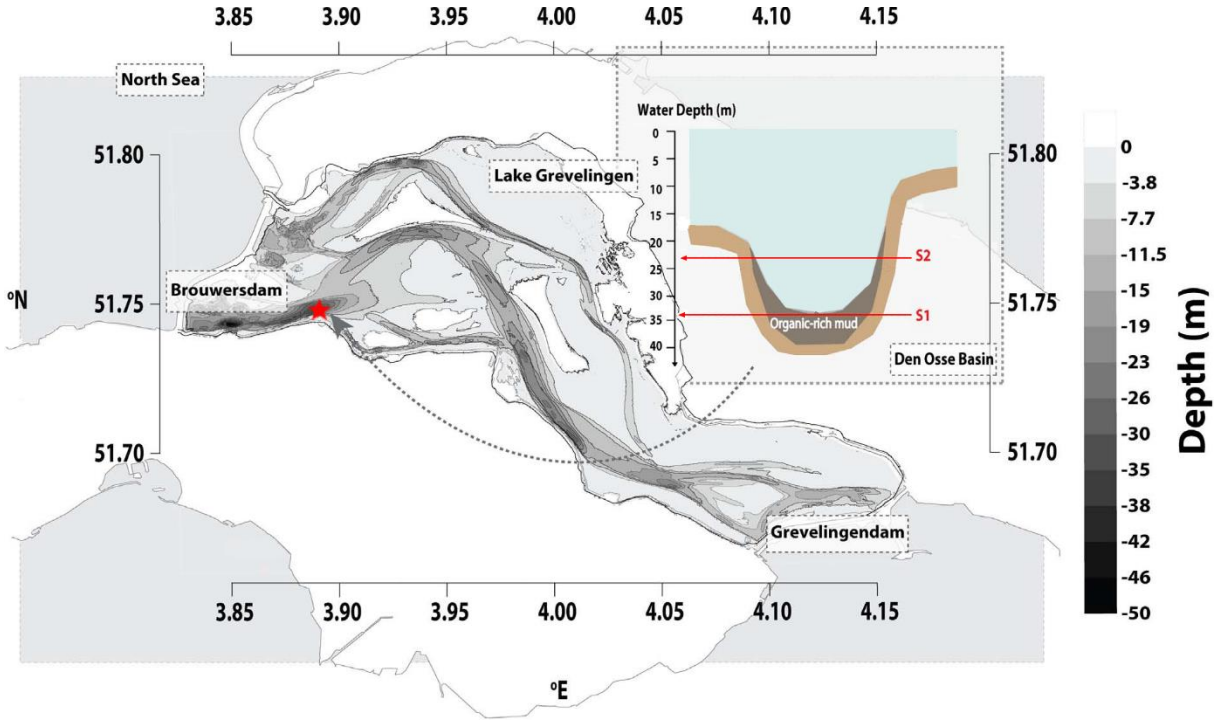

Figure 2. Map of Lake Grevelingen showing the location where the sediment core was sampled in the Den Osse basin (red star). The transversal section of the Den Osse basin (top right) shows the depth at which the sediment core was sampled at Station 1 (S1, 34 m depth). Station 2 (S2, 23 m depth), for which living assemblages were also investigated in Richirt et al. (2020), will be used later in the text. This figure was modified from Sulu-Gambari et al. 2016.

The studied site is located in Den Osse Basin (51° 44.834'N, 3° 53.401'E), the main former channel of the Grevelingen estuary (The Netherlands), at 34 m depth (Figure 2). This site is close to one of the sites which has been intensively monitored since the late 1970s (e.g. Wetsteijn, 2011) and for which detailed data are available on request at the Dutch Water Agency (DWA). Regarding the recurrent problem of seasonal anoxia in the Lake, bottom water measurements are particularly important. On the basis of the DWA data set, Sulu-Gambari et al. (2017) have summarised the bottom water oxygen concentration history close to our sampling site (Figure 3). We want to point out here that, when considering this figure, it is important to realise that the "bottom water" data have been collected in the water column about 100 m from our sampling site (at the DWA site) and sometimes about 3 m above the basin floor (and not at the sediment-water interface), where the water depth is slightly higher, about 37 m. Consequently, it seems evident that in case of (bottom water) anoxia in Figure 3 (at the DWA site), also basin floor was anoxic. However, an absence of anoxia in the water column (as

frequently recorded from late 1990s to 2010, figure 3) does not necessarily mean that the basin floor was not anoxic either.

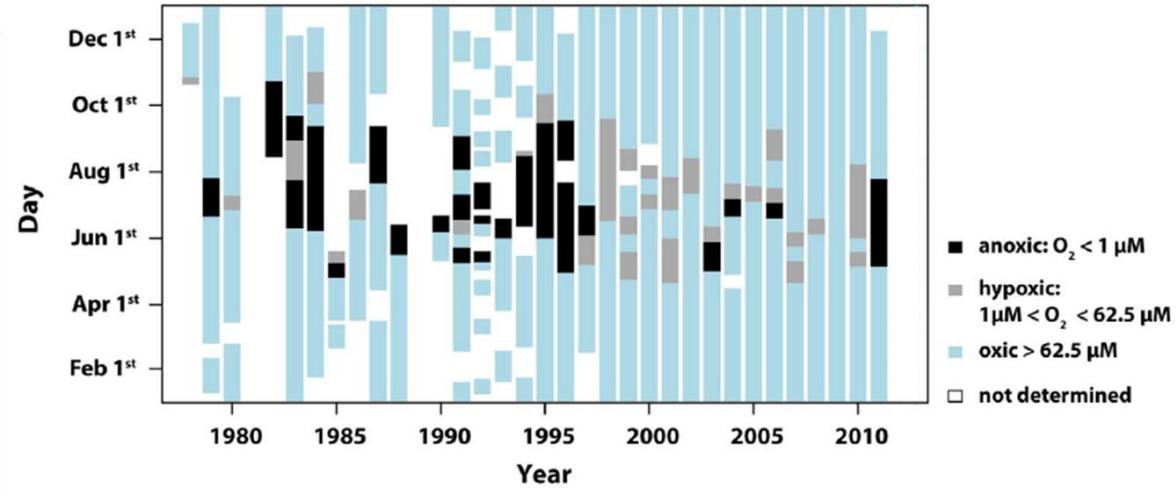

Figure 3. Periods of oxic (blue), hypoxic (grey) and anoxic (black) bottom-water conditions from 1978 to 2011 at site 1 (figure after Sulu-Gambari et al., 2017; data from DWA).

A sediment core of 90 cm length and 6 cm diameter was sampled in May 2012 with a UWITEC gravity corer. In the laboratory, the core was sliced every 0.5 cm (giving 180 samples) with an individual sample volume of 14.1 cm^3. Samples were sieved at 63, 125, 150 and 315 µm, before being dried. Foraminifera of the fraction > 125 µm were picked and stored in micropalaeontological Plummer cells. When possible, determination was made to the species level using a stereomicroscope. Samples 110, 175 and the 125–150 µm fraction of sample 180 were split into half (complete splits were counted) because of the high foraminiferal density. At 82.5 cm depth, a major change in sediment composition was observed, from sand deposits, very probably representative of the strong hydrodynamics of the former estuarine system (below 82.5 cm depth) to muddy/silty sediments, indicative of the much lower hydrodynamics of the salt lake environment (above 82.5 cm depth).

3.2. FORAMINIFERAL ANALYSES

As some samples had very low faunal abundances, two to three adjacent layers were merged (intervals 5–6, 7–8, 9.5–10.5, 12–13, 32.5–35, 57.5–60, 70–72.5 and 75–77.5 cm depth). We compromised between (1) maximising the number of individuals (to obtain a target value of at least 50 individuals) and (2) maximising sampling resolution. In fact, the total thickness of merged samples never exceeded 2.5 cm.

In order to document temporal changes in assemblage composition, a Principal Component Analysis (PCA, non-standardised) was performed on the relative abundances of the dominant

species. We considered only dominant taxa (i.e. taxon which represents at least 5% of the total assemblage in at least one sample) to decrease the signal to noise ratio.

The living assemblages (0–1 cm depth interval) of station 1 (where the sediment core was sampled, at 34 m depth, impacted by a relatively long seasonal oxygen depletion event) and station 2 (23 m depth, impacted by a shorter seasonal oxygen depletion event, Figure 2) were calculated on the basis of the sum of all seasonal samples of Richirt et al. (2020). These samples were considered as supplementary individuals in the analysis, meaning that they did not contribute to the construction of the principal component axes. The data pre-treatment and multivariate analysis procedure are summarised graphically in Figure 4.

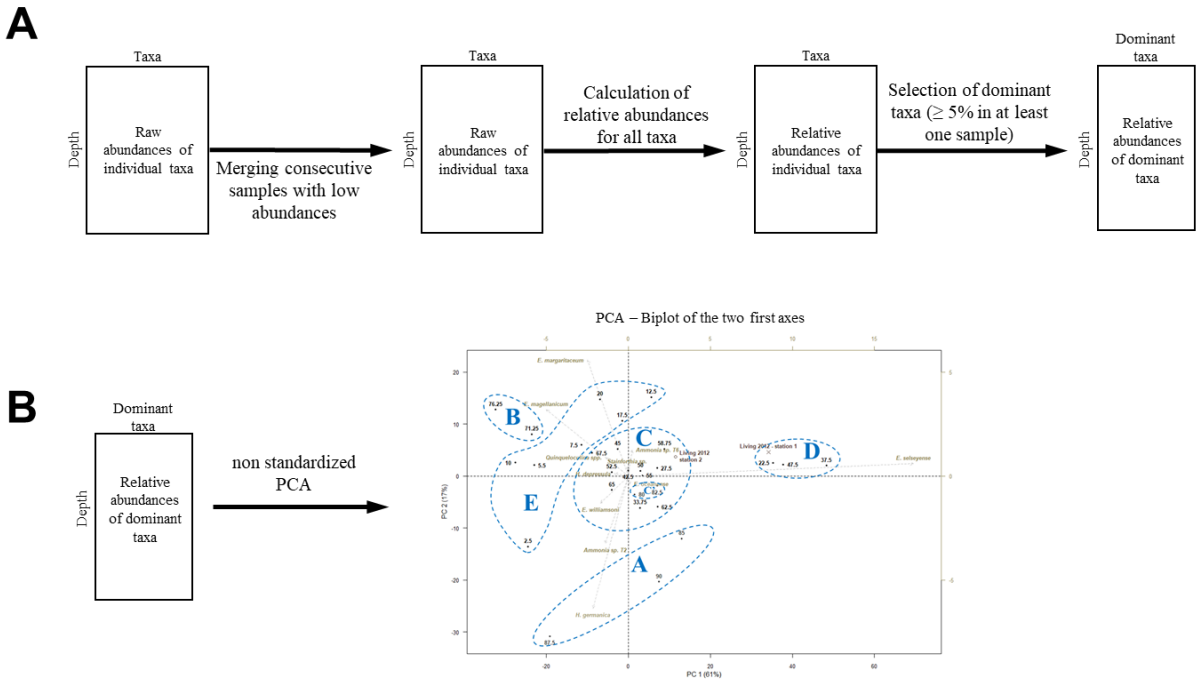

Figure 4. A: data treatment procedure performed from the initial data matrix, with lines representing samples and column taxa. B: Principal Component Analysis (PCA) procedure.

3.3. AGE MODEL

For another 90 cm long core, sampled in May 2011 at exactly the same site, an age model was developed using ^{210}Pb dating (Donders et al., 2012). The age model, which was not very well delimited, suggested an average sedimentation rate of 2.37 cm per year, meaning that the 90 cm long core covered about 37 years (1974 to 2011). This order of magnitude confirms our earlier hypothesis that the very abrupt sediment composition shift at 82.5 cm core depth corresponds to the closure of the basin in 1971.

For a third core taken at this site, sampled during the same cruise (in May 2012) as the sediment core used in this study (Sulu-Gambari et al., 2017), molybdenum (Mo) concentrations

were measured in the solid phase. In fact, Mo is sequestered when reducing conditions (i.e. presence of sulphide, Crusius et al., 1996) occur within the sediment. Therefore, the successive Mo maxima in the sediment record should reflect the yearly seasonal hypoxia/anoxia coupled with the presence of sulphides (Seitaj et al., 2015), and can therefore be used to refine the age model based on ^{210}Pb levels. This principle was earlier used for a core from another site in Lake Grevelingen with an exceptionally high sediment accumulation rate (~ 13 cm y^{-1}), slightly further to the west in Den Osse Basin (Egger et al., 2016).

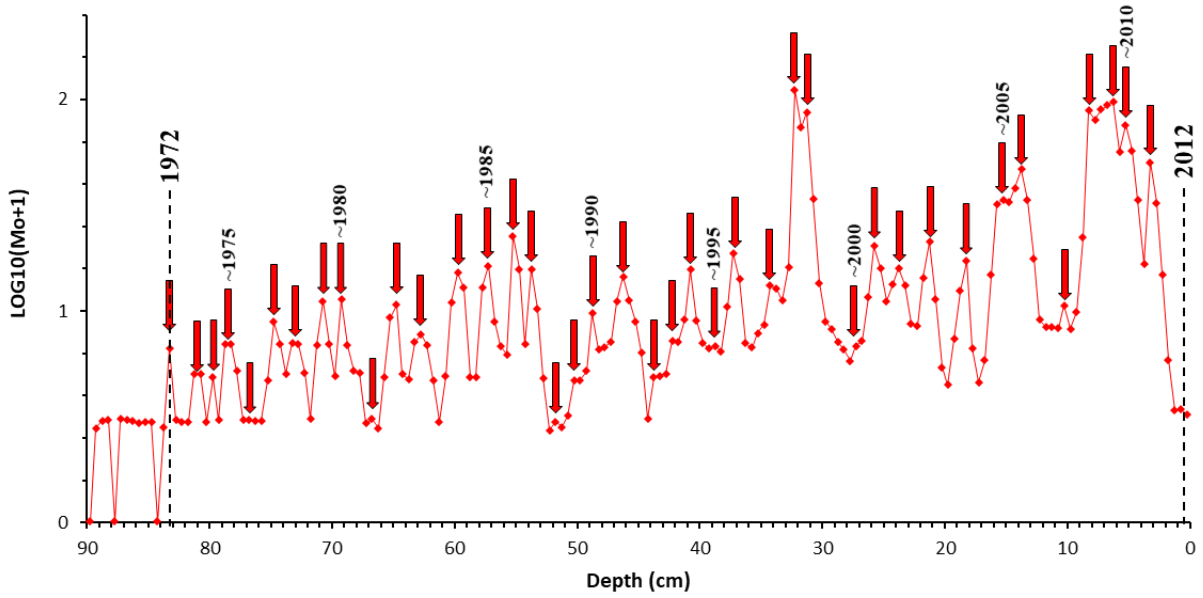

Figure 5. Molybdenum concentrations (ppm) as a function of core depth (cm). All values were LOG10(x+1) transformed to better identify peaks. Each peak is highlighted with a red arrow and is supposed to represent a yearly summer hypoxia/anoxia event. Some putative additional peaks have been added in case of broad peaks with shoulders, or broad intervals without clear peaks.

In Figure 5, a very regular, apparently cyclic alternation of maximal and minimal Mo concentrations can be observed, where Mo maxima should correspond to late summer/early autumn anoxia. The first small peak, at ~ 83 cm depth, which occurred after the closure of the estuary seaward in 1971, is supposed to represent a first anoxic/sulphidic event. Between this first peak at ~ 83 cm, thought to represent summer/autumn 1972, and the last peak, representing summer/autumn 2012, we tentatively placed 39 more annual peaks. In some years, seasonal anoxia may not have developed, or may have been very short, so that no Mo peaks have developed. Another possible explanation for the fact that we miss some Mo peaks could be that in years with somewhat lower sedimentation rates, two seasonal Mo peaks may have merged. Consequently, our tentative age model does not have the pretention to be exact; in some places it may at the maximum be two to three years off.

A further complication is that Mo concentrations were not measured in the same core as the one used for foraminiferal analysis. In fact, in the core used to construct the Mo/Al-based age model, the sedimentological shift (sand to silt/clay) characterising the closure of the estuary was observed at 84 cm depth, whereas the same transition was found at 82.5 cm in the core used for foraminiferal analysis. Consequently, when applying our Mo-based age model on foraminiferal record, there is an additional uncertainty of about 1–2 cm. In conclusion, we consider that our age model is reliable with a precision of ± 3 years, which is largely sufficient for the aims of our study.

The average sediment accumulation rate calculated using the putative age model based on the Mo peaks is 2.06 cm y^{-1}. This is consistent with the average sediment accumulation rate of 2.37 cm y^{-1} obtained with the ^{210}Pb method by Donders et al., (2012).

3.4. CALCIUM CARBONATE SATURATION STATE

In order to determine the variation of the calcium carbonate saturation state in the sediment at our station throughout the year, we used the CO2SYS software (Lewis and Wallace, 1998). Monthly temperature and salinity data are from Hagens et al. (2015) and were measured in the water column at 32 m depth. Monthly values for alkalinity and PO_4^{3-} concentrations in the pore waters are from Sulu-Gambari et al. (2016) and were measured in 0.5 cm thick sediment slices. The values of pH were obtained by profiling the first 2.5 cm of the sediment with a microsensor in three replicate cores (data from Seitaj et al., 2015). To compute the calcium carbonate saturation state, using alkalinity and PO_4^{3-} concentrations, pH values had to be averaged for 0.5 cm layers. Following Orr et al. (2015), we used the set of constant K_1 and K_2 from Lueker et al. (2000), the formula of Dickson (1990) for KSO_4 and the total boron-to-salinity ratio from Uppström (1974) for computation. The results of the calcium carbonate saturation state calculations will be presented in the discussion section because we will only use it to corroborate a hypothesis about the role of cable bacteria in the putative dissolution of foraminiferal shells.

4. RESULTS

4.1. FORAMINIFERAL FAUNAS

The black curve in figure 6 represents the total number of individuals per sample (Table 1). In cases where the total density was well below our target value of 50 individuals, individual

samples were merged (red curve in figure 6). However, even after this merging procedure, all samples in the top 17.5 cm of the core were still very poor, with less than 50 individuals (Figure 6, Table 2).

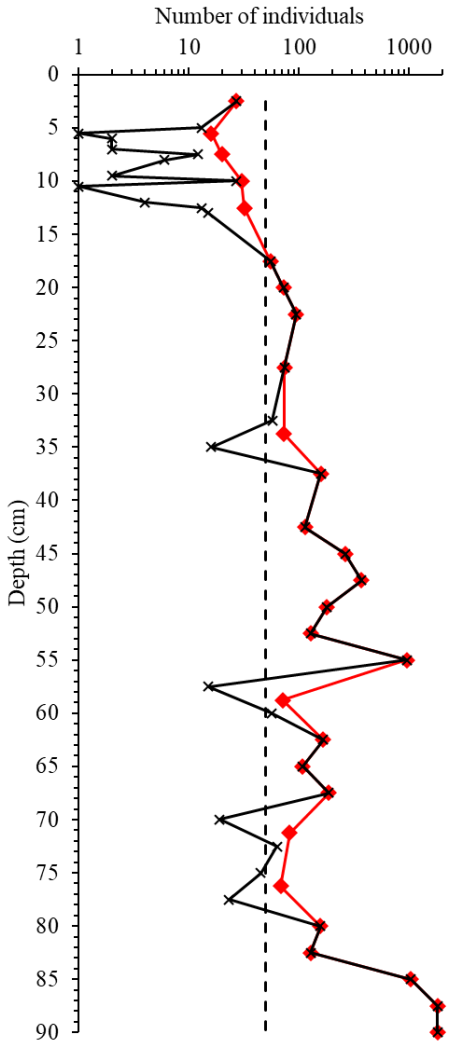

Figure 6. Total number of individuals in non-merged samples (black curve) and after merging samples (red curve). The dashed line represents the target value of 50 individuals per analysed sample.

Eleven of the 23 observed taxa were considered as dominant (≥ 5 % in at least one sample, Table 1). Together, these 11 dominant taxa represent more than 90 % of the total assemblage in almost all samples (Table 2).

Table1. Total and species abundances of foraminifera in the samples (per 14.1 cm^3). ND: Not determined.

Depth	Total abundance	*Ammonia* sp. T1	*Ammonia* sp. T2	*Ammonia* sp. T6	*Aubignyna perlucida*	*Bolivina* sp.	*Brizalina* sp.	*Bulimina* sp.	*Cassidulina* sp.	*Cibicides* sp.	*Elphidium magellanicum*	*Elphidium margaritaceum*	*Elphidium oceanense*	*Elphidium selseyense*	*Elphidium williamsoni*	*Elphidium* sp.	*Epistominella* sp.	*Haynesina germanica*	*Jadammina macrescens*	*Nonion depressulus*	*Quinqueloculina* spp.	*Rosalina* sp.	*Stainforthia* sp.	*Trochammina inflata*	ND
2.5	27	1	2	0	0	0	0	0	0	0	3	4	0	5	3	0	0	7	0	1	0	0	0	0	1
5.0	13	0	1	0	0	0	0	0	0	0	3	1	0	0	2	0	0	0	0	0	2	0	0	0	4
5.5	1	0	0	0	0	0	0	0	0	0	0	0	0	1	0	0	0	0	0	0	0	0	0	0	0
6.0	2	0	0	0	0	0	0	0	0	0	0	0	0	2	0	0	0	0	0	0	0	0	0	0	0
7.0	2	0	0	0	0	0	0	0	0	0	0	0	0	2	0	0	0	0	0	0	0	0	0	0	0
7.5	12	0	0	0	0	0	0	0	0	0	3	2	0	1	4	0	0	0	0	0	1	0	0	0	1
8.0	6	0	0	3	0	0	0	0	0	0	0	0	0	3	0	0	0	0	0	0	0	0	0	0	0
9.5	2	0	0	0	0	0	0	0	0	0	0	0	0	1	0	0	0	0	0	0	0	0	0	0	1
10.0	27	1	0	0	0	0	0	0	0	0	8	3	0	3	2	0	1	3	0	2	2	0	0	0	2
10.5	1	0	0	0	0	0	0	0	0	0	0	0	0	1	0	0	0	0	0	0	0	0	0	0	0
12.0	4	0	0	1	0	0	0	0	0	0	0	1	0	2	0	0	0	0	0	0	0	0	0	0	0
12.5	13	0	0	0	0	0	0	0	0	0	3	7	0	1	1	0	0	0	0	1	0	0	0	0	0
13.0	15	0	0	3	0	0	0	0	0	0	0	0	0	12	0	0	0	0	0	0	0	0	0	0	0
17.5	55	0	0	0	0	0	0	0	0	0	6	12	0	22	0	1	0	2	0	1	3	0	3	1	4
20.0	72	0	2	6	0	0	0	0	0	0	4	21	1	24	0	2	0	0	0	6	1	0	3	0	2
22.5	94	2	1	1	0	0	0	1	0	0	0	11	0	70	2	1	1	3	0	1	0	0	0	0	0
27.5	74	2	3	5	0	1	0	0	0	0	6	9	2	35	4	1	0	4	0	0	0	0	0	0	2
32.5	57	0	6	10	0	0	0	0	0	0	0	5	2	20	4	0	0	6	1	1	0	0	0	0	2
35.0	16	0	2	1	0	0	0	0	0	0	0	2	0	10	1	0	0	0	0	0	0	0	0	0	0
37.5	158	1	0	0	0	1	0	0	0	0	0	10	0	138	5	0	0	1	0	2	0	0	0	0	0
42.5	113	1	8	1	0	0	0	2	0	1	4	24	1	46	5	0	0	10	1	8	0	0	0	0	1
45.0	263	9	16	6	2	0	0	2	0	1	18	52	0	100	9	0	0	10	0	19	3	0	0	1	15
47.5	370	2	5	14	0	0	0	1	0	0	9	25	0	285	9	0	0	5	1	6	6	0	0	1	1
50.0	180	1	5	6	0	0	0	0	0	0	6	36	3	78	4	0	0	20	0	10	0	0	0	0	11
52.5	128	3	9	1	0	0	0	1	0	2	2	26	2	46	7	1	0	9	0	14	1	0	0	0	4
55.0	950	6	58	10	0	0	4	0	2	16	38	140	6	414	48	14	0	56	8	100	16	0	0	0	14
57.5	15	0	1	0	0	0	0	0	0	0	0	0	0	13	0	0	0	0	0	0	1	0	0	0	0
60.0	56	2	0	0	0	0	0	0	0	0	10	7	0	23	1	1	0	2	0	8	2	0	0	0	0
62.5	165	2	14	0	0	1	0	0	0	0	1	20	4	77	10	2	0	16	0	8	3	0	0	0	7
65.0	108	1	11	0	0	0	0	0	0	1	5	16	3	39	5	0	0	8	2	8	1	2	0	0	6
67.5	187	1	21	0	0	0	0	1	0	4	8	43	1	60	13	0	0	5	0	15	9	1	0	0	5
70.0	19	0	4	0	0	0	0	0	0	1	1	5	0	3	1	0	0	0	0	3	0	0	0	0	1
72.5	63	1	5	0	0	0	0	0	0	0	5	21	1	12	4	1	0	4	0	2	2	1	0	0	4
75.0	45	1	1	0	0	0	0	0	0	0	23	6	0	2	0	0	0	3	0	4	4	0	0	0	1
77.5	23	0	2	0	0	0	0	0	0	0	1	7	0	8	3	0	0	0	1	0	0	0	0	0	1
80.0	157	1	9	0	0	0	0	0	0	3	6	24	7	66	8	0	0	18	1	10	3	0	0	0	1
82.5	128	0	5	0	0	0	0	0	0	1	12	10	8	61	7	0	0	8	0	8	1	0	0	0	7
85.0	1033	18	105	0	0	0	1	0	0	29	35	8	15	540	66	8	1	105	3	47	10	9	1	5	27
87.5	1810	28	314	0	0	0	2	4	0	46	34	14	26	380	160	14	0	566	20	112	6	16	0	30	38
90.0	1805	24	245	0	0	0	0	0	0	20	16	4	17	846	128	9	0	340	17	63	9	12	0	13	42

Total faunal density is relatively high between 90 and 85 cm depth, ranging from 1033 to 1810 individuals per 14.1 cm^3 (Figure 6 and Table 1). At 82.5 cm depth, the foraminiferal density abruptly decreases by one order of magnitude. Total densities between 82.5 and 17.5 cm depth oscillate between 15 (57.5 cm depth) and 950 individuals (55 cm depth) per 14.1 cm^3, with an average of about 175 ind. per 14.1 cm^3.

Finally, in the top 17.5 cm of the core, total densities are very low, between 1 and 27 individuals per 14.1 cm^3 (Figure 6 and Table 1).

Table 2. Total abundances of the foraminiferal faunas (ind. per 14.1 cm^3) and relative abundances of the dominant species (≥ 5 % of the total assemblage in at least one sample).

Depth (cm)	Total abundance in the complete assemblage	*Ammonia* sp. T1	*Ammonia* sp. T2	*Ammonia* sp. T6	*Elphidium selseyense*	*Elphidium magellanicum*	*Elphidium margaritaceum*	*Elphidium williamsoni*	*Elphidium oceanense*	*Haynesina germanica*	*Haynesina depressula*	*Quinqueloculina* spp.	*Stainforthia* sp.	Total dominant taxa
2.5	27	3.7	7.4	0.0	18.5	11.1	14.8	11.1	0.0	25.9	3.7	0.0	0.0	92.6
5.5	16	0	6.3	0.0	18.8	18.8	6.3	12.5	0.0	0.0	0.0	12.5	0.0	75.0
7.5	20	0	0.0	15.0	30.0	15.0	10.0	20.0	0.0	0.0	0.0	5.0	0.0	95.0
10	30	3.3	0.0	0.0	16.7	26.7	10.0	6.7	0.0	10.0	6.7	6.7	0.0	83.3
12.5	32	0	0.0	12.5	46.9	9.4	25.0	3.1	0.0	0.0	3.1	0.0	0.0	100.0
17.5	55	0	0.0	0.0	40.0	10.9	21.8	0.0	0.0	3.6	1.8	5.5	5.5	89.1
20	72	0	2.8	8.3	33.3	5.6	29.2	0.0	1.4	0.0	8.3	1.4	4.2	94.4
22.5	94	2.1	1.1	1.1	74.5	0.0	11.7	2.1	0.0	3.2	1.1	0.0	0.0	94.7
27.5	74	2.7	4.1	6.8	47.3	8.1	12.2	5.4	2.7	5.4	0.0	0.0	0.0	91.9
33.75	73	0	11.0	15.1	41.1	0.0	9.6	6.8	2.7	8.2	1.4	0.0	0.0	95.9
37.5	158	0.6	0.0	0.0	87.3	0.0	6.3	3.2	0.0	0.6	1.3	0.0	0.0	98.7
42.5	113	0.9	7.1	0.9	40.7	3.5	21.2	4.4	0.9	8.8	7.1	0.0	0.0	94.7
45	263	3.4	6.1	2.3	38.0	6.8	19.8	3.4	0.0	3.8	7.2	1.1	0.0	88.6
47.5	370	0.5	1.4	3.8	77.0	2.4	6.8	2.4	0.0	1.4	1.6	1.6	0.0	98.4
50	180	0.6	2.8	3.3	43.3	3.3	20.0	2.2	1.7	11.1	5.6	0.0	0.0	93.3
52.5	128	2.3	7.0	0.8	35.9	1.6	20.3	5.5	1.6	7.0	10.9	0.8	0.0	91.4
55	950	0.6	6.1	1.1	43.6	4.0	14.7	5.1	0.6	5.9	10.5	1.7	0.0	93.3
58.75	71	2.8	1.4	0.0	50.7	14.1	9.9	1.4	0.0	2.8	11.3	4.2	0.0	95.8
62.5	165	1.2	8.5	0.0	46.7	0.6	12.1	6.1	2.4	9.7	4.8	1.8	0.0	92.7
65	108	0.9	10.2	0.0	36.1	4.6	14.8	4.6	2.8	7.4	7.4	0.9	0.0	88.9
67.5	187	0.5	11.2	0.0	32.1	4.3	23.0	7.0	0.5	2.7	8.0	4.8	0.0	93.6
71.25	82	1.2	11.0	0.0	18.3	7.3	31.7	6.1	1.2	4.9	6.1	2.4	0.0	89.0
76.25	68	1.5	4.4	0.0	14.7	35.3	19.1	4.4	0.0	4.4	5.9	5.9	0.0	94.1
80	157	0.6	5.7	0.0	42.0	3.8	15.3	5.1	4.5	11.5	6.4	1.9	0.0	96.2
82.5	128	0	3.9	0.0	47.7	9.4	7.8	5.5	6.3	6.3	6.3	0.8	0.0	93.8
85	1033	1.7	10.2	0.0	52.3	3.4	0.8	6.4	1.5	10.2	4.5	1.0	0.1	90.2
87.5	1810	1.5	17.3	0.0	21.0	1.9	0.8	8.8	1.4	31.3	6.2	0.3	0.0	89.1
90	1805	1.3	13.6	0.0	46.9	0.9	0.2	7.1	0.9	18.8	3.5	0.5	0.0	92.4

Elphidium selseyense is the dominant species in the vast majority of the samples, accounting for 14.7 to 87.3 % of the total assemblage (Figure 6, Table 2). The levels 47.5, 37.5 and 22.5 cm present peak values for this taxon, whereas the assemblages of the top 12.5 cm are rather poor in *E. selseyense*.

The relative abundance of *Elphidium magellanicum* oscillates between 0 and 35.3 %. A major peak is present at 76.25 cm (35.3 %). This species shows relatively high percentages (9.4–26.7 %) in the low density samples of the topmost 17.5 cm.

Elphidium margaritaceum is nearly absent between 90 and 85 cm. Above these levels, relative abundances vary between 6.3 and 31.7 % with maxima around 70 cm depth, from 52.5 to 42.5 cm depth, and from 20 to 12.5 cm depth.

The relative proportions of *Haynesina germanica* fluctuate generally between 1 and 10 %. This species is very abundant (18.8 and 31.3 %) in the first two samples (90 cm and 87.5 cm depth), whereas it is present in very low numbers, or even absent, in the 20–5.5 cm interval. *Haynesina germanica* shows again an elevated percentage (25.9 %) in the most recent sample (2.5 cm depth).

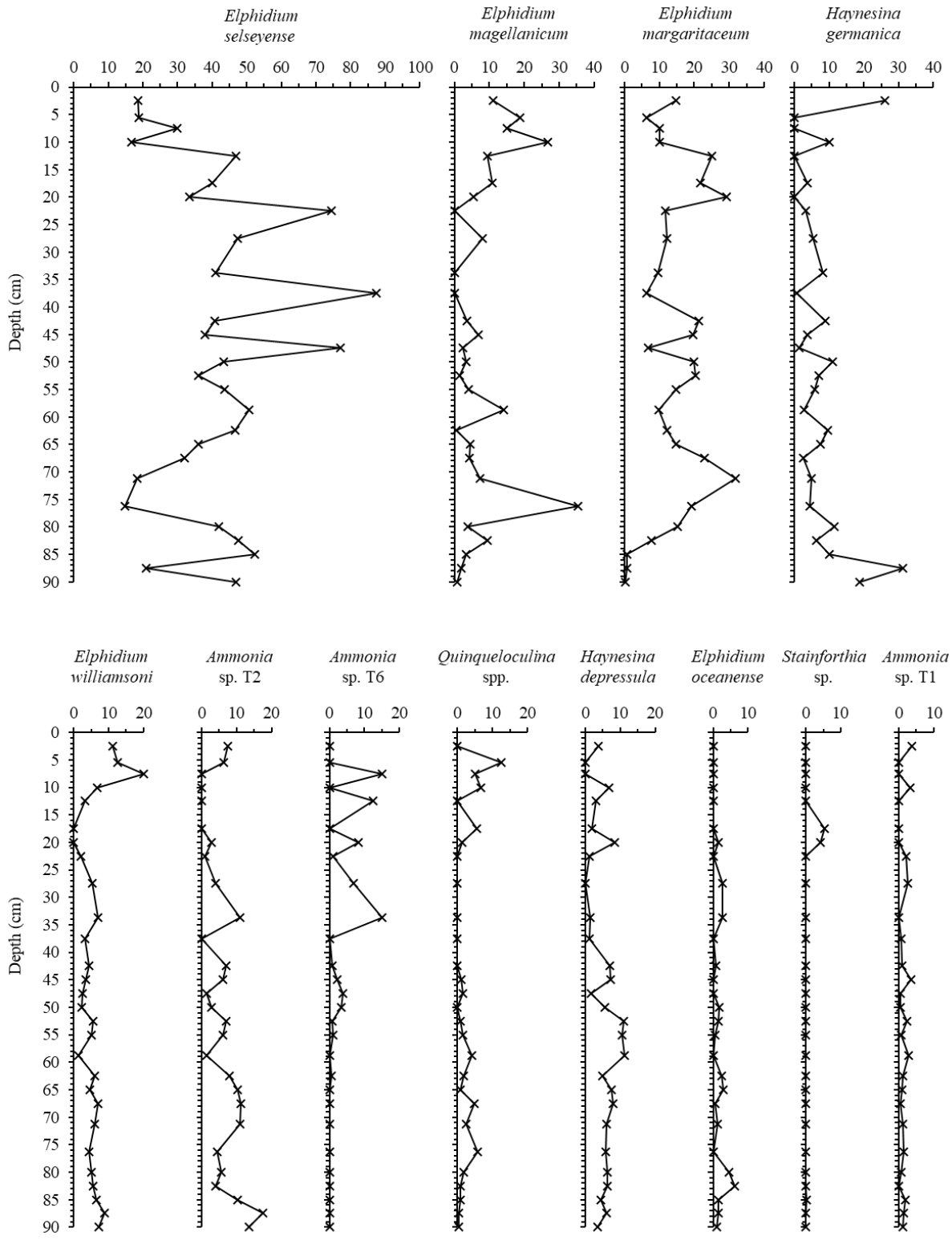

Figure 7. Relative abundances of the dominant species as a function of depth (cm). We also represented *Ammonia* sp. T1 (not considered as a dominant species), because we discuss this species later in the manuscript.

All other taxa only rarely occur with more than 10 % in the samples. *Elphidium williamsoni* shows maximum values (11.1–20 %) in the top 10 cm of the core, whereas *Elphidium oceanense* shows always low percentages (0–6.3 %), slightly decreasing upward. This taxon is

absent in the top 17.5 cm. *Ammonia* sp. T2 shows a general decrease from about 10.2–17.3 % at the bottom of the core to a near absence at about 20 cm depth. However, it shows higher percentages again (6.3–7.4 %) in the topmost two samples (5.5 and 2.5 cm depth). *Ammonia* sp. T6 is totally absent until 55 cm core depth, and fluctuates between absence and 15.1 % thereafter. *Ammonia* sp. T1 is always present in low percentages, never exceeding 4 %, without a clear pattern. *Quinqueloculina* spp. shows two main presence intervals, between 80 and 45 cm (up to 6 %) and from 20 to 5.5 cm depth (up to 12.5 %). *Haynesina depressula* (up to 11 %) tends to be more abundant in the lower 40 cm of the core. Finally, *Stainforthia* sp. is absent in most samples, but is present at 20 and 17.5 cm depth (with 4.2 and 5.5 %, respectively).

4.2. MULTIVARIATE ANALYSIS

The first two axes of our PCA based on non-standardised percentage data account for 61 % and 17 % of the total variability of the dataset, respectively (Table 3).

Table 3. Eigenvalues, explained variability (in %) and cumulative % of explained variability for the principal components of the PCA.

Principal component	Eigenvalue	Explained variability (%)	Cumulative % of variance
1	345.5	60.8	60.8
2	97.0	17.1	77.8
3	63.4	11.1	89.0
4	28.5	5.0	94.0
5	15.1	2.6	96.6
6	7.0	1.2	97.9
7	5.1	0.9	98.8
8	3.8	0.7	99.4
9	2.1	0.4	99.8
10	0.6	0.1	99.9
11	0.5	0.1	100.0

Table 4 presents the contributions of the dominant taxa to the first two PCs. *Elphidium selseyense* has a strong positive contribution to PC1, whereas *E. magellanicum* has a slight negative contribution to this axis. *Elphidium margaritaceum* and *E. magellanicum* have a positive contribution to PC2, whereas *Haynesina germanica* and *Ammonia* sp. T2 load negatively on this axis. Figure 8 presents a biplot for PC1 and PC2, in which we added the living assemblages of station 1 (same station as the long core) and of the nearby, shallower station 2 (water depth 23 m) which is less severely affected by seasonal hypoxia/anoxia (Richirt et al., 2020), as supplementary individuals.

Table 4. Taxa contributions to the first two PCs from the PCA. Values in bold are superior to the average contribution (|9.09|, if all species would contribute equally).

Species / PC contribution	PC 1	PC 2
Ammonia sp. T2	-0.6	-10.9
Ammonia sp. T6	0.0	1.6
Elphidium selseyense	87.5	0.4
Elphidium magellanicum	-7.3	10.4
Elphidium margaritaceum	-1.8	32.0
Elphidium williamsoni	-0.8	-1.8
Elphidium oceanense	0.0	-0.2
Haynesina germanica	-1.3	-41.8
Haynesina depressula	-0.2	0.0
Quinqueloculina sp.	-0.5	0.8
Stainforthia sp.	0.0	0.2

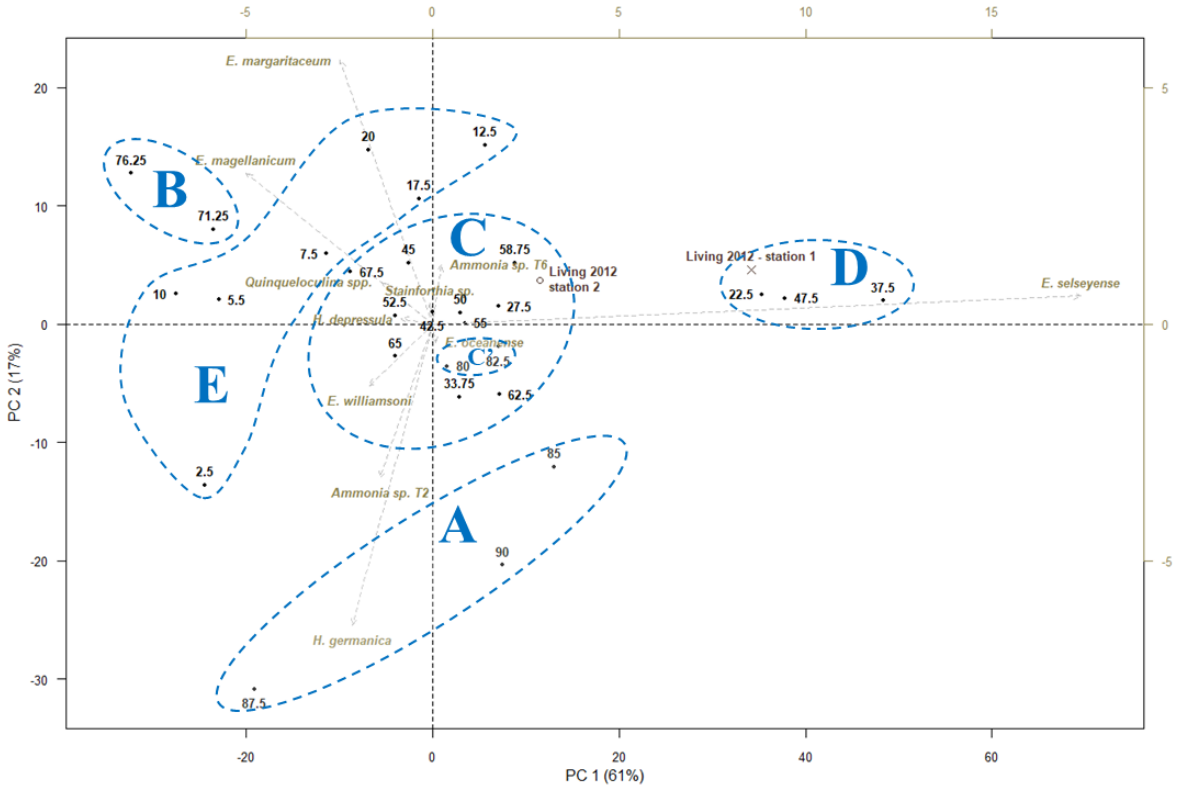

Figure 8. Biplot showing the taxa loadings and sample scores on the first two PCA axis. Core depth (cm) is indicated in black. Dominant taxa are represented by arrows. Supplementary individuals (living assemblages observed in 2012 from stations 1 and 2; Richirt et al., 2020) are indicated by a cross and a circle for station 1 and station 2, respectively. Blue dotted lines show the different, arbitrarily defined, groups of samples.

In figure 8, five groups of samples have been recognised arbitrarily on the basis of their position on the PCA biplot and their proximity in the core:

Group A is constituted of samples with high negative scores on PC2, reflecting high proportions of *Ammonia* sp. T2 and *H. germanica.* This concerns the samples from 90 to 85 cm core depth.

Group B contains samples with strongly negative scores on PC1 and positive scores on PC2, characterised by high relative abundances of *E. magellanicum* and *E. margaritaceum* and relatively low percentages of *E. selseyense*. This concerns samples from 76.25 and 71.25 cm depth. For both cases, this concerns merged samples, because the number of individuals in the separate samples was very low.

Group C is composed of samples with low scores on both PCs (i.e. centred on the biplot, figure 8), indicative of average faunas. These "typical" faunas are dominated by *E. selseyense*, have a high percentage of *E. margaritaceum*, a lower percentage of *Ammonia* sp. T2 and *H. germanica* (compared to group A), and contain *Ammonia* sp. T6 from 55 cm onward. This concerns most samples from 67.5 to 27.5 cm depth as well as the 82.5 and 80 cm depth samples (subgroup C'). The living faunas of station 2 (Den Osse Basin, 23 m water depth) plot together with this group.

Group D is composed of three samples with very high scores on PC1, reflecting uncommonly high percentages of *E. selseyense***.** This concerns samples from 22.5, 37.5 and 47.5 cm depth. The living assemblage of station 1 is very similar, as showed by its proximity on the biplot (figure 8).

Group E groups samples intermediate between groups B and C, mostly with negative scores on PC1, and positive scores on PC2. Assemblages in these samples are characterised by high relative abundances of *E. magellanicum* and *E. margaritaceum*, although lower than the samples of group B. Group E contains all samples between 20 and 2.5 cm core depth. The 2.5 cm layer is rather far away from the other samples of this group, which is due to its high percentage of *H. germanica* (Table 2). However, most samples in group E show a low absolute total abundance, so minor changes in the counts may lead to substantial changes in relative proportions.

5. DISCUSSION

5.1. TEMPORAL EVOLUTION OF THE FORAMINIFERAL COMMUNITY

Here we will focus on the temporal changes in foraminiferal densities and assemblage composition through time, and we will investigate whether it is possible to link the main faunal changes to the anthropogenic modifications of Lake Grevelingen during the last 50 years.

As explained before, our Principal Component Analysis allowed us to recognise five groups of samples, each representing different vertical intervals from the sediment core, and therefore, successive stages of the evolution of the Lake Grevelingen.

Group A includes samples from 90 to 85 cm depth (estimated period ~ 1968 to 1971). These samples contain a sandy sediment, and are situated immediately below the shift to a much finer sediment at 82.5 cm. These samples very probably represent the estuarine phase of the basin, before its seaward closure in 1971. The foraminiferal assemblages are characterised by a very high density (between 1000 and 2000 ind. in 14.1 cm^3), and by high percentages of typical estuarine/mudflat species such as *H. germanica* and *Ammonia* sp. T2 (e.g. Alve & Murray, 1994; 2001; Bouchet et al., 2007; Thibault de Chanvalon et al., 2015; Darling et al., 2016 ; Saad & Wade, 2016; 2017; Bird et al., 2020). In view of the location of station 1, in the middle of the Den Osse Basin at 34 m depth (the main former channel of the Grevelingen estuary), the sandy sediment reflects the strong hydrodynamics of this site, when it was still an estuary. Apparently, currents were too strong to allow deposits of clays and silts, so that the former channel floor was covered by a sandy lag deposit, with a very high foraminiferal density. The strong currents undoubtedly facilitated the transport of allochthonous foraminifera, such as the taxa cited above, which are typical of estuarine mudflats. However, *H. depressula*, a species typical of marine influence (Murray 1983; Darling et al., 2016) is present with substantial proportions as well, showing that foraminifera were not only transported from the inner to the outer estuary, but also from the more open sea into the outer estuary.

Subgroup C' of Group C includes the next two samples, at 82.5 and 80 cm depth (estimated period ~ 1972 to 1975). The sediment is mainly composed of clay/silt, confirming its deposition after the seaward closure of the basin, when hydrodynamics became much weaker. The strong drop of faunal density (from higher than 1000 to less than 100 ind. in 14.1 cm^3) shows that these samples no longer constitute a lag deposit, but rather that the foraminiferal populations are diluted by important supplies of fine-grained sediment (about 2 cm y^{-1}). The weaker hydrodynamics, together with the suppression of tides explain why the

foraminiferal assemblage is much less affected by transport, and probably represents an autochthonous community.

The faunas of these two samples show a strong increased percentage of the more marine taxa *E. margaritaceum* and *E. oceanense* (Darling et al., 2016), contrasting with a strong decrease of the percentages of the more estuarine species *H. germanica* and *Ammonia* sp. T2. This suggests that in the first years after the closure of the former estuary, the basin floor was still inhabited by species typical of marine influence (high salinity), whereas inner estuarine species where no longer living, or transported to the study area. Salinity, measured on surface waters, was consistently high (~ 30) in the years immediately following the closure of the basin (1972-1974, Bannink et al., 1984), allowing marine taxa to inhabit the former main channel.

Group B, which represents the 77.5 to 70 cm interval (estimated period ~ 1975–1980) contains only two merged samples (i.e. 76.25 and 71.25 cm). Their faunal composition is somewhat peculiar, because of the high relative proportions of *E. magellanicum* and *E. margaritaceum*, contrasting with the relatively low, but still substantial contribution of *E. selseyense*.

In this period, surface water salinity showed a progressive decrease, from ~ 30 in 1974 to a minimum of ~ 23 in 1978, due to the input of rain water (Bannink et al., 1984). In case these salinity values are also partly representative for the basin floor, this could suggest that *E. magellanicum* and *E. margaritaceum* are more tolerant to lower salinities than *E. selseyense*. Unfortunately, the ecology of these three species is still imperfectly known. In the literature, *E. magellanicum* is generally considered as a euryhaline species (20–30 in Fjords, Gustafsson & Nordberg, 1999; 2000; 10–20 in the western Baltic Sea, Schönfeld et al., 2018; shallow marine at Dunkirk beach, Lévy et al., 1969). *E. selseyense* appears to be opportunistic and tolerant to a large range of salinity (Darling et al., 2016). Conversely, *E. margaritaceum* has been reported as a more marine species which tolerates only slight salinity variations (Alve & Murray, 1999; Darling et al., 2016).

The transition to a lacustrine system also strongly increased the average water residence in the Lake, up to several years, compared to a few days when Grevelingen was an estuary. This strongly modified the ecosystem structure and functioning of Lake Grevelingen (Nienhuis, 1978; Saeijs & Stortelder, 1982). The strengthened water column stratification and the much longer residence times led to a progressive increase of nutrient concentrations between 1971 and 1978 (Bannink et al., 1984). The opening of the Brouwersdam in late autumn 1978, resulting in limited salt water inflow, induced a further strengthening of the salinity

stratification of the water column, which led to hypoxia/anoxia and mass mortality in the deepest parts of the basin in summer 1979 (Bannink et al., 1984).

The three *Elphidium* species that dominated the assemblages during this period apparently resisted better than other taxa to these rapidly changing conditions. Their tolerance regarding low oxygen conditions is shown by their presence in the recent faunas of this site (except for *E. margaritaceum*, Richirt et al., 2020), but also by their presence in fjord environments affected by seasonal anoxia (for *E. magellanicum*; Gustafsson & Nordberg, 1999; 2000).

The remaining samples of **Group C** represent the 67.5 to 27.5 cm interval (estimated period ~ 1980 to 2000). In order to remedy the increase of eutrophication phenomena observed in the 1970s, the basin was partly reopened by an underground sluice in 1978. This sluice was initially opened only in winter. Consequently, surface water salinity almost immediately rose to ~ 30 and nutrient concentrations showed a major decrease (Bannink et al., 1984). However, this did not solve the problem of bottom water oxygen deficiency, and in the next 20 years, an intermittent succession of major later summer/early autumn hypoxic/anoxic periods was observed, especially in the deepest parts of Lake Grevelingen (as shown by bottom water data, Figure 3). This is confirmed by the results of Lindeboom & Sandee (1984), who found anoxic conditions coupled with the presence of sulphide at a few mm depth in the sediment in May, June and December 1982, at much shallower stations, with depths < 10 m. In 1999, the sluice was opened year-round, in order to further increase water exchanges.

During this period (~ 1980 to 2000), the total faunal density showed strong variations, between ~ 70 and 950 individuals per 14.1 cm^3. This succession of richer and poorer faunas could be due to differences between successive years regarding bottom water oxygen content (Figure 3; Seitaj et al., 2015; 2017), more specifically due to inter-annual variability in the intensity and duration of the summer hypoxia/anoxia (with or without sulphide in the topmost sediment). Richirt et al. (2020) showed that in case of prolonged summer anoxia combined with the presence of sulphides in the topmost sediment, the foraminiferal community almost completely disappears, and the site is recolonised the following winter, leading to low standing stocks the next spring. The strong Mo peak at ~ 32 cm (estimated age ~ 1998, Figure 9), could indicate particularly severe euxinic conditions in the sediment (anoxia with presence of sulphides). This could explain why we observe a very low foraminiferal density (16 ind. per 14.1 cm^3) at ~ 35 cm, immediately after this period. This apparent depth shift of ~ 3 cm between these two events could be explained by the fact that Mo concentrations and foraminiferal densities were measured on two different cores (see Materials & Methods section). Conversely, layers with high foraminiferal densities (such as sample at 55 cm, estimated age ~ 1986) could

correspond to periods following weaker and/or shorter anoxic events, eventually without sulphides in the foraminiferal habitat.

Alternatively, as we look at 0.5 cm thick layers in a context where the average sediment accumulation rate is about 2 cm y^{-1}, individual layers may represent a single season, and not a complete year. Consequently, samples with high foraminiferal densities could be deposited during spring/early summer seasons, whereas samples with low foraminiferal densities could be representative of the late summer/ autumn/winter seasons.

All samples of group C are strongly dominated by *E. selseyense*, with *E. margaritaceum* being the second most important species. This seems to reflect increased salinity (more marine influence) and development of seasonal hypoxia (favouring opportunistic species such as *E. selseyense*). The arrival of *Ammonia* sp. T6, at about 55 cm core depth (~ 1986) corresponds to a progressive decrease of *H. depressula*, *Quinqueloculina* spp. and *Ammonia* sp. T2. It is interesting to note that the assemblage of group C is comparable to the composition of the living assemblage at the shallower station 2 (depth 23 m), as shown by the PCA biplot (figure 8), suggesting that the environmental conditions may have been comparable, with a rather short anoxic event in summer (maximum of 1 month, Richirt et al. 2020).

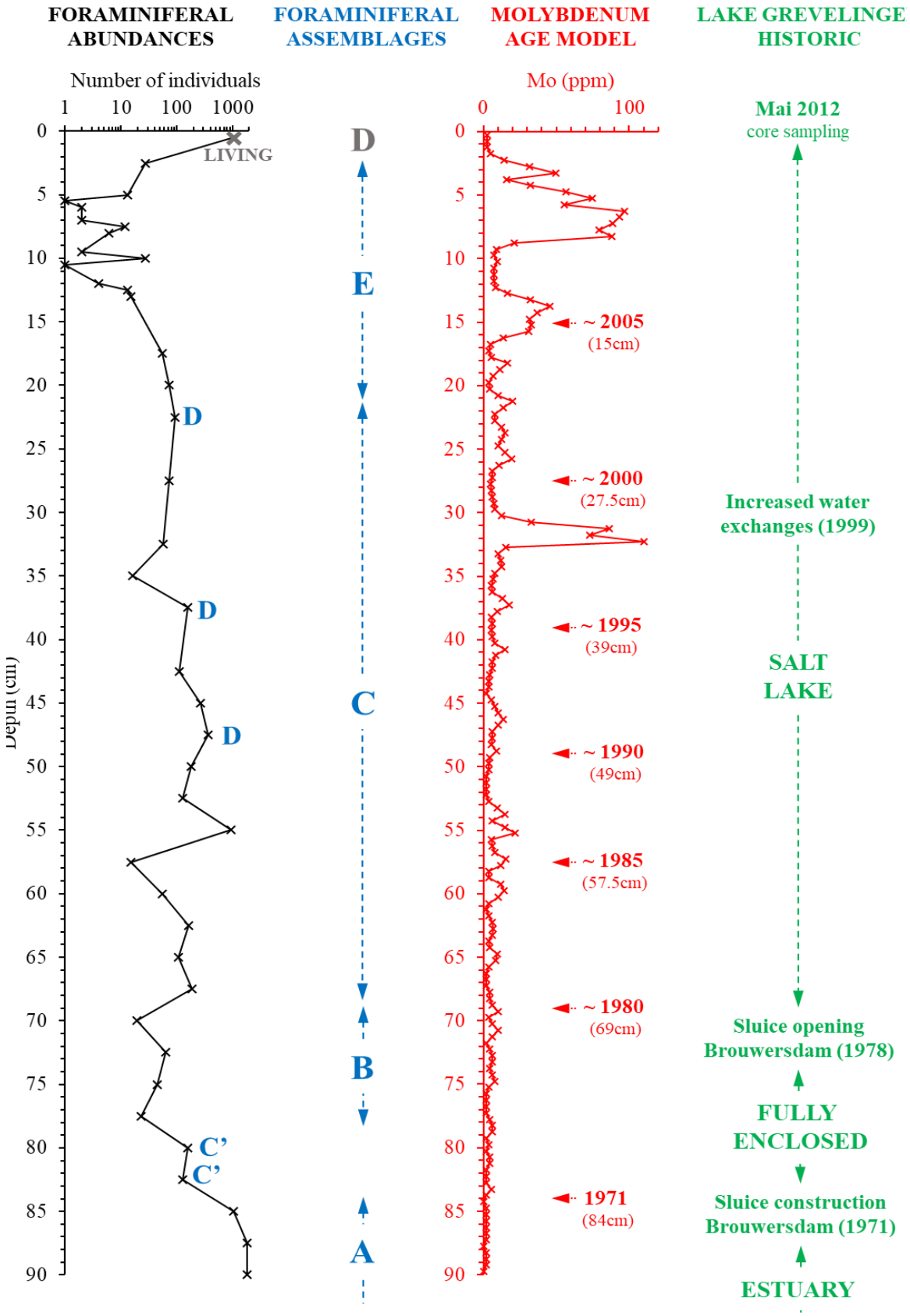

Figure 9. Timeline of the human-induced modifications following the Delta Plan at Lake Grevelingen. The sediment core used to investigate dead foraminiferal assemblage density record (black curve, excluding the top layer 0.5 cm showing living assemblage in grey) and the Mo record (red curve). Both long cores were sampled in Mai 2012. Blue letters emphasize the different groups of layers highlighted in the PCA biplot.

Group D contains only three samples, from 47.5, 37.5 and 22.5 cm core depth (deposited in ~ 1991, ~ 1996 and ~ 2003, respectively). The foraminiferal densities in these samples are comparable to densities from group C and range from 94 to 370 ind. per 14.1 cm^3. The faunal composition of these samples stands out by exceptionally high proportions of *E. selseyense* (> ~ 75 %). The composition of these assemblages is very close to the composition of the living assemblage in 2012 at the same station (Richirt et al., 2020), as shown by their proximity on the PCA biplot. This suggests that the three samples of group D reflect similar conditions, which could be characterised by a rather severe anoxic conditions with the presence of sulphides in the topmost sediment, as recorded in 2012 (Seitaj et al., 2015). It appears that *E. selseyense* could be particularly tolerant to such low oxygen conditions, as it is confirmed by its strong dominance of the living faunas sampled at this site in 2012 (Richirt et al., 2020).

Finally, **Group E** comprises all samples in the top 20 cm of the core (estimated period ~ 2003 to 2011). This group of samples has been deposited in the years after the decision had been taken to open the seaward sluice year-round (in 1999), leading to a further decrease in water residence times. The total foraminiferal densities are extremely low in this interval (rarely exceeding 15 ind. per 14.1 cm^3). Because of the low foraminiferal densities, several samples had to be merged. In spite of that, relative proportions are still based on low numbers (from 16 to 72 specimens), and should be considered with caution. Even when taking in account the high sedimentation accumulation rate at this location, the unexpected very low faunal densities strongly contrast with the elevated densities of living faunas, which attained a maximum of 634 individuals per 14.1 cm^3 in May 2012 (recalculated from Richirt et al., 2020), when the long core was sampled.

The faunal assemblages of the samples from this group are relatively poor in *E. selseyense*, whereas the percentages of *E. margaritaceum*, *E. magellanicum* and *E. williamsoni* show a strong increase. *Quinqueloculina* spp. is also somewhat more frequent (Table 2). It is surprising that the faunal composition of the group E samples is very different from the year-averaged living fauna from this site (Figure 8).

In view of the important discrepancies between the rich living faunas and poor taphocoenoses, with a very different species composition, we suspect that the dead assemblages have suffered from important taphonomic losses during early diagenesis, specifically due to carbonate dissolution. In fact, in the deepest parts of Lake Grevelingen, two antagonistic bacterial populations occur: cable bacteria develop mainly between January and May, whereas *Beggiatoceae* mats occupy the sea floor from September to December (Seitaj et al., 2015). The reasons why these two filamentous S-oxydizing bacteria show such an antagonistic seasonal

succession is not well understood yet (Seitaj et al. 2015), but it is clear that they largely affect the geochemistry of the topmost sediment layer.

5.2. CABLE BACTERIA ACTIVITY RESPONSIBLE OF FORAMINIFERAL TEST DISSOLUTION

Cable bacteria activity promotes carbonate precipitation in the oxic zone (maximum OPD about 2 mm at this site, even in winter, see Seitaj et al., 2015), and carbonate dissolution immediately below, where oxygen is absent (Risgaard-Petersen et al., 2012; Meysman et al., 2015). Consequently, the carbonate saturation state (ΩCa) is low in the first centimetres of the sediment (ΩCa < 1 at least down to 2 cm, see Table 5), which could result in the partial or complete dissolution of calcareous dead foraminiferal tests. In fact, for 2012, calculated ΩCa are < 1 from January (excluding in the top 0.5 cm) to April, when cable bacteria were active, indicating strongly increased calcium carbonate ($CaCO_3$) dissolution (Table 5). This is corroborated by a release of Ca^{2+} measured in the first centimetres in pore waters at the same station in January and March (Sulu-Gambari et al. 2016).

Table 5. Values of calcium carbonate saturation state at station 1 at different depths in the sediment for each month. Red: ΩCa < 1, indicating increased carbonate dissolution. Blue: ΩCa > 1, indicating no carbonate dissolution.

Depth (cm)	January	February	March	April	May	June	July	August	September	October	November	December
0.25	2.30	NA	NA	0.91	NA	1.93	3.08	NA	1.86	NA	2.81	3.06
0.75	0.54	0.90	0.68	0.70	NA	2.39	2.67	NA	2.30	7.46	9.62	14.68
1.25	0.29	0.41	NA	0.55	NA	2.41	2.87	NA	2.90	NA	14.76	22.66
1.75	0.20	0.27	0.24	0.51	NA	2.13	2.87	NA	NA	4.60	NA	21.11
2.25	NA	0.22	0.23	0.67	NA	1.99	2.75	NA	3.95	5.03	5.90	13.49
2.75	NA	0.21	NA	0.61	NA	2.40	2.78	NA	NA	NA	NA	7.75
3.25	NA	NA	NA	NA	NA	NA	NA	NA	NA	NA	4.29	6.98
3.75	NA	NA	NA	NA	NA	NA	NA	NA	NA	NA	4.68	NA

Living foraminifera have mechanisms to deal with lower carbonate saturation state (e.g. active control of their internal and external pH during the calcification process, intracellular storage of Ca^{2+} ions, Toyofuku et al., 2008; de Nooijer et al., 2009; Toyofuku et al., 2017). They often dwell in environments with a lower carbonate saturation state, and living specimens only rarely show serious signs of test dissolution there (e.g. Charrieau et al., 2018). However, the discrepancy between the dense living faunas, which are apparently not much affected by carbonate dissolution, and the low density dead faunas is probably explained by the fact that

the living specimens predominantly live in the thin oxic zone, which is not affected by the strongly decreased ΩCa (Seitaj et al. 2015). Only when the dead foraminiferal tests passively cross this low ΩCa zone (after the death of the individuals, due to sediment deposition at the sediment water interface), the assemblages are affected by important losses due to carbonate dissolution. The very low faunal densities in the top 20 cm of the core suggest that this situation has existed since about 2003, some years after the intensification of water exchanges. In the cartoon presented in Figure 10, the seasonal succession of events is schematised.

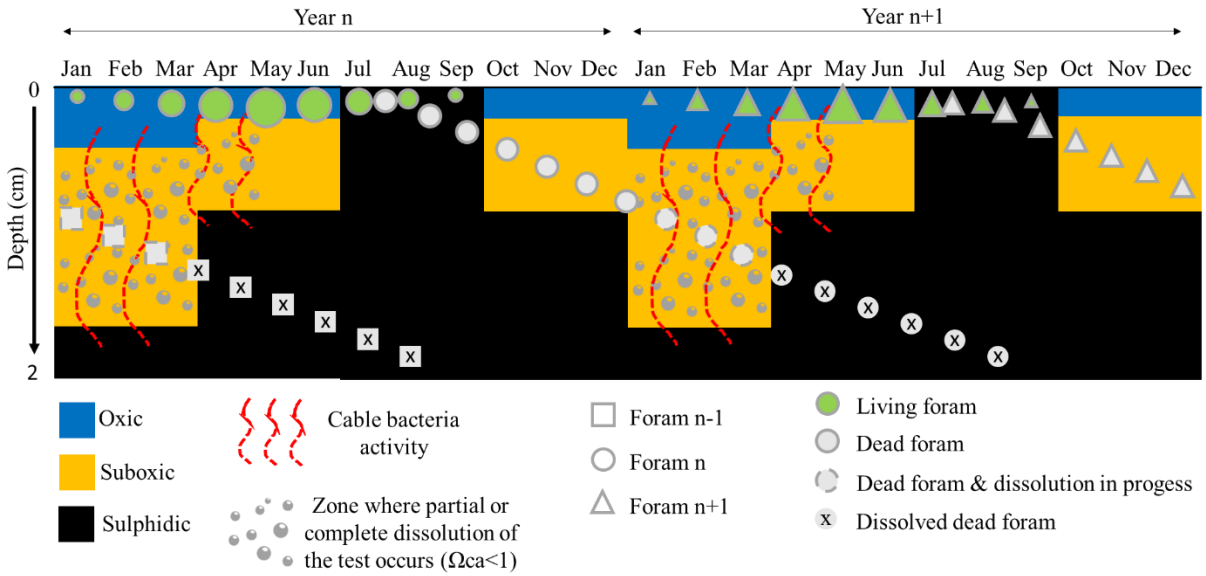

Figure 10. Conceptual scheme showing two consecutive years to explain the low density of dead faunas (in grey) in the first 20 cm of the core. The seasonal succession of oxic (blue), suboxic (orange) and sulphidic (black) zones and presence of cable bacteria (red dotted curves) are from Seitaj et al. (2015). Presence and densities (size of the signs) of living foraminifera (in green) are from Richirt et al. (2020). Squares, circles and triangles represent the yearly successive foraminifera generations.

If our hypothesis that the low density foraminiferal faunas in the top 20 cm is due to dissolution resulting from cable bacteria activity is true, this would mean that the cable bacteria activity in the Den Osse Basin started, or substantially increased between 2000 and 2005. This fits remarkably well with the year-round opening of the Brouwersdam sluice in 1999.

The increased inflow of saline, warm and well oxygenated water induced by the opening of the Brouwersdam sluice in 1999 should have improved the oxygenation and led to a reduction of the duration of anoxia events in the bottom waters compared to the situation before 1999 (Fig. 3; Wetsteijn, 2011; Sulu-Gambari et al., 2017). However, the increased concentration and large peaks in the Mo record in the last ~ 30 cm of the core suggest the presence of increased quantities of sulphides in the pore waters during the same period. Sulu-Gambari et al. (2017) explained this contradiction (better oxygenation of bottom waters but development of sulphidic conditions in sediment) by the introduction of large amounts of algae

(mainly *Phaeocystis globosa*) into Lake Grevelingen from the North Sea (Hagens et al. 2015) since ~ 2000. The intensified remineralisation of organic matter induced by this extra input of dead algal material enhanced the sulphato-reduction rate and finally resulted in an increase of sulphide concentration in the pore waters. This process culminated in the exceptionally long hypoxia/anoxia in 2011 and 2012, compared to the period 1999–2010 (Sulu-Gambari et al. 2017).

The supposed increased cable bacteria activity resulting from the increased water flow in 1999 is corroborated by the fact that the presence of an oxygen-sulphide interface is a prerequisite for the development of S-oxidising bacteria, such as cable bacteria and *Beggiatocea* (Jørgensen, 1982).

5.3. TEMPORAL SUCCESSION OF *AMMONIA* PHYLOTYPES

It has already been suggested that *Ammonia* sp. T6 could be an exotic and/or invasive species introduced in the eastern Atlantic Ocean by anthropogenic activities, and originating from east Asia (Pawlowski & Holzmann, 2008; Schweizer et al, 2011; Bird et al., 2020). Concerning the other two representatives of the *Ammonia* phylotype observed in our sediment core, *Ammonia* sp. T1 is considered cosmopolitan (Holzmann & Pawlowski, 2000) whereas *Ammonia* sp. T2 seems to be restricted to the north Atlantic (Hayward et al., 2004). The latter two species are both assumed autochthonous in Europe, and could at present be progressively replaced by the supposedly exotic phylotype *Ammonia* sp. T6 (Pawlowski & Holzmann, 2008; Schweizer et al. 2011; Richirt et al, in prep.). The historical record from the Den Osse Basin presented here shows the arrival of *Ammonia* sp. T6 at 55 cm core depth (estimated year ~ 1986), and its subsequent progressive replacement of *Ammonia* sp. T2 (Figure 11).

This species replacement suggests that phylotype T6 is more resistant than phylotype T2 to the environmental conditions found in Lake Grevelingen after the closure in 1971, especially to the seasonal hypoxia/anoxia. This hypothesis is corroborated by the much higher test porosity measured in *Ammonia* sp. T6 compared to *Ammonia* sp. T2 (22.45 ± 3.85 % versus 12.18 ± 3.8 %, respectively, Richirt et al. 2019a), suggesting that this phylotype could resist to oxygen deficiency by increasing its gas exchanges with the outer environment. The fact that *Ammonia* sp. T6 is rather poorly represented (about 5 % of the total assemblage) in the living assemblages in 2012 was explained by a phase offset between: 1) the time of repopulation of the site in winter 2011–2012 after its decimation due to euxinic conditions in summer 2011, and 2) the availability of its preferred food sources, in spring 2012 (Richirt et al. 2020).

Alternatively, the rather poor density of *Ammonia* sp. T6 could also mean that this taxon tolerates hypoxia and short phases of anoxia, but is not able to withstand prolonged periods of oxygen depletion or absence, together with a presence of sulphides in its microhabitat. This could explain the much higher percentage of this taxon in the living faunas of station 2 (shallower station in Den Osse Basin), where the duration of seasonal hypoxia/anoxia is shorter than at station 1 (Richirt et al. 2020).

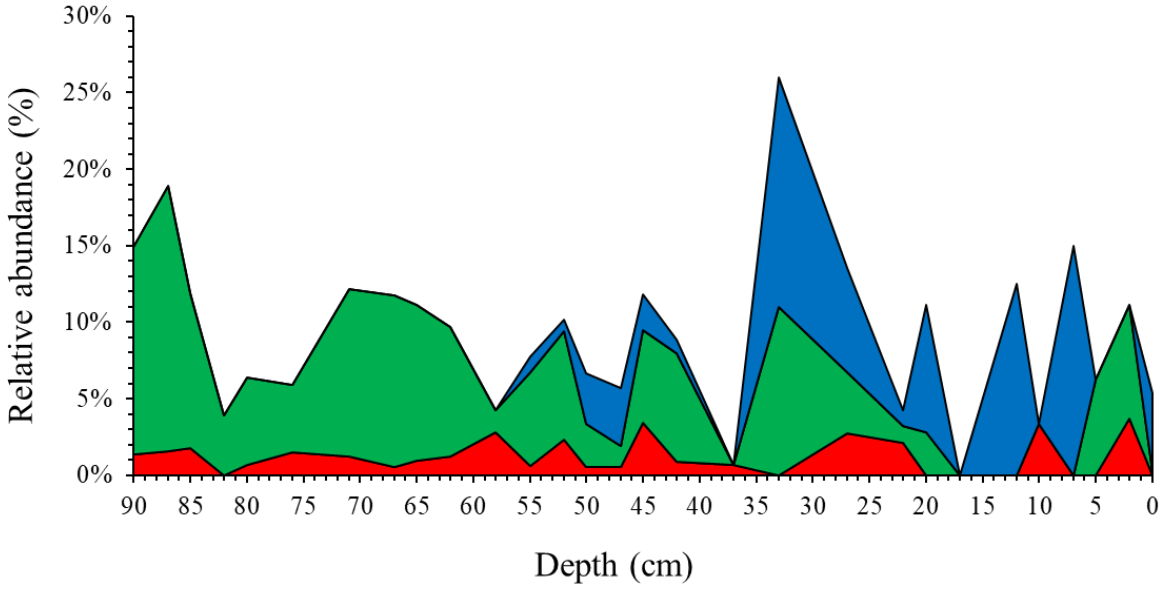

Figure 11. Relative abundances (in % of the total assemblage) of the three different *Ammonia* phylotypes T1 (red), T2 (green) and T6 (blue) as a function of depth (cm).

Finally, phylotype T6 is virtually the only *Ammonia* phylotype found in recent assemblages (~ 5.2 % of the 1044 individuals, total fauna, Richirt et al., 2020). In view of the strong anoxic events with co-occurring sulphidic conditions in 2011 and 2012 at this site (Seitaj et al. 2015; Richirt et al. 2020), this underlines the higher resistance of phylotype T6, compared to phylotypes T1 and T2, to such adverse conditions.

Today, phylotype T6 is found in all (closed or open) branches of the Rhine-Meuse-Scheldt estuary (Jorissen, unpublished data). In this context, we can consider the question of what represents the arrival of *Ammonia* sp. T6 in Lake Grevelingen (i.e. Den Osse Basin), around 1986 observed here. In our opinion, two alternative hypotheses can be envisaged:

1) *Ammonia* sp. T6 is indeed an exotic species, and its arrival in Lake Grevelingen was synchronous with its arrival on the eastern Atlantic coasts.
2) *Ammonia* sp. T6 was already present in the North Sea, either as an autochthonous species, or after a first anthropogenic introduction from eastern Asia, and its arrival in Lake Grevelingen reflects a secondary, local migration event.

In this context, it is important to notice that *Ammonia* sp. T6 was not observed in the faunas of the lower part of the core (90–85 cm) when Grevelingen was open to the North Sea. This strongly suggests that this phylotype reached this part of the eastern Atlantic facade between the closure of the Lake in 1971 and the arrival of this phylotype in the basin circa 1986. This would rather argue in favour of its exotic nature, as suggested by Pawlowski & Holzmann (2008), who hypothesized an introduction of *Ammonia* sp. T6 in North Sea in the early 19th century by means of ship ballast water. Massive importations of Japanese oysters, from 1964 to about 1980 could also represent a possible vector for *Ammonia* sp. T6, as this has been the case for a large number of different groups of organisms (e.g. Polychaeta, Amphipoda, Tunicata, Cirripedia, etc., Wolff & Reise, 2002).

Unfortunately, this study does not allow us to definitely settle whether *Ammonia* sp. T6 is an exotic and/or invasive species in Europe. Even today, *Ammonia* sp. T6 is not present in all estuaries of the mid latitude East Atlantic coast. For instance, it is absent in the French Vie and Auray estuaries (Fouet et al., in prep.). Therefore, the absence of *Ammonia* sp. T6 in the Grevelingen estuary before its closure in 1971 could also be due to the fact that this species was not present in this particular estuary. Finally, the transformation of the Grevelingen estuary to a brackish water lake with occurrence of seasonal anoxia may have facilitated the colonisation of the Den Osse Basin by *Ammonia* sp. T6, putatively more resistant to hypoxia/anoxia than its congeneric phylotypes.

6. CONCLUSION

Our investigation of the sediment record of one of the deepest basins in Lake Grevelingen highlights the important changes undergone by the foraminiferal community over the last 50 years. These changes reflect the major anthropogenic modifications of Lake Grevelingen, which was artificially turned from an estuary into a salt lake during this period. The Mo concentrations in the sediment record is supposed to mark the yearly late summer–early autumn anoxic events with co-occurring presence of free sulphides in the pore water of the sediment. This record provides a very useful tool to detail the more conventional age model based on ^{210}Pb, allowing us to obtain a higher precision of about ± 3 years.

The seaward closure of the basin in 1971 induced an important change of the foraminiferal faunas, from high proportions of *H. germanica* and *Ammonia* sp. T2, typical estuarine mudflat species, to faunas dominated by *E. margaritaceum*, typical for marine influence, *E. oceanense*, considered as an opportunistic species, and *E. magellanicum*, which seems to be tolerant to

oxygen depletion. This faunal change could be explained by the disappearance of tides, much weaker hydrodynamics, increased eutrophication phenomena and increased salinity immediately after the closure of the basin. The opening of the seaward sluice (in the Brouwersdam) in autumn 1978, to counterbalance eutrophication phenomena, increased water renewal, but did not solve the problem of seasonally occurring hypoxia/anoxia. At first, the sluice was opened only in winter and *E. selseyense* strongly dominated the foraminiferal assemblages. Around 1986, the emergence of *Ammonia* sp. T6 was observed coupled with a progressive diminution of the proportion of *Ammonia* sp. T2, *H. depressula* and *Quinqueloculina* spp. in the assemblages. After the sluice was opened almost year-round in 1999, further reducing water residence time by doubling exchanges with the North Sea, the foraminiferal assemblages became very poor, so that the assemblage composition should be interpreted very carefully. The extreme scarcity of foraminiferal tests in the top 17.5 cm of the core, which strongly contrasts with the high abundance of living foraminiferal community, is ascribed to post-mortem dissolution, resulting from the strongly diminished carbonate saturation state due to cable bacteria activity in the anoxic part of the sediment.

Our results indicate that *Ammonia* sp. T6 arrived in Lake Grevelingen around 1986 and has progressively supplanted other *Ammonia* phylotypes (T1 and especially T2) in the record. We hypothesize that this progressive takeover is the result of its better tolerance to hypoxia/anoxia events. However, our results do not allow us to definitely validate the exotic and/or invasive nature of *Ammonia* sp. T6. In fact, the absence of this taxon in the lower part of the core could either indicate that it was absent on the Dutch coast in 1971 or that it was already present at other sites, and that the important human-induced transformation of Lake Grevelingen created the environmental conditions favourable for its settlement.

ACKNOWLEDGMENTS

We acknowledge the support of P. van Rijswijk, M. Hagens, A. Tramper, and the crew of the R/V Luctor (P. Coomans and M. Kristalijn) during the sampling campaigns. We want to thanks Philip Meysman for providing datasets for pH values for carbonate saturation state calculation. This study profited from funding of Rijkswaterstaat and of the CNRS program CYBER-LEFE (project AMTEP).

REFERENCES

Alve, E., Murray, J.W., 2001. Temporal variability in vertical distributions of live (stained) intertidal foraminifera, southern England. Journal of Foraminiferal Research 31, 12–24. https://doi.org/10.2113/0310012

Alve, E., Murray, J.W., 1999. Marginal marine environments of the Skagerrak and Kattegat: a baseline study of living (stained) benthic foraminiferal ecology. Palaeogeography, Palaeoclimatology, Palaeoecology 146, 171–193. https://doi.org/10.1016/S0031-0182(98)00131-X

Alve, E., Murray, J.W., 1994. Ecology and taphonomy of benthic foraminifera in a temperate mesotidal inlet. Journal of Foraminiferal Research 24, 18–27. https://doi.org/10.2113/gsjfr.24.1.18

Bannink, B.A., Van der Meulen, J.H.M., Nienhuis, P.H., 1984. Lake grevelingen: From an estuary to a saline lake. An introduction. Netherlands Journal of Sea Research 18, 179–190. https://doi.org/10.1016/0077-7579(84)90001-2

Bird, C., Schweizer, M., Roberts, A., Austin, W.E.N., Knudsen, K.L., Evans, K.M., Filipsson, H.L., Sayer, M.D.J., Geslin, E., Darling, K.F., 2020. The genetic diversity, morphology, biogeography, and taxonomic designations of *Ammonia* (Foraminifera) in the Northeast Atlantic. Marine Micropaleontology 155, 101726. https://doi.org/10.1016/j.marmicro.2019.02.001

Bouchet, V.M.P., Debenay, J.-P., Sauriau, P.-G., Radford-Knoery, J., Soletchnik, P., 2007. Effects of short-term environmental disturbances on living benthic foraminifera during the Pacific oyster summer mortality in the Marennes-Oléron Bay (France). Marine Environmental Research 64, 358–383. https://doi.org/10.1016/j.marenvres.2007.02.007

Charrieau, L.M., Filipsson, H.L., Nagai, Y., Kawada, S., Ljung, K., Kritzberg, E., Toyofuku, T., 2018. Decalcification and survival of benthic foraminifera under the combined impacts of varying pH and salinity. Marine Environmental Research 138, 36–45. https://doi.org/10.1016/j.marenvres.2018.03.015

Crusius, J., Calvert, S., Pedersen, T., Sage, D., 1996. Rhenium and molybdenum enrichments in sediments as indicators of oxic, suboxic and sulfidic conditions of deposition. Earth and Planetary Science Letters 145, 65–78. https://doi.org/10.1016/S0012-821X(96)00204-X

Darling, K.F., Schweizer, M., Knudsen, K.L., Evans, K.M., Bird, C., Roberts, A., Filipsson, H.L., Kim, J.-H., Gudmundsson, G., Wade, C.M., Sayer, M.D.J., Austin, W.E.N., 2016. The genetic diversity, phylogeography and morphology of Elphidiidae (Foraminifera) in the Northeast Atlantic. Marine Micropaleontology 129, 1–23. https://doi.org/10.1016/j.marmicro.2016.09.001

de Nooijer, L.J., Toyofuku, T., Kitazato, H., 2009. Foraminifera promote calcification by elevating their intracellular pH. PNAS, 106, 15374–15378. https://doi.org/10.1073/pnas.0904306106

Dickson, A.G., 1990. Standard potential of the reaction: $AgCl(s) + ½H_2(g) = Ag(s) + HCl(aq)$, and and the standard acidity constant of the ion HSO_4^- in synthetic sea water from 273.15 to 318.15 K. The Journal of Chemical Thermodynamics 22, 113–127. https://doi.org/10.1016/0021-9614(90)90074-Z

Donders, T.H., Guasti, E., Bunnik, F.P.M., van Aken, H., 2012. Impact van de Brouwersdam op zuurstofcondities in de Grevelingen; reconstructies uit natuurlijke sediment archieven. TNO-rapport, TNO-060-UT-2011-02116. Geological Survey of the Netherlands.

Egger, M., Lenstra, W., Jong, D., Meysman, F.J.R., Sapart, C.J., Veen, C. van der, Röckmann, T., Gonzalez, S., Slomp, C.P., 2016. Rapid Sediment Accumulation Results in High Methane Effluxes from Coastal Sediments. PLOS ONE 11, e0161609. https://doi.org/10.1371/journal.pone.0161609

Gustafsson, M., Nordberg, K., 2000. Living (Stained) Benthic Foraminifera and their Response to the Seasonal Hydrographic Cycle, Periodic Hypoxia and to Primary Production in Havstens Fjord on the Swedish West Coast. Estuarine, Coastal and Shelf Science 51, 743–761. https://doi.org/10.1006/ecss.2000.0695

Gustafsson, M., Nordberg, K., 1999. Benthic foraminifera and their response to hydrography, periodic hypoxic conditions and primary production in the Koljö fjord on the Swedish west coast. Journal of Sea Research 41, 163–178. https://doi.org/10.1016/S1385-1101(99)00002-7

Hagens, M., Slomp, C.P., Meysman, F.J.R., Seitaj, D., Harlay, J., Borges, A.V., Middelburg, J.J., 2015. Biogeochemical processes and buffering capacity concurrently affect acidification in a seasonally

hypoxic coastal marine basin. Biogeosciences 12, 1561–1583. https://doi.org/10.5194/bg-12-1561-2015

Hayward, B.W., Holzmann, M., Grenfell, H.R., Pawlowski, J., Triggs, C.M., 2004. Morphological distinction of molecular types in *Ammonia* – towards a taxonomic revision of the world's most commonly misidentified foraminifera. Marine Micropaleontology 50, 237–271. https://doi.org/10.1016/S0377-8398(03)00074-4

Holzmann, M., Pawlowski, J., 2000. Taxonomic relationships in the genus *Ammonia* (Foraminifera) based on ribosomal DNA sequences. Journal of Micropalaeontology 19, 85–95. https://doi.org/10.1144/jm.19.1.85

Jørgensen, B.B., Postgate, J.R., Postgate, J.R., Kelly, D.P., 1982. Ecology of the bacteria of the sulphur cycle with special reference to anoxic—oxic interface environments. Philosophical Transactions of the Royal Society of London. B, Biological Sciences 298, 543–561. https://doi.org/10.1098/rstb.1982.0096

Katz, M.E., Cramer, B.S., Franzese, A., Hönisch, B., Miller, K.G., Rosenthal, Y., Wright, J.D., 2010. Traditional and emerging geochemical proxies in foraminifera. Journal of Foraminiferal Research 40, 165–192. https://doi.org/10.2113/gsjfr.40.2.165

Lévy, A., Mathieu, R., Momeni, I., Poignant, A., Rosset-Moulinier, M., Rouvillois, A., Ubaldo, M., 1969. Les représentants de la famille des Elphidiidae (foraminifères) dans les sables des plages des environs de Dunkerque. Remarques sur les espèces de *Polystomella* signalées par O. Terquem, Revue de Micropaléontologie 2, 92–98.

Lewis, E., Wallace, D.W., 1998. R: Program developed for CO2 system calculations ORNL/CDIAC-105. Carbon Dioxide Information Analysis Centre, Oak Ridge National Laboratory.

Lindeboom, H.J., Sandee, A.J.J., 1984. The Effect of Coastal Engineering Projects on Microgradients and Mineralization Reactions in Sediments. Water Science and Technology 16, 87–94. https://doi.org/10.2166/wst.1984.0046

Louters, T., Berg, J.H. van den, Mulder, J.P.M., 1998. Geomorphological Changes of the Oosterschelde Tidal System During and After the Implementation of the Delta Project. Journal of Coastal Research 14, 1134–1151.

Lueker, T.J., Dickson, A.G., Keeling, C.D., 2000. Ocean pCO_2 calculated from dissolved inorganic carbon, alkalinity, and equations for K_1 and K_2: validation based on laboratory measurements of CO_2 in gas and seawater at equilibrium. Marine Chemistry 70, 105–119. https://doi.org/10.1016/S0304-4203(00)00022-0

Meysman, F.J.R., Risgaard-Petersen, N., Malkin, S.Y., Nielsen, L.P., 2015. The geochemical fingerprint of microbial long-distance electron transport in the seafloor. Geochimica et Cosmochimica Acta 152, 122–142. https://doi.org/10.1016/j.gca.2014.12.014

Muelen, J.H.M. v d, Leentvaar, J., Rooy, N.M. de, 1984. Environmental impact statement on the problem of a fresh or salt lake Grevelingen. Water science and technology 16, 107–120.

Murray, J.W., 2006. Ecology and Applications of Benthic Foraminifera. Cambridge University Press, 426 p.

Murray, J.W., 1983. Population dynamics of benthic foraminifera; results from the Exe Estuary, England. Journal of Foraminiferal Research 13, 1–12. https://doi.org/10.2113/gsjfr.13.1.1

Nienhuis, P.H., 1978. Lake grevelingen: A case study of ecosystem changes in a closed estuary. Hydrobiological Bulletin 12, 246–259. https://doi.org/10.1007/BF02259186

Nienhuis, P.H., Veld, J.C.H. in 't, 1984. Grevelingen: From an Estuary to a Saline Lake. Water Science and Technology 16, 27–50. https://doi.org/10.2166/wst.1984.0043

Orr, J.C., Epitalon, J.-M., Gattuso, J.-P., 2015. Comparison of ten packages that compute ocean carbonate chemistry. Biogeosciences 12, 1483–1510. https://doi.org/10.5194/bg-12-1483-2015

Pawlowski, J., Holzmann, M., 2008. Diversity and geographic distribution of benthic foraminifera: a molecular perspective. Biodiversity and Conservation 17, 317–328. https://doi.org/10.1007/s10531-007-9253-8

Petersen, J., Riedel, B., Barras, C., Pays, O., Guihéneuf, A., Mabilleau, G., Schweizer, M., Meysman, F.J.R., Jorissen, F.J., 2016. Improved methodology for measuring pore patterns in the benthic

foraminiferal genus Ammonia. Marine Micropaleontology 128, 1–13. https://doi.org/10.1016/j.marmicro.2016.08.001

Richirt, J., Schweizer, M., Bouchet, V.M.P., Mouret, A., Quinchard, S., Jorissen, F.J., 2019a. Morphological distinction of three Ammonia phylotypes occurring along european coasts. Journal of Foraminiferal Research 49, 77–94.

Richirt, J., Champmartin, S., Schweizer, M., Mouret, A., Petersen, J., Ambari, A., Jorissen, F.J., 2019b. Scaling laws explain foraminiferal pore patterns. Scientific Reports 9, 9149. https://doi.org/10.1038/s41598-019-45617-x

Richirt, J., Riedel, B., Mouret, A., Schweizer, M., Langlet, D., Seitaj, D., Meysman, F.J.R., Slomp, C.P., Jorissen, F.J., 2020. Foraminiferal community response to seasonal anoxia in Lake Grevelingen (the Netherlands). Biogeosciences 17, 1415–1435. https://doi.org/10.5194/bg-17-1415-2020

Risgaard-Petersen, N., Revil, A., Meister, P., Nielsen, L.P., 2012. Sulfur, iron-, and calcium cycling associated with natural electric currents running through marine sediment. Geochimica et Cosmochimica Acta 92, 1–13. https://doi.org/10.1016/j.gca.2012.05.036

Saad, S.A., Wade, C.M., 2017. Seasonal and spatial variations of saltmarsh benthic foraminiferal communities from north Norfolk, England. Microbial Ecology 73, 539–555. https://doi.org/10.1007/s00248-016-0895-5

Saad, S.A., Wade, C.M., 2016. Biogeographic distribution and habitat association of *Ammonia* genetic variants around the coastline of Great Britain. Marine Micropaleontology 124, 54–62. https://doi.org/10.1016/j.marmicro.2016.01.004

Saeijs, H.L.F., Stortelder, P.B.M., 1982. Converting an estuary to Lake Grevelingen: Environmental review of a coastal engineering project. Environmental Management 6, 377–405. https://doi.org/10.1007/BF01871888

Schönfeld, J., 2018. Monitoring benthic foraminiferal dynamics at Bottsand coastal lagoon (western Baltic Sea). Journal of Micropalaeontology 37, 383–393. https://doi.org/10.5194/jm-37-383-2018

Schweizer, M., Polovodova, I., Nikulina, A., Schönfeld, J., 2011. Molecular identification of *Ammonia* and *Elphidium* species (Foraminifera, Rotaliida) from the Kiel Fjord (SW Baltic Sea) with rDNA sequences. Helgoland Marine Research 65, 1–10. https://doi.org/10.1007/s10152-010-0194-3

Seitaj, D., Schauer, R., Sulu-Gambari, F., Hidalgo-Martinez, S., Malkin, S.Y., Burdorf, L.D.W., Slomp, C.P., Meysman, F.J.R., 2015. Cable bacteria generate a firewall against euxinia in seasonally hypoxic basins. PNAS 112, 13278–13283. https://doi.org/10.1073/pnas.1510152112

Seitaj, D., Sulu-Gambari, F., Burdorf, L.D.W., Romero-Ramirez, A., Maire, O., Malkin, S.Y., Slomp, C.P., Meysman, F.J.R., 2017. Sedimentary oxygen dynamics in a seasonally hypoxic basin. Limnology and Oceanography 62, 452–473. https://doi.org/10.1002/lno.10434

Sulu-Gambari, F., Roepert, A., Jilbert, T., Hagens, M., Meysman, F.J.R., Slomp, C.P., 2017. Molybdenum dynamics in sediments of a seasonally-hypoxic coastal marine basin. Chemical Geology 466, 627–640. https://doi.org/10.1016/j.chemgeo.2017.07.015

Sulu-Gambari, F., Seitaj, D., Behrends, T., Banerjee, D., Meysman, F.J.R., Slomp, C.P., 2016. Impact of cable bacteria on sedimentary iron and manganese dynamics in a seasonally-hypoxic marine basin. Geochimica et Cosmochimica Acta 192, 49–69. https://doi.org/10.1016/j.gca.2016.07.028

Thibault de Chanvalon, A., Metzger, E., Mouret, A., Cesbron, F., Knoery, J., Rozuel, E., Launeau, P., Nardelli, M.P., Jorissen, F.J., Geslin, E., 2015. Two-dimensional distribution of living benthic foraminifera in anoxic sediment layers of an estuarine mudflat (Loire estuary, France). Biogeosciences 12, 6219–6234. https://doi.org/10.5194/bg-12-6219-2015

Toyofuku, T., Matsuo, M.Y., Nooijer, L.J. de, Nagai, Y., Kawada, S., Fujita, K., Reichart, G.-J., Nomaki, H., Tsuchiya, M., Sakaguchi, H., Kitazato, H., 2017. Proton pumping accompanies calcification in foraminifera. Nature Communications 8, 1–6. https://doi.org/10.1038/ncomms14145

Toyofuku, T., Nooijer, L.J. de, Yamamoto, H., Kitazato, H., 2008. Real-time visualization of calcium ion activity in shallow benthic foraminiferal cells using the fluorescent indicator Fluo-3 AM. Geochemistry, Geophysics, Geosystems 9. https://doi.org/10.1029/2007GC001772

Uppström, L.R., 1974. The boron/chlorinity ratio of deep-sea water from the Pacific Ocean. Deep Sea Research and Oceanographic Abstracts 21, 161–162. https://doi.org/10.1016/0011-7471(74)90074-6

Wetsteijn, L.P.M.J., 2011. Grevelingenmeer: meer kwetsbaar? Een beschrijving van de ecologische ontwikkelingen voor de periode 1999 t/m 2008-2010 in vergelijking met de periode 1990 t/m 1998., RWS Waterdienst. ed. Lelystad, Netherlands.

Wolff, W.J., Reise, K., 2002. Oyster Imports as a Vector for the Introduction of Alien Species into Northern and Western European Coastal Waters, in: Leppäkoski, E., Gollasch, S., Olenin, S. (Eds.), Invasive Aquatic Species of Europe. Distribution, Impacts and Management. Springer Netherlands, Dordrecht, pp. 193–205. https://doi.org/10.1007/978-94-015-9956-6_21

CHAPTER 6

SCALING LAWS EXPLAIN FORAMINIFERAL PORE PATTERNS

JULIEN RICHIRT[1,*], STEPHANE CHAMPMARTIN[2,*], MAGALI SCHWEIZER[1], AURELIA MOURET[1], JASSIN PETERSEN[3], ABDELHAK AMBARI[2] AND FRANS J. JORISSEN[1]

*Both co-authors contributed equally

[1] UMR 6112 LPG-BIAF Recent and Fossil Bio-Indicators, Angers University, 2 Bd Lavoisier, F-49045 Angers, France
[2] LAMPA, Arts et Métiers ParisTech, 2 Bd du Ronceray, BP 93525, 49035 Angers Cedex 01, France
[3] Institute of Geology and Mineralogy, University of Cologne, Zülpicher Str. 49a, 50674 Cologne, Germany

*Corresponding author: richirt.julien@gmail.com

Published in Scientific Reports, 9:9149, 24 June 2019

Received 1 February 2019
Accepted 30 May 2019

ABSTRACT

Due to climate warming and increased anthropogenic impact, a decrease of ocean water oxygenation is expected in the near future, with major consequences for marine life. In this context, it is essential to develop reliable tools to assess past oxygen concentrations in the ocean, to better forecast these future changes. Recently, foraminiferal pore patterns have been proposed as a bottom water oxygenation proxy, but the parameters controlling foraminiferal pore patterns are still largely unknown. Here we use scaling laws to describe how both gas exchanges (metabolic needs) and mechanical constraints (shell robustness) control foraminiferal pore patterns. The derived mathematical model shows that only specific combinations of pore density and size are physically feasible. Maximum porosity, of about 30%, can only be obtained by simultaneously increasing pore size and decreasing pore density. A large empirical data set of pore data obtained for three pseudocryptic phylotypes of *Ammonia*, a common intertidal genus from the eastern Atlantic, strongly supports this conclusion. These new findings provide basic mechanistic understanding of the complex controls of foraminiferal pore patterns and give a solid starting point for the development of proxies of past oxygen concentrations based on these morphological features. Pore size and pore density are largely interdependent, and both have to be considered when describing pore patterns.

1. INTRODUCTION

Marine foraminifera are unicellular eukaryotes inhabiting both the benthic and the pelagic realms. They are one of the most widespread groups of marine organisms, constitute the most diverse group of shelled microorganisms in the modern ocean and have a very rich fossil record[1,2]. Foraminifera have been intensively used in paleoceanographic studies and most of our knowledge of the response of past oceans to climate change has been obtained through geochemical measurements of foraminiferal tests[3]. Recently, porosity in benthic foraminifera has been proposed as a proxy of past bottom water oxygen[4–7] and nitrate levels[8,9]. In view of the expected future decrease in marine oxygen levels, due to global warming and increased eutrophication[10–12], a precise knowledge of oxygen levels in the past, under different climate regimes, is crucial.

Pores are important morphological features in hyaline foraminifera, but their process of formation and their functions are still very poorly known. Different functionalities have been proposed for these connexions between the cell and the surrounding environment, such as passages for pseudopods[13–15], buoyancy control[16] (i.e. in planktonic species), expulsion of gametes[16], osmoregulation[17,18], feeding[17] (intake of organic soluble substances, e. g. dissolved amino acids in sea water) or gas exchanges[17,19–22]. Foraminiferal pores show a large variability in form, size and density. The overall porosity (i.e. the percentage of the test surface covered by pores), which is determined by the latter three factors, is an integrative parameter and

studying its variability in relation to environmental parameters may help to understand the functions of pores. In fact, changes in overall porosity can be explained in two ways: (1) as a phenotypic adaptation to external (environmental) parameters, such as temperature, oxygen or nitrate concentration[8,23,24], or (2) as an internal, species specific, evolutionary adaptation of the genome[25]. In both cases, the physiology of the organism (e.g. metabolic processes) will be modified[18,20,21].

In order to cope with low oxygen concentrations, benthic foraminifera have developed a range of mechanisms such as nitrate respiration[8,26,27], sequestration of chloroplasts[28,29], bacterial symbionts[21], ultrastructural adaptations[20,21] or dormancy[30,31]. However, *Ammonia* was shown unable to sequester chloroplasts[29] and seems strictly aerobic[31]. Intensifying gas exchanges by increasing overall porosity could be another adaptation to hypoxia.

In fact, recently, the variability of pore patterns in benthic foraminifera has been increasingly attributed to differences in gas exchanges, in particular the uptake of oxygen from the surrounding sediment pore waters. The overarching idea is that, when dealing with low oxygen concentrations, a higher total porosity would allow foraminifera to increase their oxygen uptake[20,21,24,32–35]. In several studies, a correlation has been observed between the pore density (number of pores per unit of surface) and the concentration of dissolved oxygen in the surrounding waters[4,5,23]. In these studies, the authors showed that the pore density increased with lower dissolved oxygen concentrations in the surrounding water. Evidently, not only the pore density and the pore size, but also the test thickness will determine the intensity of exchanges through pores. Numerous authors already noted that thin walled species (i.e. with faster gas exchanges) strongly dominate foraminiferal assemblages in oxygen-depleted environments[33,36–38]. Finally, mechanical constraints are necessarily involved when foraminifera adapt their porosity in function of the environment. Foraminifera cannot indefinitely increase the porosity or decrease the thickness of their tests without substantially diminishing the test robustness.

Here we present a simple physical model predicting the relationship between shell porosity, metabolic needs and test robustness, for the last formed chamber of the foraminiferal test. The proposed scaling law model is built on two main assumptions: (1) overall foraminiferal porosity reflects the intensity of gas exchanges, which is determined by cell volume and gas concentrations in the surrounding seawater, and (2) there is a mechanical constraint (test robustness) that limits the increase in overall porosity. Greater porosity can essentially be achieved by increasing pore density and/or pore size. We will use a scaling law model to investigate what range of combinations of these two parameters is physically possible, and what

is the optimal response to the combined mechanical and respiratory constraints. We focus on the last formed chamber, which contains the largest volume of protoplasm and is the thinnest one, so that exchanges with the environment are maximal and test robustness is most critical. An important additional reason to use the last formed chamber is that in the foraminifera with lamellar test studied here, a thin calcite layer is precipitated over the entire test with every new chamber. Although most of the pores remain functional, these secondary calcite layers may cause slight changes of the pore characteristics of earlier chambers. Consequently, only the last chamber is fully representative of the trade-off between gas exchanges and test robustness at the time of chamber formation. Finally, we will use a large empirical data set obtained for three phylotypes of the coastal genus *Ammonia*, with very different pore patterns, to verify whether the scaling law model results correctly predict the pore patterns we observed in nature.

2. RESULTS

2.1. THE MODEL

In order to keep the manuscript as concise as possible, we only present in this section the main features of our model which is developed in detail at the end of the manuscript (see Methods section). The theoretical scaling law model is based on two constraints: the foraminifer needs a minimal respiration rate in order to ensure a nominal metabolism (i.e. “metabolic constraint”) and the mechanical resistance of the shell has to be guaranteed (i.e. “mechanical constraint”).

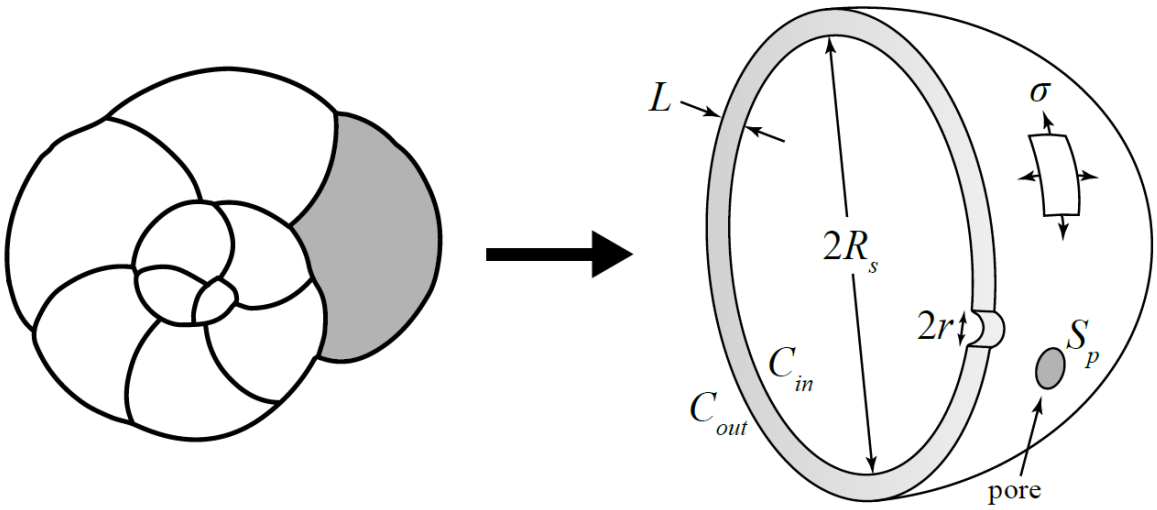

Figure 1. On the left a sketch representing an *Ammonia* sp. specimen in spiral view with the last chamber in grey. On the right, a detailed scheme of the last chamber illustrating the theoretical model. L: thickness of the test; R_s: radius of the last chamber; C_{in}: gas concentration within the cell; C_{out}: gas

concentration in the surrounding water; r: mean radius of the pores; S_p: mean surface of the pores; σ: mechanical stress.

Considering the micrometric size of the pores, passive diffusion controls the transport of gas across the shell. In case of lower oxygen concentrations, the difference of gas concentrations between the foraminiferal cell (C_{in}, Fig. 1) and the surrounding sea water (C_{out}, Fig. 1) will decrease, which according to Fick's first law of diffusion, will lead to a decrease in the mass transfer through the pores. Here we assumed that the cell adapts its morphological features (i.e. pore patterns) to maintain a constant metabolic rate. In order to compensate for this mass transfer decrease, the test porosity must increase. This can be achieved by (1) an increase in pore density N, (2) an increase in pore size (radius r), or (3) an increase of both parameters.

As shown on Figure 1, we considered the individual test chamber as a spherical shell, of radius R_s and thickness $L << R_s$. Since the test is mainly composed of calcite, we expect that only little plastic deformation is possible, and that in case of increasing mechanical stress, brittle fractures will rapidly occur, ultimately leading to breakage of the test. (see Fig. 2). The failure theory predicts that this rupture will begin at a point of maximal stress occurring at geometric discontinuities. In the present case, we assume that the pores behave like such stress concentration points. From a mechanical point of view, a fracture may happen if the stress magnitude σ in the shell exceeds a limit σ^*, the latter being related to the pore structure.

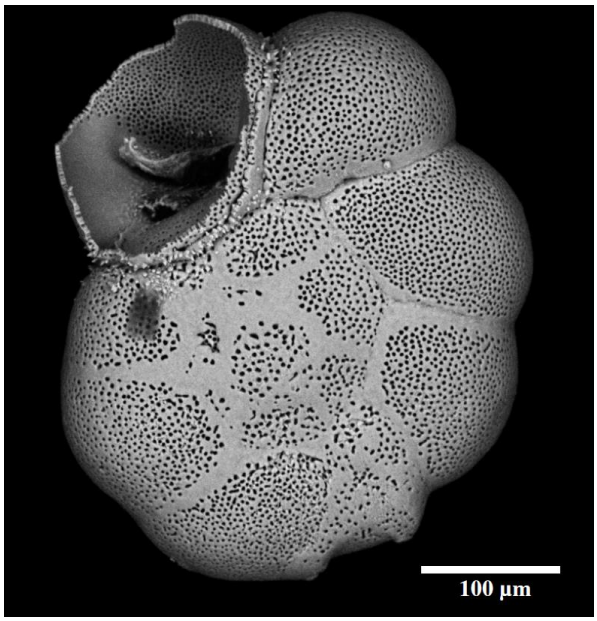

Figure 2. SEM picture of an *Ammonia* sp. specimen showing the response of the foraminiferal test to strong mechanical pressure (notice the net fracture on the last chamber).

The theoretical scaling law model presented here shows that the three basic ways to increase test porosity have very different consequences from a mechanical point of view. As detailed in the Methods section, the relationships between pore density N, pore radius r, porosity Φ and the mechanical stress at which test failure occurs σ^* can be defined as:

$$N \sim \frac{1}{r^{3/2}} \quad \text{(Eq. 1)}$$

$$\Phi \sim r^{1/2} \sim \frac{1}{N^{1/3}} \quad \text{(Eq. 2)}$$

$$\sigma^* \sim \frac{1}{r^{1/2}} \sim N^{1/3} \quad \text{(Eq. 3)}$$

We can compare these scaling laws with the results of an another simple theoretical approach, a mathematical optimisation of the three parameters above (see Methods), which gives:

$$N \sim \frac{1}{r^{5/4}} \quad \text{(Eq. 4)}$$

$$\Phi \sim r^{3/4} \quad \text{(Eq. 5)}$$

2.2. COMPARISON WITH AN EMPIRICAL DATA SET

The 1386 individuals used in this study were sampled at 36 different intertidal and subtidal locations with weak hydrodynamics, mainly along the French Atlantic and Dutch coasts (see Methods). The specimens investigated originate from living natural populations (80%), subrecent fossil samples (15%) and living specimens used in laboratory experiments (5%). The measures of the pore density N, mean pore radius r and porosity Φ were achieved following the methodology developed by Petersen et al (2016)[35]. Since in our recent specimens the last chamber is very often broken, we systematically measured pore patterns in the penultimate chamber. The range of pore radii measured on the spiral face (SEM images) shows that the three *Ammonia* sp. phylotypes T1, T2 and T6[39,40] are mixed in the present data set[41].

Figure 3 displays the empirical data obtained for the pore density N (number of pores per 562 µm²) and mean pore radius r (in µm) together with the allometric scaling. The theoretical scaling law model and the mathematical optimisation approach only predict the exponent and not the intersect. Therefore, on the figures 3 to 5, the lines representing the model outcomes can

be moved vertically in an arbitrary way, and we choose the offsets in the graphics in order to avoid superposition with empirical data to make the figures more readable. The empirical observations show a strong relationship between these two parameters described by $N \sim r^{-1.31}$. This value is intermediate between the coefficient of -1.5 provided by the model (Eq. 1) and -1.25 given by the mathematical optimisation (Eq. 4).

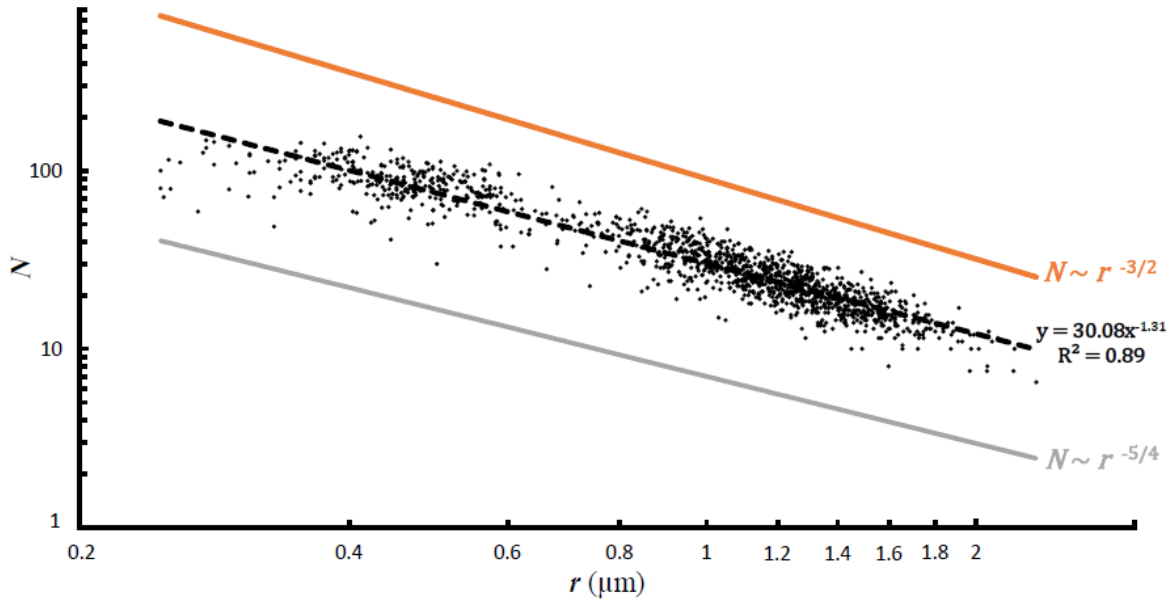

Figure 3. Pore density (N, number of pores per 562 µm²) as a function of the mean radius of the pores (r in µm). The black dots represent the empirical data. The black dotted line represents the power law model based on the empirical data ($y = 30.08 \pm 1.01x^{-1.31 \pm 0.01}$, p-value < 2^{-16}). The orange line represents the mathematical rule derived from the scaling law model ($N \sim r^{-3/2}$). The grey line represents the mathematical rule derived from the mathematical optimisation ($N \sim r^{-5/4}$).

Figure 4 shows the empirical data for total porosity using the best allometric scaling. The empirical data scale as $\Phi \sim r^{0.68}$; which is intermediate between the exponent of 0.5 predicted by the model (Eq. 2) and 0.75, given by the mathematical optimisation (Eq. 5). Again, the model and the observed data are in close agreement, given our simplified approach and uncertainties in natural settings. Similarly to what is shown in Fig. 3, porosity as observed in the empirical data set increases slightly faster with r than the predictions of the scaling law model. In fact, such minor deviations from the predicted exponents are generally interpreted as variations of the system dynamics, which can only be better understood by more exhaustive investigations.

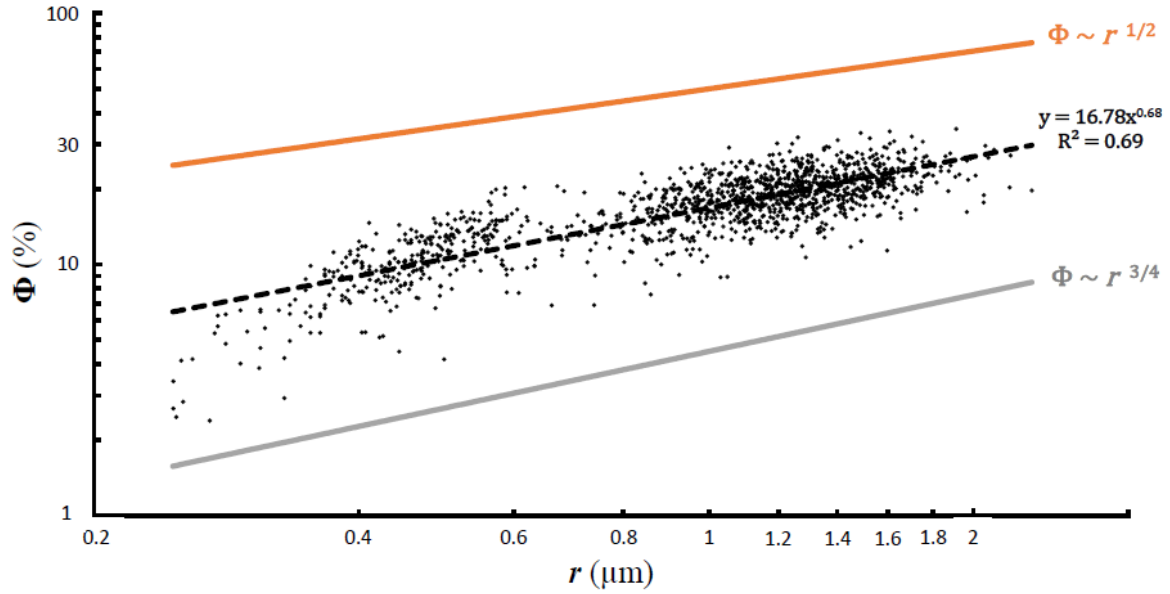

Figure 4. Overall porosity (Φ in % of total test surface) as a function of the mean radius of the pores (r in µm). The black dots represent the empirical data, the black dotted line represents the power law model based on the empirical data ($y = 16.78 \pm 1.01x^{0.68 \pm 0.01}$, p-value < 2^{-16}) and the orange line represents the mathematical rule derived from the scaling law model ($\Phi \sim r^{1/2}$). The grey line represents the mathematical rule derived from the mathematical optimisation ($\Phi \sim r^{3/4}$).

Remarkably, the model predicts that, as a result of mechanical constraint, an increase in total porosity is achieved by a concomitant increase in the pore radius r and a decrease in the pore number N. This somewhat counterintuitive finding (increased porosity is obtained by simultaneous changes with an opposed individual effect) is fully confirmed by the empirical data. There are several reasons for this. First of all, the impact of pore density and pore size on total porosity is not equivalent: since Φ is proportional to N and to r^2, porosity is much more sensitive to a change in r than in N. Concerning the decrease in N in the model results, the explanation is provided by mechanical constraints. In fact, pores act as defects, which may be the origin of fractures or shell breakage (Fig. 2). The lower the pore density is, the less likely test failure becomes. According to the theoretical model, when the pore radius grows to allow increased gas exchanges, a decrease in pore density allows preserving the same mechanical resistance of the test, with a larger overall porosity. However, according to Eq. 3, an increase in the pore radius will also weaken the mechanical resistance of the test, because the stress σ^* at which test failure occurs decreases. In fact, the response of the limit stress σ^* is more sensitive to variations in pore density N than in pore radius r.

Summarizing, the model results conclusively show that in order to increase porosity and maintain the mechanical integrity of the test at the same time, the only viable strategy is to increase the pore radius and concomitantly decrease the pore density. It is remarkable that the

empirical data set shows exactly the same pattern, strongly confirming the general outcome of the scaling law model.

3. DISCUSSION

3.1. MECHANICAL CONSTRAINTS AS PHYSICAL CONTROL OF PORE PATTERNS

Based on two simple assumptions (i.e. total porosity is controlled by metabolic demands and mechanical constraints), the obtained scaling law model fits surprisingly well with the large empirical data set of measured pore patterns. It is especially satisfactory that the counterintuitive outcome of the model, i.e. that increased porosity can best be achieved by concomitantly increasing the pore radius and decreasing the pore density, is fully confirmed by the empirical dataset. This dual result underlines the complex relationship between pore radius, pore density and overall porosity, and shows that only a limited number of combinations can be realised in nature (Fig 5).

Foraminiferal test porosity has long been considered as the critical parameter for gas exchanges[17,19–22], and empirical studies have focused on the relationship between pore parameters and water oxygen concentration[4,5,7,23,42]. Conversely, in these previous studies, the mechanical resistance of foraminiferal tests has never been considered, although it strongly influences the pore patterns, as shown by our model. To our knowledge, the only quantitative study on this topic was published by Wetmore (1987)[43]. After investigating various coastal taxa in different environmental settings, she concluded that test robustness increases with size and with increased physical stress (i.e. sediment coarseness, water turbulence). Our study confirms the major importance of resistance to mechanical constraints, and shows that the variability in pore patterns observed in *Ammonia* is not only an adaptation to increase gas exchanges (through increased overall porosity), but is at the same time strongly controlled by the mechanical resistance of the test.

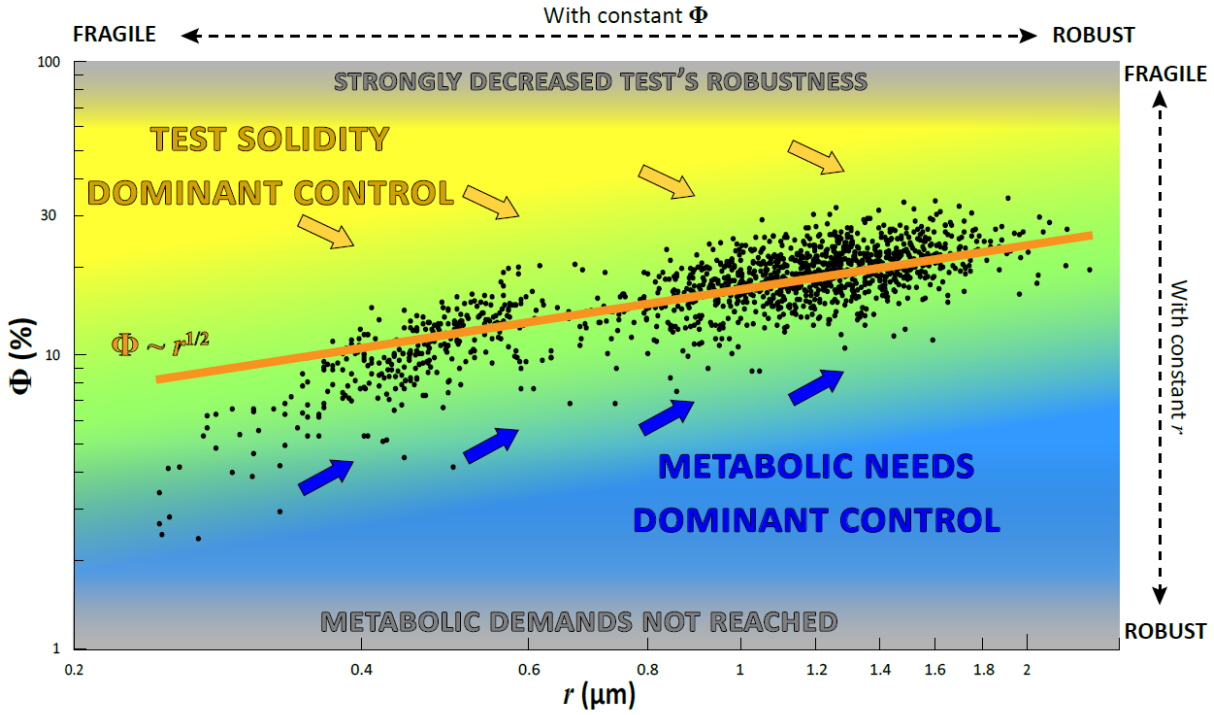

Figure 5. Overall test porosity as a function of pore radius in the empirical data set (black dots, n=1386), compared with the results of the scaling law model (the orange line $\Phi \sim r^{1/2}$). In the central part of the graph, there is an "equilibrium area" (in green) where the very large majority of individuals are plotting, in total agreement with the scaling law model. The blue area represents combinations of pore density and radius which are not encountered in nature because the metabolic demands are not fulfilled. Similarly, the yellow area represents the space where the mechanical constraints on the test are too high. The blue arrows represent the direction of the constraints imposed by the need of increased gas exchanges (toward higher porosity and increased pore radius). The yellow arrows represent the direction of the constraints imposed by the mechanical solidity of the test (toward lower porosity and larger pore radius).

3.2. THE FORAMINIFERAL DILEMMA: THE CHOICE BETWEEN GAS EXCHANGES AND TEST SOLIDITY

A higher porosity obtained by an increase in pore diameter accompanied by a reduction of pore density has been described for *Ammonia* sp. by Moodley & Hess (1992)[32] and Petersen et al. (2016)[35]. The same strategy was also highlighted for planktonic foraminifera[44,45], but has never been shown for other benthic foraminiferal taxa. Several authors have studied pore density, in relation to bottom water oxygen concentrations[4,5,7,23]. Unfortunately, in the latter studies, pore size was not investigated and the overall porosity was not taken into account. As highlighted in our study, the concomitant use of pore density and pore size is mandatory to understand foraminiferal pore patterns related to environmental conditions. In view of our results, studies that consider only one of these two parameters are potentially strongly biased. However, the study of total porosity, which represents a combination of pore number and pore size, should give an acceptable, albeit incomplete, description of pore patterns.

An alternative approach to increase porosity would be to increase both pore density and pore size. This strategy has been suggested for *Hanzawaia nitidula*, a foraminifer living in low oxygen bottom waters[24], but unfortunately, no quantitative measurements have been presented to corroborate this interpretation. However, our scaling law model strongly suggests that such a strategy is not realistic, because simultaneously increasing pore size and pore density will rapidly lead to a strong decrease of the test robustness.

Our large empirical data set suggests that a higher porosity can only be attained without substantially decreasing test robustness by concurrently increasing the pore size and decreasing pore density. In *Ammonia* sp., a porosity of 30% is the upper threshold observed in our data. This corresponds to a pore density of about 10 pores per 562 µm² and a radius of about 2 µm for individual pore. All the individuals, irrespective of their age or geographical origin, plot on the same curve; this clearly indicates that the observed relationship between total porosity, pore density and pore radius reflects a strong control of metabolic and mechanicals constraints as predicted by our scaling law model.

The scaling law model presented here is based on the pore density and pore size in the last chamber. Due to the particular calcification process of foraminifera with a lamellar test, where with every newly formed chamber, a thin calcite layer is precipitated over the entire test, pore patterns will probably change with ontogeny. For instance, Petersen et al. (2016)[35] showed that in *Ammonia*, toward earlier chambers, pore density was increasing, whereas pore size was decreasing, without a significant trend in overall porosity. However, they also noted that these ontogenetic changes were minimal compared to the differences observed between specimens from different sites. It should be noted as well that in spite of potential changes of pore patterns in successive chambers, each chamber was the last chamber when it was formed, and our model results were very probably valid at that moment.

An alternative way to adapt to low oxygen conditions would be to construct thinner tests. In fact, many calcareous taxa adapted to low oxygen environments are indeed characterised by very thin tests[34,37–39]. Just as increased porosity, also a thinner test would lead to a lower test robustness. The modelling of varying test thickness is the subject of ongoing research.

3.3. ECOLOGICAL CONSIDERATIONS

In this study, the specimens included in the dataset belong to three different pseudocryptic (morphologically distinguished only after their identification by DNA analysis) phylotypes of the genus *Ammonia*: T1, T2 and T6[39,40]. As shown by Richirt et al. (2019)[41], the phylotype T2

seems unable to attain a porosity higher than 20% and a mean pore radius larger than 0.7 µm (Figs. 3 to 5, left cluster). T1 and T6 are able to attain higher overall porosity with upper limits of about 25% and 30% and a mean pore radius larger than 1.25 µm and 1.8 µm respectively (Figs. 3 to 5, right cluster). Although these three phylotypes apparently respond to the same physical controls, as shown by the model (i.e. metabolic demand and mechanical resistance), they exhibit different values of mean pore radius, pore density and porosity, suggesting that they occupy different ecological niches. We hypothesize that these three phylotypes represent different adaptations to dissolved gas concentrations (i.e. oxygen concentration)[32,35].

At equal porosity, individuals with large pores (phylotype T6) are more robust compared to individuals with small (phylotype T2) or intermediate pore sizes (phylotype T1). In view of the limited range of pore size (and total porosity) observed for each of the three phylotypes[25,40,41], it appears that pore size is phylotype-dependant, as was already shown for other foraminiferal taxa[46,47]. However, within the limits observed for each of the three phylotypes, there is still substantial variability in porosity, which highlights a certain degree of ecophenotypic plasticity or intraspecific genetic variation. Intra-phylotype plasticity as an additional response to environmental conditions has earlier been shown in other protists[48] (i.e. the number of pores in different phylotypes of testate amoeba). Disentangling genetic and environmental controlling factors is essential to better understand the observed morphological variability.

In order to improve gas exchanges and maintain mechanical integrity of the test, the optimal solution is to increase pore size while decreasing pore density. It appears that, compared to the two other phylotypes, T6 has developed a pore pattern maximising gas exchanges, while maintaining test robustness. This should allow T6 to better perform under low oxygen conditions, which are found immediately below the sediment surface in the intertidal and subtidal mudflats where these *Ammonia* phylotypes flourish. More detailed studies have to be carried out to investigate whether T6 is able to live deeper in the sediment (i.e. where the oxygen content is lower) than T1 and T2. It has been suggested that phylotype T6 has only recently been introduced in Europe, and originates from East Asia[49]. Its higher porosity and a potential increased tolerance to hypoxic conditions, could explain why the phylotype T6 has successfully colonized mudflats along the European coasts, including areas which were not occupied by T1 and T2 before its arrival, such as the Kiel Fjord[50] or the Baltic Sea[51].

3.4. PROXY POTENTIAL OF FORAMINIFERAL PORE PATTERNS

The model developed in this study represents a first step to better understand foraminiferal pore patterns, and allowed the identification of the two main controlling factors in *Ammonia* sp. Although there is no reason to think that pore patterns in other biconvex foraminifera with a lamellar test do not follow the same systematics, the available data do not allow us to confirm this. Our study emphasizes the importance of examining both pore density and pore size when investigating foraminiferal pore patterns. Our results strongly suggest that in biconvex foraminifera with a lamellar test, different pore patterns are a morphological adaptation (genetically encoded and/or phenotypic) allowing the modulation of gas exchanges with the outer environment. Increased gas exchanges may be very beneficial in low oxygen environments. This observation has been the rationale behind the attempts to use pore patterns as a proxy for bottom water oxygen concentrations[4–7]. Our scaling law model is not restricted to exchanges of oxygen, but could also be applied to other dissolved compounds in water, such as nitrate. Recently, pore patterns in *Bolivina spissa* have been proposed as a proxy to reconstruct past nitrate concentrations[8,9]. Although the general test shape of *Bolivina* is very different compared to *Ammonia*, a theoretical scaling law model adapted to this genus, based on the same principles, should allow us to better understand how simultaneous changes of pore density and pore size will lead to maximal porosity, allowing optimisation of gas exchanges.

We are convinced that this type of modelling approach provides insight in the physical laws controlling foraminiferal porosity. Understanding the constraints controlling the foraminiferal porosity is a crucial prerequisite for the reliable calibration and successful application of paleoceanographic proxies based on foraminiferal pore patterns.

4. METHODS

4.1. SCALING LAW MODEL

Scaling arguments and dimensional analysis are extensively used to study the general characteristics of the biological world: the size and shape of plants and animals can be seen as nature's adaptation to various constraints such as gravity, surface tension, viscosity, mechanical stress and so on. Under these constraints, most living organisms exhibit the notable property of self-similarity: they are prone to scaling laws and reproduce themselves as scales change. This study proposes scaling laws for foraminifera subjected to two constraints: the foraminifera need a minimal respiration rate in order to ensure a nominal metabolism (metabolic constraint) and

the test mechanical resistance integrity (mechanical constraint). The model was developed for the last chamber, formed by a single calcite layer and which usually has the largest volume. Due to the thinner test wall, gas exchanges are more intense in this chamber, which is for the same reason also the most fragile.

4.1.1. Metabolic constraint

Considering the micrometric size of the pores, diffusion controls the transport of gas across the shell and Fick's first law for steady-state diffusion of a gas through a porous material can be used:

$$\dot{m} = S_p D \frac{\Delta C}{L}$$

with $\dot{m}$ the flow-rate of gas, D the diffusion coefficient supposed to be constant and specific to the diffusive chemical species, S_p the pore area, $\Delta C = x$ the concentration difference across the shell and L the test thickness. In order to keep a constant metabolic rate $\dot{m} = Cst$, and the equation above can be simplified to:

$$\frac{S_p x}{L} = Cst$$

The pore area depends on the number of pores N and on the pore radius r (the pore size distribution for a given test is roughly monodisperse[35]):

$$S_p = N\pi r^2$$

The metabolic constraint is thus:

$$\frac{Nr^2 x}{L} = Cst$$

We now assume that N, r and L are functions of x and scale like:

$$N \sim x^a \qquad r \sim x^b \qquad L \sim x^c$$

with a, b and c being constant to be determined. Re-writing the metabolic constraint, we obtain:

$$x^{a+2b+1-c} = Cst$$

This condition must be true for any value of x implying:

$$a + 2b + 1 - c = 0$$

At this point we need other equations to solve the problem. They are provided by the mechanical constraint based on the resistance of the shell.

4.1.2. Mechanical constraint

We consider the test chamber as a spherical thin shell of radius R_s and thickness $L \ll R_s$. From the theory of linear elasticity, we know that the wall is subject to a uniform stress σ:

$$\sigma = \frac{\Delta P\, R_s}{2L}$$

with ΔP the pressure difference across the test. The pressure jump is due to the osmotic pressure across the cell membrane and is related to the concentration difference $\Delta C = x$ by the law of Van't Hoff:

$$\Delta P = RT\, \Delta C = RTx$$

with R the ideal gas constant and T the thermodynamic temperature supposed to be constant. In bird eggs, the wall thickness L and the size of the chamber R_s are roughly proportional (i.e. $L \sim R_s$) [52,53] implying that the density of the egg is constant. Assuming a similar relation for the last chamber (which is the thinnest and most fragile chamber of the test) of foraminifera of the genus *Ammonia*, we hypothesize that the stress σ in the shell scales with the concentration difference across the shell x like:

$$\sigma \sim x$$

The key point for the mechanical constraint is the way the test is likely to break: since the test is mainly composed of calcite, only very limited plastic deformation is possible, and in case of increasing mechanical stress, brittle fractures will rapidly occur, ultimately leading to breakage of the test. The failure theory predicts that the rupture occurs from a defect of characteristic size l when the stress exceeds the limit σ^* given by:

$$\sigma^* = \frac{K_c}{\sqrt{\pi l}}$$

with K_c the stress intensity factor. We assume that the pores are such defects and that $l \sim r$. This implies that:

$$\sigma^* \sim r^{-1/2} \sim x^{-b/2}$$

The test failure is reached when $\sigma = \sigma^*$ and the mechanical constraint implies that:

$$b = -2$$

Our last hypothesis is that R_s does not depend on x. Such an argument can be understood on simple geometrical grounds: the exchanges with the surrounding medium are proportional to the cell surface $S \sim R_s^2$ whereas its needs are proportional to its volume $V \sim R_s^3$. There must be a cell size above which the cell asphyxiates because the exchanges across the cell membrane are

not fast enough. Therefore, the cell cannot grow indefinitely and reaches an optimal size R_s. Because $R_s \sim L \sim x^c$, the only acceptable solution is $c = 0$. Now the metabolic constraint gives:

$$a = -2b - 1 = 3$$

From these values, the relationships between N, Φ, σ^* and r can be obtained:

$$N \sim r^{-3/2} \qquad \Phi \sim r^{1/2} \qquad \sigma^* \sim r^{-1/2}$$

4.2. MATHEMATICAL OPTIMISATION

This approach consists in maximizing both porosity Φ (i.e. maximize transfer through the test) and mechanical resistance of the test (i.e. maximize σ^*/N). If we suppose that pore density scales as $N \sim r^a$ with a an exponent to be found, porosity scales as $\Phi \sim Nr^2 \sim r^{a+2}$ (the limit stress always scales as $\sigma^* \sim r^{-1/2}$). Thus the best compromise is obtained by solving:

$$\frac{d}{dr}\left(\Phi + \frac{\sigma^*}{N}\right) = \frac{d}{dr}\left(r^{a+2} + \frac{1}{r^{\frac{1}{2}+a}}\right) = 0$$

After simplification, we obtain:

$$r^{2a+5/2} = \frac{1+2a}{a+2} = Cst$$

The only solution to keep constant the left-hand side of the equation above is:

$$a = -5/4$$

The relationships between N, Φ, σ^* and r finally write:

$$N \sim r^{-5/4} \qquad \Phi \sim r^{3/4} \qquad \sigma^* \sim r^{-1/2}$$

4.3. EMPIRICAL DATA

The 1386 *Ammonia* sp. individuals were sampled at 36 different stations (see Fig. 6 and Table 1) around European coasts (see map), plus one station in Yokohama (Japan, three individuals) and one station at Tulear in Madagascar (one individual). Individuals come from fossil, recent and experimental material (only chambers formed in experimental conditions have been measured for specimens used in laboratory growth experiments), The measurements of the porosity features were performed following the methodology developed in Petersen et al (2016)[35]. The measured range of pore diameter shows that the three phylotypes T1, T2 and T6 are mixed in the samples[41]. Pore pattern data generated or analysed during this study have been included in the supplementary information files.

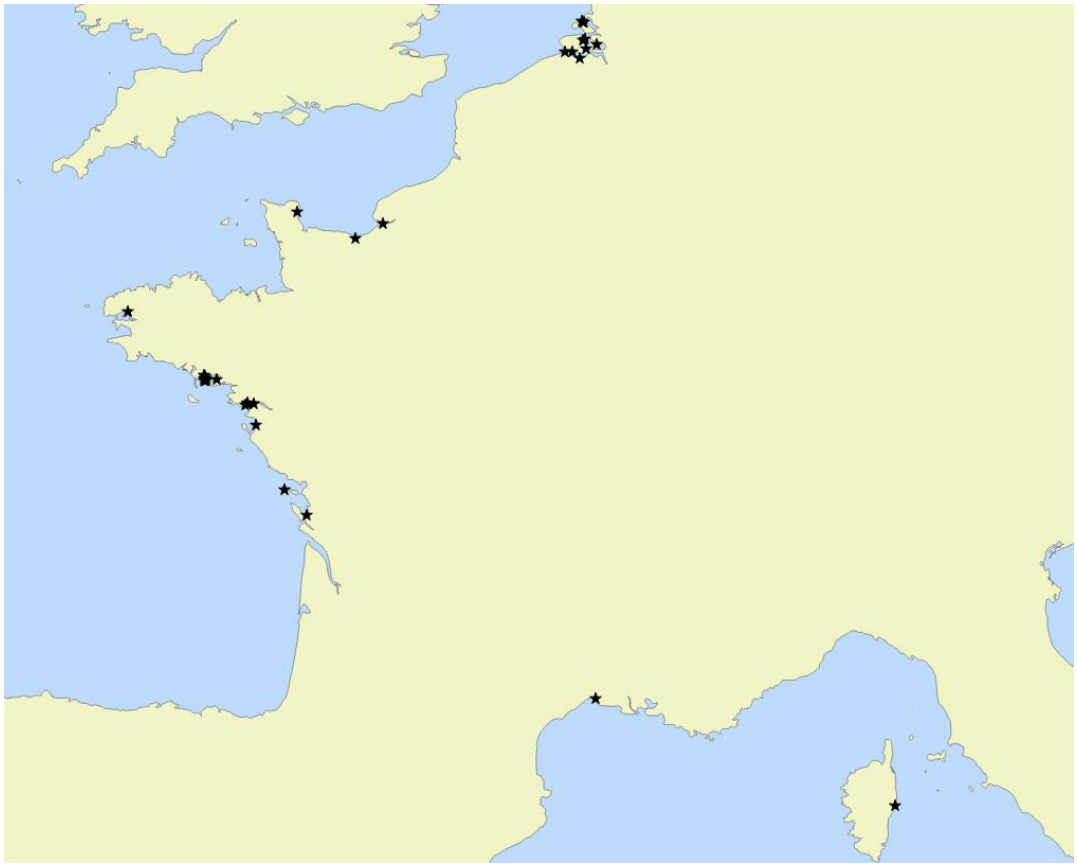

Figure 6. Map of the sampled stations.

Table 1. Location and number of individuals for each station (ordered by latitude – 1386 individuals in total).

Station	Latitude	Longitude	Number of individuals
Mokbaai, Texel	53°0'14.4"N	4°46'4.799"E	6
Grev-3	51°45'47.401"N	3°52'08.563"E	197
Grev-1	51°44'50.04"N	3°53'24.06"E	230
Grev-2	51°44.956N	03°53.826E	193
Zandkreek	51°33'12.24"N	3°52'25.34"E	107
Escault 6	51°33.401'N	3°55.082'E	2
Escault 5	51°29.888'N	4°07.915'E	5
Biezelingse Ham	51°26'53.40"N	3°55'49.79"E	73
Escault 4	51°25.208'N	3°41.783'E	32
Escault 2	51°25.134'N	3°33.804'E	3
Escault 1	51°20.881'N	3°49.365'E	20
English Channel - Saint Vaast	49°34'38.60"N	1°16'38.80"W	4
English Channel - Estuaire de la Seine	49°26'31.30"N	0°16'25.20"E	13
English Channel - Ouistreham	49°16'16.40"N	0°14'12.20"W	3
Rade de Brest	48°24'13.10"N	4°21'16.00"W	12
Gulf of Morbihan - Bono	47°38′4.71″N	2°57′36.27″W	2
Fort Espagnol	47°36'47.50"N	2°57'11.10"W	8
Gulf of Morbihan - Toulvern	47°35'39.95"N	2°55'35.80"W	3

2C2	47°35'17.7"N	2°57'50.7"W	9
Auray River - KER2	47°34'60.00"N	2°57'17.20"W	40
Auray River - LOC1	47°34'12.12"N	2°56'32.40"W	15
Auray River - LOC2	47°34'11.58"N	2°56'26.58"W	50
Auray River - LOC3	47°34'11.29"N	2°56'21.38"W	6
Gulf of Morbihan - Bailleron est	47°34′38.07″N	2°44′45.25″W	4
St Pierre Lopérec	47°33'44.8"N	2°58'23.0"W	32
Loire - core SC05	47°17'10.30"N	2°10'31.80"W	30
Loire - Semhabel	47°17.293'N	2°10.906'W	16
Loire - RS2E	47°16'58.8"N	2°3'46.8"W	28
Saint Nazaire	47°15'56.75"N	2°13'20.79"W	69
Bourgneuf	47°0'56.38"N	2°1'31.00"W	124
Ile de Ré	46°13'23.13"N	01°30'46.27"W	2
Aiguillon	45°53'60.00"N	1°7'0.00"W	40
Gulf of Lion - Camargue	43°33'9.306"N	4°6'15.112"E	2
Corsica	42°8′7.44″N	09°31′59.04″E	2
Yokohama	35°19'21"N	139°38'6"E	3

ACKNOWLEDGEMENTS

This study comprised part of the research project AMTEP, financed by the CNRS-INSU program EC2CO. We are grateful to the team of the SCIAM imaging facility at the University of Angers. We gratefully acknowledge the help of many colleagues who provided samples and/or performed measurements: Christine Barras, Eric Bénéteau, Thibaut Bernard, Vincent Bouchet, Inge van Dijk, Julie Garnier, Emmanuelle Geslin, Hélène Howa, Dylan Hurblain, Thierry Jauffrais, Liesbeth Jorissen, Charlotte LeKieffre, Edouard Metzger, Maria Pia Nardelli, Briz Parent, Jan Pawlowski, Hugo Saur, Aubin Thibault de Chanvalon, and Takashi Toyofuku.

REFERENCES

1. Gupta, B. K. S. *Modern Foraminifera*. (Springer Science & Business Media, 2007).
2. Jones, R. W. *Foraminifera and their Applications*. (Cambridge University Press, 2013).
3. Katz, M. E. *et al.* Traditional and emerging geochemical proxies in foraminifera. *J. Foraminifer. Res.* **40**, 165–192 (2010).
4. Kuhnt, T. *et al.* Relationship between pore density in benthic foraminifera and bottom-water oxygen content. *Deep Sea Res. Part Oceanogr. Res. Pap.* **76**, 85–95 (2013).
5. Kuhnt, T. *et al.* Automated and manual analyses of the pore density-to-oxygen relationship in Globobulimina turgida (Bailey). *J. Foraminifer. Res.* **44**, 5–16 (2014).
6. Rathburn, A. E., Willingham, J., Ziebis, W., Burkett, A. M. & Corliss, B. H. A New biological proxy for deep-sea paleo-oxygen: Pores of epifaunal benthic foraminifera. *Sci. Rep.* **8**, 9456 (2018).
7. Tetard, M. Dynamique de la paléo-oxygénation dans le Pacifique : reconstitution par une approche morphométrique et micropaléontologique. (Aix-Marseille, 2017).

8. Glock, N. *et al.* Environmental Influences on the Pore Density of Bolivina Spissa (Cushman). *J. Foraminifer. Res.* **41**, 22–32 (2011).
9. Glock, N. *et al.* Coupling of oceanic carbon and nitrogen facilitates spatially resolved quantitative reconstruction of nitrate inventories. *Nat. Commun.* **9**, 1217 (2018).
10. Diaz, R. J. & Rosenberg, R. Spreading Dead Zones and Consequences for Marine Ecosystems. *Science* **321**, 926–929 (2008).
11. Gilbert, D., Rabalais, N. N., Diaz, R. J. & Zhang, J. Evidence for greater oxygen decline rates in the coastal ocean than in the open ocean. *Biogeosciences* 2283–2296 (2010).
12. Helm, K. P., Bindoff, N. L. & Church, J. A. Observed decreases in oxygen content of the global ocean. *Geophys. Res. Lett.* **38**, (2011).
13. Loeblich, A. R. & Tappan, H. *Treatise on Invertebrate Paleontology, Part C: Protista 2, Sarcodina, Chiefly Thecamoebians and Foraminiferida*. (Geological Society of Amer, 1964).
14. Hansen, H. J. Pore pseudopodia and sieve plates of Amphistegina. *Micropaleontology* **18**, 223–230 (1972).
15. Dubicka, Z., Złotnik, M. & Borszcz, T. Test morphology as a function of behavioral strategies — Inferences from benthic foraminifera. *Mar. Micropaleontol.* **116**, 38–49 (2015).
16. Frerichs, W. E., Heiman, M. E., Borgman, L. E. & Be, A. W. H. Latitudal variations in planktonic foraminiferal test porosity; Part 1, Optical studies. *J. Foraminifer. Res.* **2**, 6–13 (1972).
17. Berthold, W.-U. Ultrastructure and function of wall perforations in Patellina corrugata Williamson, Foraminiferida. *J. Foraminifer. Res.* **6**, 22–29 (1976).
18. Bijma, J., Faber, W. W. & Hemleben, C. Temperature and salinity limits for growth and survival of some planktonic foraminifers in laboratory cultures. *J. Foraminifer. Res.* **20**, 95–116 (1990).
19. Hottinger, L. & Dreher, D. Differentiation of protoplasm in nummulitidae (Foraminifera) from Elat, Red Sea. *Mar. Biol.* **25**, 41–61 (1974).
20. Leutenegger, S. & Hansen, H. J. Ultrastructural and radiotracer studies of pore function in foraminifera. *Mar. Biol.* **54**, 11–16 (1979).
21. Bernhard, J. M., Goldstein, S. T. & Bowser, S. S. An ectobiont-bearing foraminiferan, Bolivina pacifica, that inhabits microxic pore waters: cell-biological and paleoceanographic insights. *Environ. Microbiol.* **12**, 2107–2119 (2010).
22. Glock, N., Schönfeld, J. & Mallon, J. The Functionality of Pores in Benthic Foraminifera in View of Bottom Water Oxygenation: A Review. in *Anoxia* 537–552 (Springer, Dordrecht, 2012).
23. Gary, A. C., Healey-Williams, N. & Ehrlich, R. Water-mass relationships and morphologic variability in the benthic foraminifer Bolivina albatrossi Cushman, northern Gulf of Mexico. *J. Foraminifer. Res.* **19**, 210–221 (1989).
24. Perez-Cruz, L. L. & Machain-Castillo, M. L. Benthic foraminifera of the oxygen minimum zone, continental shelf of the Gulf of Tehuantepec, Mexico. *J. Foraminifer. Res.* **20**, 312–325 (1990).
25. Holzmann, M. & Pawlowski, J. Molecular, morphological and ecological evidence for species recognition in Ammonia (Foraminifera). *J. Foraminifer. Res.* **27**, 311–318 (1997).
26. Risgaard-Petersen, N. *et al.* Evidence for complete denitrification in a benthic foraminifer. *Nature* **443**, 93–96 (2006).
27. Koho, K. A., Piña-Ochoa, E., Geslin, E. & Risgaard-Petersen, N. Vertical migration, nitrate uptake and denitrification: survival mechanisms of foraminifers (Globobulimina turgida) under low oxygen conditions. *FEMS Microbiol. Ecol.* **75**, 273–283 (2011).

28. Jauffrais, T. *et al.* Effect of light on photosynthetic efficiency of sequestered chloroplasts in intertidal benthic foraminifera (Haynesina germanica and Ammonia tepida). *Biogeosciences* **13**, 2715–2726 (2016).
29. Jauffrais, T. *et al.* Ultrastructure and distribution of kleptoplasts in benthic foraminifera from shallow-water (photic) habitats. *Mar. Micropaleontol.* **138**, 46–62 (2018).
30. Ross, B. J. & Hallock, P. Dormancy in the Foraminifera: A Review. *J. Foraminifer. Res.* **46**, 358–368 (2016).
31. LeKieffre, C. *et al.* Surviving anoxia in marine sediments: The metabolic response of ubiquitous benthic foraminifera (Ammonia tepida). *PLoS ONE* **12**, e0177604. (2017).
32. Moodley, L. & Hess, C. Tolerance of Infaunal Benthic Foraminifera for Low and High Oxygen Concentrations. *Biol. Bull.* **183**, 94–98 (1992).
33. Sen Gupta, B. K. & Machain-Castillo, M. L. Benthic foraminifera in oxygen-poor habitats. *Mar. Micropaleontol.* **20**, 183–201 (1993).
34. Polovodova, I., Nikulina, A., Schönfeld, J. & Dullo, W.-C. Recent benthic foraminifera in the Flensburg Fjord (Western Baltic Sea). *J. Micropalaeontology* **28**, 131–142 (2009).
35. Petersen, J. *et al.* Improved methodology for measuring pore patterns in the benthic foraminiferal genus Ammonia. *Mar. Micropaleontol.* **128**, 1–13 (2016).
36. Harman, R. A. Distribution of Foraminifera in the Santa Barbara Basin, California. *Micropaleontology* **10**, 81–96 (1964).
37. Bernhard, J. M. Characteristic assemblages and morphologies of benthic foraminifera from anoxic, organic-rich deposits; Jurassic through Holocene. *J. Foraminifer. Res.* **16**, 207–215 (1986).
38. Kaiho, K. Benthic foraminiferal dissolved-oxygen index and dissolved-oxygen levels in the modern ocean. *Geology* **22**, 719–722 (1994).
39. Holzmann, M. & Pawlowski, J. Taxonomic relationships in the genus Ammonia (Foraminifera) based on ribosomal DNA sequences. *J. Micropalaeontology* **19**, 85–95 (2000).
40. Hayward, B. W., Holzmann, M., Grenfell, H. R., Pawlowski, J. & Triggs, C. M. Morphological distinction of molecular types in Ammonia – towards a taxonomic revision of the world's most commonly misidentified foraminifera. *Mar. Micropaleontol.* **50**, 237–271 (2004).
41. Richirt, J. *et al.* Morphological distinction of three Ammonia phylotypes occurring along european coasts. *J. Foraminifer. Res.* **49**, 77–94 (2019).
42. Boersma, A. & Mikkelsen, N. 31. Miocene-age primary productivity episodes and oxygen minima in the central equatorial indian ocean. *Proc. Ocean Drill. Program Sci. Results* **115**, 21 (1990).
43. Wetmore, K. L. Correlations between test strength, morphology and habitat in some benthic foraminifera from the coast of Washington. *J. Foraminifer. Res.* **17**, 1–13 (1987).
44. Bé, A. W. H. Shell Porosity of Recent Planktonic Foraminifera as a Climatic Index. *Science* **161**, 881–884 (1968).
45. Haenel, P. Intérêt paléoocéanographique d'Orbulina universa d'Orbigny (foraminifère). *Oceanol. Acta* **10**, 15–25 (1987).
46. Morard, R. *et al.* Morphological recognition of cryptic species in the planktonic foraminifer Orbulina universa. *Mar. Micropaleontol.* **71**, 148–165 (2009).
47. Schweizer, M., Pawlowski, J., Kouwenhoven, T. & van der Zwaan, B. Molecular phylogeny of common Cibicidids and related Rotaliida (Foraminifera) based on small subunit rDNA sequences. *J. Foraminifer. Res.* **39**, 300–315 (2009).
48. Mulot, M. *et al.* Genetic Determinism vs. Phenotypic Plasticity in Protist Morphology. *J. Eukaryot. Microbiol.* **64**, 729–739 (2017).

49. Pawlowski, J. & Holzmann, M. Diversity and geographic distribution of benthic foraminifera: a molecular perspective. *Biodivers. Conserv.* **17**, 317–328 (2008).
50. Schweizer, M., Polovodova, I., Nikulina, A. & Schönfeld, J. Molecular identification of Ammonia and Elphidium species (Foraminifera, Rotaliida) from the Kiel Fjord (SW Baltic Sea) with rDNA sequences. *Helgol. Mar. Res.* **65**, 1–10 (2011).
51. Groeneveld, J. *et al.* Assessing proxy signatures of temperature, salinity, and hypoxia in the Baltic Sea through foraminifera-based geochemistry and faunal assemblages. *J. Micropalaeontology* **37**, 403–429 (2018).
52. Ar, A., Paganelli, C. V., Reeves, R. B., Greene, D. G. & Rahn, H. The Avian Egg: Water Vapor Conductance, Shell Thickness, and Functional Pore Area. *The Condor* **76**, 153–158 (1974).
53. Spaw, C. D. & Rohwer, S. A comparative study of eggshell thickness in cowbirds and other passerines. *The Condor* **89**, 307–318 (1987).

AUTHOR CONTRIBUTIONS

J.R.: compilation, analysis and interpretation of the foraminiferal pore patterns dataset. Writing of the manuscript. S.C.: development of the theoretical scaling law model and the mathematical optimisation approaches. Contribution to the discussion, interpretation of the data and writing of the manuscript. M.S.: contribution to the discussion and interpretation of the data. A.M: contribution to the discussion and interpretation of the data. J.P.: contribution to the discussion and interpretation of the data. Provided a large amount of the pore pattern data. A.A.: development of the theoretical scaling law model. F.J.: contribution to the discussion, interpretation of the data and writing of the manuscript

SUPPLEMENTARY INFORMATION

Individual ID	Pore density (per 562 µm²)	Pore surface (%)	Pore radius (µm)
Au404	36.5	22.639	1.053
Au409	33.0	13.040	0.841
Au415	41.0	16.742	0.855
Au422	27.5	17.211	1.058
Au424	37.0	20.130	0.986
Au430	34.5	18.237	0.972
Au439	25.0	22.246	1.261
Au440	28.0	20.905	1.155
Au444	32.5	19.479	1.035
Au485	33.5	18.998	1.007
Au492	38.5	23.096	1.036
Au494	43.5	23.964	0.993
Au495	51.0	16.331	0.757
Au497	40.5	17.794	0.886
Au502	40.0	19.116	0.924
Yo060	49.5	18.762	0.823
Au398	42.0	20.096	0.925
Au402	44.0	19.721	0.895
Au403	39.5	22.122	1.001
Au406	30.5	22.906	1.159
Au407	39.5	16.050	0.852
Au408	40.5	20.607	0.954
Au411	46.0	13.082	0.713
Au419	39.0	25.692	1.085
Ma027	36.0	25.340	1.122
Ma142	28.0	26.807	1.308
Md013	32.5	21.940	1.099
Mo110	47.0	23.142	0.938
RB007	73.0	9.153	0.474
Re086	30.0	25.962	1.244
Re087	38.5	17.333	0.897
Yo051	40.0	22.709	1.008
Yo052	47.5	24.260	0.956
SN044	22.0	21.163	1.256
Au442	76.0	9.438	0.471
Au452	81.5	14.960	0.573
Au461	101.5	8.691	0.391
Au467	101.0	9.524	0.411
Au487	87.0	14.048	0.537
Au501	81.5	10.969	0.491
Au503	49.5	9.570	0.588
Co005	88.5	7.376	0.386
Co006	88.0	9.011	0.428
Ma030	106.5	12.524	0.459
Mo013	85.0	7.771	0.404
Mo017	93.5	7.889	0.388
Mo099	68.0	10.487	0.525
Mo101	92.0	10.871	0.460
Au400	86.0	13.613	0.532
Au423	101.0	17.822	0.562
Au451	96.0	13.943	0.510
Au453	91.5	13.677	0.517
Au462	86.0	13.709	0.534
Au491	80.0	15.544	0.589
Au500	81.5	14.433	0.563
Ma028	72.0	8.471	0.459
Ma031	74.0	8.238	0.446
Mo014	77.0	9.876	0.479
Mo098	57.5	14.104	0.662
Mo102	93.0	12.156	0.483
ZK020	32.5	24.662	1.165
ZK023	35.0	17.664	0.950
Ma150	95.5	12.131	0.477
Mo106	74.5	13.633	0.552
RB002	82.0	10.045	0.457
RB003	94.5	20.186	0.587
Ai052	29.0	27.249	1.296
Ai055	24.0	21.431	1.264
Ai056	19.0	21.878	1.435
Ai063	22.5	19.809	1.255
BH009	23.0	16.893	1.146
BH010	17.0	22.558	1.540
BH013	27.0	22.887	1.231
BH018	28.0	15.511	0.995
Bn097	22.0	17.980	1.209
Bn099	38.0	19.502	0.958
Bn108	22.5	18.353	1.208

Bn113	27.0	24.404	1.271	**018.2 - Kerouarc'h**	83.5	11.171	0.474	**056.2 - Locmariaquer**	99.5	9.829	0.411
Bn116	39.5	21.047	0.976	**019.2 - Kerouarc'h**	76.0	12.069	0.510	**057.2 - Locmariaquer**	84.0	13.173	0.512
Bn118	35.5	18.720	0.971	**020.2 - Kerouarc'h**	33.5	20.247	0.976	**058.2 - Locmariaquer**	82.0	10.937	0.466
Bn119	35.0	30.271	1.244	**021.2 - Kerouarc'h**	25.0	21.647	1.136	**059.2 - Locmariaquer**	77.5	10.298	0.471
Bn120	31.5	19.449	1.051	**022.2 - Kerouarc'h**	79.5	7.201	0.389	**060.2 - Locmariaquer**	88.0	9.704	0.439
Li028	13.0	20.367	1.674	**023.2 - Kerouarc'h**	61.5	11.438	0.561	**061.2 - Locmariaquer**	61.0	14.932	0.622
Li035	16.5	21.216	1.516	**024.2 - Kerouarc'h**	29.5	32.083	1.263	**062.2 - Locmariaquer**	77.5	8.872	0.437
Ma080	27.0	33.440	1.488	**025.2 - Kerouarc'h**	86.5	9.376	0.432	**063.2 - Locmariaquer**	50.0	13.458	0.662
Ma083	15.5	21.644	1.580	**026.2 - Kerouarc'h**	29.5	30.395	1.196	**065.2 - Locmariaquer**	61.0	12.777	0.593
Ma084	20.5	29.109	1.593	**027.2 - Kerouarc'h (2)**	33.0	27.364	1.183	**066.2 - Locmariaquer**	77.5	12.806	0.513
Ma085	18.5	26.502	1.601	**028.2 - Kerouarc'h (2)**	71.0	15.933	0.597	**067.2 - Locmariaquer**	72.0	14.019	0.560
Ma086	23.0	19.678	1.237	**029.2 - Kerouarc'h**	68.5	19.626	0.684	**068.2 - Locmariaquer**	92.5	15.080	0.514
Ma087	19.5	26.387	1.556	**030.2 - Kerouarc'h**	23.5	20.621	1.191	**069.2 - Locmariaquer**	85.5	11.360	0.473
Ma089	13.0	22.987	1.778	**031.2 - Kerouarc'h (2)**	115.0	4.148	0.251	**070.2 - Locmariaquer**	80.0	9.647	0.451
Ma091	19.0	25.118	1.538	**032.2 - Kerouarc'h**	103.5	9.846	0.404	**071.1 - Locmariaquer**	71.0	2.468	0.248
Ma094	16.5	23.947	1.611	**033.2 - Kerouarc'h**	126.0	5.329	0.274	**071.2 - Locmariaquer**	78.5	4.031	0.293
Ma097	16.0	19.738	1.485	**034.2 - Kerouarc'h**	50.0	10.407	0.582	**072.2 - Locmariaquer**	74.0	15.042	0.573
Ma101	22.5	19.749	1.253	**035.2 - Kerouarc'h**	31.0	15.955	0.916	**073.2 - Locmariaquer**	110.5	15.224	0.487
Ma108	22.5	25.464	1.423	**036.2 - Kerouarc'h**	51.5	10.010	0.581	**074.2 - Locmariaquer**	75.5	10.623	0.473
Ma109	26.0	19.138	1.147	**037.3 - Kerouarc'h**	30.5	23.213	1.059	**075.2 - Locmariaquer**	95.5	15.228	0.522
Ma147	23.0	21.042	1.279	**038.2 - Kerouarc'h**	86.5	13.189	0.509	**076.2 - Locmariaquer**	102.5	14.512	0.495
SN051	25.5	20.342	1.194	**039.2 - Kerouarc'h**	71.0	10.528	0.491	**077.2 - Locmariaquer**	87.5	14.790	0.530
ZK043	25.5	25.384	1.273	**040.2 - Kerouarc'h**	24.5	18.775	1.095	**078.2 - Locmariaquer**	78.0	14.899	0.567
ZK047	18.5	20.052	1.339	**041.2 - Kerouarc'h**	25.0	21.343	1.110	**079.2 - Locmariaquer**	66.5	11.365	0.528
Ai045	24.0	17.034	1.025	**042.2 - Kerouarc'h**	71.5	13.781	0.555	**080.3 - Locmariaquer**	78.0	9.869	0.451
Ai047	28.0	20.896	1.098	**043.2 - Kerouarc'h**	35.0	23.731	1.005	**081.2 - Locmariaquer**	60.5	9.538	0.516
014.2 - Kerouarc'h	56.5	10.298	0.541	**044.2 - Kerouarc'h**	90.5	12.830	0.494	**082.2 - Locmariaquer**	98.0	12.956	0.472
015.2 - Kerouarc'h	71.0	12.469	0.557	**045.2 - Kerouarc'h**	71.5	9.620	0.470	**083.2 - Locmariaquer**	87.0	8.104	0.408
016.2 - Kerouarc'h	32.5	16.227	0.898	**054.2 - Locmariaquer**	83.0	8.704	0.421	**084.2 - Locmariaquer**	96.5	19.009	0.586
017.2 - Kerouarc'h	81.5	10.900	0.471	**055.2 - Locmariaquer**	92.0	7.570	0.370	**094.2 - St Pierre Loperec**	77.5	13.190	0.546

095.2 - St Pierre Loperec	40.5	11.420	0.681
096.2 - St Pierre Loperec	59.5	14.568	0.643
097.2 - St Pierre Loperec	29.0	23.953	1.106
098.2 - St Pierre Loperec	70.0	12.848	0.539
100.2 - St Pierre Loperec	37.0	25.301	1.038
101.2 - St Pierre Loperec	72.0	14.994	0.583
102.2 - St Pierre Loperec	83.5	10.233	0.444
105.2 - St Pierre Loperec	38.5	20.141	0.905
107.2 - St Pierre Loperec	35.5	14.057	0.793
108.2 - St Pierre Loperec	50.5	7.513	0.494
109.2 - St Pierre Loperec	64.5	11.009	0.506
110.2 - St Pierre Loperec	71.0	13.610	0.574
111.2 - St Pierre Loperec	72.0	13.181	0.564
113.2 - St Pierre Loperec	28.5	18.097	1.006
114.2 - St Pierre Loperec	82.0	13.121	0.502
115.2 - St Pierre Loperec	76.5	14.934	0.548
116.2 - St Pierre Loperec	35.0	18.295	0.941
117.2 - St Pierre Loperec	44.5	24.113	0.929
119.2 - St Pierre Loperec	33.5	16.767	0.888
120.2 - St Pierre Loperec	96.0	12.997	0.471
121.2 - St Pierre Loperec	73.0	14.917	0.578
123.2 - St Pierre Loperec	74.0	16.584	0.605
124.2 - St Pierre Loperec	24.0	18.733	1.094
125.2 - St Pierre Loperec	88.5	17.289	0.565
126.2 - St Pierre Loperec	72.5	13.790	0.570
127.2 - St Pierre Loperec	39.0	10.871	0.681
128.2 - St Pierre Loperec	37.5	7.755	0.589
129.2 - St Pierre Loperec	100.0	19.333	0.566
130.2 - St Pierre Loperec	98.0	5.578	0.313
131.2 - St Pierre Loperec	70.5	8.423	0.451
132.2 - St Pierre Loperec	44.5	17.875	0.816
210.2 - Kerouarc'h	50.0	14.816	0.721
211.2 - Kerouarc'h	86.5	12.186	0.458
212.2 - Kerouarc'h	37.5	18.999	0.860
214.2 - Locmariaquer	77.0	9.361	0.460
215.2 - Locmariaquer	92.0	9.605	0.427
216.2 - Locmariaquer	75.0	9.072	0.456
217.2 - Locmariaquer	81.5	10.592	0.472
218.2 - Locmariaquer	54.0	7.374	0.465
219.2 - Locmariaquer	71.5	3.870	0.308
220.2 - Locmariaquer	87.5	8.701	0.412
221.2 - Locmariaquer	64.5	8.808	0.481
299.2 - Fort Espagnol	75.5	10.227	0.464
300.2 - Fort Espagnol	75.5	11.475	0.497
301.2 - Fort Espagnol	63.5	12.115	0.561
303.2 - Fort Espagnol	129.5	12.355	0.400
304.2 - Fort Espagnol	70.5	12.275	0.541
305.2 - Fort Espagnol	69.0	11.406	0.505
306.2 - Fort Espagnol	68.5	15.488	0.620
307.2 - Fort Espagnol	93.0	10.576	0.439
332.2 - 2C2-2016	25.5	26.539	1.258
333.2 - 2C2-2016	21.0	20.179	1.178
334.2 - 2C2-2016	111.5	10.353	0.398
336.2 - 2C2-2016	75.5	15.129	0.589
337.2 - 2C2-2016	60.0	13.457	0.609
338.2 - 2C2-2016	61.0	11.507	0.550
339.2 - 2C2-2016	29.0	25.637	1.179
340.2 - 2C2-2016	26.5	19.246	1.090
341.2 - 2C2-2016	19.0	26.614	1.439
ST1A	22.5	21.250	1.300
ST1B	22.0	20.820	1.301
ST1C	18.5	21.460	1.441
ST1D	22.0	28.690	1.527
ST1E	22.0	24.960	1.424
ST1F	12.5	15.750	1.501
ST1G	24.0	17.300	1.135
ST1H	40.0	20.970	0.969
ST1I	29.0	20.330	1.120
ST1I-DL	20.5	26.620	1.524
ST1J	20.0	21.040	1.372
ST2A	15.0	25.680	1.750
ST2B	20.5	17.370	1.231
ST2C	15.0	22.070	1.622
ST2D	25.0	27.310	1.398
ST2E	30.0	23.950	1.195
ST2F	26.0	18.160	1.117
ST2G	14.5	25.740	1.781
ST2H	12.5	24.790	1.883
ST2J	24.5	22.300	1.275
ST2K	11.5	28.660	2.111
ST3A	21.0	25.210	1.465
ST3B	29.5	24.550	1.219
ST3C	19.0	20.500	1.389
ST3E	22.5	26.640	1.455
ST3F	17.5	22.220	1.507
ST3H	15.5	13.340	1.241

ST3I	23.0	16.960	1.148	**55B**	118.5	11.460	0.415	**95E**	24.5	22.470	1.280
ST3J	23.0	24.490	1.380	**55D**	87.0	11.180	0.479	**100A**	50.0	19.330	0.831
ST3L	16.5	19.910	1.469	**55E**	52.5	14.260	0.698	**100B**	97.0	10.210	0.433
ST3M	20.0	19.780	1.329	**60B**	21.0	8.430	0.846	**100C**	120.5	9.000	0.366
1A	33.0	21.880	1.090	**60C**	27.0	24.410	1.272	**100D**	96.0	10.120	0.433
1B	32.0	17.940	1.001	**60D**	100.5	12.350	0.469	**105A**	91.5	10.380	0.451
1C	106.0	16.220	0.523	**60E**	99.5	15.460	0.526	**105B**	45.0	17.060	0.823
1D	18.5	24.760	1.547	**65A**	111.0	10.100	0.403	**105C**	102.5	6.360	0.334
1E	17.5	20.950	1.464	**65B**	118.0	9.460	0.378	**105E**	115.5	13.210	0.451
5B	134.5	13.260	0.418	**65C**	24.5	20.490	1.223	**110A**	106.0	12.840	0.465
5C	113.0	6.580	0.324	**65D**	21.5	24.810	1.436	**110B**	112.5	15.950	0.505
5D	41.5	23.950	1.016	**70A**	21.0	16.600	1.189	**110E**	148.0	6.260	0.276
10A	89.5	11.170	0.472	**70B**	108.5	19.900	0.573	**110H**	79.0	10.870	0.495
15A	91.5	13.680	0.517	**70C**	86.5	12.480	0.508	**115A**	83.0	7.030	0.391
20A	37.0	18.090	0.936	**75B**	47.0	14.240	0.736	**120A**	53.5	19.130	0.800
30A	59.0	5.370	0.403	**80C**	33.5	22.230	1.090	**120B**	52.0	9.920	0.584
30B	127.5	10.990	0.391	**80D**	45.0	19.860	0.888	**120C**	41.0	16.560	0.850
40C	30.0	21.470	1.131	**80E**	25.5	24.410	1.309	**125A**	85.0	11.720	0.495
40D	28.5	17.780	1.056	**80H**	26.5	21.130	1.194	**125B**	28.0	6.880	0.663
40E	18.5	19.340	1.367	**85A**	116.5	10.170	0.395	**125D**	21.5	23.090	1.385
40F	38.0	11.410	0.733	**85B**	30.5	11.310	0.814	**125E**	41.5	20.000	0.929
45B	56.0	15.720	0.709	**85D**	38.5	22.910	1.031	**130B**	42.5	19.970	0.917
45C	72.0	12.910	0.567	**85G**	43.5	15.050	0.786	**130D**	110.0	5.410	0.299
45D	26.5	22.500	1.232	**90A**	16.0	18.110	1.423	**130E**	144.5	6.330	0.282
45E	33.0	21.460	1.078	**90B**	58.5	23.020	0.839	**130G**	128.5	8.740	0.348
50A	42.5	19.770	0.911	**90C**	133.0	11.290	0.391	**135B**	92.0	12.940	0.501
50B	128.5	11.820	0.407	**90D**	28.0	25.140	1.267	**135C**	94.5	15.200	0.535
50C	37.0	20.240	0.989	**95A**	24.5	16.700	1.104	**135D**	103.0	8.030	0.374
50E	23.5	33.890	1.606	**95B**	28.5	17.190	1.039	**135G**	43.0	19.250	0.894
55A	25.5	18.680	1.145	**95C**	29.0	23.260	1.198	**140A**	142.0	11.200	0.374

140B	100.0	9.250	0.407	**163A**	86.0	7.810	0.403	**180A**	101.0	14.440	0.505
140C	109.5	14.650	0.489	**163B**	131.0	14.360	0.444	**180B**	122.5	10.860	0.399
145A	117.5	9.310	0.374	**163C**	37.5	7.710	0.608	**180E**	130.0	11.810	0.403
145C	81.0	20.520	0.672	**163D-PA**	92.0	7.520	0.383	**b1**	27.0	20.780	1.173
145D	38.0	24.510	1.073	**164A**	96.5	12.540	0.482	**b2**	42.0	20.040	0.924
145E	119.5	8.200	0.352	**164B**	109.0	9.000	0.383	**b3**	19.5	27.030	1.575
150A	95.5	10.030	0.433	**164C**	38.0	14.790	0.835	**b4**	26.5	18.040	1.103
155A	67.0	10.370	0.526	**165A**	97.0	9.450	0.418	**b5**	31.0	17.080	0.992
155B	117.0	7.900	0.348	**165B**	112.5	10.200	0.403	**b6**	31.0	21.450	1.113
157A	42.5	21.310	0.947	**166A**	115.5	9.780	0.387	**b7**	32.0	20.680	1.075
157B	71.0	12.530	0.561	**166B**	99.0	12.720	0.479	**b8**	31.0	17.620	1.008
157C	92.5	15.070	0.541	**166C-PA**	93.0	12.400	0.475	**b9**	20.5	20.700	1.343
157D-PA	56.0	9.460	0.550	**166D-PA**	87.0	7.190	0.383	**b10**	34.0	27.560	1.203
158A	90.0	10.220	0.451	**167A**	104.0	12.240	0.458	**b11**	29.0	21.190	1.144
158B	155.0	14.650	0.411	**168A**	105.0	14.360	0.495	**z1**	17.0	18.670	1.401
158C	106.5	11.140	0.433	**168B**	89.5	12.760	0.505	**z2**	25.5	23.590	1.287
159A	80.0	12.380	0.526	**168C**	119.0	10.300	0.395	**z3**	33.0	21.460	1.078
159B	44.5	13.840	0.746	**168D**	33.0	19.340	1.023	**z4**	18.0	16.430	1.278
159C-PA	129.0	11.510	0.399	**169A**	143.0	9.880	0.352	**z5**	35.5	14.750	0.861
159D-PA	124.0	10.160	0.383	**169B**	124.0	9.410	0.370	**z6**	19.5	22.380	1.433
160C	88.0	12.370	0.501	**169C**	108.0	11.270	0.433	**z7**	20.5	27.540	1.550
160E	111.0	4.200	0.259	**169D**	52.5	5.190	0.426	**z8**	16.0	18.920	1.454
160F	48.5	12.870	0.689	**170A**	79.0	9.510	0.465	**z9**	21.0	21.300	1.347
160G	58.5	10.740	0.573	**170B**	106.0	11.350	0.437	**z10**	23.5	27.170	1.438
160I	126.5	10.670	0.387	**170D**	106.0	9.700	0.403	**z11**	33.0	28.200	1.236
161A	110.0	12.530	0.451	**170E**	88.0	11.950	0.492	**z12**	19.0	17.220	1.273
161B	44.0	9.900	0.633	**175A**	98.0	12.890	0.485	**a1**	12.0	26.450	1.985
161C	78.5	14.440	0.573	**175B**	95.0	16.000	0.550	**a2**	25.5	15.960	1.059
161D	104.5	12.180	0.455	**175C**	114.0	7.250	0.339	**a3**	41.0	4.500	0.444
162A	112.5	12.480	0.444	**175D**	98.5	6.820	0.352	**a4**	38.5	20.020	0.964

a5	29.0	21.770	1.159	**s8**	20.0	22.070	1.405	**h7-1**	37.5	17.280	0.908
a6	35.0	16.970	0.930	**s9**	19.0	20.240	1.380	**h7-2**	35.5	18.410	0.962
a7	32.5	16.660	0.957	**s10**	13.0	24.500	1.836	**h7-3**	34.0	21.850	1.072
a8	20.5	18.860	1.283	**s11**	24.0	20.770	1.244	**h7-4**	41.0	20.850	0.954
a9	23.5	19.420	1.215	**s12**	26.0	18.210	1.118	**h7-5**	46.0	18.280	0.843
a10	28.5	16.290	1.011	**f1**	24.5	10.430	0.872	**h14-1**	51.0	16.280	0.755
a11	32.0	19.100	1.033	**f4**	24.0	18.880	1.186	**h14-2**	29.0	21.980	1.164
a12	21.5	21.960	1.352	**f7**	42.5	18.780	0.888	**h14-3**	35.5	17.200	0.930
a13	29.0	22.460	1.177	**m1**	14.0	13.850	1.330	**h14-4**	46.5	18.250	0.837
a14	22.0	19.470	1.258	**m2**	25.0	18.400	1.147	**h14-5**	41.0	19.800	0.929
r1	24.0	15.540	1.076	**m3**	25.0	23.370	1.293	**h15-2**	24.5	23.500	1.310
r2	23.5	14.740	1.059	**m4**	24.5	16.430	1.095	**h15-4**	40.0	15.360	0.829
r3	33.5	20.800	1.054	**m5**	20.5	22.580	1.404	**h15-5**	37.0	25.900	1.118
r4	28.5	17.700	1.054	**m6**	30.5	18.480	1.040	**h15-6**	40.5	25.510	1.062
r5	18.5	14.760	1.194	**img42**	31.5	21.380	1.101	**h15-7**	16.0	12.800	1.195
r6	28.0	16.880	1.039	**img44**	36.5	25.330	1.114	**h17-1**	24.0	16.250	1.100
r7	18.0	18.880	1.369	**img46**	26.5	25.470	1.311	**h17-2**	32.5	16.100	0.941
r8	47.0	19.950	0.870	**img48**	26.5	26.140	1.328	**h17-3**	37.0	15.730	0.872
r9	38.0	21.320	1.001	**img50**	29.5	23.740	1.199	**h17-4**	35.0	20.910	1.034
r10	28.0	29.350	1.369	**img52**	29.0	26.450	1.277	**E1-02**	92.5	6.910	0.366
r11	39.0	20.310	0.966	**img54**	24.0	23.660	1.328	**E2-02**	86.5	5.690	0.343
r12	27.5	25.840	1.296	**img56**	48.5	22.070	0.903	**E3-02**	78.5	11.250	0.505
r13	25.5	15.320	1.036	**img58**	39.0	21.030	0.982	**E4-02**	87.5	8.580	0.418
s1	27.5	16.190	1.026	**img60**	29.0	25.790	1.262	**E5-02**	80.5	4.960	0.334
s2	28.0	18.010	1.072	**img63**	29.5	22.130	1.158	**E6-02**	124.0	6.610	0.309
s3	17.5	28.860	1.718	**am1**	47.0	29.190	1.054	**SEMA64a1-002**	18.5	27.931	1.643
s4	20.0	16.320	1.207	**am2-02**	31.5	24.170	1.171	**SEMA64a2-002**	21.5	17.718	1.214
s5	18.0	17.670	1.326	**am2-03**	36.5	16.870	0.910	**SEMA64a3-002**	32.0	20.800	1.078
s6	16.0	14.250	1.262	**am3-02**	28.5	22.860	1.198	**SEMA64a4-002**	24.0	13.460	1.001
s7	20.5	17.230	1.226	**am3-03**	33.5	21.040	1.060	**SEMA64a5-002**	39.5	17.056	0.879

SEMA64a6-002	31.0	19.689	1.066	**image14**	24.5	16.100	1.084	**image111**	42.5	13.298	0.748
SEMA64a7-002	31.0	12.400	0.846	**image16**	30.5	16.633	0.988	**image113**	22.0	19.991	1.275
SEMA64a8-002	21.5	21.142	1.326	**image18**	28.5	29.504	1.361	**image115**	18.0	22.704	1.502
SEMA64a9-002	34.5	10.209	0.727	**image20**	23.5	14.169	1.038	**image117**	33.0	20.487	1.054
SEMA64a10-002	25.0	23.073	1.285	**image22**	23.5	15.038	1.070	**image121**	19.0	17.356	1.278
GREV1A23-002	20.0	19.920	1.335	**image24**	24.0	19.640	1.210	**image123**	29.0	21.271	1.145
GREV1A24-002	18.0	18.416	1.353	**image26**	22.5	17.989	1.196	**image129**	19.5	24.044	1.485
GREV2A17-002	23.0	25.509	1.408	**image28**	31.0	12.564	0.851	**image133**	32.5	23.276	1.132
GREV2A18-002	15.5	21.962	1.592	**image30**	20.5	17.178	1.224	**image135**	23.5	21.376	1.275
GREV2A19-002	27.0	25.436	1.298	**image32**	21.0	16.180	1.174	**image137**	18.5	20.364	1.403
GREV2A20-002	16.5	22.184	1.551	**image34**	23.0	15.853	1.110	**image141**	32.0	21.409	1.094
GREV2A21-002	18.0	23.291	1.521	**image36**	21.0	14.820	1.123	**image145**	25.0	23.589	1.299
GREV2A22-002	15.5	18.327	1.454	**image38**	25.5	19.856	1.180	**image147**	33.5	12.562	0.819
GREV3B11-002	13.0	18.624	1.601	**image40**	23.0	17.147	1.155	**J1-02**	70.5	8.320	0.458
GREV3B12-002	29.5	25.856	1.252	**image75**	36.5	19.609	0.980	**J2-02**	137.5	6.580	0.293
GREV3B13-002	17.5	16.864	1.313	**image77**	31.0	15.464	0.944	**J3-02**	97.0	4.650	0.309
GREV3B14-002	13.0	22.433	1.757	**image79**	25.0	19.320	1.176	**J4-02**	121.5	6.490	0.309
GREV3B15-002	21.5	19.653	1.279	**image83**	26.0	21.131	1.206	**J5-02**	79.0	2.840	0.252
GREV3B16-002	19.5	22.367	1.432	**image85**	20.5	14.938	1.141	**J6-02**	122.0	9.170	0.366
image65	20.0	13.853	1.113	**image87**	22.5	19.369	1.241	**J7-02**	60.0	8.170	0.495
image67	18.5	17.520	1.301	**image91**	25.0	12.776	0.956	**J8-02**	79.5	2.670	0.246
image69	20.0	16.213	1.204	**image93**	17.5	16.873	1.313	**J9-02**	112.0	6.910	0.334
image71	29.0	18.800	1.077	**image95**	27.0	16.629	1.049	**J10-02**	129.0	9.550	0.366
image73	25.0	17.182	1.109	**image97**	20.0	21.918	1.400	**J11-02**	108.0	4.840	0.282
image04	31.0	19.731	1.067	**image99**	25.0	18.200	1.141	**J12-02**	77.0	5.340	0.352
image05	18.0	12.509	1.115	**image101**	34.5	14.993	0.882	**J13-02**	71.0	4.240	0.329
image06	24.0	17.222	1.133	**image103**	24.0	12.427	0.962	**J14-02**	100.0	3.430	0.246
image08	26.0	20.276	1.181	**image105**	23.5	21.476	1.278	**J16-02**	59.0	2.390	0.271
image10	23.0	10.018	0.883	**image107**	19.5	21.224	1.395	**J17-02**	50.0	6.710	0.489
image12	23.0	22.484	1.322	**image109**	23.5	13.084	0.998	**J18-02**	48.5	2.940	0.329

J19-02	127.5	11.830	0.407	**AMMONIA-022**	12.5	26.342	1.941	**AMMONIA-084**	23.5	26.120	1.410
J21-02	117.5	13.790	0.458	**AMMONIA-024**	18.5	21.349	1.437	**AMMONIA-086**	26.0	20.720	1.194
J22-02	70.0	9.760	0.498	**AMMONIA-026**	12.5	22.602	1.798	**AMMONIA-088**	35.0	19.718	1.004
J23-02	74.0	5.340	0.361	**AMMONIA-028**	18.0	22.049	1.480	**AMMONIA-090**	24.5	24.891	1.348
J24-02	90.5	6.710	0.366	**AMMONIA-030**	18.5	25.300	1.564	**AMMONIA-092**	10.0	27.158	2.204
J25-02	81.5	7.920	0.418	**AMMONIA-032**	14.5	23.558	1.704	**AMMONIA-094**	21.0	29.411	1.583
J26-02	88.5	6.180	0.352	**AMMONIA-034**	21.5	17.371	1.202	**AMMONIA-096**	11.0	26.604	2.080
J27-02	51.0	5.130	0.422	**AMMONIA-036**	19.0	20.922	1.403	**AMMONIA-098**	26.0	24.284	1.292
J28-02	82.0	10.870	0.485	**AMMONIA-038**	11.0	22.840	1.927	**AMMONIA-100**	21.5	25.002	1.442
J30-02	113.5	8.950	0.374	**AMMONIA-040**	29.0	15.458	0.976	**AMMONIA-102**	15.5	26.749	1.757
J31-02	134.0	5.680	0.276	**AMMONIA-042**	14.0	27.707	1.881	**AMMONIA-104**	24.5	31.851	1.525
J32-02	99.0	12.880	0.482	**AMMONIA-044**	21.0	22.222	1.376	**AMMONIA-106**	23.0	19.244	1.223
J33-02	95.0	8.220	0.395	**AMMONIA-046**	17.5	13.593	1.179	**AMMONIA-108**	21.0	25.169	1.464
J34-02	47.0	9.090	0.589	**AMMONIA-048**	15.5	21.629	1.580	**AMMONIA-110**	20.5	18.798	1.280
J35-02	63.5	9.120	0.508	**AMMONIA-052**	23.0	18.940	1.213	**AMMONIA-112**	23.0	26.924	1.447
J36-02	94.0	6.430	0.348	**AMMONIA-054**	20.0	22.929	1.432	**AMMONIA-114**	12.5	23.558	1.836
J37-02	77.5	9.710	0.472	**AMMONIA-056**	20.5	25.056	1.478	**AMMONIA-116**	15.0	21.864	1.615
J38-02	84.0	9.200	0.444	**AMMONIA-058**	20.5	17.731	1.244	**AMMONIA-118**	21.0	30.322	1.607
J39-02	63.5	9.860	0.526	**AMMONIA-060**	21.0	19.767	1.297	**AMMONIA1-002**	16.5	13.493	1.209
J40-02	87.0	6.350	0.361	**AMMONIA-062**	23.0	22.504	1.323	**AMMONIA1-004**	31.0	19.649	1.065
AMMONIA-002	25.0	21.762	1.248	**AMMONIA-064**	25.5	17.727	1.115	**AMMONIA1-006**	18.0	17.362	1.313
AMMONIA-004	28.5	23.540	1.215	**AMMONIA-066**	22.0	13.851	1.061	**AMMONIA1-008**	28.0	17.198	1.048
AMMONIA-006	21.0	21.073	1.340	**AMMONIA-068**	21.0	22.718	1.391	**AMMONIA1-010**	14.5	15.718	1.392
AMMONIA-008	16.0	16.424	1.355	**AMMONIA-070**	28.5	16.887	1.029	**AMMONIA1-012**	15.5	13.704	1.257
AMMONIA-010	14.0	27.029	1.858	**AMMONIA-072**	20.0	32.367	1.701	**AMMONIA1-014**	10.0	11.749	1.449
AMMONIA-012	23.5	23.358	1.333	**AMMONIA-074**	15.5	27.093	1.768	**AMMONIA1-016**	11.5	21.204	1.816
AMMONIA-014	15.0	20.369	1.558	**AMMONIA-076**	21.5	25.098	1.445	**AMMONIA1-018**	17.5	20.216	1.437
AMMONIA-016	18.5	16.931	1.279	**AMMONIA-078**	25.0	23.898	1.307	**AMMONIA1-020**	14.5	16.504	1.427
AMMONIA-018	15.0	21.129	1.587	**AMMONIA-080**	21.5	11.469	0.977	**AMMONIA1-022**	21.0	17.522	1.221
AMMONIA-020	18.0	19.609	1.396	**AMMONIA-082**	18.0	30.838	1.750	**AMMONIA1-024**	20.0	18.611	1.290

AMMONIA1-026	18.0	19.787	1.402	**AMMONIA1-088**	18.0	12.644	1.121	**E13-002**	8.0	18.896	2.055
AMMONIA1-028	8.0	11.376	1.595	**AMMONIA1-090**	19.5	19.567	1.340	**E14-002**	15.5	23.293	1.639
AMMONIA1-030	15.0	17.842	1.458	**AMMONIA1-092**	17.5	15.331	1.252	**E15-002**	24.0	22.753	1.302
AMMONIA1-032	15.0	16.933	1.421	**AMMONIA1-094**	13.5	20.067	1.630	**E16-002**	17.0	17.798	1.368
AMMONIA1-034	15.5	22.416	1.608	**AMMONIA1-096**	21.5	14.676	1.105	**E17-002**	12.0	25.933	1.966
AMMONIA1-036	14.0	18.687	1.545	**AMMONIA1-098**	16.5	18.153	1.403	**E18-002**	14.5	16.156	1.411
AMMONIA1-038	24.0	11.049	0.907	**AMMONIA1-100**	17.5	13.878	1.191	**E19-002**	17.5	22.131	1.504
AMMONIA1-040	12.5	19.842	1.685	**AMMONIA1-102**	13.0	18.484	1.595	**E20-002**	17.5	23.696	1.556
AMMONIA1-043	16.0	21.033	1.533	**AMMONIA1-104**	16.5	20.642	1.496	**E21-002**	12.5	29.744	2.063
AMMONIA1-045	13.0	11.851	1.277	**AMMONIA1-106**	24.0	17.704	1.149	**E22-002**	16.5	25.644	1.667
AMMONIA1-047	14.0	20.591	1.622	**AMMONIA1-108**	19.0	10.258	0.983	**E23-002**	21.0	26.344	1.498
AMMONIA1-049	24.5	19.056	1.179	**AMMONIA1-110**	12.0	20.367	1.742	**E24-002**	12.5	20.602	1.717
AMMONIA1-051	15.0	18.873	1.500	**AMMONIA1-112**	20.0	15.440	1.175	**E25-002**	19.0	17.142	1.270
AMMONIA1-053	13.5	13.356	1.330	**AMMONIA1-114**	17.0	18.107	1.380	**AMMONIA1-124**	27.0	12.396	0.906
AMMONIA1-055	15.5	22.136	1.598	**AMMONIA1-116**	14.0	17.262	1.485	**AMMONIA1-126**	22.5	14.722	1.082
AMMONIA1-057	14.0	15.869	1.424	**AMMONIA1-118**	15.5	23.411	1.643	**AMMONIA1-129**	19.5	14.040	1.135
AMMONIA1-059	21.5	22.258	1.361	**AMMONIA1-120**	22.5	15.202	1.099	**AMMONIA-131**	18.0	17.404	1.315
AMMONIA1-061	16.0	23.580	1.623	**AMMONIA1-122**	15.0	16.751	1.413	**AMMONIA1-133**	21.5	10.924	0.953
AMMONIA1-063	19.5	20.484	1.371	**E1-002**	12.5	21.273	1.745	**AMMONIA1-135**	14.5	8.929	1.049
AMMONIA1-065	15.5	21.242	1.565	**E2-002**	15.5	25.329	1.709	**AMMONIA1-137**	14.5	18.433	1.508
AMMONIA1-067	14.0	14.453	1.359	**E3-002**	17.0	16.771	1.328	**AMMONIA1-139**	19.0	15.673	1.215
AMMONIA1-070	13.5	17.120	1.506	**E4-002**	18.0	21.871	1.474	**AMMONIA1-141**	17.5	19.882	1.425
AMMONIA1-072	17.0	23.156	1.561	**E5-002**	19.5	10.800	0.995	**AMMONIA1-143**	22.0	17.531	1.194
AMMONIA1-074	11.5	10.676	1.288	**E6-002**	7.5	17.693	2.054	**AMMONIA1-145**	12.0	19.978	1.725
AMMONIA1-076	10.0	16.540	1.720	**E7-002**	22.0	22.367	1.348	**AMMONIA1-147**	13.0	13.876	1.382
AMMONIA1-078	17.5	18.922	1.390	**E8-002**	19.5	26.040	1.545	**AMMONIA1-149**	25.5	22.602	1.259
AMMONIA1-080	12.5	15.131	1.471	**E9-002**	25.0	19.262	1.174	**AMMONIA1-151**	14.5	19.198	1.539
AMMONIA1-082	27.5	18.324	1.092	**E10-002**	17.5	17.898	1.352	**AMMONIA1-153**	19.5	19.027	1.321
AMMONIA1-084	18.5	17.598	1.304	**E11-002**	19.0	21.591	1.426	**AMMONIA1-155**	16.5	19.631	1.459
AMMONIA1-086	16.5	18.216	1.405	**E12-002**	15.0	18.638	1.491	**AMMONIA1-157**	14.0	16.640	1.458

AMMONIA1-159	7.5	16.189	1.965	**A156**	18.0	21.711	1.469	**A216**	22.5	14.827	1.086
AMMONIA1-161	19.0	16.847	1.259	**A158**	21.5	14.522	1.099	**A218**	17.0	18.878	1.409
AMMONIA1-163	12.0	17.936	1.635	**A160**	15.5	20.191	1.526	**A220**	17.0	21.722	1.512
AMMONIA1-165	20.0	16.793	1.225	**A162**	23.5	17.029	1.138	**A222**	18.0	18.809	1.367
AMMONIA1-167	10.0	12.411	1.490	**A164**	22.0	17.218	1.183	**A224**	15.5	19.769	1.510
AMMONIA1-169	19.0	20.902	1.403	**A166**	18.0	17.393	1.314	**A226**	12.0	19.540	1.706
AMMONIA1-171	16.0	21.651	1.556	**A168**	11.5	19.122	1.724	**A228**	20.5	21.293	1.363
AMMONIA1-173	7.5	20.260	2.198	**A170**	18.0	19.713	1.399	**A230**	14.5	19.207	1.539
AMMONIA1-175	11.5	15.764	1.566	**A172**	18.0	25.147	1.581	**A232**	20.0	18.147	1.274
AMMONIA1-177	11.5	16.893	1.621	**A174**	22.5	20.522	1.277	**A234**	16.5	19.187	1.442
AMMONIA1-178A	22.5	6.896	0.740	**A176**	23.5	17.429	1.152	**A236**	23.0	27.936	1.474
AMMONIA1-180	14.5	19.360	1.545	**A178**	14.5	20.282	1.582	**A238**	31.5	20.936	1.090
AMMONIA1-182	28.0	18.424	1.085	**A180**	11.5	19.584	1.745	**A240**	28.0	18.116	1.076
A122	23.0	20.462	1.261	**A182**	18.0	18.793	1.366	**A242**	15.0	18.564	1.488
A124	28.5	27.260	1.308	**A184**	21.0	20.822	1.332	**A244**	18.5	23.764	1.516
A126	26.0	22.956	1.257	**A186**	16.0	19.796	1.487	**A246**	12.0	20.022	1.727
A128	27.0	13.082	0.931	**A188**	16.0	22.264	1.577	**A248**	15.5	20.996	1.556
A130	18.5	18.113	1.323	**A190**	17.5	16.040	1.280	**A250**	21.0	18.996	1.272
A132	13.5	20.091	1.631	**A192**	19.0	13.947	1.146	**A252**	16.0	20.222	1.503
A134	24.0	21.120	1.254	**A194**	22.0	16.858	1.171	**A254**	15.0	12.920	1.241
A136	18.0	24.669	1.565	**A196**	22.5	21.956	1.321	**A256**	21.0	17.678	1.227
A138	15.5	17.542	1.423	**A198**	15.5	18.242	1.451	**A258**	12.5	17.569	1.585
A140	24.0	18.618	1.178	**A200**	14.0	15.967	1.428	**A260**	13.5	18.524	1.566
A142	15.5	19.456	1.498	**A202**	14.0	22.587	1.698	**A262**	19.0	19.602	1.358
A144	19.5	16.664	1.236	**A204**	21.0	15.651	1.154	**A264**	20.5	16.153	1.187
A146	16.0	14.882	1.290	**A206**	18.5	14.607	1.188	**A266**	15.0	21.753	1.610
A148	17.0	17.467	1.355	**A208**	16.0	19.169	1.464	**A268**	14.5	14.671	1.345
A150	12.0	23.556	1.874	**A210**	13.5	18.704	1.574	**A270**	17.5	17.898	1.352
A152	18.5	17.184	1.289	**A212**	22.0	19.542	1.260	**A272**	18.5	16.438	1.261
A154	20.0	21.084	1.373	**A214**	21.0	18.689	1.262	**A274**	20.0	22.709	1.425

A276	14.5	22.438	1.663	**A337**	18.5	21.922	1.456	**A036**	20.0	25.373	1.506
A279	22.0	12.718	1.017	**A339**	11.5	15.564	1.556	**A038**	28.5	10.229	0.801
A281	14.0	14.062	1.340	**A341**	18.5	23.202	1.498	**A040**	21.0	17.989	1.238
A283	15.0	20.660	1.569	**A343**	26.5	23.513	1.260	**A042**	13.5	24.609	1.805
A285	18.5	22.507	1.475	**A346**	6.5	19.740	2.330	**A044**	16.5	15.438	1.293
A287	19.5	14.198	1.141	**A348**	20.5	14.598	1.128	**A046**	17.0	17.740	1.366
A289	16.0	20.471	1.513	**A350**	20.0	17.424	1.248	**A048**	20.5	17.569	1.238
A291	12.5	12.811	1.354	**A352**	22.5	16.473	1.144	**A050**	26.5	19.153	1.137
A293	16.0	15.358	1.310	**A354**	16.0	21.807	1.561	**A052**	28.5	13.044	0.905
A295	18.5	16.636	1.268	**A356**	21.0	30.978	1.624	**A054**	27.0	17.400	1.073
A297	24.5	21.824	1.262	**A358**	29.0	20.307	1.119	**A056**	28.5	18.053	1.064
A299	17.0	15.213	1.265	**A360**	18.0	13.553	1.160	**A058**	10.0	15.271	1.653
A301	15.0	20.824	1.576	**A362**	15.5	21.724	1.583	**A060**	21.0	18.056	1.240
A303	19.5	15.638	1.197	**A002**	16.5	20.138	1.477	**A062**	22.0	23.609	1.385
A305	19.5	21.056	1.390	**A004**	10.5	16.033	1.652	**A064**	20.5	19.353	1.299
A307	14.0	23.238	1.723	**A006**	19.0	12.769	1.096	**A066**	26.5	23.393	1.256
A309	21.0	14.927	1.127	**A008**	24.5	22.722	1.288	**A068**	16.5	18.587	1.419
A311	18.0	14.453	1.198	**A010**	14.5	20.818	1.602	**A070**	19.5	20.002	1.354
A313	10.0	22.596	2.010	**A012**	17.0	16.476	1.316	**A072**	28.5	12.558	0.888
A315	20.5	16.736	1.208	**A014**	15.0	8.909	1.031	**A74**	16.5	21.460	1.525
A317	21.0	13.511	1.073	**A016**	23.5	17.167	1.143	**A076**	13.5	19.889	1.623
A319	18.5	20.689	1.414	**A018**	19.5	15.280	1.184	**A078**	26.5	20.058	1.163
A321	22.5	15.664	1.116	**A020**	23.5	18.782	1.195	**A080**	12.5	19.207	1.658
A323	16.5	15.884	1.312	**A022**	26.0	24.220	1.291	**A082**	19.5	19.684	1.344
A325	24.0	21.236	1.258	**A024**	25.5	13.460	0.971	**A084**	15.5	17.300	1.413
A327	16.5	13.609	1.214	**A026**	16.0	21.560	1.552	**A086**	20.0	18.858	1.298
A329	13.5	15.460	1.431	**A028**	16.5	18.156	1.403	**A088**	19.0	9.093	0.925
A331	18.5	22.900	1.488	**A030**	18.5	22.078	1.461	**A090**	21.0	18.487	1.255
A333	16.0	20.251	1.504	**A032**	15.5	18.827	1.474	**A092**	15.5	19.898	1.515
A335	16.5	18.760	1.426	**A034**	14.5	18.236	1.500	**A094**	17.5	26.400	1.642

A096	17.0	17.071	1.340	**G18-002**	14.0	24.547	1.771	**ZK17**	24.0	20.444	1.234
A098	25.0	12.882	0.960	**G19-003**	16.0	15.858	1.331	**ZK18**	21.0	19.433	1.286
A100	23.5	18.184	1.176	**G20-003**	27.0	23.042	1.235	**ZK19**	23.0	21.407	1.290
A102	25.0	17.391	1.115	**G21-002**	31.5	25.936	1.213	**ZK20**	19.5	20.538	1.372
A104	14.5	17.544	1.471	**G22-003**	27.0	23.676	1.252	**ZK21**	74.0	12.944	0.559
A106	19.5	22.247	1.428	**G23-002**	32.0	25.053	1.183	**ZK22**	16.0	22.167	1.574
A108	24.0	11.158	0.912	**G24-003**	22.5	23.360	1.363	**ZK23**	68.0	14.256	0.612
A110	17.0	24.013	1.589	**G25-002**	18.5	28.653	1.664	**ZK24**	66.5	19.360	0.722
A112	16.5	16.153	1.323	**G26-002**	18.0	28.029	1.669	**ZK25**	24.5	17.447	1.128
A114	15.5	17.104	1.405	**G27-003**	25.5	20.931	1.212	**ZK26**	14.5	23.420	1.699
A116	17.5	15.524	1.260	**G28-002**	19.0	24.153	1.508	**ZK27**	85.5	10.160	0.461
A118	30.0	23.947	1.195	**G29-002**	41.5	23.193	1.000	**ZK28**	28.0	28.616	1.352
A120	16.0	15.698	1.325	**G30-002**	25.5	17.909	1.121	**ZK29**	18.0	24.524	1.561
G1-002	86.5	13.982	0.538	**G31-002**	27.0	21.860	1.203	**ZK30**	23.5	20.240	1.241
G2-002	28.5	31.296	1.401	**ZK1**	16.0	24.153	1.643	**ZK31**	10.0	21.729	1.971
G3-003	18.0	19.100	1.377	**ZK2**	27.5	15.804	1.014	**ZK32**	10.0	19.591	1.872
G4-003	21.0	25.649	1.478	**ZK3**	28.5	15.204	0.977	**ZK33**	36.0	24.493	1.103
G5-002	24.0	18.813	1.184	**ZK4**	20.5	27.049	1.536	**ZK34**	30.0	16.102	0.980
G6-002	18.5	21.960	1.457	**ZK5**	25.0	20.869	1.222	**ZK35**	48.0	9.573	0.597
G7-002	19.5	20.429	1.369	**ZK6**	20.0	21.913	1.400	**ZK36**	38.5	16.460	0.874
G8-002	21.0	18.393	1.251	**ZK7**	21.0	24.042	1.431	**ZK37**	15.5	21.307	1.568
G9-002	26.5	20.149	1.166	**ZK8**	18.5	27.942	1.643	**ZK38**	75.5	13.047	0.556
G10-003	24.0	21.569	1.268	**ZK9**	20.5	19.467	1.303	**ZK39**	79.5	14.978	0.580
G11-002	28.0	21.907	1.183	**ZK10**	28.5	29.109	1.351	**ZK40**	101.0	13.529	0.489
G12-002	23.5	16.656	1.126	**ZK11**	28.5	21.709	1.167	**ZK41**	23.0	20.887	1.274
G13-002	34.0	20.749	1.045	**ZK12**	16.5	19.036	1.436	**ZK42**	15.5	20.238	1.528
G14-002	17.0	25.953	1.652	**ZK13**	30.0	22.089	1.147	**ZK43**	92.0	12.024	0.483
G15-003	19.0	22.373	1.451	**ZK14**	23.0	21.389	1.290	**ZK44**	14.0	19.182	1.565
G16-003	19.0	21.000	1.406	**ZK15**	19.0	24.216	1.510	**ZK45**	23.0	20.609	1.266
G17-003	19.5	20.951	1.386	**ZK16**	26.0	14.191	0.988	**ZK46**	20.0	19.909	1.334

ZK47	22.0	14.804	1.097	**ZK77**	99.0	16.098	0.539	**SN80**	17.5	22.909	1.530
ZK48	16.0	26.447	1.719	**ZK78**	58.0	5.371	0.407	**SN81**	22.0	18.669	1.232
ZK49	29.0	20.018	1.111	**ZK79**	66.0	11.531	0.559	**SN82**	29.0	16.169	0.999
ZK50	15.0	20.591	1.567	**ZK80**	78.0	11.284	0.509	**SN83**	23.0	18.816	1.209
ZK51	33.5	17.853	0.976	**SN54**	33.5	14.642	0.884	**SN84**	29.0	13.429	0.910
ZK52	16.5	24.129	1.617	**SN55**	25.5	19.782	1.178	**SN85**	23.0	11.451	0.944
ZK53	14.5	19.569	1.553	**SN56**	29.0	12.511	0.878	**SN86**	30.5	23.893	1.184
ZK54	21.0	19.282	1.281	**SN57**	28.5	12.767	0.895	**SN87**	27.5	15.167	0.993
ZK55	21.0	18.538	1.256	**SN58**	24.5	18.271	1.155	**SN88**	35.5	17.418	0.937
ZK56	22.0	27.476	1.494	**SN59**	28.0	18.009	1.072	**SN89**	25.5	17.933	1.121
ZK57	20.0	14.638	1.144	**SN60**	13.0	22.447	1.757	**SN90**	21.0	18.469	1.254
ZK58	20.5	21.409	1.367	**SN61**	26.0	16.922	1.079	**SN91**	30.5	22.471	1.148
ZK59	19.5	19.762	1.346	**SN62**	22.5	15.402	1.106	**SN92**	23.0	20.584	1.265
ZK60	13.0	17.120	1.535	**SN63**	28.5	14.718	0.961	**SN93**	27.0	21.969	1.206
ZK61	34.0	24.807	1.142	**SN64**	23.0	20.736	1.270	**SN94**	11.0	22.371	1.907
ZK62	89.0	13.436	0.520	**SN65**	30.0	13.800	0.907	**SN95**	13.5	13.791	1.352
ZK63	53.0	14.109	0.690	**SN66**	24.0	16.371	1.104	**SN96**	16.0	19.133	1.462
ZK64	39.0	25.649	1.084	**SN67**	19.0	20.558	1.391	**SN97**	15.5	17.893	1.437
ZK65	34.0	18.889	0.997	**SN68**	18.5	15.247	1.214	**SN98**	15.5	25.069	1.701
ZK66	55.0	19.322	0.793	**SN69**	31.5	25.789	1.210	**SN100**	26.5	21.362	1.201
ZK67	85.0	6.207	0.361	**SN70**	20.0	19.560	1.322	**SN101**	28.0	20.898	1.155
ZK68	72.5	11.800	0.539	**SN71**	18.0	21.193	1.451	**SN102**	28.5	18.296	1.071
ZK69	64.5	12.442	0.587	**SN72**	29.5	20.209	1.107	**SN103**	19.0	22.722	1.462
ZK70	34.5	20.660	1.035	**SN73**	28.0	21.649	1.176	**SN104**	17.0	34.716	1.911
ZK71	27.5	25.071	1.277	**SN74**	24.5	17.227	1.121	**SN105**	30.5	20.196	1.088
ZK72	71.5	12.902	0.568	**SN75**	23.5	15.320	1.080	**SN106**	31.5	17.542	0.998
ZK73	46.5	10.464	0.634	**SN76**	27.0	20.576	1.167	**SN107**	37.0	16.551	0.894
ZK74	45.0	9.702	0.621	**SN77**	21.0	18.271	1.247	**SN108**	24.5	20.698	1.229
ZK75	25.5	24.598	1.313	**SN78**	27.5	20.711	1.160	**SN110**	21.5	12.876	1.035
ZK76	16.0	16.693	1.366	**SN79**	20.0	21.849	1.398	**SN111**	24.0	19.342	1.200

SN112	13.0	22.782	1.770	**E1-11**	30.0	18.782	1.058	**E4-18**	15.5	16.738	1.450
SN113	18.5	17.460	1.299	**E1-12**	37.0	22.993	1.054	**E4-19**	30.0	14.973	0.945
SN114	18.0	15.162	1.227	**E1-13**	40.0	16.629	0.862	**E4-20**	25.5	17.831	1.118
SN115	26.0	17.564	1.099	**E1-14**	25.0	17.051	1.104	**E4-21**	25.5	12.716	0.944
SN116	25.0	19.031	1.167	**E1-15**	27.5	20.756	1.162	**E4-22**	31.0	15.580	0.948
SN118	22.5	18.769	1.221	**E1-16**	27.5	14.736	0.979	**E4-23**	30.0	19.060	1.066
SN119	22.5	15.082	1.095	**E1-17**	34.0	17.751	0.966	**E4-24**	20.5	22.147	1.390
SN120	19.0	18.349	1.314	**E1-18**	44.5	14.504	0.763	**E4-25**	20.0	16.838	1.227
SN121	23.0	17.342	1.161	**E1-19**	44.0	9.864	0.633	**E4-26**	31.0	17.693	1.010
SN122	17.0	19.407	1.429	**E1-20**	57.0	13.667	0.655	**E4-27**	37.5	13.358	0.798
SN123	26.0	12.711	0.935	**E2**	27.0	16.733	1.053	**E4-28**	34.0	15.364	0.899
RD1	90.0	13.011	0.508	**E2-2**	14.5	21.302	1.621	**E4-29**	29.0	19.549	1.098
RD2	81.0	13.264	0.541	**E2-3**	21.5	16.538	1.173	**E4-30**	24.5	19.220	1.184
RD3	95.5	20.324	0.617	**E4**	22.5	19.680	1.251	**E4-31**	22.0	23.947	1.395
RD4	76.0	10.313	0.493	**E4-2**	22.5	15.416	1.107	**E4-32**	35.0	11.638	0.771
RD5	90.0	16.051	0.565	**E4-3**	22.5	21.878	1.319	**E5-1**	60.0	7.333	0.468
RD6	60.0	8.229	0.495	**E4-4**	30.0	13.589	0.900	**E5-2**	73.0	7.956	0.441
RD7	35.5	27.273	1.172	**E4-5**	27.5	19.358	1.122	**E5-3**	69.0	7.109	0.429
RD8	68.0	10.362	0.522	**E4-6**	20.5	17.467	1.234	**E5-4**	68.5	7.971	0.456
RD9	55.0	8.002	0.510	**E4-7**	29.5	16.493	1.000	**E5-5**	30.0	4.193	0.500
E1	17.0	23.898	1.585	**E4-8**	24.0	16.900	1.122	**E6-2**	62.5	6.811	0.441
E1-2	27.0	17.513	1.077	**E4-9**	27.0	18.658	1.112	**E6-3**	80.0	13.320	0.546
E1-3	30.5	18.007	1.027	**E4-10**	25.0	18.262	1.143	**BH**	36.0	17.516	0.933
E1-4	29.0	17.351	1.034	**E4-11**	31.0	13.404	0.879	**BH2**	25.0	28.018	1.416
E1-5	29.5	20.184	1.106	**E4-12**	22.5	22.440	1.335	**BH3**	27.0	18.562	1.109
E1-6	30.0	16.073	0.979	**E4-13**	35.0	15.342	0.885	**BH4**	13.5	13.536	1.339
E1-7	26.5	19.942	1.160	**E4-14**	22.0	19.078	1.245	**BH5**	25.0	17.551	1.120
E1-8	39.0	20.567	0.971	**E4-15**	19.5	19.229	1.328	**BH6**	34.0	19.996	1.025
E1-9	29.0	17.360	1.035	**E4-16**	24.0	15.809	1.085	**BH7**	47.0	12.536	0.691
E1-10	39.0	16.173	0.861	**E4-17**	22.0	19.587	1.262	**BH8**	21.5	20.571	1.308

BH9	27.5	24.729	1.268	**BH39**	26.5	15.338	1.017	**L41**	34.5	16.278	0.919
BH10	24.5	16.629	1.102	**BH40**	46.5	18.336	0.857	**L42**	74.0	7.209	0.417
BH11	28.5	18.360	1.073	**L1**	78.5	14.344	0.572	**Plot0008_01_Aq1_ N-1**	36.0	18.144	0.986
BH12	33.5	21.991	1.083	**L5**	79.5	10.776	0.492	**Plot0008_04_Aq1_N-1**	24.0	12.351	0.951
BH13	32.5	17.056	0.969	**L6**	79.0	8.642	0.442	**Plot0008_06_Aq1_N-1**	24.0	18.377	1.239
BH14	26.5	22.069	1.220	**L7**	93.0	10.224	0.443	**Plot0008_07_Aq1_ N-1**	18.0	13.347	1.243
BH15	42.0	18.424	0.886	**L8**	73.0	7.749	0.436	**Plot0008_11_Aq1_N N-1**	51.0	13.140	0.724
BH16	20.0	13.569	1.101	**L10**	73.0	8.298	0.451	**Plot0008_17_Aq2_N-1**	36.0	15.186	0.946
BH17	31.0	18.124	1.022	**L11**	98.0	9.860	0.424	**Plot0008_28_Aq3_N N-3**	43.0	17.061	0.964
BH18	26.0	21.062	1.204	**L12**	87.0	7.787	0.400	**Plot0008_44_Aq5_N**	48.0	14.527	0.798
BH19	20.5	21.347	1.365	**L13**	94.0	9.680	0.429	**Plot0008_45_Aq5_N-1**	34.0	16.358	0.998
BH20	32.5	22.220	1.106	**L14**	81.0	8.567	0.435	**Plot0008_46_Aq5_N N-1**	21.0	12.142	1.116
BH21	26.0	14.216	0.989	**L15**	84.0	8.429	0.424	**Plot0008_47_Aq5_N-1**	22.0	7.597	0.859
BH22	30.0	12.136	0.851	**L16**	90.5	10.256	0.450	**Plot0008_48_Aq5_N N-1**	30.0	18.420	1.186
BH23	25.5	19.062	1.156	**L17**	73.0	7.393	0.426	**Plot0008_49_Aq5_N N-1**	22.0	12.543	1.061
BH24	28.5	16.580	1.020	**L19**	71.0	8.798	0.471	**Plot0008_50_Aq5_N-1**	24.0	14.763	1.166
BH25	28.5	18.233	1.070	**L20**	27.5	25.829	1.296	**Plot0008_51_Aq5_N N-1**	31.0	11.518	0.959
BH26	33.5	18.024	0.981	**L23**	75.0	12.842	0.553	**Plot0008_52_Aq5_N N-1**	35.0	15.921	0.993
BH27	26.0	21.062	1.204	**L24**	79.0	9.418	0.462	**Aq1 21_01 F-1**	39.0	15.992	0.912
BH28	29.5	13.771	0.914	**L25**	88.5	10.422	0.459	**Aq1 21_02 F-1**	45.0	18.097	0.950
BH29	39.0	23.053	1.028	**L27**	31.0	17.422	1.002	**Aq1 21_03 F-1**	35.0	16.190	0.961
BH30	37.5	17.207	0.906	**L29**	83.0	8.518	0.428	**Aq1 21_04 F-1**	49.0	18.399	0.892
BH31	27.0	15.313	1.007	**L30**	112.0	13.527	0.465	**Aq1 21_05 F-1**	53.0	16.491	0.820
BH32	23.5	20.531	1.250	**L32**	74.0	8.224	0.446	**Aq1 21_09 F-1**	57.0	15.976	0.750
BH33	26.5	18.256	1.110	**L33**	19.5	23.271	1.461	**Aq1 21_10 F-1**	55.0	15.930	0.793
BH34	30.5	17.791	1.021	**L34**	22.0	21.236	1.314	**Aq1 21_11 F-1**	47.0	15.680	0.897
BH35	21.0	15.547	1.151	**L35**	25.0	24.044	1.311	**Aq1 21_12 F-1**	50.0	14.193	0.757
BH36	26.5	22.438	1.230	**L38**	70.0	7.738	0.445	**Aq1 21_13 F-1**	33.0	16.331	1.006
BH37	32.5	20.600	1.065	**L39**	62.0	6.538	0.434	**Aq1 21_14 F-1**	36.0	19.706	1.068
BH38	33.0	18.704	1.007	**L40**	86.0	8.960	0.432	**Aq1 21_15 F-1**	45.0	18.339	0.943

Aq2 21_17 F-1	58.0	15.859	0.758
Aq2 21_18 F-1	40.0	18.637	1.039
Aq2 21_19 F-1	41.0	15.335	0.893
Aq2 21_21 F-1	54.0	25.060	0.984
Aq2 21_22 F-1	52.0	20.849	0.912
Aq2 21_24 F-1	59.0	18.632	0.858
Aq2 21_26 F-1	51.0	15.645	0.786
Aq2 21_27 F-1	40.0	15.314	0.950
Aq2 21_29 F-1	43.0	16.776	0.941
Aq3 21_34 F-1	38.0	12.622	0.855
Aq3 21_36 F-1	36.0	20.477	1.116
Aq3 21_37 F-1	48.0	18.051	0.918
Aq3 21_38 F-1	39.0	16.773	0.941
Aq3 21_39 F-1	61.0	21.305	0.846
Aq3 21_42 F-1	55.0	18.670	0.854
Aq4 21_45 F-1	49.0	12.174	0.744
Aq4 21_46 F-1	46.0	15.542	0.857
Aq4 21_47 F-1	46.0	18.447	0.916
Aq4 21_48 F-1	48.0	20.051	0.910
Aq4 21_49 F-1	29.0	16.516	1.068
Aq4 21_50 F-1	42.0	19.354	0.996
Aq4 21_51 F-1	50.0	15.411	0.793
Aq4 21_52 F-1	48.0	15.520	0.874
Aq4 21_53 F-1	41.0	14.386	0.853
Aq4 21_54 F-1	45.0	21.440	0.981
Aq4 21_55 F-3	39.0	17.389	0.973
Aq4 21_58 F-1	41.0	17.501	0.915
Aq1 25_42 F-2	42.0	17.362	0.958
Aq1 25_43 F-1	35.0	17.631	1.054
Aq1 25_44 F-1	46.0	14.690	0.828
Aq1 25_49 F F-1	46.0	13.037	0.775
Aq1 25_50 F F-1	34.0	16.071	1.034
Aq1 25_51 F F-1	37.0	12.763	0.846
Aq1 25_52 F-1	31.0	17.704	1.075
Aq1 25_53 F-1	45.0	14.483	0.868
Aq1 25_54 F-1	34.0	20.404	1.096
Aq1 25_55 F-1	29.0	10.967	0.897
Aq 5 26_40 F-1	44.0	13.721	0.822
Aq 5 26_41 F-1	55.0	13.078	0.711
Aq 5 26_42 F-1	47.0	14.584	0.804
Aq 5 26_43 F-1	56.0	12.595	0.679
Aq 5 26_44 F-1	44.0	9.051	0.742
Aq 5 26_45 F-1	47.0	14.956	0.825
Aq 5 26_46 F-1	47.0	22.908	0.990
Aq 5 26_47 F-1	57.0	14.236	0.734
Aq 5 26_49 F-1	33.0	11.181	0.818
Aq 5 26_50 F-1	36.0	12.391	0.861
Aq 5 26_51 F-1	43.0	13.482	0.798
Aq 5 26_52 F-1	29.0	14.516	1.011
Aq 5 26_53 F-1	48.0	14.608	0.815
Aq1 25_02 F-2	31.0	21.958	1.231
Aq1 25_03 F-2	40.0	21.660	1.047
Aq1 25_05 F-1	35.0	23.538	1.218

CHAPTER 7

SYNTHESIS

1. SYNTHESIS

The general aim of this PhD research was to better understand the role of the phylotypes T1, T2 and T6, which are traditionally identified as the morphospecies *Ammonia tepida* in European Atlantic coastal ecosystems. This PhD thesis is divided into five chapters, each of them investigating a different aspect of these three phylotypes. The articulations between the topics and the main conclusions of the five chapters are summarised in Figure 1.

C**hapter 2** investigates the morphological variability of the three phylotypes and proposes a simple and efficient morphometric method to discriminate them. The method is based on two criteria, the pore size and the suture elevation on the spiral side. This new method opens the possibility to generate large datasets on recent specimens, but also to work on fossil material. In C**hapter 3** the morphometric method of the previous chapter is tested on an independent dataset from a previous publication which studied the biogeographic distribution of T1, T2 and T6 around the British Isles. This chapter shows that the morphometric identification developed in Chapter 2 is highly reliable. The newly acquired distribution showed the emergence of a coherent but previously unnoticed distribution pattern around the British Isles, which suggests that the supposedly exotic phylotype T6 is still spreading and replacing autochthonous phylotypes T1 and T2. **Chapter 4** investigates the response of a modern foraminiferal community to seasonal anoxia and the presence of sulphide (euxinia) in Lake Grevelingen (The Netherlands), where *Ammonia* sp. T6 is presently among the dominant species. It is shown that phylotype T6 is able to cope with short seasonal anoxia and presence of sulphide, but disappears in case of prolonged euxinia. **Chapter 5** focuses on a historical record (~ 50 years) from Lake Grevelingen, including the transition from estuary to salt lake. The changes of the foraminiferal community are explained as a response to the human-induced modifications, including the closure of the estuary and its partial re-openings. In the mid-1980s, phylotype T6, completely absent in older sediment layers, replaced the congeneric *Ammonia* sp. T2, possibly because of its higher tolerance of hypoxia. Finally, combining the conclusions and hypotheses proposed in the previous four chapters, **Chapter 6** proposes a theoretical approach based on scaling laws to explain the pore patterns observed in *Ammonia* sp. T1, T2 and T6. This chapter points out that the pore patterns are mainly controlled by two constraints: metabolic demands and mechanical integrity. A large empirical data set, which fits the theoretical model remarkably well, shows that phylotype T6 has fewer but much bigger pores compared to other phylotypes. This pore pattern represents the best compromise between the two constraints, explaining the potential success of T6 in replacing autochthonous phylotypes T1 and T2.

In the following sections, we develop in more detail the outcome of each of these five chapters and present some additional data.

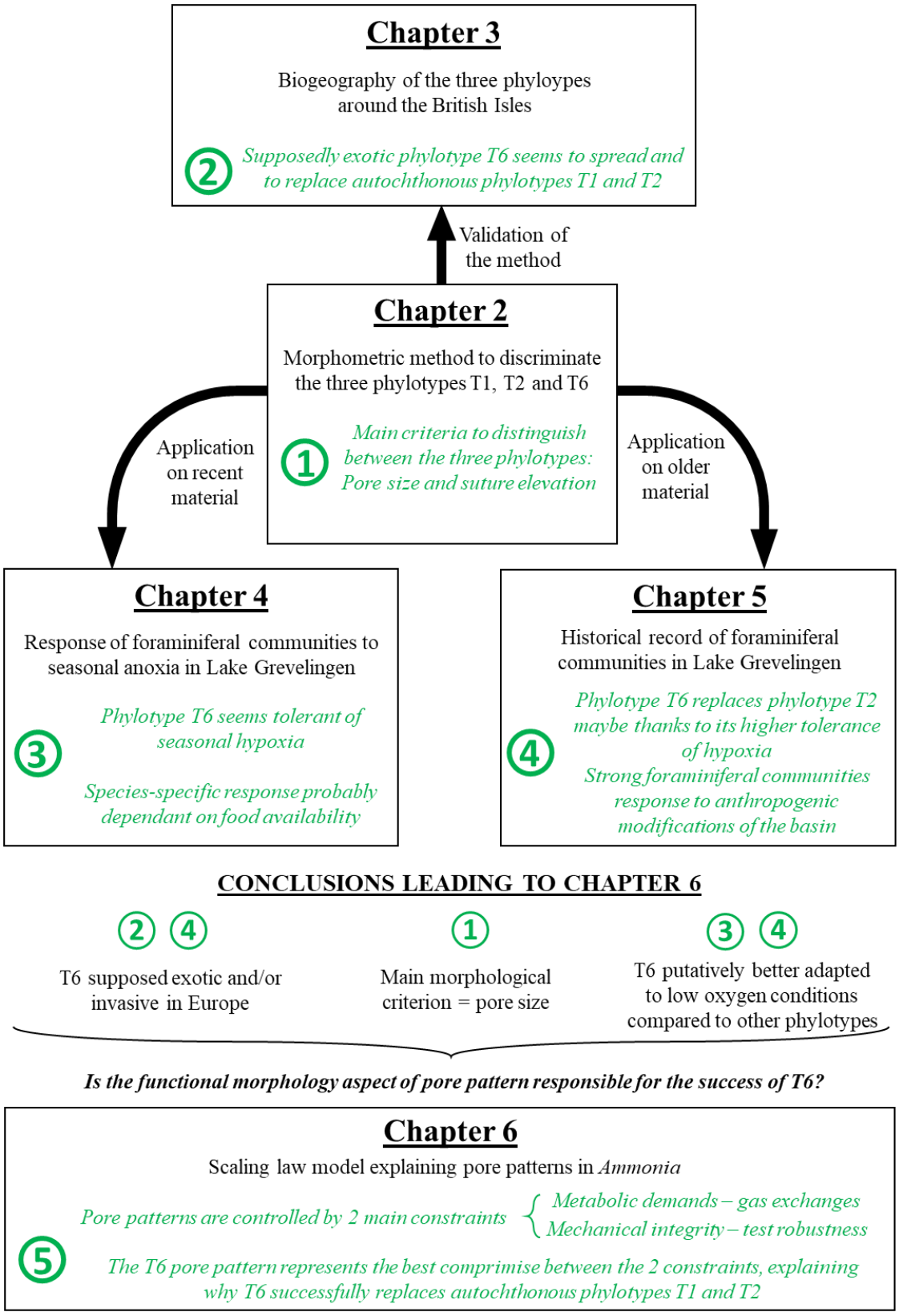

Figure 1. Main connections (arrows) between the chapters (boxes) of this PhD thesis. Each chapter is represented by a separate box. The main investigated subjects and the obtained conclusion(s) are indicated by numbers in green circles (in green).

1.1. RECONCILING TRADITIONAL TAXONOMY AND MOLECULAR IDENTIFICATION

In **Chapter 2,** we investigated the morphological variability of molecularly identified phylotypes T1, T2 and T6. To select reliable morphometric parameters measured on SEM images allowing to discriminate between the three phylotypes, we used a step-by-step multivariate approach. Our results show that the use of two main criteria allows the morphological identification of specimens with a high consistency: the average pore size (T2: smaller pores, T1: intermediate pore size and T6: larger pores) and the suture elevation on the spiral side (raised in T1 but flush in T2 and T6). The possibility to identify the different phylotypes based only on morphological features under a stereomicroscope makes it possible to quickly generate large datasets and opens the possibility to recognise these phylotypes in historical or fossil records, which is difficult or impossible to achieve with molecular methods. Chapters 3, 4 and 5 present direct applications of the morphometric method developed in Chapter 2 to discriminate the phylotypes T1, T2 and T6. These applications would have been impossible with molecular analyses alone. The opportunity to discriminate the different phylotypes using morphological features was widely applied during my entire PhD research, and whenever possible, we attempted to confirm the determinations by molecular methods.

1.2. APPLICATION OF THE MORPHOMETRIC DETERMINATION TO MATERIAL COLLECTED AROUND THE BRITISH ISLES – BIOGEOGRAPHY

The first aim of **Chapter 3** was to test the reliability of the morphometric method on an independent dataset. For this purpose, we used the preserved material molecularly identified in an earlier study of Saad & Wade (2016), which investigated the biogeographical distribution of phylotypes T1, T2 and T6 around the British Isles. Our results show that the morphometric method is consistent, if we assume that the specimens at two sites (Thornham and Shoreham by Sea) were genetically misidentified due to a permutation of samples. We have three main reasons to consider morphometric identification more reliable than molecular identification in this case. First, molecular and morphometric identifications give exactly opposite results between both sites (T6 instead of T2 and vice versa), so that the misidentifications are systematic. Second, the main criterion to discriminate these two phylotypes is the pore size, which we identified as the most efficient criterion to discriminate between T2 (very small pores) and T1/T6 (bigger pores) with a very high accuracy (about 97 %, calculated in the second chapter). Third, eight new individuals from Thornham were sequenced and molecularly

assigned to phylotype T6, in accordance with previous morphometric identification. These three arguments corroborate the hypothesis that the samples from both sites were inverted during the first molecular study.

Finally, after a careful examination of the morphometric assignations and the addition of supplementary datasets to increase the spatial coverage, a rather clear and coherent biogeographical distribution pattern emerged for the three phylotypes. The obtained distribution pattern at a larger spatial scale suggests that the putatively invasive *Ammonia* sp. T6 is currently spreading out over large areas, and is supplanting autochthonous phylotypes T1 and T2 at the outskirt of its present distributional areas along the coastlines of Great Britain and Northern France. We hypothesise that the general current circulation pattern in the English Channel and the Irish Sea could delay, or even inhibit, the further expansion of *Ammonia* sp. T6. Our results also suggest that *Ammonia* sp. T2 may have found refuges in the inner parts of estuaries, which are not easily reached by phylotype T6. The distribution pattern revealed in this study strongly suggests that the different phylotypes must have different ecological preferences that remain to be discovered.

When we consider a smaller spatial scale, preliminary data comparing different sites within a single estuary suggest that the three phylotypes show a complex distribution pattern. When entire estuaries are considered, the co-occurrence of several phylotypes (at different locations within the estuary) appears to be rather common. In the next paragraphs, we present the Auray and Loire estuaries as examples. These two estuaries show very different distribution patterns for the three phylotypes.

In the Auray estuary in the Gulf of Morbihan, sites where sampled at various locations in March and May 2016 along an upstream–downstream gradient (Garnier, 2016, Figure 2A) and in October 2016 along two bathymetrical transects perpendicular to the axis of the estuary (in the context of my PhD thesis, Figure 2B & 2C). In this estuary, where *Ammonia* sp. T6 is absent, *Ammonia* sp. T1 and *Ammonia* sp. T2 show a different distribution pattern (samples from March and May considered). Phylotype T2 is present at all sites and is the only phylotype occurring at the more upstream site (Fort Espagnol) and closer to the estuary mouth (LOC 2), while the phylotype T1 is present in the middle part (2C2 and KER2) and outside the estuary (St Pierre Lopérec, Figure 2A). Furthermore, in October 2016, these phylotypes were present in varying proportions along bathymetrical transects (onshore – offshore) at Kerouarc'h and Locmariaquer (Figure 2B & 2C) with *Ammonia* sp. T2 and *Ammonia* sp. T1 co-occurring at all sites (KER 1–3 and LOC 1–3). At these two transects, phylotype T2 better represented at the deepest sites (KER3 and LOC3). Finally, it appears that the absolute and relative abundances of phylotypes

T1 and T2 showed important temporal variability in 2016 (Figure 2D). At KER 2, *Ammonia* sp. T1 was strongly dominant in October (about 98 %) while phylotype T2 was representing about 40 % in March. At LOC 2, *Ammonia* sp. T1 was dominant in October (more than 75%), while only T2 was occurring in March (Figure 2D).

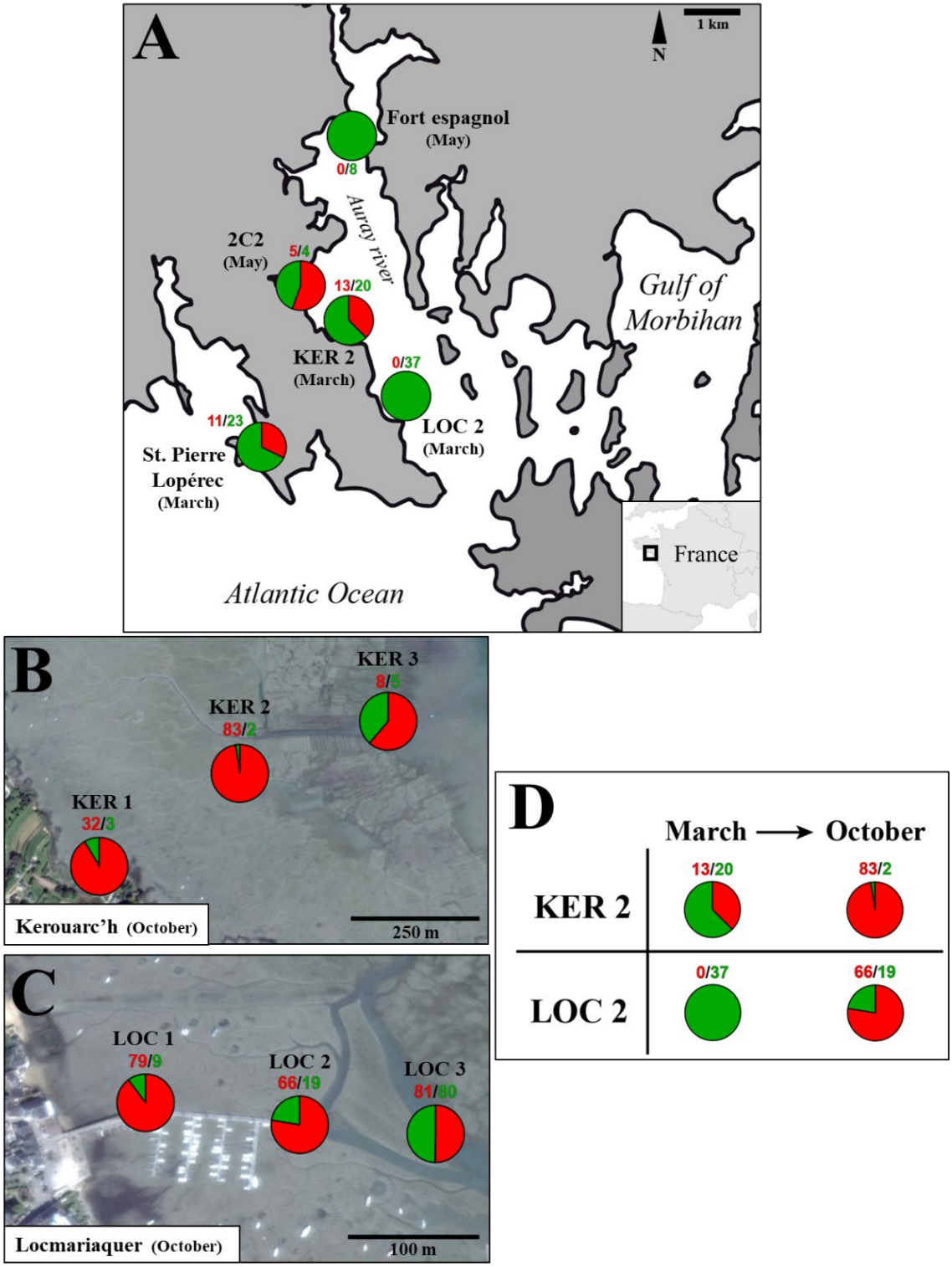

Figure 2. A: Distribution of *Ammonia* phylotypes T1 (red) and T2 (green) in the Auray river (Gulf of Morbihan, France). B: Distribution of *Ammonia* phylotypes T1 (red) and T2 (green) along a transect at Kerouarc'h. C: Distribution of *Ammonia* phylotypes T1 (red) and T2 (green) along a transect at

Locmariaquer. D: Comparison of the proportion of Ammonia phylotypes T1 (red) and T2 (green) between March and October 2016 at KER 2 and LOC 2 sites. The colour of the circles represents the respective proportions of *Ammonia* phylotypes T1 and T2, with the number of specimens indicated (T1/T2). The name and sampling month of each site are indicated, all samples were taken in 2016.

In the same estuary, Diz et al. (2009) hypothesised on the basis of stable isotopic measurements on *Ammonia tepida* tests that specimens of this morphospecies had different calcification seasons in the upper and lower estuary. Their results suggest that one of the two phylotypes, which tends to dominate in the inner estuary, is rather growing in autumn–winter (supposedly T2), whereas the other phylotypes, more frequent in the outer part of the estuary, is preferentially calcifying in summer (supposedly T1). This would explain why we observed a higher proportion of T2 at both sites in March (after the calcification period of this phylotype, supposed to be in autumn–winter), whereas T1 was strongly dominant in October, following its putative summer calcification period.

In the Loire estuary, only phylotypes T6 and T1 were recorded in the live (Rose Bengal stained) assemblages, with relative proportions of about 90 % for T6 and 10 % for T1 at all sites. The map (Figure 3) has been produced using morphological identification of the material published in Mojtahid et al. (2016). *Ammonia* sp. T2 is absent from all samples, suggesting that its ecological preferences are not met in this estuary. Alternatively, if we assume that *Ammonia* sp. T6 is invasive in Europe, the observed distributional pattern could also mean that T6 has completely replaced T2 and that the progressive replacement of T1 by T6 is still going on. In order to gain more insight into this matter, it would be very interesting to sample the same sites again in a few years, to see whether *Ammonia* sp. T6 is the only phylotype remaining in the estuary. A study of sub-recent assemblages preserved in sediment cores, which is in progress (Xu et al., in prep.) should also shed more light on the putative arrival of T6 in the estuary in recent times, and the progressive replacement of the autochthonous phylotypes (as we did in Chapter 4 for the Lake Grevelingen).

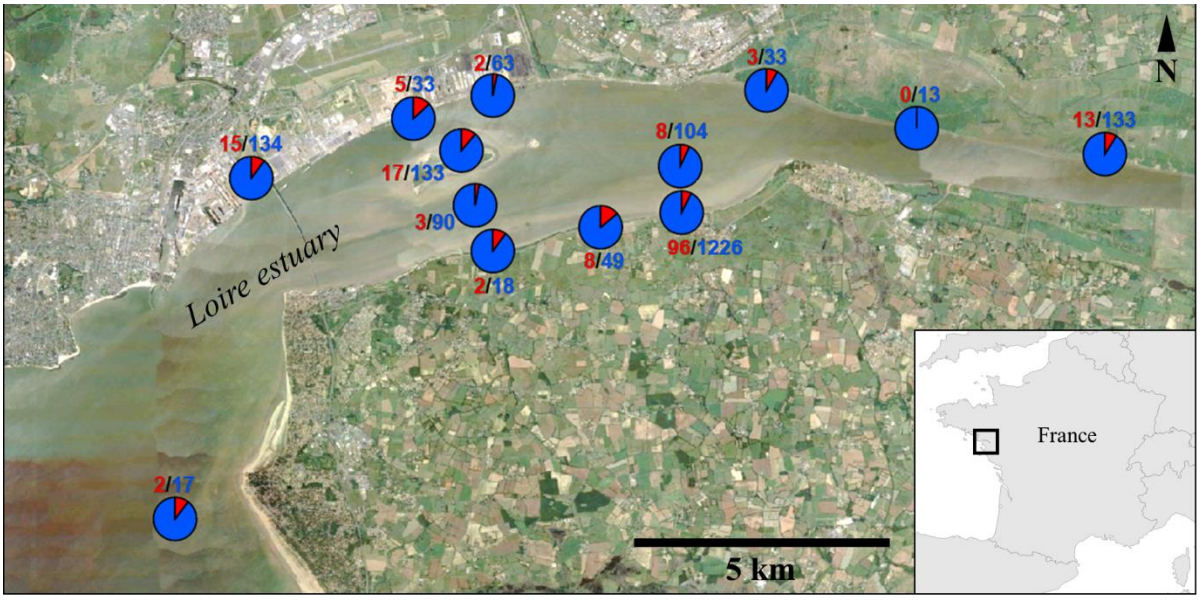

Figure 3. Distribution of *Ammonia* phylotypes T1 (red) and T6 (blue) in the Loire estuary, France. Circles represent the proportions of *Ammonia* phylotypes T1 and T6, the number of specimens per site are indicated (T1/T6). Specimens were assigned to a phylotype using the morphometric method developed in Chapter 2. These sites were sampled in September 2012 in the context of the SEMHABEL project (Mojtahid et al., 2016).

In summary, we obtain very different pictures when comparing the distributions of the three *Ammonia* phylotypes between two very close estuaries (about 70 km between the Auray and Loire estuaries). In the Auray estuary, the two phylotypes T1 and T2 show a complex distributional pattern within the same estuary (a few kilometers), at even smaller spatial scales when a bathymetric transect is considered (a few hundred meters), but also on a seasonal scale (with major differences between March and October 2016). Conversely, we observed almost no spatial variability in the distribution pattern within the Loire estuary (unfortunately no observations on temporal variability are available yet). These two very different situations clearly highlight that the biogeographic distribution must be considered with caution, at both temporal and spatial scales. The preliminary results for the Auray and Loire estuaries makes us also question the validity of the large scale distribution pattern around the British Isles described in Chapter 3 (in which most of the sites are separated by tens of kilometers), and underline the need to very carefully consider the interpretations and conclusions we present in this chapter.

In the Auray river, the complex distribution pattern of phylotypes T1 and T2 (a seasonally moving mosaic) seems to be largely controlled by the ecological requirements of each phylotype (possibly related to the seasonal salinity pattern), and maybe by their different seasonal timing. Phylotypes T1 and T2 are considered autochthonous in Europe, suggesting that they are rather finely adapted to the environmental conditions of their seasonally changing

respective habitats. Consequently, they have different ecological niches, explaining the complex mosaic distribution pattern observed at different seasons in the Auray estuary.

In the Loire estuary, conversely, the distribution pattern of phylotypes T1 and T6 is rather homogeneous. This cannot be explained by a low spatial variability of the environmental parameters, which is clearly not the case in this estuary (Mojtahid et al., 2016). Phylotype T6 is strongly dominant in the whole estuary, indicating that it is highly tolerant regarding the range of ecological conditions found in the estuary. If we hypothesise that this phylotype is indeed exotic and could be invasive in Europe, the relatively homogeneous distribution pattern observed in this estuary suggests that T6 shows an opportunistic behaviour and is probably supplanting its congeneric phylotypes at present. This is in accordance with unpublished data acquired on a sediment core sampled in the same estuary, which indicate that in the deeper sediment layers (i.e. in the past) phylotype T6 was absent (Xu et al., in prep.). This corroborates our hypothesis that, due to its greater tolerance to a larger range of environmental conditions, phylotype T6 outcompetes and replaces phylotypes T1 and T2.

Finally, we could ask why phylotype T6 is absent in the Auray estuary, considering its putative very opportunistic behaviour? This could be due to its ecological preferences, which do not fit the environmental conditions found in this peculiar estuary. A more detailed study of the distribution of the various *Ammonia* phylotypes in the Auray river is in progress and could help to answer this question (Fouet et al., in prep). However, it seems more likely that the absence of T6 in the Auray river can be explained by the semi-enclosed nature of the Gulf of Morbihan, which could have delayed the entrance of T6 for the time being (other locations in the Gulf have been sampled and did not show any T6 either, Schweizer et al., in prep.). The latter hypothesis is in agreement with the hydrodynamic pattern at a large spatial scale we proposed in this chapter, which may also hamper the spreading of T6 in the Gulf of Morbihan.

1.3. RESPONSE OF FORAMINIFERAL COMMUNITIES TO EUXINIA IN LAKE GREVELINGEN

In **Chapter 4**, we investigated the response of foraminiferal communities to seasonal anoxia with the presence of sulphides (i.e. euxinia) in their environment, by studying samples taken bimonthly in 2012 at two sites in Lake Grevelingen (the Netherlands). Both sites are situated at different water depths (23 and 34 m respectively), and show different durations of seasonal anoxia (one month or less at 23 m depth versus one to two months at 34 m depth). The results show that (1) the foraminiferal communities are more strongly impacted when the duration of euxinia increases, with an almost total disappearance of foraminifera at the deepest site and (2)

these adverse conditions impede reproduction instead of causing direct mortality. We finally hypothesise that the different responses of the dominant taxa are rather the consequence of the seasonal succession of food availability, than the expressions of different tolerance levels regarding anoxia and presence of sulphides.

Initially, we intended also to investigate the population dynamics for the dominant morphospecies (*Elphidium selseyense*, *Elphidium magellanicum*, *Trochammina inflata* and *Ammonia* sp. T6) at these two locations, in order to better understand their ecological preferences. However, our available morphometric data for the >125 µm fraction were insufficient to clearly identify successive cohorts. This would have necessitated at least the morphometric study of the 63–125 µm fraction for which taxonomical issues may arise, as well as a higher temporal resolution (e.g. one sample per month), which would have both increased the picking time. The different phylotypes of *Ammonia* are now considered as separated species. Consequently, they may exhibit differences in life traits such as the reproduction period for example, as it is suggested by the data from the Auray estuary (Figure 2), where at the Locmariaquer site, *Ammonia* sp. T1 was dominant in October whereas *Ammonia* sp. T2 strongly dominated the assemblages in March.

Investigations of individual species responses in laboratory experiments could also yield new insights and a better understanding of the foraminiferal responses to stressing conditions in natural settings. Experimental controlled studies in the laboratory with different durations of anoxic conditions and especially with different concentrations of sulphide could be realised to confirm our hypothesis that the progressively decreasing standing stocks after the summer euxinia are not the consequence of strongly increased mortality but mainly the consequence of inhibited reproduction. Although this kind of experiments was already done (with other species and in situ settings, see Chapter 4), we insist on the fact that it is crucial to carefully check the vitality of foraminifera in these low-oxygen environments where organic matter (foraminiferal protoplasm) degradation might take years. Moreover, because *Ammonia* was shown to be able to enter a dormancy state under anoxic conditions (LeKieffre et al., 2017), activity checks such as movement, feeding, reproduction and growth are needed.

At the deepest station in Lake Grevelingen, where the duration of euxinia is the most extended, T6 is almost the only *Ammonia* phylotype present in the recent faunas. However, previous investigations of a sediment core at the same station showed that, in older layers, specimens of *Ammonia* exhibited small pores (associated with low porosity, because pore size is positively correlated with porosity). This strongly suggested that T2 was the dominant *Ammonia* phylotype somewhere in the past (Petersen et al., 2016). This historical shift from

morphotypes with smaller pores (lower porosity) to morphotypes with larger pores (higher porosity) could very well reflect different tolerance levels with respect to oxygen concentrations and/or presence of sulphide in their microhabitat. If one of the main functions of pores is indeed to exchange gases with the outer environment, it could be expected that phylotypes with bigger pores are more resistant to euxinia than phylotypes with smaller pores.

1.4. HISTORICAL EVOLUTION OF THE FORAMINIFERAL COMMUNITY IN LAKE GREVELINGEN

Chapter 5 investigates the foraminiferal community changes related to the human-induced modifications of Lake Grevelingen in a sediment core sampled in 2012 at a location where the living foraminiferal community was also studied (Den Osse Basin, 34 m depth, see Chapter 4). We used sediment molybdenum (Mo) concentrations to refine a pre-existing age model based on ^{210}Pb (each Mo peak is supposed to represent a yearly euxinic event in the sediment). The sediment core of 90 cm length covered about ~ 50 years, and allowed us to characterise the foraminiferal community changes which took place since the time that Lake Grevelingen was still an estuary, before its closure seaward in 1971. We could identify different foraminiferal assemblages, which were typical for the successive periods, with high proportions of typical estuarine mudflat morphospecies before closure of the estuary, replaced mainly by opportunistic morphospecies and/or morphospecies supposed to be tolerant to low oxygen conditions when the Lake was completely closed (1971–1978). The seaward closure in 1971 had disastrous consequences for macrofauna, because the system rapidly showed eutrophication phenomena, with development of anoxic conditions in the bottom waters due to diminished hydrodynamics and water renewal. To solve these environmental problems, a sluice was opened seaward in 1978, to increase water exchanges with the North Sea and counterbalance eutrophication phenomena. However, this management decision did not solve the problem of seasonally occurring hypoxia/anoxia. At this time, the foraminiferal community was strongly dominated by *Elphidium selseyense*, similarly to the living community observed in 2012 (described in Chapter 4). From 1999 onward, this sluice was therefore opened almost year-round, to further enhance oxygen renewal in the bottom waters, by doubling exchanges with the North Sea. Surprisingly, after this new management change, the foraminiferal assemblages became very poor in the top part of the sediment core, with very low dead foraminiferal densities, strongly contrasting with the high abundances of the living foraminiferal communities described in Chapter 4. We ascribed this near absence of foraminiferal tests to

post-mortem dissolution, resulting from the cable bacteria activity in the anoxic part of the sediment, which leads to a strongly diminished carbonate saturation state.

To our knowledge, dissolution of foraminiferal tests due to cable bacteria activity has not been suggested before. This phenomenon could also explain the presence of living specimens with partly and/or completely dissolved shells in other sites such as in the Baltic Sea (Charrieau et al., 2018). Another example is in the Arcachon Bay, where some of the pH profiles are typical of cable bacteria activity, with a minimum of 6.2 at about 2 cm below the sediment surface (Cesbron et al. 2016). At nearby sites in the same bay, Le Campion (1966) showed earlier that the proportion of dead tests was surprisingly small compared to the number of living specimens. However, we still lack studies integrating observations of cable bacteria, geochemical profiles and foraminifera, which are necessary to confirm the causative relationship between foraminiferal test dissolution and cable bacteria activity. Laboratory experiments under controlled conditions would be another strategy to investigate this topic. At Lake Grevelingen, if foraminiferal dissolution is indeed mainly due to cable bacteria activity, the preservation of foraminiferal tests in sediment cores could give information about the cable bacteria activity in the past. Although the absence of dead foraminiferal assemblages is not necessary an indication of cable bacteria activity, our findings strongly suggest that in environments where cable bacteria are occurring, foraminiferal records (densities and/or composition) should be interpreted with caution.

Finally, the results obtained through the study of the sediment core reveal that *Ammonia* sp. T6 (identified using the morphometric method of Chapter 2) arrived in Lake Grevelingen in the mid 1980's and has progressively supplanted other *Ammonia* phylotypes (T1 and especially T2). We hypothesise that this progressive takeover is the result of the better resistance of T6 to hypoxia/anoxia events, which could be a direct consequence of its much larger pores.

1.5. POROSITY MODEL – WHAT IS DRIVING POROSITY IN *AMMONIA*?

As shown in Chapter 2, the pore pattern is an important discriminating feature for phylotypes T1, T2 and T6. All previous studies on *Ammonia* have suggested that the three phylotypes seem strictly aerobic. This means that in order to cope with low oxygen concentrations, individuals must increase their contact surface with the surrounding media to increase gas exchanges (metabolic demand). This can be achieved by increasing porosity. Evidently, there must be an upper limit for porosity, because the test must maintain a certain robustness (mechanical constraint). Based on these two ideas, in **Chapter 6** we developed a

theoretical scaling law model that represents the optimal compromise between these two constraints.

Our results show that the pore pattern measurements obtained for sampled specimens of *Ammonia* are fully in accordance with the model obtained by our theoretical approach. This emphasises the dilemma faced by these three *Ammonia* phylotypes: the need to increase porosity while not decreasing test robustness too much. Our study shows that for an equal porosity, the optimal solution is to increase pore size while simultaneously decreasing pore density. Following these physical laws, by building tests with fewer but larger pores, *Ammonia* sp. T6 has developed a pore pattern that maximises gas exchanges, while maintaining as much as possible test robustness. This pore pattern (large but few pores) could allow phylotype T6 to better perform under low oxygen conditions than *Ammonia* sp. T1 and especially T2, as we suggested in Chapters 4 and 5. In a world where the frequency and duration of hypoxia are increasing, due to increased anthropogenic activities, this could explain why *Ammonia* sp. T6 is very successful in replacing phylotypes T1 and T2 (Chapter 3).

2. PERSPECTIVES

2.1. SPECIES IDENTIFICATION - TAXONOMY AND MOLECULAR IDENTIFICATION

Reliable identification of foraminiferal species is a keystone for all studies involving this group of organisms. Molecular identification represents a rather new, rapidly developing method to delineate species and classify foraminifera. This new method is considered to be more objective to classify species, and more in accordance with the biological species concept than the traditionally used morphological methods. Although the molecular identification has its own limitations, it seems to be the most reliable solution to discriminate species efficiently, and to detect cryptic diversity. However, a classification based on morphological criteria will continue to exist because of its ease of use, particularly for dead or fossil material. Consequently, it is important to reconcile traditional taxonomy and molecular identification and to develop a classification system which includes both ways to determine species.

In this PhD thesis, we propose a simple dichotomous method for discrimination between *Ammonia* sp. T1, T2 and T6, the three phylotypes of the morphospecies *Ammonia tepida* occurring on the northeast Atlantic coasts. It is probable that other phylotypes identified within this morphospecies, occurring in other regions, such as T7, T10 or T11 from Hayward et al. (2004), could also be discriminated on the basis of a detailed analysis of their morphology.

However, this would certainly increase the number of morphological characters used to discriminate them. Moreover, 30 individuals from the dataset of Chapter 2 belonging to sub-phylotypes T2A and T2B (20 T2A and 10 T2B) were analysed morphometrically, but no discriminating criterion was found to distinguish them. This may be explained by the low number of individuals (especially for T2B), or because the morphometric parameter(s) which would allow their discrimination was (were) not considered. It is also possible that the discrimination of these sub-phylotypes is impossible on the basis of morphological criteria (case of truly cryptic species). The method developed to discriminate phylotypes T1, T2 and T6 can be used with a stereomicroscope, but there is no guarantee that this will also be possible for other phylotypes. However, the increasing availability of high quality table Scanning Electron Microscopes (SEM) makes it now possible to study almost routinely minute morphological details, which are not visible on conventional stereomicroscopes. In this context, two relatively recent developments are especially important, which both allow to study the molecular composition and morphological characteristics of the shell for the same specimens. First, the development of environmental SEM, which allows to take high quality pictures of uncoated specimens under partial vacuum, make it easier and faster to image specimens before DNA extraction; this is the method used for most of the specimens we analysed. Next, the development of non-destructive methods to extract foraminiferal protoplasm from the tests (Saad & Wade, 2016), which offers the possibility to preserve the test after DNA extraction.

Whether they are pseudocryptic (as phylotypes T1, T2 and T6 studied here) or truly cryptic species (impossible to discriminate morphologically), the different *Ammonia* phylotypes are now considered as separate species, and should therefore have different ecological niches. Consequently, it is logical to expect that the different phylotypes have adapted their functional morphology to their peculiar environmental preferences, as we suppose that this is the case with the pore patterns of *Ammonia* sp. T1, T2 and T6.

The two most reliable criteria to discriminate between phylotypes T1, T2 and T6 are the pore size and the suture elevation on the spiral side of the test. Although the morphofunctional role of pores is apparently related to the need of the cell to exchange gases (or other dissolved compounds) with the surrounding media (especially oxygen in the case of *Ammonia*), the function of the raised sutures on the spiral side is less evident. We think that this thickening of the sutures could be linked to mechanical resistance again, since this seems to be a major constraint in *Ammonia*. Strengthening the suture between whorls and individual chambers would very probably increase the robustness of the whole test. This hypothesis still has to be tested experimentally, by using for instance a comparable methodology as used by Wetmore

(1987), who measured the compressive strength of individual foraminiferal tests using strain gauges.

Molecular analyses of *Ammonia* are rather recent, and are ongoing as is shown by the rapidly increasing number of phylotypes distinguished in the last years. In view of the newly revealed (pseudo-)cryptic species diversity in coastal ecosystems, it seems particularly important to couple molecular analyses and morphometric measurements with statistical approaches. This is not only the case for *Ammonia*, but also for *Elphidium*, for which many studies have already been performed (e.g. Pillet et al, 2013, Voltski et al., 2015; Darling et al. 2016, Roberts et al., 2016), for miliolids such as *Quinqueloculina* (Kaushik et al., 2019) or for *Uvigerina* (Schweizer et al., 2005). However, as for *Ammonia*, the harmonisation between molecular identification and traditional, morphology-based, taxonomy is in its infancy and needs to be continued.

Identification of the various phylotypes is only a stepping stone toward the characterisation of their ecological preferences (and ultimately the ecological niches). Only when the ecology of the different phylotypes is known, will it be possible to exploit the environmental information offered by the taxonomical composition of the foraminiferal community, either in studies regarding environmental quality, or in palaeorecords. The ecological characteristics of different phylotypes can be obtained by observations of their distribution in nature or by laboratory experiments. For example, at a site where various phylotypes occur together, an in situ approach combining the characterisation of their vertical and/or lateral distribution and the geochemistry of the sediment at fine resolution, could allow us to describe the micro-environment inhabited by each phylotypes (e.g. Thibault de Chanvalon et al., 2015; Cesbron et al., 2016). Laboratory experiments should be performed on each of the three phylotypes separately to obtain a better knowledge of their ecological preferences. For instance, it should be possible to investigate differences in their tolerance levels for main stress parameters, such as oxygen and sulphide concentration or salinity.

Finally, the geochemical composition of the test can yield precious information concerning the foraminiferal ecology. Because it seems to be largely dependent on the biogeochemistry of the site of calcification, the geochemistry of the shell therefore should be representative of the foraminiferal microhabitat. For this reason, measurements of the elemental ratios in the shell performed on the different phylotypes of *Ammonia* could give us some more insight about their specific microhabitats. For instance, the Mn/Ca ratio can inform us about the presence of reducing conditions in the microhabitat (e.g. Koho et al., 2017; Petersen et al., 2018). Alternatively, stable isotopes measurements ($\delta^{18}O$ and $\delta^{13}C$) may give us indications about the

period of growth or reproduction during the year (Diz et al., 2009). Consequently, it should be possible to simultaneously obtain information about the calcification period and the geochemical characteristics of the foraminiferal microhabitat during this period. We expect that the different phylotypes live in slightly different microhabitats, particularly regarding the oxygen levels (with phylotype T6 having a higher tolerance to low oxygen concentrations), but they may also have different reproduction and/or calcification periods (as hypothesised by Diz et al., 2009). *Ammonia* is a promising biological model for calibration of proxies based on shell elemental ratios in coastal settings, but the application of this kind of methods needs further investigations. More particularly, the intra-phylotype variability of these proxies must be tested in controlled conditions, for instance in laboratory experiments with clones (De Nooijer et al., 2014).

2.2. INVASIVE SPECIES IN *AMMONIA*?

The recognition of previously cryptic species (which become pseudocryptic, when their morphological identification becomes possible) reveals new biogeographical patterns such as for phylotype T6 in this PhD thesis, which is often considered as exotic and/or invasive in Europe (Pawlowski & Holzmann, 2008; Schweizer et al, 2011; Bird et al., 2020). By outcompeting native taxa, invasive species may represent a potential threat to native biodiversity, with cascading effects on overall ecosystem functioning. This may especially be a problem in changing environments, for instance in response to climate change, in which the native species may approach the limits of their ecological tolerance levels. Ultimately, the replacement of native species by invasive ones may lead to a loss of biodiversity and ecosystem services.

Introduced species with an invasive behaviour are well known in benthic foraminifera. The spreading and rapid progression of the genus *Amphistegina* in Mediterranean Sea, after the opening of the Suez Canal in 1869, is probably the most famous example of a supposedly invasive species. At present, the further westward expansion of this taxon in the Mediterranean Sea seems to be facilitated by climate-driven temperature increase (Langer et al., 2012). The introduction of *Trochammina hadai* (Uchio, 1962) in Padilla Bay (western coast of the United States of America) was related to the decline of *Elphidium excavatum*, one of the most common native morphospecies (McGann & Sloan, 1996; McGann et al., 2012). The authors suggested that *T. hadai* could have been introduced in the bay in the 1930s together with oysters imported from Japan, or by other vectors such as ballast waters or anchor mud. Another example is the

putative invasion of *Haynesina germanica* in the Bahia Blanca estuary (Argentina), where the species was never recorded until its recent introduction through human-mediated activities, with ship ballast water and ballast sediment considered as the most plausible vectors (Calvo-Marcilese & Langer, 2010). Phylotype *Nonionella* sp. T1 is another example of a recent introduction in the Skagerrak, with marine currents or ship ballast tanks as supposed vectors (Swedish fjord in the Skagerrak in Polovodova Asteman & Schönfeld, 2015; Oslofjord in Deldicq et al., 2019).

The putatively exotic and invasive nature of *Ammonia* sp. T6 has not been fully confirmed yet. In fact, the available data do not allow us to definitely discard the possibility that phylotype T6 has its origins in Europe and is invasive in Asia (the reverse situation), or is distributed in other parts of the world (it occurs in eDNA from the Gulf of Mexico, Schweizer, personal communication). Furthermore, it has not yet been shown that this phylotype has negative effects on the supposedly native European communities. Several aspects of the results presented in this PhD thesis support the theory that *Ammonia* sp. T6 is an exotic phylotype in Europe and that it could be invasive in the environments where it progressively replaces autochthonous phylotypes T1 and T2. We can especially mention the large-scale biogeographical distribution pattern (Chapter 3), the historical record of Lake Grevelingen (Chapter 5), and the higher tolerance of phylotypes T6 for low oxygen conditions (Chapter 4), which increased in extent and severity in the last decades. The invasive behaviour of phylotype T6 is rather clear in the historical record of Lake Grevelingen (Chapter 5), because of its well documented recent arrival and very rapid replacement of the congeneric, supposedly autochthonous, phylotype T2.

Since a morphometric method is now available to recognise this potentially exotic phylotype, alive or dead as it is based on the test morphology, an increased sampling effort within and between the two disjoint distributional areas (Europe and eastern Asia) should allow us to definitely statue about its exotic nature. The morphological determination method, which requires only limited technological means (basically a high magnification 80x stereomicroscope), represents also a good opportunity to implicate scientists from countries where foraminiferal studies are developing, and where more advanced material may be a limiting factor.

In order to definitely settle whether T6 is indeed an exotic phylotype in Europe, we should study a large number of well-dated sediment cores from different locations where phylotype T6 is currently occurring. If *Ammonia* sp. T6 is exotic, we should observe its complete absence in the older layers, and its arrival somewhere in more recent layers. The precise dating of its arrival in the different sites could provide clues about the potential vector responsible for its

introduction. The same approach should be applied in Asia at places where T6 is occurring. If the phylotype is indeed originating from Asia, it should be present throughout the sediment cores, and not appearing recently.

Another way to obtain more information about the potential origin of *Ammonia* sp. T6 in Asia and to verify if its recent spread in the northeast Atlantic is indeed the result of an anthropogenic introduction, would be to characterise the pattern of genetic differentiation between populations in European and Asian coasts. With population genetics analyses, we could infer the relative importance of short-distance (between nearby sites) and long-distance (between distant sites in Europe or between Europe and Asia) dispersal. If the dispersal happened naturally during a long time, we expect significant genetic differences between populations in Asia and populations in Europe, because direct genetic material exchanges would be rather limited between the two distant regions. Conversely, if the dispersal happened recently and quickly through anthropogenic means, we expect little or no genetic differentiation between Asia and Europe (because genetic material exchanges would have happened recently) and maybe a lower genetic diversity in the place where the species arrived recently (due to the founder effect). However, this would require to identify DNA markers showing enough polymorphism (e.g. microsatellites or other regions showing a high polymorphism) to allow differentiation at the population level (intra-specific). For the moment, the most variable region known for foraminifera is the ITS (Internal Transcribed Spacer) region of the ribosomal DNA, but it is not sure that this region shows enough variation in this case. Although we need the suitable genetic markers and more knowledge about the sequencing and the mapping of the foraminiferal genome to apply this kind of tool, this is theoretically possible if no methodological obstacles arise.

Finally, it appears difficult to definitely prove that phylotype T6 is indeed invasive, and alters (even only locally) ecosystem functioning. A better understanding of the functional/ecological differences between *Ammonia* sp. T6 and other phylotypes in ecosystems, for example, by studying their physiology and/or their role in food web, might help to settle this question.

2.3. PORE FUNCTIONS AND DEVELOPMENT OF PALAEOCEANOGRAPHICAL PROXIES?

The pore pattern is an important morphological feature in hyaline foraminifera and it has already been proposed as a proxy for oxygen and nitrate concentrations in the surrounding environment (Glock et al., 2011; Kuhnt et al., 2013; Tetard, 2017; Rathburn et al., 2018; Glock

et al., 2018). The identification and consideration of the mechanical constraints on the pore pattern highlight the fact that this parameter must be taken into consideration if we want to fully understand the morphofunctional role of the pore pattern in *Ammonia*. Although our empirical data fit very well with the theoretical predictions, our model suffers from some intermediate approximations which are possible to improve. For example, the shell thickness, which was considered as constant in our model, must be an important parameter, and its potential variability should be taken into account. A next step could then be to consider not only of the last chamber, but the general shape of the whole test, which was considered spherical in our model. Ornamentation could also be taken into account, such as the thickened sutures on the spiral side of *Ammonia* sp. T1, which could play a role in the test robustness. In order to develop such more complex models, precise empirical measurements are needed for additional parameters (e.g. shell thickness, thickened parts as sutures, internal structures…), which have still to be developed.

The development of palaeoceanographical proxies based on foraminiferal pore patterns is relatively recent, and has been suggested for bottom water oxygen as well as nitrate concentrations, using different species (Glock et al., 2011; Kuhnt et al., 2013; Tetard et al., 2017; Rathburn et al., 2018; Glock et al., 2018). The first results are promising, although a precise mechanistic understanding of the constraints controlling the foraminiferal pore pattern, which were not considered until now, seems to be a crucial prerequisite for the reliable calibration and successful application of such palaeoceanographical proxies. It seems evident that more knowledge about the metabolism of the concerned taxa is needed, especially because different types of metabolic adaptations to stressed conditions (anoxia, euxinia) have been described for foraminifera (e.g. denitrification, dormancy, kleptoplasty). In facultative anaerobic taxa, which can alternate between different types of respiration (oxygen or nitrate), such as *Globobulimina turgida* (Piña-Ochoa et al., 2010) or *Bolivina argentea* (Bernhard et al., 2012), the pore pattern would be controlled by both exchanges of gas (oxygen) and ions (nitrate). Alternatively, in the previously believed aerobic coastal species *Haynesina germanica*, which is in fact mixotrophic (because it possesses functional kleptoplasts, Jauffrais et al., 2018), gas exchanges may be (much) less important than mechanical constraints since this species can obtain oxygen and energy from the activity of its kleptoplasts.

Finally, it should be kept in mind that gas exchanges through the pores have never been experimentally demonstrated yet, and remain therefore hypothetical. Laboratory experiments are needed to test different *Ammonia* phylotypes in different oxygen concentrations, in order to see whether the foraminiferal tolerance to low oxygen concentrations differs between the

phylotypes, and is correlated with pore density. In case of a positive result, this would largely support the idea that it should be possible to use the pore patterns of *Ammonia* as a basis for a proxy of oxygen concentration.

3. CONCLUDING REMARKS

Coastal ecosystems are valuable for human societies, and there is an urgent need to take reasonable, suitable and efficient management decisions to preserve the services and goods they provide. For this reason, it is necessary to understand how the different entangled components and processes are functioning in these ecosystems. Yet, coastal ecosystems represent a challenge to understand because they are prone to great natural variability but also to important anthropogenic pressure, which together are threatening their correct functioning. In these coastal ecosystems, foraminifera are a major component. Among them, *Ammonia* is one of the most widespread and abundant genera and often dominates assemblages, making it a good biological model to study the interaction of biota and their environment.

This PhD thesis aimed to study and understand how three *Ammonia* phylotypes interact with their environment in the Northeast Atlantic. We demonstrated that it was possible to discriminate phylotypes T1, T2 and T6 based only on morphological features. Previously, these phylotypes were considered as cryptic species and commonly identified as the morphospecies *Ammonia tepida* in Europe. The use of this refined morphological recognition allowed us to consider this pseudo-cryptic diversity, previously accessible only by molecular analyses. Using this method, we highlighted a coherent distribution pattern at large spatial scale around the British Isles for these phylotypes, but we also unveiled the complexity of their distribution at lower spatial scale in estuaries for instance. Our investigations of their historical succession over the last 50 years and their seasonal response to euxinia in an artificially enclosed lake in the Netherlands strongly suggest that they show different tolerance to oxygen levels in their habitat. Moreover, our work strongly supports the putative exotic and invasive nature of the phylotype T6, which is supposed to originate from East Asia. Based on our previous findings and using a theoretical approach, we propose that the pore pattern of their test is reflecting differential tolerances for low oxygen conditions, possibly explaining the spreading success of T6. We finally hypothesise that the pore pattern could serve as a proxy for past oxygen concentrations in coastal area.

In this thesis, we demonstrated the importance of refining species recognition in order to better understand the relations between biota and their environment, which in turn could have

possible applications for proxy development for past conditions or biomonitoring in recent coastal ecosystems. In view of the current accelerated climate change and increased anthropogenic impacts on ecosystems, which in most cases are already altered, a better knowledge about how coastal ecosystems are functioning today, but also how they were functioning in the past, will help us to resolve crucial ecologic, economic and societal questions.

REFERENCES

Bernhard, J.M., Casciotti, K.L., McIlvin, M.R., Beaudoin, D.J., Visscher, P.T., Edgcomb, V.P., 2012. Potential importance of physiologically diverse benthic foraminifera in sedimentary nitrate storage and respiration. Journal of Geophysical Research: Biogeosciences 117, G03002. https://doi.org/10.1029/2012JG001949

Bird, C., Schweizer, M., Roberts, A., Austin, W.E.N., Knudsen, K.L., Evans, K.M., Filipsson, H.L., Sayer, M.D.J., Geslin, E., Darling, K.F., 2020. The genetic diversity, morphology, biogeography, and taxonomic designations of *Ammonia* (Foraminifera) in the Northeast Atlantic. Marine Micropaleontology 155, 101726. https://doi.org/10.1016/j.marmicro.2019.02.001

Calvo-Marcilese, L., Langer, M.R., 2010. Breaching biogeographic barriers: the invasion of *Haynesina germanica* (Foraminifera, Protista) in the Bahía Blanca estuary, Argentina. Biological Invasions 12, 3299–3306. https://doi.org/10.1007/s10530-010-9723-x

Cesbron, F., Geslin, E., Jorissen, F.J., Delgard, M.L., Charrieau, L., Deflandre, B., Jézéquel, D., Anschutz, P., Metzger, E., 2016. Vertical distribution and respiration rates of benthic foraminifera: Contribution to aerobic remineralization in intertidal mudflats covered by *Zostera noltei* meadows. Estuarine, Coastal and Shelf Science, Special Issue: Functioning and dysfunctioning of Marine and Brackish Ecosystems 179, 23–38. https://doi.org/10.1016/j.ecss.2015.12.005

Charrieau, L.M., Filipsson, H.L., Ljung, K., Chierici, M., Knudsen, K.L., Kritzberg, E., 2018. The effects of multiple stressors on the distribution of coastal benthic foraminifera: A case study from the Skagerrak-Baltic Sea region. Marine Micropaleontology 139, 42–56. https://doi.org/10.1016/j.marmicro.2017.11.004

Darling, K.F., Schweizer, M., Knudsen, K.L., Evans, K.M., Bird, C., Roberts, A., Filipsson, H.L., Kim, J.-H., Gudmundsson, G., Wade, C.M., Sayer, M.D.J., Austin, W.E.N., 2016. The genetic diversity, phylogeography and morphology of Elphidiidae (Foraminifera) in the Northeast Atlantic. Marine Micropaleontology 129, 1–23. https://doi.org/10.1016/j.marmicro.2016.09.001

de Nooijer, L.J., Hathorne, E.C., Reichart, G.J., Langer, G., Bijma, J., 2014. Variability in calcitic Mg/Ca and Sr/Ca ratios in clones of the benthic foraminifer *Ammonia tepida*. Marine Micropaleontology 107, 32–43. https://doi.org/10.1016/j.marmicro.2014.02.002

Deldicq, N., Alve, E., Schweizer, M., Asteman, I.P., Hess, S., Darling, K., Bouchet, V.M.P., 2019. History of the introduction of a species resembling the benthic foraminifera Nonionella stella in the oslofjord (Norway): morphological, molecular and paleo-ecological evidences. https://doi.org/10.3391/ai.2019.14.2.03

Diz, P., Jorissen, F.J., Reichart, G.J., Poulain, C., Dehairs, F., Leorri, E., Paulet, Y.-M., 2009. Interpretation of benthic foraminiferal stable isotopes in subtidal estuarine environments. Biogeosciences 6, 2549–2560. https://doi.org/10.5194/bg-6-2549-2009

Ganier, J., 2016. Le rôle du complexe d'espèces cryptiques *Ammonia tepida* dans les écosystèmes côtiers de la façade Atlantique. Cas de la rivière d'Auray. Master thesis, University of Angers, 29 p.

Glock, N., Eisenhauer, A., Milker, Y., Liebetrau, V., Schönfeld, J., Mallon, J., Sommer, S., Hensen, C., 2011. Environmental Influences on the Pore Density of *Bolivina Spissa* (Cushman). Journal of Foraminiferal Research 41, 22–32. https://doi.org/10.2113/gsjfr.41.1.22

Glock, N., Erdem, Z., Wallmann, K., Somes, C.J., Liebetrau, V., Schönfeld, J., Gorb, S., Eisenhauer, A., 2018. Coupling of oceanic carbon and nitrogen facilitates spatially resolved quantitative

reconstruction of nitrate inventories. Nature Communications 9, 1217. https://doi.org/10.1038/s41467-018-03647-5

Jauffrais, T., LeKieffre, C., Koho, K.A., Tsuchiya, M., Schweizer, M., Bernhard, J.M., Meibom, A., Geslin, E., 2018. Ultrastructure and distribution of kleptoplasts in benthic foraminifera from shallow-water (photic) habitats. Marine Micropaleontology, Benthic Foraminiferal Ultrastructure Studies 138, 46–62. https://doi.org/10.1016/j.marmicro.2017.10.003

Kaushik, T., Murugan, T., Dagar, S.S., 2019. Morphological variation in the porcelaneous benthic foraminifer *Quinqueloculina seminula* (Linnaeus, 1758): Genotypes or Morphotypes? A detailed morphotaxonomic, molecular and ecological investigation. Marine Micropaleontology 150, 101748. https://doi.org/10.1016/j.marmicro.2019.101748

Koho, K.A., de Nooijer, L.J., Fontanier, C., Toyofuku, T., Oguri, K., Kitazato, H., Reichart, G.-J., 2017. Benthic foraminiferal Mn/Ca ratios reflect microhabitat preferences. https://doi.org/10.5194/bg-14-3067-2017

Kuhnt, T., Friedrich, O., Schmiedl, G., Milker, Y., Mackensen, A., Lückge, A., 2013. Relationship between pore density in benthic foraminifera and bottom-water oxygen content. Deep Sea Research Part I Oceanographic Research Papers 76, 85–95. https://doi.org/10.1016/j.dsr.2012.11.013

Langer, M.R., Weinmann, A.E., Lötters, S., Rödder, D., 2012. "Strangers" in paradise: modeling the biogeographic range expansion of the foraminifera *Amphistegina* in the Mediterranean Sea. Journal of Foraminiferal Research 42, 234–244. https://doi.org/10.2113/gsjfr.42.3.234

Le Campion, J., 1966. Contribution à l'étude des foraminifères du Bassin d'Arcachon et du proche océan. Université d'Aix-Marseille, Aix Marseille.

LeKieffre, C., Spangenberg, J., Mabilleau, G., Escrig, S., Meibom, A., Geslin, E., 2017. Surviving anoxia in marine sediments: The metabolic response of ubiquitous benthic foraminifera (*Ammonia tepida*). PLOS ONE 12, e0177604. https://doi.org/10.1371/journal.pone.0177604

McGann, M., Grossman, E.E., Takesue, R.K., Penttila, D., Walsh, J.P., Corbett, R., 2012. Arrival and Expansion of the Invasive Foraminifera *Trochammina hadai* Uchio in Padilla Bay, Washington. Northwest Science 86, 9–26. https://doi.org/10.3955/046.086.0102

McGann, M., Sloan, D., 1996. Recent introduction of the foraminifer *Trochammina hadai* Uchio into San Francisco Bay, California, USA. Marine Micropaleontology 28, 1–3. https://doi.org/10.1016/0377-8398(95)00077-1

Mojtahid, M., Geslin, E., Coynel, A., Gorse, L., Vella, C., Davranche, A., Zozzolo, L., Blanchet, L., Bénéteau, E., Maillet, G., 2016. Spatial distribution of living (Rose Bengal stained) benthic foraminifera in the Loire estuary (western France). Journal of Sea Research, Recent and past sedimentary, biogeochemical and benthic ecosystem evolution of the Loire Estuary (Western France) 118, 1–16. https://doi.org/10.1016/j.seares.2016.02.003

Pawlowski, J., Holzmann, M., 2008. Diversity and geographic distribution of benthic foraminifera: a molecular perspective. Biodiversity and Conservation 17, 317–328. https://doi.org/10.1007/s10531-007-9253-8

Petersen, J., Barras, C., Bézos, A., La, C., de Nooijer, L.J., Meysman, F.J.R., Mouret, A., Slomp, C.P., Jorissen, F.J., 2018. Mn/Ca intra- and inter-test variability in the benthic foraminifer *Ammonia tepida*. Biogeosciences 15, 331–348. https://doi.org/10.5194/bg-15-331-2018

Petersen, J., Riedel, B., Barras, C., Pays, O., Guihéneuf, A., Mabilleau, G., Schweizer, M., Meysman, F.J.R., Jorissen, F.J., 2016. Improved methodology for measuring pore patterns in the benthic foraminiferal genus *Ammonia*. Marine Micropaleontology 128, 1–13. https://doi.org/10.1016/j.marmicro.2016.08.001

Pillet, L., Voltski, I., Korsun, S., Pawlowski, J., 2013. Molecular phylogeny of Elphidiidae (foraminifera). Marine Micropaleontology 103, 1–14. https://doi.org/10.1016/j.marmicro.2013.07.001

Piña-Ochoa, E., Koho, K.A., Geslin, E., Risgaard-Petersen, N., 2010. Survival and life strategy of the foraminiferan *Globobulimina turgida* through nitrate storage and denitrification. Marine Ecology Progress Series 417, 39–49. https://doi.org/10.3354/meps08805

Polovodova Asteman, I., Schönfeld, J., 2016. Recent invasion of the foraminifer *Nonionella stella* Cushman & Moyer, 1930 in northern European waters: evidence from the Skagerrak and its fjords. Journal of Micropalaeontology 35, 20–25. https://doi.org/10.1144/jmpaleo2015-007

Rathburn, A.E., Willingham, J., Ziebis, W., Burkett, A.M., Corliss, B.H., 2018. A New biological proxy for deep-sea paleo-oxygen: Pores of epifaunal benthic foraminifera. Scientific Reports 8, 9456. https://doi.org/10.1038/s41598-018-27793-4

Roberts, A., Austin, W., Evans, K., Bird, C., Schweizer, M., Darling, K., 2016. A new integrated approach to taxonomy: the fusion of molecular and morphological systematics with type material in benthic foraminifera. PLOS ONE 11, e0158754. https://doi.org/10.1371/journal.pone.0158754

Saad, S.A., Wade, C.M., 2016. Biogeographic distribution and habitat association of *Ammonia* genetic variants around the coastline of Great Britain. Marine Micropaleontology 124, 54–62. https://doi.org/10.1016/j.marmicro.2016.01.004

Schweizer, M., Pawlowski, J., Duijnstee, I.A.P., Kouwenhoven, T.J., van der Zwaan, G.J., 2005. Molecular phylogeny of the foraminiferal genus *Uvigerina* based on ribosomal DNA sequences. Marine Micropaleontology 57, 51–67. https://doi.org/10.1016/j.marmicro.2005.07.001

Schweizer, M., Polovodova, I., Nikulina, A., Schönfeld, J., 2011. Molecular identification of *Ammonia* and *Elphidium* species (Foraminifera, Rotaliida) from the Kiel Fjord (SW Baltic Sea) with rDNA sequences. Helgoland Marine Research 65, 1–10. https://doi.org/10.1007/s10152-010-0194-3

Tetard, M., Beaufort, L., Licari, L., 2017. A new optical method for automated pore analysis on benthic foraminifera. Marine Micropaleontology 136, 30–36. https://doi.org/10.1016/j.marmicro.2017.08.005

Thibault de Chanvalon, A., Metzger, E., Mouret, A., Cesbron, F., Knoery, J., Rozuel, E., Launeau, P., Nardelli, M.P., Jorissen, F.J., Geslin, E., 2015. Two-dimensional distribution of living benthic foraminifera in anoxic sediment layers of an estuarine mudflat (Loire estuary, France). Biogeosciences 12, 6219–6234. https://doi.org/10.5194/bg-12-6219-2015

Voltski, I., Korsun, S., Pillet, L., Pawlowski, J., 2015. *Protelphidium niveum* (Lafrenz, 1936) and the taxonomy of "lower" elphidiids. Journal of Foraminiferal Research 45, 250–263. https://doi.org/10.2113/gsjfr.45.3.250

Wetmore, K.L., 1987. Correlations between test strength, morphology and habitat in some benthic foraminifera from the coast of Washington. Journal of Foraminiferal Research 17, 1–13. https://doi.org/10.2113/gsjfr.17.1.1

COMMUNICATIONS

TALKS

Morphological distinction between three *Ammonia* phylotypes along European Atlantic coasts
Presented at FORAMS2018, 17-22 June 2018, Edinburgh, Scotland.

Modelling foraminiferal pore patterns: how to reconciliate gas exchanges and test robustness
Presented at The Micropalaeontological Society's Joint Foraminifera and Nannofossil Meeting, 1–4 July 2019 – Fribourg, Switzerland.

POSTERS

Morphological traits of selected phylotypes identified as *Ammonia tepida* (Cushman, 1926) along the European coast
Presented at The Micropalaeontological Society's Joint Foraminifera and Nannofossil Meeting, 19–23 April 2017 – Birmingham, UK.

Scaling laws explain pore patterns in foraminifera (Rhizaria)
Presented by Magali Schweizer at the VIII European Congress of Protistology – ISOP joint meeting– 28 July–2 August 2019 – Rome, Italy.

Foraminiferal community response to seasonal anoxia in Lake Grevelingen (Netherlands)
Presented at The Micropalaeontological Society's Joint Foraminifera and Nannofossil Meeting, 1–4 July 2019 – Fribourg, Switzerland.

MORPHOLOGICAL TRAITS OF SELECTED PHYLOTYPES IDENTIFIED AS *AMMONIA TEPIDA* (CUSHMAN, 1926) ALONG THE EUROPEAN COAST

RICHIRT Julien[1], SCHWEIZER Magali[1], and JORISSEN Frans[1]

[1]Université d'Angers, UMR6112 LPG-BIAF – Bio-Indicateurs Actuels et Fossiles, 49045 Angers, France

Corresponding author: richirt.julien@gmail.com

Ammonia is one of the most abundant genera worldwide exhibiting a very high morphological variability, although commonly researchers use one to three morphospecies. Even if they are not often used, a plethora of species/subspecies descriptions of recent *Ammonia* exist and has led to "taxonomical chaos". The tendency to consider the morphotypes as ecophenotypes belonging to a strongly reduced number of species has been challenged by molecular studies, showing that many supposed ecophenotypes were in reality well separated genetically and can/should be considered as different species. This study aims to investigate morphological characteristics of phylotypes belonging to the genus *Ammonia*. We are particularly interested in three phylotypes widely encountered along the European coasts which are difficult to distinguish morphologically (T1, T2 and T6). For this purpose, about 360 *Ammonia* specimens were sampled and SEM (Scanning Electron Microscopy) imaged of the spiral, umbilical and lateral sides were obtained to perform morphometric measures. Pore features were investigated using 1000x magnified images of the penultimate chamber on the spiral side. In order to assign each specimen to a phylotype, a fragment of the 5' terminal region of the SSU rDNA (14F-N6) was sequenced and compared to previous data. Linking morphometric analyses and molecular identification will allow us to determine morphological traits useful to effectively distinguish these three phylotypes. The revision of the traditional nomenclature in the light of molecular data is urged to reach a taxonomic standardisation. We strongly believe that molecular identification combined with morphological analyses will help to disentangle these taxonomic issues.

Morphological traits of selected phylotypes identified as *Ammonia tepida* (Cushman, 1926) along the European coast

RICHIRT Julien[1], SCHWEIZER Magali[1], and JORISSEN Frans[1]

[1] Angers University, UMR6122 LPG-BIAF – Recent and Fossil Bio-Indicators, 49045 Angers, France

CONTEXT

Ammonia **is one of the most abundant genera worldwide. Cosmopolitan and neritic, *Ammonia* is also one of the first foraminiferal genera described (Plancus, 1739). Showing a very high morphological variability which led to « taxonomical chaos », more than 40 recent species/subspecies were described, although researchers commonly used one to three morphospecies considered as ecophenotypes. This « lumping » tendency has recently been challenged by molecular studies, showing that many supposed ecophenotypes are well separated genetically and can be regarded as different species.**

This study aims to investigate three phylotypes (T1, T2 and T6) widely encountered along the European coast which are usually grouped as « *Ammonia tepida* » and difficult to distinguish morphologically.

Diagram of the number of species considered since the discovery of the genus until recent time

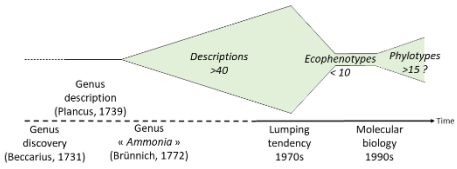

MATERIAL AND METHOD

About 360 *Ammonia* specimens were sampled from 30 sites along the European coast during the AMTEP project (EC2CO) to perform morphometric and molecular analysis.

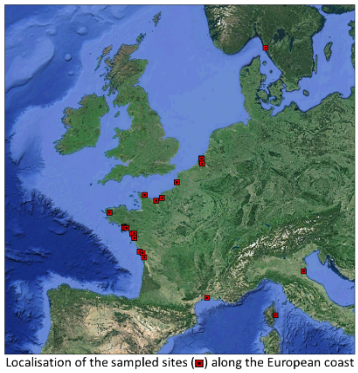

Localisation of the sampled sites (■) along the European coast

SAMPLING

Surface of the sediment sampling

Sieving at 100µm
Picking of living specimens

MORPHOMETRY

For each specimen, Scanning Electron Microscopy (SEM) images of the 3 sides and a 1000x magnified image of the penultimate chamber were taken.

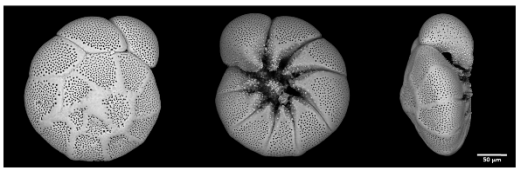

Spiral side | Umbilical side | Apertural side

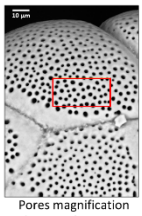

Pores magnification
Red rectangle represent the measuring area.

More than 70 morphometric parameters were measured to determine a set of criteria, allowing to discriminate each phylotype morphologically

PHYLOTYPE DETERMINATION

Live specimens were firstly crushed into DOC buffer. Two DNA amplifications by Polymerase Chain Reaction (PCR) were performed sequentially using respectively s14F3/J2 and s14F1/N6 primers to amplify a part of the SSU rDNA. Fragments (about 500 nt) were then sequenced and each specimen was assigned to a phylotype.

Location of the primers used to amplify the SSU fragments

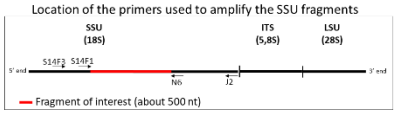

Phylogenic tree (neighbourg joining, Kimura 2 parameters) constructed with some specimens from Auray river (Gulf of Morbihan, France – annoted « Au ») and known individuals issued from GenBank database considered as reference

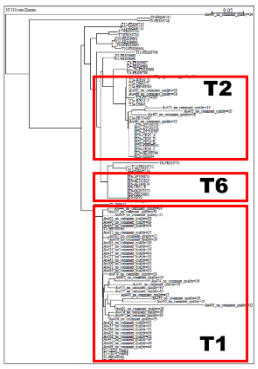

PRELIMINARY RESULTS

Porosity of the penultimate chamber (ellipses represent the confidence interval at 95%) **1**

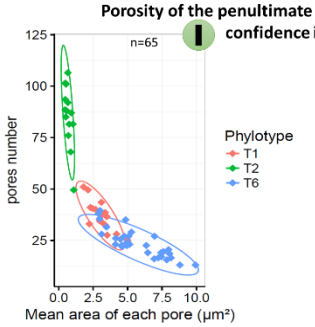

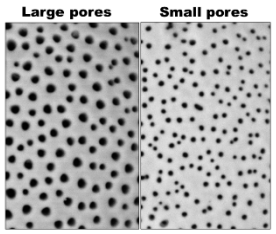

Sutures in central part of the spiral side **2**

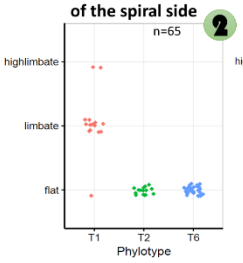

Convexity of spiral part on apertural side **3**

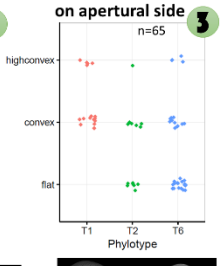

Number of chambers with depressed sutures in last whorl **4**

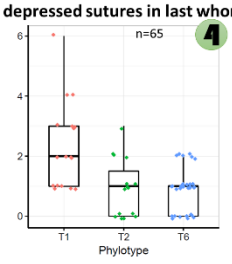

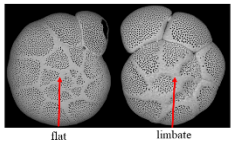

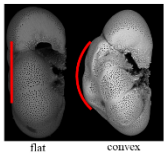

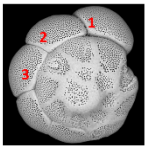

MAJOR POINTS

Morphometric measurements were performed for 65 specimens (17 T1, 15 T2 and 33 T6), work still in progress, to increase the number of analysed individuals. Results seem to indicate that :

1. **The POROSITY OF THE TEST (of the penultimate chamber) allows to discriminate between T2 (small pores) and T1 & T6 (large pores).**
2. **T1 exhibits LIMBATE SUTURES on the spiral side (also apparent in lateral view).**
3. **T1 never shows a FLAT SPIRAL PART in apertural view.**
4. **T1 has at least 1 CHAMBER WITH DEPRESSED SUTURES in the last whorl on the spiral side (and in general shows more depressed sutures than other phylotypes).**

All these criteria are well distinguishable with a stereomicroscope, even when looking for the porosity of the test, and have to be used in combination to discriminate T1, T2 and T6.

We strongly believe that molecular identification combined with morphological analysis will help to disentangle taxonomic issues.

ACKNOWLEDMENTS

This work is part of the AMTEP project, we thank the many people involved in the sampling of the specimens and the Service Commun d'Imagerie et d'Analyses Microscopiques (SCIAM) for the SEM images.

SCALING LAWS EXPLAIN PORE PATTERNS IN FORAMINIFERA (RHIZARIA)

Julien RICHIRT[a,*], Stéphane CHAMPMARTIN[a,*], Magali SCHWEIZER[a], Aurélia MOURET[a], Jassin PETERSEN[b], Abdelhak AMBARI[c], Frans J. JORISSEN[a]

[a] LPG-BIAF, UMR 6112-CNRS, UNIV Angers, Université de Nantes, Angers Cedex, France
[b] Institute of Geology and Mineralogy, University of Cologne, Cologne, Germany
[c] LAMPA, Arts et Métiers ParisTech, Angers Cedex 01, France

*Both coauthors contributed equally

E-mail of the corresponding Authors: richirt.julien@gmail.com; magali.schweizer@univ-angers.fr

Due to climate warming and increased anthropogenic impact, a decrease of ocean water oxygenation is expected in the near future, with major consequences for marine life. In this context, it is essential to develop reliable tools to assess past oxygen concentrations in the ocean, to better forecast these future changes. Recently, foraminiferal pore patterns have been proposed as a bottom water oxygenation proxy, but the parameters controlling these pore patterns are still largely unknown. Here we use scaling laws to describe how both gas exchanges (metabolic needs) and mechanical constraints (shell robustness) control foraminiferal pore patterns. The derived mathematical model shows that only specific combinations of pore density and surface are physically feasible. Maximum porosity can only be obtained by simultaneously increasing pore surface and decreasing pore density. A large empirical data set containing three pseudocryptic phylotypes of *Ammonia*, a common intertidal genus of foraminifera from the eastern Atlantic, strongly supports this conclusion. These new findings provide basic mechanistic understanding of the complex controls of foraminiferal pore patterns and give a solid starting point for the development of proxies of past oxygen concentrations based on these morphological features. Pore surface and pore density are greatly interdependent, and both have to be considered when describing pore patterns.

SCALING LAWS EXPLAIN FORAMINIFERAL PORE PATTERNS

JULIEN RICHIRT, STÉPHANE CHAMPMARTIN, MAGALI SCHWEIZER, AURÉLIA MOURET, JASSIN PETERSEN, ABDELHAK AMBARI AND FRANS J. JORISSEN

CAUSES

Human activity

Global warming

T°

CONSEQUENCES

Increasing eutrophication

Decreasing oxygen solubility

Events of deoxygenation

Duration

Frequency

Coastal hypoxic systems

(modified from Diaz & Rosenberg, 2008)

GENERAL QUESTION

Effects of **hypoxia** events on **present ecosystems**?

Reconstruction of former hypoxias

Extremely diversified **SHELLED ORGANISMS**

& Very complete **FOSSIL RECORD**

FORAMINIFERA (Rhizaria)

Hypothesis: **pores** on the shell **allow them to breath**

➡ Utilisation of the **porosity** to assess **[O_2]**

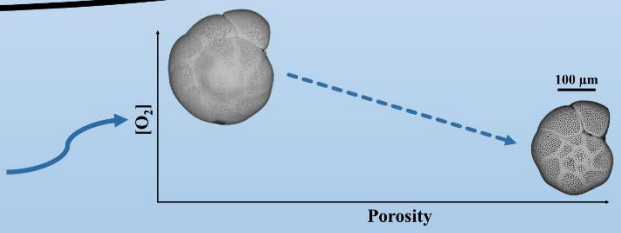

Is oxygen concentration the only factor controlling the porosity?

Hypothesis: porosity is also controlled by a **second factor, the mechanical resistance** of the shell

EMPIRICAL APPROACH

Measurement of different porosity features

on 1386 individuals belonging to the genus *Ammonia*

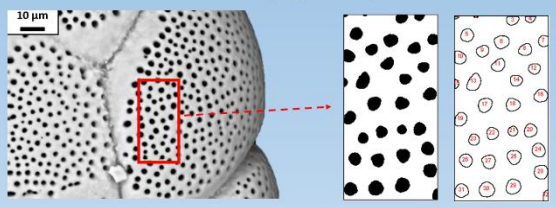

Acquisition of porosity parameters (density and size of pores, overall porosity) with ImageJ using a standardised methodology (Petersen et al., 2016)

THEORETICAL APPROACH

Scaling laws model: 2 constraints

① **Minimum respiration rate** to ensure metabolism

For a given thickness, density and radius of the pores are dependent of the differences between extra and intracellular dissolved oxygen concentrations

② **Mechanical resistance** of the shell must be **preserved**

When hemispherical chamber and $L \ll R_s$, density of the chamber is constant, calcite breaks by brittle fractures with negligible plastic deformations

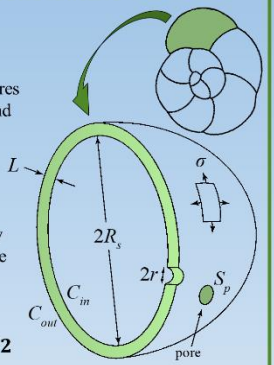

MODEL PREDICTIONS

$N \sim r^{-3/2}$ $\Phi \sim r^{1/2}$ $\sigma^* \sim r^{-1/2}$

N = density of pores, Φ = overall porosity, L = thickness of the shell, R_s = radius of the chamber, C_{in} = intracellular concentration, C_{out} = extracellular concentration, r = radius of the pores, S_p = surface of the pores, σ = mechanical stress on the shell

PREDICTIONS *vs.* MEASUREMENTS

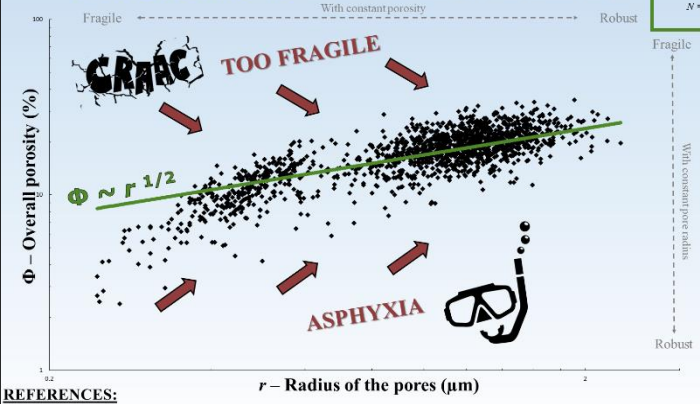

Best **strategy** to preserve the **mechanical integrity** of the shell & increase the **porosity**?

➚ **Surface of the pores** ➘ **Density of the pores**

Potentially applicable to any:

- **Species of foraminifera** (with similar morphology)
- **Dissolved chemical species** (ex: nitrates)

➡ 1st step toward the development of an [O_2] **proxy** based on the **morphology** of foraminifera

REFERENCES:

Richirt *et al.* Scaling laws model explain foraminiferal pore patterns, *Scientific Reports* 9, 9149 (2019) - Diaz, R. J. & Rosenberg, R. Spreading Dead Zones and Consequences for Marine Ecosystems. *Science* 321, 926–929 (2008) - Petersen, J. *et al.* Improved methodology for measuring pore patterns in the benthic foraminiferal genus Ammonia. *Mar. Micropaleontol.* 128, 1–13 (2016)

FORAMINIFERAL COMMUNITY RESPONSE TO SEASONAL ANOXIA IN LAKE GREVELINGEN (NETHERLANDS)

Julien RICHIRT[1], Bettina RIEDEL[2], Aurelia MOURET[1], Magali SCHWEIZER[1], Dewi LANGLET[3], Filip J. R. MEYSMAN[4,5], Caroline P. SLOMP[6] and Frans J. JORISSEN[1]

[1] UMR 6112 LPG-BIAF Recent and Fossil Bio-Indicators, University of Angers, 2 Boulevard Lavoisier, F-49045 Angers, France
[2] Natural History Museum Vienna, 1. Zoology, Fish Collection
[3] UMR 8187 LOG Laboratory of Oceanology and Geosciences, Univ. Lille, CNRS, Univ. Littoral Côte d'Opale, Marine Station of Wimereux, 28 Avenue Foch, 62930 Wimereux, France
[4] Department of Biology, University of Antwerp, Universiteitsplein 1, B-2610 Wilrijk, Belgium
[5] Department of Biotechnology, Delft University of Technology, Van der Maasweg 9, 2629 HZ Delft, The Netherlands
[6] Department of Earth Sciences (Geochemistry), Faculty of Geosciences, Utrecht University, Princetonlaan 8a, 3584 CB Utrecht, The Netherlands

Corresponding author e-mail: richirt.julien@gmail.com

Oxygen depleted bottom waters are observed with increased frequency, intensity, extent and duration, and such events have very deleterious consequences for ecosystem functioning. Benthic foraminifera are fairly tolerant to low oxygen concentrations, which makes them ideal to develop environmental quality indices for these oxygen-stressed environments. Lake Grevelingen (Netherlands) is an artificial saltwater lake, experiencing seasonal anoxia/hypoxia in summer. At this location, two groups of bacteria (*Beggiatoaceae* and cable bacteria) have a profound impact on biogeochemical cycles and show contrasting population dynamics throughout the year. In 2012, two sites showing a variable duration of hypoxic/anoxic events during the year were sampled bimonthly in order to characterize the population dynamics of foraminifera over the seasonal cycle. We used CellTracker Green (CTG) to focus on living specimens in our investigations, as it is known that in low oxygen conditions, Rose Bengal does not efficiently discriminate living from dead individuals. Our results show that the benthic foraminiferal communities are strongly dominated by *Elphidium selseyense*, *Ammonia* T6, *Elphidium magellanicum* and *Trochammina inflata*. These dominant taxa exhibit different responses to the seasonal hypoxia/anoxia. Our data suggest that *Elphidium selseyense* is more resistant to oxic stress than *Ammonia* T6. The better understanding and characterization of the response of foraminiferal populations to seasonal hypoxia/anoxia, as obtained in this study, will help to design environmental quality indices using foraminifera.

FORAMINIFERAL COMMUNITY RESPONSE TO SEASONAL ANOXIA IN LAKE GREVELINGEN (THE NETHERLANDS)

JULIEN RICHIRT[1], BETTINA RIEDEL[1,2], AURELIA MOURET[1], MAGALI SCHWEIZER[1], DEWI LANGLET[1,3], DORINA SEITAJ[4], FILIP J. R. MEYSMAN[5,6], CAROLINE P. SLOMP[7] AND FRANS J. JORISSEN[1]

[1] UMR 6112 LPG-BIAF Recent and Fossil Bio-Indicators, Angers University, 2 Boulevard Lavoisier, F-49045 Angers, France
[2] Now at Natural History Museum Vienna, 1. Zoology, Fish Collection
[3] Now at UMR 8187 LOG Laboratory of Oceanology and Geosciences, Marine Station of Wimereux, 28 Avenue Foch, 62930 Wimereux, France
[4] Department of Ecosystem Studies, Royal Netherlands Institute for Sea Research (NIOZ), Yerseke, The Netherlands
[5] Department of Biology, University of Antwerp, Universiteitsplein 1, BE-2610 Wilrijk, Belgium
[6] Department of Biotechnology, Delft University of Technology, 2629 HZ Delft, The Netherlands
[7] Department of Earth Sciences (Geochemistry), Faculty of Geosciences, Utrecht University, Princetonlaan 8a, 3584 CB Utrecht, The Netherlands

The Micropalaeontological Society
Foram – Nanno
1st – 4th July 2019
Fribourg

LAKE GREVELINGEN

Former estuary **artificially closed** (1965 – 1971)

↳ Strongly reduced water circulation

↓

Thermal **stratification** + Benthic **respiration**

Seasonal anoxia + **H_2S at sediment surface**

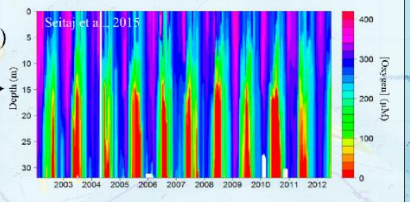

BENTHIC FORAMINIFERA

Tolerance to **anoxia** well documented

?

Information about tolerance of **H_2S** less clear

MATERIAL & METHODS

OPD: Oxygen Penetration Depth
BWO: Bottom Water Oxygen
H_2S: Hydrogen sulphide presence

FORAMINIFERA (1cm – fraction >125µm)

Monthly — **2011** — **August & November**
Monthly — **2012** — **Bi-monthly**

CellTracker Green stained – 2 replicates

Donders et al., 2012; Seitaj et al., 2017

Station 1

STRONG RESPONSE

Almost **complete disappearance** of foraminifera
Delayed response ~ 2 months
Long recovery time ~ 6 months

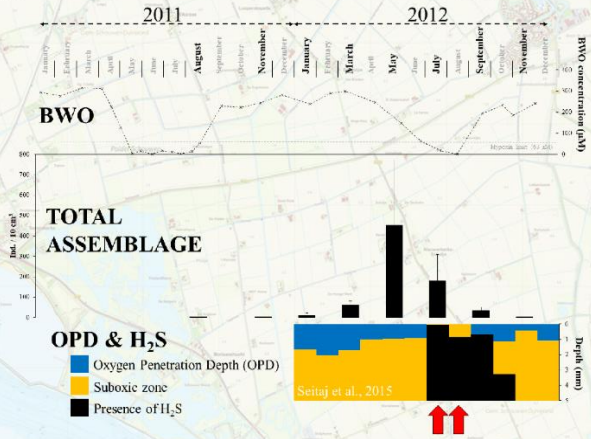

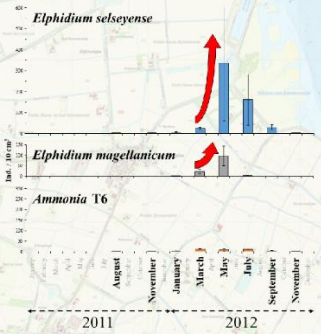

Station 2

MODERATE RESPONSE

Decrease of total abundances
Delayed response ~ 2 months
Fast recovery time = 1 month

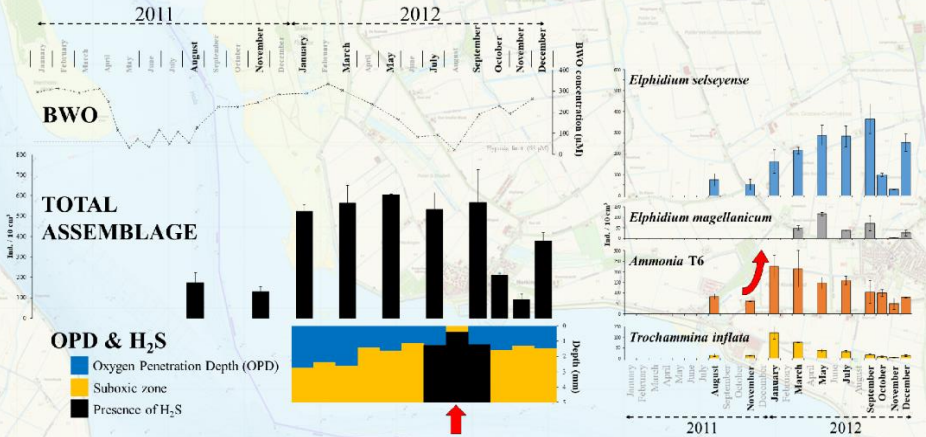

Species specific response ≠ **Species specific** response

Favourable for *Elphidium* in spring/summer ↓ **FOOD** Favourable for *Ammonia* in winter

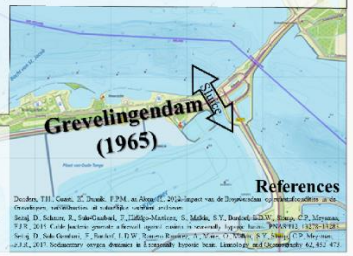

1 Communities strongly **impacted** by the **duration** of **anoxia** & **H_2S**
➡ Station 1 = almost **extinction** of foraminifera

2 **Food source** causes interspecific **differences** in population dynamics

3 **Delayed response** of ~ 2 months
➡ **Stop of reproduction** & maybe increased mortality

References

Donders, T.H., Cleveringa, J., Dusseldorp, E.P.M., van Arkel, J.C., 2012. Impact van de Brouwersdam op de Grevelingen: veranderingen in de overstromingsfrequentie en de zuurstofhuishouding in de waterkolom en in de bodem. Rapport 2012-01, Utrecht University, Utrecht, The Netherlands, 1–57.

Seitaj, D., Schauer, R., Sulu-Gambari, F., Hidalgo-Martinez, S., Malkin, S.Y., Burdorf, L.D.W., Slomp, C.P., Meysman, F.J.R., 2015. Cable bacteria generate a firewall against euxinia in seasonally hypoxic basins. PNAS 112, 13278–13283.

Seitaj, D., Sulu-Gambari, F., Burdorf, L.D.W., Tramper, A., Polerecky, L., Slomp, C.P., Meysman, F.J.R., 2017. Sedimentary oxygen dynamics in a seasonally hypoxic basin. Limnology and Oceanography 62, 452–472.

UNIVERSITE SCIENCES BRETAGNE DE LA MER LOIRE ET DU LITTORAL

université angers

Titre : Le genre *Ammonia* (Foraminifères) dans les écosystèmes côtiers de la façade atlantique

Mots clés : *Ammonia*, phylotype, biogéographie, diversité (pseudo-)cryptique, anoxie, porosité

Résumé : L'objectif principal de cette thèse est l'étude de trois phylotypes, *Ammonia* sp. T1, T2 et T6, sur les littoraux de l'Atlantique nord-est. Ces phylotypes étaient auparavant impossibles à distinguer sans l'utilisation d'outils moléculaires et souvent identifiés comme la morpho-espèce de foraminifère cosmopolite *Ammonia tepida*. Nous montrons ici à l'aide d'une analyse morphométrique qu'il est maintenant possible de différencier ces trois phylotypes en se basant sur deux critères morphologiques : la taille des pores et l'élévation des sutures sur la face spirale. En utilisant cette nouvelle méthode, nous examinons leur distribution autour des Îles Britanniques et nos résultats suggèrent que le phylotype T6 étend son aire de répartition et remplace les phylotypes T1 et T2. Au lac de Grevelingen (Pays-Bas), fortement artificialisé, nous étudions leur réponse à une euxinie saisonnière ainsi que leur succession sur un enregistrement sédimentaire couvrant les 50 dernières années. Nos résultats montrent que T6 est arrivé dans le lac au milieu des années 1980 et a progressivement remplacé T1 et T2 jusqu'à aujourd'hui, potentiellement grâce à une meilleure tolérance à de faibles concentrations d'oxygène. Finalement, à l'aide de relations allométriques, nous proposons que le motif des pores du test reflète une différence de tolérance aux concentrations en oxygène, expliquant le succès invasif de T6 en Europe et insistant sur son utilisation potentielle pour la reconstruction des concentrations passées d'oxygène dans les zones côtières. Les résultats obtenus indiquent que les trois phylotypes semblent montrer des différences de tolérance aux concentrations en oxygène et appuient l'hypothèse de la nature exotique et invasive du phylotype T6, supposé originaire d'Asie de l'est.

Title: The genus *Ammonia* (Foraminifera) in the ecosystems of the Atlantic coasts

Keywords: *Ammonia*, phylotype, biogeography, (pseudo-)cryptic diversity, anoxia, porosity

Abstract: The overall aim of this PhD thesis is to investigate the three phylotypes *Ammonia* sp. T1, T2 and T6 in mid-latitude Eastern Atlantic coastal areas. Previously, as they were impossible to distinguish without molecular analyses, these phylotypes were often merged together and identified as the cosmopolitan foraminiferal morphospecies *Ammonia tepida*. Here we show with a morphometric study that it is possible to discriminate the three phylotypes based on two morphological features: the pore size and the suture elevation on the spiral side. Using this new method, we study their large scale biogeography around the British Isles and highlight a coherent distribution pattern, which suggests that T6 is currently spreading out over large areas and supplanting phylotypes T1 and T2. In the artificially enclosed Lake Grevelingen (the Netherlands), we investigate their seasonal response to euxinia and their historical succession over the last 50 years. Our results show that T6 arrived in the lake only in the mid 1980s and progressively replaced T1 and T2, possibly thanks to its higher tolerance to low oxygen concentrations. Using a theoretical approach, we finally propose that the pore pattern of the test reflects differences in tolerance for low oxygen conditions, which possibly explain the spreading success of T6 in Europe, and highlight its potential use as a proxy for the reconstruction of past oxygen concentrations in coastal areas. Our results strongly suggest that the three phylotypes show different tolerance levels for low oxygen concentrations, and support the putative exotic and invasive nature of the phylotype T6, supposedly originating from East Asia.